PALAEOMAGNETIC STUDIES OF THE MESOZOIC-TERTIARY TECTONIC EVOLUTION OF CYPRUS, TURKEY AND GREECE

A. MORRIS B.Sc M.Sc

DEPARTMENT OF GEOLOGY AND GEOPHYSICS, JAMES CLERK MAXWELL BUILDING, KINGS BUILDINGS, THE UNIVERSITY OF EDINBURGH

THESIS SUBMITTED FOR THE DEGREE OF
DOCTOR OF PHILOSOPHY
AT THE UNIVERSITY OF EDINBURGH,
SEPTEMBER, 1990.

DECLARATION.

I declare that this thesis has been composed by myself, and that the work is my own except where otherwise stated and duly acknowledged.

ABSTRACT.

Palaeomagnetic studies have been carried out in three key regions of the eastern Mediterranean part of the Tethyan orogenic belt.

Within the Troodos ophiolite of Cyprus, samples were collected from extrusives and sediments exposed along the Arakapas fault belt and around the periphery of the Limassol Forest block. These areas represent crust which formed in the Upper Cretaceous within a 'leaky' oceanic transform fault, and also a small fragment of crust generated at an 'Anti-Troodos' spreading axis. Significant clockwise intra-crustal rotations of small fault-bounded blocks have been identified within the inferred transform zone. These rotations are shown to be synchronous with crustal genesis and indicate a probable dextral sense of shear along the transform. In contrast, the 'Anti-Troodos' crust appears to have undergone an identical rotation to the non-transform tectonised Troodos crust to the north. Variations in declination upwards through the umber-radiolarite sequences overlying the extrusives demonstrate that 45° of the 90° palaeorotation of the Troodos microplate occurred within 15 Ma of formation of the Troodos crust.

A wide-spread remagnetisation event has been identified in the Isparta angle region of SW Turkey. Sites were located both within the Tauride carbonate platform massifs and in the overthrust units of the Antalya Complex. The latter consists of an assemblage of continental margin and ophiolitic rocks which originated in a strand of the Neotethys located to the south of the carbonate platforms. The secondary nature of the remanence at most sites is demonstrated by several negative fold tests. The magnetisation is carried by magnetite of presumed authigenic origin. The remagnetisation event was probably triggered by the migration of orogenic fluids ahead of the Antalya Complex during its emplacement onto the adjacent platforms in the Lower-Middle Miocene. Subsequent to remagnetisation, a large segment of the area underwent an anticlockwise rotation of 30°. This rotation was probably related to the Neotectonic bending of the Hellenic arc and the emplacement of the Lycian Nappes during the Middle-Upper Miocene.

A detailed palaeomagnetic study within the Argolis Peninsula of the southern Greek Hellenides has demonstrated that the northern and southern halves of this area have undergone significantly different tectonic rotations. The results support the suggestion that the Asklipion Unit exposed within Argolis represents the sedimentary infill of intra-platformal deep-water basins and not a far-travelled continental margin assemblage. The data also indicate that the emplacement of the Jurassic Migdhalitsa Ophiolite Unit may have had a strong strike-slip component. A combination of the Argolis data, preliminary results from the Gavrovo-Tripolitza and Ionian Zones further to the west and previously published data from other Greek areas suggests that a 25-40° clockwise rotation affected much of the Hellenides in the Pliocene. The large rotation of the northern half of the Argolis Peninsula does not represent the isolated rotation of a small fault-bounded block. Instead, there is evidence for large (*ca.* 70°) clockwise rotations in areas both to the north and south of the Gulf of Corinth, which may in part be related to fault block activity within a distributed shear zone linking the North Anatolian Fault with the Hellenic trench to the west. Additional results from the Pindos thrust sheets, which overlie the Gavrovo-Tripolitza platform, indicate varying amounts of rotation. These variations may be related to local rotations due to break-up of the thrust sheets during emplacement over a topographically uneven footwall and/or to local variations in the Late Tertiary rotation of the underlying autochthon. Removal of an average rotation of the basement suggests that the thrust sheets experienced an overall anticlockwise rotation during their emplacement, which may relate to the diachronous closure of the Pindos basin in the Eocene.

This research has identified block rotations in a variety of geological settings. These range from rotations active during oceanic crustal genesis to those associated with the

late stages of continental collision. These rotations would have been impossible to identify by means of field structural studies alone. An awareness of such rotational deformation is essential if the geological evolution of complex areas is to be fully understood.

Acknowledgements.

This work was carried out under the tenure of a studentship from the Natural Environmental Research Council. Additional fieldwork support was provided by Amoco Production Company, Houston.

I am greatly indebted to my supervisors, Professor K. M. Creer and Dr. A. H. F. Robertson, for their encouragement and assistance during my time in Edinburgh. Especial thanks go to Alastair for always finding time to visit me in the field.

This project owes a great deal to Tristan Clube, for teaching me how to drill straight cores and for demonstrating the geology of Cyprus to me. Especial thanks also go to Fred Vine for getting me interested in Geophysics as an undergraduate at U.E.A. and for informal discussions, to Simon Allerton for explaining the intricacies of his net tectonic rotation technique, and to Peter Clift for stimulating discussions on the geology of Argolis.

I have benefited from informal discussions with many other scientists from Britain, Greece, Turkey, Canada and the United States, including W. Birch (Liverpool), H. Brown (Edinburgh), P. Condon (Chevron), P. Degnan (Edinburgh), E. Follows (Edinburgh), D. Galanopoulos (Edinburgh), B. Goodman (2-G Enterprises, California), G. Jones (Edinburgh), F. Liakopoulou (Edinburgh), C. MacLeod (Open University), B. Murton (Open University), P. Pal (India), D. Piper (Canada), D. Stone (Alaska), M. Stewart (Edinburgh), I. Snowball (Edinburgh), R. Thompson (Edinburgh), H. Turnell (BP Research), I. Turton (Edinburgh), T. Ustaomer (Edinburgh), V. Valiant (NERC Pool, Edinburgh), J. Waldron (Newfoundland), D. Watson (Edinburgh), and W. Williams (Edinburgh).

I thank Professors K. M. Creer and G. S. Boulton for making the resources at the Department of Geology and Geophysics freely available to me. In Edinburgh, technical help and facilities were provided by A. Pike, A. Jackson, C. Grandison, H. McKeating, M. Macdonald, and D. Baty. I am especially grateful to Alan Pike for keeping the magnetometers running and cheering me up at times of difficulty in the laboratory.

Palaeomagnetic field assistance was provided by K. Creer, A. Robertson, S. Gray, C. Kelly and H. Livingston, while S. Law, M. Manson, M. Tolstoy, C. Kelly, H. Livingston and Y. Hague have helped with measuring. I. Snowball performed several thermomagnetic experiments for me.

I thank the Cyprus Geological Survey, and Soteris Varnavas of Patras University, Greece, for providing permits for fieldwork.

Finally, I would like to thank my parents and family for always encouraging me to move on to the next stage in my career and for their love, and Fotini for her love and support during the writing of this thesis.

CONTENTS.

PART FOUR - GREECE.

CHAPTER SEVEN - GEOLOGY AND PALAEOMAGNETISM OF GREECE: A REVIEW.

CHAPTER EIGHT - A PALAEOMAGNETIC STUDY OF THE RELATIVE AUTOCHTHONS OF THE PELOPONNESOS.

PART ONE - INTRODUCTION.

CHAPTER ONE - INTRODUCTION.

1.1 Introduction.

This thesis presents the results of palaeomagnetic studies of the Mesozoic and Tertiary units exposed in three important areas of the eastern Mediterranean part of the Tethyan orogenic belt.

Although the palaeomagnetic technique is best known for continental-scale tectonic studies, it is also uniquely suited to the identification of rotations about steeply inclined axes and horizontal translations which have affected smaller, microcontinental-scale crustal units. The data provided by palaeomagnetic studies within complex orogenic belts can greatly assist interpretation of their tectonic evolution. For example, reconstructions of the various strands of the Neotethyan ocean (see Chapter 2) during the Mesozoic and Tertiary are particularly dependent on knowledge of the direction and timing of the emplacement of allochthonous units, such as ophiolite nappes. Without information on the rotations which have affected the underlying relative autochthons, structural data concerning the direction of transport of such units may be misinterpreted and lead to erroneous palinspastic reconstructions.

The original aim of the present research was to examine the tectonic evolution of the Isparta angle region of southwestern Turkey, a critical suture zone which appears to separate the Tauride and Hellenide segments of the Tethyan orogenic belt. An analysis of a pre-existing set of samples from this region is presented in Part Three of this thesis. However, logistical problems prevented further fieldwork in Turkey. Instead a short period of fieldwork in Cyprus was undertaken, and the research was then shifted further west, into the Peloponnesos of southern Greece. This final move was prompted by the establishment in Edinburgh of a large research group studying the geological evolution of the Greek Hellenides. It was felt that the palaeomagnetic research of the present study and the research of the geological group would complement each other, and lead to a better understanding of the tectonic evolution of this complex region.

A project of this kind, which is involved in several different geological provinces within the overall Tethyan orogenic belt, necessarily has to draw heavily on published geological studies for background information and to obtain an overall understanding of the tectonics of the areas in question. Thus many of the review sections of this thesis do not include any new data acquired as part of the research, but instead deal with the geological arguments which must be considered before any reasonable and geologically consistent interpretations can be made of the palaeomagnetic results. I stress, however,

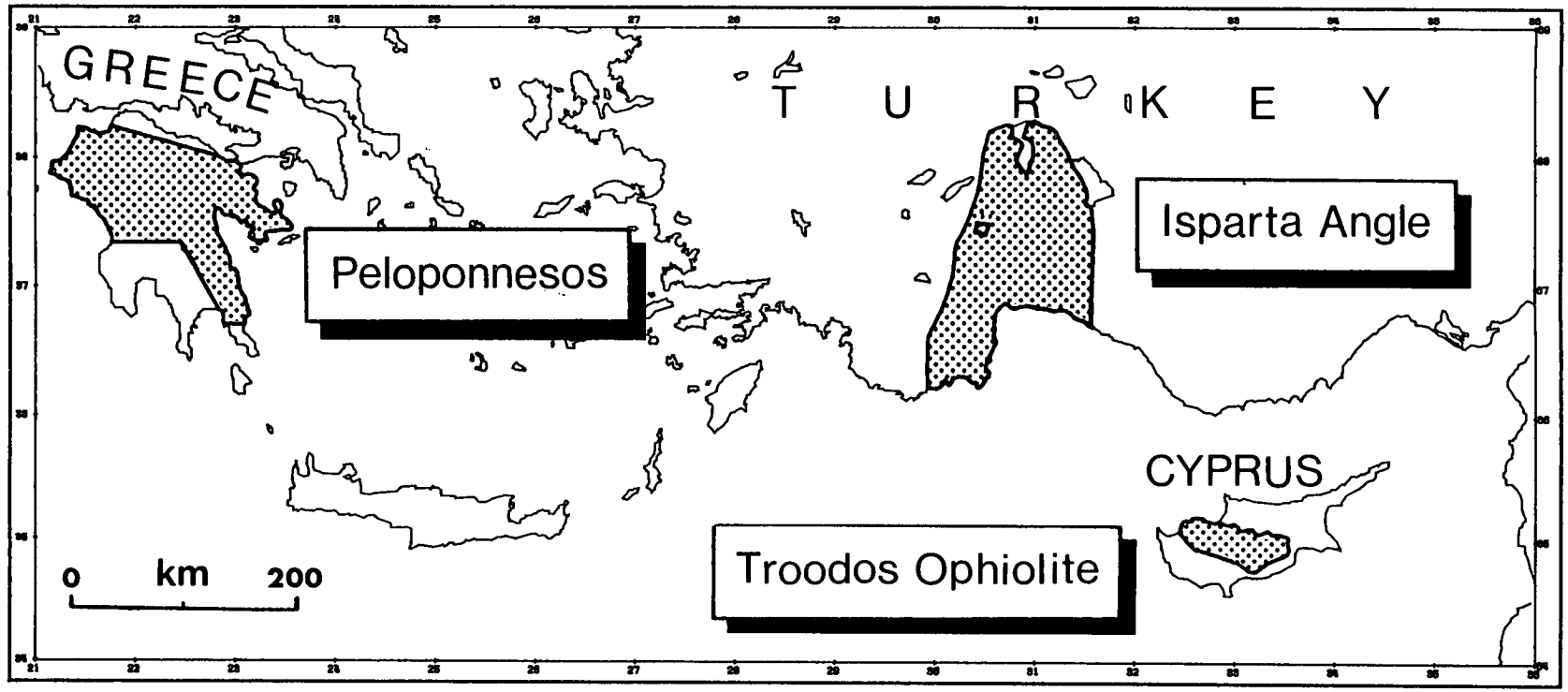

Figure 1.01. Map of the eastern Mediterranean region showing the location of the three study areas where palaeomagnetic sampling has been carried out in the present study.

that all such interpretations and discussions of the geological significance of the results are based on my own ideas.

This thesis could have been made considerably shorter by the exclusion of much of the information on the geological setting of the study areas. However, I feel that this would result in a less coherent thesis, and reduce the interest of the work to those unfamiliar with the eastern Mediterranean Tethys.

The locations within the eastern Mediterranean region of the three areas examined in this thesis are shown in Figure 1.01. The objectives of the research within each of these areas are outlined below.

1.2 Objectives of this research.

1. To establish the sense of motion along a fossil oceanic fracture zone preserved within the Arakapas fault belt and Limassol Forest sub-terranes of the Troodos ophiolite, Cyprus.

2. To place further constraints on the timing of the Upper Cretaceous-Lower Eocene 90° anticlockwise rotation of the Troodos microplate.

3. To determine whether the continental margin and ophiolitic assemblage of the Antalya Complex, exposed within the centre of the Isparta angle region of southwestern Turkey, experienced relative block rotations during its strike-slip dominated emplacement onto the adjacent Tauride platform units in the Upper Cretaceous and Lower Tertiary.

4. To determine whether the Tauride carbonate platform massifs exposed around the Isparta angle have behaved as a single tectonic unit, or have rotated independently of each other, and to what extent the observed rotations have been influenced by the strike-slip regime.

5. To establish the pattern of rotation within the Argolis Peninsula of the Subpelagonian Zone of the southern Greek Hellenides, and to test palaeomagnetically several tectonic models which have been proposed for the area.

6. To determine whether the autochthonous units of the Gavrovo-Tripolitza and Ionian Zones to the west of Argolis have also experienced significant tectonic rotations, and to what extent such rotations can be related to the Neotectonic deformation of the Hellenic arc and trench system.

7. To examine the thrust sheets of the Pindos Zone to determine whether they have been subjected to significant rotation during their emplacement over the relative autochthon of the Gavrovo-Tripolitza platform.

1.3 Assumptions of the palaeomagnetic method.

The objective of palaeomagnetic studies when applied to tectonic problems is to recover the direction of the geomagnetic field at known points in the geological history of a crustal unit. This data can then give us information on the amount of rotation and translation which has affected the unit since it acquired its magnetisation. An important assumption of such studies is, therefore,that the sampled lithologies accurately retain a record of the past orientation of the geomagnetic field. This retention is due to the inclusion in the rock of a mineral fraction exhibiting a form of ferromagnetic behaviour.

For palaeomagnetic studies to be of use for palaeotectonic purposes, however, the orientation of the field itself must be shown to vary in a systematic fashion with respect to the geographic poles both at the present and during previous periods of geological time.

At present, approximately 90% of the Earth's magnetic field can be ascribed to a geocentric magnetic dipole inclined at about 11.5° to the axis of rotation. This is termed the dipole field. The 10% of the total field which remains after the best-fitting geocentric dipole has been subtracted is known as the non-dipole field. Historical, archaeomagnetic and geomagnetic records indicate that the magnetic field has constantly changed over several thousands of years. These changes are described as secular (i.e. slow) variation, and they appear to be roughly cyclic, with a periodicity of several hundreds of years, such that they will be averaged out given a sufficient time sampling of the field.

When combined with palaeomagnetic studies covering the last few million years, the collective observations conform to a model in which the time-averaged magnetic field may be represented by an axial geocentric dipole, such that the geographical and geomagnetic axes coincide. In this model, the field is directed downwards at the north geographic pole and upwards at the south pole (during a normal polarity period), and is horizontal at the equator. Providing that i) palaeosecular variation is sufficiently time-averaged by the palaeomagnetic sampling, and ii) the inclination of the remanence identified within a sampled unit corresponds accurately to the inclination of the geomagnetic field at the time of magnetisation, the axial geocentric assumption allows the inclination to be related to the latitudinal position of the sampled unit at that time through the following relationship:

$$\tan I = 2 \tan \lambda$$

where I is the inclination of the remanence, and λ is the palaeolatitude of the sampling site.

There now follows a description of the laboratory techniques and instrumentation used to determine the characteristics of the natural remanent magnetisation (NRM) at each of the sites analysed in this study.

1.4 Demagnetisation techniques.

NRM is the remanent magnetisation present in a rock sample prior to any laboratory treatment. The NRM depends upon the geomagnetic field and geological processes affecting the rock during its formation and subsequent history. The NRM is typically composed of more than one component. The component acquired during rock formation is referred to as the *primary* NRM and is the component sought in most palaeomagnetic investigations. However, *secondary* NRM components can be acquired subsequent to rock formation and can alter or obscure the primary NRM.

The two routine 'cleaning' techniques currently employed to isolate the primary components of magnetisation within rock specimens are the thermal and alternating magnetic field methods. They operate by using thermal and magnetic energy respectively to overcome magnetic energy barriers within particles carrying secondary remanences. In this way, the magnetic moments of these particles are randomised.

1.4.1 Thermal demagnetisation.

This technique relies upon the strong inverse dependence of magnetic relaxation time upon temperature. If the temperature of rock is raised until the relaxation time of some fraction of the particles carrying a secondary component of magnetisation has been reduced to a few minutes or less, the remanence of these particles will be 'unblocked' and their contribution to the NRM lost. If the rock is then cooled in a zero field environment a random orientation of particle or domain moments will be produced at room temperature, and components of NRM with blocking temperatures less than the maximum heating temperature will be removed.

To progressively demagnetise a rock specimen, therefore, we raise its temperature to successively higher levels and measure its remaining NRM after cooling in zero field. In this way, lower blocking temperature components are removed, hopefully leaving the primary component with a higher blocking temperature relatively unaltered.

Thermal cleaning has proved successful when applied to sediments, in which partial thermoremanent magnetisation (PTRM) acquired during burial and viscous remanent magnetisation (VRM) acquired in the recent geomagnetic field are common sources of secondary NRM. It is particularly useful when dealing with haematite bearing rocks, for which alternating field treatment is ineffective because of high remanent coercivities.

The thermal demagnetisation oven used in the present study was manufactured by Magnetic Measurements Ltd. A single heating/cooling chamber is surrounded by a four-layer Mumetal magnetic shield to produce a very low field environment. The oven is capable of holding 18 standard palaeomagnetic cores, and is fully programmable with two heating ramps and one cooling cycle. The mouth of the oven projects into a set of Helmholtz coils surrounding the cryogenic magnetometer (section 1.7.1), to reduce the acquisition of spurious components of magnetisation when removing samples. In this study thermal demagnetisation has been successful in recovering primary remanences from many carbonate sites located in southern Greece.

1.4.2 Alternating field demagnetisation.

The variable grain size and shape distribution of magnetic minerals in naturally occurring samples gives rise to a similarly variable distribution or spectrum of coercive forces. This fact is utilised in the stepwise alternating field (AF) demagnetisation process, in which samples are cycled through hysteresis loops of gradually decreasing amplitude from an initial field setting, H_1. In the stepwise technique, the value of H_1 is increased from one treatment to the next, thus affecting particles of sequentially higher coercive force.

The behaviour of single-domain (SD) and multi-domain (MD) particles during AF demagnetisation is somewhat different. SD grains with a coercive force less than H_1 will follow the alternating field direction until the external field drops below the coercive force, leaving the SD moments randomised in the sample. On the other hand, MD grains will demagnetise to form 'closed' domain patterns which, in the absence of a magnetic field, will have no magnetic moment. Imperfect MD and PSD grains may retain a residual moment which, like the SD grains, is random throughout the sample.

In practice, AF demagnetisation is usually used in the treatment of samples containing remanences carried by magnetite and titanomagnetite grains. The strong crystalline anisotropy of haematite produces a coercivity well in excess of presently available pure peak fields.

The AF demagnetisation unit used in this study was manufactured by 2-G Enterprises, and consists of a single coil surrounded by a three-layer Mumetal shield. Each axis of the specimen to be demagnetised is presented in turn to the axis of the coil. A fourth demagnetisation step at half the peak field value, with the sample orientated antiparallel to the third position, is used to reduce any possible acquisition of an anhysteretic magnetisation, following the method of Snape (1971).

In the present study, AF demagnetisation has been applied to all igneous and sedimentary samples collected from southern Cyprus. It has also been successfully

used to recover primary and 'ancient secondary' remanences from many carbonates from south-western Turkey and southern Greece, in cases where the remanence is carried by magnetite and titanomagnetite particles.

Two types of magnetometer have been used in the present study for the measurement of all remanences. Details of these are given in the next sections.

1.5 The Molspin spinner magnetometer.

Spinner magnetometers utilise the alternating voltage produced by the continuous rotation of a magnetised sample within a fluxgate system, consisting of two flux-sensitive probes stationed in opposition (Figure 1.02). The amplitude of the output voltage is proportional to the component of magnetic moment perpendicular to the rotation axis (which is itself perpendicular to the fluxgate axis), to the distance between the specimen and the probes, and to the sensitivity of the probes themselves. As the specimen rotates, the fluxgate sensors are subjected to a fluctuating magnetic field, and the resulting signal is compared with a reference signal. The phase difference between the reference and signal voltages is proportional to the angle between the direction of the measured component and a fixed direction in the sample holder. The holder fiducial direction is orientated such that the phase difference is zero when the component of magnetisation is parallel to the fiducial direction. In the Molspin system, the phase information is used to resolve the signal voltage into orthogonal components proportional to components of magnetisation parallel and perpendicular to the reference direction on the holder.

In the present study, the Molspin magnetometer was used to measure natural and isothermal remanences which were too intense to measure on the more sensitive cryogenic systems (section 1.6). Measurements were made using a sequence of four specimen orientations, identical to those used with the cryogenic magnetometer (section 1.6.2; Figure 1.05). The direction and total moment (measured in μAm^2) of each specimen was obtained from the average values of specimen x, y and z components.

All NRM and demagnetisation data for extrusive and intrusive samples collected from southern Cyprus were obtained using this instrument (Chapter 4).

1.6 The cryogenic magnetometers.

The 'workhorse' magnetometers used in the present study for the measurement of weak natural and laboratory grown remanences were cryogenic systems manufactured by Cryogenic Consultants Ltd of London and 2-G Enterprises of San Francisco.

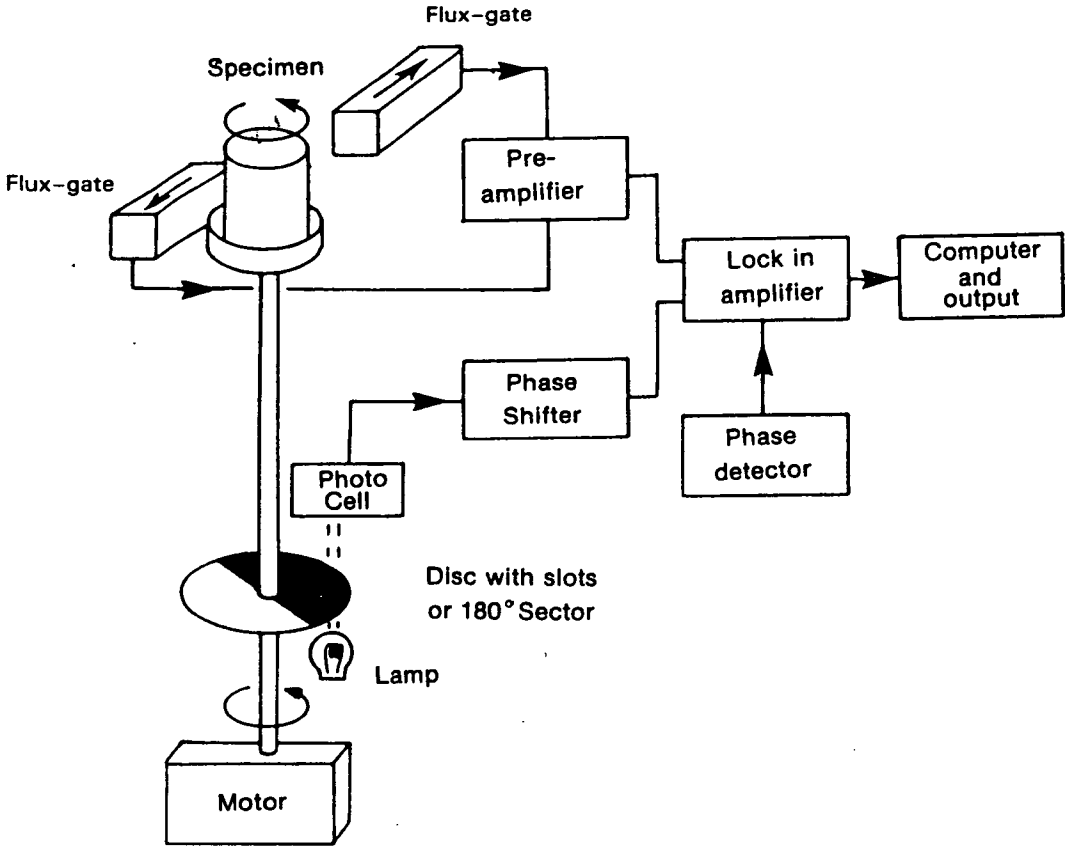

Figure 1.02. Block diagram of a spinner magnetometer. The sensing device is a system of two fluxgate probes in an astatic configuration. The whole is surrounded by magnetic shielding so that variations in direct and alternating ambient fields do not effect the sensors. (from Piper, 1987).

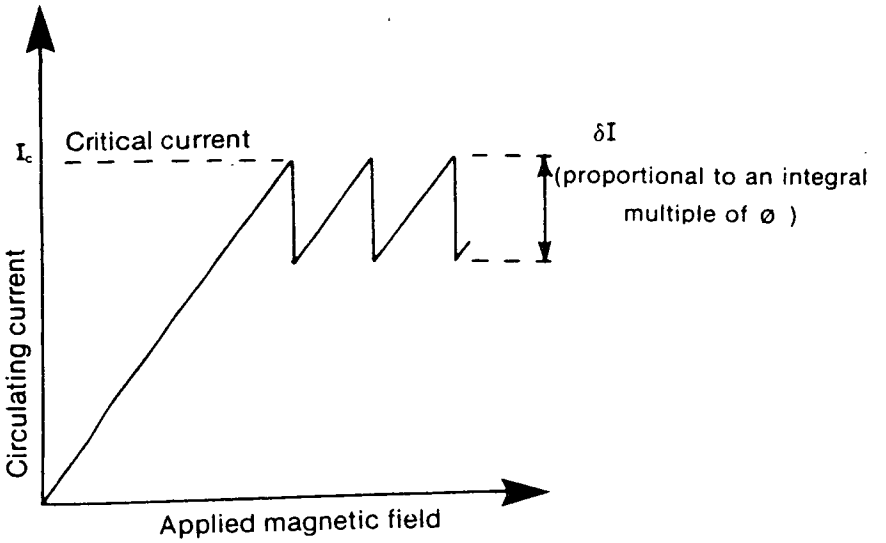

Figure 1.03. Current/field relationship for a superconducting cylinder with a weak link.

The development of cryogenic magnetometers in the 1970's led to an increase in sensitivity of approximately three orders of magnitude over existing spinner and parastatic systems. This has permitted study of a wider range of rock types than was previously possible. In particular the accurate determination of the magnetisations carried by carbonate facies can now be routinely carried out. These limestones typically have intensities of magnetisation at or below the noise level of the most sensitive spinner systems. Since in many cases the intensity of the facies analysed in the present study approaches the instrumental noise level of even available cryogenic magnetometers, it is apparent that special care during measuring and rigorous statistical testing are required to ensure that measured remanences are of acceptable quality. Detailed discussions of sources of instrumental noise and of techniques used to assess the reliability of weak NRM measurements are therefore given in sections 1.7.1 to 1.7.3. Firstly, however, I present a brief discussion of the principles of operation of cryogenic magnetometers, together with an outline of the procedures involved in using the two systems available in Edinburgh. A detailed description of the physics involved in these systems is beyond the scope of the present study. A more thorough treatment of the subject is given by Goree and Fuller (1976).

1.6.1 Operating principles of superconducting magnetometers.

Cryogenic (superconducting) magnetometers are based on the properties of a superconducting ring made of a metal with perfect diamagnetism, which causes the expulsion of all magnetic flux from the ring below a certain temperature. Such a ring has the property that when an external magnetic field is applied along its axis while it is in the superconducting state, superconducting circulating currents are set up in the material of the ring, the magnitude and sense of which exactly cancel the applied flux (Goree and Fuller, 1976). Thus, all magnetic flux is excluded from the interior of the metal, but not from the hole within the ring. This means that induced currents flow in one direction on the outer face of the ring and in the opposite direction on the inner face. If the applied field is removed, the currents on the outside of the ring disappear, but the current on the inside face persists to maintain the field within the ring at the same value. In this way the magnetic field in which the ring was initially cooled below the superconducting temperature is effectively trapped within the hole. Consideration of quantum mechanics shows that this trapped flux cannot take any arbitrary value, but instead is quantised into integral multiples of h/2e, where h is Planck's constant and e is the charge on an electron. This unit is known as the flux quantum, ϕ, and has a value of 2.07×10^{-15} Weber.

This ability of the superconductor to trap and maintain magnetic fields to better than one part in 10^9 is used in cryogenic magnetometers to trap a zero field within the loop. This volume is then used for measurements. The trapping ability is exploited by causing the ring to operate at the superconducting:resistive boundary, and employing a device known as a SQUID (Superconducting Quantum Interference Device). This state is achieved by increasing the field applied to the ring until the circulating current exceeds the critical current of the superconducting material from which the ring is made. The ring then reverts to the normal state and an integral number of flux quanta may enter the material of the ring (Figure 1.03). For low circulating currents only one flux quantum will be admitted. This reduces the circulating current to below the critical value, and the ring becomes superconducting again. The response of the loop to the increasing field therefore has the sawtooth form shown in Figure 1.03. The magnitude of the critical current is a function of the cross-sectional area of the ring, and can be made very small (i.e. comparable to the current equivalent to ϕ) if the current is concentrated through a small cross-sectional area (weak link) at one point.

In practice, the loop is inductively coupled to a tuned coil which is externally excited at its resonant frequency in the radio-frequency (RF) range. This coil is used to produce an a.c. field which drives the loop and also acts as a pick-up coil. Each time the circulating current exceeds the critical current, a flux quantum enters the ring. This generates a voltage spike in the RF coil. When a d.c bias field is present, such as that produced by introducing a rock specimen into the system, the flux quanta enter the ring at different points in the drive field cycle. This effect is measured by applying a feed-back current to a system known as a 'flux locked loop' such that this d.c. shift is cancelled. This current is proportional to the bias field produced by the sample along the axis of the loop.

The magnetometer consists of one, two or three SQUID sensors and pick-up coils, to simultaneously measure sample magnetisations along one, two or three mutually perpendicular axes. The assembly is placed in a superconducting shield to isolate the sensor from all magnetic field changes except that from the field coil, and the whole is surrounded by an insulated evacuated space cooled by liquid helium to produce a cryogenic environment.

1.6.2 The CCL cryogenic magnetometer.

A diagram of the CCL two-axis cryogenic magnetometer is shown in Figure 1.04. The instrument is precooled with liquid nitrogen, contained in the upper tank, which cools the helium chamber and assists in reducing the boil-off of more expensive liquid helium during operation. Both the nitrogen and helium chambers are surrounded by

vacuum spaces which are evacuated prior to cooling. The pick-up coils and SQUID detectors are shielded from external magnetic fields by a niobium superconducting shield and by a magnetic shield of Mumetal. The vertical sample access tube is 35 mm in diameter. The helium chamber capacity is approximately 25 litres and one fill of helium lasts between 15 and 19 days. Helium gas is exhausted from the top of the chamber and passes via a flowmeter to a gas recovery system, where it is collected and compressed into cylinders for resale to offset running costs.

The Edinburgh system is equipped with two pairs of pick-up coils, for simultaneous measurement along two mutually perpendicular axes. One pair of coils is mounted on the side of the access tube to detect radial components of NRM, while the second pair are coaxial with the tube and are symmetrically placed about the measuring position for the axial NRM component. Each coil pair is connected to its own SQUID detector. The output signal from each SQUID is proportional to the flux change produced by the appropriate NRM component.

The sample handling system is mounted vertically on the top of the cryostat. It consists of a carriage moving on vertical guides. A nylon specimen holder is attached to the bottom of a 1 metre long perspex rod of 6 mm diameter which is connected to the carriage by a flexible joint. A circular nylon guide mounted halfway along the rod and a tapered cup on top of the cryostat aid correct insertion of the rod into the access tube. The whole system is interfaced to a Sirius microcomputer, which controls movement of the carriage and reduces data to a declination, inclination and intensity format.

The specimen is inserted into the holder in a specified orientation with its axis aligned with the radial SQUID 'zero declination' direction (see below), and a command is sent via the Sirius to initiate the automatic measuring sequence. The specimen is then lowered to a 'background' measuring position. This is a position where the specimen magnetisation does not couple significantly with the pick-up coils and where readings of the 'zero-level' SQUID outputs can be recorded immediately before and after measurement of the specimen. After readings of the background SQUID voltages are obtained, the specimen is lowered further to the measuring position. The holder is then rotated into four orthogonal azimuths about the vertical axis, to give two pairs of readings for the specimen x and y coordinates and four readings for the axial z component. A final reading at the background position completes the specimen insertion sequence. The output voltages from the SQUIDs in each position are then combined by the microcomputer to yield mean specimen x, y and z components and the corresponding declination, inclination and intensity of the specimen magnetisation vector. The control program is described in detail in Smith (1985).

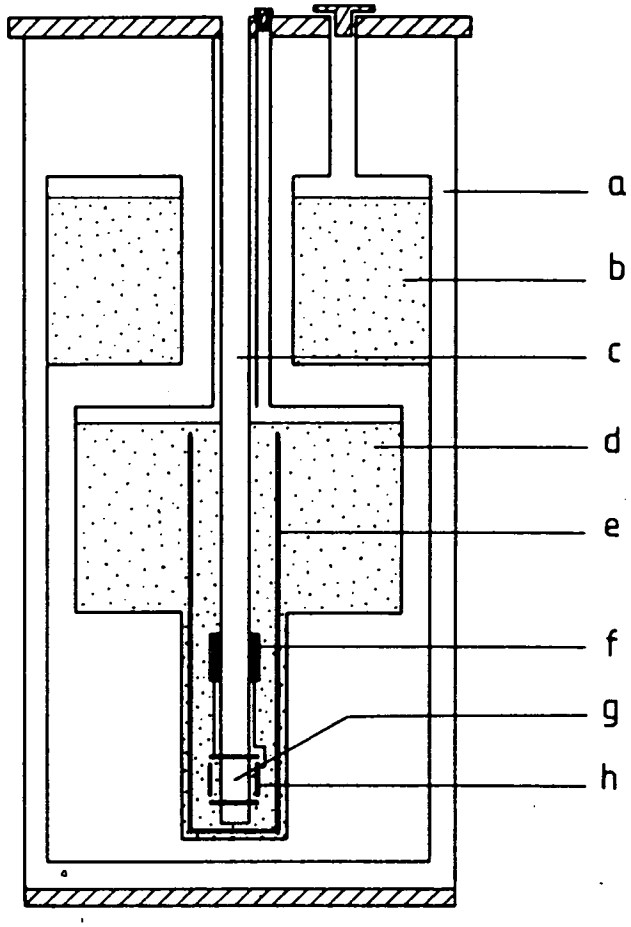

Figure 1.04. Cross-section of a CCL cryogenic magnetometer.

As standard practice in the present study, repeat measurements of every specimen were made in four orientations, arranged to partially cancel the effects of holder remanence. In each position, the specimen was inserted on its side to avoid errors arising from badly sliced specimen ends (i.e. those samples whose end surfaces were not perpendicular to their axes). With reference to the fiducial line marked on the top of the specimen, and looking along the radial SQUID zero declination direction, these positions were; front down, front left, back down, back right (Figure 1.05). This gave an amount of redundancy in the estimation of the orthogonal components of magnetisation of each specimen, which was used to assess the quality of the measurements (see section 1.7.3 below) and to insure that instrumental noise was cancelled out. Experiments demonstrated that no significant increase in the accuracy of NRM determination was achieved by using six sample orientations, designed to completely cancel the effects of sample holder remanence.

On occasions, a fault developed with the axial SQUID of the CCL equipment. When this SQUID was out of operation, the four measurement positions became essential to obtain sufficient information to allow accurate determination of the specimen remanence. Additionally, this SQUID exhibited significantly more 'noise' than the radial SQUID and was therefore switched off when measuring very weakly magnetic samples (see section 1.7.1).

1.6.3 The 2-G cryogenic magnetometer.

In November, 1989, a new 2-G Enterprises cryogenic magnetometer became available in Edinburgh. The new system exhibits some significant design differences compared to the CCL magnetometer outlined above. It is a horizontally mounted magnetometer with a 7.5 cm diameter sample access tube which is open at both ends. The helium dewar has a maximum capacity of 100 litres, and with the aid of a cryopump refrigeration system the boil-off rate of liquid helium is between 0.15 and 0.20 litres per day. A complete helium fill lasts between 500 and 660 days. It is therefore 7 times more economical to run than the CCL magnetometer.

The 2-G instrument is equipped with three sets of SQUID's and pick-up coils, allowing the complete determination of sample remanence after just one insertion into the magnetometer. The carriage system is controlled by stepper motors and is mounted separately from the main cryostat. The sample holder designed for the present project consists of three nylon pins attached to a base which screws onto the holder rod. The holder is designed to have a minimum mass with respect to a standard sample. The whole system is interfaced to an IBM-clone microcomputer running commercially purchased software. The control program automatically applies geographic (field) and

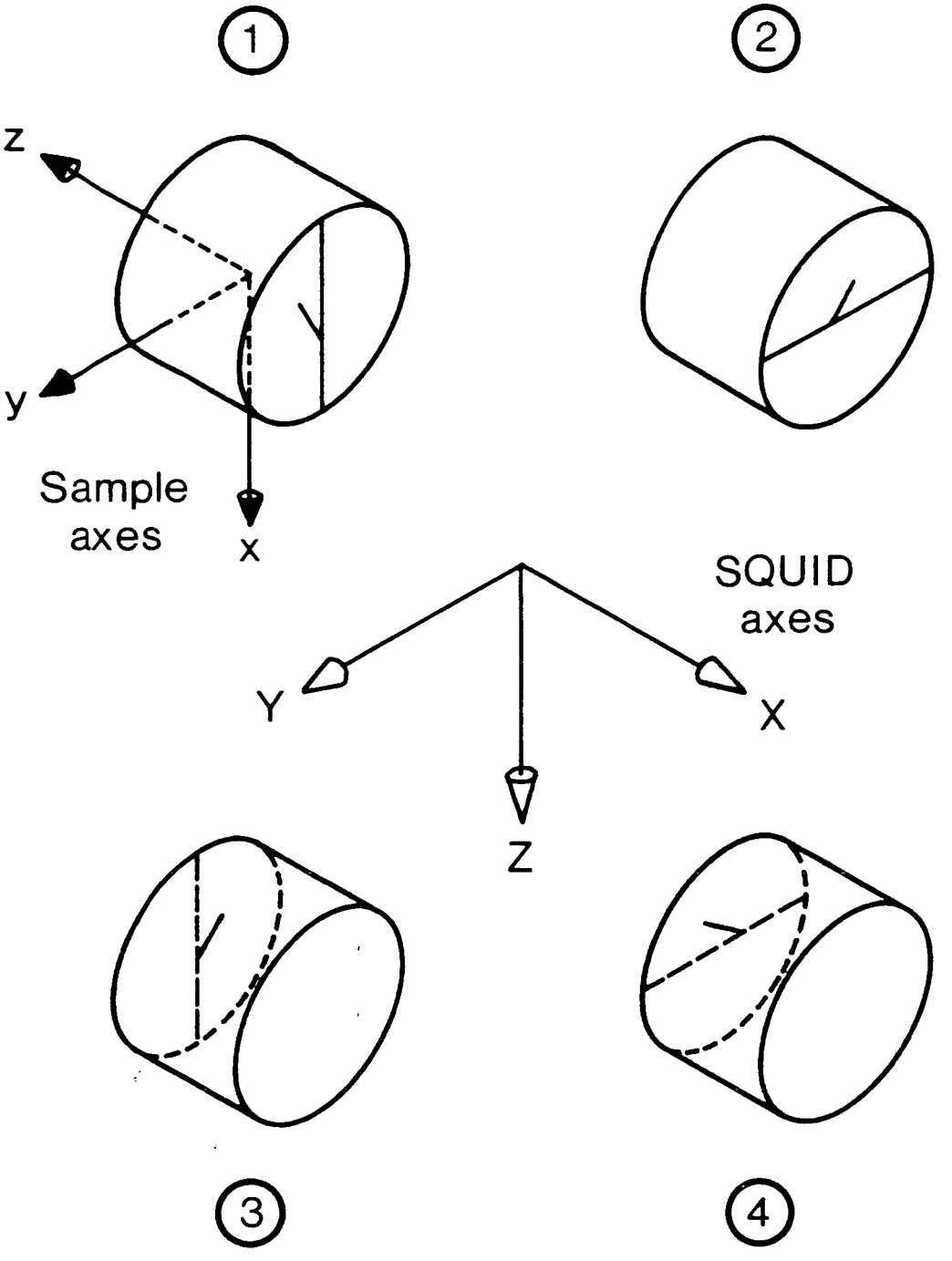

Figure 1.05. Sample orientations used in the present study. With respect to the fiducial line on the top of the sample, these are: a) front down; b) front left; c) back down; d) back right.

stratigraphic (bedding) corrections to remanence data obtained on the system, and can optionally plot data as measurement takes place. At present the system is programmed for just two sample orientations, but in each position either two or four measurements of the remanence direction can be obtained by rotating the sample by 180° or 90° steps about its axis. Additionally, the number of SQUID readings which are averaged to yield each measurement can be increased to any desired level. In the present study, four readings were averaged in each of two orientations for each sample insertion. The control program outputs a statistic based upon the agreement between the positive and negative values of the sample x, y and z components of magnetisation for each measurement, which can be used to identify unreliable data immediately and allow remeasurement to take place if desired.

Three sets of orthogonally arranged demagnetisation coils are installed inside one end of the Mumetal shielding surrounding the cryostat assembly. The peak field achievable is 30 mT. It is therefore possible to program the system with a complete AF demagnetisation sequence, up to this peak field, which can be run automatically. The advantages of this are a saving in time and, more importantly, the ability to demagnetise a sample without removing it from the holder or the magnetic shielding, thereby reducing the acquisition of viscous components of magnetisation during demagnetisation.

Since this new system only came 'on-line' during the final months of this project, the majority of measurements were made using the CCL magnetometer. Thus the next section, dealing with the effects of noise on the measurement of weak remanences, relates specifically to this latter instrument, although many of the points raised apply equally to the 2-G magnetometer.

1.7 The measurement of weakly magnetised samples.

There are many problems inherent in the measurement of weakly magnetised samples such as carbonates, the NRM of which often approaches the noise level of both CCL and 2-G magnetometers. Throughout the present study, much care has been taken to ensure that sources of random and systematic errors were minimised during measuring. There follows a discussion of the steps taken to reduce these problems, a detailed examination of the effects of noise on measured remanence directions, and finally a discussion of statistical analyses used to check the quality of measurements made in the present study.

1.7.1 Sources and effects of instrumental noise.

Under ideal conditions of very low external magnetic and radio-frequency noise, the noise level of a typical cryogenic system is stated to be (5-10) x 10^{-12} Am^2 total moment (Collinson, 1983). For a standard cylindrical sample 2.5 cm in diameter and 2.2 cm high, this noise level is equivalent to an intensity of magnetisation of approximately (4.5-9.0) x 10^{-7} Am^{-1}. However, this is the upper limit of sensitivity and is not achievable in practice. Instead, the useful limit of performance of cryogenic systems depends on the level of external sources of both random and systematic noise.

Probably the most frequent cause of random noise are fluctuations in the ambient laboratory magnetic field. Even though the superconducting and Mumetal shields provide a high degree of protection against field variations, SQUID detectors are sensitive enough to still respond to residual variations. Both the Edinburgh magnetometers are therefore housed inside 3-layer Mumetal cylinders to further decrease these variations, and both are further surrounded by Helmholtz coil systems adjusted to back-off the main Earth's magnetic field in the laboratory. These have the additional effect of reducing the enhanced magnetic field at the mouth of the Mumetal shielding, thereby providing a low ambient field at the sample during loading and reorientation. This is particularly important when measuring samples which are susceptible to acquiring viscous components of magnetisation (e.g. limestones which have been thermally demagnetised to temperatures in excess of 400°C).

Other possible sources of noise are mechanical vibration and RF interference. Both magnetometers have been insulated from vibrations transmitted through the floor, caused by activities in the building and strong winds outside; the CCL system is mounted on a bed of sand which acts to dampen such vibrations, whereas the horizontal 2-G magnetometer stands on anti-vibration padding. A potential source of vibration in the CCL system is the sample touching the side of the access tube during insertion and withdrawal. This has been reduced by attaching a guide to the carriage system above the sample holder which maintains the assembly in a central position. The 7.5 cm diameter access tube of the 2-G magnetometer effectively removes this source of noise. Additionally, in this system the carriage assembly is not directly coupled to the cryostat, thereby reducing vibrations caused by movement of the sample holder along the carriage guide rods.

When the ultimate sensitivity of the magnetometers is approached, for example while measuring weakly magnetised limestones, sources of random and systematic noise which are negligible when measuring intensely magnetised facies must be eliminated. Among the former are magnetisation of the sample holder and the residual magnetic field at the measuring position. The effect of sample holders was reduced by

keeping their mass to a minimum, and ensuring that they were frequently cleaned (see next section). The method of achieving a low residual field in the measuring space (and hence low induced magnetisations in samples being measured) differed between the two systems used in the present study.

In the CCL magnetometer, the Helmholtz coils normally used to back-off the ambient field surrounding the whole system were used during initial 'cool-down' of the cryostat to finely adjust the field at the appropriate point in the access tube immediately before the superconducting shield reached its critical temperature. Only the axial component of the field could be adjusted in this way because of the limited diameter of the access tube. The field was measured using an astatic ('back to back') configuration of two fluxgate probes. This procedure could only be carried out at the time of the first helium fill of a magnetometer run, since the trapped field could not be altered once superconducting temperatures were reached. Once the magnetometer was cold the Helmholtz coils were then used to back-off the magnetic field at the top of the cryostat.

The 2-G magnetometer is equipped with a heater surrounding the superconducting shield. To trap a known magnetic field at the measurement position, this heater is activated for two minutes to raise the shield temperature to approximately 10 Kelvin and switch it to a non-superconducting state. Three coils mounted outside the helium dewar vacuum jacket are then used in conjunction with a three component fluxgate system to establish the required low field environment. Current to the coils is maintained for 20 minutes to allow superconducting conditions to be reestablished. With this system it is therefore possible to create a known field environment while the magnetometer is still cold.

In the CCL magnetometer an axial magnetic field at the measuring position of approximately 10-15 nT could be achieved at each cool-down, whereas in the 2-G system a total field of the order of 30 nT was obtained.

Throughout the period of this project, various experiments were performed to monitor the 'working' noise level of both cryogenic systems. At intervals, repeat measurements of the residual magnetisation of the empty sample holder (i.e. the magnetisation obtained after the stored value of holder remanence is removed) were obtained to investigate the background noise which may be superimposed on sample remanences during a measuring session. On the CCL equipment, the procedure followed was:

1. the sample holder was carefully cleaned and then aligned on the carriage system,
2. ten measurements were made of the empty holder to define an average holder remanence which was stored on the Sirius microcomputer,

3. one hundred successive dummy sample insertions were made of the empty holder to obtain estimates of the residual signal after automatic removal of the stored holder magnetisation,

4. the x, y and z components of these readings were plotted, along with the 'horizontal' component $(x^2 + y^2)^{\frac{1}{2}}$, at equal intervals.

Figure 1.06 shows a typical result of this analysis at a time when the radial SQUID of the CCL magnetometer was functioning correctly, but when the axial SQUID was found to be excessively noisy. It can be seen that the residual signal on the radial SQUID is typically less than 0.03 nAm^2 with no preferred direction of magnetisation. However, the axial SQUID signal exhibits large variations with amplitudes greater than 0.2 nAm^2, and with occasional peaks exceeding 0.3 nAm^2. This noise appears to occur in discrete packets separated by periods of noise of similar amplitude to that observed on the radial SQUID. The source of these large amplitude variations cannot be identified with certainty. They cannot be attributed to RF interference or mains current supply 'spikes', since the introduction of a filter designed to protect against such interference had no effect in reducing either the amplitude or frequency of occurrence of the noise packets. It seems more likely that these variations are due to either a fault with the axial SQUID itself, or to magnetic interference from equipment operating in other laboratories within the building. The latter would be expected to effect the axial SQUID more than the radial SQUID, as the radial SQUID is better protected by the superconducting and magnetic shielding in the magnetometer.

To test the probable effect of this noise level on the measurement of sample remanences, the 100 noise estimates were used to simulate a four position measuring sequence for 25 fictitious samples with a constant remanence direction of declination = 45°, inclination = 45°. Intensities were increased in 0.1 nAm^2 total moment steps from 0.1 nAm^2 to 5.0 nAm^2, thereby yielding 25 estimates of the fictitious sample remanence at each of 50 intensity levels. The results were plotted as scatter diagrams of estimated declination and inclination against intensity, and as x-y plots of the percentage error in the estimates of intensity against 'true' intensity (Figure 1.07). All three parameters display an exponential increase in accuracy with increasing intensity. It can be seen from these simulated results that the 'measured' declination and inclination of remanence may be expected to be more than 20° away from their true directions on a significant number of occasions for a sample intensity of 0.1 nAm^2. Scatter in declination is greater than that for inclination because the declination is more dependant upon axial SQUID readings for the four positions used in the calculation. Both declination and inclination are only consistently within 5° of their true directions for intensities ≥ 0.8 nAm^2. Percentage errors in the estimation of intensity are greater

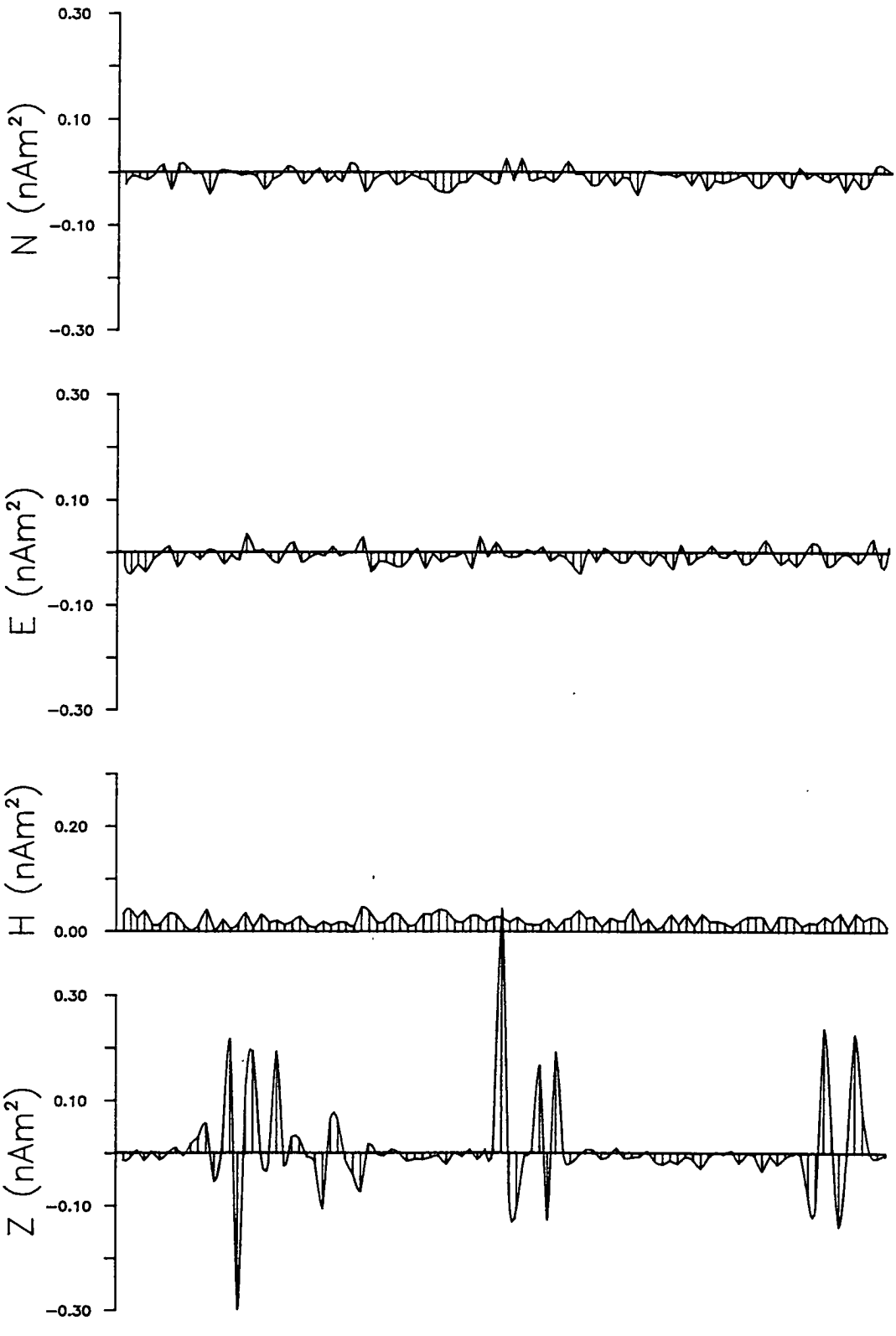

Figure 1.06. Residual SQUID signals from the CCL magnetometer, found by repeatedly measuring an empty sample holder while removing the stored holder remanence. Note the highly noisy signal from the axial SQUID.

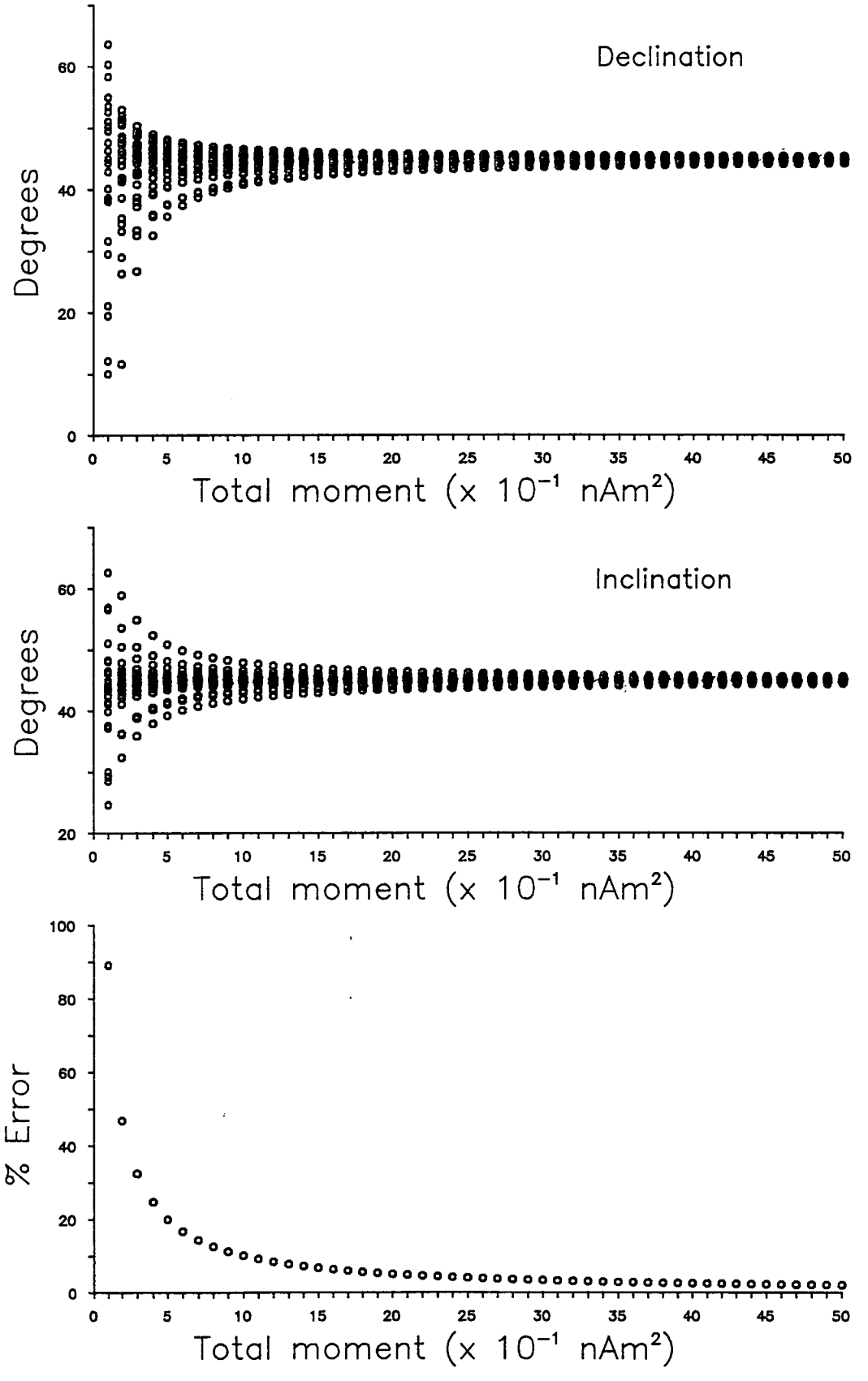

Figure 1.07. Simulated four-position remanence data found by superimposing the noise levels shown in Figure 1.07 onto a fictitious sample remanence (declination = 45°, inclination = 45°) with a total moment ranging from 0.1 nAm^2 to 5.0 nAm^2. In this case, data from both radial and axial SQUID's has been used.

than 30% for intensities ≤ 0.3 nAm^2, and only drop to below 10% for intensities ≥ 1.1 nAm^2.

Figure 1.08 shows the effect of excluding the axial SQUID data from the calculations, i.e. equivalent to measuring sample remanences in the same four positions but using just the radial SQUID. A dramatic increase in the quality of estimates of sample remanence is observed. Calculated declination and inclination are typically within 15° of their true directions, even at the lowest intensity level used in the calculations (0.1 nAm^2). This error reduces to 5° at an intensity of 0.3 nAm^2. Percentage errors in the estimation of intensity are below 10% for intensities ≤ 0.4 nAm^2, and only rise above 30% at an intensity level of 0.1 nAm^2.

Once the presence of this problem with the axial SQUID of the CCL magnetometer had been identified, this SQUID was switched down while measuring all specimens with total magnetic moments less than 2.0 nAm^2. The results of the above simulation demonstrate that, using the radial SQUID alone, one four-position measuring sequence should be capable of defining the direction of remanence of a specimen with a total moment of 0.1 nAm^2 with an accuracy of 15°. To further increase the accuracy of measurement in the present study, all specimens with total moments below 0.3 nAm^2 were measured a minimum of three times (in four positions each time) and vector averages calculated. It is estimated that the resulting specimen mean directions of magnetisation were within 5° of the true direction.

1.7.2 Measuring precautions.

The following steps were taken to reduce errors arising from sample and holder sources during measurement:

1. Specimens were kept dust-free to avoid contamination by ferromagnetic dust particles. Many of the carbonate facies sampled contain just a few parts per million of magnetite. The effect of any magnetic dust particles adhering to the surface of a specimen could totally swamp the signal from its natural remanence. Samples were stored on plastic trays in a low field environment to minimise the acquisition of viscous components of magnetisation. Storage space was provided by either a rectangular Mumetal shield or a set of Helmholtz coils adjusted to null the ambient magnetic field in the laboratory.
2. The access tubes of the magnetometers were cleaned at regular intervals to remove accummulations of dust and particles derived from samples. This was particularly important with the CCL magnetometer since the sample holder frequently came into contact with the side of the access tube because of its small diameter. Debris from samples tended to accummulate in the base of the CCL system. Cleaning of this system

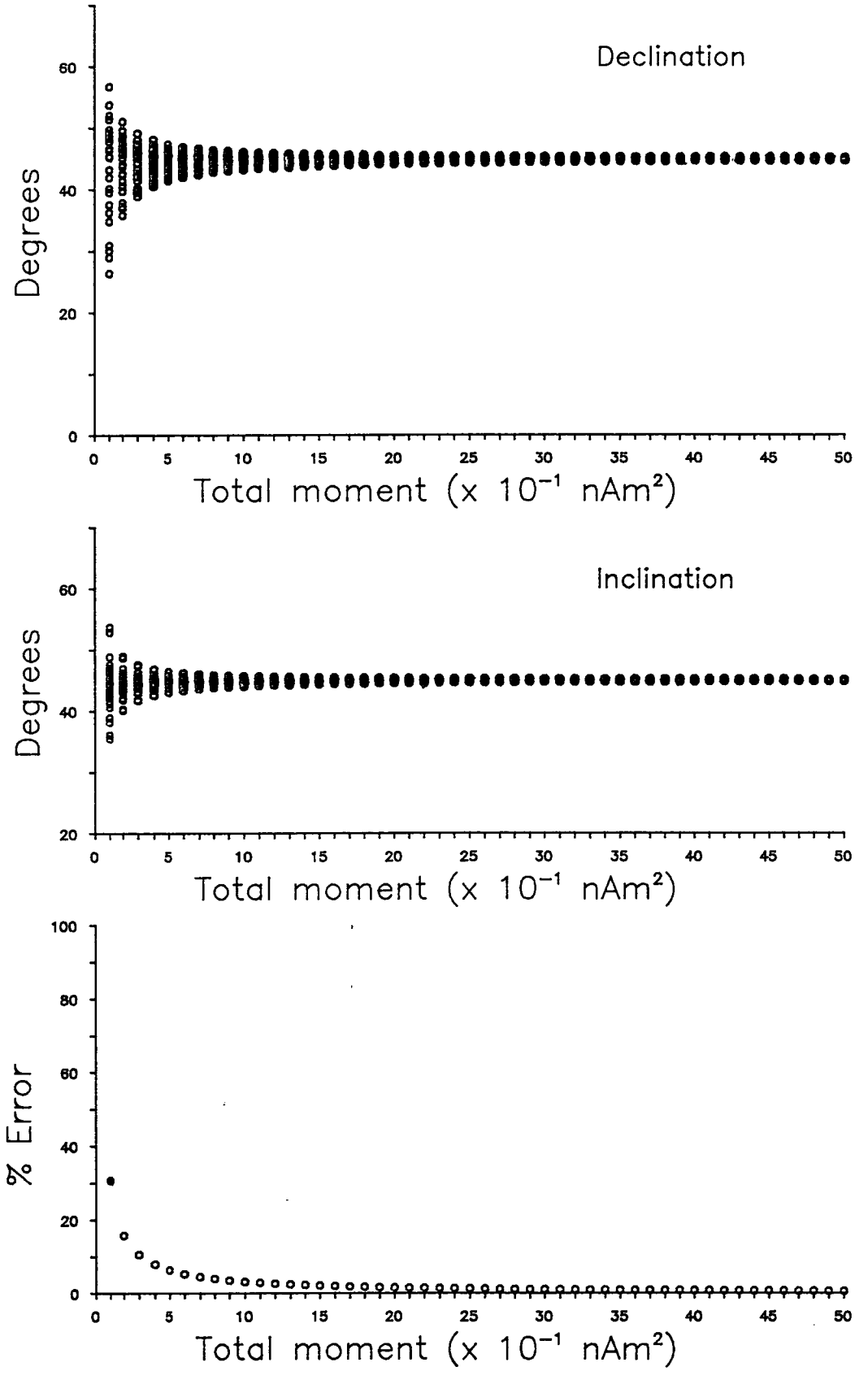

Figure 1.08. As Figure 1.07, but using data from the radial SQUID only. Note the reduction in scatter compared to the case when both SQUID were used.

was carried out with a cotton swab soaked in acetone and attached to a two metre rod. The 2-G magnetometer was easier to keep in a clean condition because of its open-ended access tube. Rock particles accummulating at the measuring position in this system were removed by using a compressed air source to blow through the tube.

3. The nylon sample holders used in both systems were cleaned at the start of each measuring session. At less frequent intervals, holders were immersed in a soap solution in an ultrasonic cleaning bath. Occasional AF demagnetisation along three orthogonal axes was used to reduce the effect of the residual remanence of the sample holder material.

4. The sample holder remanence was routinely subtracted from the specimen remanence during measurement, even though the measuring sequence was designed to reduce the effect of holder remanence. On both systems this was achieved by storing an average of ten readings of the remanence of the empty holder within the magnetometer control program at the start of each measuring session. This was then automatically removed from each estimate of the specimen remanence.

5. During each measuring period, the empty holder was measured after every ten specimens. If the residual magnetisation left over after removal of the stored holder remanence became too high then the holder was removed, cleaned, realigned and its new remanence stored.

With these precautions being taken, samples with total magnetic moments of less than 0.1 nAm^2 could be measured with repeatable results on both systems.

1.7.3 The reliability of weak NRM measurements.

The procedure used in the present study of measuring each specimen in four orientations results in an over-definition of specimen remanent magnetisation, since each orthogonal component of the magnetisation is measured several times. For the most common situation in this project (i.e. use of the CCL magnetometer with the axial SQUID switched off), two estimates of each of the specimen x and y components and four estimates of the z component were obtained for each measurement. Equal numbers of positive and negative estimates of each component were obtained (e.g. two estimates where z was aligned along the radial SQUID zero axis, and two estimates where z was aligned along the 180° axis). It is hoped therefore that the errors of measurement, whether instrumental or due to specimen instability, were distributed equally among the remanence components, and that these errors cancelled each other when the measured values were combined to compute intensities and directions of rock magnetisations.

However, since the intensity of many of the carbonates sampled in the present study approaches the noise level of the magnetometer system, especially during the later stages of specimen demagnetisation, an objective method of assessing the reliability of each measurement and defining an acceptance criterion was considered to be essential.

A good criterion of reliability is the repeatability of a measurement. From an over-defined remanence the repeatability can be easily determined from the scatter of the estimates of the magnetisation direction about their mean (Heller, 1977; Channell, 1977). To achieve this, for the case outlined above, the 16 possible vectors corresponding to all combinations of the estimates of the specimen x, y and z components are calculated, following the procedure of Channell (1977). The 16 estimates of the magnetisation vector are then treated as unit vectors and broken into directional cosines (l_i, m_i, n_i), where i = 1 to 16, and the resultant vector, R, is found where

$$R^2 = (\Sigma l_i)^2 + (\Sigma m_i)^2 + (\Sigma n_i)^2$$

The circular standard deviation ω about the mean of these unit vectors is then computed

$$\psi = 81/[(N - 1)/(N - R)]^{\frac{1}{2}}$$

where N = 16.

If the individual estimates of the remanence vector are randomly distributed, then the value of R will be less than if the vectors are significantly aligned. Perfect alignment will give R = N. Watson (1956) defined critical values of R_o for various values of N, such that if R is less than R_o there is a greater than 5% probability that the individual vectors were drawn from a random population and thus do not record a coherent magnetisation. For N = 16 the value of R_o is 6.4. Substituting this value of R_o for R in the equation for ψ above gives a critical value ψ_o for the circular standard deviation of 64.8°. Therefore, if for a specimen $\psi > 64.8°$ that specimen may be rejected as unreliable at the 95% confidence level.

This procedure can be criticized (Harrison, 1980) on the grounds that the sixteen values of the magnetisation vector are not independent. When only the radial SQUID is in operation just two independent measurements are provided by the four positions used here. A stricter determination of the critical value for ω would result in more data being rejected. However, Lowrie, Channell and Heller (1980) point out that their method, though not based on rigorous statistical principles, does provide a criterion which appears in practice to be satisfactory. They object to the computation of a statistically based parameter ω from only two observations, and point out that although the higher cut-off threshold allows some individual measurements of marginal quality to pass the

elimination procedure, the poorest quality data are eliminated at an early stage of analysis. Further rejection can then be made subjectively, as is often the case at a higher hierarchical level in many palaeomagnetic investigations (Lowrie *et al.*, 1980).

The programs used in the present study to process magnetometer output automatically calculate the value of the statistic ω for each sample, following the method of Lowrie *et al.* (1980). Comparison of these values with the critical value has then been used to reject poor quality data before further analysis at site level.

Figure 1.09 illustrates the dependence of the circular standard variation on the intensity of the remanence. The data shown derives from replicate measurements at various stages of demagnetisation of carbonate rocks from the Isparta Angle region of southwest Turkey and the Peloponnesos of southern Greece. Each value was computed from four measurements using just the radial SQUID of the CCL cryogenic magnetometer. The internal dispersion of each determination (ω) increases as the intensity decreases. However, relatively few points fail the rejection test. Furthermore, an acceptable value of 15° for the α_{95} statistic, the standard measure of confidence in palaeomagnetic studies, corresponds to a value of ψ of 30.6°, for N = 16 vectors. It can be seen from Figure 1.09 that the majority of sample remanence determinations have ω values less than this, even at intensities of 0.06-0.07 nAm^2 total moment. Thus measurements made down to this level will frequently be significant at the 95% confidence limit.

1.7.4 Summary.

Various sources of noise become important when working with weakly magnetised sediments. An analysis of the effects of the level of noise exhibited by the magnetometer used for the majority of this project demonstrates that the direction of remanence in samples with total magnetic moments of 0.1 nAm^2 should be measurable to within 15° of the true value. Statistical analysis of actual data indicates that an acceptable degree of accuracy can be obtained when measuring samples with total moments down to 0.06-0.07 nAm^2. Repeat measurements of these very weakly magnetised rocks further improve the reliability of determined remanence directions.

Finally, the satisfactory measurement of samples close to the noise level of a magnetometer system and the derivation of meaningful directional data requires constant vigilance to minimise the effects of holder contamination, viscous remanent magnetisations and sources of random noise.

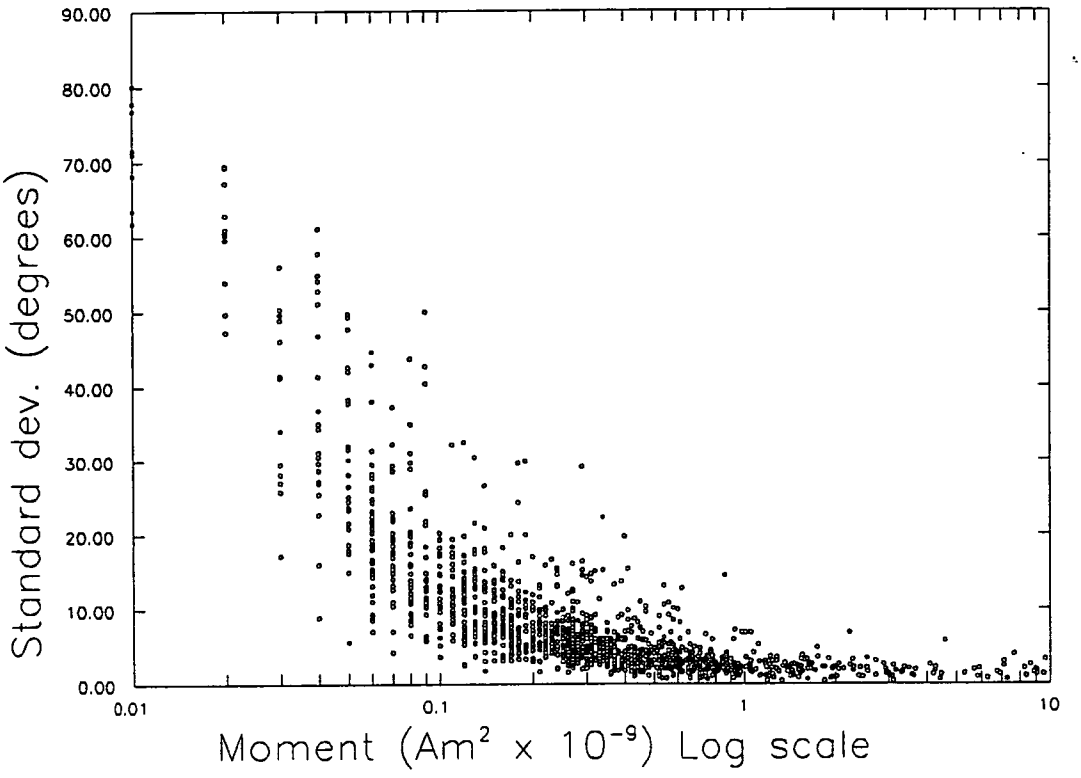

Figure 1.09. Log-normal plot of circular standard deviation, ψ, against intensity (total moment). Data derives from measurements made at various stages of demagnetisation of carbonate samples from the Isparta angle of S. W. Turkey and the Peloponnesos of Greece (see Figure 1.01). Note the increase in ψ at lower intensity levels.

1.8 Thesis layout

This thesis is divided into five parts. The remainder of this first part is devoted to an overview of past and current ideas on the geological evolution of the eastern Mediterranean part of the Tethyan orogenic belt. This acts as a basis for more detailed discussions of the geological setting of each of the study areas given in subsequent chapters.

Part Two is concerned with the Southern Troodos Transform Fault of southern Cyprus. In Chapter 3 I present a review of the geology of Cyprus and a discussion of previous palaeomagnetic studies carried out on the island. Chapter 4 then deals with the palaeomagnetic research undertaken for the present project.

Part Three is devoted to a study of the Mesozoic and Tertiary units of the Isparta Angle of southwest Turkey. Again, the first chapter in the section gives a summary of previous geological and palaeomagnetic studies in the area, while Chapter 6 concerns the results obtained in this study.

The first chapter of Part Four describes the plate tectonic setting and geological history of the Peloponnesos, southern Greece. Chapter 8 describes a palaeomagnetic study of the carbonate platforms exposed in the area, with emphasis on the Argolis Peninsula, while Chapter 9 concerns a complementary study of the Pindos thrust sheets, which overlie the platform over much of the area of the Peloponnesos.

Finally, Part Five of the thesis presents a brief summary of the findings of the project in each of the above areas, and some suggestions for further work.

CHAPTER TWO - THE TECTONIC FRAMEWORK OF THE EASTERN MEDITERRANEAN.

2.1 General.

One of the most interesting results to emerge from studies of crustal deformation over the last two decades has been the recognition that large regions of continental crust undergo rotations about vertical axes during deformation. Key evidence for such rotations has been provided by the palaeomagnetic method; rotations are identified when declinations within deforming zones are compared with those from adjacent stable areas. One of the most intensely studied areas has been the Mediterranean region, which forms part of the Tethyan orogenic belt. This region has behaved as a collision zone from at least early Mesozoic time to the present day (Robertson and Dixon, 1984) between the converging continents of Africa and Eurasia. Geological studies have shown that the eastern Mediterranean represents a mosaic of microcontinental and ophiolitic terranes, resulting from a sequence of strike-slip and closure movements between the African and Eurasian margins of the Tethyan Ocean. Numerous palaeomagnetic investigations suggest that many of these terranes have undergone local rotations with respect to the major continents, e.g. the Iberian peninsula (Van der Voo, 1969), Sardinia and Corsica (Westphal, 1977), the Italian peninsula (Lowrie and Alvarez, 1975), and the Ionian Islands (Laj *et al.*, 1982).

In this chapter I will present a review of the various tectonic models proposed for the geological evolution of the eastern Mediterranean part of the Tethyan belt. This section will form the basis of the more detailed discussions of the geological setting of individual study areas presented in Chapters 3, 5 and 7. The rotations identified in the present study occur in a variety of geological settings, ranging from rotations active during oceanic crustal genesis to those associated with the late stages of continental deformation. In the final section of this chapter I therefore present a brief discussion of the possible mechanisms of block rotations in deforming zones, with emphasis on those processes which operate during the deformation of continental crust.

As noted above, the geological evolution of the Tethyan belt has been controlled by the relative motion history of the African and Eurasian plates. I begin this chapter then with an examination of the apparent polar wander paths for these plates (Section 2.2) and the kinematic framework derived from the Atlantic Ocean spreading record (Section 2.3). Interpretation of the palaeomagnetic results described later must be consistent with the plate tectonic framework defined by these data.

2.2 The African and European apparent polar wander paths.

Polar wander paths are denoted as 'apparent' because it is not the pole that wanders but the continent that moves relative to the pole. The drift of a continent means that the palaeomagnetic pole appears to wander with respect to that continent, thus producing an apparent polar wander path (APWP).

Irving (1977) gave apparent polar wander curves relative to northern Eurasia and relative to North America from the Devonian until recent times. Irving arranged the palaeomagnetic data from these continental blocks according to their absolute ages. Beginning with the oldest data he calculated running mean values for overlapping 40 Ma windows, moving the window limits forward by 10 Ma at each step. In this way smooth polar wander paths were obtained.

For Eurasia (Figure 2.01 solid circles) Irving (1977) included data from Western Europe, and also from the U.S.S.R. in order to overcome the scarcity of Mesozoic data from Western Europe. To ensure that this predominantly Soviet curve could be applied to stable Western Europe, VandenBerg and Zijderveld (1982) plotted the Late Carboniferous, Permian and Late Permian/Early Triassic mean pole positions derived exclusively from Western European data on to the Eurasia path obtained by Irving (1977) (open squares in Figure 2.01). An excellent agreement was found, confirming the Late Palaeozoic/Early Mesozoic segment of Irving's path.

More recently, Westphal *et al.* (1986) produced a mean synthetic APWP for Eurasia, as part of a joint French-Soviet project aimed at establishing a series of palaeogeographic maps of the Tethys belt. They initially selected the most reliable data for stable Eurasia (north of the Alpine belt). They then used the kinematics of the major plates around the Atlantic given by Savostin *et al.* (1986) to transfer their polar wander curves to Eurasia and calculated the mean curve (Figure 2.01 open circles). This curve can be divided into four different segments. In the first segment, from the Permian to the Lower Jurassic the pole moves more or less northward. Then, from the Lower Jurassic to the Cretaceous it moves along a parallel to the east. It describes a loop in the Middle Cretaceous. Then the pole moves westwards and finally approaches the present geographic pole position. This path displays several differences from the that of Irving (1977). In the latter curve the Cretaceous loop is absent, and its final Tertiary part lies along a different line of longitude (about 190°E instead of 150°E). These differences result from a more selective use of Soviet results by Westphal *et al.* They did not include any Soviet Tertiary results which were considered to be unreliable. Additionally, Irving (1977) used rotated poles related to the mobile belt from Sardinia, Iberia and Spitzbergen.

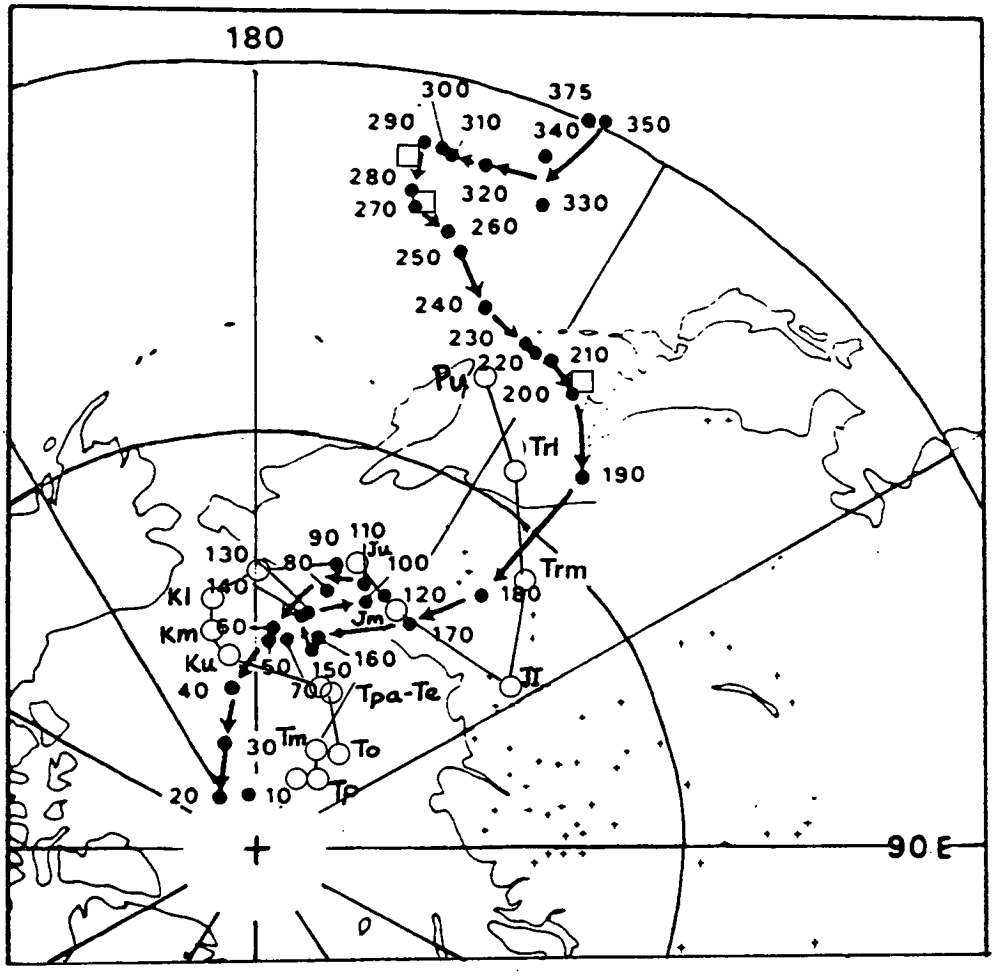

Figure 2.01. The Eurasian apparent polar wander path of Irving (1977) (solid circles) (Figure 2), with the Western European palaeomagnetic poles listed by VandenBerg and Zijderveld (1982) overlain (open squares). Also shown is the synthetic European polar wander curve of Westphal *et al.* (1986), used as a reference path in the present study (open circles).

Palaeomagnetic data from the African continent are not abundant enough to allow a reliable continuous APWP to be constructed. In particular, there is ambiguity about the position and shape of the Late Palaeozoic part of the curve. In order to overcome this scarcity of data, Van der Voo and French (1974) transferred palaeomagnetic data from other continents to Africa with the aid of continental drift reconstructions. The pole positions obtained by Van der Voo and French (*op. cit.*) are shown in Figure 2.02 (solid circles). A further indirect 'African' APWP was calculated by VandenBerg and Zijderveld (1982). They used the well documented sea-floor spreading history of the Atlantic between Africa and North America to transfer the detailed APWP of North America from Irving (1977). The resulting curve is shown in Figure 2.02 (open triangles). Since the initial fit of Africa and North America used by VandenBerg and Zijderveld (1982) was only slightly different from the Bullard fit of Pangaea used by Van der Voo and French (1974), the indirect African curves shown in Figure 2.02 are in good agreement. The final curve of Figure 2.02 (solid triangles) shows the synthetic African path defined by Westphal et al. (1986), using the more up-to-date kinematics of Savostin et al. (1986).

There are several discrepancies between the paths of Figure 2.02 and Palaeozoic poles calculated from the palaeomagnetic data from Africa itself. For a detailed discussion of these problems, the reader is referred to VandenBerg and Zijderveld (1982). Fortunately there is no doubt about the Mesozoic and Tertiary part of the indirect African polar wander curve. A Bullard-fit Pangaea during the Late Triassic until the beginning of North Atlantic spreading is generally accepted, and the stages of the opening of the North Atlantic are sufficiently well determined (VandenBerg and Zijderveld, 1982; Savostin et al., 1986). Also, real African mean poles for the Late Mesozoic and Early Tertiary (Figure 2.02 open circles) coincide very well with the indirectly derived polar wander curves, not only in position but also in age. We can deduce the following movements of Africa with respect to the pole from the Mesozoic and Tertiary segments of the curves of Figure 2.02 (VandenBerg and Zijderveld, 1982): (i) Africa remained essentially stationary during the latest Triassic and Early Jurassic; (ii) palaeomagnetic data with absolute ages ranging between 120-106 Ma reveal a southward movement in the Early Cretaceous; (iii) this southward movement is followed by a counterclockwise rotation of approximately 25o during the Late Cretaceous; (iv) an additional northward movement took place during the Late Cretaceous to Early Tertiary interval.

The synthetic Eurasian and African APWPs of Westphal *et al.* (1986) have been used as reference curves for the palaeomagnetic results obtained in this project. The preferred method of comparing these results to the reference curves has been to plot the

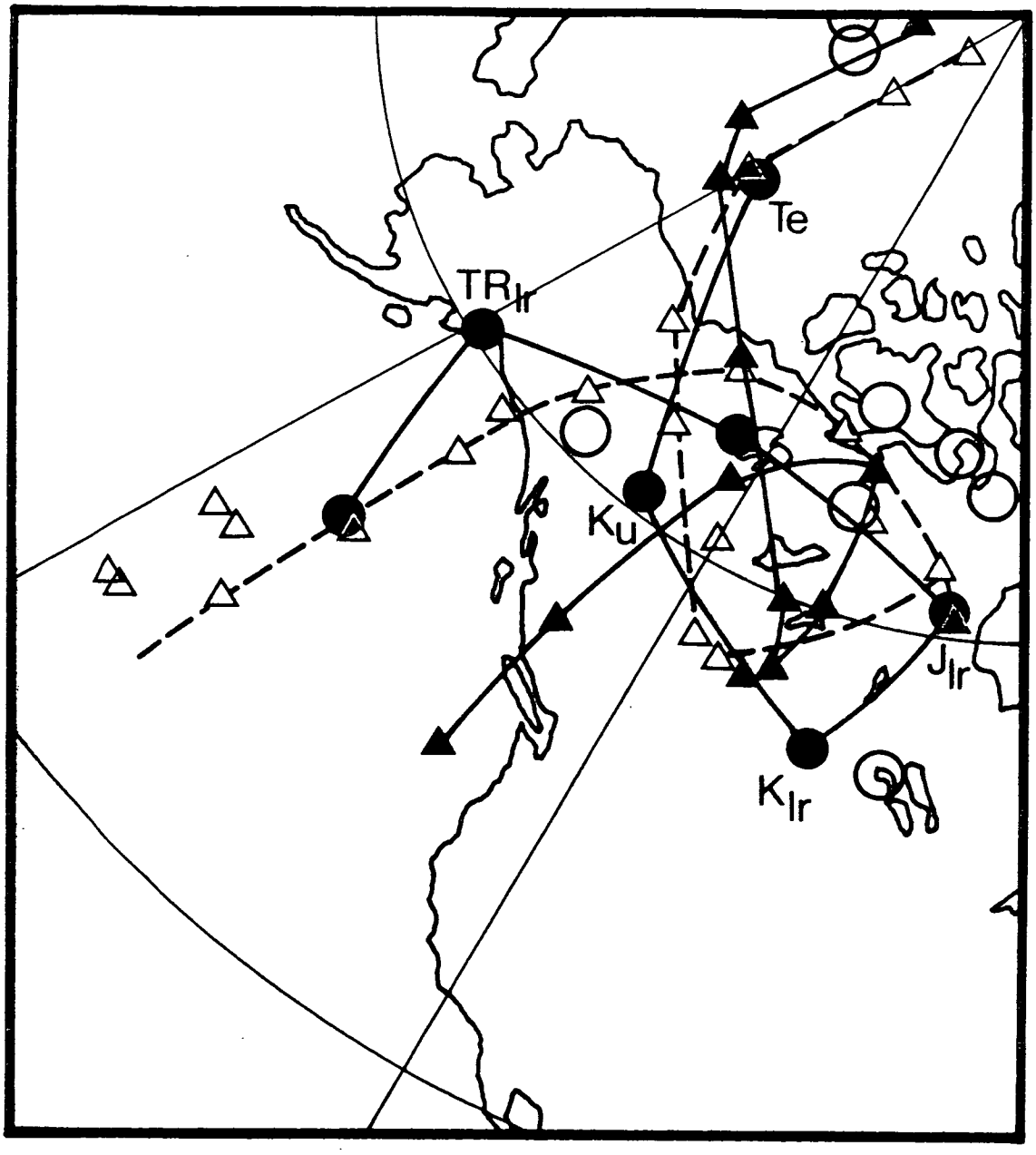

Figure 2.02. The indirect African apparent polar wander curves of Van der Voo and French (1974) (solid circles), VandenBerg and Zijderveld (1982) (open triangles) and Westphal *et al.* (1986) (solid triangles). Open circles represent real African poles, listed by Vandenberg and Zijderveld (1982). Note the general agreement between the reference curves during the Mesozoic and Tertiary. The synthetic African polar wander curve of Westphal *et al.* (1986) is used as a reference path in the present study.

declination and palaeolatitude expected from the Eurasian and African paths at a central point in each study area as a function of time. The latter reference curves then show the declination and palaeolatitude of these points as if they were rigidly attached either to Eurasia or to Africa in its present position. Differences between these curves and the declination and palaeolatitude calculated from site mean data found in the present study indicate relative rotations and latitudinal changes with respect to the major continents. An example of such a set of reference curves is shown in Figure 2.03 for a site in the central Peloponnesos, Greece (lat.= 37.5 °N, long.= 22.5°E).

2.3 The relative motion history of the African and Eurasian plates.

After the early kinematic attempt of Le Pichon (1968), the first comprehensive plate tectonic model of the development of the Tethyan system was proposed by Smith (1971) who pointed out that the evolution of the Africa-Eurasia plate system could be derived from the relative motion of these plates with respect to North America. Smith (*op. cit.*) defined the relative motion between Africa and North America since 180 Ma as a single rotation around the pole of Bullard *et al.* (1965), while the relative motion between Eurasia and North America was divided into two stages: a first stage from the Santonian (81 Ma) to the Late Eocene (42 Ma) at a constant spreading rate of 2 cm/yr and a second stage since the Late Eocene at a constant rate of 1 cm/yr. Thus, three main phases were used to describe the motion between Eurasia and Africa: (i) from the Early Jurassic to the Late Cretaceous, Africa moved left-laterally with respect to Eurasia; (ii) from the Late Santonian to the Late Eocene, there was a change to right-lateral motion; (iii) finally, northward movement of Africa in the Late Eocene initiated the main collision between the continents.

The first comprehensive kinematic model of the relative motion of the African-North American and Eurasian-North American lithospheric plates to be based on the identification and fit of magnetic anomalies in the North and Central Atlantic oceans was made by Pitman and Talwani (1972). Their reconstruction enabled a refinement of the relative motion history of Africa and Eurasia, and suggested that Africa moved past Eurasia in a left-lateral sense during the period from the Late Triassic to the Late Cretaceous. A right-lateral relative motion then occurred between the Late Cretaceous and the earliest Oligocene. Hence the more robust method used by Pitman and Talwani (*op. cit.*) confirmed the general result of Smith (1971).

Subsequent modifications to Pitman and Talwani's Atlantic ocean floor spreading data by various authors were combined with continental palaeomagnetic data by Smith and Woodcock (1982). They produced a new series of palaeocontinental maps showing

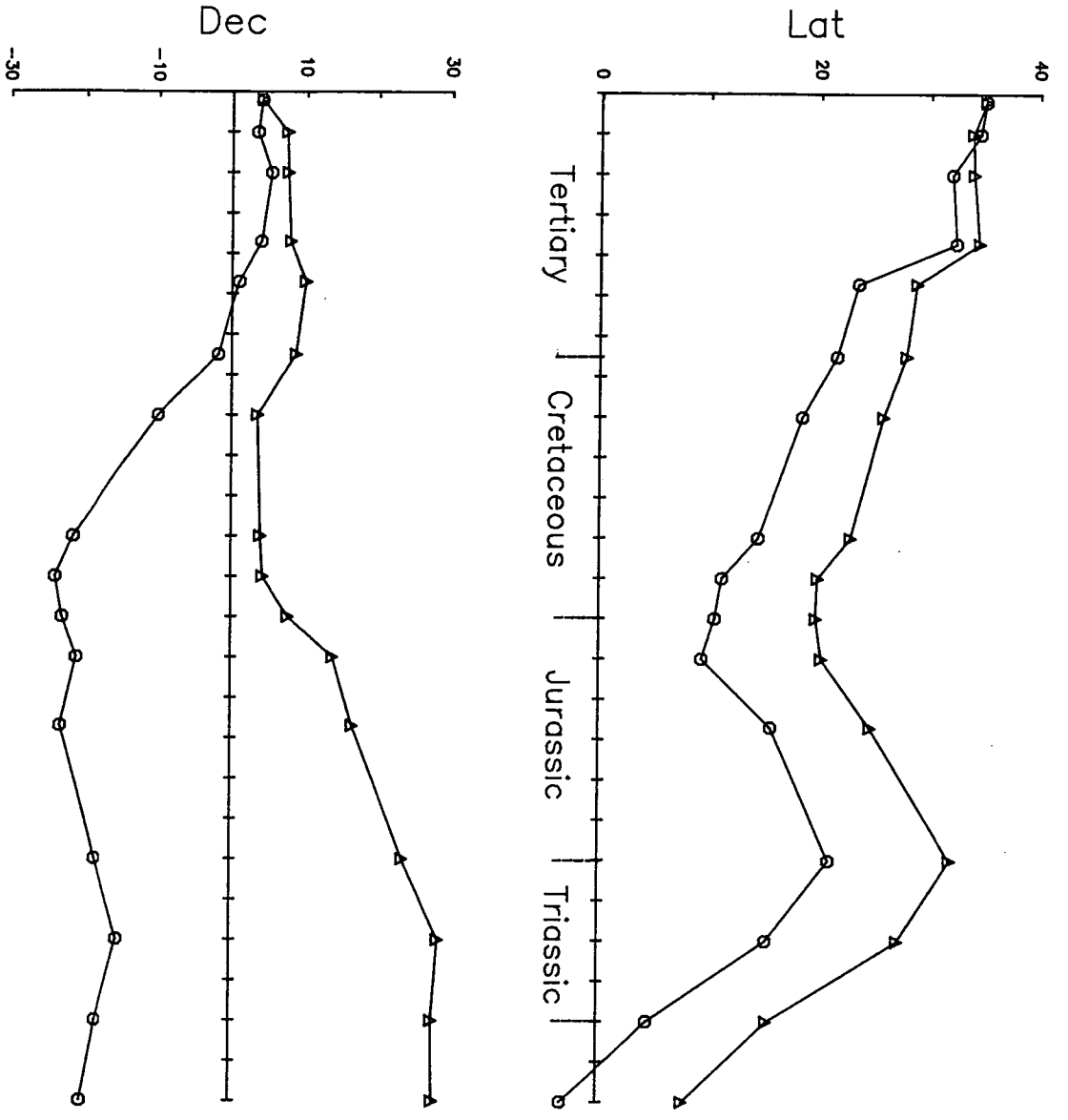

Figure 2.03. Reference declination and palaeolatitude curves calculated from Westphal *et al.*'s (1986) Eurasian and African polar wander curves for a site in the central Peloponnesos (lat.= 37.5^{o}N, long.= 22.5^{o}E). Circles = African data; Triangles = Eurasian data.

the relative positions of Africa and Europe and their inferred palaeolatitudes. These were created automatically by computer in two stages. In the first, the finite rotations required to produce a continental reassembly for the time concerned were calculated from the available ocean-floor spreading data. Secondly, the reassemblies were reorientated using palaeomagnetic poles from the stable continental areas so that the mean pole for each assembly corresponded to the geographic pole of the maps. Quite correctly, Smith and Woodcock (*op. cit.*) made no attempt to use their data to constrain the position of the continental fragments which now make up the eastern Mediterranean region. The ten reconstructions of Smith and Woodcock (*op. cit.*) are shown in Figure 2.04, and clearly show the postulated switch from left-lateral to right-lateral relative motion between Africa and Eurasia in the Late Cretaceous.

However, recent correlations by Livermore and Smith (1984) and Savostin *et al.* (1986), based on more accurate sea-floor spreading data and robust methods of analysis, do not support a change in the sense of relative motion at this time. Instead, both these studies (Figure 2.05a, b) indicate a smooth, more arcuate, first sinistral then convergent path of Africa relative to Eurasia. Periods of accelerated motion are observed at around 170 Ma and 100 Ma, related to the opening of the central and north Atlantic respectively. The only major anomaly within these frameworks occurs during the Eocene in Livermore and Smith's path and during the Oligocene in that of Savostin *et al.* when a brief period of reversed shear occurs. Savostin *et al.* relate this event to a decrease by a factor of 1.5 in the spreading rate between Africa and North America during the Oligocene, whereas no corresponding change in spreading rate between Eurasia and North America occurred. As a result, Africa moved right-laterally with respect to Eurasia along the whole Tethys boundary at this time.

The reconstructed positions of Africa and Eurasia from the Lias to the Present according to Savostin *et al.* (1986) are shown in Figure 2.06., with palaeolatitudes calculated by Westphal *et al.* (1986) superimposed.

Major events in the geodynamic evolution of the eastern Mediterranean Tethys can be related elegantly to the kinematic framework provided by these recent studies. In a synthesis which is discussed in greater detail in Section 2.4.4, Robertson and Dixon (1984) suggest that ophiolite emplacement during the Mid-Jurassic in the Greek Neotethyan area coincides with the rapid westward shift of Eurasia relative to Africa at about 170 Ma, produced by the initiation of spreading in the central Atlantic. The subsequent slow change to north-south convergence allowed opening of east-west basins in the Turkish area, which were previously 'locked' by the Arabian margin and the Pelagonian microcontinent. Later rapid convergence in the Late Cretaceous and

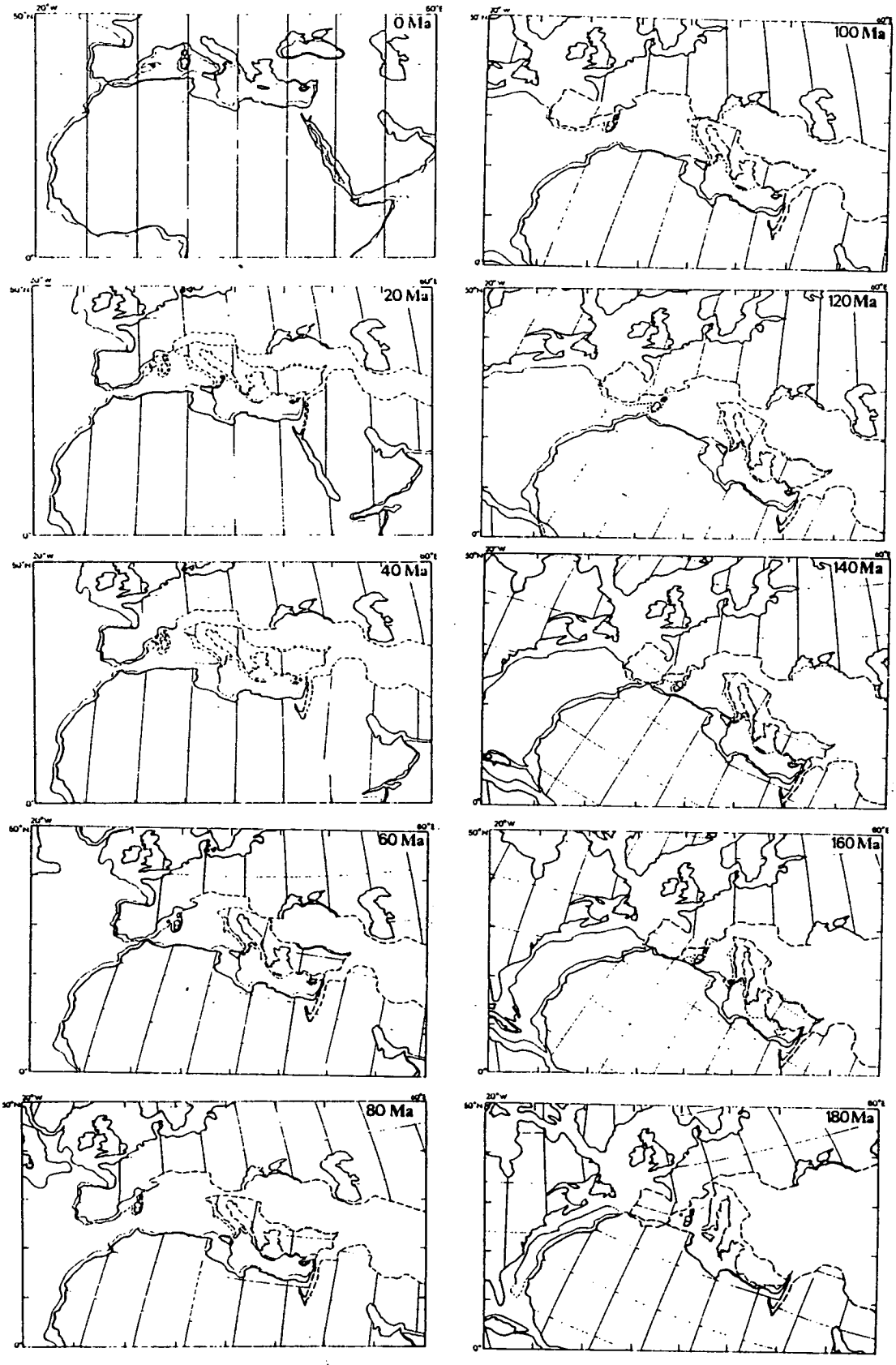

Figure 2.04. The palaeocontinental maps of Smith and Woodcock (1982) showing the relative positions of Africa and Europe and their inferred palaeolatitudes. Relative motions between Africa and Europe were determined entirely from Atlantic-floor spreading data. Note the postulated change from left-lateral to right lateral relative motion in the Late Cretaceous (compare the 120, 100, 80 and 60 Ma reconstructions).

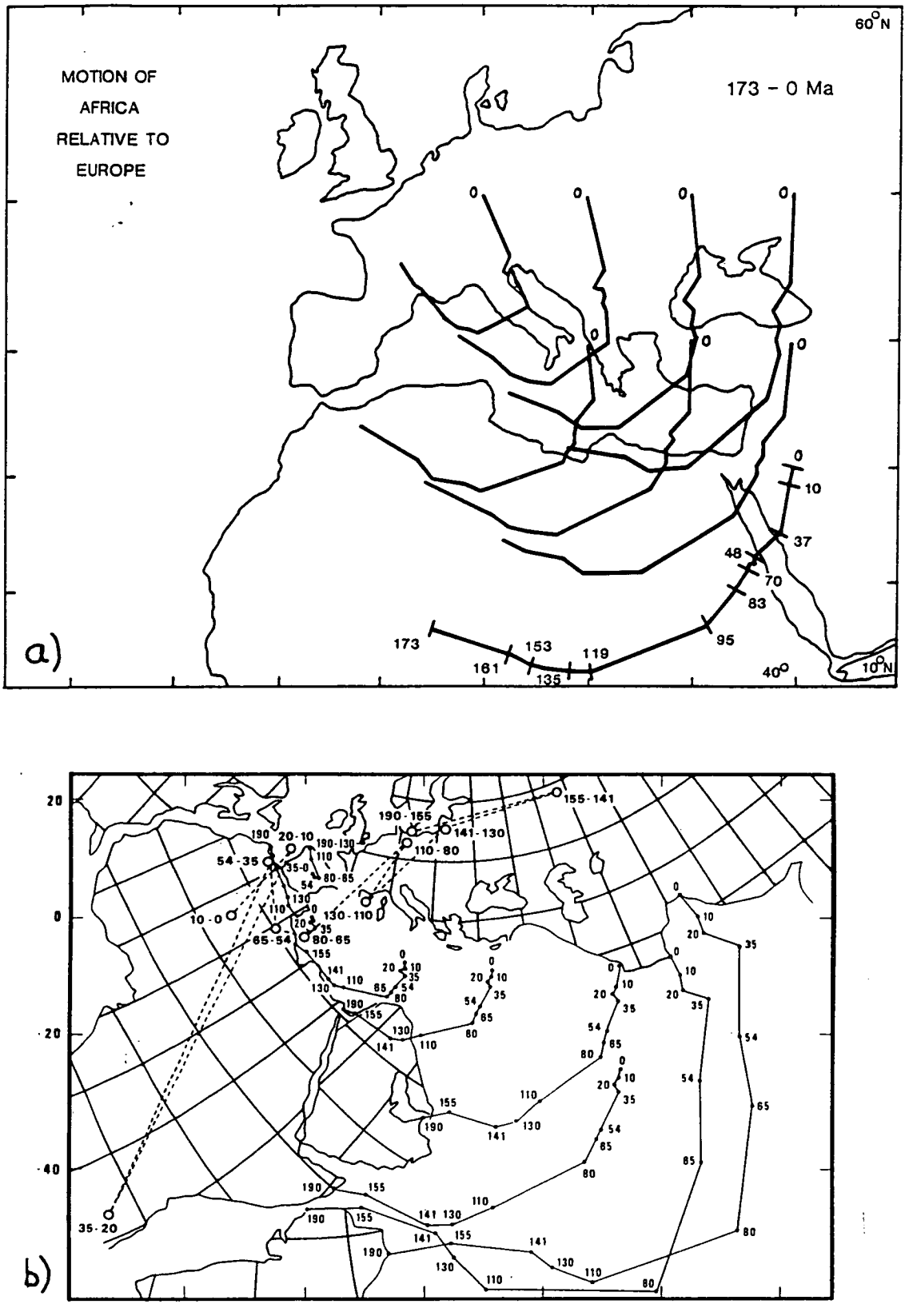

Figure 2.05. The relative motion history of Africa with respect to Eurasia according to a) Livermore and Smith (1984), and b) Savostin *et al.* (1986).

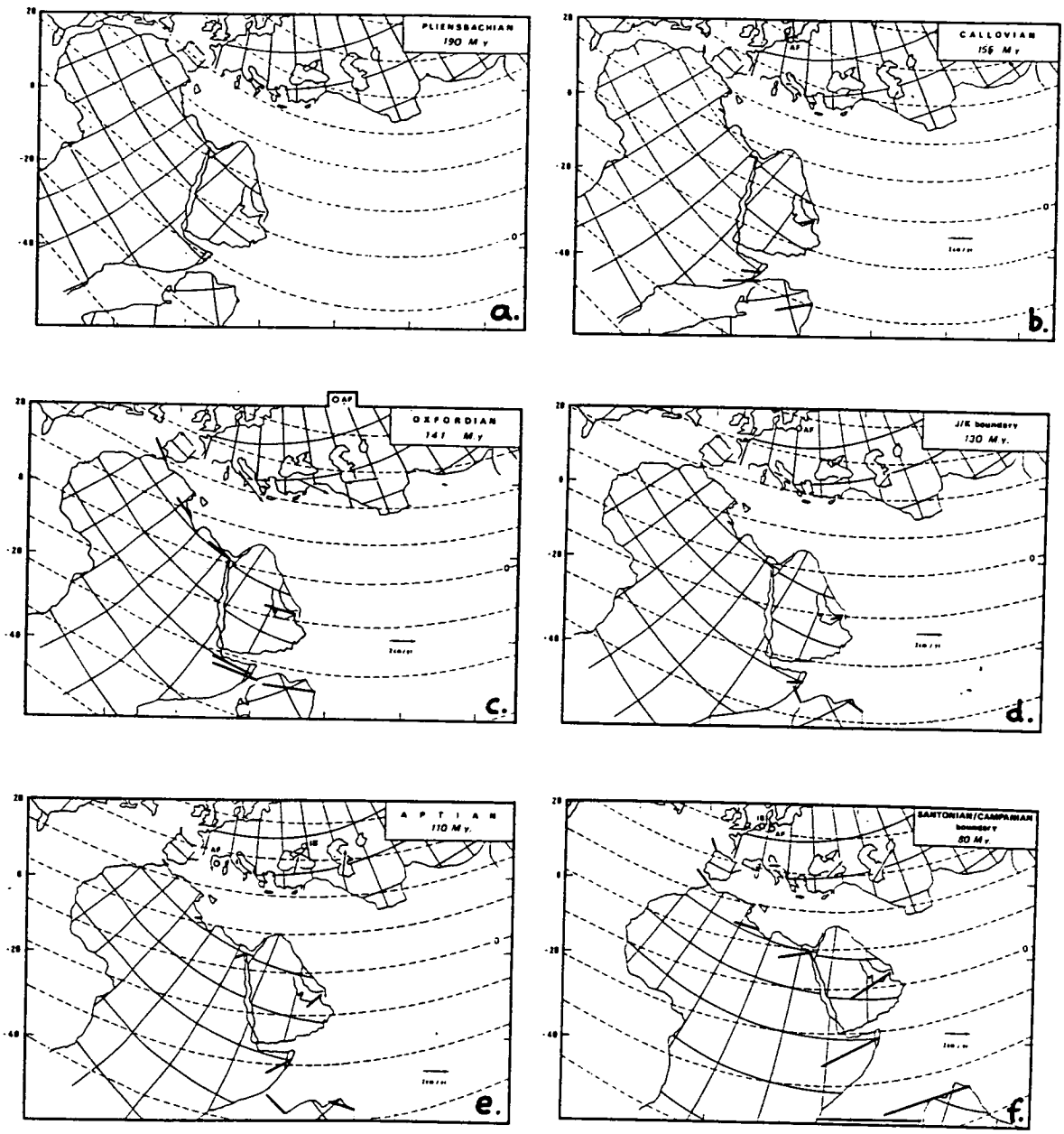

Figure 2.06 a-l. Reconstructed positions of Africa, Arabia, India and Eurasia from the Lias to the Present according to Savostin et al. (1986). Palaeolatitudes calculated by Westphal et al. (1986) are superimposed in 10° intervals. The palaeoequator is marked. Present latitudes and longitudes on the continents are shown at 10o intervals. The stages shown are as follows: a) Pliensbachian, Early Jurassic (190 Ma); b) Callovian, Middle Jurassic (155 Ma); c) Oxfordian, Late Jurassic (141 Ma); d) Jurassic-Cretaceous (130 Ma); e) Aptian, mid-Cretaceous (110 Ma); f) Santonian-Campanian boundary, Late Cretaceous (80 Ma); g) Cretaceous-Tertiary boundary (65 Ma); h) Ypresian, early Eocene (54 Ma); i) Priabonian, late Eocene (35 Ma); j) Aquitanian, early Miocene (20 Ma); k) Tortonian, late Miocene (10 Ma); and l) Present day.

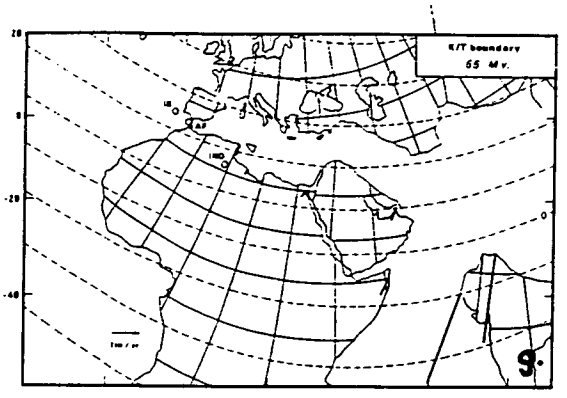
K/T boundary
65 M.y.
g.

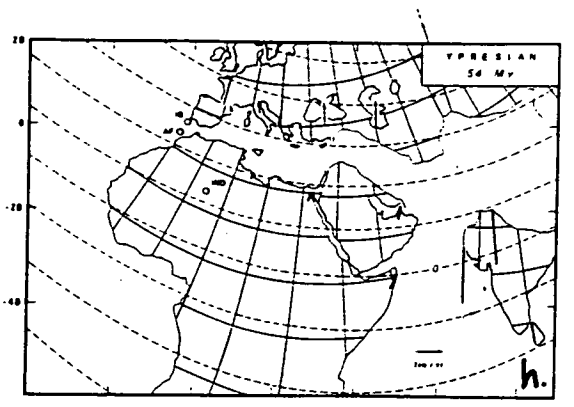
YPRESIAN
54 M.y.
h.

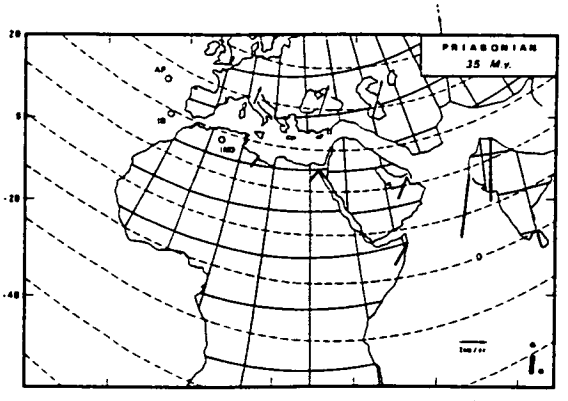
PRIABONIAN
35 M.y.
i.

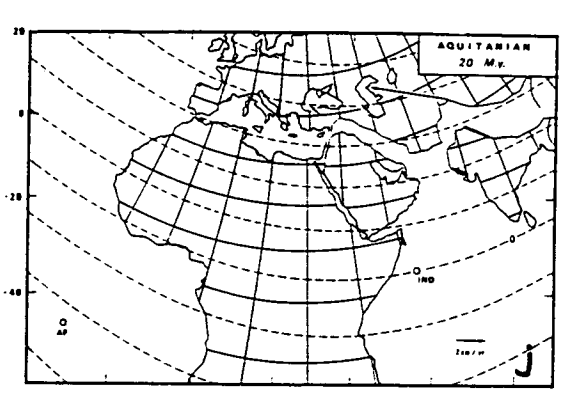
AQUITANIAN
20 M.y.
j

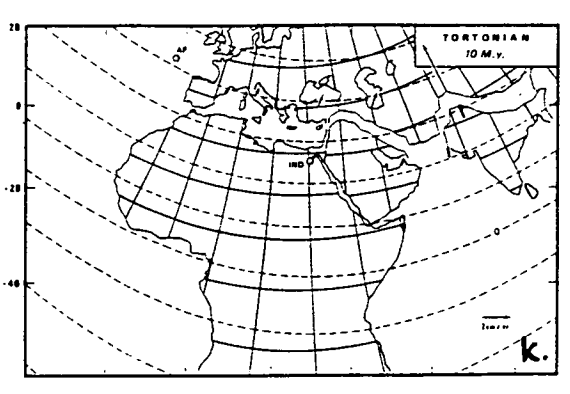
TORTONIAN
10 M.y.
k.

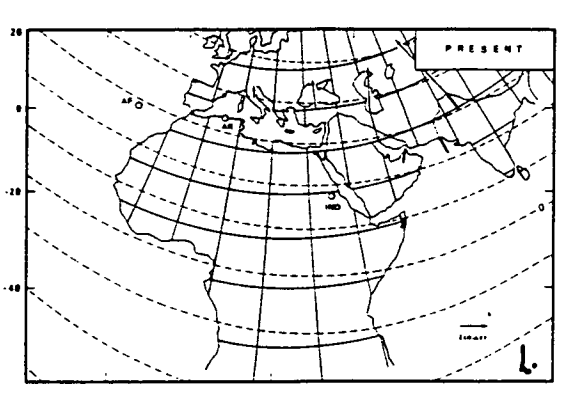
PRESENT
l.

Tertiary led to compression and the generation and emplacement of ophiolitic terranes in this area (see Figure 2.19a-f).

2.4 The tectonic framework of the eastern Mediterranean.

The existence of a former ocean between Africa and Eurasia was first postulated by Suess (1904-1924), who named it 'Tethys'. Argand (1924) and Carey (1955) proposed that the disappearance of the Tethys was due to continental drift and consequently that the geological evolution of the Mediterranean region resulted from the relative motion of Africa and Eurasia. Following the earth sciences revolution of the 1960's and the availability of kinematic solutions for the past motions of the African, Eurasian and North American lithospheric plates (Section 2.3 above), numerous geological models for the evolution of the Tethyan system have been proposed. These range from models involving a single Tethyan embayment separating Gondwanaland (Africa) from Eurasia (e.g. Ricou *et al.*, 1984), to those invoking an anastomosing series of small ocean basins separating microcontinental terranes, which rifted off the northern margin of Gondwanaland at various times during the Mesozoic (e.g. Sengör and Yilmaz, 1981; Robertson and Dixon, 1984). In this section I give a brief description of the main controversies which have arisen from these reconstructions. I begin, however, with an examination of the present day plate tectonic setting of the eastern Mediterranean, which must form the end point of any valid model for the evolution of the region. Figure 2.07 gives an outline sketch of the eastern Mediterranean showing the important tectonic units mentioned in the text.

2.4.1 The present plate tectonic framework.

Active deformation in the eastern Mediterranean area is primarily controlled by the mutual interaction of the major African and Eurasian lithospheric plates and the smaller Anatolian plate, which forms the majority of the area of Turkey. The overall pattern was established by the collision of the Adriatic and Arabian promontories with Eurasia (Tapponnier, 1977).

In south-eastern Turkey this collision resulted in the expulsion of the Anatolian plate westward away from the zone of crustal thickening and incipient collision between the Eurasian and Arabian plates in the Zagros thrust belt (Le Pichon and Angelier, 1979). The Anatolian block is thus bounded along its northern and eastern margins by major continental transform zones; the North and East Anatolian Faults respectively (Sengör, 1979; Figure 2.08). It is estimated that 25 km of dextral motion has taken

place along the North Anatolian transform fault since the Late Miocene (Barka and Hancock, 1984). Dextral strike-slip motion along the fault extends westward as far as the North Aegean Trough. However, this transform does not extend across Central Greece. Instead, motion is taken up on a large active normal fault system, which forms a zone of distributed shear linking the North Anatolian Fault to the Hellenic Trench in the west (McKenzie and Jackson, 1983; Figure 2.08; see also Section 2.5).

In the west of the area, progressive north-eastwards subduction of up to several hundred kilometres of Neotethyan oceanic crust in the Ionian Sea has occurred beneath Crete, along the Hellenic arc and trench system (Le Pichon and Angelier, 1979; Figure 2.08). The down-going slab is well-defined by seismic activity. Further east, the more V-shaped Pliny and Strabo trenches represent a transform plate boundary (Figure 2.08).

Subduction has resulted in north-south back-arc extension in the Aegean Sea and Central Greece, with the formation of grabens and troughs related to large-scale normal faulting. Estimates of the overall crustal extension vary greatly from 30-50% by Le Pichon and Angelier (1979) to up to three times this amount by McKenzie (1982).

In contrast to the Hellenic arc region, no well-defined Benioff zone is observed along the Cyprean Arc, which forms the boundary between the African and Anatolian plates, although bathymetric and seismic data clearly define a subduction trench (Figure 2.09). Here seismicity is sporadic and generally at a shallow level. The trench curves around the northern margin of the Eratosthenes Seamount, and broadens and shallows to the east. Crust to the south of Cyprus could either be oceanic crust with a thick sediment blanket or attenuated continental crust, i.e. African continental margin (Makris *et al.*, 1983). Normal subduction may be being disrupted by the collision of the major Anaximander and Eratosthenes seamounts with the active trench.

2.4.2 Single vs. multiple ophiolite root-zone models.

One of the diagnostic features of eastern Mediterranean geology is the abundance of Mesozoic ophiolitic rocks. These occur in variable states of preservation along a series of anastomosing suture zones, often in close spatial association with rift-related and passive continental margin sediments (Figure 2.10). Assuming that the ophiolites represent some form of oceanic crust (Anonymous, 1972; Moores and Vine, 1971; Robertson and Dixon, 1984), their presence must indicate the existence in the Mesozoic of one or more ocean basins, which have since been destroyed by subduction. A controversial question in Tethyan geology has been the number and location of these ophiolitic root-zones. Proposals range from suggestions that all the Turkish and Greek ophiolites originated in a single basin (Ricou *et al.*, 1979, 1984; Marcoux *et al.*, 1989), to

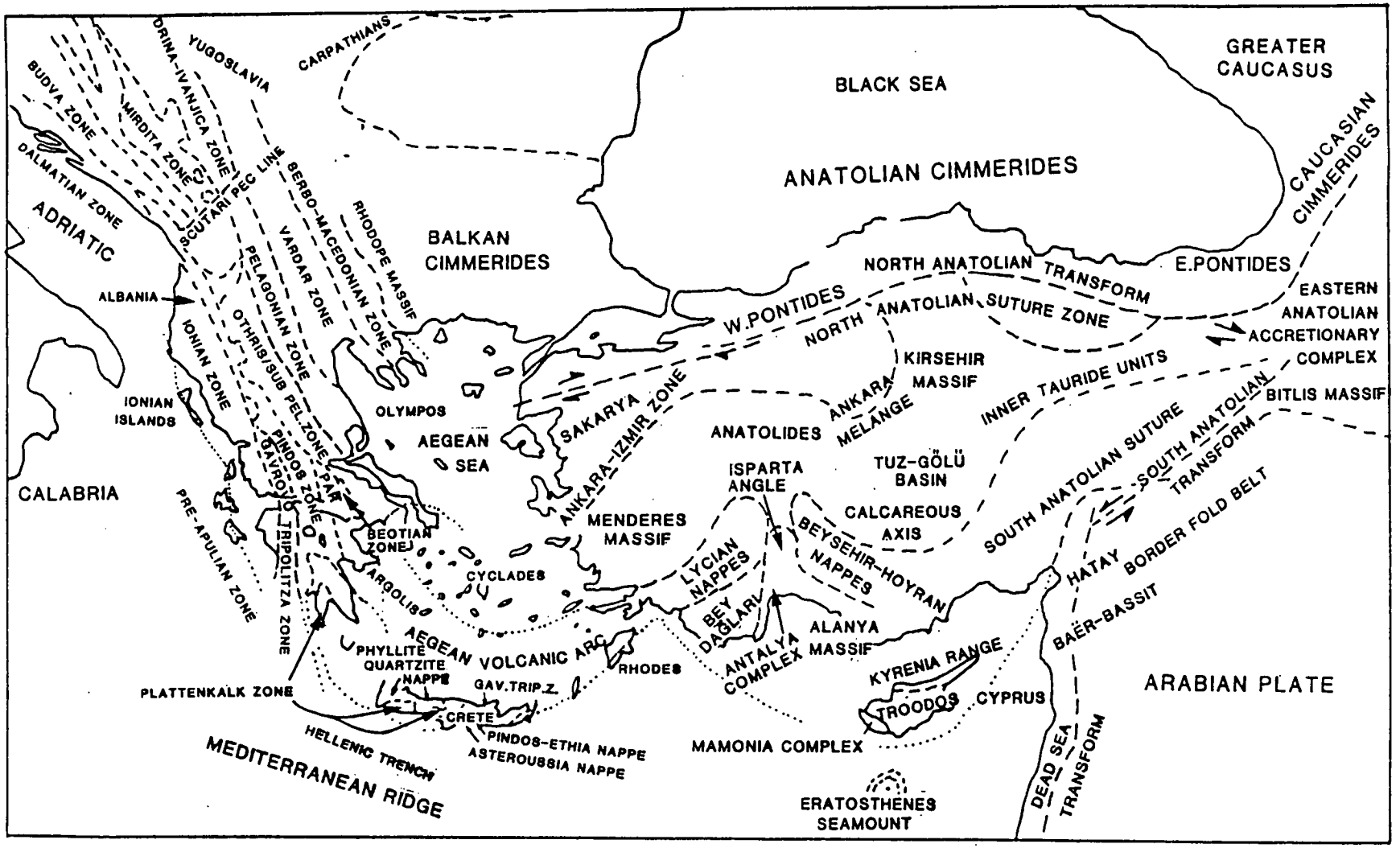

Figure 2.07. Outline tectonic map of the eastern Mediterranean, showing the tectonic units mentioned in the text (from Robertson *et al.*, in press).

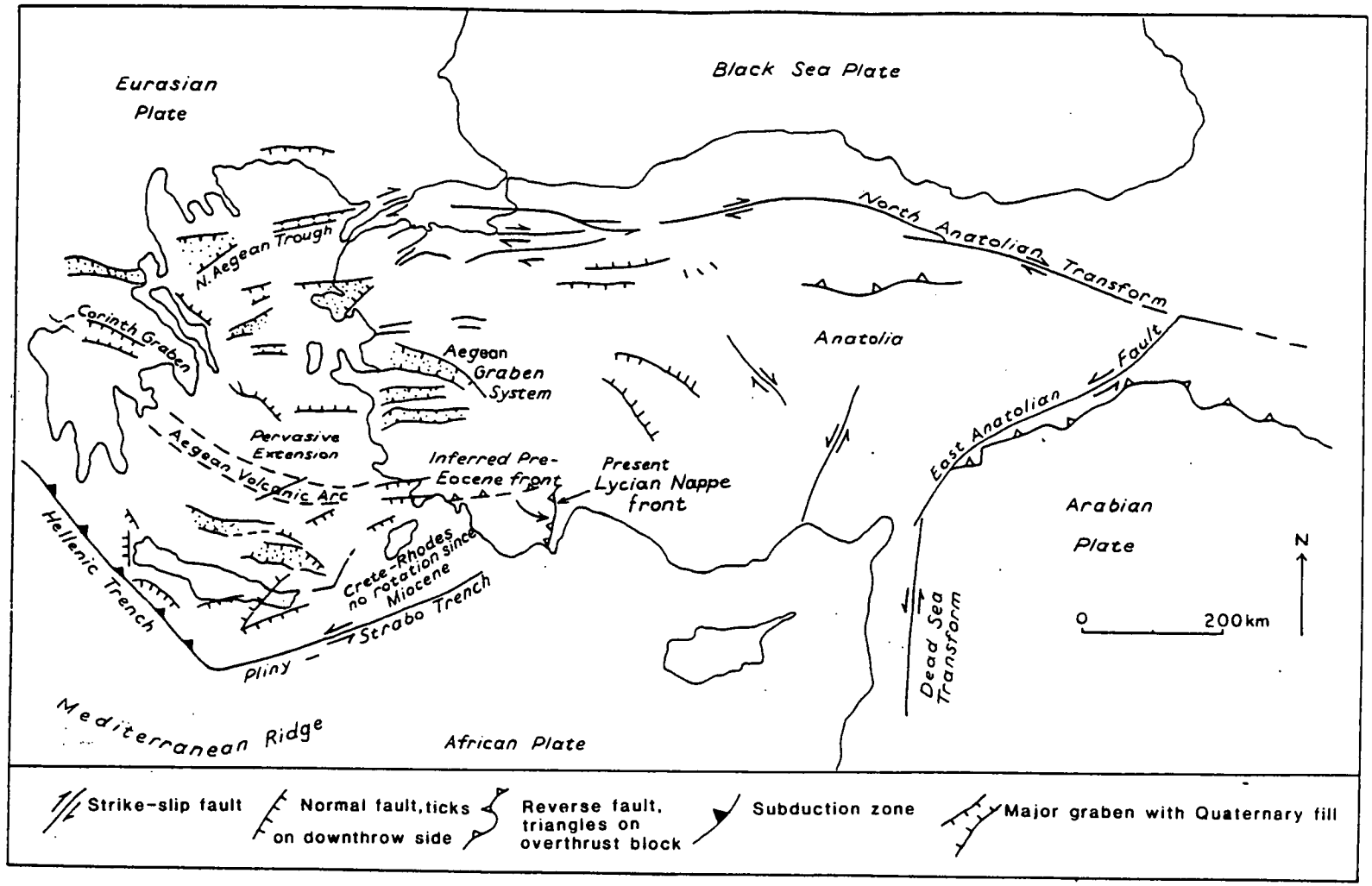

Figure 2.08. Main Neotectonic elements in the eastern Mediterranean (from Robertson and Dixon, 1984).

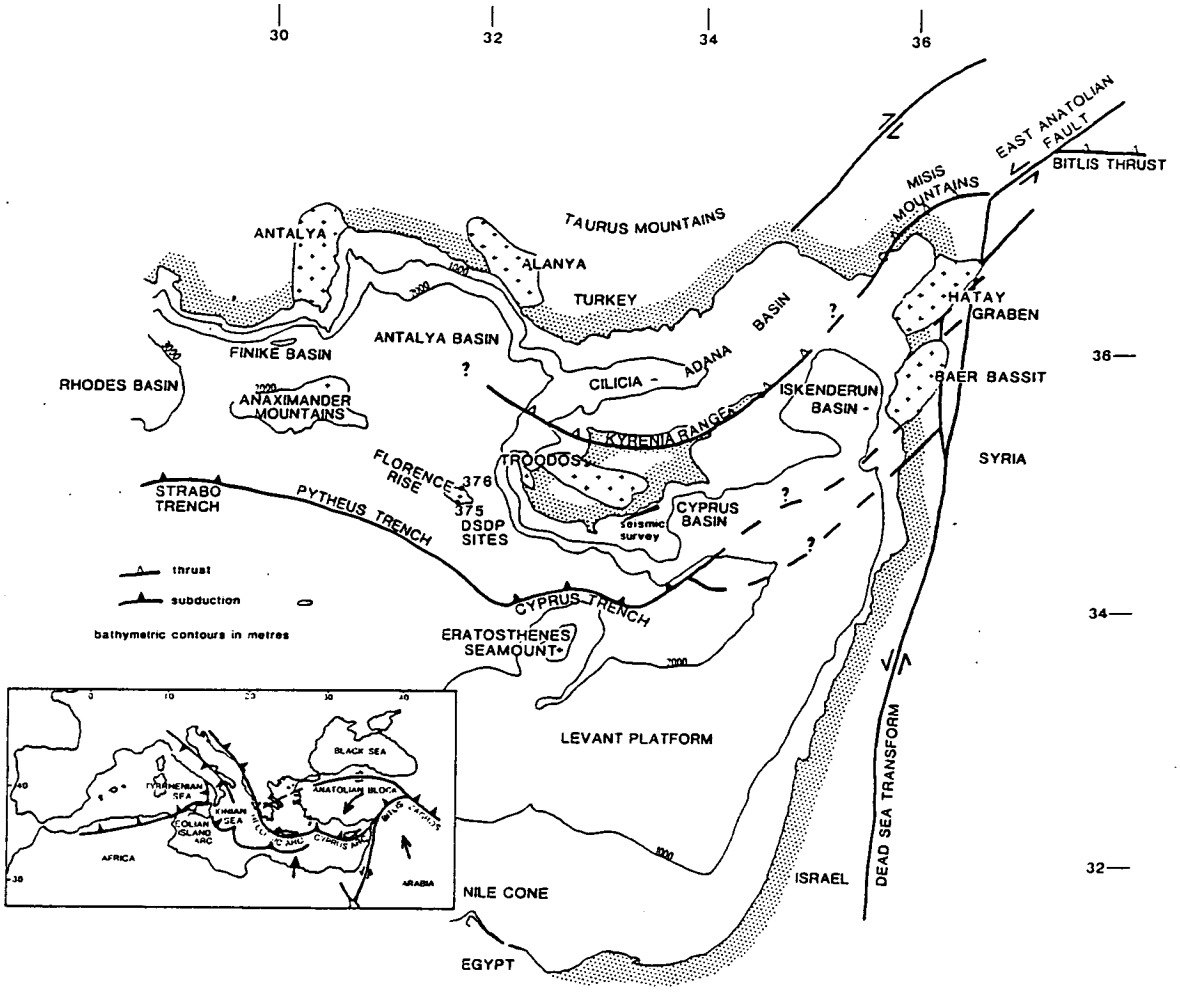

Figure 2.09. Outline map of the easternmost Mediterranean, showing the present day Cyprus active margin and inset showing the trends of active margins in the Mediterranean.

ones in which almost every ophiolite body is considered to be rooted *in situ* in a separate basin (Sengör *et al.*, 1984; Robertson and Dixon, 1984). The question of the number of separate oceanic basins which existed in the Greek area is deferred until Section 2.4.4, where it is discussed in relation to two recent tectonic reconstructions of the eastern Mediterranean Tethys. In this section, I will examine evidence mainly related to the Turkish area.

In the Turkish area, Ricou *et al.* (1984) suggested that the general similarity of many marginal sedimentary successions preserved within separate ophiolite belts indicates that all of the allochthonous ophiolite-related units, including the Troodos ophiolite of Cyprus, were derived from a single root-zone in North Anatolia (Figure 2.11b). In this model, after the Hercynian orogeny, rifting took place in the Triassic to form a single Mesozoic ocean basin, with the Tauride carbonate platforms forming part of the northern passive continental margin of Gondwana. The ocean then began to close by progressive *northward* subduction beneath the Pontides (which formed the Eurasian margin in this model) from Mid-Cretaceous onwards. This led to the rapid collapse of platforms to pelagic depths, followed by deposition of ophiolitic olistostromes, heralding the emplacement of ophiolitic nappes in the Late Cretaceous from the principal Tethyan suture zone in northern Turkey. After successive stages of southward transport over the Tauride and Arabian platforms, the nappes reached their final positions by Late Eocene to Late Miocene times. Subsequent erosion then led to the formation of windows through to the underlying platform carbonates to yield three ophiolite belts (Figure 2.11b).

An alternative multiple root-zone model, illustrated in Figures 2.11c and 2.12, has been proposed by Sengör *et al.* (1984) in which each ophiolite belt derives from its own separate basin. Here, *southward* subduction of 'Palaeotethyan' oceanic crust during the Triassic resulted in the rifting of an east-west trending continental sliver, the 'Cimmerian continent', away from the Gondwanan margin and the opening of a strand of the 'Neotethys' to the south. This sliver then migrated northwards towards Eurasia. Continued southward subduction resulted in rifting off of the Sakarya, Kirsehir and Tauride-Anatolide blocks from Gondwanaland. Subsequent closure yielded four Neotethyan sutures, which merge in a complex region in eastern Anatolia. The model of Sengör *et al.* (1984) therefore derives the Pontides from Gondwana, and also opens a Triassic ocean basin between the Taurides and the African margin, then another bifurcating one further north from the Early Jurassic onwards (Robertson and Dixon, 1984).

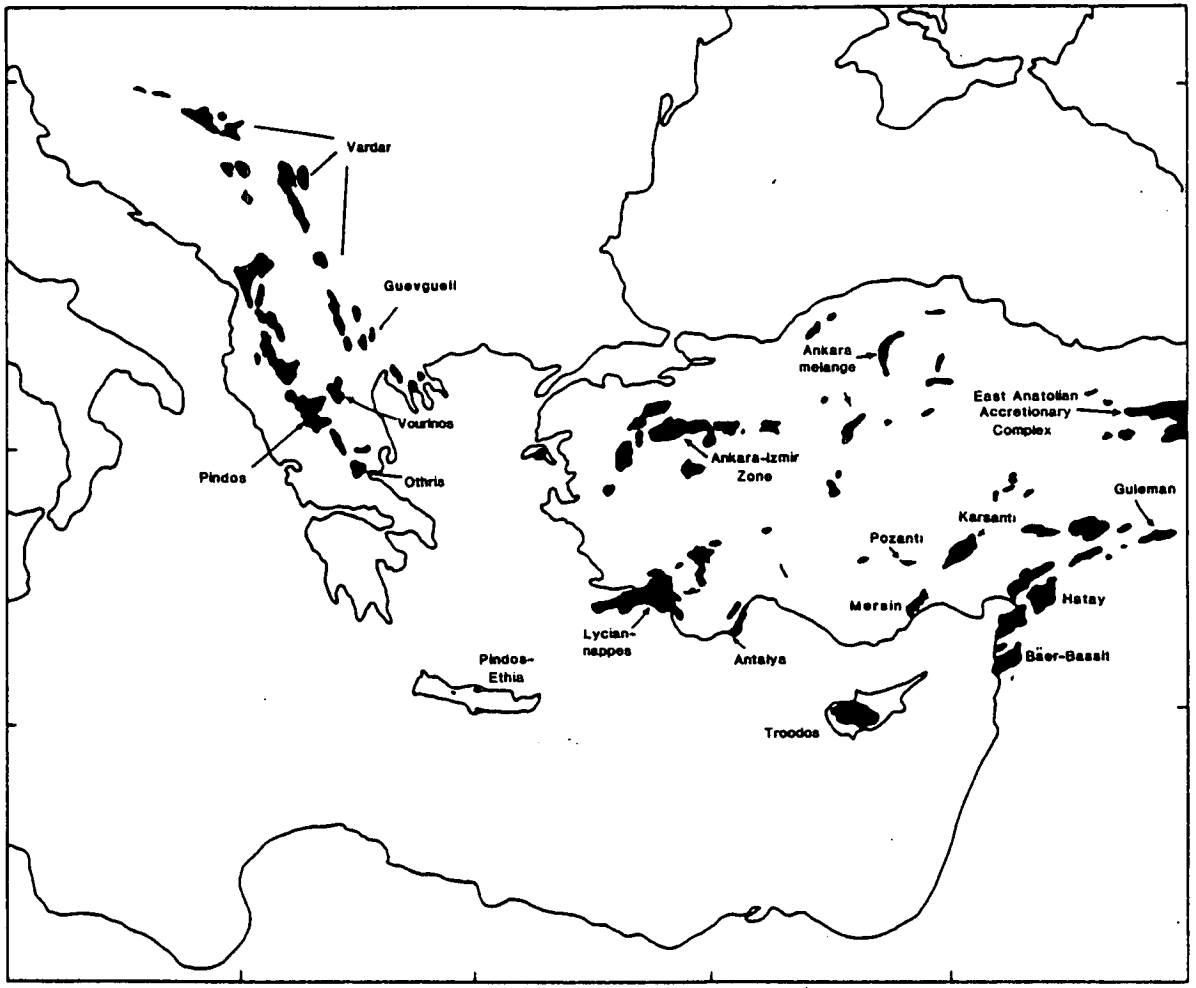

Figure 2.10. Location of the main ophiolites in the eastern Mediterranean (from Robertson and Dixon, 1984).

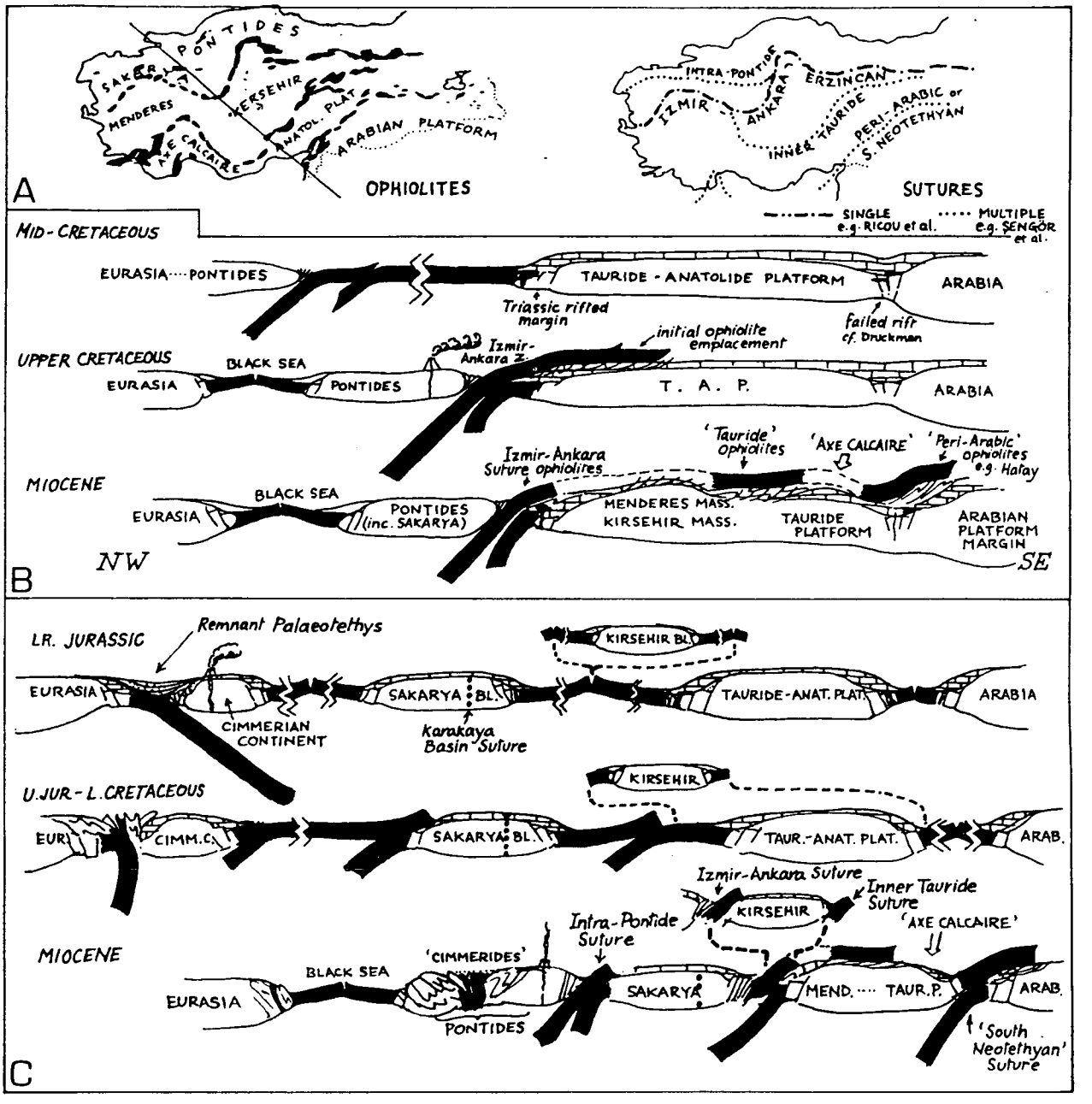

Figure 2.11. The origin of Neotethyan ophiolites in the Turkish area (from Robertson and Dixon, 1984).

(A) shows location of principal ophiolite belts in relation to major autochthons. Postulated suture zones for 'single' and 'multiple' root-zone models are also indicated, as is approximate line of section represented by (B) and (C). (B) shows the main features of the single (Izmir-Ankara-Erzican) root model of Ricou et al. (1979, 1984). In this model, the northern margin of the Afro-Arabian plate extends as far north as the Sakarya and Pontide units of northern Turkey. A major ophiolite nappe, emplaced initially on to the northern margin of the Tauride-Anatolide platform in the Late Cretaceous, is differentially disrupted and transported southward in episodic Tertiary thrusting events, to create three independent ophiolite belts stranded on the northern margin of the African plate. (C) shows multiple root-zone model favoured by Sengör and Yilmaz (1981) and Sengör et al. (1984). Schematic diagram shows the Sakarya, Kirsehir, Tauride-Anatolide and Cimmerian blocks being rifted-off the northern margin of Gondwanaland as a result of southward subduction of the Palaeotethys. Each rift acted as an ophiolite source once an individual basin experienced compression. Following incipient collision, a complex braided network of four suture zones were preserved in Turkey (Intrapontide, Izmir-Ankara-Erzican, Inner Tauride and Peri-Arabic sutures). The multiple root-zone model of Robertson and Dixon (1984) again adopts a separate block configuration, but maintains a northward-subducting Palaeotethys between the Sakarya-Kirsehir blocks and the Pontides until the Mid-Tertiary.

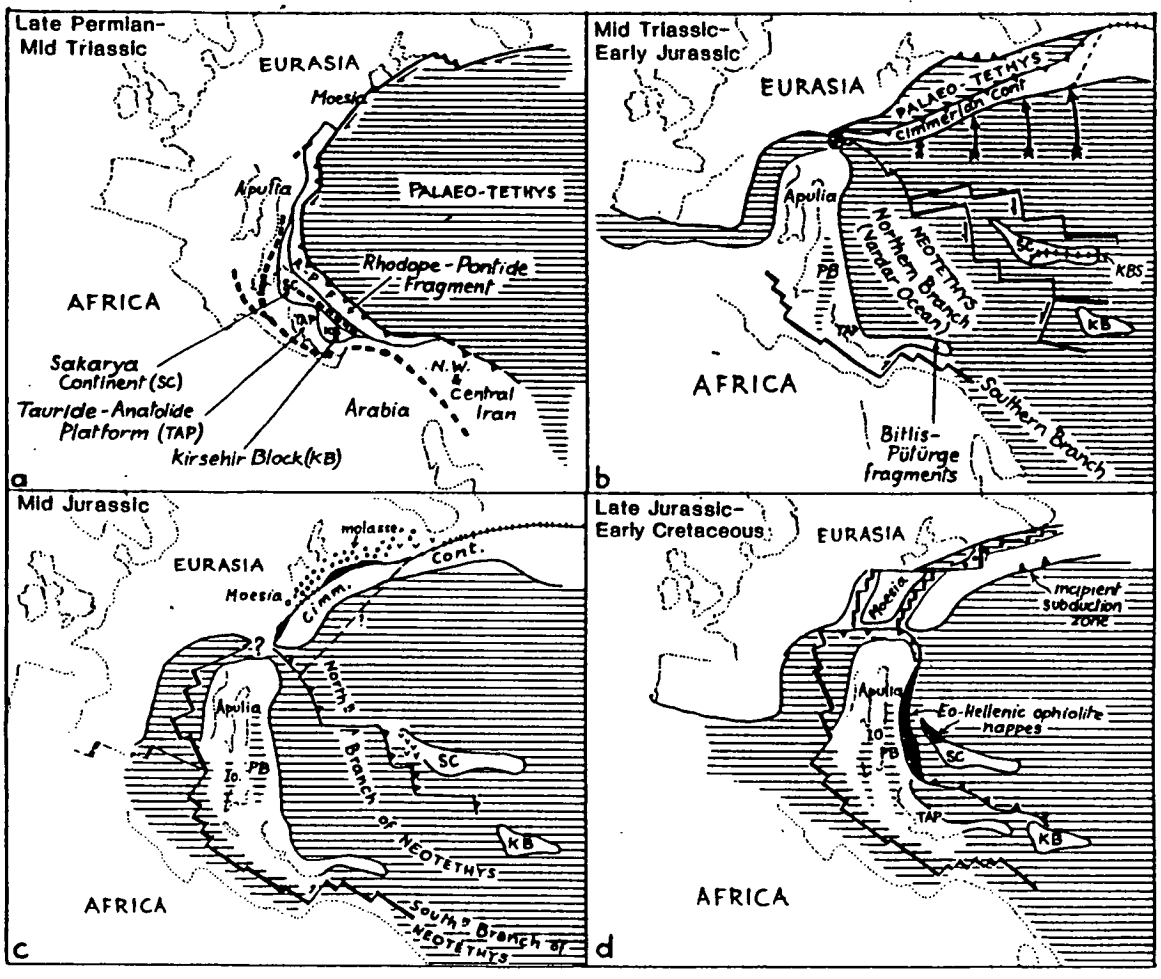

Figure 2.12. Schematic illustration of the concept of the geological evolution of the Palaeotethys according to Sengör et al. (1984).

PB = Pindos-Budva basin; IO = Ionian Zone; SC = Sakarya continent; KBS = Karakaya Basin suture. a) a wide Late Permian-Mid Triassic Palaeotethys undergoes southward subduction under Gondwanaland; b) Mid-Triassic to Early Jurassic, a Cimmerian continent is rifted off Gondwanaland and sweeps northward opening a 'Northern Branch of the Neotethys'. Note the inferred pole of rotation; c) Mid-Jurassic, the Cimmerian continent has collided with the Eurasian margin; the 'Southern Neotethyan Branch' opens; intra-oceanic subduction of the Northern Neotethys is initiated; d) Late Jurassic to Early Cretaceous, subduction of the Northern Neotethyan Branch leads to ophiolite emplacement in Greece and establishes the mechanism for future Tauride ophiolite obduction. The Southern Neotethyan Branch remains unaffected at this stage.

The single versus multiple root-zone controversy is highlighted when considering the origin of the Antalya Complex, southwest Turkey (Robertson and Woodcock, 1982; the Antalya Nappes of Brunn *et al.*, 1970; Figure 2.07). The Antalya Complex crops out in a critical suture, the Isparta angle, which separates the main Tauride (to the east) and Hellenide (to the west) segments of the eastern Mediterranean Tethyan belt. The various outcrop areas of the complex are shown in Figure 2.13. The Antalya terranes consist of large Mesozoic carbonate platforms and overthrust allochthonous units which include deep-water sediments, volcanics, passive continental margin facies and dismembered ophiolitic rocks. These allochthonous units were first seen as having been emplaced long distances (i.e. hundreds of km) northwards from a southerly ocean, the 'Pamphylian basin' (Dumont *et al.*, 1972). Subsequently, a palaeogeographically complex southerly basin was reconstructed in some detail by Robertson and Woodcock (1980b, 1981a, b, c, 1982, 1984) and Waldron (1984a, b), comparable with, for example, the modern Caribbean area. In this model, the Antalya Complex is seen as recording the initiation, construction, and later tectonic disruption of the continental margin of this southern strand of the Neotethys. Final emplacement of the allochthonous units on to the adjacent carbonate platforms was dominated by collisional and strike-slip tectonics. This reconstruction is discussed fully in Chapter 5, in relation to the palaeomagnetic sampling carried out for the present study.

The alternative view of the origin of the Antalya Complex is that of Ricou *et al.* (1979, 1984), in which all the ophiolitic and associated deep-water sediments were thrust hundreds of kilometres southwards from a single Neotethyan suture zone in northern Turkey (Izmir-Ankara Zone) to their present positions, beginning in the Late Cretaceous. In this scenario, the ophiolitic nappes would have to be transported over the 'Axis Calcaire', the east-west trending zone of carbonate platforms which stretches across central Turkey (Figure 2.07). In the latest version of this model, Marcoux *et al.* (1989) maintain that the 'Antalya Nappes' were thrust generally southwards in stages, from Late Cretaceous-Early Tertiary to Late Miocene time. In accordance with Ricou *et al.* (1979), they claim that the relatively autochthonous Bey Daglari platform (Figure 2.13) was in fact subdivided into two separate units; a relatively autochthonous basement to the southwest ('Western Bey Daglari') and an elongate, allochthonous unit further northeast ('Eastern Bey Daglari'). In their view, the Antalya oceanic rocks were first emplaced southwards, in the Late Cretaceous-Early Tertiary, on to the 'Eastern Bey Daglari'. This unit was then located to the northwest of the 'Western Bey Daglari' platform unit. In the Late Miocene, the 'Eastern Bey Daglari' was detached and thrust

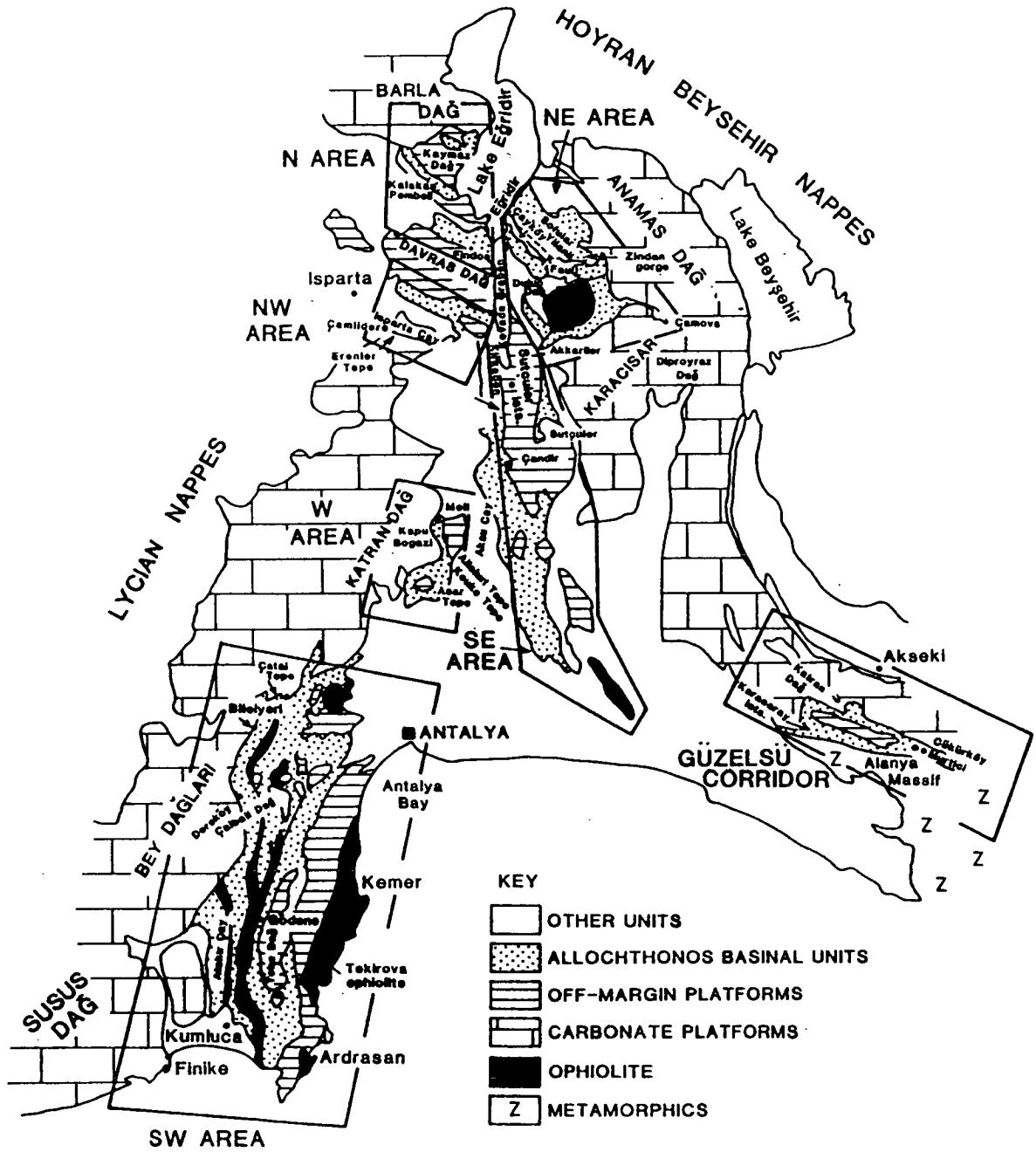

Figure 2.13. Sketch map to show the division of the Antalya Complex into specific areas and the locations of features mentioned in the text (from Robertson et al., in press).

southwards over the larger 'Western Bey Daglari' unit, along with final emplacement of the Lycian Nappes (Figure 2.13).

There is a substantial amount of evidence from local geological studies which supports the southerly basin concept. The key evidence is as follows:

(i) Reconstructed passive margins faced generally southeastwards in the westerly outcrop areas of the Antalya Complex, and southwestwards in the easterly outcrop areas, i.e. inwards into the Isparta angle, the site of the proposed Neotethyan ocean basin (Robertson *et al.*, in press). The northeast (Egridir) and northwest (Isparta) areas of the complex (Figure 2.13) are critical since they would have lain in the path of thrust sheets derived from the north, as in Ricou *et al.*'s (1979, 1984) model. Evidence from the northeast area, however, confirms the presence of a large carbonate platform (the Anamas Dag), which passed *southwestwards* across a passive margin into a coeval ocean basin (Waldron, 1984a, b). In general, Mesozoic basinal sediment thrust sheets become more distal towards the southwest, i.e. towards the inferred ocean basin. Also, para-autochthonous slope carbonates beneath the Antalya Complex thrust sheets are interpreted as the western margin of the adjacent Anamas Dag platform (Waldron, 1984 a, b). Elsewhere, platform edge units are mostly concealed by the overthrust Antalya Complex. However, base-of-slope carbonates are found in the lowest structural units of the southwestern segment of the Antalya Complex (Çatal Tepe unit and Bilelyeri Group; Robertson and Woodcock, 1981a, 1982). The systematic facies distribution, including proximal carbonate platform margin units (e.g. Çatal Tepe unit) could not be easily explained if the whole of the Antalya Complex were thrust hundreds of kilometres from the north, as in Ricou *et al.*'s (1984) model (Robertson *et al.*, in press).

(ii) The strike and dip of imbricate fans, thrust duplexes and large and small scale folds indicate thrust emplacement generally towards the adjacent carbonate platforms. In the northeast area of the Antalya Complex, six thrust sheets south of a major high-angle fault (Yilanli-Pazarköy Fault, Figure 2.13), consisting of slope and basinal sediments, are deformed by thrust duplexes and folds of Late Cretaceous-Early Tertiary age. These structures indicate emplacement towards the *north and northeast* (Waldron, 1984a, b). By contrast, thrust imbrication and fold facing within basinal sediments in the northwest area (Isparta Çay unit, Figure 2.13) indicate displacement towards the southwest in pre-Late Eocene time. Within the southwest Antalya Complex area, thrusting was mainly to the northwest in the north (Çatal Tepe unit; Robertson and Woodcock, 1982), to the west further southwest (Bilelyeri Group), and also to the west in the south (Kumluca Group; Woodcock and Robertson, 1982; Figure 2.13). Sedimentation ended in the Late Cretaceous in all of the transported successions, and

thrusting apparently took place in Maastrichtian-Palaeocene time (Robertson *et al.*, in press).

(iii) The sedimentary succession on the major carbonate platform of the Bey Daglari to the southwest of the Isparta angle (Figure 2.13) is unbroken from the latest Cretaceous through to the Palaeocene. Therefore, allochthonous units to the northwest, the Lycian Nappes (Figure 2.13) cannot simply be correlated with the Antalya Complex to the east (Hayward, 1984). Also, south of Isparta the Antalya Complex is unconformably overlain by Lower and Middle Miocene sedimentary cover rocks. This precludes thrusting of the complex through the Isparta angle to reach its present position in the southwestern area by Middle to Late Miocene.

Marcoux *et al.* (1989) reported shear-sense structural evidence which they claimed confirmed a northerly origin for the Antalya Complex and supported their two-stage thrusting model. Their data are summarised in Figure 2.14. However, their data do not unambiguously indicate a southward emplacement direction, for the following reasons:

(i) Many of the structural features recognised by Marcoux *et al.* (e.g. slickensides, shear bands, friction grooves in pebbles, normal and reverse small faults) deform Eocene and Miocene sedimentary rocks and are thus not related to the critical Late Cretaceous-Palaeocene initial emplacement.

(ii) Palaeomagnetic data indicate that the Bey Daglari platform underwent 30° of anticlockwise rotation during the Neogene (Kissel and Laj, 1988). In Chapter 6 of the present work, I show that this rotation has not been confined to the autochthon itself, but has also affected the southwestern segment of the Antalya Complex. Thus, after stripping off this later rotation, Marcoux *et al.*'s (1989) shear-sense data from this area implies thrusting from the northeast. This contrasts with the inferred directions of thrusting of the supposedly correlative Lycian nappes; south-southeastward in the Middle Miocene, and southeastward in the Late Miocene.

(iii) Striations on the basal thrust plane of the Antalya Complex in the Çatal Tepe unit outcrop indicate emplacement mainly towards the present southwest. After removal of the Neogene 30° anticlockwise rotation of these units, this direction becomes more westerly, which is consistent with emplacement from within the Isparta angle.

(iv) In inferring southward displacement of units within the Antalya Complex (e.g. 'Upper Antalya Nappe'; Antalya-Finike road; Kemer gorge), Marcoux *et al.* (1989) assumed that deformation took place when the rocks were sub-horizontal, and rotated structures back to the palaeohorizontal, essentially in the same way that standard stratigraphic corrections are applied to palaeomagnetic data. However, it is well known that the application of this type of simple correction to directional data obtained from

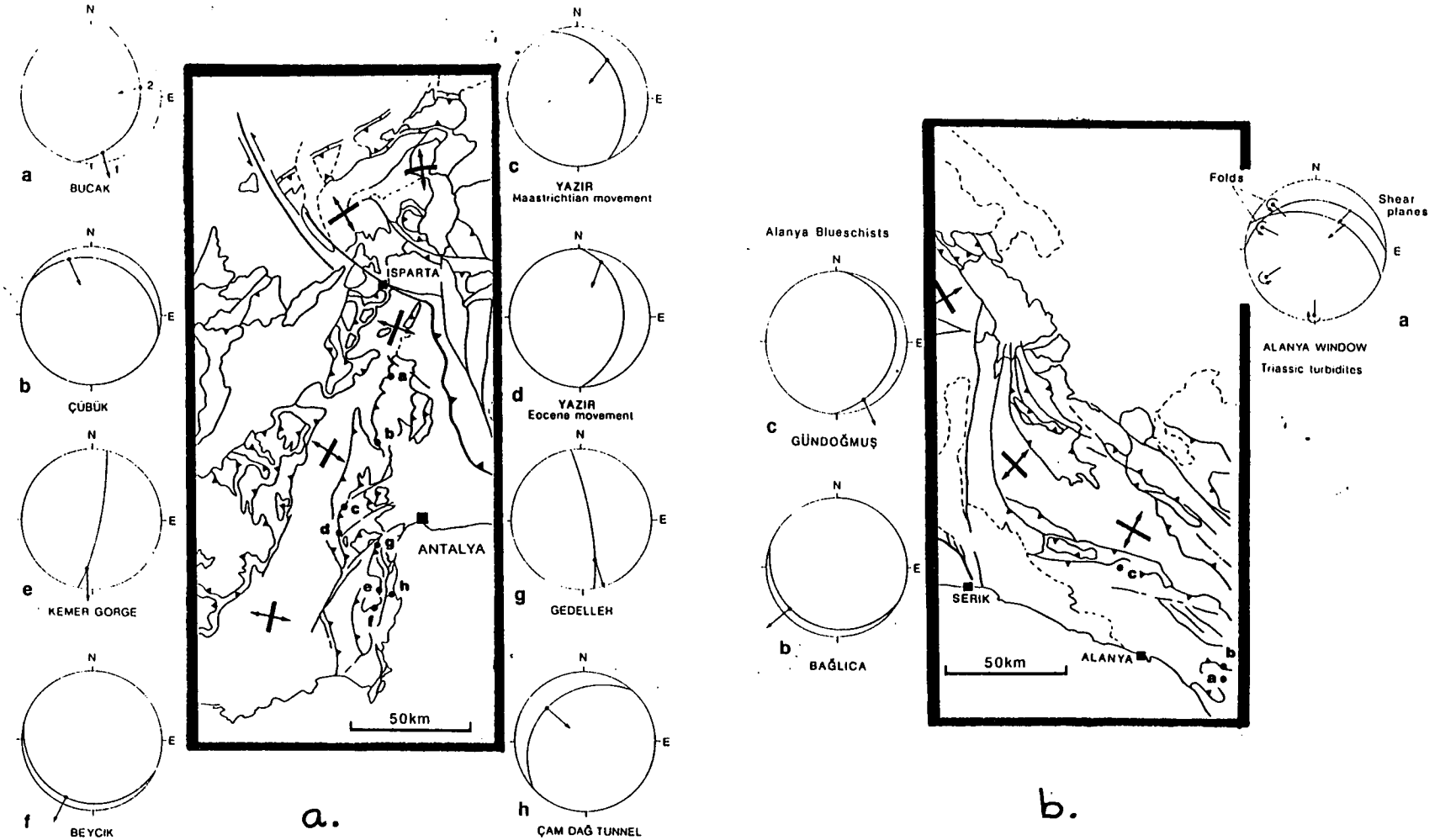

Figure 2.14. Observed senses of displacement along shear zones in a) the type area for the Antalya Nappes, and b) the type area for the Alanya blueschists and marbles, according to Marcoux *et al.* (1989).

such steeply dipping strata can lead to the generation of large declination anomalies (MacDonald, 1980). Also, Reuber (1984) interprets the contact between the Tekirova ophiolite and the subjacent Kemer limestones (Figure 2.13) as a sinistral strike-slip fault, and moreover, much evidence has been presented that the entire structure of the southwest area of the Antalya Complex (Gödene, Kemer and Tekirova Zones) was the result of pervasive strike-slip faulting (Robertson and Woodcock, 1980b; Woodcock and Robertson, 1982). Emplacement directions in these areas cannot, therefore, be determined by application of a tilt correction to small-scale structures.

(v) Finally, Marcoux *et al.* (1989) quote supporting evidence of southward emplacement from blueschists in the Alanya Massif (Figs. 2.13 and 2.14), further east, but these structures presumably developed at depth in a subduction zone and cannot be used to indicate the direction of thin-skinned thrusting (Robertson *et al.*, in press).

In conclusion, the shear-sense data of Marcoux *et al.* (1989) do not prove a northern derivation of the Antalya Complex.

When considering the possibility of complex multi-stage southward thrusting from a single basin as an origin for all Turkish and Middle Eastern ophiolites, including the Troodos massif of Cyprus, it should be noted that from the Late Cretaceous to the Lower Tertiary the northern and eastern margins of the Troodos massif remained undeformed. Throughout this time a continuous pelagic sediment cover accummulated over the ophiolitic crust (see Chapter 3). It seems unlikely that the Troodos underwent over 400 km of tectonic transport without disturbing the quiet, unbroken pelagic deposition. This is in contrast with the Semail ophiolite nappe to the east, which is known to have been emplaced on to the Arabian margin in the Late Cretaceous (Glennie *et al.*, 1973). In this case pelagic sedimentation above the ophiolitic extrusives ended abruptly, and was followed by overthrusting of various allochthonous units of continental margin affinities (Woodcock and Robertson, 1982).

The majority of field geological data therefore support a root-zone model for the southern ophiolites (Antalya, Troodos, Baër Bassit and Hatay) involving at least two oceanic basins, contrary to the hypothesis of Ricou *et al.* (1984) and Marcoux *et al.* (1989). The model adopted here, that of Robertson and Dixon (1984), retains the separate blocks of Sengör *et al.* (1984) but maintains a *northward-subducting* Palaeotethys (see Section 2.4.4). It incorporates the reconstruction of the Turkish segment of the southern strand of the Neotethys proposed by Robertson and Woodcock (1980b, 1981a, b, c, 1982, 1984).

2.4.3 Lauer's hypothesis for the Turkish microblocks.

Having concluded that the present distribution of sub-parallel ophiolite belts in Anatolia cannot be easily explained by overthrusting, I now go on to look at the possibility that some of the component blocks of Turkey may represent suspect terranes which have travelled long distances along strike to reach their present positions. Supporting evidence for such a theory is provided by the palaeomagnetic studies of Lauer (1981, 1984).

According to Lauer (*op. cit.*), the available palaeomagnetic data allow Turkey to be sub-divided into three blocks; A - the Pontides, B - the Western Taurides, and C - the Eastern Taurides (Figure 2.15a). In the model suggested by Lauer (*op. cit.*), each of these blocks has moved independently until continental collision and eventual accretion against the leading edge of the African plate in the Neogene. Although he suggests that the spatial extent of each block has been defined solely on palaeomagnetic criteria, the specific boundaries to each unit were in fact chosen so that they correspond to important suture zones (i.e. the southern boundary of block A runs east-west along the northern Anatolian suture, while the boundary between blocks B and C coincides with the axis of the Isparta angle lineament). Discrepancies in remanence declinations between rock units of the same age in any one of these three 'rigid' blocks were attributed to localised internal 'block rotations' or large scale plastic deformation.

Although no palaeomagnetic data exist for autochthonous units in block B, the low inclinations recorded in Triassic and Jurassic successions in both blocks A and C 'requires' these blocks to have been originally located at equatorial latitudes to the east of the Arabian plate, whose northern margin can be independently constrained to have lain between 10° and 20° to the north of the equator (Savostin *et al.*, 1986; Figure 2.06). Not unexpectedly, inclination data for allochthonous units in blocks A and C do not differ considerably from contemporaneous autochthonous successions in the same block, implying that within the resolution of the palaeomagnetic data there has not been a significant displacement of nappe sheets relative to underlying basement units. Similarly, the low inclinations recorded in allochthonous units above block B are assumed to imply that, like the other blocks, the Western Taurides also have an equatorial origin.

Assuming that the sparse pre-Cretaceous palaeoinclination data used are reliable, Lauer's hypothesis would require each of the three separate blocks to have rifted off adjacent areas of the eastern Arabian margin in the Triassic, possibly with block A originating from the lowest latitudes. The Turkish blocks then migrated northward (Figure 2.15a, b), but probably never drifted far from the Arabian margin. Each of the

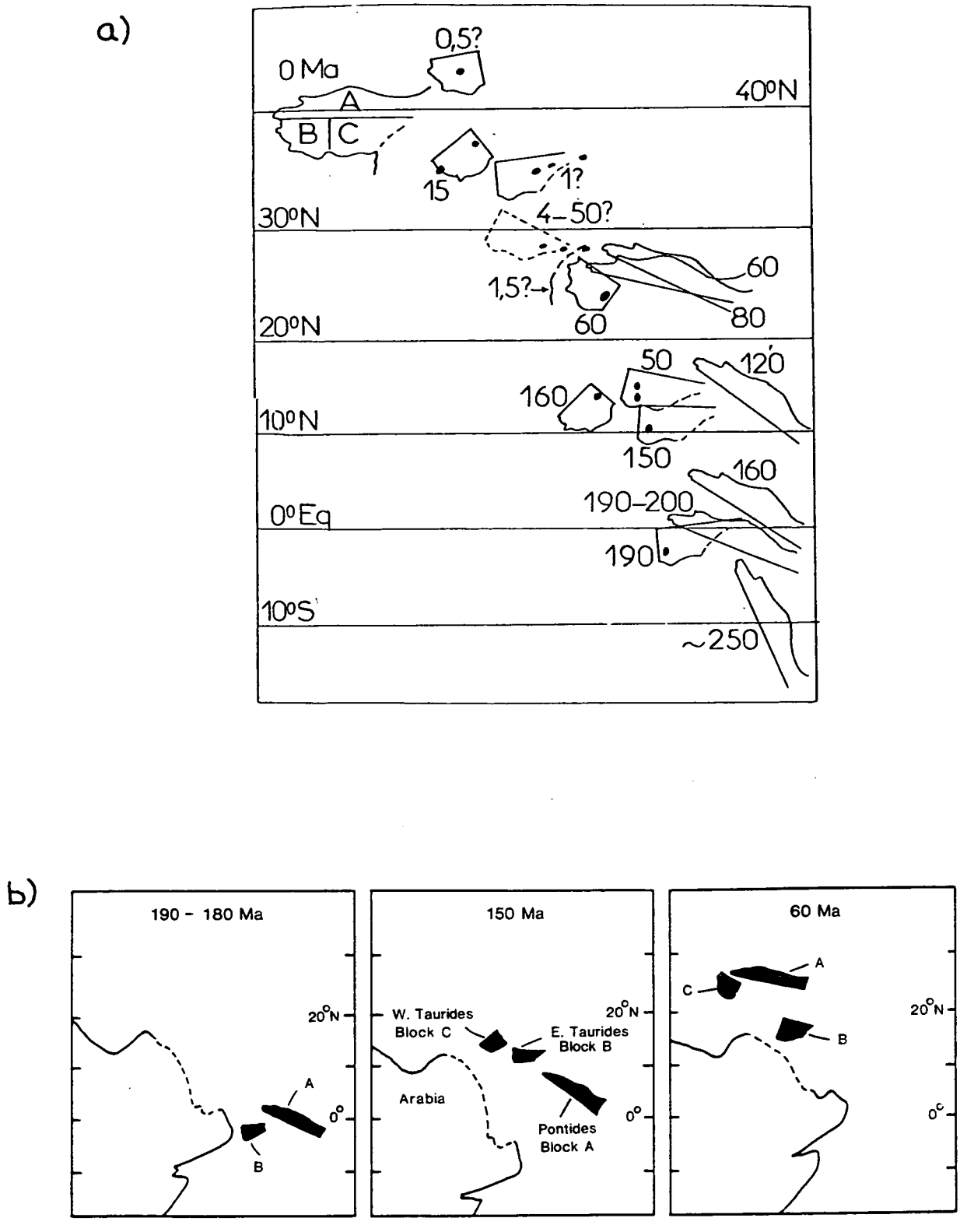

Figure 2.15. Lauer's hypothesis of the division of Turkey into 3 separate blocks. a) Latitudinal reconstruction of positions of the Turkish blocks A, B, and C at various periods (average ages, Ma) according to Lauer (1984). The black dots on B and C represent sites for which data are used. The present position of Turkey is not deduced from the palaeomagnetism. Longitudes are arbitrary. b) Reconstruction of the position of the three blocks defined by Lauer (1981, 1984) relative to the Arabian plate for three selected periods (modified from Lauer, 1984), illustrating the proposed northwestwards drift from an initial position off southeastern Arabia.

three independent units were then juxtaposed close to their present position, prior to the emplacement of ophiolites in the Late Cretaceous.

When evaluating Lauer's hypothesis it is first necessary to consider how accurately the palaeolatitudinal positions of each of the three independent blocks relative to the Arabian plate can be determined from the available data. Importantly, the inferred equatorial palaeolatitudes for blocks B and C were primarily based on remanence directions isolated from pillow lava formations where appropriate structural corrections are difficult to determine (see Chapter 4, Section 4.3.2). For example, even in an allochthonous 250m thick coherent succession on block B (Çalbali Dag succession), remanence inclinations measured for over 50 samples were found to vary between -32.6° and +15.1°, leading to wide errors in the Fisherian mean*. Similarly, the equatorial origin for block A relies heavily on the Permian inclination data of Gregor and Zijderveld (1964) and the Jurassic data of Van der Voo (1968), supplemented by two localities sampled by Lauer (1981). As noted by Lauer (1984), the Permian data are open to alternative interpretations (they may be of either normal or reverse polarity), while the Lower Jurassic result from Bayburt was not considered reliable by Van der Voo as the stable remanence was carried by haematite of possible secondary origin. Only a thorough analysis of 191 samples from Upper Jurassic limestones in the western Pontides (Bilecik limestones, Evans *et al.*, 1982) has provided a reliable remanence direction with a mean inclination of +53°, corresponding to a palaeolatitude of 33.5°N, and a declination of 093°. Significantly, Saribudak *et al.* (1989) reported preliminary results from Lower Triassic volcanic and sedimentary rocks of the western Pontides which indicated that at least this part of the Pontide belt was formed close to the Eurasian margin during the Triassic. Clearly more palaeomagnetic data are needed to assess whether block A of Lauer (1981, 1984) originated close to Africa or Eurasia.

If it is assumed that the Turkish basement elements were derived from the eastern Arabian margin, then the model of Lauer (*op. cit.*) implies that the independent blocks should be bordered on at least one edge by passive continental margin successions with a long Palaeozoic history, and that during the Mesozoic they were translated by several thousand kilometres along major transforms bounding the leading margin of Arabia (Robertson and Dixon, 1984). Unfortunately there is little definitive evidence for either of the prerequisites. In addition, if the sparse pre-Cretaceous palaeoinclination data are deemed unreliable and removed from the analysis, the palaeolatitudes calculated by Lauer (*op. cit.*) for the Cretaceous onwards for all three blocks are also consistent with a

---

* Note - Lauer's data from the Çalbali Dag section will be discussed in detail in Chapters 5 and 6.

subequatorial location within the north African embayment, according to the reconstructions of Savostin *et al.* (1986) (compare Figure 2.15a with Figure 2.06a-l). This African margin affinity is in agreement with recent reconstructions of the palaeogeography of the eastern Mediterranean Tethys by Dercourt *et al.* (1986), Robertson and Dixon (1984) and Robertson *et al.* (in press).

In conclusion, more data are needed to test the hypothesis of Lauer (*op. cit.*), but it seems that the available data do not preclude an original location of the Turkish blocks against North Africa rather than southeast Arabia. I shall return to Lauer's theory in Chapter 6, in relation to the data obtained in the present study from southwest Turkey. I will now discuss various other aspects of the geological evolution of the Tethys region, including the question of the number of oceanic basins which existed in the Greek area, within the context of two recent Mesozoic-Tertiary reconstructions of the region.

2.4.4 Tectonic reconstructions of the eastern Mediterranean Tethys.

In general, reconstructions of the evolution of the eastern Mediterranean segment of the Tethyan orogenic belt may be divided into two classes; those involving southward subduction of Palaeotethyan crust beneath the Gondwanan margin, and those which invoke northward subduction beneath Eurasia. The most important model of the former classification is that of Sengör and others (Sengör and Yilmaz, 1981; Sengör *et al.*, 1984), which was discussed briefly in Section 2.4.2 above and illustrated in Figures 2.11 and 2.12. This model will not be discussed further here. Instead, this section will be limited to those models involving northward consumption of Palaeotethyan oceanic crust along a Eurasian margin, acting as an active, eastern Pacific-type margin. Within this category, there have been two important recent reconstructions; that of Dercourt *et al.* (1986), and that of Robertson and Dixon (1984). The latter was further refined by Robertson *et al.* (in press). Both models describe the break-up of the northern passive margin of Gondwanaland, but differ in the number of microcontinental blocks which rift off this margin during the Mesozoic.

The plate tectonic scheme of Dercourt *et al.* (1986) was constructed as part of a joint French-Soviet project, aimed at producing a series of palaeogeographic maps for various time periods from the Lias to the Present. The palaeomagnetic and kinematic data used by this group has already been discussed in Sections 2.2 and 2.3, respectively. The ten colour plates produced by this collaboration are not reproduced here, but Figures 2.16 to 2.18 represent simplified versions of the reconstructions, as given by Dercourt *et al.* (*op. cit.*).

By the Lias (Pliensbachian, 190 Ma), the time period represented by the first of these reconstructions, several microcontinental blocks had already rifted off the Gondwana margin and drifted northwards to collide with the Eurasian active margin, thereby forming a new Neotethyan (or Neo-Tethyan (Dercourt *et al.* (*op. cit.*)) ocean to the south. The subsequent tectonic evolution is characterised by Dercourt *et al.* (*op. cit.*) in terms of a change from convergence through subduction (Figure 2.16a) to convergence through continental collision (Figure 2.18h). This transition to a collision régime was believed to have occurred during the Oligocene, with the progressive development of a 500-1000 km wide convergence zone in which oceanic basins were still trapped (Figure 2.18f).

During the pre-Oligocene subduction dominated stage of this model, from the Lias to the Upper Cretaceous (190 - 80 Ma, Figs. 2.16 and 2.17), the basic plate tectonic system involved three plates. The African and 'Neo-Tethys' plates were separated by an accreting plate boundary, whereas the 'Neo-Tethys' plate was being subducted below the Eurasian plate (Figure 2.16a). As subduction was only occurring to the north of the Neo-Tethys spreading axis, this axis migrated northward with respect to Eurasia at a relative velocity equal to the spreading rate plus the Africa/Eurasia convergence rate, i.e. at about 5-6 cm/yr or 50-60 km/Ma. Assuming a half-width of the ocean of approximately 1500 km in the Middle Jurassic, Dercourt *et al.* (*op. cit.*) estimate that the spreading axis must have reached the subduction zone towards the end of the Jurassic (Figure 2.16b). Because of the eastward widening nature of the Neo-Tethys, subduction of this ridge was probably diachronous, with the age of subduction decreasing eastward.

As a consequence of this subduction, Dercourt *et al.* (*op. cit.*) suggest that the system changed briefly to one involving two plates in the Early Cretaceous (Figure 2.16b), with a decrease in the subduction rate to the Africa/Eurasia motion rate of 2 cm/yr. As the new slab in the subduction zone increased in length, the slab-pull force increased and the velocity of subduction picked up again. This increased velocity is believed by Dercourt *et al.* (*op. cit.*) to have been accommodated by a new accreting plate boundary to the south of the Neo-Tethys (Figure 2.16c), and the rifting off from the Gondwanan margin of a microcontinental fragment, which included Apulia and much of the present area of Greece and Turkey. The new accreting boundary propagated westward south of Apulia, which had just collided with Eurasia along its northwestern border and begun to rotate anticlockwise. The southern 'Mesogean' seaway formed an oceanic connection between the widening Atlantic Ocean and the shortening Neo-Tethys from the Aptian-Albian to the Middle Eocene (110-45 Ma).

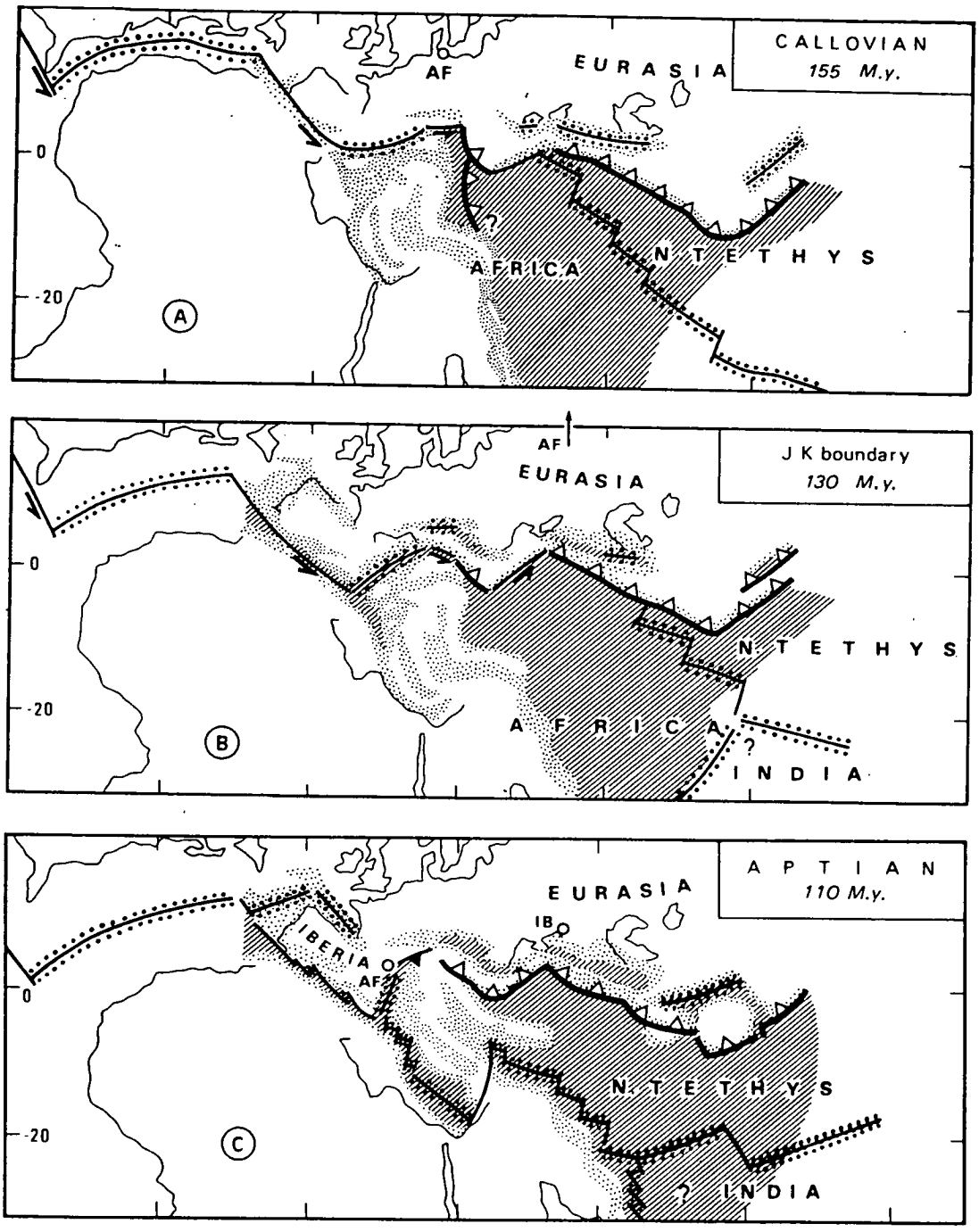

Figure 2.16. Simplified plate tectonic scheme of Dercourt *et al.* (1986) during the early three-plates stage (A: 155 Ma; B: 130 Ma; C: 110 Ma). Each figure applies to the immediately preceding geological period (e.g. between 155 and 130 Ma in Figure 2.16B). The three plates are Africa, the Neo-Tethys and Eurasia. Apulia moved from Africa to the Neo-Tethys in the Aptian at a time when Iberia was identified as a plate. Collision began to the north of Apulia in the Aptian. Schematic plate boundaries: continuous line = transform; open triangles = oceanic subduction; closed triangles = continental collision; double dotted line = accretion; hatchured pattern = oceanic crust; dotted pattern = thinned continental crust.

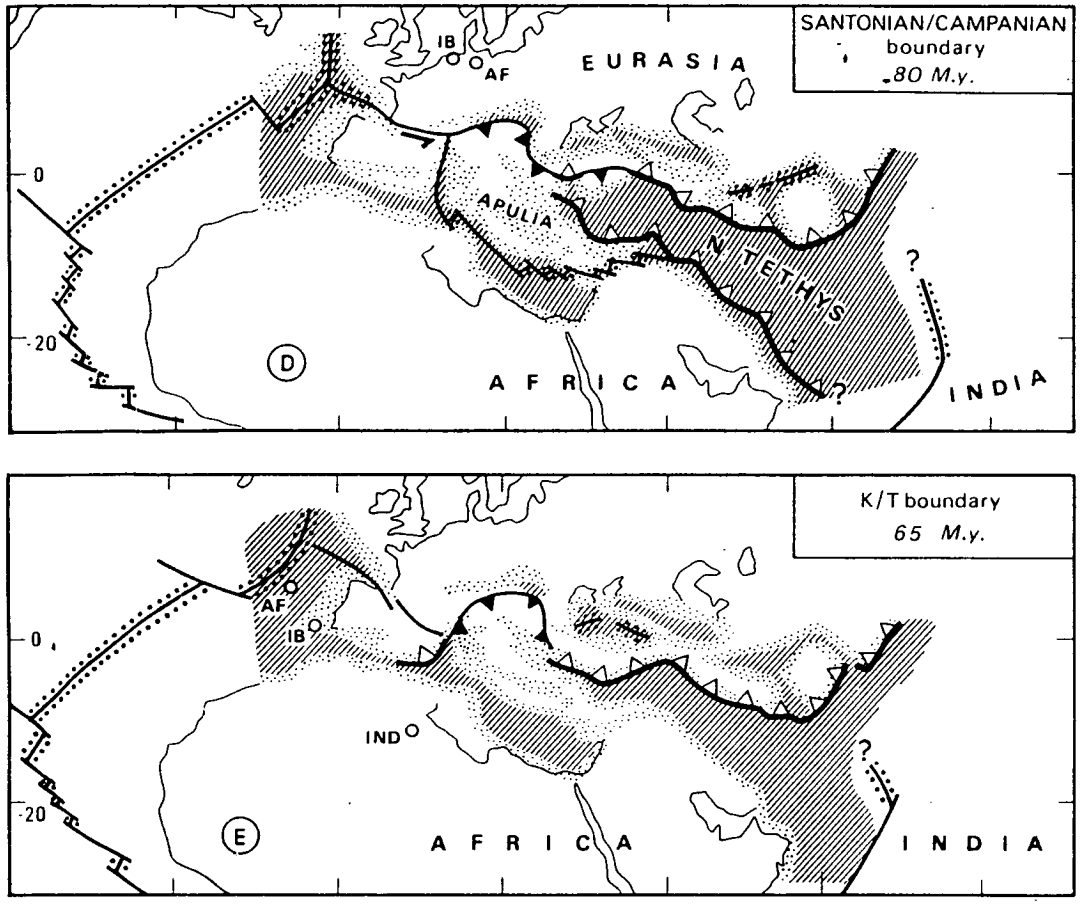

Figure 2.17. Simplified plate tectonic scheme of Dercourt *et al.* (1986) during the two plates stage (D: 80 Ma; E: 65 Ma). The two plates are Africa and Eurasia. Apulia was identified as a plate during the Upper Cretaceous at a time when Iberia was a part of Africa.

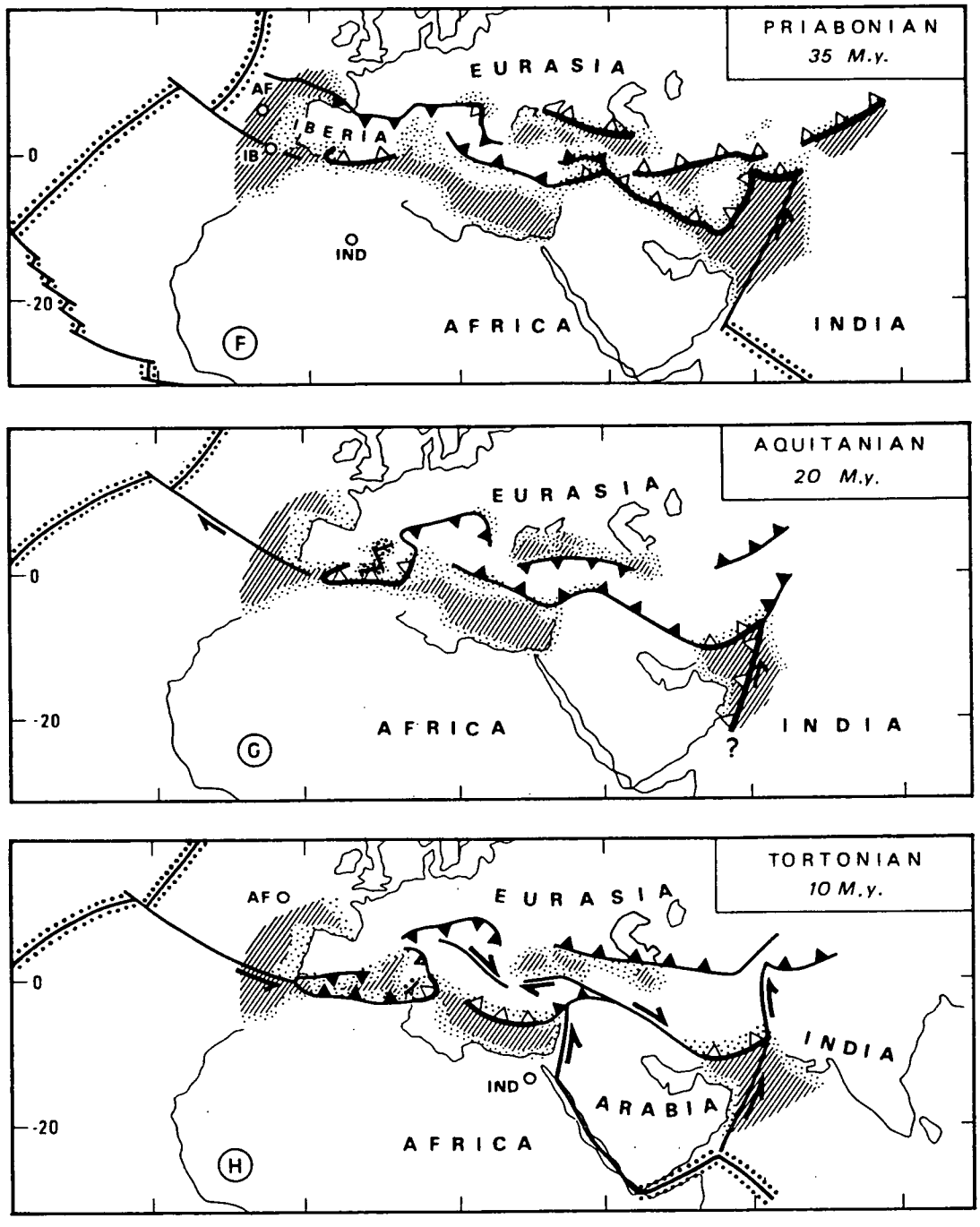

Figure 2.18. Simplified plate tectonic scheme of Dercourt *et al.* (1986) during the collision stage (F: 35 Ma; G: 20 Ma; H: 10 Ma).

The new spreading axis was destroyed 80 Ma ago (Upper Cretaceous) along a southern subduction zone formed on or very close to it, a situation which led to the emplacement of young oceanic crust and mantle on to the Arabian margin along a 3000 km long zone stretching from Turkey to Oman. In this model, all Turkish and Middle Eastern ophiolites, including the Troodos massif, were therefore derived from a single root-zone, in accordance with the hypothesis of Ricou *et al.* (1984). Subsequently, a system involving relatively slow subduction between the African and Eurasian plates was established. Finally, 35 Ma ago, closure of the Neo-Tethys to the north of India was completed and a pattern dominated by continental collision was established (Figure 2.18). The last fragments of Mesogea are still being subducted below the Calabrian and Hellenic arcs (Dercourt *et al.*, 1986).

To summarise, this model involves: (i) migration of the spreading axis from north to south across the Neo-Tethys, (ii) subduction of this spreading axis beneath Eurasia, (iii) rifting of a *single* microcontinent from Gondwanaland, and the formation of a new spreading axis to the south leading to the formation of a new ocean basin (Mesogea) as the older one disappeared by subduction to the north, and (iv) collision of the microcontinent with Eurasia, emplacement of ophiolites from a single root-zone, and subsequently final closure of the Neo-Tethys.

The scheme of Dercourt *et al.* (1986) suffers from several major drawbacks, mainly related to the number of Neotethyan basins created in the Jurassic and Cretaceous. In this model, all Turkish and Middle Eastern ophiolites, including the Troodos massif of Cyprus, were derived from a single oceanic basin located between the Pontide-Kirsehir and Menderes-Tauride blocks in the Late Cretaceous. As discussed above (Section 2.4.2), although this single root-zone concept is appealing in its simplicity, it does not agree well with regional geological studies. Also in this model, the Pindos basin in the Greek area is considered to be an intra-continental rift within the single Apulian microplate which separated from the Gondwanan margin. Thus this basin would be floored by thinned continental crust. However, geochemical studies of basaltic blocks within a tectonic mélange underlying thrust sheets of pelagic limestones derived from the Pindos basin and emplaced westwards onto the Gavrovo-Tripolis platform in southern Greece indicate a more MORB-like than within plate (WPB) signature (P. Degnan, pers. comm., 1989). This provides evidence for oceanic crust within the Pindos basin. More importantly, there is growing evidence for *eastwards* emplacement of the Jurassic ophiolites of the Greek area onto an adjacent Pelagonian microcontinental sliver from a Pindos root-zone (Robertson *et al.*, *in press*). Key evidence for this

emplacement direction, rather than an easterly derivation from an inferred Vardar ocean (from the Neo-Tethys of Dercourt *et al.*, 1986) includes:

(i) High temperature fabrics preserved within the depleted mantle section of the Pindos ophiolite in northwest Greece indicate tectonic displacement towards the northeast or east (Jones and Robertson, 1990; Jones, 1990).

(ii) Within the Sub-Pelagonian (Othris) Zone (Figure 2.07) abundant structural evidence from deformed continental margin successions below the Othris ophiolite indicate emplacement towards the northeast (Smith *et al.*, 1979).

(iii) On the island of Evvia, structures in the metamorphic sole beneath the harzburgitic ophiolite mainly indicate displacement towards the east (A. H. F. Robertson, unpublished data; Robertson *et al.*, in press).

Thus there is good evidence that the Jurassic ophiolites were derived from a root-zone to the west of a separate Pelagonian microcontinent (Robertson *et al.*, in press). It seems then that the Pindos basin must represent a small Red Sea-type ocean basin floored by oceanic crust, and not an intra-continental rift as in the model of Dercourt *et al.* (1986).

An alternative scheme which resolves these problems was proposed by Robertson and Dixon (1984). The salient points of this model are: (i) the older Palaeotethyan ocean remained open until the Early Tertiary, (ii) the Adriatic 'promontory', including the Apulian platform of Dercourt *et al.* (1986), remained an undisturbed part of Africa until sometime in the Tertiary, when it rotated anticlockwise to its present position (Channell *et al.*, 1979), (iii) rifting of the northern margin of Gondwanaland produced a braided system of Neotethyan ocean basins separating various microcontinental blocks, (iv) the constituent blocks of Turkey were derived from essentially within the Mediterranean basin, and do not represent terranes which moved long distances along strike to their present positions (cf. the hypothesis of Lauer, Section 2.4.3), and (v) the Adriatic/Apulian and Arabian promontories of Africa exerted a strong influence on the development of the rift system.

The cartoons of Figures 2.19a to 2.19f illustrate various stages in the tectonic evolution of the region according to the reconstruction of Robertson and Dixon (1984). This model retains the separate blocks defined by Sengör and Yilmaz (1981) and Sengör *et al.* (1984), but in contrast to this latter model it maintains a *northward* subducting Palaeotethys, to the south of the Pontides, until the Mid-Tertiary. Here the Pontides are considered to have always been a part of the northern Tethyan margin.

During the Late Permian to Mid Triassic (Figure 2.19a), Palaeotethyan oceanic crust was undergoing subduction under an active Eurasian margin of Pacific-type with a long

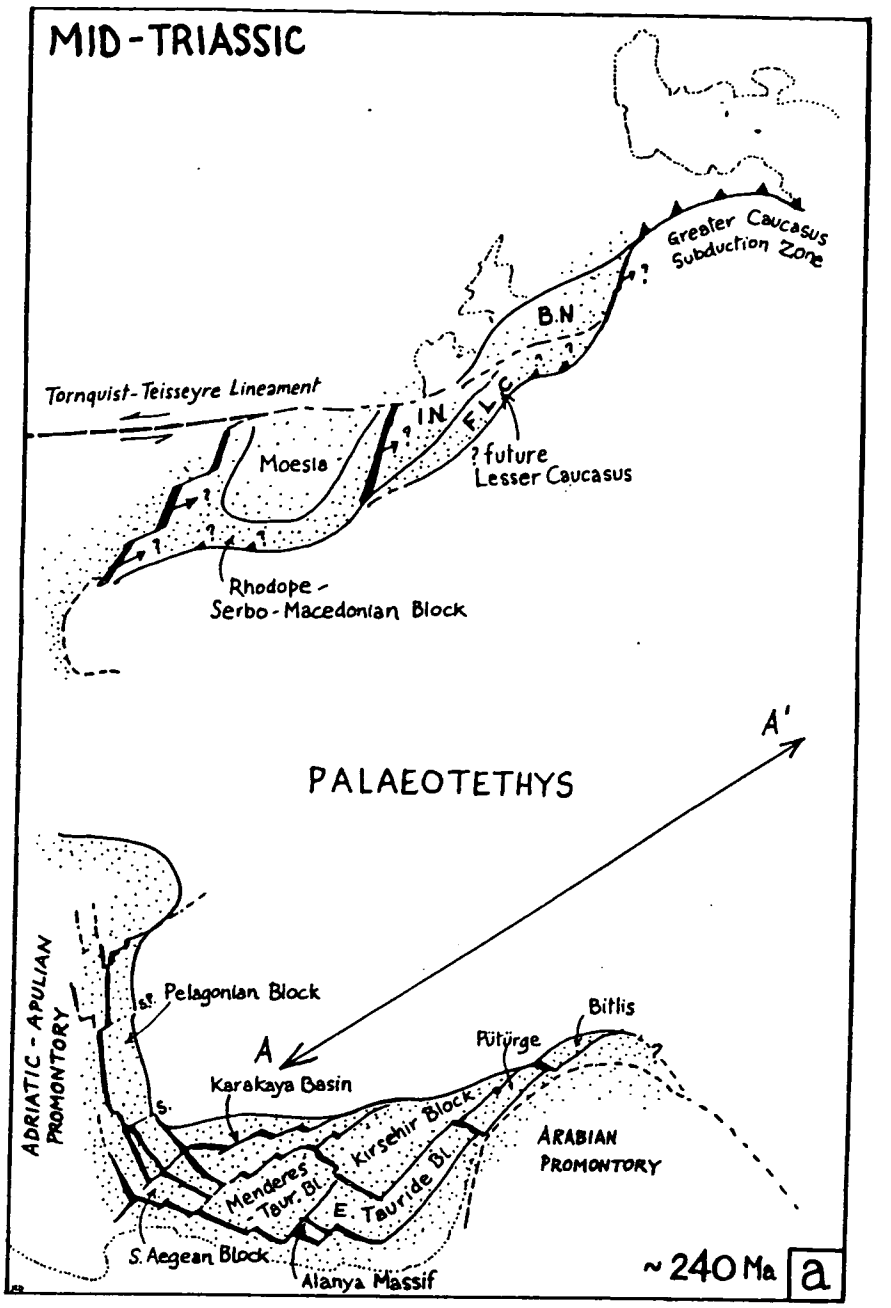

Figure 2.19a-f. The reconstructions of Robertson and Dixon (1984).

General key.

All cartoons show motion relative to a fixed Africa, with Arabia restored to a pre-Red Sea position. Continental blocks are shown idealised and un-stretched. The Adriatic-Apulian promontory has been restored to a more N-S position by being rotated 25° clockwise about a pole near its NW end. Thrust-barb symbols imply a subduction zone complete with calc-alkaline magmatism. All cartoons from Robertson and Dixon (1984).

Figure 2.19a. Mid-Triassic. 240 Ma.

The positions of Eurasia and Gondwana are those for 245 Ma and 173 Ma. The vector AA' gives the approximate magnitude and direction of the displacement of the Eurasian plate to the NE, in the Lower-Mid Triassic interval, and back to the SW in the succeeding Upper Triassic to Mid Jurassic interval, that will account for the separate N. American and African APWP's at this time and also keep the NW African Atlantic margin as a transform zone. Coupling of Palaeotethys to Eurasia during the NE-ward phase generates the Gondwanan margin braided rift network. Palaeotethyan spreading, subduction, and/or strike-slip zones if they existed, will have added components to the relative motion across the north and south margins. The configuration of continental fragments along the northern, 'E Pacific-type' margin is conjectural.

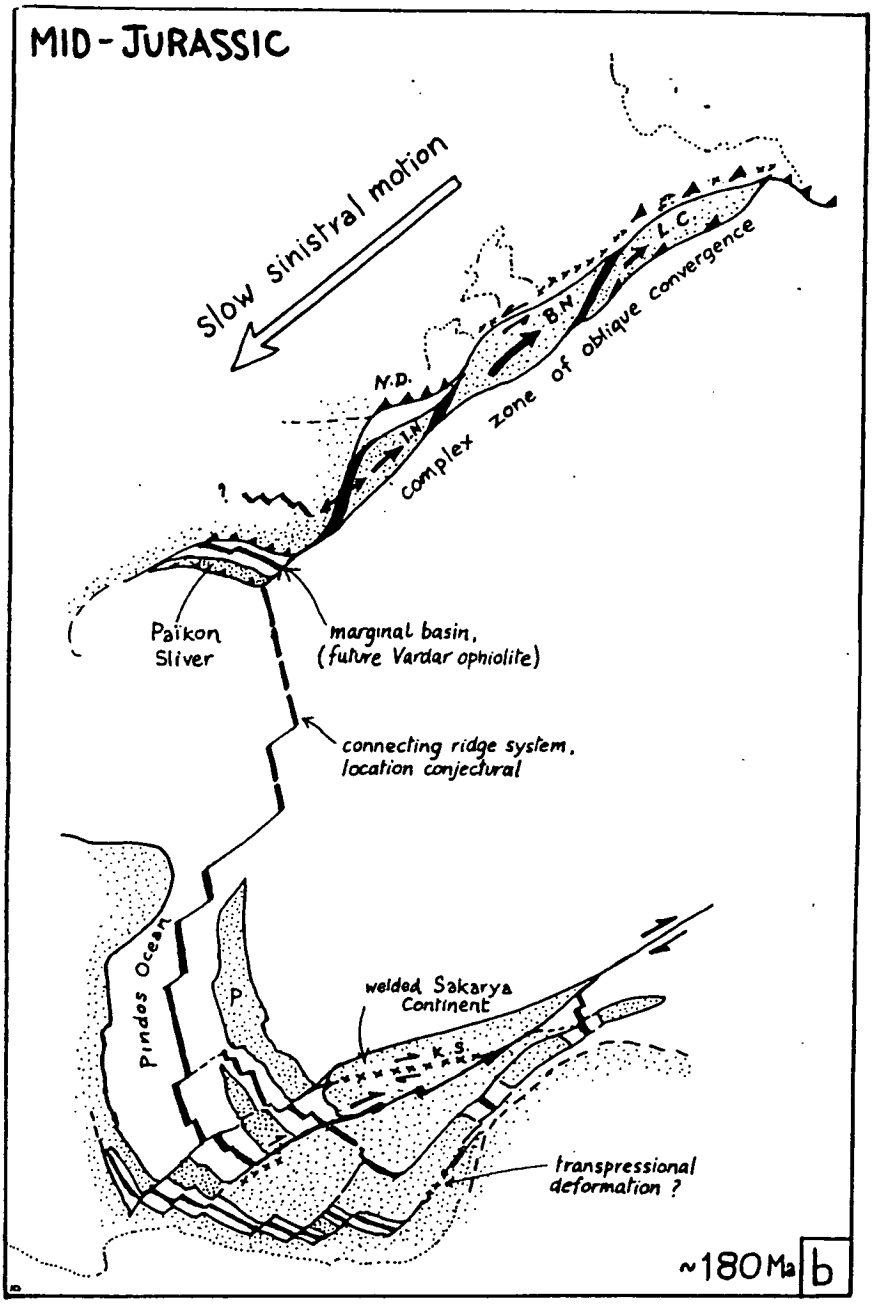

Figure 2.19b. Mid-Jurassic. 180 Ma.

The earlier NE-ward extensional motion established the N-S trending Hellenide-Dinaride rifts as ocean basins (Pindos). S. Turkey remains largely 'unexpanded' in the shadow of the Arabian promontory. Dextral shear propagating intermittently into the Turkish mosaic during the Late Triassic-Early Jurassic causes local transpressional deformation in the Taurides. The most northerly E-W continental sliver of Gondwana is welded by dextral shear along the Karakaya suture in Late Triassic to form the Sakarya continent. At least three major plates now exist, implying a connecting spreading system from the Neotethyan Pindos ocean, through Palaeotethys, to the northern complex margin. The Istanbul Nappe (IN), Bayburt Nappe (BN) and Lesser Caucasus (LC) blocks are emplaced NE-wards by strike-slip processes in the Late Triassic-early Jurassic, to form the Eurasian margin 'collage zone'.

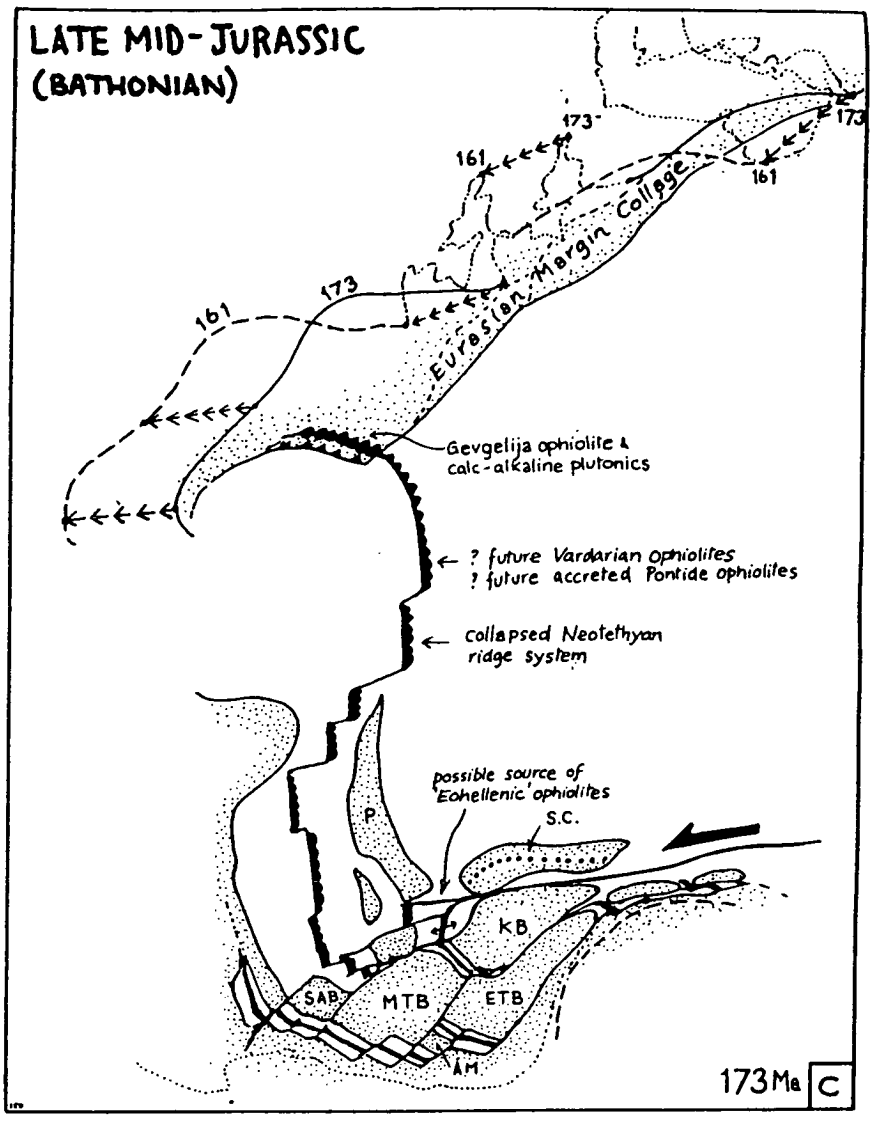

Figure 2.19c. Late Mid-Jurassic (Bathonian). 173 Ma.

Relative to Africa, Eurasia shifts rapidly westwards as the central Atlantic begins to open. The position of the boundary of 'stable' Europe at 161 Ma (Oxfordian) is shown dashed as an indication of the scale and rate of this motion. The Pindos-Budva ocean ridge and linking ridges to the north are driven into compression and collapse at the crest generating emplaceable ophiolites with 173 Ma soles. An E-W transform bounds the Turkish Gondwana mosaic to the south along the future Izmir-Ankara zone. Pull-apart basins along this zone provide future Eohellenic ophiolites for the eastern Pelagonian zone margin. Rifts within the Turkish mosaic and south of the South Aegean block remain undisturbed. The Sakarya continent (SC) is transported passively westwards with the Pelagonian microcontinent.

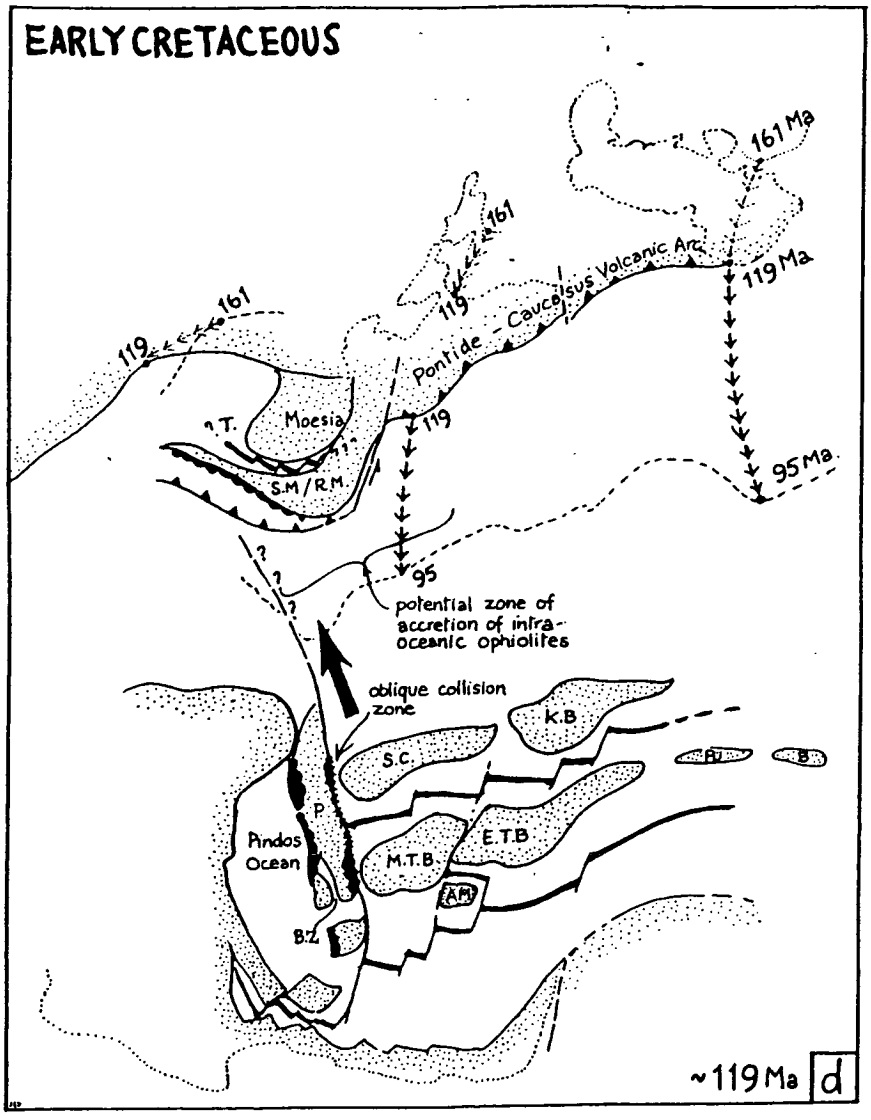

Figure 2.19d. Early Cretaceous (the position of the Pontide margin is shown for 119 Ma - Barremian/Aptian - with the motion in the preceding 42 Ma and succeeding 24 Ma shown by the arrows).

Collapse of N-S spreading ridges and continued westward motion of Palaeotethys with the Pelagonian and Sakarya blocks led to emplacement of ophiolites on the western Pelagonian margin in the latest Jurassic-early Cretaceous. E-W rifts in the Turkish mosaic began actively spreading; the E-W leaky transform south of the Sakarya and Kirsehir blocks also became an active spreading zone. The Sakarya and Menderes-Tauride blocks travelled northwards, deforming the eastward Pelagonian margin and emplacing ophiolitic mélange on to it. The Pindos ocean became an inactive basin but was connected to the main active southern Neotethyan strand and thence to Palaeotethys. In the north a progressive change in Africa-Eurasia motion to convergent, plus the spreading in the south, led to enhanced subduction and associated magmatism spreading from E to W. Intra-oceanic ophiolites and island-arcs created in the Upper Jurassic were accreted along the Eurasian margin.

The accelerated convergence from 108 Ma on results from N. Atlantic opening and causes collapse of the E-W ridges.

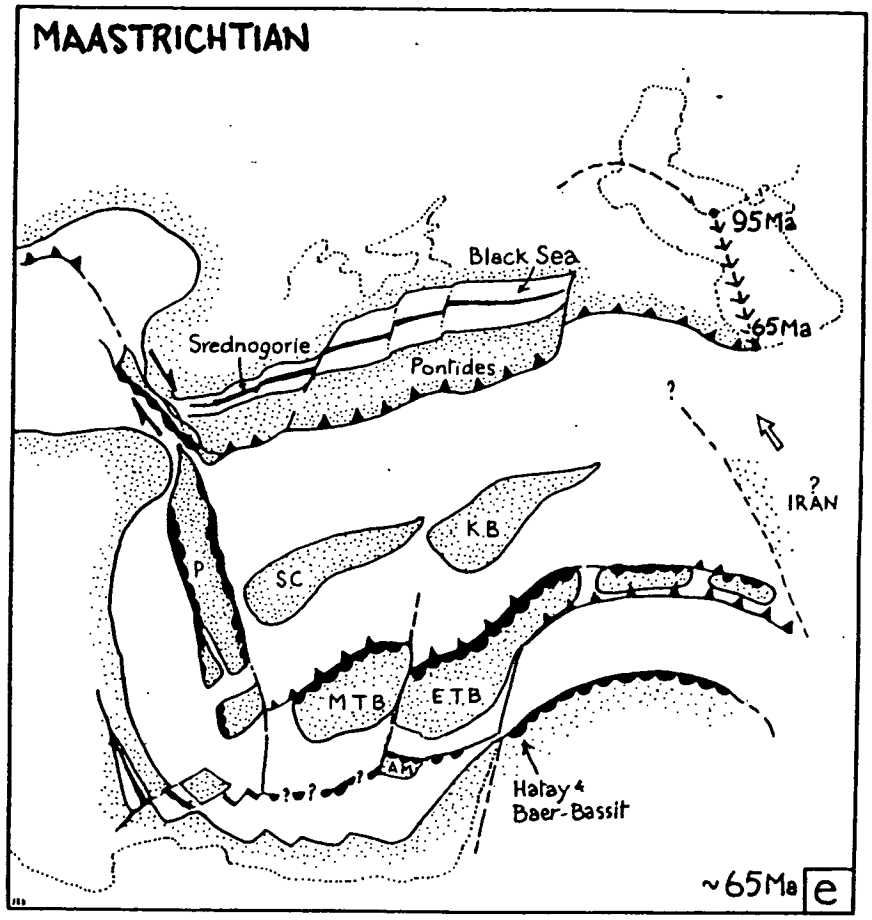

Figure 2.19e. Maastrichtian. 65 Ma.

Collapse of E-W ridges in the period 108-85 Ma, following the opening of the N. Atlantic, led to Maastrichtian emplacement of ophiolites southwards onto adjacent continental margins and the development of northward-dipping subduction zones.The Pindos basin and most of the future Aegean remained unaffected. Earlier ridge collapse in the main Palaeotethyan-Neotethyan basins caused oblique convergence along the Pelagonian margin to cease and to go into reverse, leading to widespread subsidence. In the north, the Srednogorie and Black Sea basins may have been initiated behind the Pontide arc following the drop in net convergence rates. An independently advancing Iran plate kept the Caucasus active and compressed. Impingement of the Eurasian margin began at the northern end of the Apulian promontory.

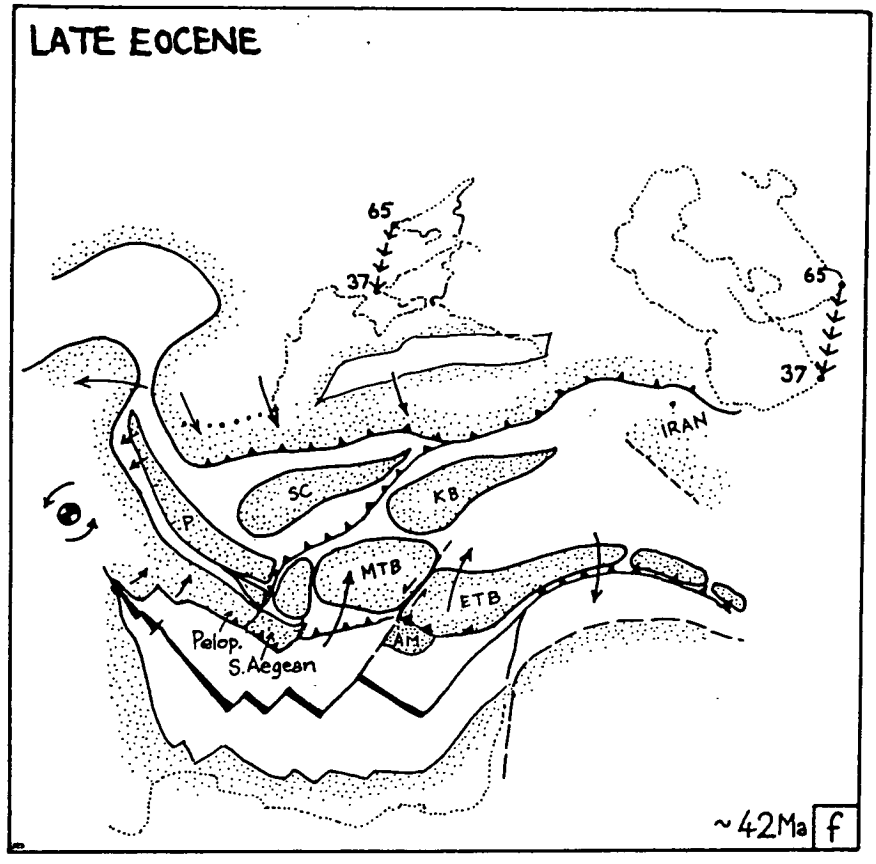

Figure 2.19f. Late Eocene. 42 Ma.

The Pontide 'front' is shown at its 37 Ma (Lower Oligocene) position, with its previous Maastrichtian position indicated. The state of microplate collision to the south is shown for Mid to Late Eocene times. The advance of Eurasia closes the Pindos basin and initiates the rotation of the Adriatic promontory anticlockwise about a pole lying within it. The south-westernmost Neotethyan rifts now spread actively and propagate eastwards swinging the Peloponnesian and S. Aegean blocks northwards to create a complex proto-Hellenic arc. The Neotethyan remnant lying between the S end of the Pelagonian block and the N. Aegean block is destroyed by NW-ward subduction, creating the Aegean blueschist belt. Further E, the Alanya Massif (AM) collides with the E. Tauride block, which rotates clockwise. The Sakarya and Kirsehir blocks are relatively independent and can be positioned to suit local geological or palaeomagnetic constraints. The Srednogorie basin within the Rhodope closes, but the Black Sea remains open.

history of accretion and strike-slip faulting, subduction and marginal basin formation. To the south, the northern edge of Gondwana was undergoing active extension and volcanism to generate a braided intra-continental rift network. These rifts are presumed to be floored by stretched continental crust, and were probably narrower than the modern Gulf of California (Robertson and Dixon, *op. cit.*). Because all the southern continental fragments were located in a major Gondwanan margin embayment between the Adriatic and Arabian promontories (Figure 2.19a), the sense and direction of shear between the African and Eurasian continents favoured the establishment of active spreading on the north-south aligned rifts in the Greek-Yugoslavian area during the Mid Triassic to Mid Jurassic (Figure 2.19b). The Turkish fragments were generally locked together since the Arabian promontory prevented easy eastward escape of these blocks at this stage, although periodic propagation of shear into the braided Turkish rifts may have occurred. The elongate Pelagonian microcontinent rifted away from the Adriatic promontory, with the development of the Pindos ocean basin. The Pindos spreading axis presumably connected with the Eurasian margin plate boundary to the north.

A significant change in the direction of relative motion between Africa and Eurasia occurred when the central Atlantic began to open at 173 Ma (Livermore and Smith, 1984; Section 2.3 above), from southwestwards convergence to a more westerly motion. The rate of relative motion also increased at this time. This sudden burst of sinistral east-west motion had the effect of throwing the north-south spreading centres between the Pelagonian zone and the Eurasian margin into compression. This resulted in progressive asymmetrical spreading and ridge collapse (see Robertson and Dixon, 1984, for details), and the generation of emplaceable ophiolites (Figure 2.19c). These ophiolites were later emplaced during the latest Jurassic to Early Cretaceous. The Turkish microplate mosaic remained tucked into the North African embayment and was effectively decoupled from the Hellenides and Dinarides to the west by a transform zone (Figure 2.19b).

The rate of sinistral motion between Africa and Eurasia declined steadily from the Early to mid-Cretaceous. A subsequent change to north-south convergence occurred with another accelerated period of relative motion around 108 Ma when the North Atlantic began to open (Section 2.3; Figure 2.05). The Arabian margin and the Pelagonian zone then no longer impeded opening of the east-west basins in the Turkish area and the older Triassic rifts were reactivated, thereby converting the attenuated Tauride-Anatolide platform into a series of microplates (Figure 2.19d). Several separate Neotethyan ocean strands developed. An active southern strand connected the inactive

Pindos basin to the Palaeotethys in the east, and was the site of creation of the Troodos, Antalya, Hatay and Baër-Bassit oceanic crust.

In the Upper Cretaceous (Figure 2.19e), the accelerated north-south convergence between Africa and Eurasia caused the spreading axes separating the Turkish blocks from each other and from Arabia, and the active ridge segments in the remaining part of the Palaeotethys to all come under compression. They underwent the process of asymmetrical spreading decline, collapse and generation of ophiolites that had befallen the north-south Hellenic ridges in the Upper Jurassic. Northward-dipping subduction zones were initiated to the south of the Kirsehir block and the Tauride platform, with north-south segments acting as transform margins (e.g Antalya Complex, see Chapter 5). Some of these consuming margins may have begun at the ridge-collapse zones themselves as intra-oceanic arcs, leading by the Maastrichtian to collision of the southern passive margins with the trenches and emplacement of ophiolites southwards onto the continental margins. Oceanic tracts would have remained after ophiolite emplacement in all the ophiolite-generating Neotethyan strands. Also at this time, impingement of the Eurasian margin began at the northern end of the Apulian promontory (Figure 2.19e). This collision thus occurs substantially later than in the model of Dercourt *et al.* (1986), i.e. in the Late Cretaceous rather than the Early Cretaceous.

During the Early Tertiary (Figure 2.19f), a complex pattern of progressive convergence and collision developed as Africa and Eurasia continued their rapid approach. The advance of Eurasia closed the Pindos basin and initiated the anticlockwise rotation of the Adriatic promontory. The south-westernmost Neotethyan rifts began to spread actively and propagate eastwards, swinging the Peloponnesian and South Aegean blocks northwards to create a complex east-west proto-Hellenic arc. From the Late Eocene to the Miocene a series of collisions occurred differing in timing and geometry until the northern Neotethyan and Palaeotethyan strands closed completely, leaving only a remnant southern strand south of Turkey, Crete and the Peloponnesos.

The reconstruction of Robertson and Dixon (1984), therefore, resolves several of the difficulties presented by that of Dercourt *et al.* (1986). In particular, this model is consistent with evidence for the existence of oceanic crust in the Pindos basin until the Eocene. Also, as discussed in Section 2.4.2, this multiple basin model gives a more plausible explanation for the origin of the Turkish and Troodos ophiolites than the model of Dercourt *et al.* (*op. cit.*), which incorporates the single root-zone theory of Ricou *et al.* (1984).

The model of Robertson and Dixon (1984) has therefore been chosen as the working model for the evolution of the eastern Mediterranean region used in the present study. A more recent synthesis of the tectonic development of the southern Neotethys by Robertson *et al.* (in press) has led to refinement of this model. The most notable differences between the reconstructions are that i) Robertson *et al.* (*op. cit.*) accept that an ocean basin existed to the south of Apulia during the Mesozoic. This basin formed along a pre-existing southern Tethyan seaway produced by initial Late Permian rifting; ii) the basins which separated the Turkish blocks in the Late Triassic were more extensive than the narrow rifts proposed by Robertson and Dixon (1984), and were probably small ocean basins; and iii) transform faults played an important role in offsetting the mosaic of Turkish blocks.

I now move on to the more general problem of the mechanisms by which tectonic rotations about vertical axes can occur within deforming zones.

2.5 Tectonic rotations in deforming zones.

In contrast to oceanic crust, in which deformation is generally restricted to narrow linear belts, continental crust deforms in a widespread and diffuse way, typically along zones of distributed deformation which separate stable, non-deforming regions. In the last fifteen years palaeomagnetic observations have revealed large and systematic tectonic rotations with components about vertical axes in many diverse regions of such distributed deformation, e.g. western North America (Beck, 1980; Luyendyk *et al.*, 1980), northern Israel (Ron *et al.*, 1984), and the Mediterranean (Horner and Freeman, 1983; Kissel and Laj, 1988; the present study).

There has been considerable discussion about the nature of the structures which can accommodate such rotations about vertical axes. A brief description of some of the more important models which have been proposed seems appropriate here before going on to discuss the evidence for the rotations identified in the present study in subsequent chapters.

One of the earliest proposals (Beck, 1976) was concerned with distributed strike-slip deformation, and suggested that circular blocks may rotate like ball-bearings between two plates on either side of a deforming zone (Figure 2.20). This model suffers from several problems. Rigid circular blocks have never been identified in regions undergoing distributed deformation. The motion of such blocks would be expected to generate very characteristic fault plane solutions, which again have never been reported (McKenzie and Jackson, 1988). Instead, earthquake fault plane solutions indicate that a combination of strike-slip faulting and extension (or thrusting) is more common in zones

of distributed deformation (McKenzie and Jackson, 1983). However, the rotation mechanism shown in Figure 2.20 conserves area and therefore cannot describe a zone undergoing stretching or shortening. It may still be a valid mechanism for rotations observed in very narrow zones of strike-slip deformation.

An alternative scheme attempts to take up the distributed deformation on systems of strike-slip faults. Freund (1970) was the first to recognise that the fault blocks which occur in strike-slip tectonic domains must progressively rotate on vertical axes as the overall strike-slip motion continues. Two direct consequences of this deformation mechanism are that:

1. slip on each of the faults within a domain must be related to the rotation of the blocks bounded by these faults, and
2. the faults themselves must also rotate because they are the boundaries of the blocks (Ron *et al.*, 1984) (Figure 2.21).

One of the most basic aspects of this rigid fault and block rotation model (Freund, 1970) is that the sense of block rotation must be opposite to the sense of the fault slip, with sinistral slip associated with clockwise rotation, and dextral slip with counterclockwise rotation (Figure 2.21).

A constraint on the amount of fault rotation which can occur through this mechanism is imposed by the mechanical condition of faulting, namely that shear stress on the plane of the fault must exceed the shear resistance to slip along the fault (Nur *et al.*, 1988). *Therefore, lateral stresses control the rotation process.* Theoretical considerations show that the angle to which a fault set can rotate before a new set must appear to accommodate further block rotation ranges from 25° to an absolute maximum of 45°. Importantly, if the fault blocks are rigid, this model predicts a quantitative relationship between fault spacing, slip, and amount and sense of block rotation. Thus in areas where fault spacing and net slip can be determined geologically, palaeomagnetic measurements may be used to test the amount and sense of rotation predicted by the model. Such a test was performed in northern Israel by Ron *et al.* (1984), where good structural data were available and good palaeomagnetic material yielded reliable and accurate declination data (Figure 2.22a). The results revealed several domains of fault sets, some with clockwise rotation and sinistral fault slip, others with counterclockwise rotation and dextral slip, as predicted by the model of Freund (1970). Figure 2.22b shows how closely the rotations calculated from the structural data agree with those determined independently using the palaeomagnetic technique, both in magnitude and sense. The model has also been successful in explaining fault patterns and palaeomagnetic rotations in both the central Mojave

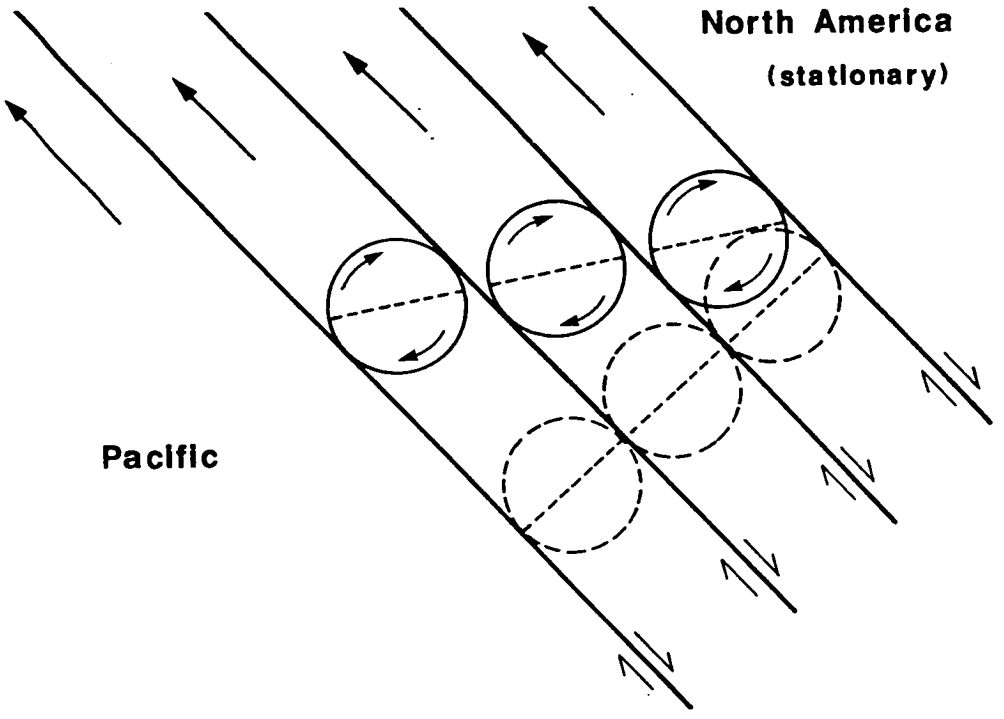

Figure 2.20. Sketch illustrating the clockwise rotation of circular blocks within a distributed right-lateral shear zone. The heavy lines represent individual strike-slip faults (Beck, 1976).

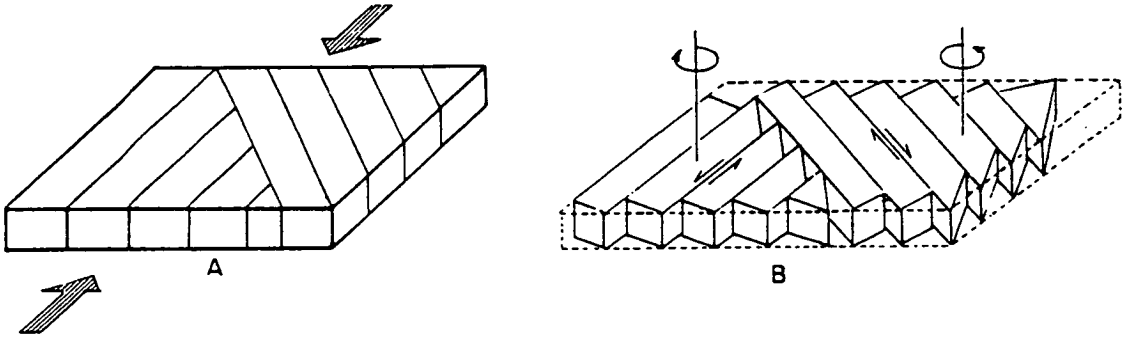

Figure 2.21. Sketch illustrating the simultaneous activity of two systems of strike-slip faults, (a) initial geometry, and (b) after deformation. The blocks bounded by left-lateral faults rotate clockwise, those bounded by right-lateral faults anticlockwise (Ron et al., 1984).

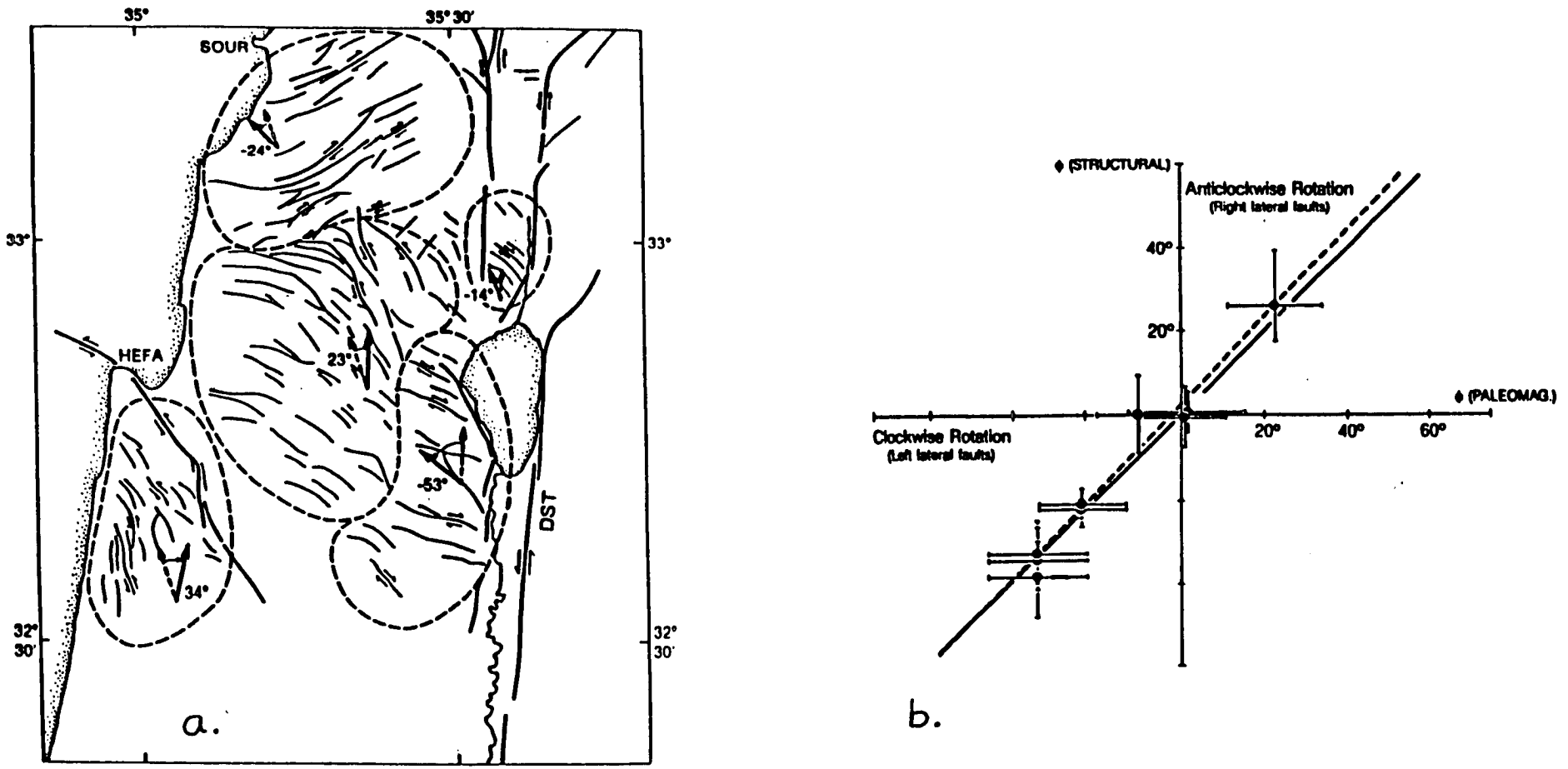

Figure 2.22. a) Fault domains in northern Israel, showing fault sets, directions of slip, and palaeomagnetically determined rotations in these domains. b) Comparison between structurally derived and palaeomagnetically determined rotations in northern Israel. Solid line represents perfect agreement; dashed line is linear best fit to data (from Nur *et al.*, 1988).

Desert domain and the Lake Mead fault system, Nevada (Nur *et al.*, 1988). This suggests that the rigid fault rotation process may be generally applicable to such systems.

However, a geometric problem associated with the scheme shown in Figure 2.21 results from the fact that the deformation conserves surface area, and is therefore a form of plane strain. Shortening (or extension) can only be achieved by pushing (or pulling) material out of (or into) the ends of the deforming zone. The deformation within the zone then becomes complicated (McKenzie and Jackson, 1988). Also, neither the model of Beck (1976) nor that of Ron *et al.* (1984) can explain deformation involving rotations about inclined axes, which must occur in reality since deformation invariably alters the dip of strata.

McKenzie and Jackson (1983, 1986) proposed a scheme which avoids these difficulties. They show that blocks floating on a deforming lithosphere will rotate with the angular velocity of the underlying 'liquid', and suggest that such rotations are the cause of disparate declinations observed in palaeomagnetic studies of deforming zones. *Therefore, fluid vorticity controls the rotation process.* Their model involves movement on inclined faults (Figure 2.23) which cut through the thin brittle layer at the top of the lithosphere. These faults attempt to take up the distributed uniform creep in the underlying ductile lithosphere. McKenzie and Jackson (*op. cit.*) suggest that the fault geometry illustrated in Figure 2.23 is most able to accommodate this deformation, and that movement on the faults can be related to the movements of the plates on either side of the deforming zone through a series of simple equations derived using a fluid dynamical approach.

Since the faults shown in Figure 2.23 are inclined to the vertical, the rotation of the fault blocks relative to the flanking plates must be described by rotations about axes which are not vertical. These rotation axes lie in the vertical plane containing the long axes of the blocks. Fault block rotation in this model will therefore have components about both vertical and horizontal axes, and, unlike the motions in Figures 2.20 and 2.21, can result in a change of the dip of strata.

Although the blocks rotate relative to the zone boundary, they remain parallel to each other and hence translate. McKenzie and Jackson (1983) demonstrate that the horizontal projection of the slip vectors on the faults will always be perpendicular to the zone boundaries. An important consequence of this is that the faults will exhibit a component of sinistral strike-slip motion, even though the motion of the bounding plates involves a component of dextral shear (plus an extension). The total motion on each fault is a combination of this shear component and a dip-slip component, although only the dip-slip component may be discernible from structural studies in the field.

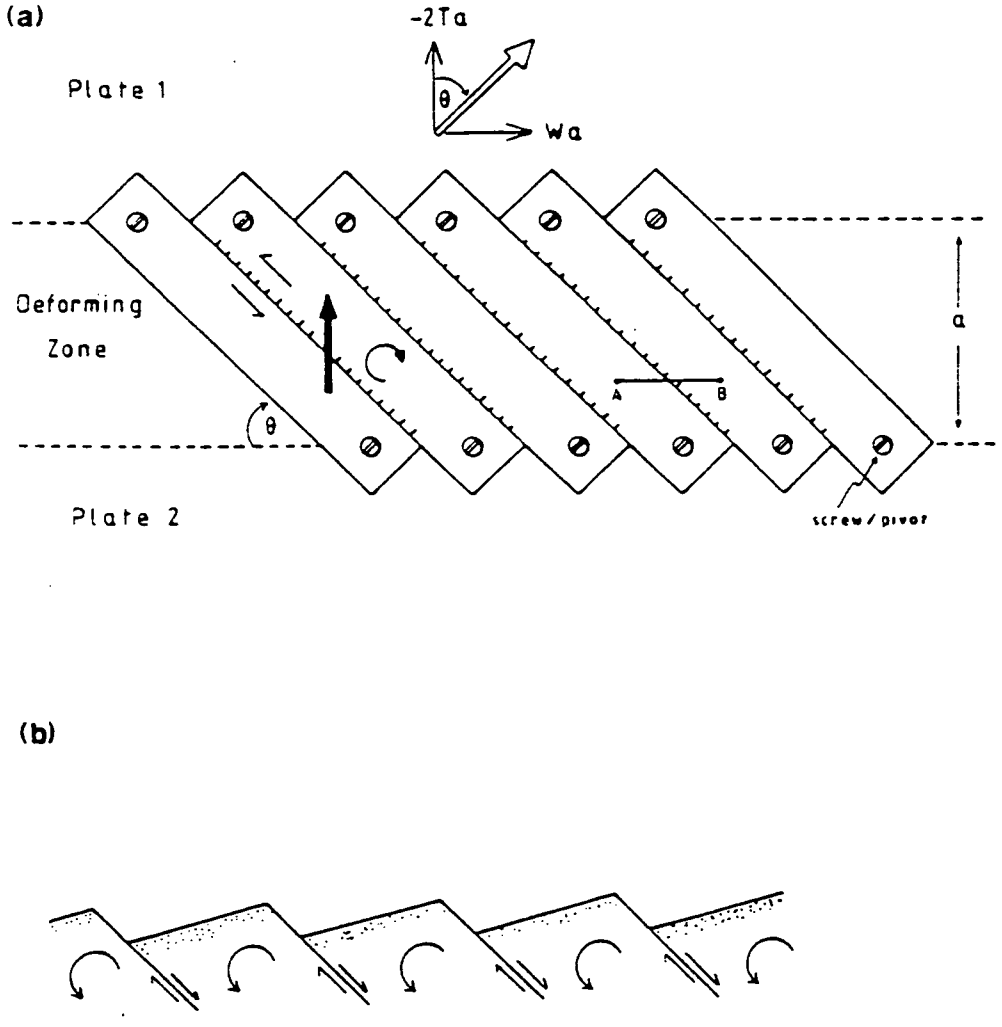

Figure 2.23. The model of distributed deformation by faulting of McKenzie and Jackson (1983, 1986, 1988). Plan view, (a), and section, (b), of blocks bounded by normal faults. The motion of plate 1 with respect to plate 2 is shown by the large white arrow, and requires the zone to take up normal and right-lateral strike-slip movement. The heavy black arrow shows the relative movement between individual blocks, and the movement on the normal faults bounding the blocks therefore has a left-lateral component, and the blocks rotate about both vertical and horizontal axes (from McKenzie and Jackson, 1988).

A second variant of the model of McKenzie and Jackson (1983) involves fault-bounded blocks which are not pinned to the boundaries of the deforming zone, as in Figure 2.23, but contains blocks which are small compared to the width of the zone and are floating in it. McKenzie and Jackson (op. cit.) show that in both systems, the rate of rotation of fault blocks is controlled by the relative movement across the whole zone, but the floating blocks will rotate at half the velocity of the pinned blocks. In both cases, the slip vectors on the faults will be normal to the zone boundaries.

An important feature of this model is that it is two dimensional, in that material is not moved in or out along the strike of the zone. The model is therefore simple in the sense that the relative motion between the plates is taken up locally. There is an intimate relationship between the strike-slip and dip-slip components of motion along the faults bounding the blocks. The strike-slip component indicates the presence of a simple shear component, but it is the dip-slip component which is responsible for distributing this simple shear across the width of the zone (McKenzie and Jackson, 1986).

This model has been applied by McKenzie and Jackson (1983, 1986) to the central Aegean graben system, which forms a shear zone linking the dextrally-slipping North Anatolian Fault and North Aegean Trough with the Hellenic Arc to the west (see Section 2.4.1 above). The major normal faults in the area (Figure 2.24) form an *en échelon* group similar to that shown in Figure 2.23. McKenzie and Jackson (*op. cit.*) calculate that since the slip vector across this zone is at about 45° to the strike of the zone, the inter-block faults should be orientated at either 45° or 27° to the boundary of the zone, depending on whether the blocks are pinned or floating respectively. Both are comparable to the strike of the faults in the zone (Figure 2.24). Fault plane solutions reported by McKenzie and Jackson (1983) for earthquakes on the Gulf of Corinth and Skyros faults indicate slip vectors with a northerly azimuth. This is consistent with the model of Figure 2.23. Furthermore, a small left-lateral component of motion is implied for these earthquakes. This direction is in contrast to the right-lateral slip across the zone as a whole and may result from clockwise rotation of blocks between the faults (Figure 2.23). Assuming a slip rate across a 50 km wide zone of 5 cm/yr, McKenzie and Jackson (1983, 1986) calculated an instantaneous rotation rate for these fault blocks of 40° (pinned block model), or 20° (floating block model) per million years, and suggested that these rotations should by easily detected by palaeomagnetic measurements.

Subsequently, palaeomagnetic sampling within the proposed shear zone has indicated that large clockwise rotations have indeed occurred in this area (Kissel *et al.*, 1986, 1988). These studies have demonstrated that the island of Evvia has experienced

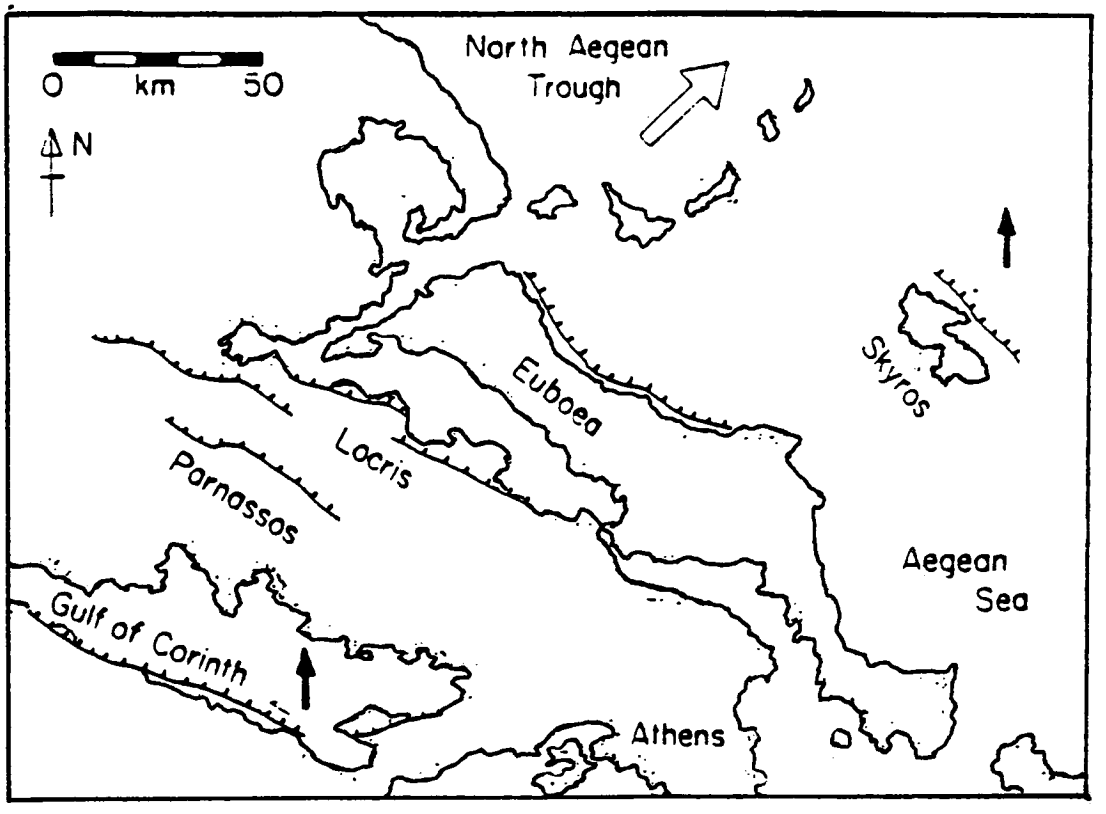

Figure 2.24. The geometry of the main zone of distributed normal faulting in central Greece. Major active normal faults that dip NNE and dominate the topography and bathymetry are shown by heavy lines with ticks on their down-thrown sides. All are known or inferred to have moved in historical or recent earthquakes. Slip vectors for recent earthquakes on the Gulf of Corinth and Skyros faults are shown by black arrows. Both involved small left-lateral components of motion on the normal faults. The motion of the top of the figure relative to the bottom is shown by the large white arrow in the North Aegean Trough. For clarity, many smaller, mostly antithetic, normal faults have been omitted (from McKenzie and Jackson, 1986).

a 48° clockwise rotation during the Plio-Quaternary, while the island of Skyros has only been rotated by 26°. Kissel *et al.* (1988) have calculated that using a more realistic width of 90 km for the shear zone than the 50 km used by McKenzie and Jackson (1983, 1986), their 48° rotation implies a reasonable slip rate of 1.5-2.5 cm/yr over the last 5 Ma. They also note that the difference between the rotations of Evvia and Skyros may be explained in terms of the model of McKenzie and Jackson (1983, 1986, 1988), assuming that Skyros belongs to a block more loosely attached to the borders of the shear zone or entirely floating within it.

It seems then that the model of distributed deformation by faulting proposed by McKenzie and Jackson (*op. cit.*) may be used to account for both the fault plane solutions and the large rotations suggested by the palaeomagnetic data in the central Aegean area. Also, McKenzie and Jackson (1983) refer to several other examples where the pinned and floating block variants of their model may be applicable (e.g. the Las Vegas Shear Zone in the Basin and Range of the western U.S.A.). One drawback of the model, however, is that if the deformation has to be approximated by the movement of perfectly rigid blocks separated by faults which move both normal and parallel to their strike, then a definite angular relationship must exist between the strike of the faults, the trend of the zone and the velocity gradient. For a given trend and velocity only a particular orientation of the faults will fulfil the conditions of the model (McKenzie and Jackson, 1983). This angular relationship can however be satisfied only instantaneously, so that if the fault-bounded blocks rotate through a finite angle, either the trend of the zone or the velocity gradient must change, or else internal deformation of the blocks must occur. McKenzie and Jackson (1983) state that such deformation can be taken into account to produce a more complicated theoretical model, but that this 'obscures the essential simplicity of the motions'.

In conclusion, the simple rotation of fault bounded blocks about vertical axes, as envisaged by Beck (1976), is unlikely to be an important mechanism of continental deformation, except in regions experiencing almost pure strike-slip motion taken up over a narrow zone. Both the rigid fault and block model of Ron *et al.* (1984) and the more involved model of McKenzie and Jackson (1983, 1986, 1988) appear to be applicable to wider zones of continental distributed deformation. The former model may only describe those situations where the amount of crustal extension or shortening is limited, for example in northern Israel (Ron *et al.*, 1984), or where it is accommodated by movement of material along the strike of the zone of deformation, for example in the Zagros collision zone, eastern Turkey (Le Pichon and Angelier, 1979). A serious shortcoming of this model is its failure to explain components of rotation about

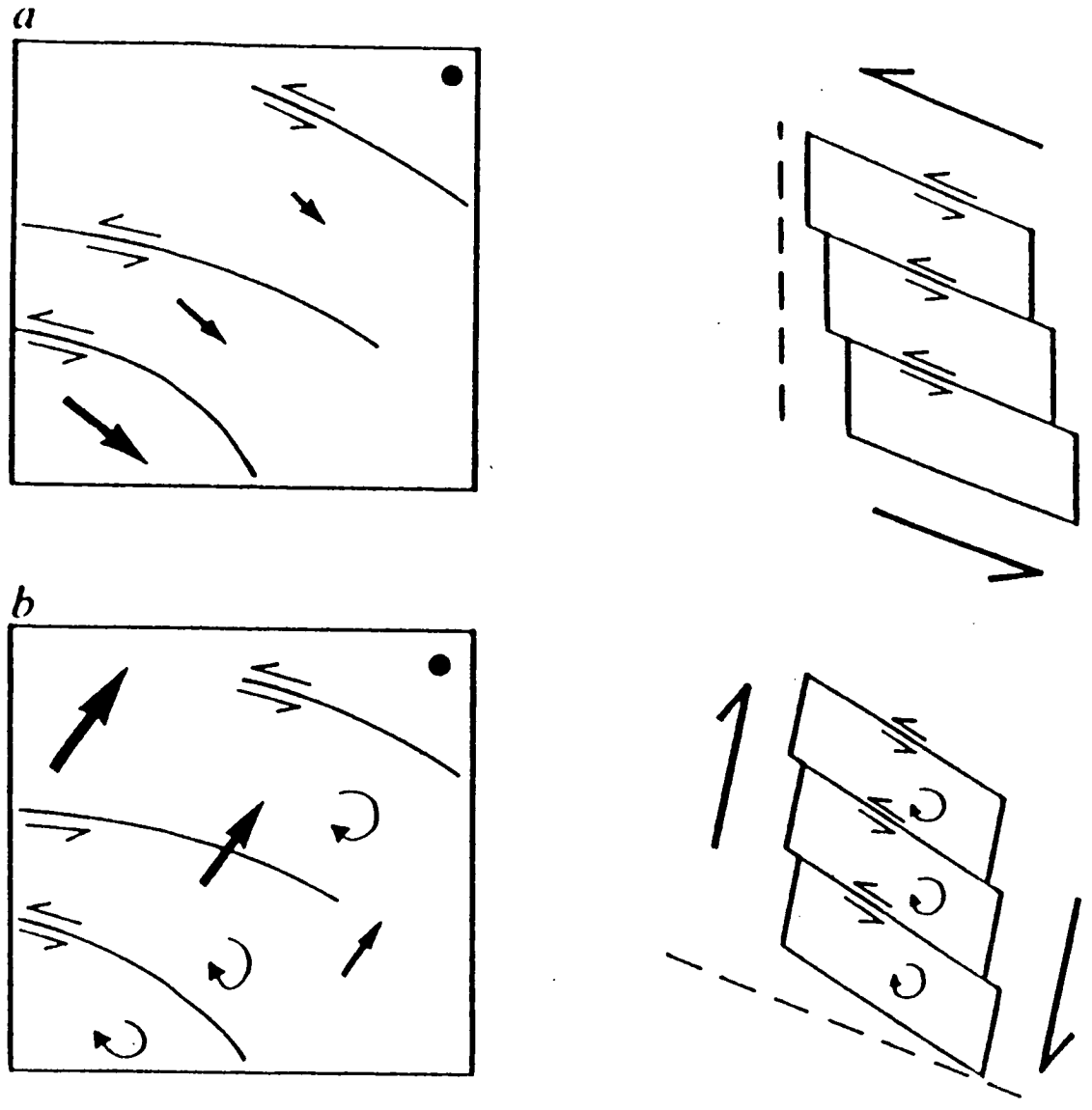

Figure 2.25. Sketches of contrasting interpretations of the faulting in eastern Tibet (from England and Molnar, 1990). For a) and b), the left figure shows locations and senses of slip on idealised faults with the inferred velocity field corresponding to the simple interpretation on the right. The velocities are drawn with respect to a fixed point in the upper right-hand corner. In a), as slip occurs, the faults do not rotate with respect to the surrounding material. Left-lateral slip leads to an east-southeastward translation of material on the south side of each fault relative to material on the north side. The sum of slip rates on the faults would give the rate at which material in the south is translated east-southeastward with respect to material in the north. In b), the eastern boundary of the region defines the fixed reference frame, and the left-lateral slip is a manifestation of north-trending right-lateral shear of the region and clockwise rotation of the blocks between the left-lateral faults. Note that for the east-southeasterly strikes of the faults, the continued rotation and slip on these faults leads to a shortening of the east-west dimension and a lengthening of the north-south dimension.

horizontal axes. McKenzie and Jackson's model is more successful in describing areas where no movement along strike is known to occur, for example in the central Aegean graben system. Common to both models is the realisation that block rotation must be accompanied by a rotation of the faults that define the blocks, and that the sense of shear between individual fault blocks is opposite to the sense of shear along the zone of deformation as a whole. Both also share a common problem, in that space problems occur at the margins of the fault blocks. Internal deformation of these blocks must then occur at the boundaries of the deforming zone. No such deformation is required at the base of rotating blocks in the model of McKenzie and Jackson (*op. cit.*) since faults extend down as far as the underlying ductile layer.

Finally, perhaps the largest shear zone structure yet proposed (McKenzie, 1990) has been described by England and Molnar (1990) in an attempt to explain the presence of large east-west left-lateral strike-slip faults on the eastern margin of the Tibetan collision zone. Previously, these faults were believed to be systematically displacing material eastward (Figure 2.25a), away from the locus of collision between the Indian and Eurasian plates (Molnar and Tapponnier, 1975). This interpretation was based on the assumption, unrecognised at the time, that the faults separating the crustal blocks do not rotate. England and Molnar (1990) now propose that these faults form the margins of blocks that are rotating clockwise at a rate of 1-2° /Ma, and that the whole system forms a huge north-south right-lateral shear zone (Figure 2.25b). This simple system then allows both the eastward motion of Tibet relative to Asia and India and its northward motion relative to southeastern China to be taken up locally on the eastern margin of the Tibetan Plateau (McKenzie, 1990). England and Molnar (1990) conclude that the previous lack of recognition of this north-south shear zone with its inferred clockwise block rotations points to a fundamental weakness of structural geology and seismology in the study of tectonics; both are poorly equipped to detect rotations of faults and fault blocks about vertical axes. A unique property of the palaeomagnetic technique is that it can be used to document such rotations. This is one of the central themes of this thesis.

PART TWO - CYPRUS.

CHAPTER THREE - GEOLOGY AND PALAEOMAGNETISM OF CYPRUS: A REVIEW.

3.1 General.

Recent plate tectonic studies have demonstrated the difficulty of measuring deformation and strain taking place in ocean basins. While the development of side-scan sonar and other remote sensing techniques have made direct observations of the ocean floor possible (Searle, 1983), much important information about processes at present-day constructive margins and transform faults can also be gained by studying ancient ophiolitic terranes. However, field structural studies frequently only tell us about horizontal crustal movements (i.e. thrusting), since rotations about steeply inclined axes are often not apparent in the field. Only the palaeomagnetic technique can be used to obtain information about these rotations.

In this section I will present the results of a palaeomagnetic study of the fossil Southern Troodos (Arakapas) Transform Fault, preserved within the Troodos ophiolite of Cyprus. I will demonstrate that substantial rotations of fault bounded blocks occurred within the transform zone during crustal genesis, thereby confirming the importance of rotational deformation along oceanic fracture zones. The data also allow an important choice to be made between alternate spreading configurations for the Troodos axis system.

This chapter is devoted to a review of the geology of Cyprus and a summary of palaeomagnetic research to date. Cyprus may be divided into several tectonostratigraphic terranes (Figure 3.01). However, discussion here will be limited to the Troodos terrane, with emphasis on the Southern Troodos Transform sub-terrane; no detailed discussion of the Mamonia and Kyrenia terranes will be given. These terranes represent the preserved fragments of a generally south-facing continental margin to the Neotethyan Troodos ocean basin. For a review of the geology of these units, the reader is referred to Robertson (1990) and Clube (1986).

Chapter four presents the results of the palaeomagnetic work carried out in the present study. This research forms the basis of a paper entitled 'Palaeomagnetic evidence for clockwise rotations related to dextral shear along the Southern Troodos Transform Fault' by Morris, Creer and Robertson, to be published in Earth and Planetary Science Letters.

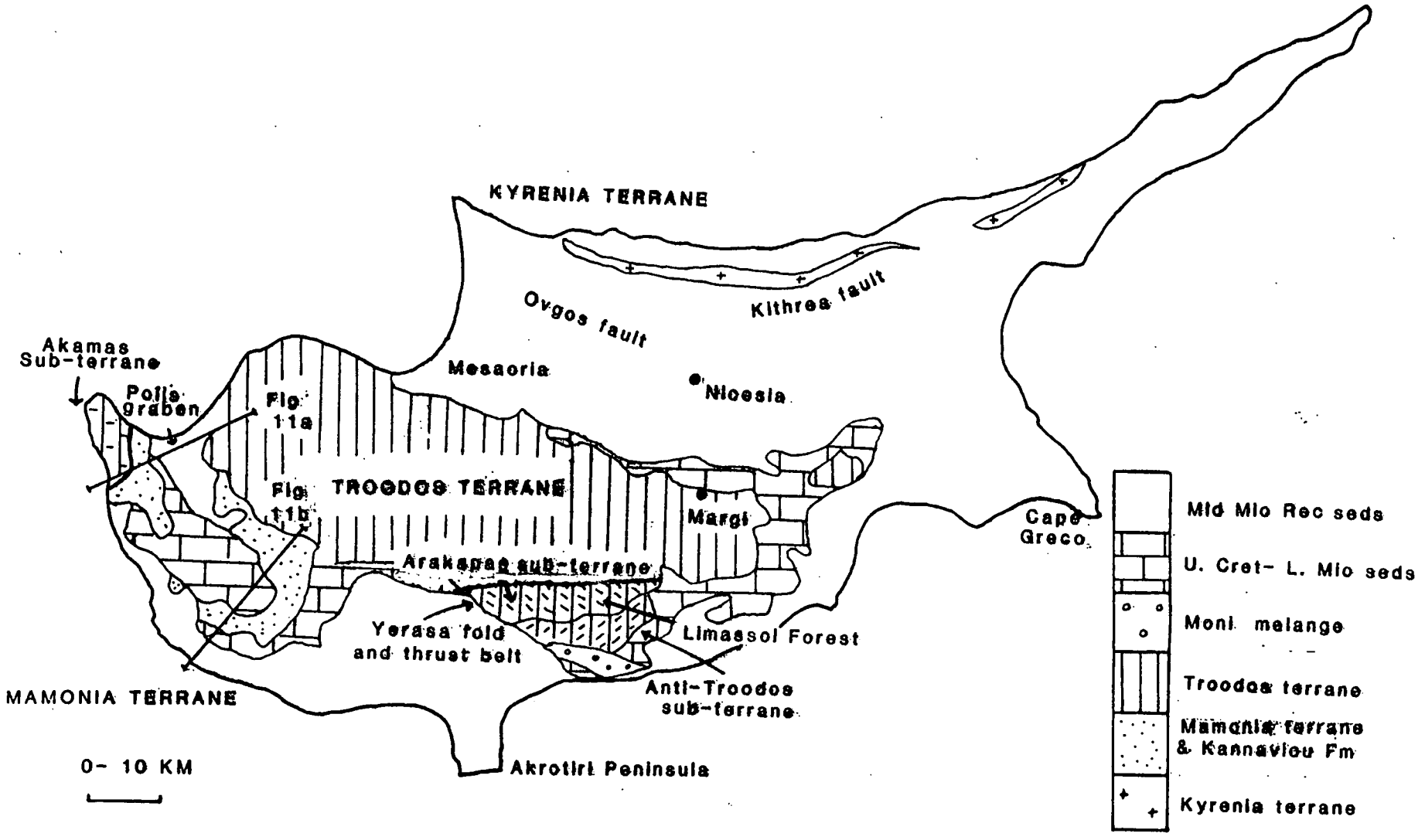

Figure 3.01. Outline geological map of Cyprus showing the Troodos, Mamonia and Kyrenia terranes, the ophiolitic Anti-Troodos and Akamas sub-terranes, and the Arakapas sub-terrane which represents a preserved oceanic transform zone (from Robertson, 1990).

3.2 The Troodos Ophiolite.

It is now well established that the Troodos massif represents an uplifted fragment of Late Cretaceous Neotethyan oceanic crust which formed in a supra-subduction zone setting (Robertson, 1990). Subsequently, the Troodos ophiolite underwent a 90° anticlockwise rotation as a distinct microplate during the Late Cretaceous (Campanian) to Early Eocene (83.0-50.0 Ma) (Clube *et al*, 1985; Clube and Robertson, 1986). A complete ophiolite stratigraphy is preserved within the massif, with tectonised harzburgites, cumulate gabbros, sheeted dykes, mafic extrusives and an *in situ* pelagic sedimentary cover (Figure 3.02; Anonymous, 1972; Moores and Vine, 1971; Gass, 1980). Recent rapid uplift has resulted in a concentric outcrop pattern with the deepest structural levels exposed in the centre (Figure 3.01).

The existence of a well-developed sheeted dyke complex provides unequivocal evidence of formation of the massif at a linear spreading axis (Gass, 1968; Moores and Vine, 1971). In the past it was believed that the Troodos ophiolite was generated in a small Red Sea-type basin above a heterogeneous mantle source (Gass and Smewing, 1973; Robertson and Woodcock, 1980a). However, geochemical studies (Pearce, 1975; Schmincke *et al*, 1983; Robinson *et al*, 1983; McCulloch and Cameron, 1983) now suggest that the ophiolite formed in a spreading setting that lay above a Late Cretaceous subduction zone (i.e. in a supra-subduction zone setting).

In the western and central parts of the massif dykes trend predominantly north to south. However, significant deviations away from this azimuth are observed in the north and in the vicinity of a major fracture zone known as the Arakapas fault belt (Figure 3.01; Simonian and Gass, 1978). Dyke deviations in the north will be discussed below (section 3.5.2), while a detailed discussion of those adjacent to the Arakapas fault belt will be given in chapter four (section 4.1).

The sheeted dyke complex passes up into a thick (1.0 - 1.5 km) extrusive succession, dominated by pillowed and massive lava flow units, with subordinate volcanic breccias and hyaloclastites (Figure 3.02; Schmincke *et al*, 1983). This extrusive series has been subdivided into a lower andesite to dacitic-andesite series (c. 1.0 km thick) that is similar geochemically to evolved island arc tholeiites, and an upper picrite to basaltic andesite series (c. 0.5 km) comparable with modern day extrusives close to island arcs in a forearc setting (Robinson *et al*, 1983). However, whereas there appears to be a distinct compositional break between the 'Upper' and 'Lower' Pillow Lava Series, there is no strong evidence for either structural or metamorphic disconformities (Gass and Smewing, 1973). Together with a general absence of major sedimentary sequences within the lava succession, this evidence supports a cogenesis of the lava suites close to

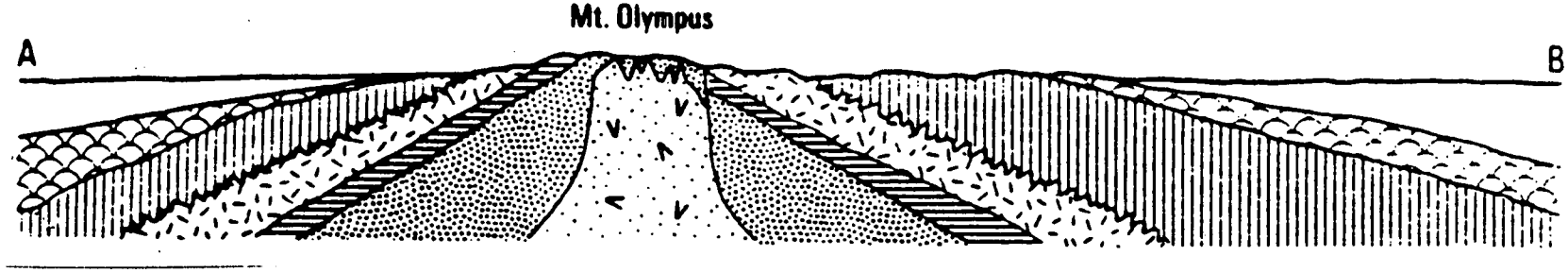

Figure 3.02. Generalised section through the Troodos massif showing the coherent Penrose stratigraphy. Note also the dome-like structure produced by rapid Tertiary uplift centred on Mount Olympos.

a single spreading axis, which probably lay above a subducting oceanic slab (Smewing et al, 1975).

Verosub and Moores (1981) separated the sheeted dyke complex along the northern margin of the Troodos massif into several domains of uniform strike and dip. They suggested that tilting of originally vertical dykes was caused by extensional faulting near a ridge crest. Further work by Varga and Moores (1985) identified three structural grabens defined by listric and planar normal faults and rotated dykes that dip symmetrically toward graben axes (Figure 3.03). Varga and Moores (*op. cit.*) suggested that these grabens represented fossil axial valleys produced by successive eastward jumps of an approximately north-trending (present coordinates), *slow-spreading* ridge crest. Palaeomagnetic research within one of these grabens (the Solea graben) by Allerton and Vine (1987) has identified rotations of up to 78° around subhorizontal axes which are subparallel to the original dyke strikes, consistent with an axial process for the development of the structure. Allerton and Vine's preferred model involves formation of the Solea graben by antithetic faulting on the west flank of an *intermediate- to fast-spreading* axis during a time of reduced magma supply (Figure 3.04). Subsequently, normal dyke intrusion resumed, generating the typical, simple structures observed over much of the complex.

More recent work by Allerton (1988a; *in prep.*) on greenschist and zeolite facies dykes exposed in the Lefkara region has demonstrated that a ridge-jump boundary is preserved within the complex, to the east of the Arakapas fault belt. The boundary separates a zone to the west, where dykes have experienced clockwise rotation about steeply inclined axes, from an area to the east, where dykes have been simply tilted about sub-horizontal axes.

These studies suggest that the Troodos spreading system experienced complex, non-steady state spreading, although the nature of the spreading process is still in debate.

3.3 The Limassol Forest Complex and the Southern Troodos Transform Zone.

The main ophiolitic massif is bounded to the south by the Arakapas fault belt (Figure 3.01). This major east-west valley is an intensely faulted zone of lavas and sheeted dykes. The lineament has a strike that is perpendicular to the general dyke trend observed in the sheeted dyke complex of the main massif, and represents the remnants of a Late Cretaceous oceanic transform fault (Moores and Vine, 1971). The volcanic and sedimentary infill of the fault belt includes basaltic lava breccias, volcaniclastic sandstones, pillow lavas, massive lava flows, and intercalated iron-rich

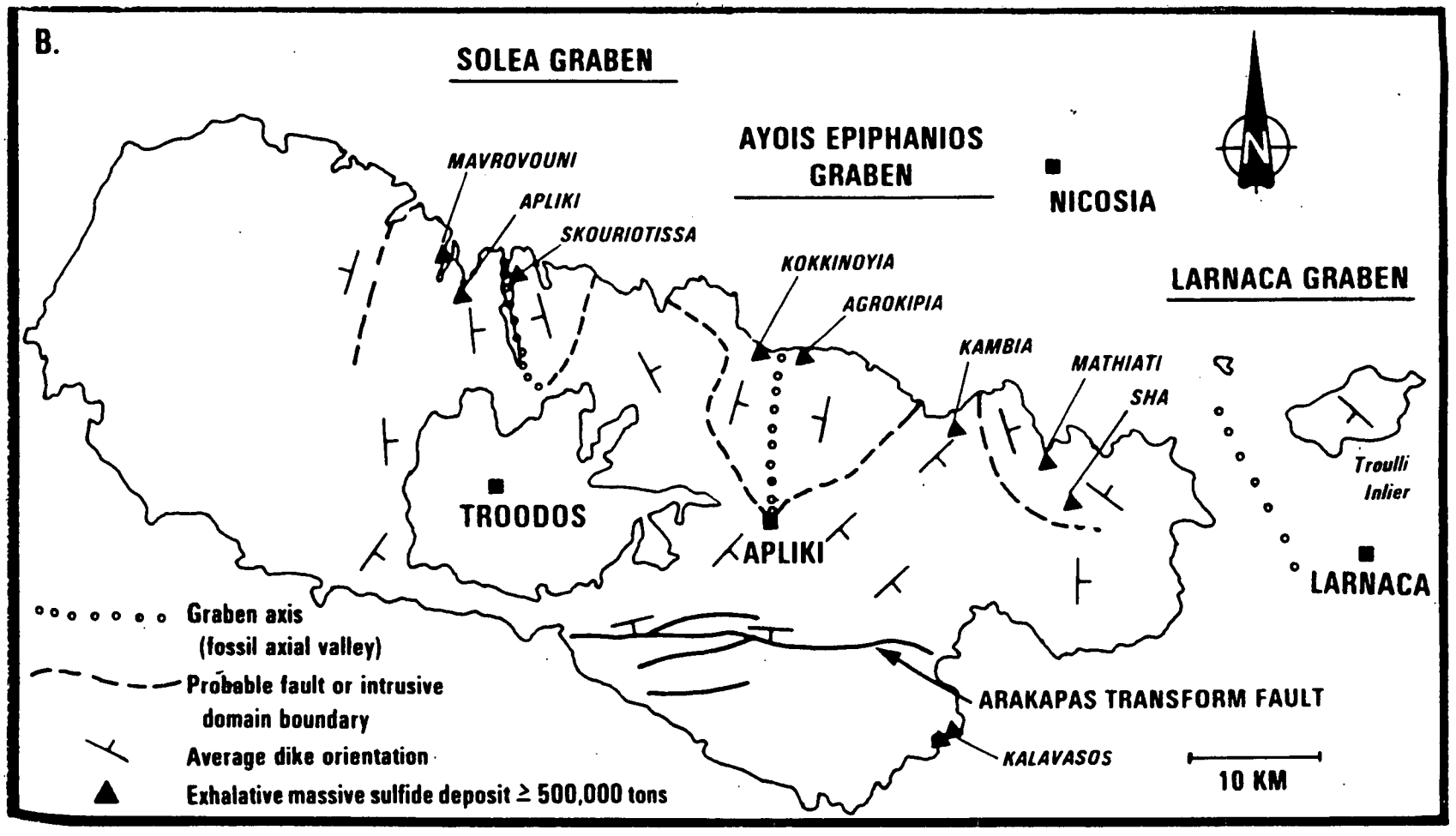

Figure 3.03. Map showing the location of dyke domains identified by Varga and Moores (1985), and the average orientation of dykes within the sheeted dyke complex and extrusive sequence exposed in each domain.

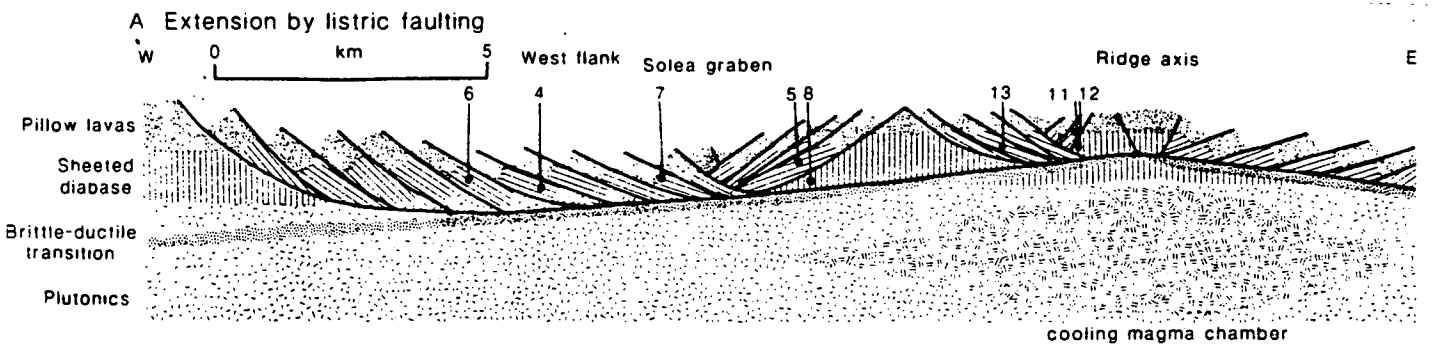

Figure 3.04. Model for the formation of the Solea graben proposed by Allerton and Vine (1987). A: Upper part of normal oceanic crust formed at an intermediate- to fast-spreading ridge anomalously extended by listric-normal faulting (here shown with about 40% extension of the graben area). The brittle-ductile transition is shown at the approximate position of the 600°C geotherm (numbers indicate the relative positions of the sampling sites of Allerton and Vine). The Solea graben is formed by antithetic faulting on the west flank of the spreading system, with rotations of up to 70°-80°; B: Subsequently, normal spreading resumes with extension of upper oceanic crust being accommodated mainly be extrusion and dyke intrusion. Minor faulting, with typical throws of 100m, gives comparatively gentle topography (tilts on fault blocks are up to about 30°). From Allerton and Vine (1987).

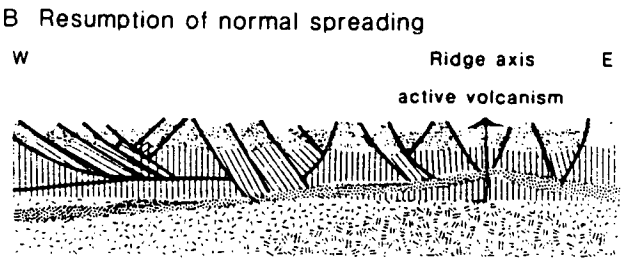

mudstones (Simonian and Gass, 1978). Lava flows, together with volcaniclastic sediments derived from the submarine erosion of fault scarps, accumulated over an irregular horst and graben style basement of strongly faulted sheeted dykes, which were mechanically brecciated by east-west strike-slip faulting (Simonian and Gass, *op. cit.*; Figure 3.05). By contrast, the iron-rich mudstones originated as chemical precipitates from hydrothermal solutions generated by leaching of basalt by seawater (Robertson, 1978). This same hydrothermal activity produced pervasive greenschist facies metamorphism in the underlying sheeted dyke complex.

To the south of the fault belt lies the ophiolitic crust and mantle of the Limassol Forest Complex subterrane (Figure 3.01). Simonian and Gass (1978) suggested that the whole Limassol Forest block formed within the transform domain, with the Arakapas fault belt as its northern boundary. The complex can, however, be subdivided into western and eastern parts, each of which has its own distinct history.

3.3.1 The Western Limassol Forest Complex.

The Western Limassol Forest Complex consists of strongly deformed, predominantly mantle sequences generated within a 'leaky' transform zone (Simonian and Gass, 1978; Murton, 1986; Murton and Gass, 1986). The igneous part of the complex was divided by Murton (1986) into two major parts (Figure 3.06). In the north and the far south a Troodos-type stratigraphy is preserved. This consists of pillowed and massive lavas overlying an east-west trending sheeted dyke complex, which roots into massive gabbro. This forms the 'Axis Crustal Sequence' of Murton (*op. cit.*). Below the gabbros are layered mafic and ultramafic cumulates forming the base of the crustal sequence. The palaeo-Moho is represented by a transition from cumulate gabbros into a tectonised harzburgite/dunite mantle sequence. The whole Axis Crustal Sequence in the Western Limassol Forest Complex is only 3 km thick (Murton, *op. cit.*), in contrast to the 5 km thick Troodos sequence.

The Axis Crustal Sequence is cut by multiple mafic and ultramafic plutons and dykes, termed the 'Transform Active Sequence' by Murton (*op. cit.*). This intrusive suite forms a plutonic core complex within a tectonised harzburgite host, and forms the central area of the Western Limassol Forest Complex. The Transform Active Sequence magmas form a sequence of lavas and breccias in the south-eastern and western parts of the complex.

Murton and Gass (1986) proposed a multiple stage model for the structural evolution of the Western Limassol Forest Complex. The earliest phase of tectonic activity produced east-west trending, ductile, vertical mylonite zones in both gabbro and

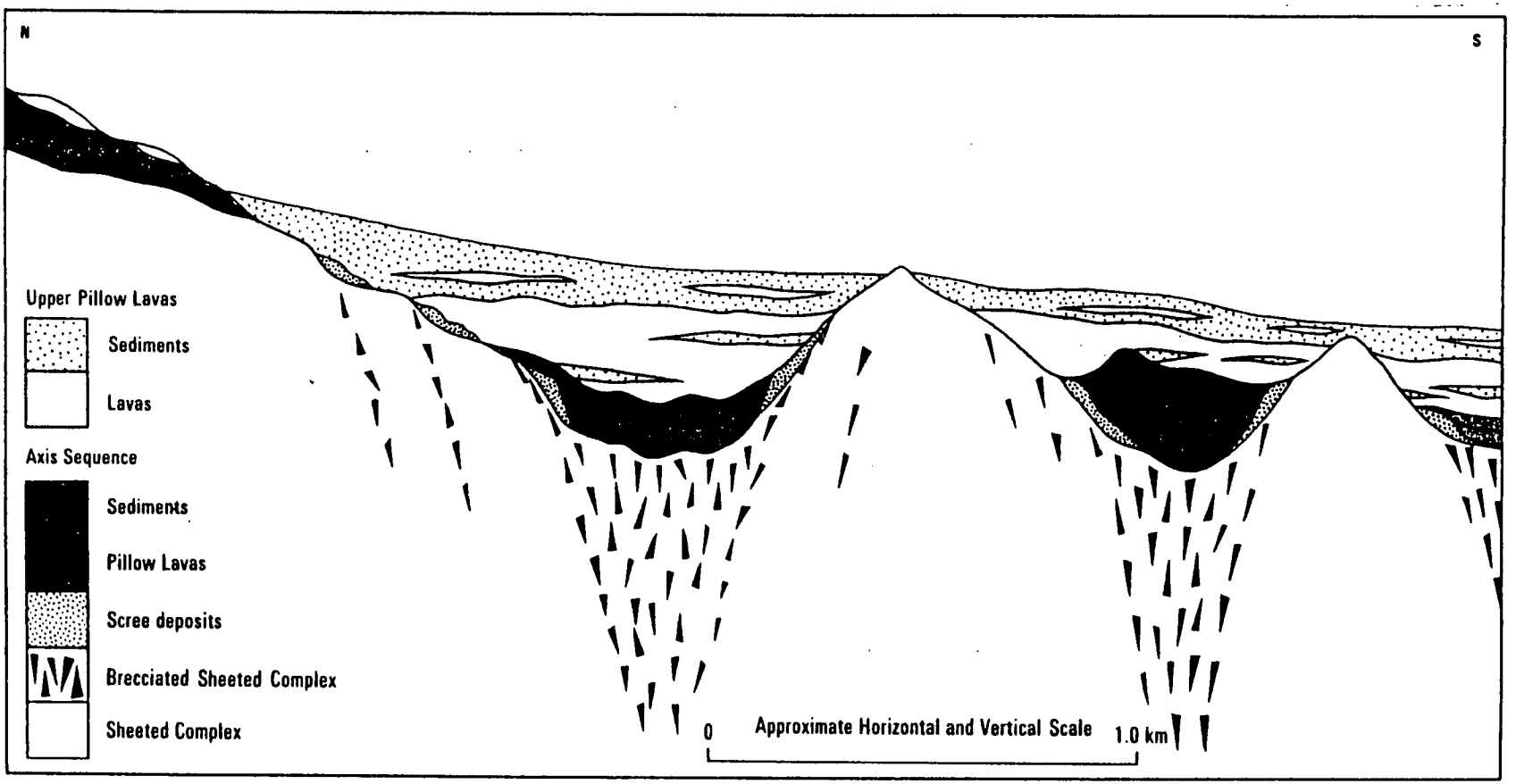

Figure 3.05. Composite schematic north-south section across the Arakapas fault belt according to Simonian and Gass (1978), showing rugged brecciated basement and disposition of the volcanic and sedimentary infill.

harzburgite (Figure 3.07). Fabrics within the mylonites indicate the dominance of east-west transcurrent movement. The next tectonic episode gave rise to a brittle, bifurcating fault system, with an 080°-110°N orientation. Mafic dykes were injected and serpentinite mélanges were formed along these faults. The serpentinite mélange zones are up to 500 m in width and up to 4 km long, and contain blocks of principally harzburgite entrained in a sheared serpentinite matrix. The orientation of the serpentinite mélange zones and the internal fabrics in the mylonites led Murton (1986) to suggest that the transform acted as a sinistral shear zone. The serpentinite shear zones cut across the older mylonite zones, while mafic and picritic dykes are found both crosscutting and being cut by the shear zones. This gives clear evidence of a sea-floor setting for this tectonic activity (Murton, 1986; Murton and Gass, 1986).

An unusual feature of the Western Limassol Forest Complex is that the tectonised harzburgite-dunite mantle suite, which is normally found at the base of the ophiolite succession, occurs at a high structural level. The mantle suite has a history of decreasing temperature and uplift while being intruded by several sets of dykes (Murton and Gass, 1986). It is known that oceanic crust thins toward fracture zones and transform faults (Stroop and Fox, 1981). It seems likely, therefore, that the high structural level of the Limassol Forest mantle suite is due to a combination of this thinning effect and dilatational and isostatic forces acting across the transform domain (Murton and Gass, 1986).

Postmagmatic deformation of the Western Limassol Forest crust includes tensional reactivation of earlier east-west faults, later north-south faulting, and finally north-south compression along low angle, reverse faults (Murton and Gass, 1986). The deformation of Late Cretaceous and Miocene sediments in the Yerasa fold belt to the south of the Limassol Forest indicates that north-south compression continued until the late Miocene (late Tortonian to early Messinian; Eaton, 1986).

In summary, the existence of a tectonised harzburgite, acting as a host to intrusive wehrlites and gabbros, cut by mylonite and serpentinite shear zones, and subsequently cut by dykes, indicates that intrusion of the Western Limassol Forest Complex took place within the active part of a 'leaky' transform domain (Murton and Gass, 1986; Figure 3.07).

3.3.2 The Eastern Limassol Forest Complex.

There is some evidence within the northern part of the Eastern Limassol Forest of mantle tectonites, serpentinite mélange zones and transform sequence magmatism similar to those described by Murton (1986) to the west. This area was deformed in a 5

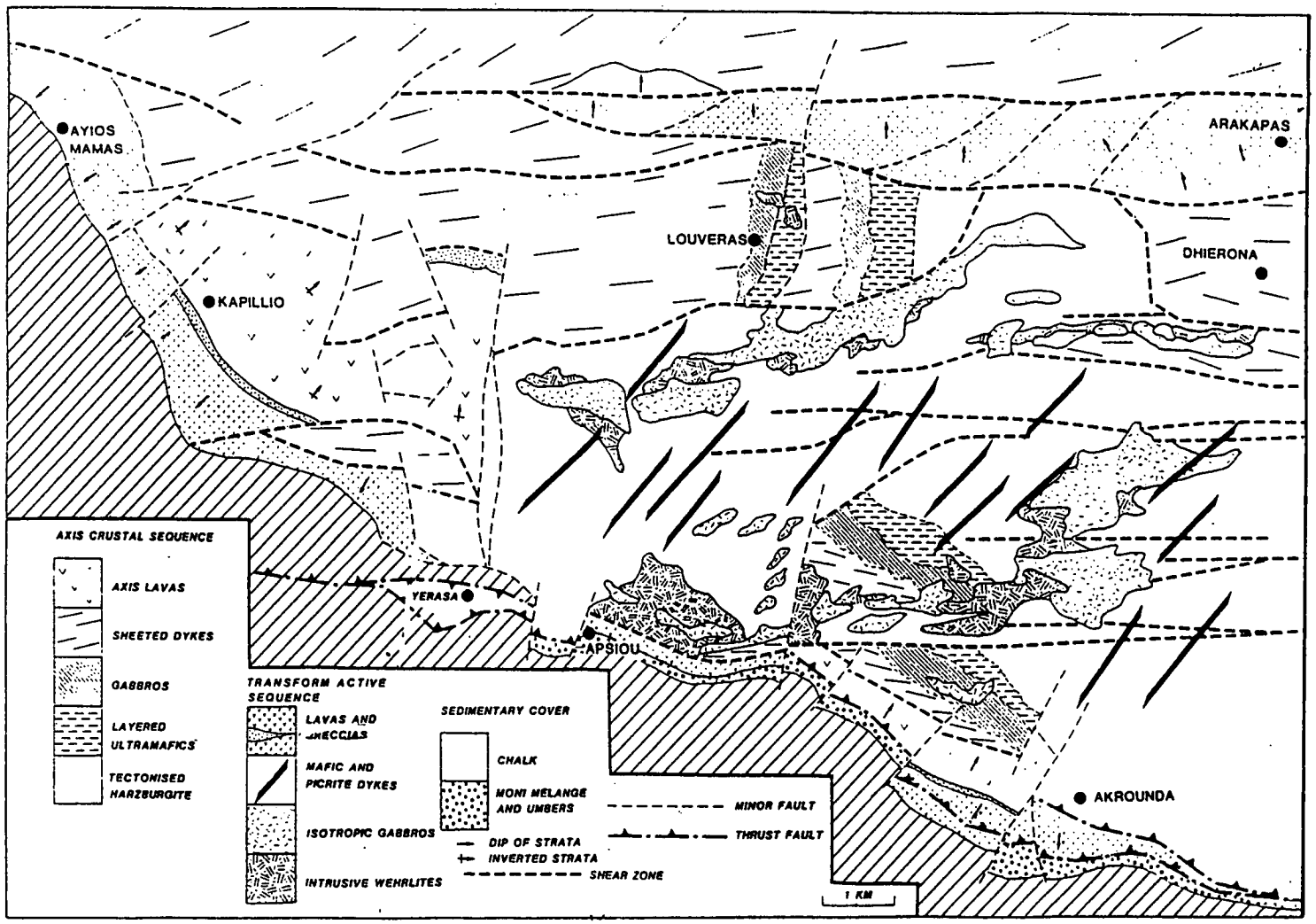

Figure 3.06. Generalised geology of the Western Limassol Forest Complex (from Murton, 1986). The plutonic core complex of this area is dominated by both a tectonised harzburgite of upper mantle origin, and multiple mafic and ultramafic intrusions. Major shear zones (heavy dashed lines) impose a strong E-W tectonic fabric on the area.

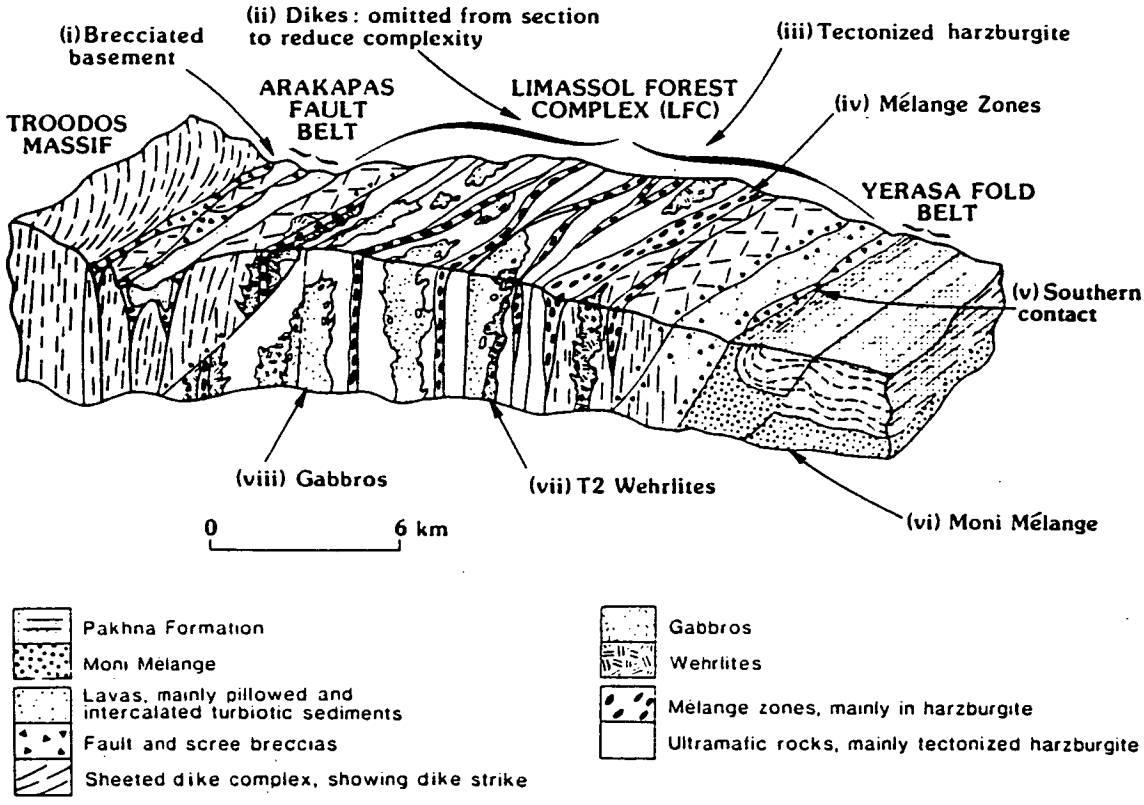

Figure 3.07. North-south block diagram showing the main petrological and structural features of the Western Limassol Forest complex, identified by Murton and Gass (1986).

(i) Arakapas fault belt - intensely brecciated basement of sheeted dykes overlain by scree deposits and mafic lavas intercalated with clastic basaltic sediments. (ii) Dykes - Three main trends, from oldest to youngest: 100o-110o near-vertical greenschist facies; 030o-040o subvertical basaltic dykes, commonest trend in the Western Limassol Forest Complex, associated with gabbro plutons; and 000o-040o sinuous brownstone facies dolerites. (iii) Host lithologies - tectonised harzburgite, and mafic and ultramafic cumulates of a high-level axis magma chamber(s). (iv) Serpentinite shear zones - E-W elongated, phacoidal blocks of tectonised harzburgite, dunite and gabbro in completely serpentinised flaky matrix of comminuted harzburgite. (v) Southern contact - inverted unconformable contact with either umbers of the Perapedhi Fmn. or Moni mélange resting on basaltic scree breccias and/or pillow lavas of the Western Limassol Forest complex. (vi) Moni mélange - large allochthonous blocks of quartzose sandstone, Triassic limestone, jasper, chert, and basic volcanics in Upper Cretaceous bentonitic clay matrix. (vii) Wehrlites - oldest phase of intrusive plutonism. (viii) Gabbros - petrologically similar to high-level gabbros of Troodos and other ophiolites.

km wide transform zone. However, to the south, across most of the Eastern Limassol Forest Complex, blocks of a brittely disrupted ophiolite sequence are exposed (MacLeod, 1990), in contrast to the predominantly mantle lithologies of the Western Limassol Forest Complex. Detailed mapping of the area by MacLeod (1988; 1990) has shown that the southern margin of the transform domain is preserved within the Eastern Limassol Forest Complex, and that the exposed ophiolitic sequence represents a small fragment of crust generated at an 'Anti-Troodos' spreading axis.

Approximately 70 km^2 of the Anti-Troodos plate is preserved to the south of the transform domain (MacLeod, 1990). Pillow lavas are exposed across much of this area (Figure 3.08). These include some highly primitive boninitic lavas, which are normally considered to have been generated only close to the transform (MacLeod, 1990; Cameron, 1985). However, MacLeod (*op. cit.*) also reports dacitic glasses found in the Anti-Troodos area which are similar to those from the main Troodos massif, and which are rare amongst the transform related lavas. Thus, there appears to be a geochemical as well as a structural similarity between the Anti-Troodos sequences and the non transform-tectonised Troodos crust (MacLeod, 1990).

The crustal sequence of the Eastern Limassol Forest Complex has been broken up by locally extreme brittle faulting into semi-coherent blocks (MacLeod, *op. cit.*). The absence of angular unconformities in the uppermost lava units, together with the lack of volcanic features cutting or utilising the brittle structures, led MacLeod (*op. cit.*) to suggest that this deformation was entirely post-volcanic in origin. Maastrichtian - Miocene chalks of the Lefkara Group (see section 3.4.2) which overlie the ophiolite to the east of the Limassol Forest are not affected by the faulting, confirming that the deformation took place in the Upper Cretaceous. The hydrothermal umbers in this area were partly mapped by Robertson (1975). Detailed studies of stratigraphic relationships within the umbers and radiolarites overlying the lava sequences reveal evidence of progressive tilting during deposition (MacLeod, *op. cit.*). This further constrains the initiation of regional extension to the period of umber deposition (i.e. the Turonian; 90.4-88.5 Ma), and indicates that deformation occurred soon after the cessation of volcanic activity. This extensional disaggregation of the crustal sequence was accommodated above a major sub-horizontal shear zone. This serpentinite-lubricated basal detachment horizon is known as the 'Akapnou Forest Décollement' (MacLeod, *op. cit.*).

According to MacLeod (*op. cit.*), extension in the northern part of the Eastern Limassol Forest Complex caused the reactivation of transform structures, and resulted in a rotation of fault blocks about sub-horizontal axes. MacLeod (*op. cit.*) has suggested that subsequent post-décollement faulting, active in the Campanian-Maastrichtian

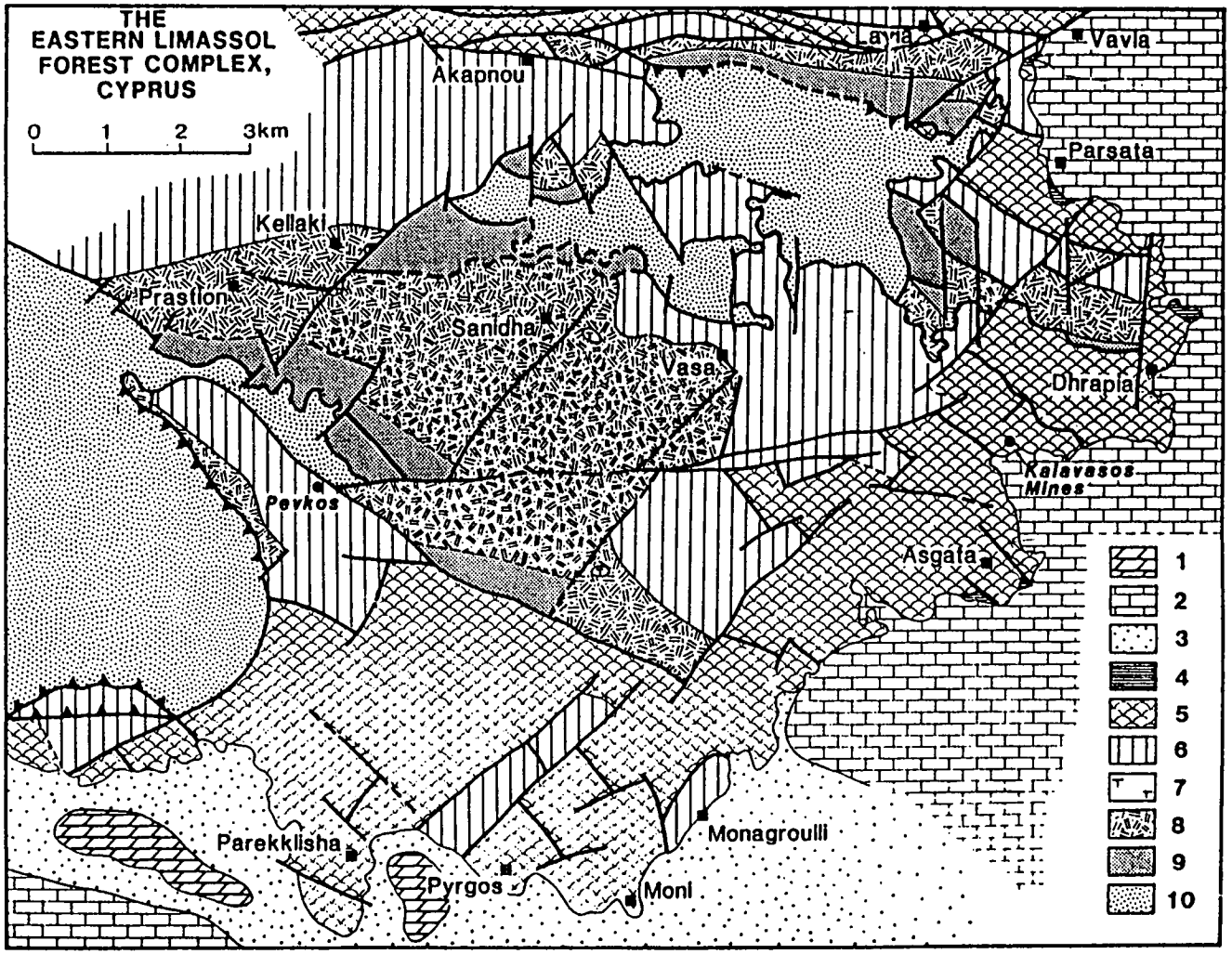

Figure 3.08. Geological map of the Eastern Limassol Forest Complex (from MacLeod, 1990).

Sediments: (1) Miocene-Recent; (2) Maastrichtian-Miocene; (3) Campanian-Maastrichtian Moni mélange; (4) Turonian-Maastrichtian Perapedhi Formation.

Igneous rocks: (5) pillow lavas; (6) sheeted dyke complex; (7) plagiogranite bodies; (8) gabbros; (9) ultramafic rocks; (10) tectonised harzburgites and dunites.

interval (83.0-65.0 Ma), was triggered by initial palaeorotation of the Troodos microplate, and gave rise to dextral reactivation of previously extensional structures and an associated clockwise rotation of fault-bounded blocks. This model will be discussed in detail in the next chapter (section 4.4).

3.3.3 The Southern Troodos Transform Fault.

It is now accepted that the Arakapas fault belt and a large part of the Limassol Forest Complex were formed within a 'leaky', transtensional oceanic fracture zone which separated the Late Cretaceous Neotethyan crust of the Troodos and 'Anti-Troodos' plates. The spreading system may have been unstable, and several ridge-jumps may be preserved within the Troodos ophiolite (Varga and Moores, 1985; Allerton, 1988a,b). The transform domain was locally disrupted during the initial stages of the Late Cretaceous-Eocene palaeorotation of the Troodos microplate (section 3.5.2). No concensus of opinion exists at present regarding the sense of shear along the transform during its active phase.

The term 'Southern Troodos Transform Fault' has been proposed (MacLeod, 1988) to describe the combination of the Arakapas fault belt and that part of the Limassol Forest Complex to the south which was formed within the transform zone (i.e. excluding the Anti-Troodos crust of MacLeod (1988; 1990)). In accordance with this, the terms 'Arakapas fault belt' and 'Limassol Forest Complex' are used in the present study only in a geographical context.

3.4 The pre-Miocene sedimentary cover.

At specific localities around the periphery of the Troodos massif and Limassol Forest block, the stratigraphically highest pillow lavas are overlain by umbers, metal enriched clays, and radiolarites of the Perapedhi Formation of Turonian-Campanian age (90.4-74.0 Ma). These pass up into variable volcanogenic facies and then into Maastrichtian to mid-Miocene (74.0-10.4 Ma) successions of pelagic chalks with subordinate cherts of the Lefkara Formation (Figure 3.02; Robertson and Hudson, 1974).

3.4.1 The Perapedhi and Kannaviou Formations.

The first deposits to accumulate above the topographically irregular pillow lavas of both the Troodos and 'Anti-Troodos' crust were the ferromanganiferous umbers of the

Perapedhi Formation. Umbers are chemical precipitates which are derived from hot Fe, Mn and trace metal enriched hydrothermal fluids circulating at spreading axes.

In the field, umbers are pale, brown, or almost black, low density, fine grained mudstones which contain almost no calcium carbonate. Robertson (1975) divided the umber outcrops of Cyprus into five types of deposit related to a variety of depositional settings:

1. Umbers encountered in small hollows on the Upper Pillow Lava surface. These are the most common type of deposit, and are almost always finely laminated and undisturbed. They vary in thickness from 0.5 m to 7 m, with an average thickness of 2.5 m.
2. Umbers intercalated between the uppermost lava flows, demonstrating that umber formation took place during, and immediately after, the final phase of Upper Pillow Lava volcanism.
3. Substantial umber formations related to large fault-controlled depressions within the Upper Pillow Lavas.
4. Umbers associated with lava breccias.
5. Umbers spatially related with massive sulphide ores.

Of specific interest in the present study are those umbers which are found in association with lava breccias, as these have been palaeomagnetically sampled at several sites (along with some exposures of small hollow umbers; see Chapter 4). They are restricted in occurrence to the southern margin of the Troodos massif, but form some of the thickest umber deposits in Cyprus. The lava breccias crop out extensively between Vavla and Ayios Mamas, parallel to the Arakapas fault belt, and at Dhrapia and Asgata along the eastern edge of the Limassol Forest block (Figure 3.08). The breccias are interpreted as due to slumping and disintegration of pillow lavas down slopes during the culminating phases of Upper Pillow Lava volcanism, the time when umbers first began to accummulate (Boyle and Robertson, 1984). Post-depositional slumping is common within the umbers. At Asgata, lava breccias interdigitate with chaotically slump-folded brown umbers. This may be explained in terms of the collapse of unstable lava debris into unconsolidated or partly consolidated umber pools (MacLeod, 1990). At other localities, progressive unconformities have been observed between the lower and upper parts of the umber sequences (e.g. at Dhrapia, MacLeod, 1990; and at Mavridhia, in the Kalavasos Mines, Robertson, 1975). These observations provide evidence of tectonic instability during the period of umber deposition, probably related to the onset of the regional extension documented by MacLeod (1988; 1990).

The topmost umbers become increasingly clay-rich and change from dark brown to grey in colour (Robertson, 1975). They are succeeded by pink, carbonate-free radiolarite and radiolarian mudstone (Figure 3.02).

On the northern, eastern and southern flanks of the Troodos massif, the radiolarian sediments pass into discontinuous deposits of bentonitic (illite-montmorollonitic) clays which fill the upper parts of hollows floored by umbers and radiolarian bearing rocks (Boyle, 1984; Clube, 1986). In the Paphos District (south-west Cyprus), these clays are interbedded with a varied succession of volcaniclastic sandstones and siltstones. This sequence, the Kannaviou Formation, reaches a total thickness in excess of 750 m (Robertson, 1977a). The sandstones include 'arc', terrigenous and ophiolitic components. They are interpreted as a pyroclastic sediment wedge, of Campanian-mid Maastrichtian age (83.0-75.0 Ma), mostly derived from mafic-acidic calc-alkaline volcanic centres to the west and northwest of the present outcrop of the Troodos ophiolite (Clube and Robertson, 1986; Robertson, 1990).

3.4.2 The Lefkara Group.

Conformably overlying the Perapedhi and Kannaviou Formations are the pelagic sediments of the Lefkara Group (Figure 3.02), which can be divided into Lower, Middle and Upper units on the basis of lithological and micropalaeontological criteria (Mantis, 1970).

The Lower Lefkara marls and chalks are of Maastrichtian age (74.0-65.0 Ma), and rarely exceed 25 m in total thickness. They discontinuously outcrop around the Troodos massif, either above Campanian aged sediments that have been ponded in topographic hollows, or directly above the extrusives in broad shallow troughs in the pillow lava surface (Robertson and Hudson, 1974).

On the northern margin of the ophiolite complex, the Upper Palaeocene-Lower Eocene (60.5-50.0 Ma) Middle Lefkara forms a highly condensed sequence of chalks with bedded and nodular cherts, which conformably overlies the Lower Lefkara unit. To the south of the ophiolite the sequence is represented by a thick (>300 m), deep water succession containing both pelagic and turbiditic components (Robertson, 1976).

The stratigraphically lower parts of the Upper Lefkara succession consist of massive, normally chert-free chalks of Middle to Late Eocene age (50.0-35.4 Ma). Younger chalks of Oligocene to Early Miocene age (35.4-16.3 Ma) are less well consolidated and lithologically more variable. Locally these chalks toward the top of the Upper Lefkara are chaotically slumped, and it appears that at this time the Troodos massif underwent differential uplift resulting in folding, slumping and erosion of the overlying sediments (Robertson, 1977b).

3.5 Palaeomagnetic studies.

Cyprus forms an excellent natural laboratory for the study of the physical properties of oceanic crust and of the processes involved in its generation (Vine and Moores, 1972; Varga and Moores, 1985; Smith and Vine, 1990). Palaeomagnetic research within the Troodos ophiolite has provided key information on the tectonic evolution of the Eastern Mediterranean region, particularly with regard to rotational deformation occurring within the Neotethyan ocean basin (Clube and Robertson, 1986; Allerton and Vine, 1987; Robertson, 1990).

3.5.1 Early work.

Following the development in the mid to late 1960's of a working sea-floor spreading hypothesis (Vine, 1966), and the recognition that the Troodos ophiolite represented a fragment of oceanic crust preserved on land (Gass, 1968), the primary objective of early palaeomagnetic investigations on Cyprus was to determine the distribution and extent of interfingering of normally and reversely magnetised material within the Troodos complex. It was hoped that such a study would simultaneously confirm the Vine-Matthews hypothesis and provide compelling evidence that the massif was indeed formed by the process of sea-floor spreading.

Thus, with this intention in mind, Vine and Moores measured the direction and intensity of the natural remanent magnetisation (NRM) of over 900 hand specimens from 150 localities within the Troodos complex, using a portable fluxgate magnetometer (Vine and Moores, 1969; Moores and Vine, 1971). It was estimated that the direction of NRM could be assessed in the field to within 20° of the true direction. This approach was justified as the mean NRM intensity of Troodos rocks is high, and a complementary laboratory study of 200 orientated drill cores from a further 27 sites indicated that the remanence vectors of pillow lava and gabbro samples change very little on progressive demagnetisation.

To the disappointment of Vine and Moores, no areas of convincingly reversely magnetised material were found over the whole outcrop of the Troodos massif and the two major inliers at Akamas and Troulli. Only shallow positive inclinations (mean 32° down) were recorded in the pillow lavas (Vine and Moores, 1969) indicating an origin for the Troodos at a palaeolatitude of 17°N, consistent with a location intermediate between Africa and Eurasia during the Late Cretaceous.

The declination of the primary thermo-remanent magnetisation retained by the pillow lavas was consistently orientated approximately due west (mean azimuth 276°).

Such an azimuth for the palaeomagnetic vector was completely unexpected, and was interpreted by Moores and Vine (1971) as indicating an anticlockwise rotation of the whole Troodos massif through approximately 90° since its formation. This implied that the original spreading axis was orientated in an east-west direction, more in line with the general Tethyan trend (Gass, 1968).

The intensity of NRM for the zeolite facies pillow lavas was typically found to be 1-10 Am^{-1}, with a Köenigsberger ratio (ratio of NRM intensity to intensity of induced magnetisation) of approximately 10. In contrast, the greenschist facies sheeted dyke complex were found to have much lower NRM intensities of 0.01-0.5 Am^{-1}, and a correspondingly lower Köenigsberger ratio of 0.5. This drastic reduction in mean intensity of NRM within the sheeted dyke complex was attributed to the metamorphic destruction of titanomagnetite phases into Ti-poor titanomagnetites during hydrothermal circulation of fluids at the spreading ridge crest. Free titanium was presumed to be taken up in newly formed sphene (Moores and Vine, 1971; Vine and Moores, 1972). The underlying plutonics exhibited NRM intensities similar to those of the sheeted dykes, but with a slightly higher Koenigsberger ratio of 1.

Pursuing the sea-floor analogue for the Troodos ophiolite, Moores and Vine (1971) concluded that the most potent source rocks on Cyprus capable of contributing to marine magnetic anomalies were the pillow lavas (seismic layer two). This was confirmed by an aeromagnetic survey of southern Cyprus which clearly indicated that the steepest magnetic anomaly gradients correlated closely with the outcrop area of the peripheral pillow lavas (Vine *et al*, 1973). In addition, the systematic association of positive anomalies with pillow lava outcrops suggested that the extrusives were uniformly normally magnetised.

In contrast to the strong, single component thermoremanent magnetisations recorded by the Troodos pillow lavas, samples collected from the greenschist facies sheeted dyke complex were often dominated by secondary viscous components with a coercive force spectrum which overlapped that of the primary magnetisation. Therefore, prior to structural tilt correction, NRM directions within the dyke complex were spread between the due westerly directed vectors obtained from the pillow lavas and the direction of the ambient magnetic field over Cyprus (Dec=003°, Inc=54.4°) (Lauer and Barry, 1976). However, recent work within the sheeted dyke complex (Allerton, 1988a) has demonstrated that alternating field demagnetisation is capable of recovering primary remanences from these rocks.

Following the discovery of the stable, westerly directed primary remanence recorded in the extrusive sequences of the Troodos crust, palaeomagnetic investigations were extended into the continuous Late Cretaceous to Recent sedimentary cover to the

ophiolite. The intention of these studies was to constrain the timing of the rotation of the ocean crust. This approach was justified as the sediments lie *in situ* upon the ophiolite. Thus any rotation of the underlying basement must necessarily be reflected by a change in the azimuth of primary magnetisation recorded within the sedimentary sequence.

In the first investigation of this type, Shelton and Gass (1980) measured the NRM of a small suite of samples collected principally from the pelagic chalks of the Lefkara Group. However, the NRM intensities of these sediments were found to be comparable in many instances with the noise level of their magnetometer (a slow spin balanced fluxgate instrument). Thus, no absolutely reliable vectors could be defined. Even when using high spin numbers (2^7-2^8) and measuring all samples in six orientations there were large variations in the directions of magnetisation obtained. No attempt was made to investigate the stability of remanence in these samples.

In addition, Shelton and Gass (1980) collected a limited number of samples from the ferromanganiferous umbers of the Perapedhi Formation, the volcaniclastic sandstones of the Kannaviou Formation, and from a sequence of Pliocene marls. These all had measurable NRM intensities. Declinations were found to cluster in the northwest quadrant, although the limited sample population, the scatter of inclination values, and a lack of stability tests leaves any interpretation of these vectors open to debate. Shelton and Gass were certainly not justified in concluding that rotation was confined to a single Late Miocene event (Clube, 1986).

3.5.2 Recent studies.

By the early 1980's, several important palaeomagnetic issues had still to be resolved in Cyprus. While it was accepted that the Troodos massif had undergone a 90° anticlockwise rotation, the exact timing of rotation remained unknown. Importantly, the size of the rotated unit had not been defined and no satisfactory model for a rotation mechanism had been proposed. On a more local scale, various anomalies identified by early studies had still to be investigated. Variations in the strike of sheeted dykes away from the predominant north-south alignment were known to occur along the northern margin of the ophiolite (Moores and Vine, 1971). Also, deviations in dyke trend in the vicinity of the Arakapas fault belt had been noted. However, it was not known whether these variations represented a primary feature of the Troodos crust or were the result of tectonic rotation of large fault blocks subsequent to crustal accretion.

With these questions in mind, a major palaeomagnetic study of the Troodos extrusive sequences and the overlying sedimentary cover was undertaken by Clube (1986).

Table 3.1. Summary of the palaeomagnetic results obtained by Clube (1986).

	Age	N	n	Dec	Inc	α_{95}
TR	Turonian	11	663	274	36	12.3
AK	Turonian	3	217	276	41	14.1
UM	Turonian	5	56	279	6	28.6
RA	Campanian	1	25	289	13	23.9
PE	Maastrichtian-Palaeocene (No)	5	116	336	32	13.2
PE	Maastrichtian-Palaeocene (Re)	6	101	152	-14	15.3
PE	Lower Eocene	5	136	357	38	10.1

TR = Troodos Pillow Lavas (north Troodos, Akamas and Southern Limassol Forest areas).

AK = Akamas.

UM = Umbers (north Troodos and Southern Limassol Forest areas).

RA = Radiolarites (north Troodos).

PE = Pelagic chalks.

N = number of localities; n = number of samples; Dec = declination; Inc = inclination; α_{95} = radius of the 95% cone of confidence; No = normal polarity; Re = reversed polarity.

Almost without exception the 880 extrusive samples collected from the main massif and the Akamas peninsula to the west by Clube were found to record stable westerly directions of magnetisation (see table 3.1). Secondary viscous components of magnetisation were removed by low alternating demagnetisation fields to leave stable primary components of presumed thermoremanent origin. No systematic swings in declination occurred across the strike of the ophiolite complex, demonstrating that the Troodos crust experienced bulk-rotation by approximately 90° anticlockwise, in agreement with the earlier findings of Vine and Moores (1969).

Along the northern margin of the massif, Clube discovered that remanence declinations in areas where dykes deviated markedly away from the predominant north-south direction were not significantly different from those recorded in areas where dykes are aligned north-south. This implies that major discontinuities in the orientation of dykes along the northern margin of Troodos cannot be attributed to major post-intrusion tectonic rotations about vertical axes. Therefore, the general complexity in dyke trends in this area must be a primary feature of the original oceanic crust (Clube, 1986). It seems then that the zone of crustal accretion could not always have been a simple north-south trending symmetrical spreading ridge. Some areas of crust preserved in the east of the massif must have been created at a spreading centre that was orientated at a considerable angle to the principal ridge crest. This is in keeping with the suggestion by Varga and Moores (1985) that the Troodos spreading system may have been unstable.

A preliminary study of the Southern Troodos Transform Fault system was also carried out by Clube (Clube, 1986; Clube and Robertson, 1986). Upper Pillow Lava pillows and interlava sediments were sampled at five sites along the Arakapas fault belt. Two sites were located close to Arakapas village, whereas the other three sites were located at the western end of the fault belt, in the Ayios Mamas region. At four of these sites cleaned remanence vectors, after application of a simple tilt correction, fell in the northwest quadrant, while the remaining site exhibited a southwesterly directed magnetisation. These results were significantly different from those obtained from the Troodos massif to the north and from a complementary study of several sites in the Limassol Forest block, where westerly directed remanences were found. The results were interpreted in terms of localised clockwise rotation of intra-crustal fault blocks relative to ophiolitic basement both to the north and south, and were used to support the suggestion that the transform acted as a dextral shear zone (Clube, 1986; Clube and Robertson, 1986; Robertson, 1990). However, the limited sampling area necessarily made this interpretation tentative.

The most important contribution of the studies of Clube (1986) was the constraining of the timing of rotation of the Troodos ophiolite by detailed palaeomagnetic measurements made through its *in situ* sedimentary cover. The stable remanent magnetisation retained by the umbers and lowermost radiolarites of the Perapedhi Formation was found by Clube to be indistinguishable from that of the underlying extrusives (table 3.1). Hence, rotation of the ophiolite complex must have been initiated after the deposition of these sediments. Declination data from the overlying Lefkara Group pelagic chalks indicated that the Troodos crust was rotated through at least 60° between the Upper Campanian (c. 75 Ma) and the end of the Late Palaeocene (57 Ma), and that rotation was complete by the end of the Lower Eocene (50 Ma) (Clube *et al.*, 1985; Clube and Robertson, 1986). Younger, Miocene sediments were found to consistently retain a stable remanent magnetisation orientated close to north, suggesting that only minor rotation of the underlying ophiolitic basement took place after the end of the Lower Eocene (Clube, 1986).

Furthermore, the detailed studies of Clube identified several high-angle lineaments within Cyprus which probably acted as boundaries to the rotated area (Clube, 1986; Clube and Robertson, 1986).

The palaeomagnetic data on the timing of rotation and related geological data from the Eastern Mediterranean region were then synthesised into a tectonic model for the palaeorotation of the Troodos microplate within the regional plate tectonic framework (Clube and Robertson, 1986; Robertson, 1990). This model will be discussed in section 3.6.

A complementary investigation of the rotation history recorded by the circum-Troodos sedimentary succession was carried out by Abrahamsen and Schönharting (1987). The majority of their samples were collected from two successions; an Upper Palaeocene-Lower Eocene section of Lefkara Group pelagic chalks, and an Upper Eocene-Upper Miocene section of Lefkara chalks and reefal limestones of the Koronia Formation. The results were of variable quality due to scatter ascribed to the low intensities of these sediments (c. 10^{-4} Am^{-1}). However, mean directions were found to cluster between north and northwest for the majority of sites, and the data obtained were thus in agreement with the results of Clube (1986).

With the overall framework of the palaeorotation of Troodos established (Moores and Vine, 1971; Clube et al, 1985; Clube, 1986; Clube and Robertson, 1986; Abrahamsen and Schönharting, 1987), the most recent palaeomagnetic work carried out in Cyprus has been aimed at more specific, genetic problems associated with the structure and configuration of the Troodos spreading system. In addition to the palaeomagnetic and structural modelling of the Solea graben along the northern margin

of Troodos by Allerton and Vine (1987), outlined in section 3.2 above, several studies carried out within the zone of dyke deviation to the north of the Arakapas fault belt have been published (Bonhommet et al, 1988; Allerton, 1988b; Allerton, *in prep*). These investigations will be discussed in Chapter 4 (section 4.4), in relation to the findings of the present study.

3.6 The palaeorotation of the Troodos ophiolite.

A number of potential settings have been proposed in which the palaeorotation of a small oceanic microplate within a narrow Neotethyan ocean basin undergoing regional compression might be accommodated.

A popular idea is that the palaeorotation was driven by a collision between a seamount or microcontinent with a subduction zone (Figure 3.09a; Moores *et al*, 1984). In one scenario (Robinson, 1987), the microcontinent was thrust beneath the Troodos completely explaining the present day existence of continental crust below Cyprus (Makris *et al*, 1983). Alternatively, rotation was initiated by a glancing blow from the microcontinent (Murton, 1987). The Troodos was certainly *not* emplaced onto the Arabian continental margin in the Late Cretaceous, in contrast to ophiolites further east, from Hatay and Baër-Bassit to Oman (Robertson, 1990). The continuous Cretaceous to Tertiary pelagic sedimentary cover of the Troodos contrasts markedly with the tectonic disruption and emergence of these other ophiolites during their emplacement. Indeed, the Troodos terrane shows little evidence of regional compression or fault disruption, as expected from forceful collision and underthrusting, with partial or complete subduction of a seamount or microcontinent. Also, the palaeorotation of Troodos has been shown to have occurred during the Late Cretaceous to Early Eocene interval (a period of 25-30 Ma), and not during a short-lived collisional event (Robertson, 1990).

An alternative mechanism of rotation is that the Troodos crust was formed by spreading about an Eulerian pole of rotation located close to the south-eastern coastline of Antalya Bay (Figure 3.09b). This setting is broadly analogous to the Neogene opening of the Ligurian Sea marginal basin, where both Sardinia and Corsica rotated anticlockwise away from the stable European craton (Clube and Robertson, 1986). However, no regional declination swings have been detected within the Troodos basement, suggesting that no rotation occurred during crustal genesis (Clube, 1986). A further problem with this model is that it implies that spreading occurred into the Tertiary, yet ophiolites of this age are not known in the Eastern Mediterranean area. Also, the Early Tertiary sedimentary cover of the Troodos massif (Lefkara Formation)

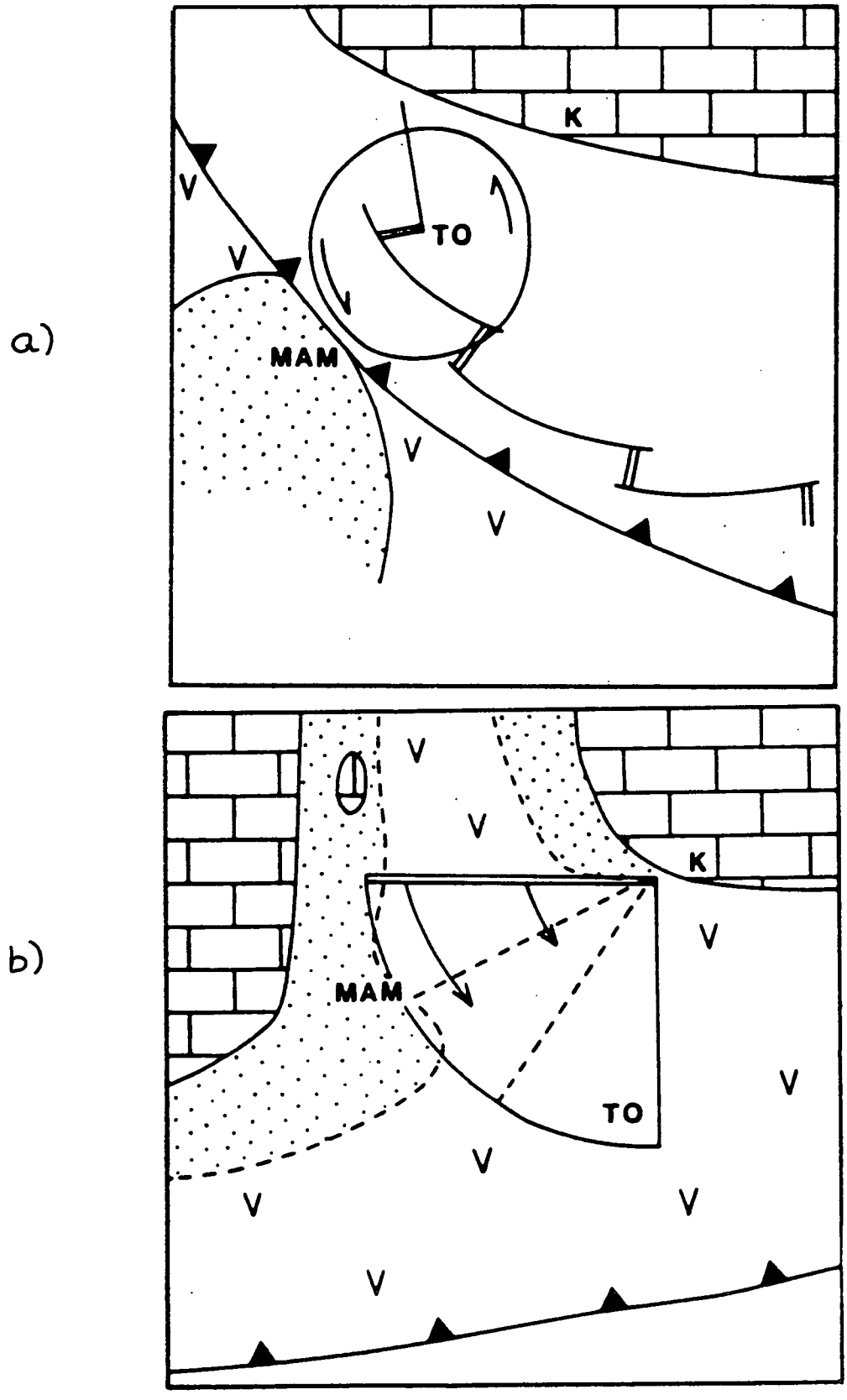

Figure 3.09. Theoretical, but unsatisfactory models for the Troodos palaeorotation. (a) rotation driven by collision of a microcontinent with a subduction zone; (b) opening of a small marginal basin about a local pole of rotation. TO = Troodos, K = Kyrenia Range, MAM = origin of Mamonia (from Clube and Robertson, 1986).

does not suggest proximity to a spreading centre (e.g. there are no dispersed hydrothermal sediments) (Robertson, 1990).

Clube *et al* (1985) invoked oblique subduction beneath the Troodos ophiolite as a driving mechanism for the palaeorotation. The main problem with this is that oblique subduction alone does not obviously provide the required rotational torque. In a revised model, Clube and Robertson (1986) favoured northward subduction beneath Troodos, combined with collision outside Cyprus to provide the necessary rotational force (Figure 3.10).

Clube and Robertson (*op. cit.*) noted the near coincidence of the timing of the initiation of palaeorotation and the emplacement of the Hatay and Baër-Bassit ophiolites in the Campanian. These ophiolites represent fragments of supra-subduction zone crust which formed to the east of the Troodos spreading centre and which subsequently collided with the offset Levant continental margin. The emplaced Hatay ophiolite was transgressed by upper Campanian neritic carbonates (cf. the Campanian onset of rotation in Cyprus).

Collision to the east of Troodos effectively pinned one segment of the supra-subduction zone ophiolite, while the Troodos spreading centre still remained above a downgoing slab. Continued northward movement of the African plate resulted in the trench pivoting about the intersection of the transform passive margin with the subduction front (Figure 3.10; Robertson, 1990). Southwards "roll-back" of the trench to the west of the pivot point exerted a pull on the overriding plate. As a consequence, an anticlockwise rotational torque was developed in the forearc region. The Troodos microplate then became detached and began to rotate about an irregular ring of dextral strike-slip faults and associated relay faults (Figure 3.10; Clube and Robertson, 1986; Robertson, 1990). Fragments of the northern continental margin (Mamonia Complex, Moni Mélange) became attached to the rotating microplate along strike-slip lineaments and were then carried southward to their present position.

Some of the microplate boundary faults are preserved in southwest and south Cyprus, and possibly in north Cyprus as well. Pre-existing zones of crustal weakness were exploited, particularly the westward extension of the South Troodos Transform Zone in southwest Cyprus. The curved microplate boundary must have cut across the pre-existing, more linear oceanic fracture zone (Robertson, 1990). In south Cyprus, microplate boundary faults are located close to the present coastline, south of the fossil transform zone (Clube and Robertson, 1986).

This model for the palaeorotation is more consistent with the geology of Cyprus and the regional tectonic setting than models which invoke 'push' mechanisms involving microcontinental collision.

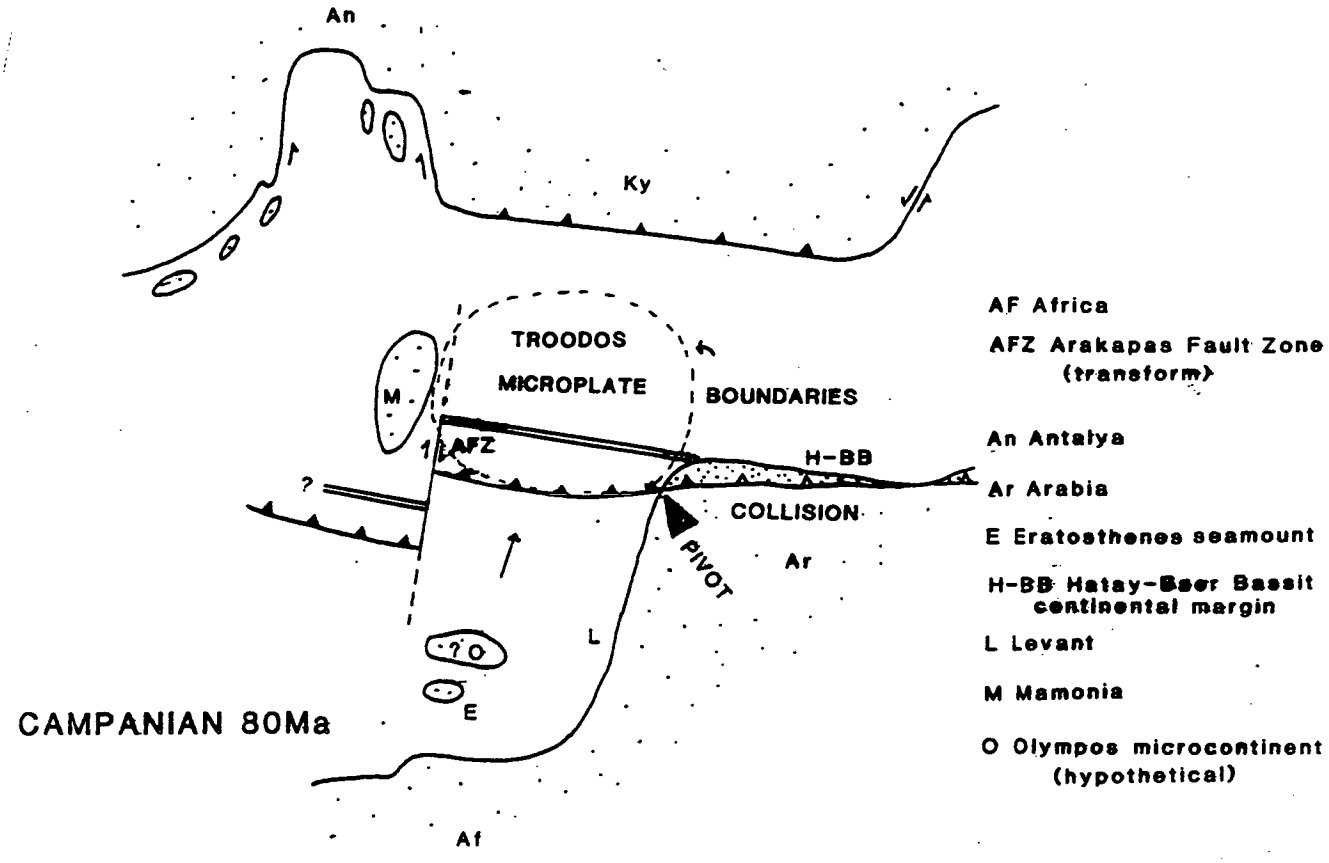

Figure 3.10. The preferred plate tectonic setting for initiation of the palaeorotation of the Troodos microplate in upper Campanian time (from Robertson, 1990). The Troodos formed above a subduction zone in the Cenomanian (97-91 Ma), offset by a dextrally slipping Southern Troodos transform zone and its extension in SW Cyprus. Prior to upper Campanian time, supra-subduction ophiolite crust collided with the Arabian promontory to the E, emplacing the Hatay and Baër Bassit ophiolites. Northward convergence of Africa continued and the Troodos began to pivot anticlockwise above a relict subduction zone. An irregularly shaped Troodos slab then detached and began to rotate.

3.7 Summary.

The Troodos massif represents an uplifted fragment of Neotethyan oceanic crust which formed above a northward dipping intra-oceanic subduction zone in the Late Cretaceous. Fabrics preserved within the ophiolite indicate that the Troodos system experienced non-steady state spreading. The Limassol Forest Complex and Arakapas fault belt sub-terranes exposed along the southern margin of the massif were formed within a 'leaky' oceanic fracture zone. Ophiolitic crust in the south-eastern part of the Limassol Forest represents a small fragment of the 'Anti-Troodos' plate, which lay to the south of the transform (present coordinates).

Palaeomagnetic research has demonstrated that the ophiolite underwent a 90° anticlockwise rotation subsequent to its formation (Moores and Vine, 1971). Detailed studies of the circum-Troodos sedimentary cover constrain the timing of this rotation to the Campanian to Early Eocene interval (Clube, 1986; Abrahamsen and Schönharting, 1987). The favoured model for the palaeorotation (Clube and Robertson, 1986; Robertson, 1990) involves continental margin-trench collision and ophiolite emplacement to the east of Troodos generating an anticlockwise torque upon the supra-subduction zone Troodos crust. As a consequence, a small Cyprus-sized microplate detached and rotated around an irregular ring of dextral wrench faults.

CHAPTER FOUR - A PALAEOMAGNETIC STUDY OF THE SOUTHERN TROODOS TRANSFORM FAULT.

4.1 Introduction and aims.

There has been much lively debate concerning the sense of shear along the fossil Southern Troodos Transform Fault, and hence the sense of offset of the Troodos spreading axes. The aims of the palaeomagnetic study detailed in this chapter are to address this problem and at the same time to demonstrate that rotational strain plays an important part in deformation occurring within transform zones.

At present, within the sheeted dyke complex of the Troodos massif there is a general north-south orientation of dykes, as noted in the previous chapter. However, as the Arakapas fault belt is approached a progressive change in dyke trend into eventual alignment with the transform lineament is seen (Figure 4.01). This observation led to the suggestion (Simonian and Gass, 1978) that the dykes were injected into a sigmoidal stress field that operated across the transform zone (Figure 4.02a). This would imply that the transform operated as a sinistral fault system between dextrally displaced spreading axes. This interpretation was supported by a suggestion that abundant NE-SW orientated mafic and picritic dykes within the Western Limassol Forest Complex were injected along *en echelon* fractures oblique to the principal east-west direction of shear, in response to sinistral transform movement (Murton, 1986). In addition, large phacoidal blocks with NE long axis orientations were found entrained within serpentinite shear zones. The obliquity of these blocks to the predominantly east-west trending shear zones was believed to be due to rotation associated with sinistral shearing (Murton, 1986).

An alternative explanation for the swing in dyke trend is that right-lateral movement along the transform has frictionally rotated originally north-south striking dykes around vertical axes into alignment with the fault lineament (Figure 4.02b). This would therefore require sinistral offset of ridge segments along the transform. This spreading configuration is more consistent with the geology of Cyprus and was incorporated into the tectonic model for the palaeorotation of the Troodos microplate within the regional plate tectonic framework of the Eastern Mediterranean outlined in Chapter 3 (Robertson, 1990; Clube *et al*, 1985; Clube and Robertson, 1986).

The geological arguments are therefore conflicting but palaeomagnetic studies provide a direct method of determining whether either of the models apply. The first palaeomagnetic data obtained from the Troodos ophiolite (Vine and Moores, 1969) demonstrated that a stable westerly directed magnetisation vector was retained by the

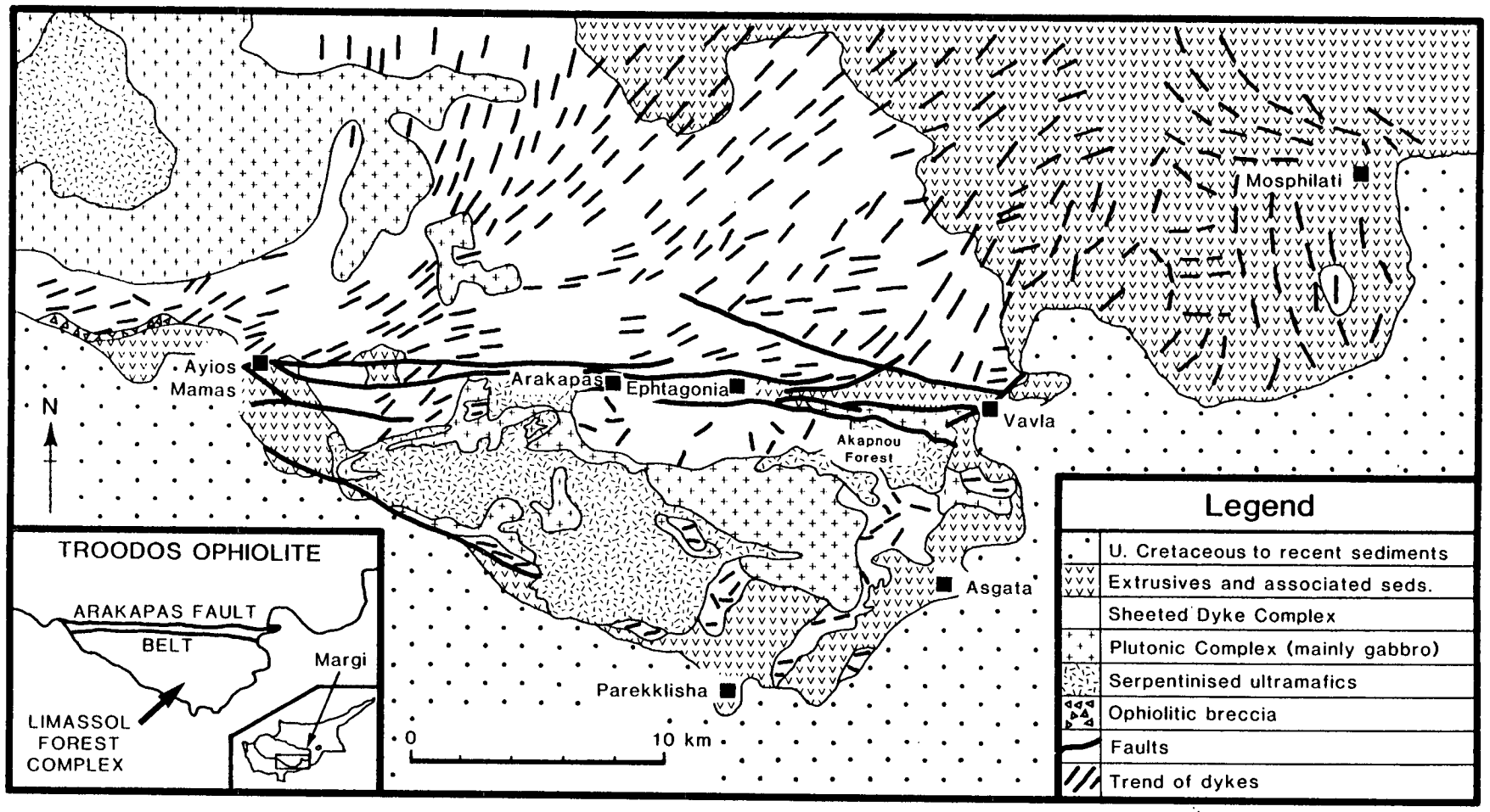

Figure 4.01. Simplified geological map of the Limassol Forest Complex and the southern margin of the main Troodos ophiolite (adapted from Simonian and Gass (1978)), showing the locations referred to in the text. Note the progressive change in the trend of dykes into near parallelism with the Arakapas fault belt over a distance of 10 - 15 km.

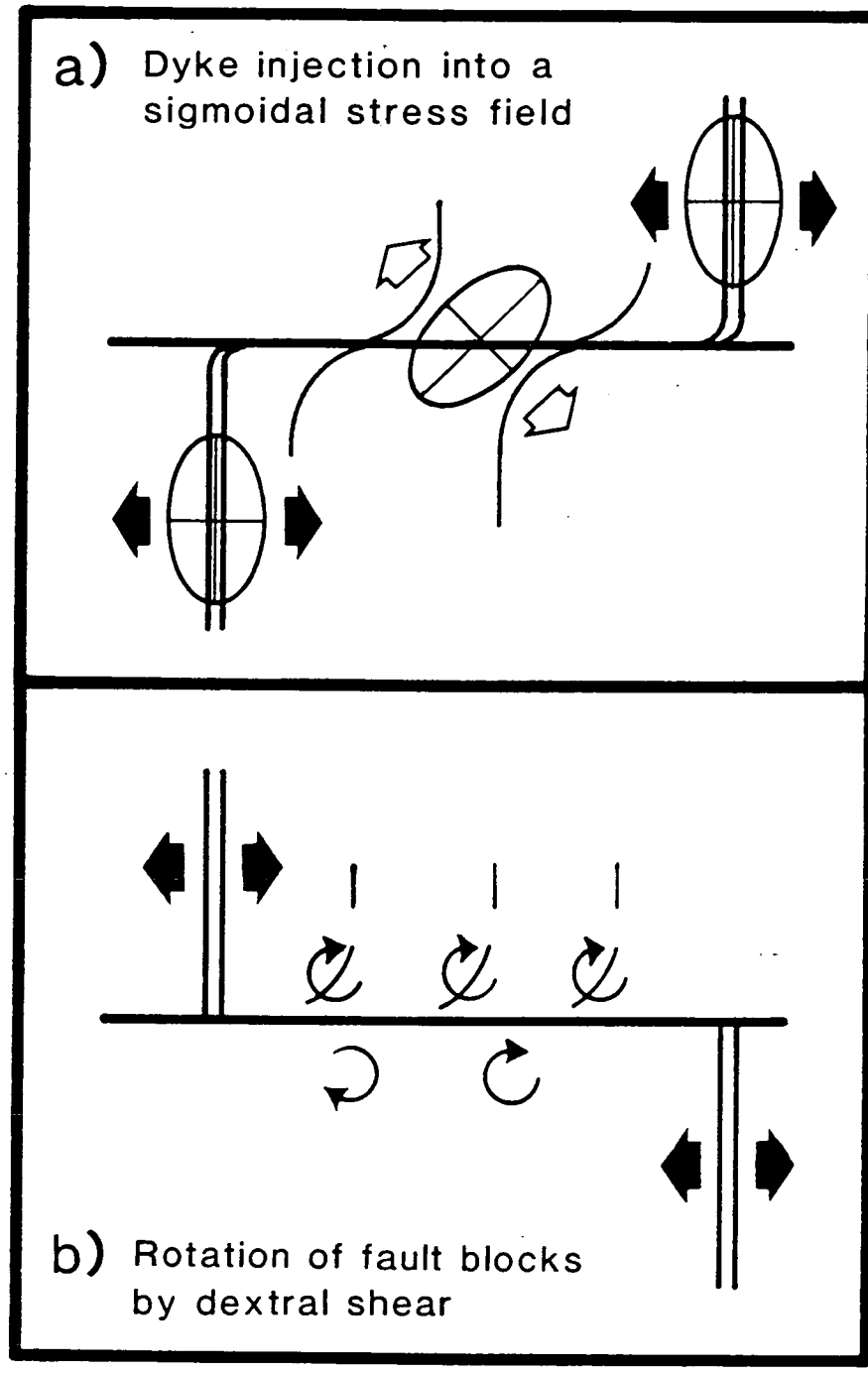

Figure 4.02. Possible alternative settings in which deviations in dyke trend could occur close to the Southern Troodos Transform Fault (adapted from Clube and Robertson, 1986): (a) shows dyke injection into a sigmoidal stress field operating across a *sinistrally slipping* transform between dextrally offset spreading axes; (b) shows dyke deviation attributed to frictional rotation of fault blocks related to *dextral slip* along the active transform domain. In this model, clockwise rotation of fault blocks would be expected to occur between the sinistrally offset spreading axes.

extrusive series, indicating that a 90° anticlockwise rotation had taken place. Subsequent studies (Clube *et al*, 1985) have confirmed this result and have further shown that there was no rotation of the ophiolite during its formation in the Late Cretaceous (Clube and Robertson, 1986). The structurally corrected remanence direction of declination 276°, inclination 32° (Vine and Moores, 1969) may therefore be assumed to represent the geomagnetic field direction at the time of magnetisation of the ophiolite. This direction is hereafter referred to as the Troodos magnetisation vector (TMV) (Allerton and Vine, 1987).

If the deviations in dyke trend observed to the north of the Arakapas fault belt are a primary feature of the oceanic crust, as required by the sigmoidal stress field model, then magnetisation vectors obtained from units within the deviation zone and along the transform should cluster around the TMV. In contrast, a deviation of magnetisation vectors away from the TMV would indicate that significant tectonic rotations have taken place.

I present here new palaeomagnetic results obtained from the extrusive and sedimentary sequences of the Arakapas fault belt and the Limassol Forest Complex to the south. These data confirm that tectonic rotations of fault-bounded blocks have occurred within the transform zone and yield important information concerning the sense of offset along the Troodos spreading axis. In addition, I report data that further constrain the timing of the initial stages of palaeorotation of the Troodos microplate as a whole.

4.2 Sampling and methods.

I have obtained orientated cores mainly from zeolite facies pillow lavas, massive lava flows, dykes, sills and interlava sediments exposed around the periphery of the Limassol Forest block and at a single site on the eastern flank of the Troodos ophiolite (see Figure 4.03). The sampled units form part of the Lower Pillow Lava (LPL) and Upper Pillow Lava (UPL) units and are assumed to be of Turonian age (90.4-88.5 Ma) (Mukasa and Ludden, 1987). Cores were taken using a standard petrol-driven rock drill, with water cooled, 1" diameter diamond-tipped drill bits. Between 5 and 20 samples were drilled at each site. Each sample was orientated with both magnetic and sun compasses (Creer and Sanver, 1967). In the laboratory, 22 mm long subsamples were prepared from each core.

In addition, samples were taken from the overlying metalliferous umbers and radiolarites of the Perapedhi Formation, of assumed Turonian to Campanian age (90.4-74.0 Ma) (Blome and Irwin, 1985). Standard coring techniques could not be used to

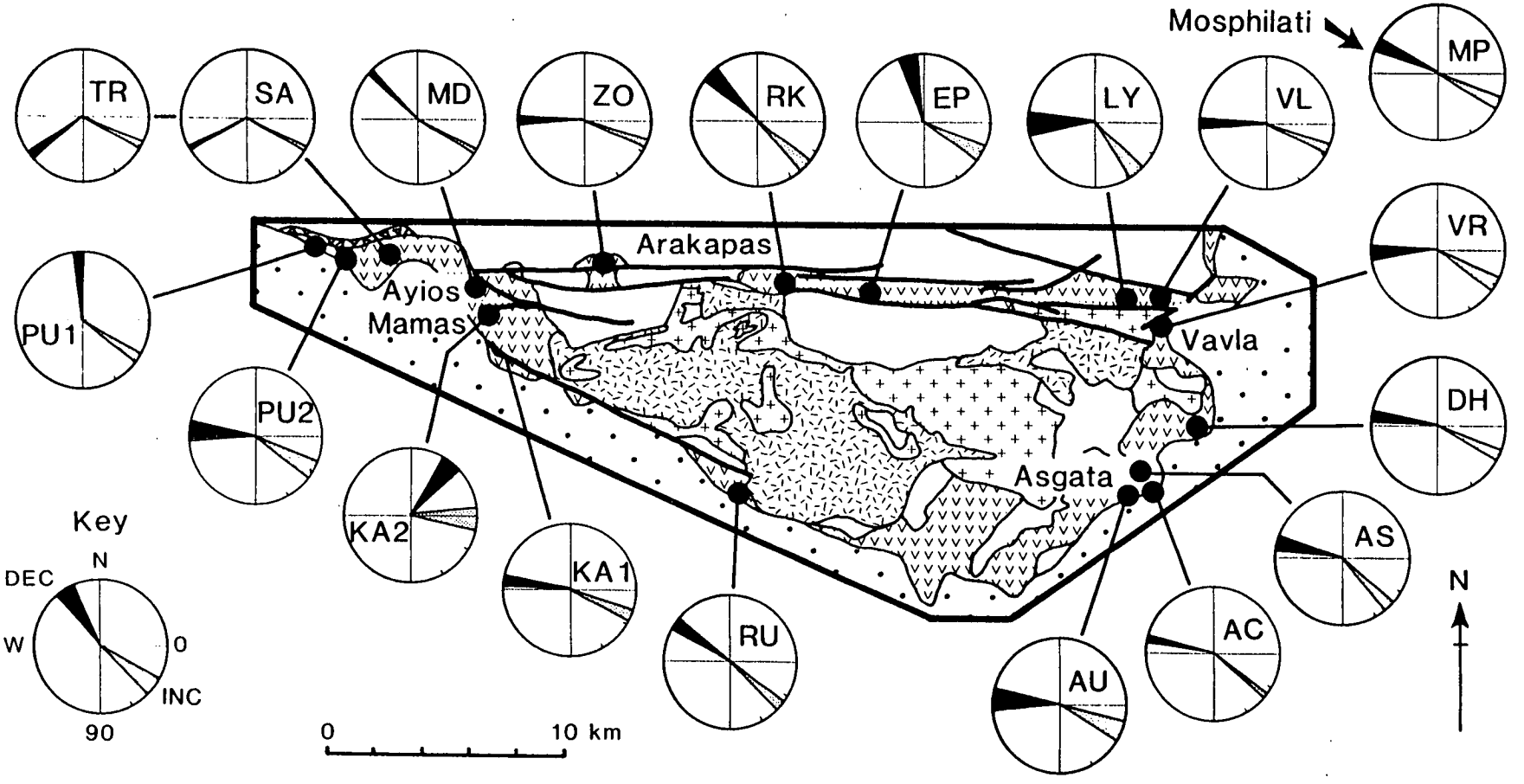

Figure 4.03. Geological map showing the location of the 19 palaeomagnetic sites. The 'clock' diagrams show the 95% confidence limits associated with the tilt corrected mean declination and inclination at each site (see Figure 1 for the location of site MP at Mosphilati on the eastern flank of the Troodos ophiolite).

collect samples from these lithologies, since both generally occur in thin beds which fracture upon drilling. Umbers do occur in thicker beds but become muddy when drilled. To overcome these problems, small independently orientated rock chips were collected. The sampling method involved locating beds less than 1cm thick which could be cleared to expose flat areas of approximately 20 cm^2. A line of strike was then marked on the bedding surface, and the strike and dip recorded using a magnetic compass and clinometer. After carefully removing the large rock chip, additional strike lines were drawn. Each chip was broken into smaller pieces of c. 1 cm^2 in the laboratory, and finally each fragment was mounted inside a plastic sample box with its strike lines parallel with one side of the box. Between 5 and 20 specimens were prepared in this way for each "chip" site.

Sites were located away from areas of intense shearing and brecciation. Visibly weathered and altered exposures were avoided. Samples were only collected when an accurate structural tilt correction could be defined. Sites with only minor structural tilt were preferred (normally less than 40°), to minimise any declination errors due to tectonic rotation about inclined axes (MacDonald, 1980). Tilt corrections were based on the attitude of massive lava flow units, together with primary lamination in interlava sediments and in the overlying umbers and radiolarites. The orientation of the margins of any dykes and sills present were also recorded.

A total of 24 sites were collected, 19 of which yielded reliable palaeomagnetic results. Five sites were rejected because of sample instability and/or large within site dispersion (K<10).

Magnetic measurements were carried out using a Molspin fluxgate spinner magnetometer for the pillow lava, massive flow, sill and dyke samples, and a 2-axis CCL superconducting magnetometer for the more weakly magnetised interlava sediments, umbers and radiolarites. Details of these instruments were given in Chapter 1.

4.3 Palaeomagnetic results.

4.3.1 Rock magnetic characteristics.

The frequency distributions of the natural remanent magnetisation (NRM) intensities of the igneous samples and the sediments show clear log-normal distributions (Figure 4.04). The mean intensity of the lava samples is 1.3 Am^{-1} which is substantially lower than the values of 13.0 Am^{-1} found for the extrusives of the main Troodos ophiolite by the Cyprus Drilling Project (Smith and Vine, 1990) and 6.0 Am^{-1}

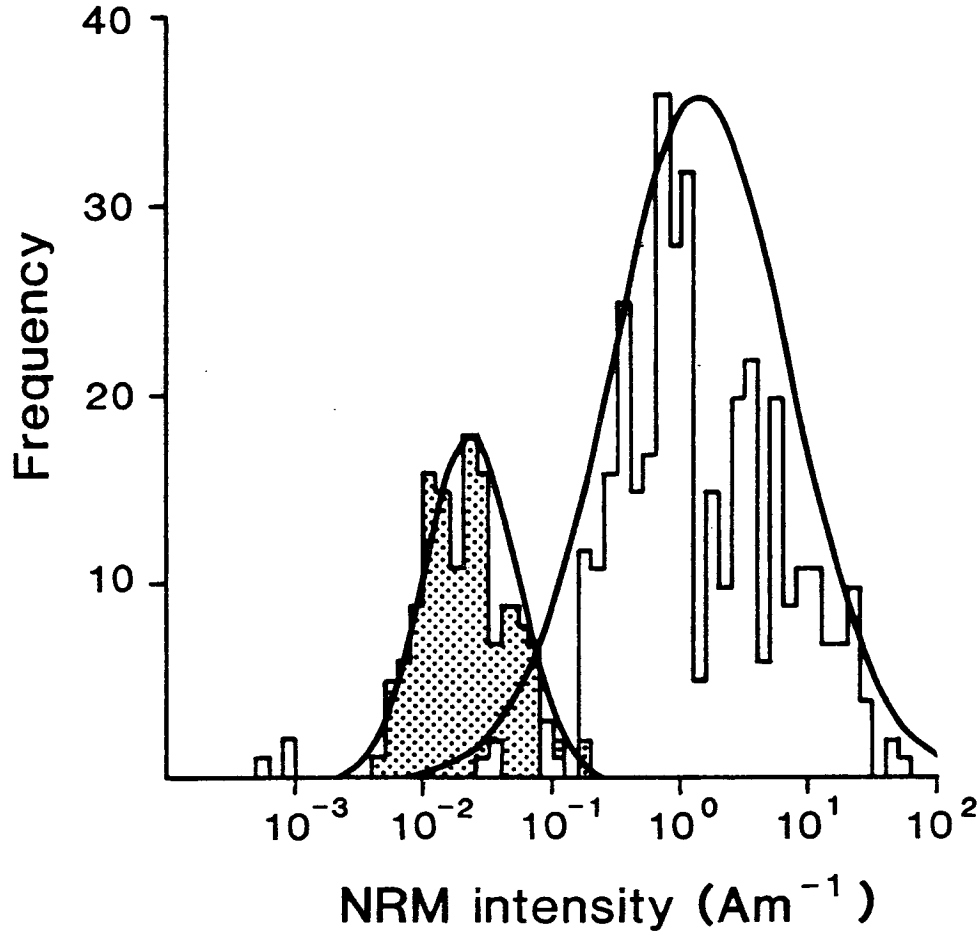

Figure 4.04. Histograms illustrating the frequency distributions of the NRM intensities of igneous and sediment samples measured in the present study of the Southern Troodos Transform Fault (sediments shaded). Note the clear log-normal distributions for both sample sets.

found for the upper levels of oceanic layer 2 sampled by DSDP Leg 83 (Smith, 1985). However, this value is comparable to the mean intensity of 1.16 Am^{-1} found for the Upper Pillow Lava unit by Vine et al (1973). The mean intensity of the sediments is two orders of magnitude lower than that of the lavas, but is much greater than the noise level of the cryogenic magnetometer (5.0 μAm^{-1}).

The rate of acquisition of isothermal remanence (IRM) in fields up to 1.0 T - 1.5 T has been studied for at least two samples per site. The method involved repeatedly exposing each sample to successively higher direct magnetic fields produced by a water-cooled high-field electromagnet and measuring the IRM induced in the sample using either a spinner or cryogenic magnetometer, according to the intensity of magnetisation produced. Fields above 1 T were achieved using a pulse magnetiser. This technique provides a rapid and effective method for distinguishing the presence of Ti-poor titanomagnetites and Ti-poor ilmenohaematites (Tarling, 1983). Single and multi-domain titanomagnetite (and maghemite) grains reach saturation in fields of 0.05 - 0.2 T, although single domain needle-shaped magnetite grains may have peak coercivities of up to 0.3 T. Haematite and goethite, on the other hand, do not saturate until fields of over 1 - 3 T. If d.c. magnetic fields are applied in incremental steps, therefore, the saturation moment becomes constant before 1 T for low coercivity magnetite and maghemite, but continues to increase at higher fields for haematite and goethite. An advantage of this technique of identifying the possible carriers of natural remanence in samples is that it does not involve chemical changes in the rock, since no heating is required.

Dunlop (1972) described a method of deriving the remanent coercivity spectra of a sample from the IRM vs. applied field characteristic. Dunlop (*op. cit.*) demonstrated that the coercivity spectrum may be approximated by the incremental isothermal remanent moment, Δm_r, in equal applied field intervals, ΔH, as determined from the IRM acquisition curve. This incremental spectrum is easier to calculate than the continuous spectrum determined from the point-by-point slope of the IRM curve, which in any case may not be justified by the limited number of measurements which are normally made.

Typical results of the IRM analyses are shown in Figure 4.05. In each graph the solid curve represents the stepwise increase in isothermal remanent moment produced by successively increasing applied fields, while the histogram shows the rate of change of IRM, i.e. the incremental coercivity spectrum (Dunlop, 1972). The rapid initial rise and subsequent flattening off of curves below 0.3 T indicates that magnetite is the main magnetic mineral present in all the sampled lithologies. An exception, however, are the interlava sediment samples analysed, where a continuous increase in the IRM for fields higher than 0.3 T indicates the presence of a higher coercivity fraction, which is

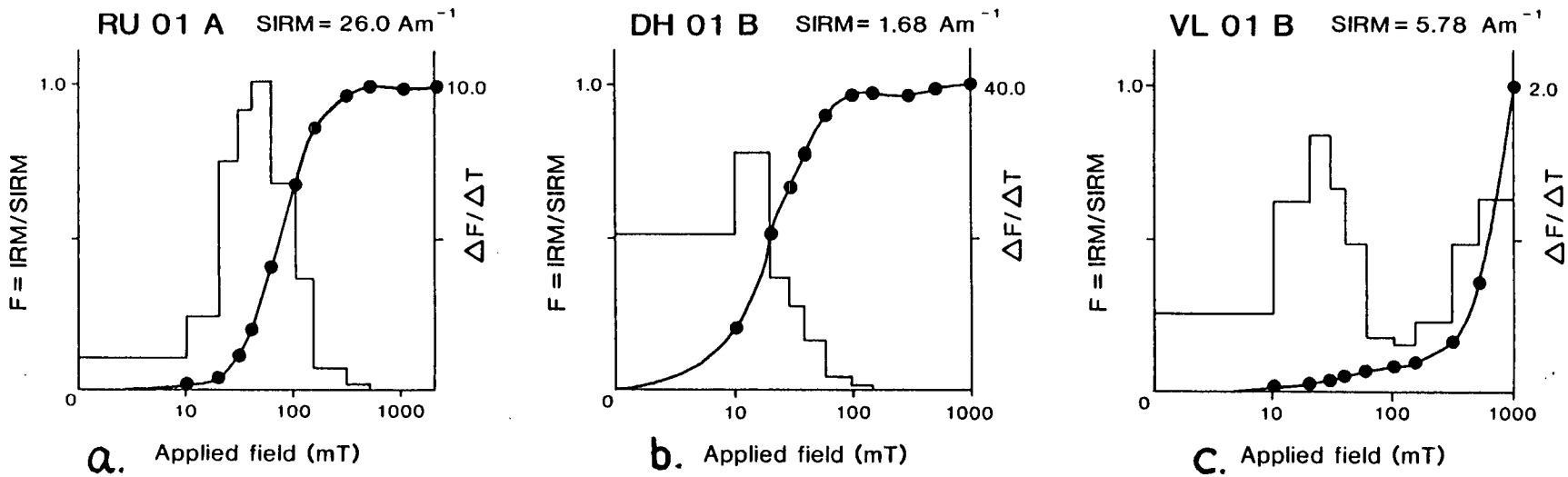

Figure 4.05. Examples of normalised IRM acquisition curves and coercivity spectra for (a) pillow lava, (b) umber and (c) interlava sediment specimens. Magnetite is the main magnetic mineral present in all the sampled lithologies except for the interlava sediments, where a higher coercivity fraction also occurs but which does not contribute to the NRM.

probably haematite. It seems possible that this haematite fraction contributes to the reddish colouration of these samples.

Magnetic extracts for thermomagnetic analysis have been prepared from lava samples from several sites. Samples were crushed using a jaw-crusher and Teamer mill. The powdered lavas were then added to water and extracts obtained using a strong bar magnet placed inside a rubber sheath suspended in the constantly stirred solution. The Curie point of each extract was found using a horizontal translation balance (Collinson, 1983).

Figure 4.06a shows a typical thermomagnetic curve, obtained from sample EP 001 A. Well defined Curie temperatures of between 560°C and 580°C were found for all the samples studied. This corresponds to a relatively pure magnetite composition, with only minor amounts of titanium present. An irreversible chemical change is also visible in the curves as a reduction of up to 40% in the room temperature value of the induced magnetisation upon cooling. This change could be due to oxidation of magnetite or to the inversion of maghemite to haematite at 350°C. Heating the samples in an inert nitrogen atmosphere did not alter the irreversible nature of the thermomagnetic curves, but did increase the room temperature induced magnetisation after cooling to 80% of its initial value (Figure 4.06b).

The thermomagnetic analyses confirm the dominant presence of magnetite as a remanence carrier in the lava units. The Curie points obtained may, however, indicate that the lavas have been altered by sea-floor weathering, since unaltered lavas tend to include titanomagnetites with significantly lower Curie temperatures (Beske-Diehl and Banerjee, 1980; F. J. Vine, pers. comm., 1990).

Magnetite Curie points have also previously been obtained for the umbers of the Perapedhi Formation (Clube, 1986).

Stepwise alternating field (AF) demagnetisation of a minimum of two samples per site was carried out up to peak fields of 100 mT to define cleaning fields for the remaining samples. AF treatment was found to be effective in removing all the magnetisation, even in the interlava sediment samples where high coercivity minerals were identified by the IRM analyses. This indicates that any high coercivity minerals present do not contribute significantly to the NRM of these samples.

Typical Zijderveld demagnetisation diagrams (Zijderveld, 1967) are shown in Figure 4.07 for sites situated along the Arakapas fault belt, in the Eastern Limassol Forest Complex and at Mosphilati on the eastern flank of the Troodos ophiolite. Apart from a minor north-dipping secondary component, attributed to viscous magnetisation in the present field direction, single stable components of magnetisation were isolated in fields of less than 20 mT for almost all samples studied. Exceptionally a further higher

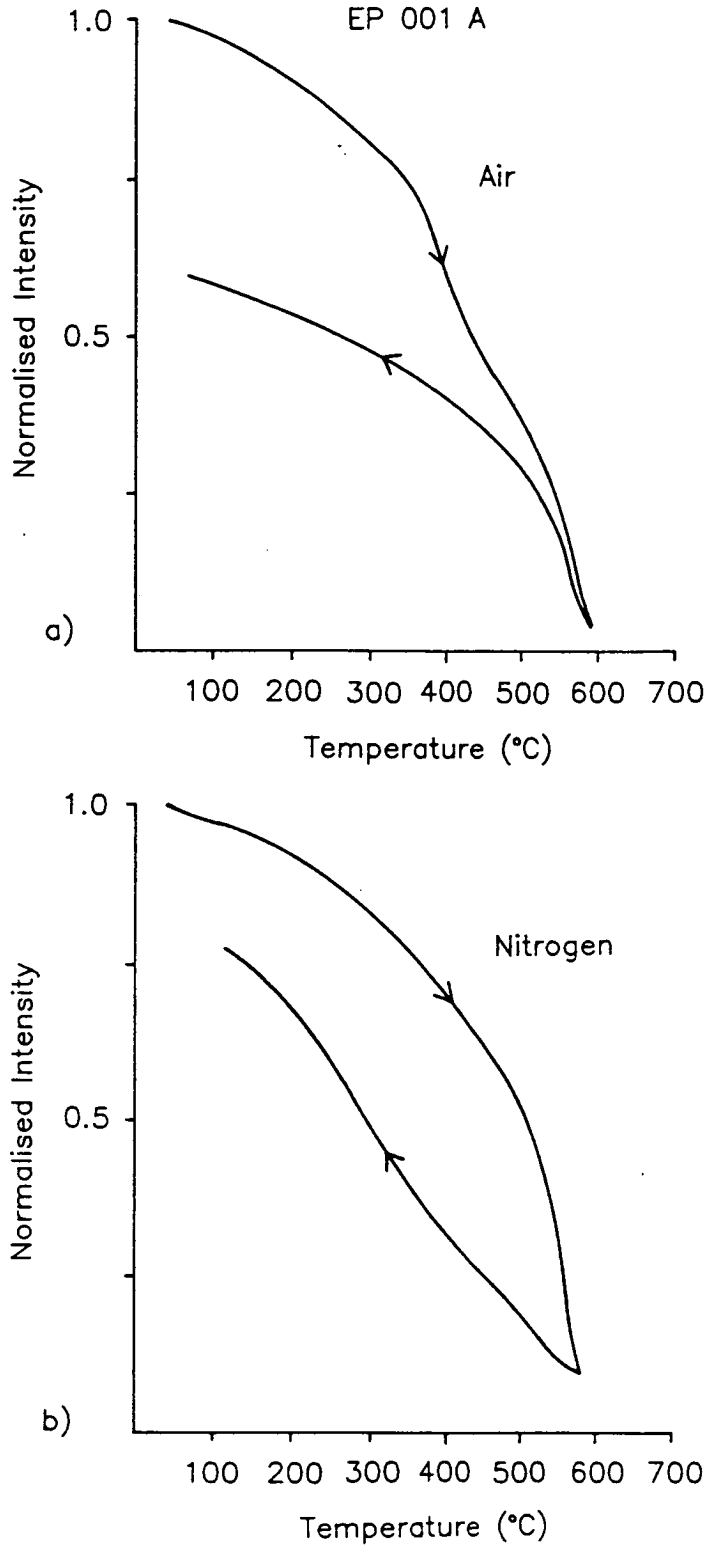

Figure 4.06. Thermomagnetic analysis of a powdered lava sample from site EP: a) thermomagnetic curve obtained by heating sample in air. Note the well defined Curie temperature between 560°C to 580°C, typical of a relatively pure magnetite composition, and the irreversible nature of the curve; b) curve obtained by heating in an inert nitrogen atmosphere. Note the reduction of the drop in intensity upon cooling.

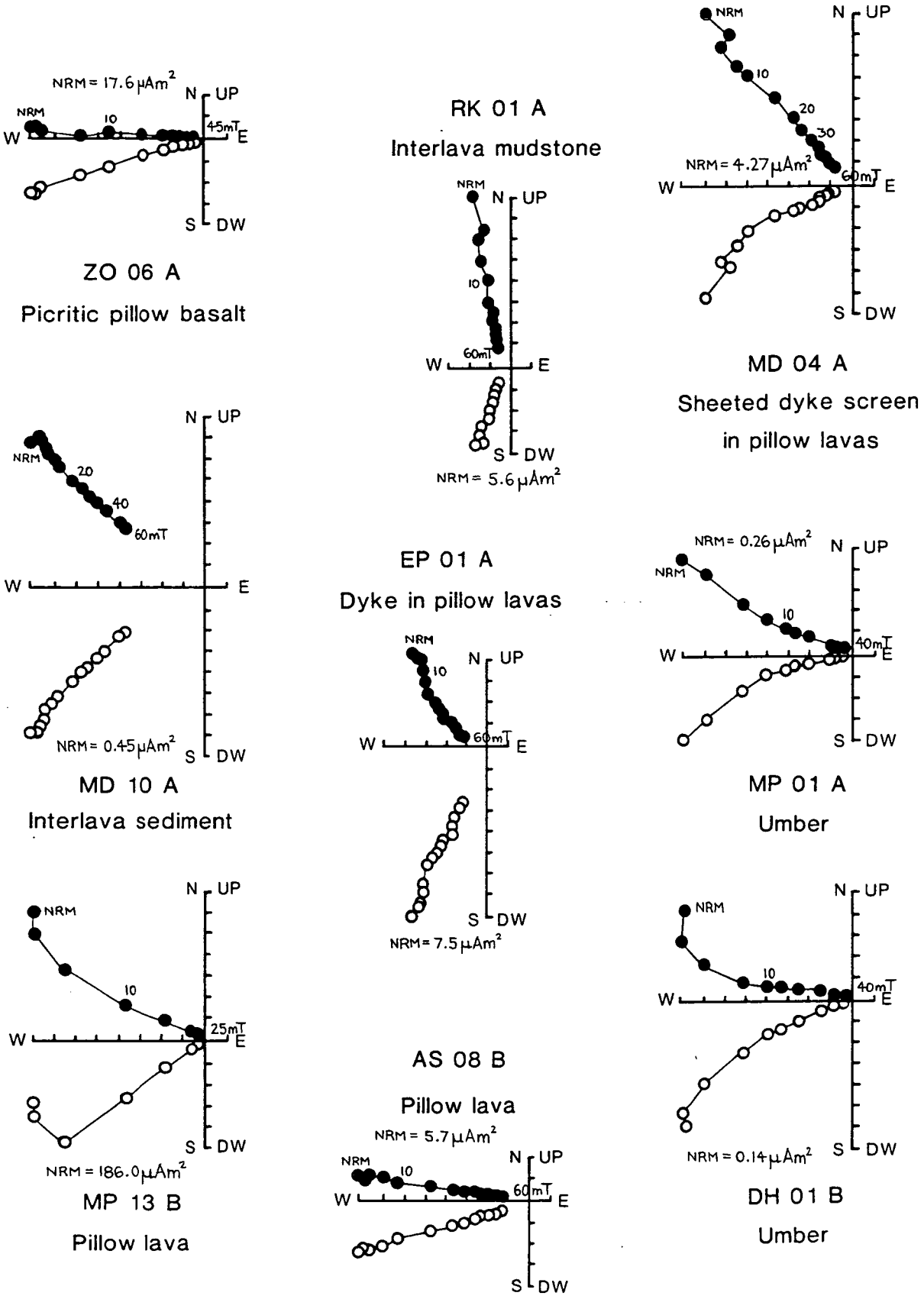

Figure 4.07. Typical Zijderveld plots of AF demagnetisation data for a range of lithologies. Single stable components of magnetisation were isolated for all samples. A minor north-dipping secondary component seen in some cases was removed in fields of less than 20 mT.

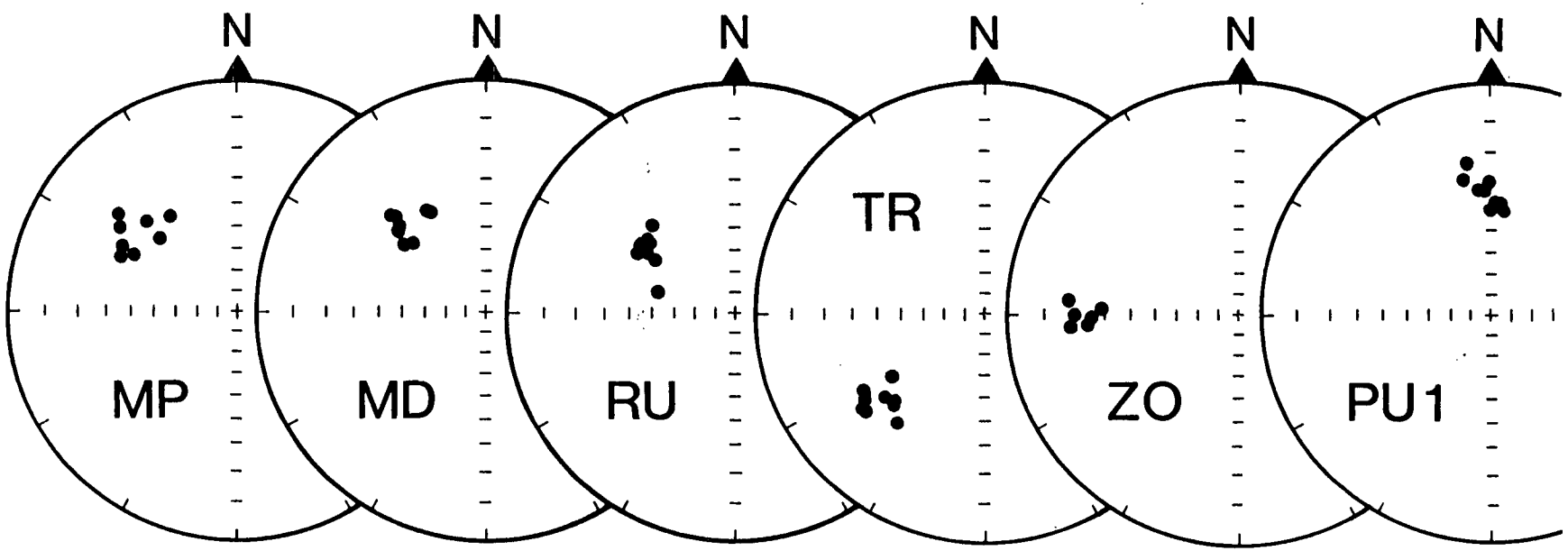

Figure 4.08. Stereographic projections of cleaned sample directions at six typical sites. After demagnetisation, within-site scatter is small. Significant deviations of magnetisation directions away from the Troodos magnetisation vector (TMV) are attributed to predominantly clockwise block rotations occurring within the transform domain.

coercivity component with a westerly declination remained after AF cleaning. This component may represent a secondary CRM acquired by submarine weathering soon after formation.

Cleaning fields of 10, 15 or 20 mT were subsequently applied to the remaining samples at each site.

After demagnetisation, within-site scatter is small, as shown by the stereographic projections of Figure 4.08. A reduction in α_{95} and increase in the precision parameter K after tilt correction at sites where variations in palaeohorizontal orientation were recorded indicates that magnetisation predates folding (Graham, 1949).

No reversed sample polarities were identified, as may be expected for units formed during the long Cretaceous normal polarity period (Moores and Vine, 1971).

4.3.2 Palaeomagnetic results.

The results obtained from the 19 reliable sites before and after application of a standard tilt correction are reported in Table 4.1. Results have been grouped into four sub-areas and the site means for each area are shown in the 'clock' diagrams of Figure 4.03. These diagrams show the 95% confidence limits associated with the mean declination and inclination at each site. Demarest (1983) demonstrated that such limits cannot be simply found by constructing tangential lines of equal declination and small circles of equal inclination around the standard α_{95} cone of confidence. The probability that the true mean direction of magnetisation lies within the region defined by these lines must exceed 95%, since this region includes the 95% cone of confidence plus an additional area. Error bars found by this construction will be exaggerated by approximately 25%. Demarest (*op. cit.*) gave correction factors based on an analytical calculation for varying values of N which can be used to remove this effect when α_{95} is less than 15° and the mean inclination is less than $90° - 2\alpha_{95}$. The confidence limits shown in Figure 4.03 were calculated using this technique.

Considerable variations in the declination of cleaned remanence directions occur between sites along the Arakapas fault belt, the western margin of the Limassol Forest Complex and the eastern flank of the Troodos ophiolite at Mosphilati (Figure 4.03). Seven sites show more northerly declinations than the TMV, indicating that these sites have experienced a net clockwise rotation with respect to the Troodos ophiolite. Two adjacent sites at the western end of the Arakapas fault Belt have declinations in the SW quadrant, indicating a net anticlockwise rotation of the sampled block. Declinations at the remaining six sites are indistinguishable from that of the TMV.

Table 4.1. Palaeomagnetic results from the Southern Troodos Transform Fault.

Site	Age	N	Geographic				Stratigraphic			
			Dec	Inc	α_{95}	K	Dec	Inc	α_{95}	K
Troodos Reference Direction										
TMV							276	32		
Arakapas Fault Belt										
TR	UPL Pillows	10	232	14	4.4	121	231	28	4.4	121
SA	UPL Pillows	6	224	18	2.4	773	240	30	2.4	773
MD	UPL Dykes	8	317	49	9.6	34	317	36	5.5	101
	UPL Sediments	17	313	45	3.4	112	311	29	2.6	193
ZO	UPL Pillows	6	267	33	4.8	198	269	22	4.8	198
RK	UPL Seds/dyke	13	338	59	7.4	33	314	45	7.4	33
EP	UPL Pillows/dyke	11	167	75	9.5	24	345	30	9.5	24
LY	LPL Sediments	7	270	15	9.0	46	267	51	8.7	49
VL	LPL Haem. Shales	17	266	-3	6.1	35	270	23	5.9	38
VR	Perapedhi Umbers	5	268	11	8.0	92	266	30	8.0	92
	Perapedhi Rads	17	307	-5	3.7	95	304	28	3.2	127
PU1	Perapedhi Umbers	9	358	33	5.1	101	358	34	5.1	101
PU2	Perapedhi Umbers	7	284	21	10.9	31	274	29	9.8	39
Western margin of Limassol Forest Complex										
KA1	Flows/Sills	7	343	57	6.2	95	277	22	6.2	95
KA2	TAS Pillows	4	26	29	12.3	57	39	3	12.3	57
RU	UPL Pillows	8	292	46	5.9	88	304	40	5.9	88
Eastern flank of Troodos massif										
MP	UPL Pillows	9	294	4	6.3	68	305	33	6.3	68
	Perapedhi Umbers	10	284	-3	7.1	47	286	17	7.1	47
Eastern Limassol Forest Complex										
AS	UPL Pillows/seds	14	266	2	6.2	42	282	46	6.2	42
AC	Perapedhi Umbers	5	293	41	3.1	597	282	39	3.1	597
DH	Perapedhi Umbers	9	269	21	8.2	40	277	26	5.8	81
AU	Perapedhi Umbers	4	285	26	11.8	61	274	23	11.8	61
	Perapedhi Rads	8	304	23	7.0	63	306	20	7.0	63

N = number of samples; α_{95} = semi-angle of 95% cone of confidence; K = Fisher precision parameter

By contrast, sites located further south in the Eastern Limassol Forest Complex, near Asgata (in the 'Anti-Troodos' plate (MacLeod, 1990)), exhibit consistent westerly directed declinations. No relative rotation has therefore occurred between these sites and the Troodos microplate to the north. Three previously reported sites at Asgata, Kalavasos and Parekklisha (Clube, 1986) gave similar results.

The mean inclination of all sites (36°) is comparable to the inclination of the TMV (32°). However, significant variations are seen within the extrusives and interlava sediments, whereas the inclinations of the umbers and radiolarites are generally low. These discrepancies cannot be attributed to latitudinal drift during crustal genesis since the variations are unsystematic. Alternative possibilities are that:

(1) physical rotation of remanence carriers has occurred during compaction of the sediments studied. This could explain the shallow inclinations observed in the Perapedhi Formation umbers and radiolarites. Similar inclinations have been found in umbers and radiolarites exposed at Margi on the northeastern margin of the Troodos ophiolite (Clube, 1986). It has been shown that in this area the umbers underwent compaction into hollows in the surface of the Troodos lavas, reducing thicknesses by up to 50% (Boyle, 1984).

(2) the attitude of the palaeohorizontal relative to the palaeofield was incorrectly identified at several sites. Tilt corrections are difficult to define in submarine extrusive sequences. Seafloor lava slopes can be inclined at a considerable angle to the horizontal so that recorded palaeohorizontals frequently represent palaeoslopes. It is known that lavas along the Arakapas fault belt were erupted down significant slopes into hollows in the brecciated basement (Simonian and Gass, 1978). The application of a simple tilt correction may therefore be unjustified in such cases.

A further criticism of the standard structural correction in palaeomagnetic studies is that it is assumed that tilt took place about the line of strike of bedding. Thus the total motion experienced at a site is arbitrarily divided into a tilt plus a rotation about a vertical pole. The assumption of simple tilting is incorrect where tectonic rotations have taken place about non-horizontal, inclined axes. In such cases the conventional correction gives rise to declination anomalies (MacDonald, 1980). These resemble the effects of tectonic rotation, but are more appropriately termed 'apparent tectonic rotation'. Variations in declination along the transform may therefore be partially due to apparent rotation, arising from the use of simple tilt corrections in this structurally complex terrain.

To overcome these problems, a method of resolving net tectonic rotation parameters (Allerton and Vine, 1987) has been applied to the data in the present study.

4.3.3 Derivation of net tectonic rotation parameters.

Allerton and Vine (1987) describe an analysis which yields both the initial orientation of a sampled unit and the pole and amount of tectonic rotation which has affected the unit in one operation. The method was originally used in the sheeted dyke terrain of the Solea graben on the northern flank of the Troodos ophiolite (Allerton and Vine, 1987), but is also applicable to the palaeohorizontal case (Allerton, 1988a).

There are four assumptions in the method: (1) the observed stable magnetisation was acquired before deformation took place; (2) a reference magnetisation vector can be found which represents the geomagnetic field direction at the time of magnetisation; (3) dykes are intruded vertically and original bedding/sill orientations are as close to horizontal as possible and (4) no internal deformation of the sampled unit has occurred so the angle β between the magnetisation vector and the pole to the dyke/bed is constant during deformation (Allerton and Vine, 1987).

The analysis involves finding a single pole of rotation which simultaneously restores the sample magnetisation vector (i.e. the *in situ* remanence direction) back to the Troodos magnetisation vector *and* the present bedding (dyke) pole as close to the vertical (horizontal) as possible, while conserving the angle β. The net tectonic rotation is described by the declination and inclination of this pole of rotation, and the angle of rotation; a positive angle representing an anticlockwise rotation (Allerton and Vine, 1987).

An example of this analysis for the palaeohorizontal case is given in Figure 4.09, using data obtained from site AS (located in the Eastern Limassol Forest Complex).
The cleaned *in situ* magnetisation vector for this site (SMV; dec = 266°, inc = 2°) makes an angle β of 44° with the present pole to the bedding (PBP). If this angle is conserved during deformation then a circle of radius β centred on the TMV gives the locus of all possible initial bedding poles. The pole chosen in the analysis (IBP) is that which is closest to the origin of the stereonet and corresponds to the most horizontal initial bedding dip possible. The position of the net tectonic rotation pole which restores the SMV to the TMV and the PBP to the IBP is then found by constructing the great circle bisectrices of both pairs of vectors; the intersection of the great circles gives the pole of rotation and the angle of rotation is readily measured. In this case, 45° of clockwise rotation has occurred about a horizontal axis.

The net tectonic rotation parameters found by applying this technique to the data obtained in the present study are given in Table 4.2, while the stereonet of Figure 4.10 shows the distribution of rotation poles.

Table 4.2. Net tectonic rotation parameters for sites along the transform zone.

Site	Pole of rotation	Angle of rotation
TR	170/67	48
SA	091/42	51
MD dykes	204/67	-44
sediments	193/69	-37
ZO	078/55	8
RK	178/48	-52
EP Stage 1	281/54	-118
EP Stage 2	247/54	-92
LY	201/25	20
VL	149/05	41
PU1	205/89	-82
PU2	252/06	23
KA1	326/03	64
KA2	335/66	-141
RU	239/54	-33
MP pillow lavas	325/33	-51
umbers	352/16	-38
AS	311/01	-45
AC	138/23	-18
DH	302/07	-22
AU	266/09	24

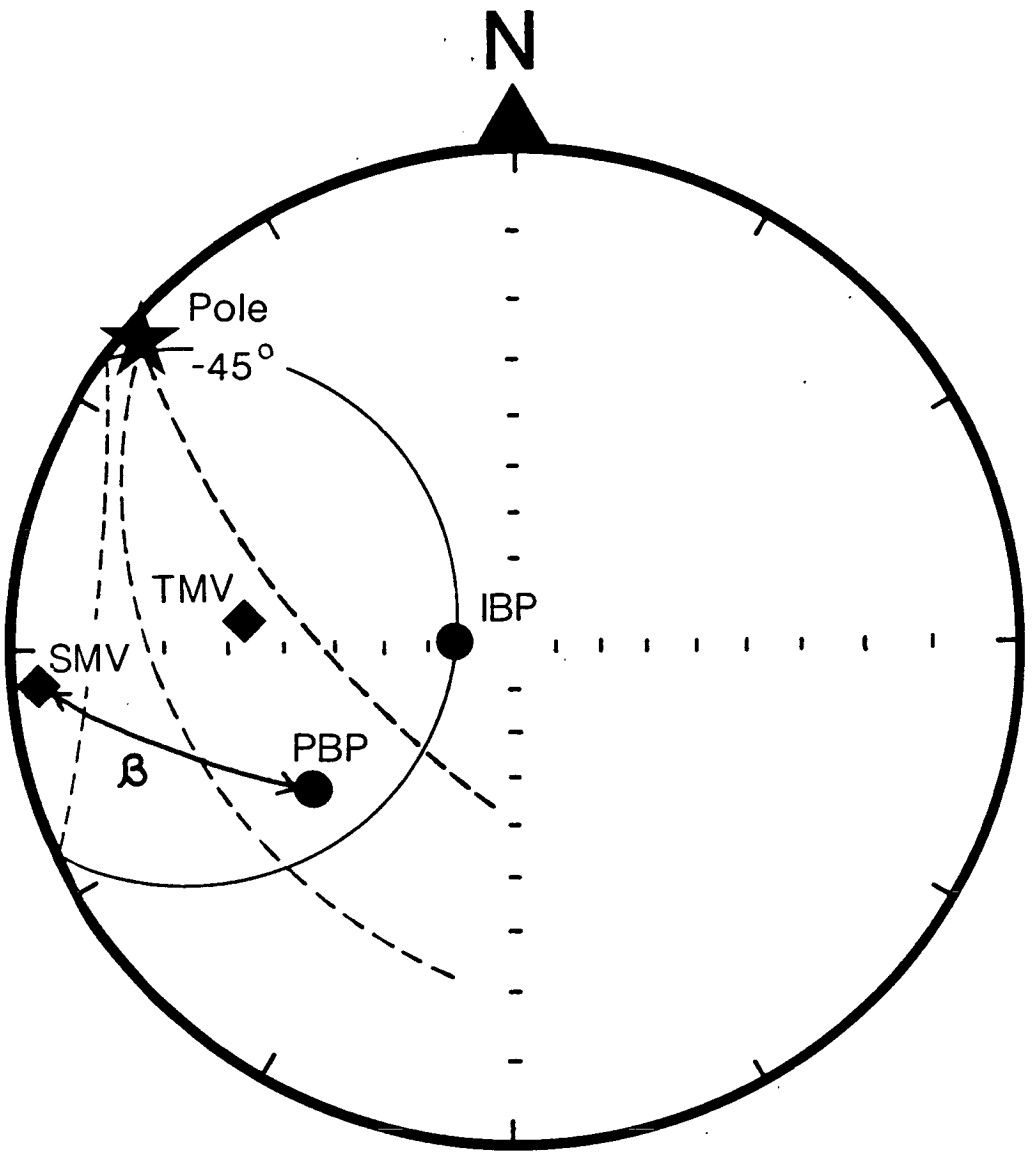

Figure 4.09. An example of the palaeohorizontal case of the technique of Allerton and Vine (1987) using data from site AS. The cleaned *in situ* magnetisation vector for this site (SMV; dec = 266°, inc = 2°) makes an angle ß of 44° with the present pole to the bedding (PBP). If this angle is conserved during deformation then a circle of radius ß centred on the TMV gives the locus of all possible initial bedding poles. The pole chosen in the analysis (IBP) is that which is closest to the origin of the stereonet and corresponds to the most horizontal initial bedding dip possible. The position of the net tectonic rotation pole which restores the SMV to the TMV and the PBP to the IBP is then found by constructing the great circle bisectrices of both pairs of vectors; the intersection of the great circles gives the pole of rotation and the angle of rotation is readily measured. In this case, 45° of clockwise rotation has occurred about a horizontal axis.

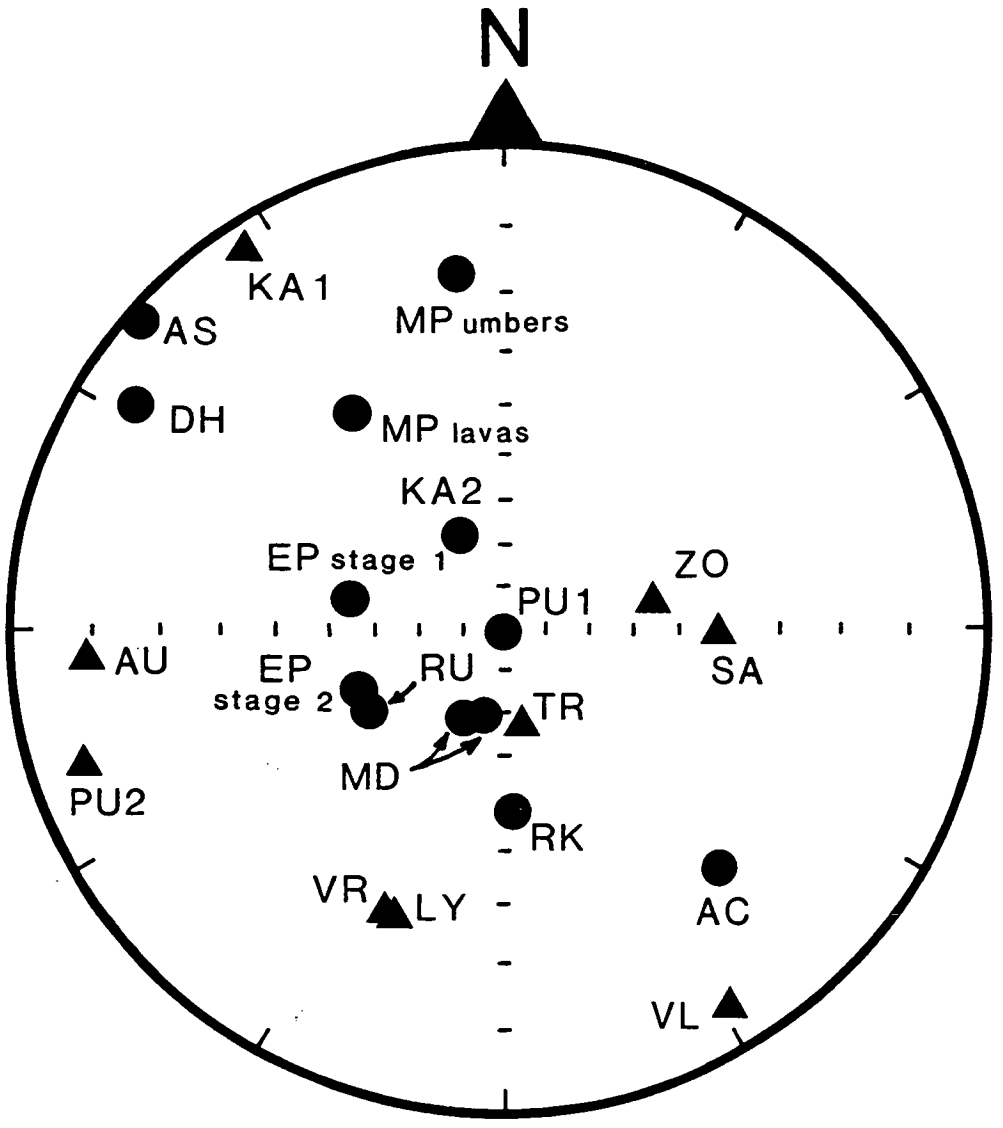

Figure 4.10. Stereographic projection showing the poles of net tectonic rotation derived for each site using the method of Allerton and Vine (1987) (circles = poles of clockwise rotation, triangles = poles of anticlockwise rotation). Poles close to the primitive indicate simple tilting about near-horizontal axes. Poles close to the origin of the stereonet indicate rotation about near-vertical axes.

Sites located along the Arakapas fault belt which exhibited significant tilt corrected declination anomalies, with respect to the TMV, have experienced large mainly clockwise rotations about intermediate to steeply inclined axes. In some cases rotation angles exceed 100°. Rotation poles for these sites cluster in the south-west quadrant, except for site MP on the eastern flank of the Troodos ophiolite where more northerly axes are found.

Those sites with tilt corrected declinations close to that of the TMV have poles of net tectonic rotation close to the primitive of the stereonet of Figure 4.10 and angles of rotation comparable to the structural dips at the sites. Rotational deformation here has been limited to simple tilt about sub-horizontal and mainly strike-parallel axes.

At three sites along the Arakapas fault belt (MD, RK, EP), it has been possible to determine the initial strike of single and sheeted dykes within the Upper Pillow Lavas. For each site the analysis yielded two solutions for the dyke orientation and net tectonic rotation. To decide which solution was correct, the pillow lavas and sediments at the sites were restored to their original orientations using both solutions. In each case one solution gave overturned palaeoslopes and was rejected.

The calculated initial dyke strikes were 320°, 315° and 317° for sites MD, RK and EP respectively. Assuming that dykes were injected perpendicularly to the minimum principal stress axis, this indicates that the stress ellipsoid had an orientation consistent with *dextral* slip along the transform.

The net tectonic rotation analysis can be taken one stage further at site EP, along the Arakapas fault belt between Arakapas and Ephtagonia. The exposure here consists of a road-cutting through Upper Pillow Lava pillow basalts and a sheeted dyke screen. The pillow lavas have well developed toes and pronounced lateral lobes which enable the palaeoslope at the time of eruption to be accurately defined. The orientation of the dyke margin could also be accurately measured. Samples were collected from both the sheeted dyke screen and the host pillow lavas. Detailed alternating field demagnetisation experiments reveal a significant difference in the cleaned remanence directions obtained from the sampled dyke and the surrounding pillow lavas (Figure 4.11). It seems therefore that tectonic rotation at this site was occurring at the same time as dyke injection, i.e. rotation was synchronous with crustal genesis. Using the technique of Allerton and Vine (1987), the complete rotational history for this site may be determined (Figure 4.12):-

(1) pillow lavas were erupted and then rotated by 118° clockwise about an inclined axis (declination 281°, inclination 54°);

(2) dyke injection occurred along a strike of 317° and

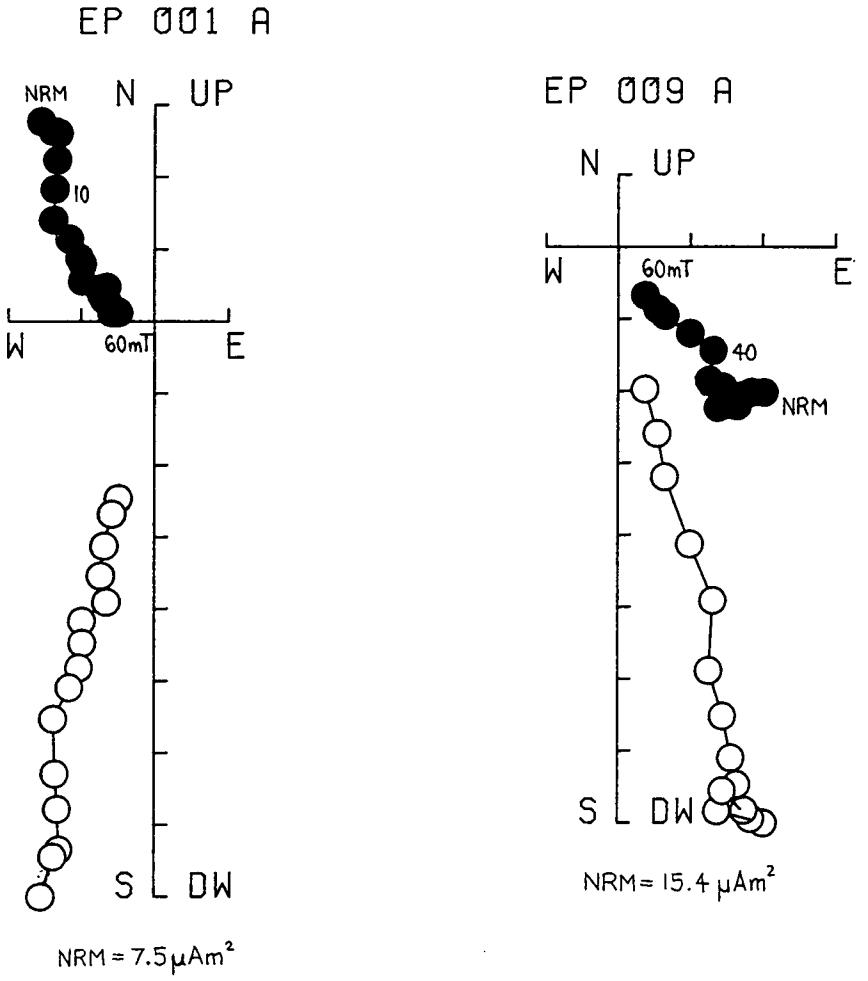

Figure 4.11. Zijderveld diagrams showing alternating field demagnetisation of dyke and pillow lava samples from site EP. Note the significant difference in recorded declinations between the two lithologies, indicating that rotation must be synchronous with dyke injection and lava extrusion (Geographic coordinates).

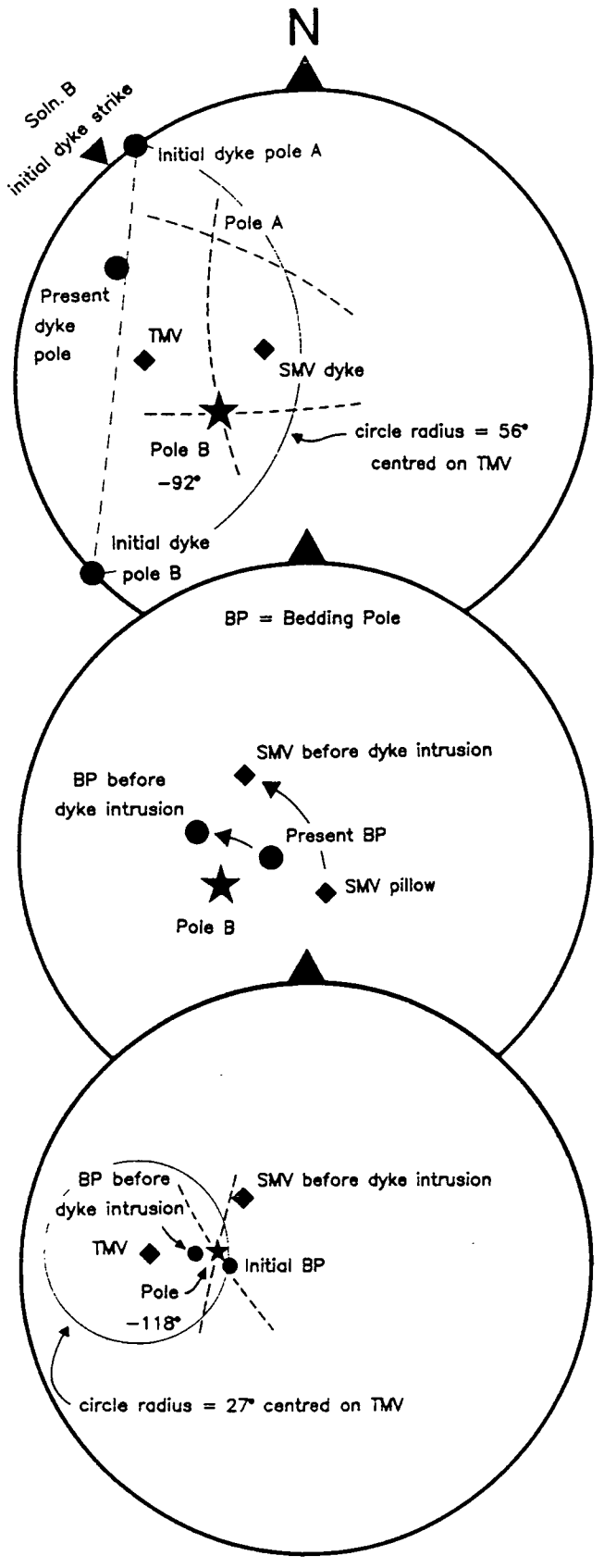

Figure 4.12. Determination of the net tectonic rotation history at site EP, using the technique of Allerton and Vine (1987). Results indicate that 118° of clockwise rotation about an inclined axis occurred prior to dyke injection. A subsequent clockwise rotation of 92° then affected both the pillow lavas and the sampled dyke.

(3) a further clockwise rotation of 92° about an inclined axis (declination 247°, inclination 54°) affected both the pillows and the dyke.
The poles of rotation for this site are shown on Figure 4.10 as EP Stage 1 and EP Stage 2.

In summary, the more robust net tectonic rotation analysis applied here confirms that substantial clockwise rotations of small-scale fault blocks (100's metres to several km in size) about steeply inclined axes have occurred within the transform zone. Cross-cutting relationships revealed by the analysis at site EP demonstrate the synmagmatic nature of these rotations. On the other hand, rotational deformation at sites in the Eastern Limassol Forest Complex to the south of the fault belt has been shown to be restricted to simple tilt about sub-horizontal axes.

4.3.4 Constraints on the timing of palaeorotation.

Previous palaeomagnetic data have established that the 90° palaeorotation of the Troodos microplate began soon after its oceanic genesis in the Turonian (90.4-88.5 Ma), with at least 60° of rotation occurring by the end of the Late Palaeocene (60.5-56.5 Ma). Rotation was essentially complete by the end of the Early Eocene (50.0 Ma) (Clube and Robertson, 1986; Clube, 1986). It appears then that the time period represented by the Perapedhi Formation (Turonian to Campanian; 90.4-74.0 Ma) is a critical interval during which much of the rotation may have taken place.

At two sites (AU, 0.5 km southwest of Asgata and VR, 0.5 km southwest of Vavla) I have sampled both the metalliferous brown umbers and the stratigraphically overlying radiolarites of the Perapedhi Formation. Cleaned remanence directions for both sites are listed in Table 4.1, whereas Figure 4.13 shows Zijderveld demagnetisation plots for both lithologies. The mean declination of the stable remanent magnetisation carried by the umber samples is indistinguishable from that of the TMV (i.e. 276°). This is in contrast to the more northerly directions recorded by the radiolarite samples (Figure 4.13).

No relative rotation has occurred between these sites and the main ophiolitic massif to the north. Therefore, since the umber-radiolarite sequences sampled are stratigraphically continuous, it may be assumed that the observed declination difference is due to a 30° anticlockwise rotation of both the Troodos microplate and the sampled area of the Eastern Limassol Forest Complex. In addition, radiolarite sequences exposed near Margi on the northeastern margin of the Troodos ophiolite (Clube, 1986) yielded a mean declination of 296°. Significantly, two samples from within the top three metres of the radiolarite interval at Margi showed stable magnetisations with even more northerly declinations of 321° (Clube, 1986).

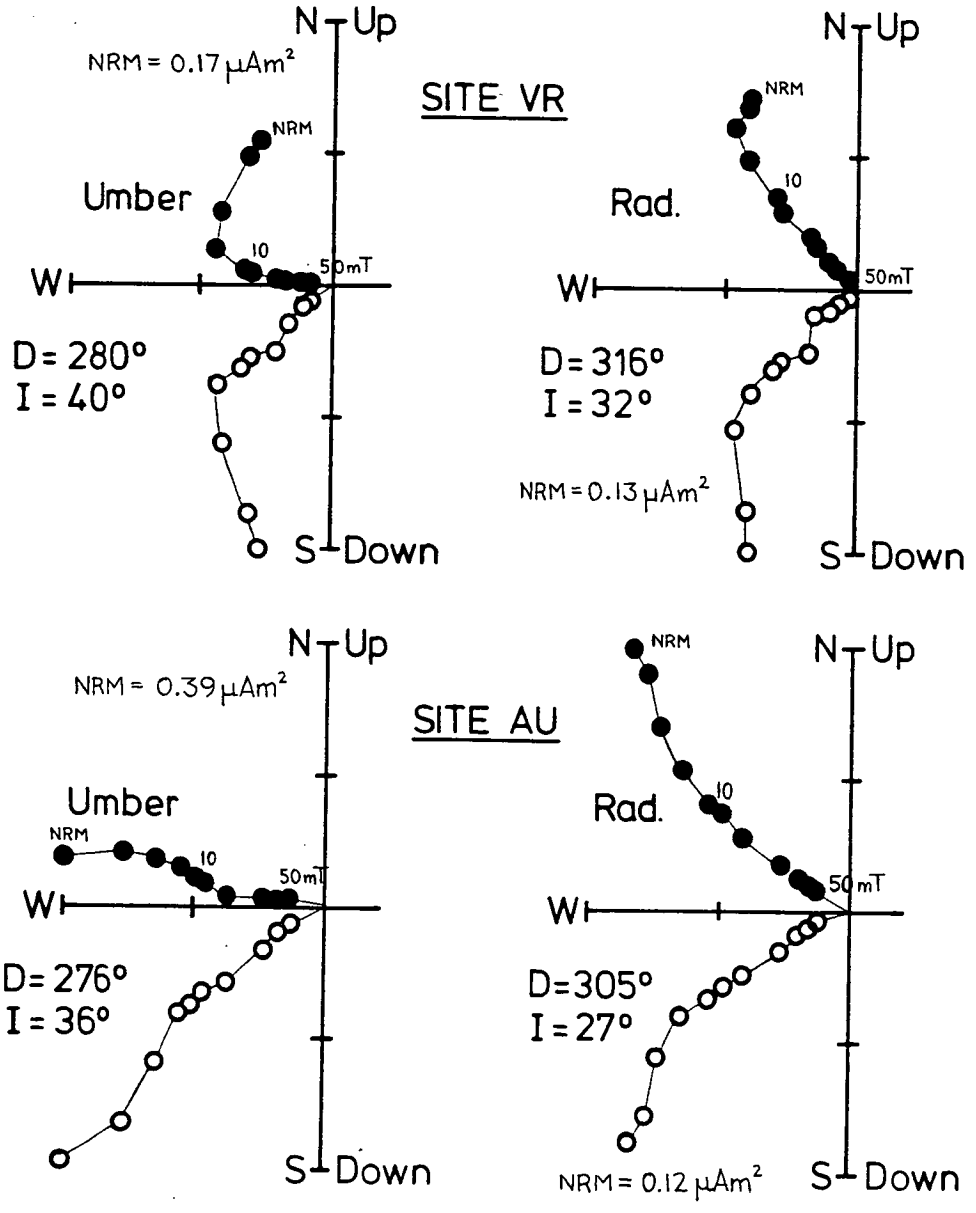

Figure 4.13. Zijderveld diagrams showing alternating field demagnetisation of umber and radiolarite samples from sites VR and AU. Note the more northerly declinations recorded by the radiolarite samples. Stratigraphic coordinates.

These results therefore indicate that at least 30° and possibly up to 45° of the 90° anticlockwise rotation of the Troodos microplate took place over a maximum of 15 Ma, between Turonian umber deposition and the end of Campanian radiolarite deposition.

4.4 Discussion of spreading axis configuration

It is now widely accepted that the Southern Troodos Transform Zone represents a fossil fracture zone which linked originally east-west orientated segments of a Neotethyan spreading axis (Simonian and Gass, 1978). I have shown that significant variations in declination of primary magnetisation between sites located within the transform zone are due to real tectonic rotations and not apparent rotations caused by the application of inappropriate structural corrections. Results obtained here demonstrate that predominantly *clockwise rotation* of small fault-bounded blocks about steeply inclined axes has occurred within the fracture zone. These results are consistent with *dextral shear* along the transform and hence a *sinistral offset* between the Troodos and 'Anti-Troodos' ridge segments. Original dyke orientations recovered at three sites along the Arakapas fault belt indicate that dykes were injected along a NW strike direction (present coordinates). This orientation is consistent with dyke intrusion in a sigmoidal stress system at a *dextrally* slipping transform.

These results are in agreement with a preliminary study of five sites located along the Arakapas fault belt (Clube and Robertson, 1986; Clube, 1986) in which north-westerly remanence directions were recovered from Upper Pillow Lavas pillows and interlava sediments. In addition, significant variations in the direction of magnetisation vectors have been reported (Bonhommet et al, 1988) at 13 dyke sites located in the zone of dyke deviation to the north of the Arakapas lineament. Cleaned remanence directions were found to cluster in the north-west and north-east quadrants and became more tightly grouped with a westerly declination after reorientating the dyke strikes to a north-south direction. The tilt-corrected inclination values found in this latter study were significantly higher than the inclination of the TMV (32°), with a mean value of 48°. This may indicate that the structural corrections applied were invalid as the technique of Allerton and Vine (1987) was not used to determine the net tectonic rotation affecting each site. Even so, an overall clockwise sense of dyke motion would still be required to account for the deviation of the magnetisation vectors with respect to the TMV.

More recent work by Allerton (1988b) on greenschist and zeolite facies dykes exposed further to the east in the Lefkara region, to the north of the eastward extension of the Arakapas fault belt, has also demonstrated the presence of major clockwise block rotations about steeply inclined axes.

All four studies therefore show that substantial clockwise tectonic rotations have occurred in the vicinity of the Southern Troodos Transform Zone. Palaeomagnetic evidence therefore does not appear to support a dextral offset configuration for the Troodos axis system.

A modern day analogue of the Southern Troodos Transform Zone is the Tjörnes Fracture Zone, Iceland. This transform is known to have an overall right-lateral sense of motion (Young, 1985). However, to the south of the transform a progressive change in the strike of lava units is seen, similar to that observed to the north of the Arakapas fault belt (Figure 4.14). Left-lateral strike-slip along the fracture zone could be inferred if this curvature is compared with similar lineations seen in GLORIA sonograph studies of the Quebrada-Gofar fracture zones along the East Pacific Rise (Searle, 1983) (Figure 4.15). However, the known slip direction and preliminary palaeomagnetic data indicating significant tectonic rotations within the Tjörnes Fracture Zone clearly show that the observed swing in the orientation of lava units is not a primary feature of the spreading process (Young, 1985).

The extent of the zone along the Southern Troodos transform system where the observed rotations could take place is not clear at present. Recently, Allerton (1989) has pointed out that in both the Tjörnes Fracture Zone and the Southern Troodos Transform Zone a 10 km wide strip of crust has been affected by simple shear, with associated rotation of fault blocks extending outside the transform domain. By contrast, studies of contemporary oceanic transforms suggest that deformation is restricted to a single fault trace within the transform domain (Fox and Gallo, 1984). Allerton (*op. cit.*) has proposed a model which attempts to reconcile this apparent inconsistency by suggesting that rotations occur at the ridge-transform intersection during accretion of crust. The strains calculated by Allerton in this model indicate extension at the ridge, simple shear at the transform, and composite strains in a region of distributed deformation in the ridge-transform corner. Faults at this intersection would be dominantly dip-slip with a small but significant component of strike-slip movement, sufficient to produce the required rotations. Such a model would elegantly explain synchronous rotation and dyke intrusion (e.g. at site EP in this study). However, the possibility that rotations occur along a longer zone within the transform domain cannot be excluded.

Following recent detailed remapping of the Eastern Limassol Forest Complex, MacLeod (1990) has proposed that the Southern Troodos Transform Zone was locally disrupted during the early stages of palaeorotation of the Troodos microplate. The model of MacLeod (*op. cit.*) involves initial genesis of the Eastern Limassol Forest Complex crust at an 'Anti-Troodos' spreading axis adjacent to a sinistrally slipping transform, accepting the conclusions of Murton (1986). This 'Anti-Troodos' crust exhibits a similar

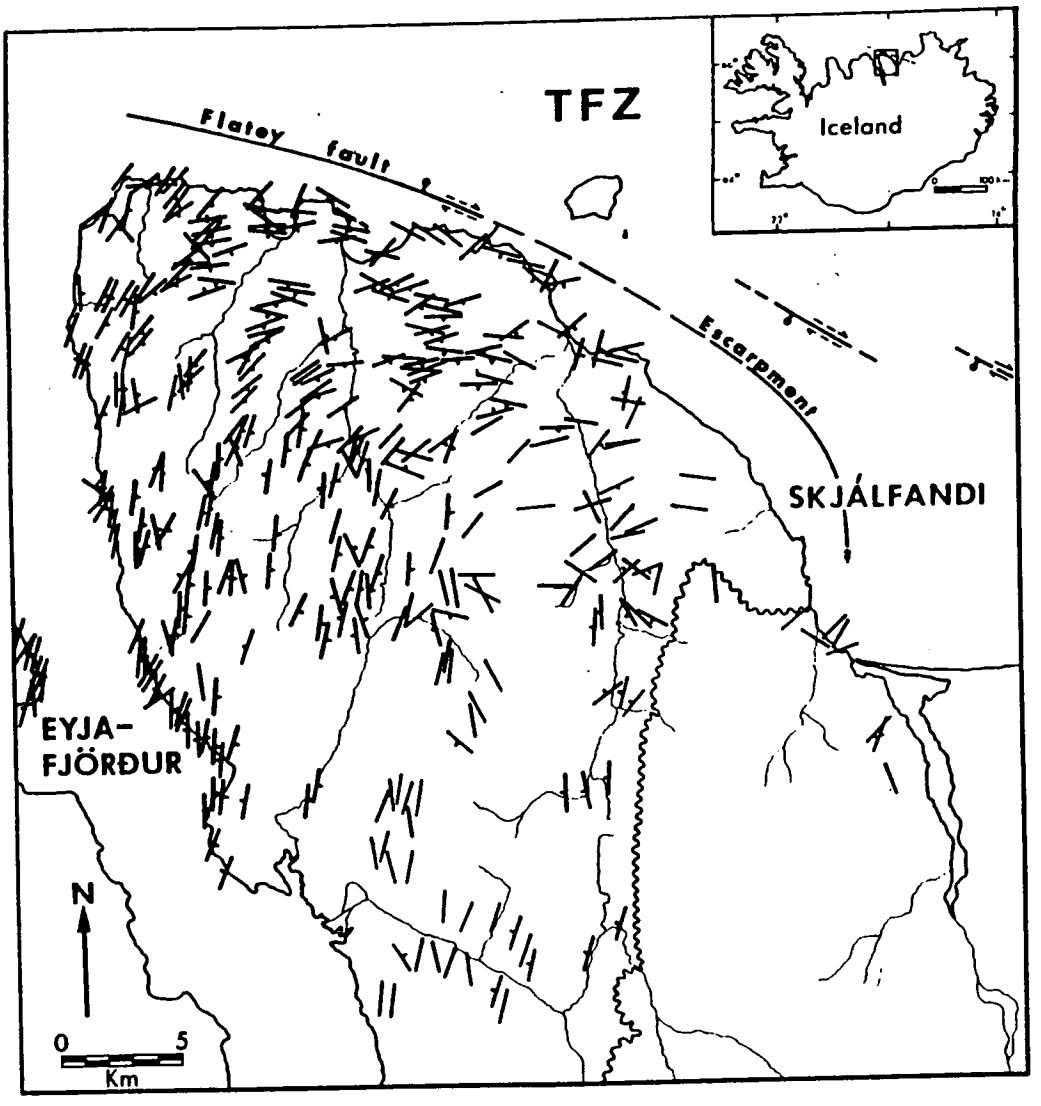

Figure 4.14. Basaltic dyke orientations in Flateyjarskagi, adjacent to the dextrally slipping Tjörnes Fracture Zone (TFZ). Note the change in dyke orientation as the transform zone is approached from the south. Frequencies of dykes shown do not rigourously reflect actual dyke densities in the field (from Young *et al.* 1985).

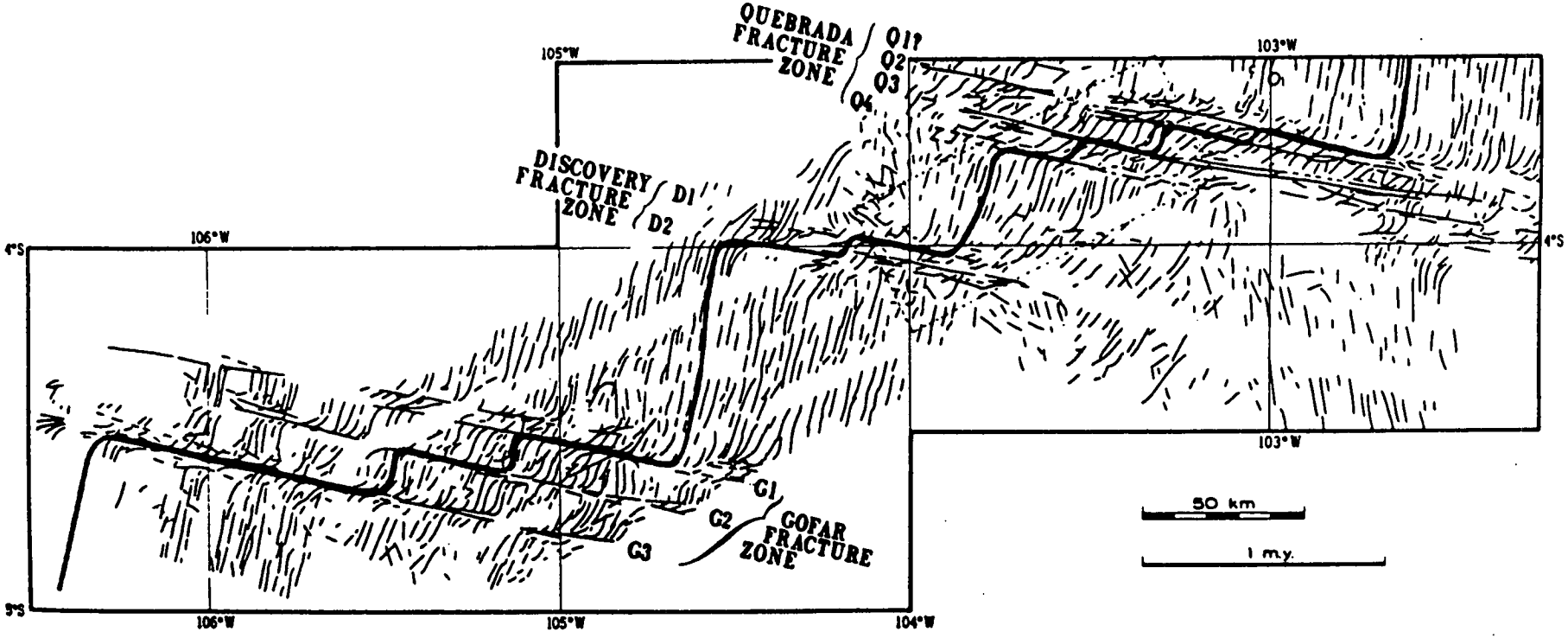

Figure 4.15. Tectonic lineaments in the vicinity of the Quebrada and Discovery fracture zones, along the East Pacific Rise, inferred from GLORIA sonographs. Heavy line indicates inferred plate boundary (from Searle, 83).

stratigraphy and geochemistry to that of the Troodos ophiolite as a whole. Post-oceanic disruption of the transform domain is then believed to have occurred in two stages. Firstly, regional extension was initiated during deposition of the umbers and radiolarites, which show evidence of progressive tilting. Extension in the northern part of the Eastern Limassol Forest Complex was primarily accommodated by reactivation of transform structures. At this stage fault blocks were rotated about north-west axes above a sub-horizontal décollement surface located in the lower part of the layered plutonic complex (the Akapnou Forest Décollement, Figure 4.16). During the second stage, initial rotation of the Troodos microplate in the Campanian-Maastrichtian interval imposed a frictional drag along the southern margin of the microplate. The Arakapas fault belt lay close to the inferred position of this margin, and this drag resulted in dextral reactivation of previously developed extensional structures. MacLeod (1990) believes that the clockwise block rotations observed within the transform zone are related to this second stage of deformation (Figure 4.16).

MacLeod (1988) reports palaeomagnetic data from seven sites within the Eastern Limassol Forest Complex which are used to support this model of post-oceanic rotational deformation. The application of the method of Allerton and Vine (1987) to these data yielded inclined poles of clockwise rotation clustering in the southwest quadrant for five sites, while the remaining two sites showed sub-horizontal rotation axes.

Data obtained at site EP in the present study indicate that rotations were occurring while dykes were still being injected. This clearly shows that rotation of blocks along the Arakapas fault belt was concurrent with Turonian crustal genesis. Thus, block rotation there cannot reflect dextral reactivation of originally sinistral east-west transform lineaments by later anticlockwise rotation of the microplate. In addition, the Turonian lavas, interlava sediments and umbers sampled at my four sites in the Eastern Limassol Forest Complex, and at three previous sites analysed by Clube (1986), exhibit only simple tilting about nearly strike-parallel sub-horizontal axes. A further site at Monagroulli studied by Clube (*op. cit.*) showed a tilt corrected declination of 313°. If these data are considered in conjunction with those from the seven sites reported by MacLeod (1988) then the style of rotational deformation in the Eastern Limassol Forest is not palaeomagnetically distinguishable from that found along the Arakapas fault belt. A suggestion of MacLeod (1988) which cannot be excluded is that the rotations occurring about inclined poles in the *Eastern Limassol Forest Complex* are due to local reactivation of extensional structures during microplate rotation. However, I prefer a model in which both the mapped transform fault and adjacent oceanic crust both to the north (Bonhommet *et al*, 1988) and to the south was the site of a complicated system of

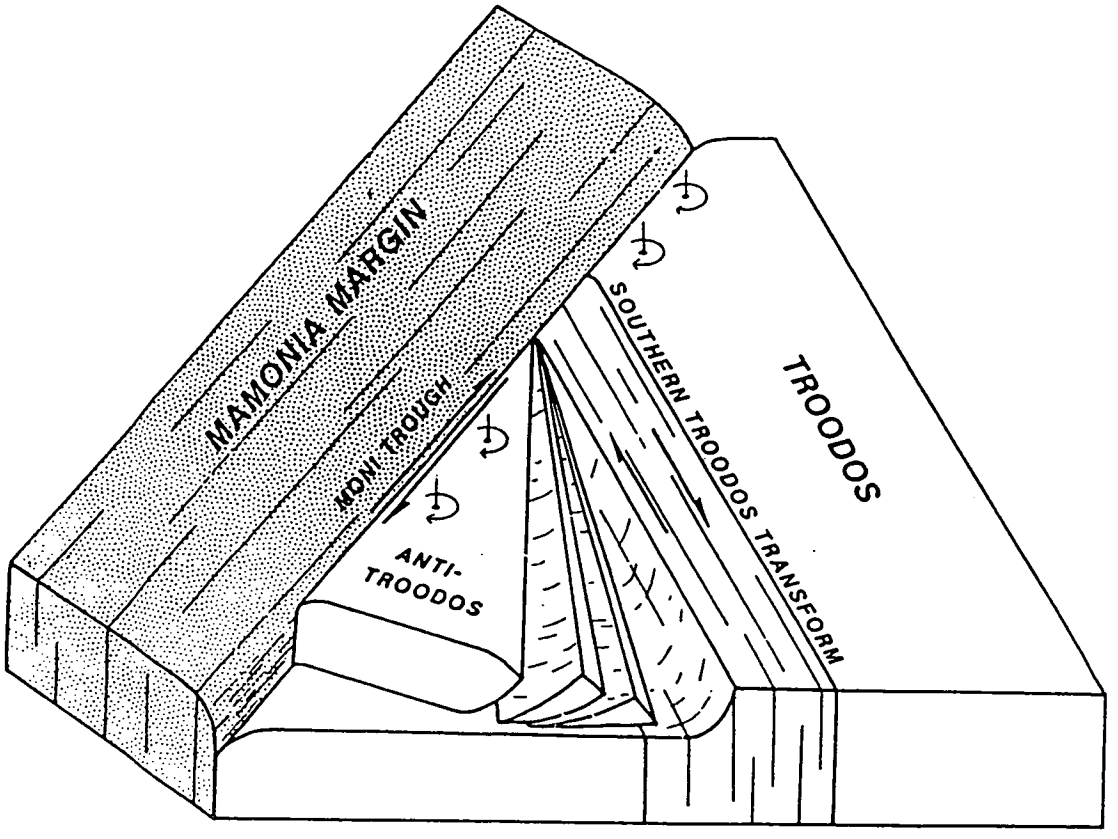

Figure 4.16. The configuration of the southern Troodos margin in the late Campanian-early Maastrichtian as suggested by MacLeod (1990). The Troodos oceanic crust has been brought close to the fragmented Mamonia continental margin by dextral strike-slip along a major lineament blanketed by the Moni mélange, and significant angular rotation of the ophiolite is now commencing. The lineament is inferred to be slightly oblique to the trend of the Southern Troodos Transform Fault, thus incorporating transform-tectonised blocks into the Mamonia Complex to the present day west, and preserving a fragment of the 'Anti-Troodos' plate to the east. In this model, frictional drag along the southern boundary of the Troodos microplate is responsible for clockwise block rotations and reactivation of originally sinistrally-slipping transform lineaments in a dextral sense (from MacLeod, 1990).

localised, predominantly clockwise block rotations; some areas were rotated by over 100° about steeply inclined axes, whereas others experienced only simple tilting. Rotations outside of the immediate fault zone may have occurred at the ridge-transform intersection (Allerton, 1989). The whole area underwent later passive anticlockwise rotation by 90° as part of the Troodos microplate.

Finally, structural (Varga and Moores, 1985) and palaeomagnetic (Allerton and Vine, 1987) studies along the northern margin of the Troodos ophiolite suggest that the Troodos spreading system may have experienced non-steady state spreading, possibly involving ridge jumping. If correct this could have given rise to a complex situation with areas of crust being incorporated within or stranded outside the region of active slip between the two plates. The possibility of reversals of motion along the Southern Troodos Transform therefore could not be excluded. However, the extensive palaeomagnetic evidence of widespread clockwise rotation of lavas, dykes and sediments points to a dominance of right-lateral slip within the transform domain. Such rotations could not have been identified by field structural studies alone and confirm the importance of rotations about steeply inclined axes in deformed oceanic crust adjacent to transform faults.

4.5 Conclusions.

Significant intra-crustal rotations of small fault-bounded blocks have taken place within the Southern Troodos Transform Zone. These rotations are considered to represent primary features of crustal genesis and can not be attributed simply to post-oceanic disruption of the fracture zone. The predominantly clockwise sense of block rotation suggests that the Troodos ridge system had a sinistral offset configuration. This is supported by original north-west dyke strikes found along the Arakapas fault belt which are consistent with a stress field operating across a dextrally slipping transform.

Additional palaeomagnetic data obtained from the umbers and radiolarites of the Perapedhi Formation confirm that the Campanian period was a time of rapid rotation of the Troodos microplate, with up to 45° of rotation occurring over 15 Ma.

PART THREE - TURKEY.

CHAPTER FIVE - GEOLOGY AND PALAEOMAGNETISM OF S. W. TURKEY: A REVIEW.

5.1 General.

This section is devoted to a palaeomagnetic study of the Mesozoic and Tertiary units which occur in the 'Isparta angle' region of southwestern Turkey. This area forms a critical suture which separates the main Tauride (to the east) and Hellenide (to the west) segments of the eastern Mediterranean Tethyan belt.

The samples analysed for the present study were collected by T. M. M. Clube (with the assistance of A. H. F. Robertson, K. M. Creer and R. Sutherland) in 1984, during the final field-season of his doctoral studies. The aim of the sampling was to discover whether the autochthonous and para-autochthonous basement elements exposed in this part of southern Turkey experienced a different palaeorotation history to that of the adjacent Troodos ophiolite complex (discussed in Chapter 3), and to test the hypothesis that the southwestern area of the Antalya Complex was a strike-slip zone in the Late Cretaceous to Early Tertiary. However, time constraints prevented Clube from making more than a few preliminary measurements. Thus, as a starting point for the laboratory work in the present study, the complete sample collection and accompanying field notes were made available to me for detailed palaeomagnetic analysis. As mentioned in the introductory chapter to this thesis, the original purpose of the present doctoral study was to continue sampling within the Isparta angle on the basis of the results of this analysis, and to extend this work to other critical areas in Turkey, such as the Pontides. However, it subsequently became difficult to obtain the necessary permits for working in Turkey, and so the project was broadened to encompass a much wider geographical area, and sampling was carried out in other key areas within the Tethyan belt. Nevertheless, analysis of the preliminary sample collection obtained by Clube has yielded some interesting and important data.

I begin this section of the thesis then with a brief review of the geology of southwestern Turkey, and a discussion of previous palaeomagnetic work within the region. I go on in Chapter 6 to present the palaeomagnetic data obtained in this study, and to discuss their bearing on the evolution of the Isparta angle.

5.2 Regional geology

The study area forms part of the Tauride mountain chain, which lies to the south of the Anatolian plateau and runs for some 1500 km between the Aegean Sea and Iran (see Figure 2.07). The Taurides form an arcuate belt divided into two limbs either side of the Gulf of Antalya (Figure 5.01). The junction of the two limbs to the north of Antalya is termed the 'Coubure d'Isparta' or 'Isparta angle'.

5.2.1 Eastern Taurides.

To the east of Antalya, the Eastern Taurides comprises a series of para-autochthonous slices dominated by Mesozoic shallow water carbonates. Erosion to a deep structural level reveals that the carbonates are underlain by a Triassic sequence, including thick turbiditic sandstones and shales, resting on Palaeozoic sedimentary rocks. Resting upon these slices are the Beysehir-Hoyran-Hadim nappes (Figure 5.01; Brunn *et al.*, 1970; Monod, 1977). These nappe units contain an ophiolite unit, together with a diverse assemblage of Mesozoic and Permian sedimentary rocks, including shallow water carbonates, flysch and volcaniclastic sandstones overlain by Mesozoic pelagic limestones. The nappe's root-zone lies to the northeast beneath a thick cover of Neogene fluvial and lacustrine sediments of the Anatolian plateau. These nappes were emplaced during the Eocene and are now preserved along the axis of a later gentle syncline.

5.2.2 Western Taurides.

The Western (or Lycian) Taurides have been considered as an extension of the Hellenide orogenic belt of Greece (Brunn *et al.*, 1976; Bernoulli *et al.*, 1974). On a regional scale, the Lycian Taurus consists of a central para-autochthonous unit, the 'Tauride autochthon' (Brunn *et al.*, 1970; Dumont *et al.*, 1972), either side of which lie two allochthonous units; the Lycian Nappes to the northwest and the Antalya Complex to the east.

The Lycian Nappes form an edifice of allochthonous sheets believed to have been transported from the northwest towards the southeast in a number of phases during the Early Tertiary, ending with emplacement into their present position in Miocene times. Within the nappes, Brunn *et al.* (1970, 1971) and Poisson (1977) have described a number of distinct stratigraphic sequences of Mesozoic to Early Tertiary age, showing

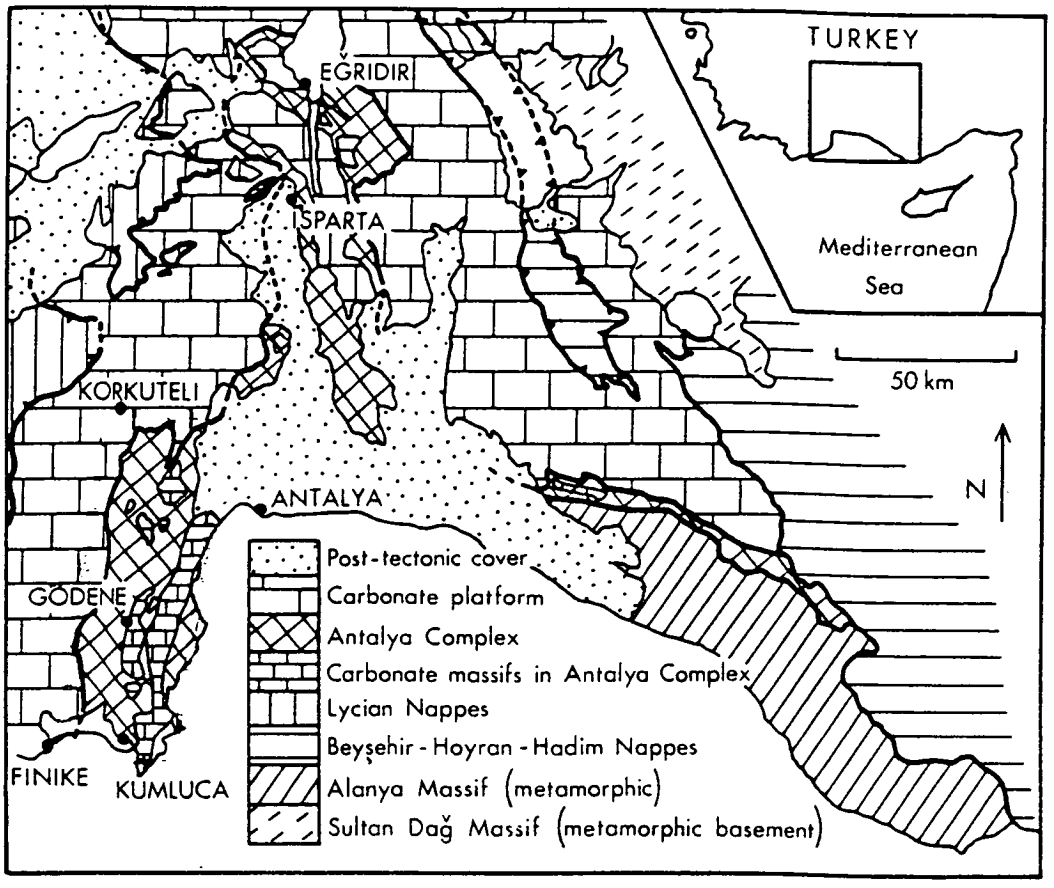

Figure 5.01. Map showing location of the Tauride platform units, Beysehir-Hoyran-Hadim nappes and Alanya massif.

facies ranging from shallow-water platform carbonates, through redeposited slope breccias, to pelagic limestones and cherts. Some of the sequences terminate in flysch, varying in age from Turonian to Late Eocene. Delaune-Mayere *et al.* (1977) interpret these sequences as different parts of a Mesozoic continental margin, which was subsequently telescoped during Late Cretaceous and Early Tertiary orogeny. So-called 'ophiolitic' units, consisting of slivers of peridotite and diabase, are intercalated between the nappes, and the edifice is capped by the 'Peridotite Nappe', which consists mainly of harzburgite cut by pyroxenite and dolerite dykes.

To the northwest of the Lycian nappes lies the Menderes Massif, composed of gneisses overlain by mica-schists and marbles of probable Palaeozoic age. Its structural relationship to the Lycian Nappes is uncertain.

The Lycian Nappes rest upon the central unit of the Lycian Taurus, the Taurus autochthon. This consists of a regionally extensive unit of shallow water limestones of a carbonate platform ranging in age from Liassic to Lower Miocene (Aquitanian) (Poisson, 1977). This unit forms the limestone massifs of the Susuz Dag and Bey Daglari. The carbonates are capped by detrital sediments, related to emplacement of the Antalya Complex. During Maastrichtian to Palaeocene times, ophiolite-derived clastic sediments were deposited all around the Isparta angle. After a period of local non-deposition during the Oligocene, carbonate sedimentation resumed in the Early Miocene, and was followed by an influx of flysch-type terrigenous sediments, on top of which rest the Lycian Nappes.

5.2.3 The Antalya Complex

A third group of allochthonous rocks are present in the centre of the Isparta angle, in a relatively 'external' position in the orogenic belt. These constitute the Antalya Nappes of Lefèvre (1967), or the Antalya Complex of Woodcock and Robertson (1977a). In addition, to the east of Antalya is a large area of variably metamorphosed Palaeozoic sediments known as the Alanya Massif (Figure 5.01). This too is located in a relatively external position and appears also to be allochthonous, resting tectonically above the Antalya Complex (Okay and Özgül, 1984)

In the Antalya Complex, Brunn *et al.* (1971), Marcoux (in Delaune-Mayere *et al.*, 1977), Allasinaz *et al.* (1974), Monod (1977, 1978), Dumont (1976), and Robertson and Woodcock (1982) have distinguished a great variety of Mesozoic sedimentary facies, including turbiditic sandstones, pelagic limestones, radiolarites, redeposited limestones, and ophiolite-derived sandstones. Massive limestones of shallow-water origin also occur, overlying Ordovician to Permian sandstones, mudstones and limestones (Kemer unit). In

addition, an ophiolite suite (Tekirova unit) is represented by pillow lavas, dolerites, gabbros, dunites, and peridotites (Juteau, 1975). Minor occurrences of metamorphic rocks are also known (Juteau, 1975; Woodcock and Robertson, 1977b).

Sedimentological and structural work by Robertson and Woodcock (1980b, 1981a, b, c, 1982, 1984) and Woodcock and Robertson (1977a, 1982) has established a zonal scheme for the southwestern segment of the Antalya Complex. These workers have demonstrated that strike-slip movements, as well as thrust faulting, played an important part in the emplacement of the Complex onto the adjacent Bey Daglari carbonate platform. Hayward (1984) describes Tertiary foredeep sediments derived from the Complex during this emplacement. The less well-organised northern segment of the Complex has been reconstructed in some detail by Waldron (1984a, b), who demonstrated that in this area a complex mosaic of carbonate platforms and intervening basins existed during the Mesozoic and Tertiary. These studies have demonstrated that the Antalya Complex records the initiation, development and tectonic disruption of a segment of a Mesozoic/Cenozoic continental margin. They are now discussed in detail in the next section, which also outlines the preferred model for the tectonic history of the area.

5.3 Tectono-sedimentary model for the evolution of the Antalya Complex.

5.3.1 Original ocean.

As noted above, the Antalya Complex occurs in a relatively external position in the Tauride mountain belt, to the south of the major Mesozoic-Tertiary carbonate platforms. This is in common with the other southern ophiolites of the area (Troodos, Hatay, and Baër Bassit). Ricou *et al.* (1979, 1984) and Marcoux *et al.* (1989) proposed a tectonic explanation for this distribution, in which the external ophiolites and pelagic sediments of Antalya, Troodos and Baër Bassit are interpreted as klippen of a Late Cretaceous nappe transported southwards over the carbonate platform. However, the results of detailed field studies rule out such an origin for the Antalya Complex, as discussed in section 2.4.2. Also, in Cyprus the presence of a continuous pelagic sedimentary sequence above the Troodos ophiolite (Robertson and Hudson, 1974) rules out Cretaceous long distance nappe transport from the north. The external ophiolites must therefore have originated in an ocean basin between the northern Tauride carbonate platform autochthons (Bey Daglari, Anamas Dag, Akseki) and the continental massif of Africa and Arabia. This basin has been referred to as the 'Troodos Ocean' (Robertson and Woodcock, 1980a) or the 'southern strand of the Neotethys' (Robertson and Dixon, 1984). It is in part equivalent to the 'Pamphylian Basin' of Dumont *et al.* (1972), 'Tethys

2' of Dewey *et al.* (1973), and to parts of the 'Mesogean ocean' of Dercourt *et al.* (1986) (see section 2.4.4).

5.3.2 Zonation of the SW Antalya Complex.

Robertson and Woodcock (1980b, 1981a, b, c, 1982, 1984) subdivided the SW Antalya Complex area (Figure 2.13) into five north-south trending structural zones, usually bounded by tectonic contacts (Figure 5.02). These represent a Mesozoic continent-ocean transition (Robertson and Woodcock, 1981a, c). From west to east these zones are:

(i) *Bey Daglari Zone*: a relatively autochthonous Mesozoic carbonate platform unit, founded on continental crust, which became pelagic by mid-Late Cretaceous time (Poisson, 1977), and which passes conformably up into Miocene ophiolite-derived clastics (Hayward and Robertson, 1982; Hayward, 1984).

(ii) *Kumluca Zone*: a north-south trending imbricate thrust unit of Upper Triassic to Upper Cretaceous quartzose clastics, hemi-pelagic and pelagic sediments. The Kumluca Zone is interpreted as the former passive margin of the Bey Daglari carbonate platform (Robertson and Woodcock, 1981a, b).

(iii) *Gödene Zone*: a complexly deformed, mostly steeply dipping zone of Upper Triassic alkalic mafic extrusives and associated Late Triassic to Late Cretaceous deep sea sediments, plus intrusive ophiolitic rocks, mountain-sized shallow water carbonate massifs, and minor metamorphic rocks (Juteau, 1975; Delaune-Mayere *et al.*, 1977; Robertson and Woodcock, 1981c). This zone represents an Upper Triassic ophiolite formed during the initial stages of continental separation to form a Mesozoic ocean basin. The carbonate massifs within the zone are interpreted as substantial carbonate build-ups founded on continental slivers rifted from the parent margin during this separation (Robertson and Woodcock, 1981c). The Gödene marginal oceanic crustal zone is dominated by an array of north-south striking vertical faults, often serpentinite-filled, separating lozenges of more coherent rocks. The anastomosing fault pattern, steeply plunging asymmetric folds and sigmoidal and oblique intra-lozenge structures have been interpreted as indicating a strong strike-slip deformation component (Woodcock and Robertson, 1982).

(iv) *Kemer Zone*: a zone dominated by again mostly steeply dipping north-south trending masses of Ordovician to Upper Cretaceous sedimentary rocks, plus smaller volumes of mafic lavas and basinal sediments similar to the Gödene Zone. This zone represents the largest of the continental slivers to rift off the parent margin in the Triassic (Woodcock and Robertson, 1982).

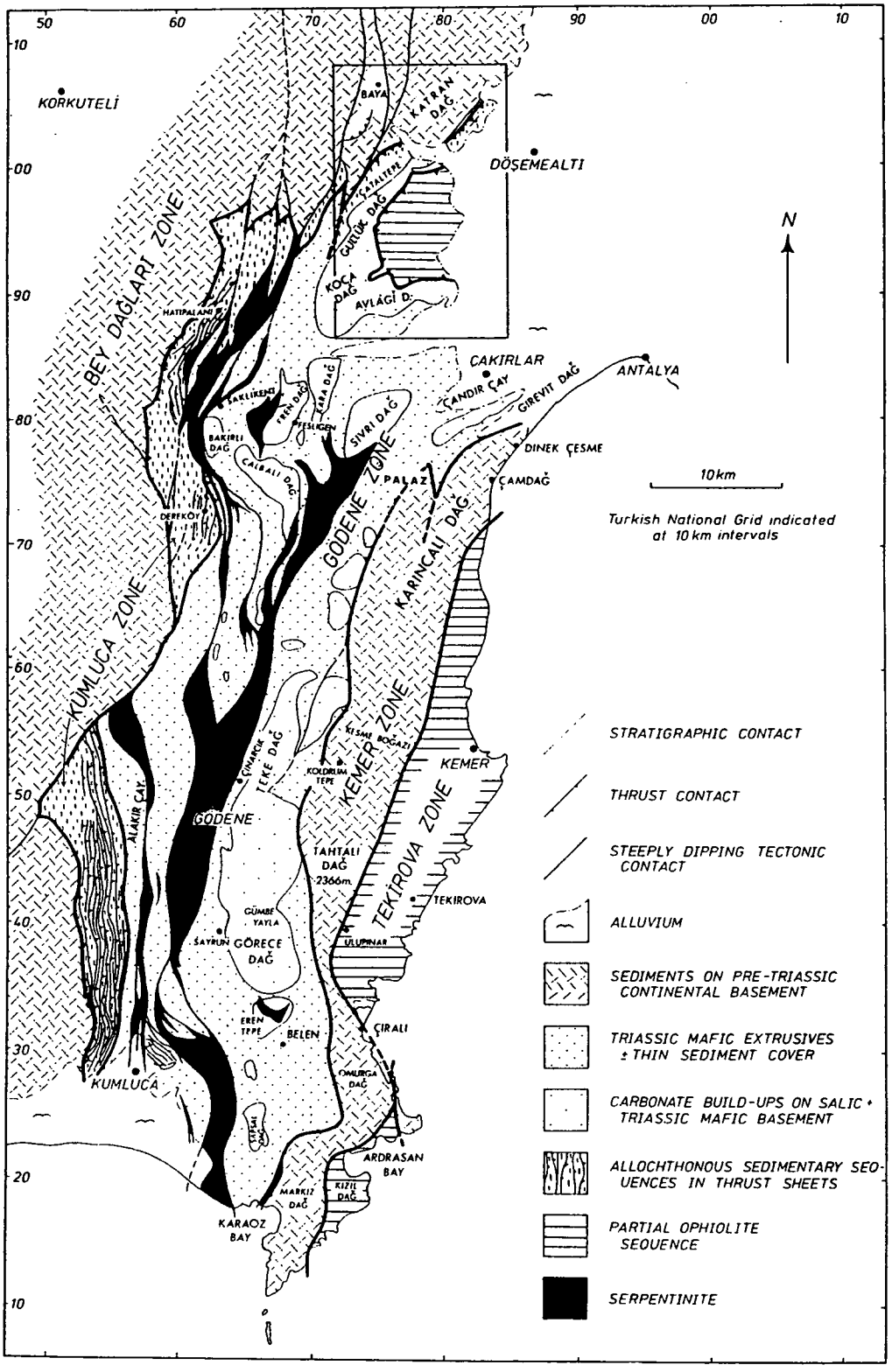

Figure 5.02. Map of the SW Antalya Complex showing the tectonic zonation of Robertson and Woodcock (1980b, 1981a, b, c, 1982, 1984). From west to east, the zones are: (i) *Bey Daglari Zone* - a relatively autochthonous Mesozoic carbonate platform, topped by Miocene ophiolite-derived clastics; (ii) *Kumluca Zone* - the tectonically imbricated former passive margin of the Bey Daglari platform; (iii) *Gödene Zone* - Late Triassic marginal oceanic crust, with carbonate-topped off-margin continental slivers, formed during the initial stages of continental separation; (iv) *Kemer Zone* - the largest off-margin continental sliver; (v) *Tekirova Zone* - a Late Cretaceous partial ophiolite sequence.

(v) *Tektrova Zone*: a major ophiolite complex exposed along the present coast. Only intrusive parts of the ophiolite are preserved. This represents a remnant of Late Cretaceous oceanic crust, more comparable with the Troodos massif of Cyprus than with the now adjacent Late Triassic marginal crust of the Gödene Zone (Woodcock and Robertson, 1982).

Figure 5.03 shows a series of summary logs of the chief sedimentary successions in each of the zones (from Robertson and Woodcock, 1984).

5.3.3 Tectonic interpretation of the SW Antalya Complex.

The sedimentological and structural features of the five zones defined by Robertson and Woodcock (1980b, 1981a, b, c, 1982, 1984) were used by these authors to reconstruct the palaeogeography of the SW Antalya area during the Mesozoic and Tertiary. In this model, this segment of the Antalya Complex is interpreted as the eroded remnants of a Mesozoic continental margin destroyed in latest Cretaceous to Miocene times by a combination of wrench and thrust tectonics (Woodcock and Robertson, 1982). The palaeogeographic schemes of Robertson and Woodcock (*op. cit.*) are illustrated in Figure 5.04, and their model is outlined below.

The Antalya Complex originated as a braided Triassic intra-continental rift located along the northern margin of Gondwanaland, comparable to the Neogene Gulf of Suez (Figure 5.04a; Figure 2.19a). Crustal extension was probably achieved by large-scale listric faulting generating both deep pelagic basins into which thick piles of mafic alkalic lavas were erupted, and basement highs forming seamounts capped by carbonate complexes (Gödene and Kemer Zones; Robertson and Woodcock, 1981c). To the west, the Bey Daglari carbonate platform became defined. After the end of volcanism the area subsided progressively under thermal control. Reefs on the main margin and on the off-margin highs grew apace. In the model of Robertson and Woodcock (1984), the area was interpreted as an elongate sediment-starved gulf during Early and Mid Jurassic time, comparable to the Neogene Red Sea prior to ocean spreading. However, new geochemical data now suggest that the Antalya basin at this time was wider and formed a small ocean basin, floored by crust with a transitional to MORB-like geochemistry (Robertson *et al.*, in press).

In the Late Jurassic to Early Cretaceous, a regime dominated by north-south strike-slip faulting was initiated (Woodcock and Robertson, 1982). This was marked by fresh volcanism. From this time onwards the basin progressively widened, becoming comparable in size to the Gulf of California by the Mid Cretaceous.

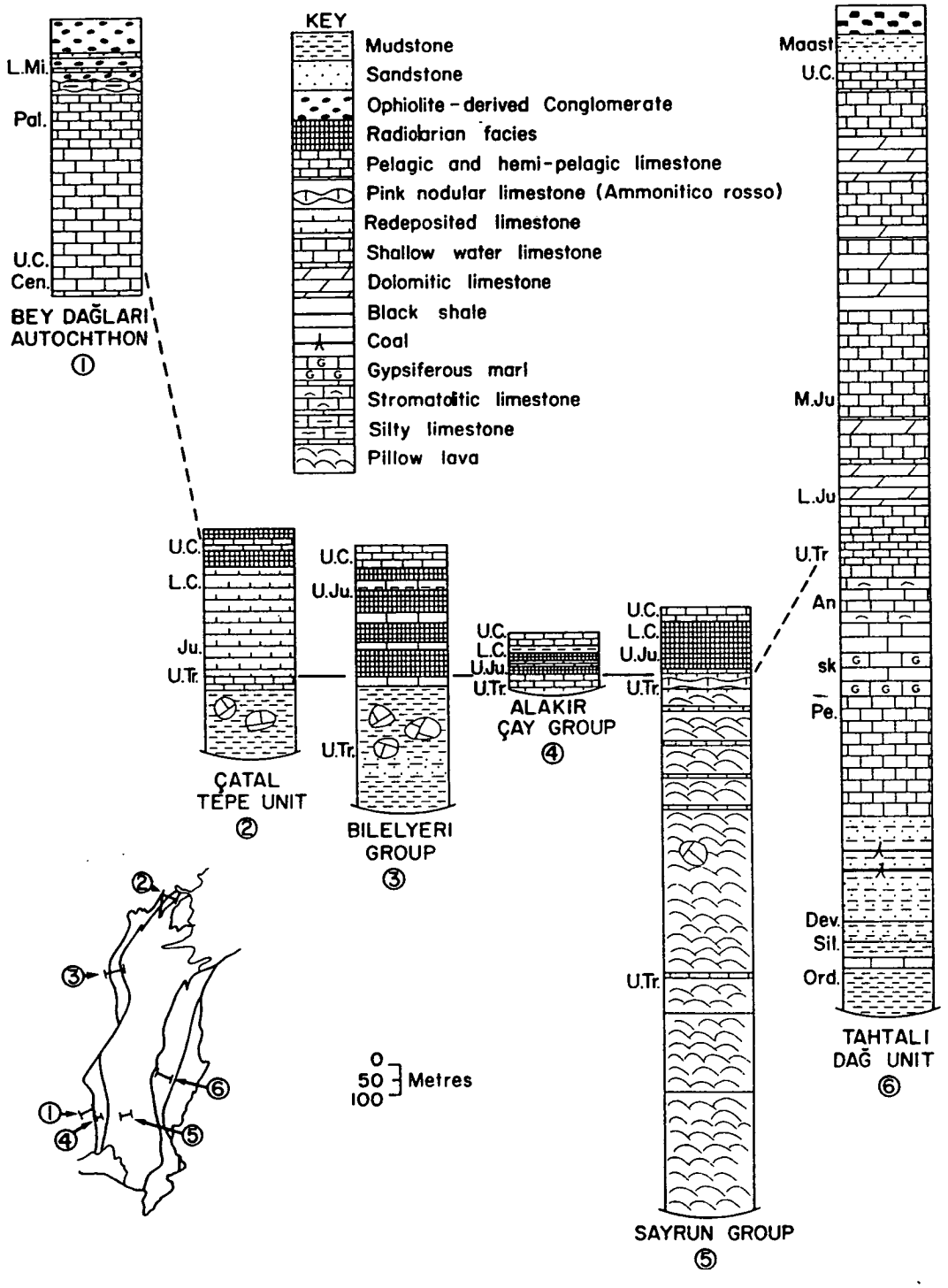

Figure 5.03. Composite sedimentary logs summarising the main sedimentary succession in each of the tectonic zones of the SW segment of the Antalya Complex (excluding the Late Cretaceous ophiolite of the Tekirova Zone). The location of the composite logs are shown (from Robertson and Woodcock, 1984).

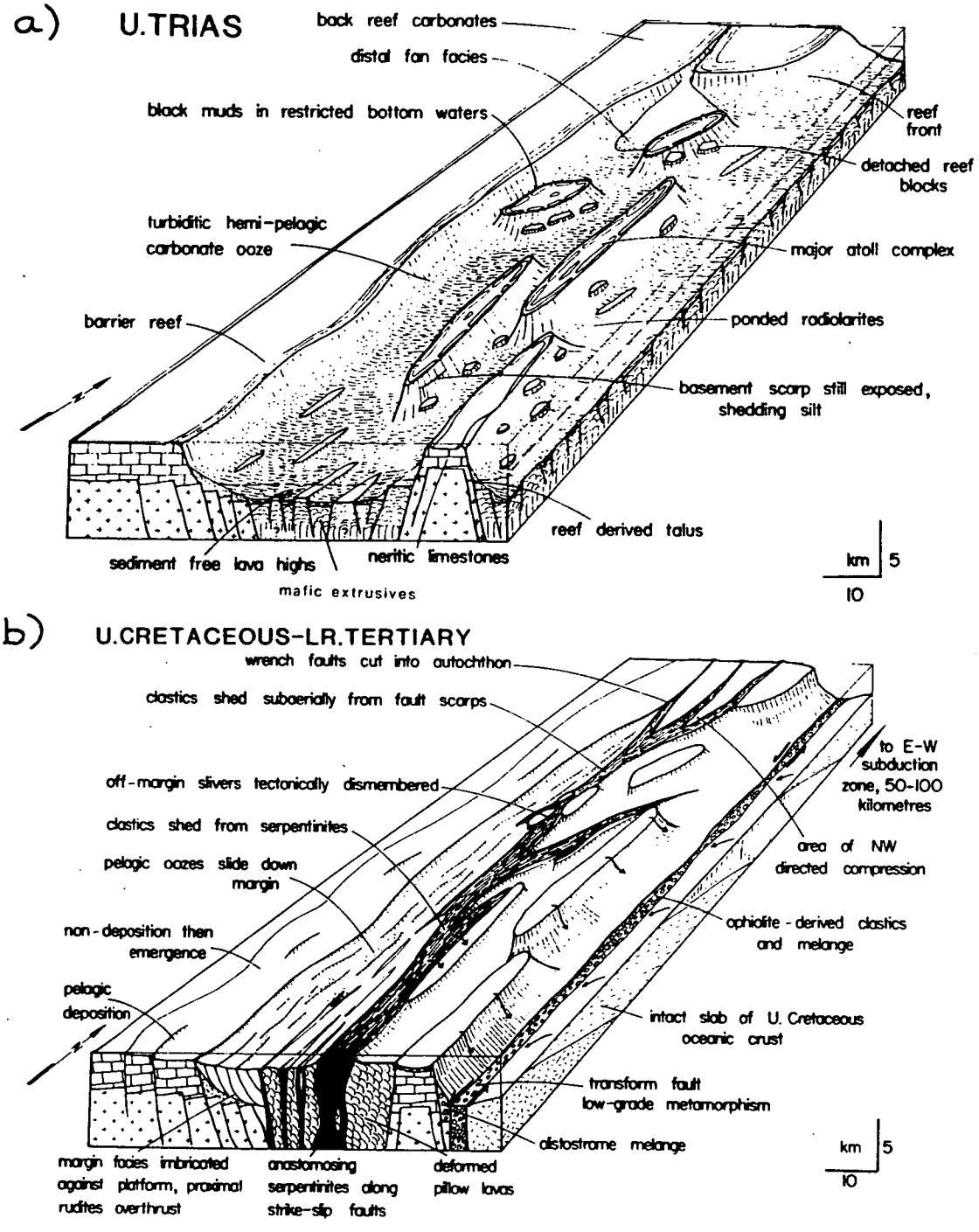

Figure 5.04. Block diagrams showing the SW Antalya palaeogeography during Upper Triassic and Upper Cretaceous to Early Tertiary time (from Robertson and Woodcock, 1984). a) shows the pattern of off-margin carbonate build-ups on basement highs formed in a wide extensional rift. Strike-slip faulting played little role until the onset of oblique ocean floor spreading, possibly in Upper Jurassic to Lower Cretaceous time; b) by Latest Cretaceous to Early Tertiary the carbonate margin was stacked against, but not over, the carbonate platform. The Tekirova coastal ophiolite was emplaced by sinistral strike-slip which also effected the ophiolites further west, where anastomosing strands of serpentinite were protruded. It should be noted that these diagrams illustrate the style of the margin and are not accurate palinspastic reconstructions.

During the Mid to Late Cretaceous the small ocean basin of the southern Neotethys opened (see Section 2.4.4 and Figure 2.19d), in response to the change to north-south convergence between Africa and Eurasia. The edge of a major basement high within the Antalya basin accommodated a submarine strike-slip controlled fault scarp during the final crustal separation. During strike-slip opening the former off-margin highs may have been strung out along the margin (Robertson and Woodcock, 1984). Oceanic crust, now represented by the Tekirova Zone ophiolite, formed at essentially east-west spreading axes. Primary structures preserved within the ophiolite indicate that the spreading axes were offset by sinistral transform faults (Reuber, 1984). The basin was closing northwards by latest Cretaceous times. The Antalya margin acted as a sinistral strike-slip fault zone (Figure 5.04b). During closure, slivers of oceanic crust were entrained between the carbonate platform (Bey Daglari Zone) and the former off-margin slivers to the east (Gödene and Kemer Zones). Close to the former continent-ocean boundary (the contact between the Kemer Zone and the Tekirova ophiolite), the ophiolite was intensely sheared, brecciated, uplifted and eroded to form shallow water breccias of Maastrichtian age. Low grade metamorphism took place along key strike-slip faults. Further west, the edge facies of the Bey Daglari platform were imbricated (Kumluca Zone).

Strike-slip faulting continued either continuously or episodically from the Upper Cretaceous throughout Palaeogene into Neogene time. Previously imbricated zones were cut by sub-vertical anastomosing strands of sheared serpentinite. These are interpreted as low temperature protrusions up strike-slip faults (Gödene Zone; Robertson and Woodcock, 1981c). Ophiolite-derived clastics accummulated in short-lived pull-apart basins (Robertson and Woodcock, 1980b). During Early to Mid Miocene time the deformed Antalya allochthon was thrust westwards over the edge of the carbonate platform (Bey Daglari Zone), shedding large volumes of first turbiditic, then alluvial fan clastics (Haywood, 1984). Miocene thrusting was possibly related to regional shortening connected with the emplacement of the Lycian Nappes further northwest. Only later in the Neogene did deformation cease. This was followed by drastic uplift of the limestone massifs of the Gödene and Kemer Zones, possibly isostatically controlled. By this time, the southern strand of the Neotethys had probably completely closed explaining why continental crust is now apparently present beneath the Antalya Bay area. The whole of the Antalya Complex is allochthonous with respect to the original parent carbonate platform and basement, except locally in the northeast area where a faulted contact between a carbonate platform (Anamas Dag) and its passive margin is still preserved (Waldron, 1984 a, b).

5.3.4 Palaeogeographic interpretation of the N Antalya Complex.

In contrast to the southwestern segment of the Antalya Complex, which was dominated by wrench and thrust tectonics during its development and subsequent emplacement onto the adjacent autochthon, the northeast segment of the Complex exhibits larger scale polyphase thrusting. This area was mapped in detail by Waldron (1984a, b). Between the major carbonate platforms of the Bey Daglari and Anamas Dag-Karacahisar, several smaller scale carbonate build-ups can be identified (Barla Dag, Dulup Dag, Davras Dag), separated tectonically by slices of more basinal facies. The structure and sedimentology of these intervening units led Waldron (1984b) to conclude that the carbonate massifs cannot be interpreted as fragments of a single continuous platform, but must represent a number of separated carbonate banks similar to the modern Bahamas (Figure 5.05). This model has been refined recently by Robertson *et al.*, (in press), who have reinterpreted the Dulup Dag and Sutculer Limestone units as a single shallow-water carbonate platform. They also correlate the Karacahisar platform with the much larger Anamas-Akseki unit.

5.3.5 Overall synthesis: development of the Isparta angle.

The Isparta angle shows no evidence to suggest major oroclinal bending of an originally straight mountain chain. Instead, it originated as two regions of continental crust, on which were developed carbonate platforms, separated by a zone of Cretaceous oceanic crust (Waldron, 1984a). A reconstruction of the area in Late Cretaceous time is shown in Figure 5.06 (see figure caption for details). During the Late Cretaceous, major changes in the relative motion of Africa and Eurasia (Livermore and Smith, 1984; Savostin *et al.*, 1986; see Sections 2.3 and 2.4.4) led to emplacement of the Antalya Complex between the carbonate platforms of the Anamas Dag and the Bey Daglari. Emplacement involved mainly thrust tectonics along the margin of the Anamas Dag (Waldron, 1984a, b), but strike-slip processes played an important role in the emplacement of the southwest segment of the Complex along the Bey Daglari margin (Woodcock and Robertson, 1982). As pointed out by Robertson and Woodcock (1984), it should not be thought at all surprising that the histories of the southwestern and northeastern segments of the Antalya Complex should differ so markedly. Both areas document originally complex Mesozoic palaeogeography with carbonate build-ups of various scales with intervening pelagic basins. Such variety in structural styles is exactly as expected from knowledge of modern passive and active continental margins.

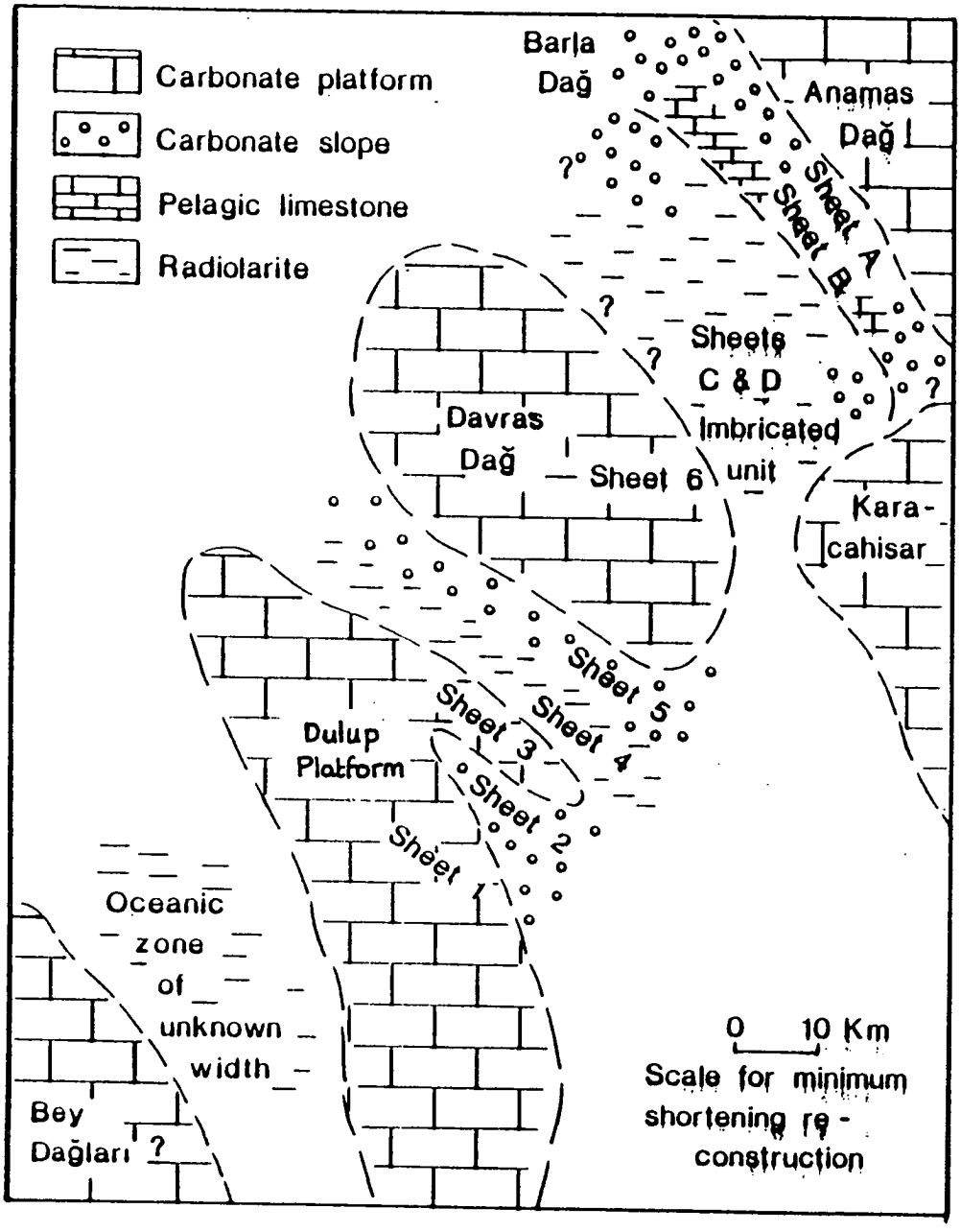

Figure 5.05. Schematic Late Cretaceous (Senonian) palinspastic map for units in the Northwestern Antalya Complex and adjacent areas. Units have been unstacked without rotation and assuming minimal translation for consistency with the outcrop. Actual size of banks and/or basins may have been much larger (from Waldron, 1984a).

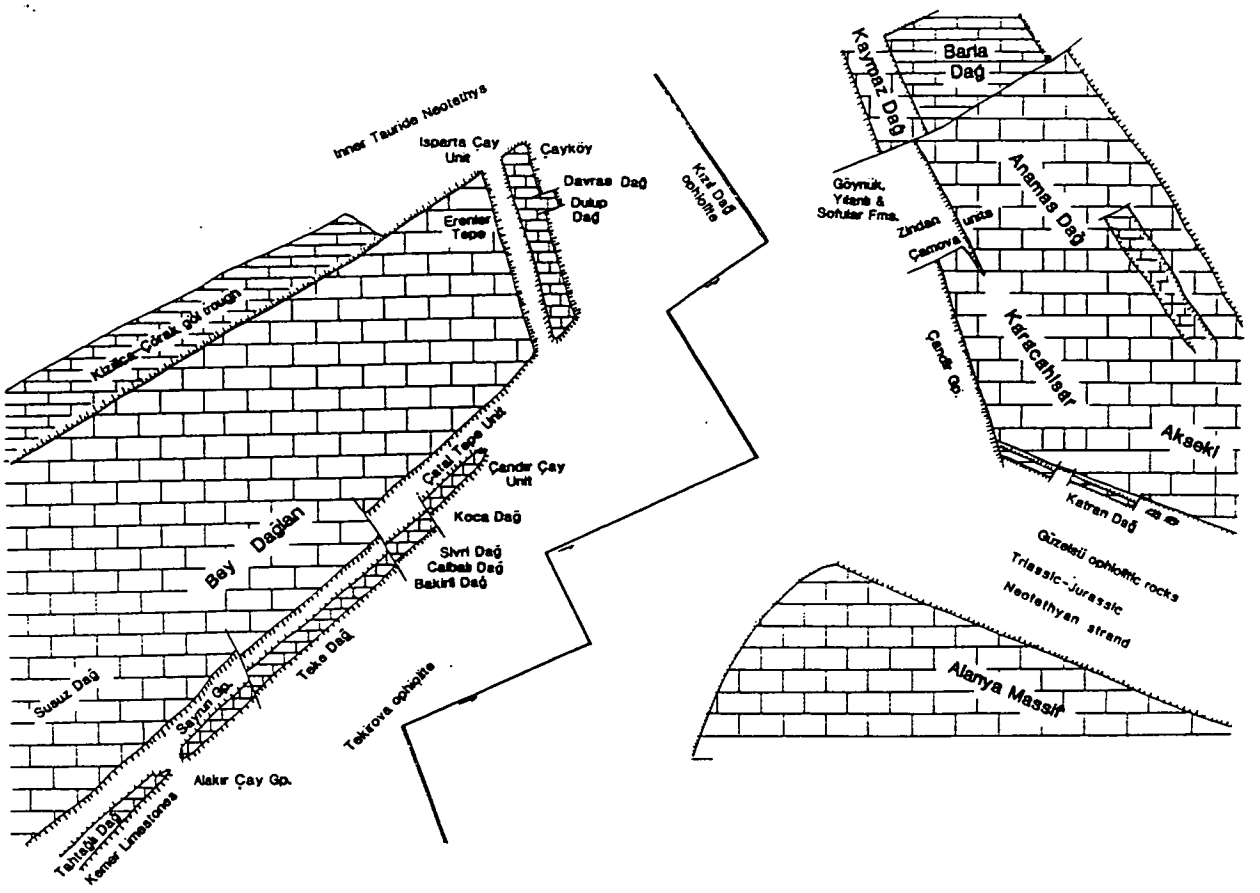

Figure 5.06. Reconstruction of the Isparta angle area in Late Cretaceous time, according to Robertson *et al.* (in press). The Bey Daglari is interpreted as a promontory of Apulia. This was fringed by smaller carbonate platforms and dissected by intra-platform basins. To the east was a separate large carbonate platform, also fringed by smaller submerged platforms. A microcontinent (Alanya Massif) was located to the SE with another small Neotethyan strand to the N (Guzelsu corridor). The E margin of the Bey Daglari was a strike-slip (shear) dominated margin. In the Late Cretaceous oceanic crust formed at a spreading axis offset by sinistral transform faults (Tekirova complex), probably in a supra-subduction zone setting. *Note - in this reconstruction the Bey Daglari platform has been restored to its pre-Neogene position by removing the 30° anticlockwise rotation identified by Kissel and Poisson (1987) and in this study (Chapter 6). This rotation is discussed in Section 5.4.2.*

Following emplacement of the Antalya Complex, convergence resulting from the Palaeocene to Miocene northward movement of Africa (Livermore and Smith, 1984; Savostin *et al.*, 1986) was taken up along the northern margins of the newly-joined platform massifs, resulting in the emplacement of the Lycian and Beysehir-Hoyran-Hadim nappe systems southward across their relative autochthons (Delaune-Mayère *et al.*, 1977; Waldron, 1984a). Finally, thrusting took place in Upper Miocene time along a narrow belt to the south of the Davras Dag, in the Aksu phase of Poisson (1977). This represented the last stage of compressive movement between the Anamas Dag and Bey Daglari blocks, leaving the Isparta angle essentially in its present-day configuration, modified only by a switch to extension and development of the north-south Kovada graben in the north.

5.4 Palaeomagnetic studies in S. W. Turkey.

Previous palaeomagnetic studies within the Mesozoic and Tertiary sequences of the Isparta angle region have been carried out by two French groups with differing objectives. Firstly, J. P Lauer (Strasbourg University) carried out sampling of carbonates and igneous rocks of the Antalya Complex and underlying autochthons as part of a study and review of Turkish palaeomagnetism, aimed at placing constraints on the positions of various Turkish blocks during the Mesozoic and Tertiary. I have already discussed the model for the evolution of Turkey put forward by Lauer on the basis of his research in Chapter 2 (Section 2.4.3). Here, therefore, I will only review the palaeomagnetic database compiled by Lauer (1981, 1984) for the Isparta angle area, and assess the reliability of these data. The second group of French workers, consisting of C. Laj, C. Kissel and others (C.N.R.S., Gif-sur-Yvette), have been concerned with the more recent geodynamic evolution of the Hellenic arc and trench system. Their work on the eastern termination of this system has involved sampling of Tertiary and Quaternary formations exposed on either side of the Bey Daglari platform, as well as parts of the platform itself (Kissel and Poisson, 1986, 1987). Here I will discuss fully only those data obtained by this group in southwestern Turkey; the results of their research at the western termination of the Hellenic arc and trench will be discussed in Chapter 7.

5.4.1 The work of Lauer.

The data obtained by Lauer (1981) in southwestern Turkey are of variable quality and reliability. One shortcoming of Lauer's database is that it does not include many determinations of the magnetic mineralogy of the sampled lithologies, to complement the demagnetisation experiments carried out. However, perhaps the most serious

problem with the data compiled by Lauer is the indiscriminate application of standard structural tilt corrections. I shall return to this point in Chapter 6. While the analyses carried out by Lauer have not been comprehensive, there are still some interesting data from the Isparta angle region contained in his thesis. Here I will discuss these data in two sections: firstly I will examine those sites located in the Bey Daglari platform massif; secondly I will look at Lauer's sites in the overlying Antalya Complex.

Sites in the Bey Daglari relative autochthon.

Lauer (1981) reports four sites located in Maastrichtian to Palaeocene sequences of the Bey Daglari, near to the top of the platform succession (sites 10 to 13; Lauer, *op. cit.*). In all cases, the intensities of remanent magnetisation were predictably low, and the quality of demagnetisation data which Lauer (*op. cit.*) could obtain was thus limited by the sensitivity of the available Digico spinner magnetometer.

Site 10 (Lauer, *op. cit.*) is located along the main Korkuteli-Antalya road, approximately 10 km east of the village of Yazir, in purple, muddy carbonates of Upper Palaeocene age. This site is very close to site YA of the present study (see Chapter 6). Thermal demagnetisation carried out by Lauer (*op. cit.*) was successful in eliminating an important viscous component of magnetisation. However, determination of the precise direction of the higher blocking temperature component carried by the samples was difficult because of the low intensities involved. The cleaned magnetisation vectors obtained were therefore widely dispersed. Stratigraphic corrections were determined individually for each sample, with bedding tilts varying between 40° and 53°. The final site mean given by Lauer (*op. cit.*) was:

Dec = 325°, Inc = 05°, K = 7.6, α_{95} = 29°, n = 5 (geographic coordinates).

Dec = 342°, Inc = 43°, K = 8.1, α_{95} = 28°, n = 5 (stratigraphic coordinates).

The dispersion of vectors at this site, both before and after stratigraphic correction, is unacceptably high and thus interpretation of this result should not be attempted.

Site 13 of Lauer (1981) is also of poor precision. This site is located approximately 4 km northwest of Bucak, in purple carbonates of Maastrichtian age. At this site alternating field demagnetisation up to a peak field of 70 mT was effective in removing a viscous component of magnetisation. Subsequent thermal demagnetisation revealed the presence of a single component of magnetisation of reversed polarity. The stratigraphic corrections applied to the data were variable, with dips ranging between 11° and 26° and strikes ranging from 198° to 249°. The final site mean reported by Lauer (*op. cit.*) was:

Dec = 132°, Inc = -37°, K = 10, α_{95} = 22°, n = 6 (stratigraphic coordinates).

Dispersion at this site is also too high for the site mean to be considered reliable.

The remaining two of Lauer's sites in the Bey Daglari platform are located further north, close to Isparta. Site 11 consists of pink carbonates of Palaeocene age. At this

site a combination of alternating field and thermal demagnetisation revealed single components of magnetisation of normal polarity only. Approximately the same stratigraphic correction was applied to all samples (22°/155°, strike measured 90° anticlockwise from dip). The final direction obtained by Lauer (*op. cit.*) of
Dec = 327°, Inc = 51°, K = 40.4, α_{95} = 8.8°, n = 8 (stratigraphic coordinates)
is the most reliable of the four Bey Daglari site mean directions.

Site 12 consists of Maastrichtian pink pelagic carbonates. Lauer (*op. cit.*) collected a total of 42 samples from this site taken uniformly through the section. Samples were found to be of predominantly reversed polarity. Stratigraphic corrections were carried out individually for each sample, and had dips ranging from 13°-30° and strikes from 131°-196°. Dispersion of sample vectors remained high after these tilt corrections had been applied, and was not improved by repeatedly measuring the samples on the Digico magnetometer used by Lauer (*op. cit.*). This dispersion reflects the fact that the intensity of magnetisation of these samples is close to the limit of sensitivity of the instrument used. The average directions after stratigraphic correction found by Lauer (*op. cit.*) were as follows:

	Dec	Inc	K	α_{95}	n
Normal polarity	328°	40°	13.3	17.0°	7
Reverse polarity	130°	-35°	11.0	7.6°	35
Combined	133°	-34°	9.2	7.7°	42

In addition, Lauer (*op. cit.*) gives the site mean of the reverse polarity group in geographic coordinates as:
Dec = 145°, Inc = -43°, K = 11.0, α_{95} = 7.7°, n = 35.

The precision parameter, K, for this site is again quite low. However, the site mean is probably meaningful since, with such high sample numbers, measurement errors would be expected to cancel out (assuming they are randomly distributed).

In summary, the four sites analysed by Lauer (*op. cit.*) from the Bey Daglari carbonate platform massif are generally of poor palaeomagnetic quality, with large dispersions of cleaned sample remanences being observed at three sites. Although it is not advisable to attempt a geological interpretation of such data, the overall northwesterly trend of most vectors (after inverting reversed polarities through the origin) may indicate a significant anticlockwise rotation of the sampled sequences. However, although Lauer (*op. cit.*) has applied stratigraphic corrections to all four sites, he presents no evidence concerning the age of magnetisation. The question of whether Lauer (*op. cit.*) was justified in applying these corrections to this data will be discussed in Chapter 6.

Sites in the allochthonous units of the Antalya Complex.

The majority of sites studied by Lauer (1981) in the Isparta angle region were within the ophiolitic sequences of the Antalya Complex. Sites located within the gabbros and mantle-related rocks of the coastal Tekirova ophiolite complex exhibited large intra-site dispersions and no inter-site consistency. These results are not considered further here. However, consistent, good quality data were obtained from the Çalbali Dag massif, in the marginal oceanic crust of the Gödene Zone of Robertson and Woodcock (1980b, 1981a, b, c, 1982, 1984). The massif consists of a 650m thick sequence of mafic pillow lavas, with interbedded thin pelagic carbonates containing a Late Triassic (Norian-Carnian) *Halobia* fauna (Robertson and Woodcock, 1981c). Lauer (1981) sampled the pillow lavas at 11 sites spread throughout the lava pile. Stratigraphic corrections were determined from the orientation of the interbedded limestones. As in the case of the Upper and Lower Pillow Lava series of the Troodos ophiolite sampled in the present study (Chapters 3 and 4), Lauer (*op. cit.*) found that alternating field demagnetisation was successful in recovering characteristic magnetisation directions from these sites. The demagnetisation curves obtained were simple, with only minor viscous magnetisations superimposed upon single stable remanence components. The stratigraphically corrected site mean directions listed by Lauer (*op. cit.*) for these 11 sites were as follows:

	Dec	Inc	K	α_{95}	n
Site 43	347°	-33°	33	10.7°	7
Site 44	346°	-02°	18	16.1°	6
Site 45	324°	-16°	28	12.9°	6
Site 46	312°	-22°	72	7.1°	7
Site 47	329°	-04°	47	13.5°	4
Site 48	323°	-09°	55	16.8°	3
Site 49	329°	-16°	53	10.6°	5
Site 50	335°	-01°	104	9.0°	4
Site 51	000°	-05°	16	19.7°	5
Site 52	342°	-07°	43	14.1°	4
Site 53	001°	+15°	50	11.0°	5

We can see from these results that intra-site dispersion in these sites is substantially less than that found by Lauer (*op. cit.*) in the Bey Daglari sequences. The site mean directions cluster well in the northwest quadrant, but the reversed polarity of all but one site makes any formation mean calculated from these data difficult to interpret. I shall return to the data from these sites in Chapter 6, in the light of the results obtained in the present study.

5.4.2 The work of Kissel and Poisson.

The palaeomagnetic research group at Gif-sur-Yvette have been concerned in the eastern Mediterranean region primarily with the reconstruction of the geodynamical evolution of the successive Ionian-Lycian and Aegean arcs. Previous work by them (Laj *et al.*, 1982; Kissel *et al.*, 1985) demonstrated that the northwestern extremity of the arc system was subjected to a clockwise rotation which occurred in two separate phases of approximately the same amplitude (around 20-25°). The first phase occurred in the Middle Miocene, contemporaneous with the Langhian tectonic phase, whereas the second rotational event was of Plio-Quaternary age. The aim of this group in southwestern Turkey was to determine whether complementary rotations had occurred at the other extremity of the arc. To achieve this, they sampled Tertiary formations of the Bey Daglari and overlying Lycian Nappes, and Neogene to Quaternary deposits of the Antalya basin, north of Antalya Bay.

In the Antalya basin, Kissel and Poisson (1986) collected from a total of fourteen sites, predominantly within marls and carbonates of Langhian to Late Pliocene age, but also within the Gölcük lavas of Early Pliocene age and Pleistocene ignimbrites in the north of the basin, near Isparta (Figure 5.07). In the case of the sedimentary sites, only fine-grained, blue-grey, unaltered rocks with well-defined bedding were sampled. For the volcanics near Isparta, tilt corrections were estimated from the regional trend.

Primary depositional magnetic fabrics were observed in the majority of samples collected by Kissel and Poisson (*op. cit.*). Isothermal remanence studies carried out on two samples per site demonstrated that magnetite was the only carrier of natural remanence in all the sampled lithologies. Remanence measurements were carried out using a spinner magnetometer for the igneous sites and a three-axis LETI cryogenic magnetometer for the sediments. All samples were subjected to stepwise thermal demagnetisation.

Stable components of magnetisation were obtained at ten sites (Figure 5.08). A fold test carried out on site mean directions was positive at the 95% confidence level, indicating that the magnetisation predates folding. Also, site mean directions for two reversely magnetised sites were found to be antiparallel to those exhibiting a normal polarity (Figure 5.08).

The Fisherian mean of the site directions from the Antalya basin, after inverting the reversed polarity sites through the origin, was calculated to be:
Dec = 001.5°, Inc = 50°, K = 80, α_{95} = 4.5°, N = 10 (stratigraphic coordinates).

The calculated mean inclination (50°) is lower than that expected at the latitude of Antalya, assuming an axial geocentric dipole field (56°). Kissel and Poisson (*op. cit.*) point out that this deviation could either be the result of northward drift of the Antalya region,

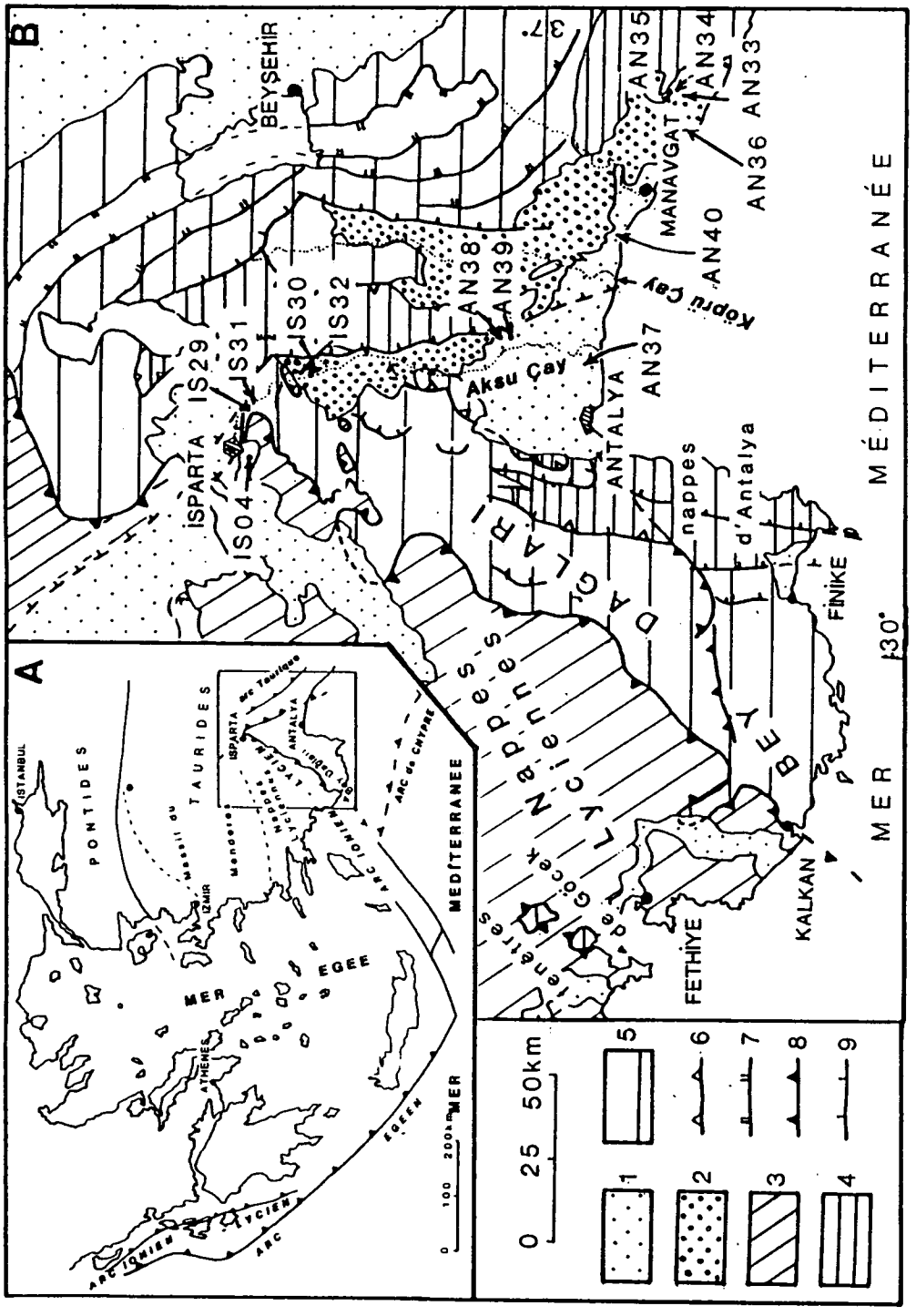

Figure 5.07. Geological map of the Antalya basin and the location of the sites sampled by Kissel and Poisson (1986). Key: *Neogene sequences*: 1 - Post-tectonic sequences (Upper Messinian to Plio-Quaternary); 2 - Pre-tectonic sequences (Late Oligocene to Lower Messinian); 3 - Lycian Nappes; 4 - Antalya Nappes (Antalya Complex of Robertson and Woodcock (1980b); 5 - Autochthonous and para-autochthonous Tauride carbonate platforms. *Compressive phases of deformation*: 6 - Palaeocene to Lower Eocene (Antalya Nappes); 7 - Late Eocene (Beysehir Nappes - Tauric arc); 8 - post-Lower Langhian - pre-Tortonian (Lycian Nappes - Ionian-Lycian arc); 9 - Post-Tortonian - pre-Lower Pliocene (Aksu thrust) (from Kissel and Poisson, 1986).

Sites	Age	n	D°	I°	K	α_{95}
IS 29	Pleistocène	8	5.3	59.0	170	3.7
IS 31	inférieur	9	358.0	58.0	288	2.7
AN 37	Plioc. sup.	9	186.0	-48.0	270	2.8
AN 40	Pliocène	10	358.0	52.0	107	4.0
IS 04	Pliocène	9	12.5	46.6	221	3.0
AN 39	inférieur	8	182.0	-52.0	19	11.0
IS 32	Serravallien-	8	352.0	43.0	163	4.0
AN 33	-Tortonien	9	359.0	45.4	24	9.5
AN 34	Langhien	4	11.3	38.4	23	14.0
AN 35		9	347.0	59.0	49	7.0

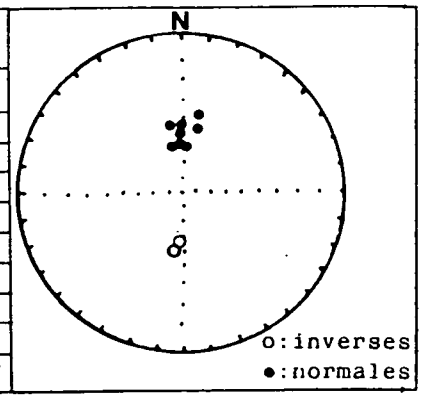

Figure 5.08. Palaeomagnetic mean directions found by Kissel and Poisson (1986) for sites in the Antalya basin (tilt corrected directions). Note the antiparallel normal and reverse polarity groups.

Sites	Age	n	Da	Ia	Db	Ib	K	α_{95}
L I		5	325	5	342	43	8	28
L II	(Ks)	6	132	-52	132	-37	10	22
L III		42	145	-43	133	-34	11	7
L IV	(Pa)	8	352	48	327	50	40	9
EL 83		6	130	-33	115	-16	19	13
EL 84	(E)	8	151	-53	154	-29	61	6
EL 71		1 8 7	176 2 2	-63 51 49	149 340 341	-40 32 31	.. 54 58	.. 6 7
EL 67	(O)	5 7 2	158 339 342	-49 46 48	152 333 336	-42 40 34	60 55 ..	8 7 ..
EL 65*		10	36	64	40	29	37	7
EL 70		10	171	-34	161	-30	39	7
EL 73	(M)	9	319	24	324	39	57	6
EL 78		7	338	64	359	68	39	18
EL 76*	(P)	10	353	59	331	49	134	4

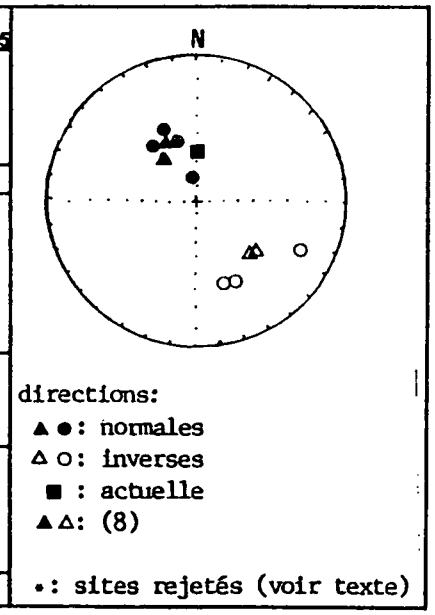

Figure 5.10. Palaeomagnetic directions obtained by Kissel and Poisson (1987) from the Bey Daglari, before (Da, Ia) and after (Db, Ib) application of a standard structural tilt correction, together with a stereographic projection of the tilt corrected directions (stratigraphic coordinates). Sites LI, LII, LIII and LIV are the sites previously reported by Lauer (1981) from the Bey Daglari (his sites 10, 13, 12 and 11 respectively). Ks = Cretaceous: Pa = Palaeocene: E = Eocene: O = Oligocene: M = Miocene: P = Pliocene.

Figure 5.09. Geological map and location of the sites studied by Kissel and Poisson (1987) in the Bey Daglari and Lycian Nappes.

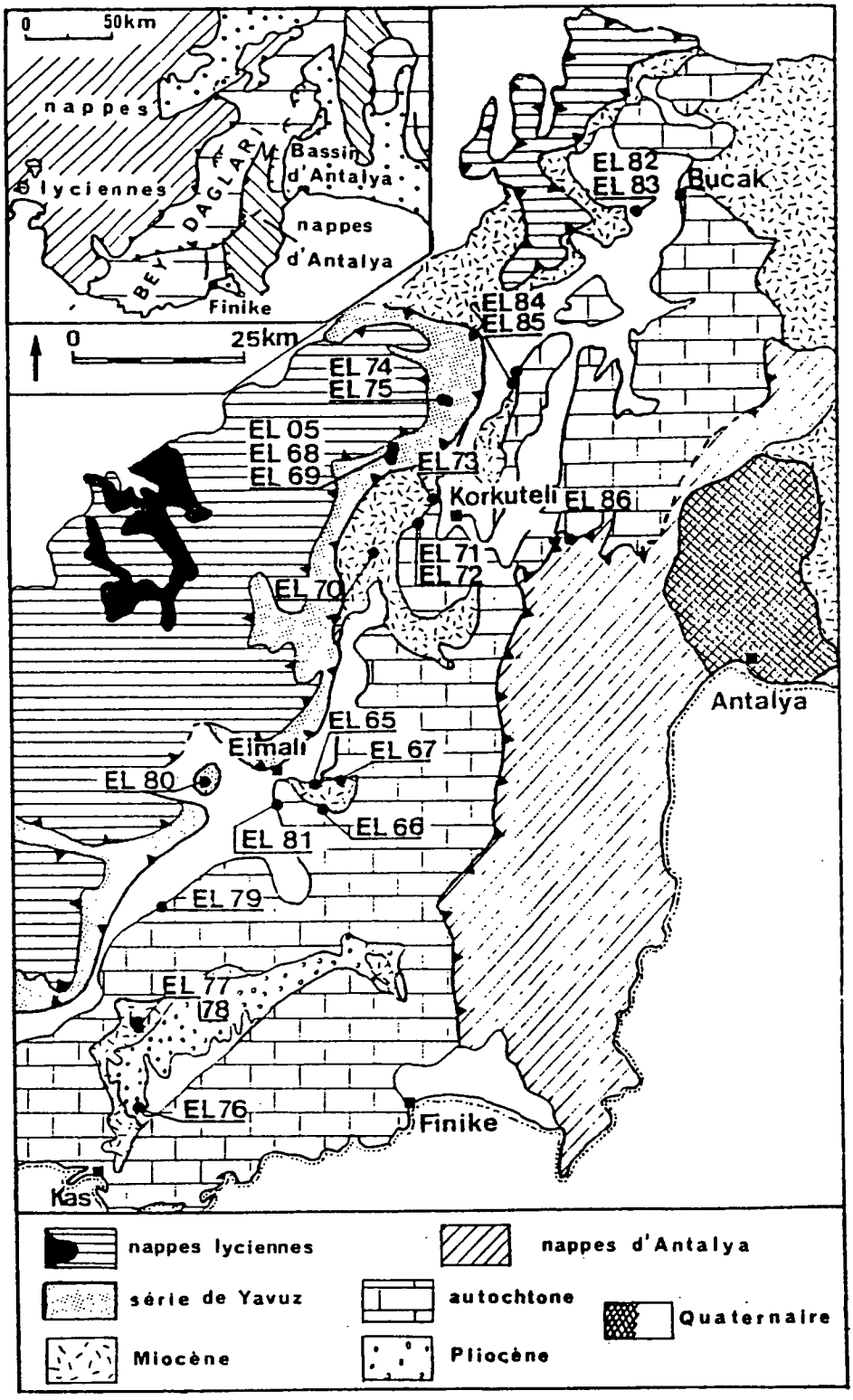

or the result of an inclination error produced by compaction of the sampled sedimentary formations. This latter mechanism was invoked by Laj *et al.* (1982) to explain a larger deviation between expected and observed inclinations seen in the sedimentary formations of the external sedimentary arc in northwestern Greece.

The mean declination of 001.5° indicates that the Antalya basin has not been subjected to any significant rotation since at least the Langhian.

Having established that this area had not been involved in any rotational deformation at the eastern extremity of the Ionian-Lycian arc, Kissel and Poisson (1987) went on to attempt to determine whether the Bey Daglari massif, situated between the Lycian Nappes and the Antalya basin, had itself been affected by such deformation. They collected from 17 sites located in sedimentary formations on the western flank of the Bey Daglari platform, and from a further six sites located in the Eocene carbonates of the Yavuz Series in the Lycian Nappes (Figure 5.09). In the Bey Daglari sequences, Kissel and Poisson (*op. cit.*) sampled pink and white micritic limestones of Late Cretaceous age, calcareous marls of Eocene age, Oligocene marls, and Lower to Mid Miocene (Burdigalian to Langhian) marls and calcareous marls.

As in the Antalya basin sequences, Kissel and Poisson (*op. cit.*) identified primary depositional magnetic fabrics through studies of the anisotropy of susceptibility, and magnetite remanence carriers were identified by IRM acquisition experiments. All remanence measurements were made using a three axis LETI cryogenic magnetometer. The majority of samples were subjected to stepwise thermal demagnetisation.

Of the six sites within the Yavuz Series of the Lycian Nappes studied by Kissel and Poisson (*op. cit.*), three were rejected because the intra-site dispersion was found to be too high (K<10). Mean remanence directions for the remaining three sites were very different from each other, and hence these sites were rejected as well.

Reliable mean directions were obtained from 7 of the 17 sites located in the sequences of the Bey Daglari platform. These sites ranged in age from Eocene to Lower Miocene (Figure 5.10). After inverting the directions from reversed polarity sites through the origin, the mean direction obtained from these 7 sites was:

Dec = 334°, Inc = 45°, K = 18, A_{95} = 12.5°, N = 7 (geographic coordinates)

Dec = 329°, Inc = 37°, K = 14, A_{95} = 14.0°, N = 7 (stratigraphic coordinates).

No conclusion concerning the age of magnetisation was drawn by Kissel and Poisson (*op. cit.*), as no real fold test was carried out. However, the results both before and after application of the structural tilt correction are very different from the present field direction in the Isparta angle area. In both cases, the mean inclination is significantly less than that expected at the mean latitude of the Bey Daglari for an axial geocentric dipole field (Inc = 56°), but is similar to the values of around 45° obtained in

other studies in the Aegean region (Kissel *et al.*, 1985; Kissel and Poisson, 1986; Horner and Freeman, 1983). This suggests that the Aegean region as a whole has undergone a northward drift since the Lower Miocene (Kissel and Poisson, 1987; Kissel and Laj, 1988).

The mean regional declination, both before and after tilt correction, indicates an anticlockwise rotation of the Bey Daglari of approximately 30° with respect to present day north (Figure 5.10). This result is in agreement with those obtained by Lauer (1981) from three Maastrichtian sites and one Palaeocene site (sites 10 to 13 of Lauer, *op. cit.*; see section 5.4.1 above). These latter data were combined by Kissel and Poisson (1987) with those obtained from their seven sites to yield an overall mean direction in stratigraphic coordinates of:

Dec = 327°, Inc = 39°, K = 19, A_{95} = 9.0°, N = 11.

However, as discussed in section 5.4.1, the reliability of two of the sites of Lauer (1981) is questionable (sites 10 and 13 of Lauer, *op. cit.*, see section 5.4.1; sites LI and LII as listed by Kissel and Poisson, 1987, see Figure 5.10). Also, Kissel and Poisson (*op. cit.*) incorrectly report the precision parameter for site 12 of Lauer (1981) as K = 11, whereas this is listed by Lauer (*op. cit.*) as K = 9.2. If Kissel and Poisson (1987) had applied the same rejection criterion to the data of Lauer (1981) as they had to their own data, then all three of these sites would have been excluded from the regional mean because of large intra-site dispersion (K<10). This would have given an overall mean direction in stratigraphic coordinates of:

Dec = 329°, Inc = 39°, K = 15, A_{95} = 14.6°, N = 8.

The rotation indicated by these data is entirely post-Lower Miocene in age. Kissel and Poisson (1987) propose that the rotation occurred about a pole located near Isparta, which would imply a horizontal displacement at the southern end of the platform of approximately 90 km towards the southeast.

Kissel and Poisson (1987) conclude that the anticlockwise rotation of the Bey Daglari platform is 'absorbed' in the overlying Antalya Complex (Antalya Nappes), since the Neogene Antalya basin to the east has experienced no rotation since the Langhian (Kissel and Poisson, 1986).

Finally, the results of the palaeomagnetic studies carried out in southwestern Turkey by Kissel and Poisson (1986, 1987) have been incorporated into a larger database for the Aegean region compiled by the French group. This has been used by Kissel and Laj (1988) to produce a model for the development of the curvature of the Hellenic arc through the Tertiary. This model will be discussed in detail in Chapter 7.

5.5 Summary.

The Isparta angle region forms a critical testing ground for various models proposed for the geodynamical evolution of Turkey. Detailed local geological studies do not support thrusting of the allochthonous units of the Antalya Complex over the carbonate platforms of the Tauride 'Axe Calcaire' from an original basin to the north, as proposed by Ricou *et al.* (1979, 1984) and Marcoux *et al.* (1989). Instead, the Mesozoic continental margin and ophiolitic rocks of the Antalya Complex originated in a strand of the Neotethys located to the south of the carbonate platforms which form the cusp of the Isparta angle. The palaeogeographically complex margins of this ocean basin were affected by a combination of strike-slip and thrust faulting during a sequence of closure movements which took place from the Late Cretaceous onwards (Robertson and Woodcock, 1980b, 1981a, b, c, 1982, 1984; Waldron, 1984 a, b).

Previous palaeomagnetic work carried out by Lauer (1981) within the Antalya Complex have yielded results which are not easily interpreted within the known tectonic framework of the region. The inclinations obtained have, however, been incorporated into the mobilistic theory for the development of Turkey proposed by Lauer (1981, 1984), discussed in Chapter 2. These results are re-evaluated in the next chapter. Results obtained by Kissel and Poisson (1987) from the sequences of the underlying Bey Daglari carbonate platform (during the period between sample collection and analysis in the present study) indicate that this unit has undergone an anticlockwise rotation of 30° since the Middle Miocene. The conclusions of Kissel and Poisson (1987) are also reassessed in Chapter 6, in the light of the data obtained in this study.

CHAPTER SIX - A PALAEOMAGNETIC STUDY OF MESOZOIC AND TERTIARY UNITS IN THE ISPARTA ANGLE.

6.1 Introduction and aims.

In this chapter, I will describe the results of the analyses carried out in the present study on a suite of samples collected from the Mesozoic and Tertiary units of the Isparta angle.

The main aims of this work were: i) to determine whether carbonate platforms in the Isparta angle have been subjected to any rotation, and if so whether they have behaved independently or as a single tectonic unit; ii) to determine whether rotational deformation has affected the overthrust Antalya Complex, and whether such deformation has been influenced by strike-slip tectonics; and iii) to determine the palaeolatitude of formation of units within the Isparta angle, thereby testing Lauer's hypothesis that these units originated close to the equator, to the east of the Arabian promontory.

However, I will show here that the palaeomagnetic usefulness of these sequences for the determination of Mesozoic tectonic rotations and for distinguishing between independent platform units is severely limited by a strong Tertiary magnetic overprint. The possible origins of this pervasive secondary remagnetisation will be discussed. Finally, the implications of the identification of a remagnetisation event upon the data obtained by previous workers in the area will be examined.

6.2 Sampling and methods.

As mentioned in the introductory section to Chapter 5, the samples analysed in this section were collected by T. M. M. Clube and others during the summer of 1984. I have not visited this field area.

The sampling strategy adopted by Clube differs markedly from that used in the present study in Cyprus (Chapter 3) and Greece (Chapters 8 and 9); instead of sampling from a large number of sites spread throughout the study area with an average of 10 samples collected at each site, Clube collected large numbers of samples (over 100 in some cases), mainly from continuous sections, at a reduced number of 'critical' localities. Over long sections it was hoped that this sampling procedure would result in the identification of both normal and reversed polarity intervals (Clube, 1986). Retrospectively, this strategy was not the most appropriate to use in a tectonically complicated region like the Isparta angle. In such areas, higher site numbers are desirable to identify local variations in rotational deformation and to obtain a degree of

statistical reliability. Once secular variation of the geomagnetic field has been averaged out, increased sample numbers do not necessarily improve the accuracy of calculated site mean directions. Indeed, very little decrease in the calculated value of the 95% cone of confidence, α_{95}, and increase in the precision parameter, K, is obtained when more than 8 to 10 samples are analysed per site (see figure 6.5 in Tarling, 1983).

Within the relative autochthons of the Isparta angle area (the Bey Daglari, Anamas-Akseki, Karacahisar, Davras Dag, Dulup Dag and Barla Dag massifs), sites were located in thick, structurally coherent platform and pelagic limestone successions. These were dated on the basis of combined lithological and palaeontological criteria (Clube, 1986). Although some sites were located in Triassic, Jurassic and Lower Cretaceous sections, sampling was concentrated in the Upper Cretaceous-Lower Tertiary stratigraphic interval for two main reasons (Clube, 1986):

i) Upper Cretaceous-Lower Tertiary pelagic successions are thinly-bedded and fine-grained, in contrast to many earlier Mesozoic platform limestones which are massively bedded, coarse-grained and recrystallised. The regular bedding planes of the pelagic facies allowed the accurate determination of appropriate structural tilt corrections at each site. Also, fine-grained sediments are generally considered to be more useful for palaeomagnetic studies since: a) their sedimentation rate is low enough to average out secular variations of the geomagnetic field over the thickness of the sample; b) remanence directions within such sediments are not affected significantly by the physical processes operating during deposition and are therefore most likely to reflect accurately the geomagnetic field direction; and c) fine-grained particles are more stable magnetically than coarser particles (Tarling, 1983).

ii) Intuitively, one might expect important tectonic rotations to occur between independent basement blocks during the Upper Cretaceous and Tertiary phase of crustal convergence and collisional tectonics, rather than in the Triassic to Mid Cretaceous 'passive margin' phase (see Chapter 5, Section 5.3).

Additionally samples were taken from the allochthonous units of the Antalya Complex, especially within the well known exposures of its southwestern segment, adjacent to the Bey Daglari carbonate platform massif. Here, sites were located: i) in the passive margin sequences of the Kumluca Zone imbricate fan of thrust sheets; ii) in the Upper Triassic lavas of the Gödene Zone marginal oceanic crust; iii) along a complete Ordovician to Upper Cretaceous section in the carbonate massif of the Kemer Zone, interpreted as a small off-margin platform (Robertson and Woodcock, 1980b, 1981a, b, c, 1982, 1984); and iv) in Upper Cretaceous ophiolite-derived sandstones preserved near the contact between the Kemer and Tekirova Zones (see Chapter 5, Section 5.3.2 for a definition of these units).

Sampling was carried out by Clube using a standard petrol-driven rock drill, with water cooled, 1" diameter diamond-tipped drill bits. Each sample was orientated with both magnetic and sun compasses (Creer and Sanver, 1967). Visibly weathered material was avoided, together with sections close to faults, landslides and zones of penetrative veining. A total of 28 sites were drilled. The location of all sites is shown in Figure 6.01.

In the laboratory, 18 mm long subsamples were prepared from each core, for analysis using the 2-axis CCL superconducting magnetometer. This is the maximum sample length which this magnetometer can accommodate with the sample inserted on its side (Chapter 1, Section 1.6.2).

The data presented in this chapter have all been obtained from analyses carried out for this thesis. None have been reported previously elsewhere. As discussed below, the NRM intensities of many of the carbonate samples collected from the platform massifs were at or close to the limit of sensitivity of the cryogenic magnetometer. Special care was taken when measuring these samples (see Chapter 1, Section 1.7). Even so, reliable results were only obtained from 13 of the 28 sites collected by Clube. Good quality demagnetisation data were obtained at these sites, and only those samples which yielded stable endpoints have been included in the site mean directions given below. This has necessarily involved a reduction in the number of samples included in these mean directions, but also, hopefully, an increase in the credibility of the results.

6.3 Palaeomagnetic results from the Tauride carbonate platforms.

6.3.1 Rock magnetic characteristics.

The limestones of the Tauride platforms are very weakly magnetic. The frequency distribution of the natural remanent magnetisation (NRM) intensities of these samples is shown in Figure 6.02. The mean intensity is 7.6×10^{-5} Am^{-1}. A significant proportion of the samples have intensities which are only one order of magnitude greater than the noise level of the cryogenic magnetometer (approximately 5.0×10^{-6} Am^{-1}). In Chapter 1, I demonstrated that when adequate steps are taken to reduce the effects of instrumental and other noise, an acceptable degree of reliability can be obtained when measuring samples with intensities of approximately 10.0×10^{-6} Am^{-1}. However, even when statistically acceptable NRM measurements were obtained, many samples became too weakly magnetised to measure after the initial stages of demagnetisation. Measurements carried out on other samples frequently passed the statistical rejection criteria based on the sample 'internal' standard deviation (detailed in Chapter 1, Section 1.7.3), but showed large variations in remanence direction between successive

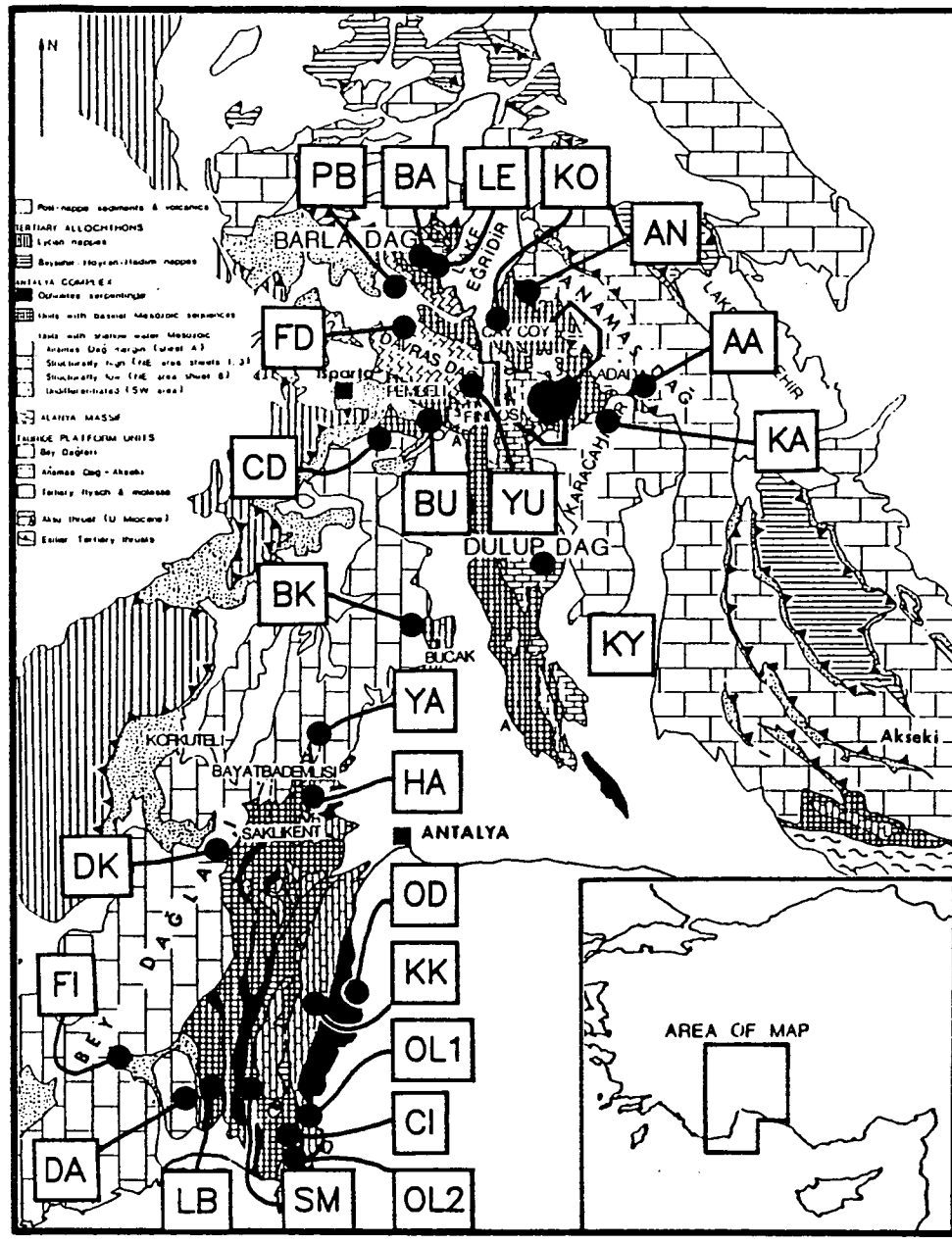

Figure 6.01. Geological map of the Isparta Angle showing the location of the sampling sites.

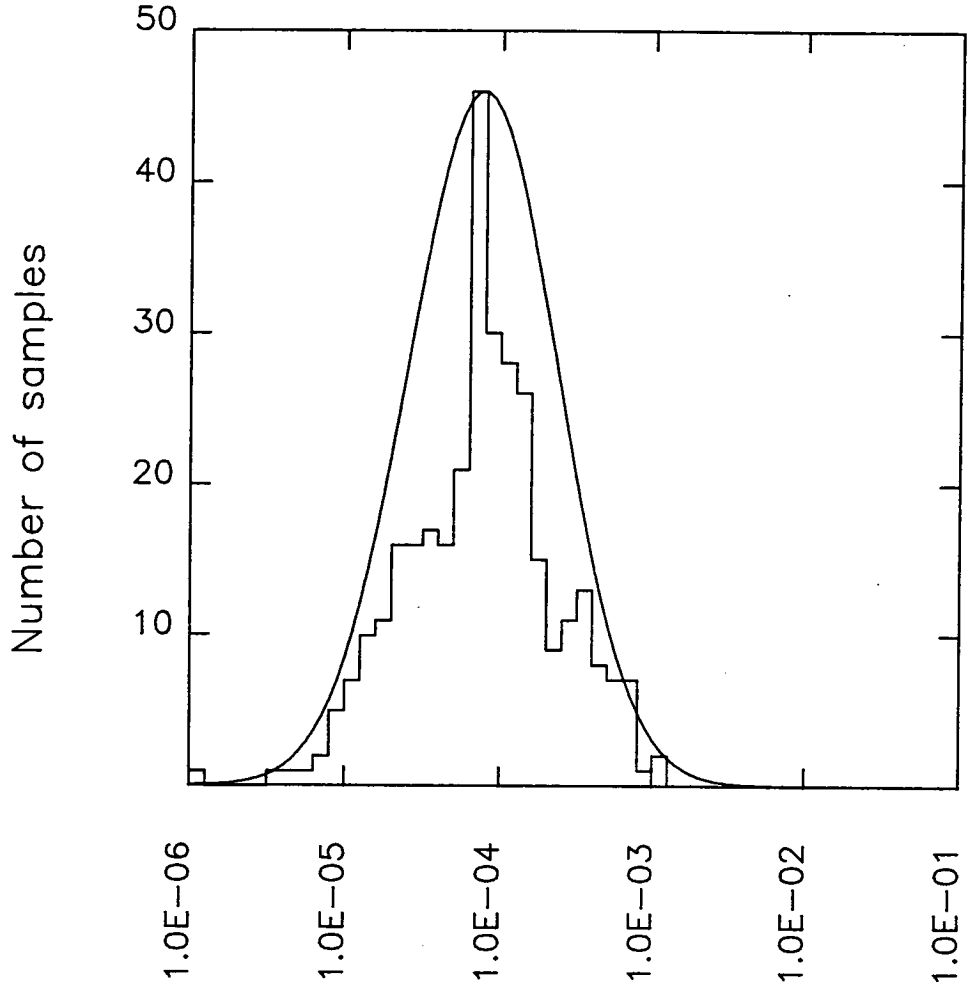

Figure 6.02. Histogram showing the clear log-normal frequency distribution of the NRM intensities of the Tauride platform samples. The mean intensity of magnetisation is 7.6 x 10^{-5} Am^{-1}.

demagnetisation steps. Thus, a large number of samples were rejected at an early stage in the analysis.

No attempt has been made to obtain magnetic extracts from these carbonate samples because of the low concentration of magnetic minerals implied by the very weak NRM intensities. In general, separation techniques which have been tried by other workers on such carbonates have only been partially successful in enriching a pure and representative sample for thermomagnetic analysis (Lowrie and Heller, 1982, and references therein). Instead, the magnetic mineralogy of the sampled lithologies has been determined from the coercivity and blocking temperature characteristics of both natural and laboratory-grown remanences.

The rate of acquisition of isothermal remanence (IRM) in fields up to 1.0 - 2.0 T has been studied for at least two samples per site. Details of the experimental procedure involved have been previously given in Chapter 4, Section 4.3.1. Typical results of the IRM analyses are shown in Figure 6.03. In each graph the solid curve represents the stepwise increase in isothermal remanent moment produced by successively increasing applied fields, while the histogram shows the incremental coercivity spectrum (Dunlop, 1972). In the majority of samples studied, a rapid initial rise and subsequent flattening off of curves below 0.3 T indicates that magnetite is the main magnetic mineral present. In some cases, however, a continuous increase in the IRM for fields higher than 0.3 T is observed. This indicates the presence of a higher coercivity mineral.

To confirm the presence of magnetite and to identify the higher coercivity fraction, one sample from each site was given an IRM at 2.0 T along the -Z sample axis, and an IRM at 0.3 T along the +Z axis. The samples were then thermally demagnetised, following the example of Channell *et al.* (1982). Figure 6.04 shows typical normalised intensity against temperature curves obtained upon stepwise demagnetisation of these composite IRMs. Figure 6.04a illustrates the type of curves found in those samples where only magnetite was identified by the IRM acquisition analyses. The IRM grown at 0.3 T along the +Z sample axes, which affected only the low-coercivity grains, is removed continuously up to temperatures of 520-580°C. These unblocking temperatures are consistent with the IRM being carried by relatively titanium-free titanomagnetite.

More complicated demagnetisation paths are observed in those samples where a high coercivity mineral was identified by the IRM analyses (Figure 6.04b). In these cases, the 0.3 T IRM is preferentially destroyed up to temperatures of about 550°C. At approximately 400°C, the normalised intensity reaches zero, indicating that the remaining intensities of the two antiparallel IRM's cancel each other out. The 0.3 T IRM is completely destroyed at 550°C, when minima in the curves are observed. Again, this indicates that these IRMs are carried by relatively pure titanomagnetite. At

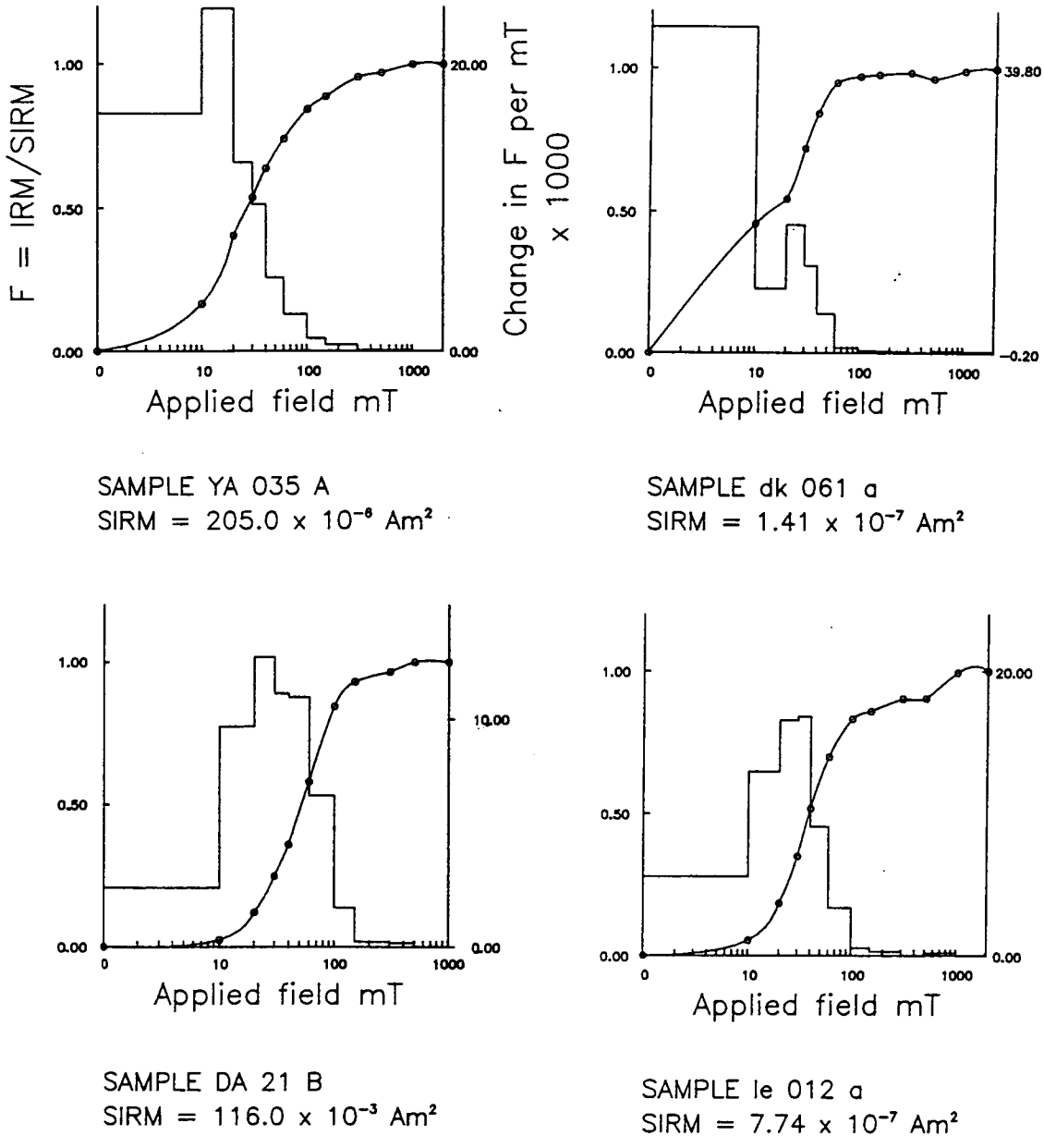

Figure 6.03. Typical IRM acquisition curves for the Tauride platform carbonate samples, indicating the dominance of magnetite as a potential remanence carrier. In some cases a magnetic mineral with a coercivity higher than that of magnetite is also present.

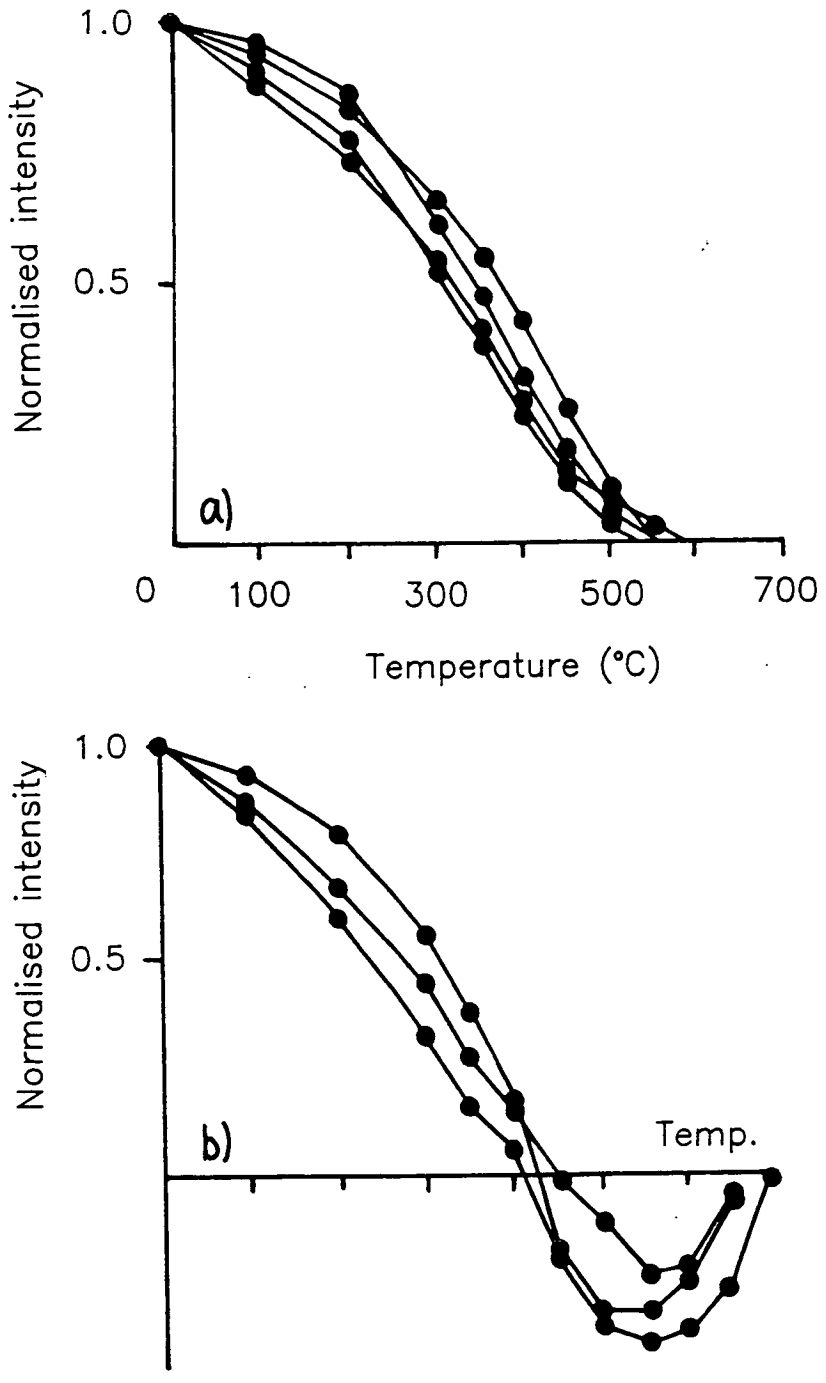

Figure 6.04. Thermal demagnetisation of composite IRMs, following the example of Channell *et al.* (1982), for typical Tauride platform carbonate samples. Low coercivity carriers have a positive magnetisation, and high coercivity carriers have a negative one. (a) In the majority of samples, a continuous reduction in the intensity of magnetisation up to maximum unblocking temperatures of 520-580°C confirms the presence of magnetite as the dominant magnetic mineral present. (b) In those cases where a higher coercivity mineral was identified by the IRM analyses, a decrease in the normalised intensity up to temperatures of 550°C indicates the presence of magnetite, whereas maximum unblocking temperatures of approximately 650°C for the 2.0 T IRM indicate that haematite is also present.

temperatures above 550°C, only the higher-coercivity (2.0 T) IRMs remain. These are destroyed by approximately 650°C, indicating haematite to be the carrier.

The domain structure of the titanomagnetite carriers, identified by both the IRM acquisition and thermal demagnetisation experiments outlined above, has been examined by determining the relative resistance of laboratory-induced isothermal and anhysteretic remanences to alternating field (AF) demagnetisation. Lowrie and Fuller (1971) were the first to propose that thermoremanent magnetisation (TRM) is more stable than high-field IRM against AF demagnetisation in single-domain (SD) magnetite-titanomagnetite (i.e. grain sizes < 0.5 λm), but that the reverse relationship of the stabilities holds in multidomain (MD) magnetite-titanomagnetite; grains in the size range 0.5-0.15 λm are pseudo-single domain (PSD) and give results identical to SD grains. Subsequently, Johnson *et al.* (1975) showed that a weak field anhysteretic remanence (ARM) could be substituted for the TRM in this test, thus obviating the problem of chemical changes during heating experiments.

Figure 6.05 shows characteristic results of the application of this modified Lowrie-Fuller test to the platform limestones samples collected for the present study. In every instance the weak-field ARM was found to be more resistive to AF demagnetisation than the IRM, indicating that single-domain-sized grains dominate the magnetite fraction of the samples.

Stepwise AF demagnetisation of a minimum of ten samples per site was carried out up to peak fields of 100 mT. In many cases, the intensity of magnetisation decreased below a level at which accurate measurement could be made (approximately 10.0×10^{-6} Am^{-1}) before final endpoints were obtained. In samples where stable components of magnetisation were recovered, AF demagnetisation was found to be effective in removing all the magnetisation. This indicates that the haematite fraction identified by the thermal demagnetisation of composite IRMs, described above, does not carry any significant natural remanence. Typical Zijderveld demagnetisation diagrams (Zijderveld, 1967) are shown in Figure 6.06. A common north-dipping component, attributed to viscous magnetisation in the present field direction, was removed by fields of less than 15-20 mT to leave single stable components of magnetisation.

Very few stepwise thermal demagnetisation experiments were carried out on these samples. This was mainly due to the lack of a suitable furnace during the first half of this project. After the arrival of a new furnace, a limited number of samples were subjected to thermal treatment to investigate the blocking temperature spectra of the natural remanence carried by the platform carbonates. Two examples of the Zijderveld demagnetisation diagrams obtained are shown in Figure 6.06. Maximum unblocking temperatures of between 350°C and 500°C were found (see Figure 6.07). These data, in

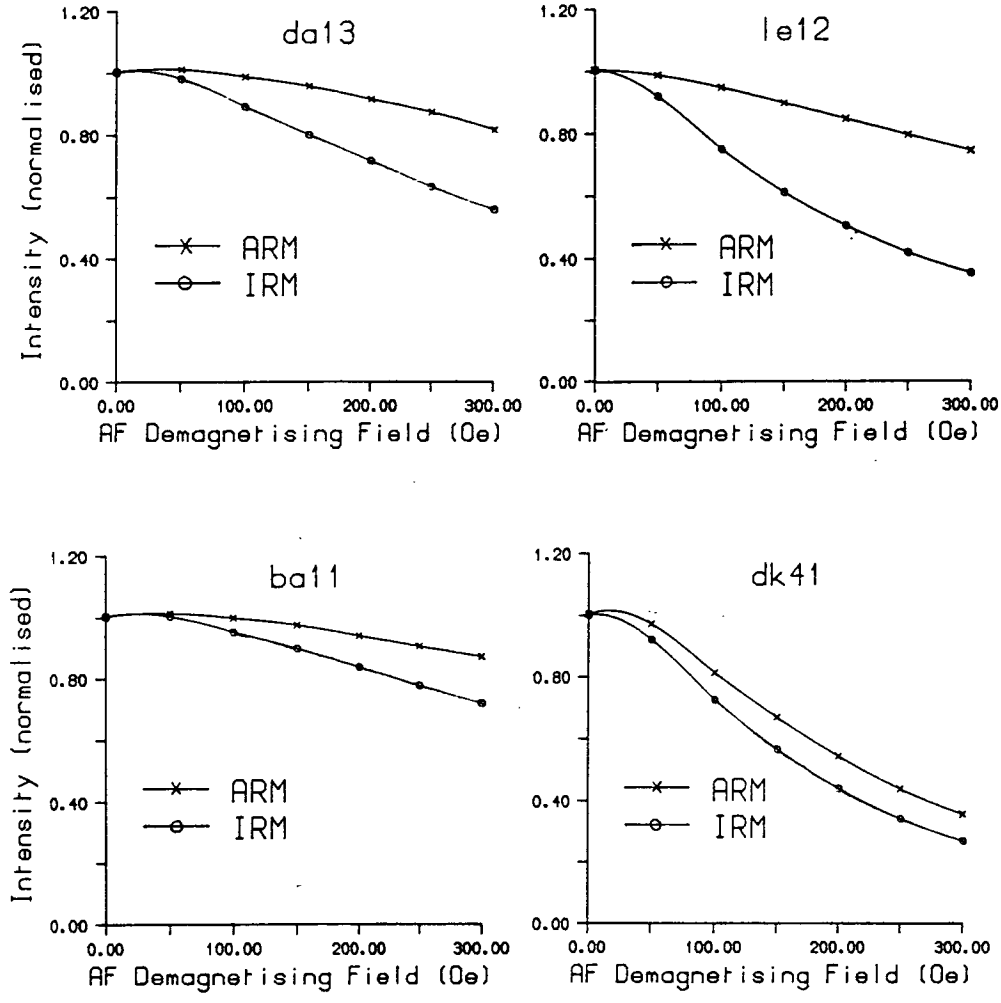

Figure 6.05. Typical results of the domain size test carried out to determine the domain state of the titanomagnetite fraction within the Tauride platform samples. In all cases, the weak field ARM was found to be more resistant to alternating field demagnetisation than the induced IRM, indicating the single-domain nature of the titanomagnetite grains.

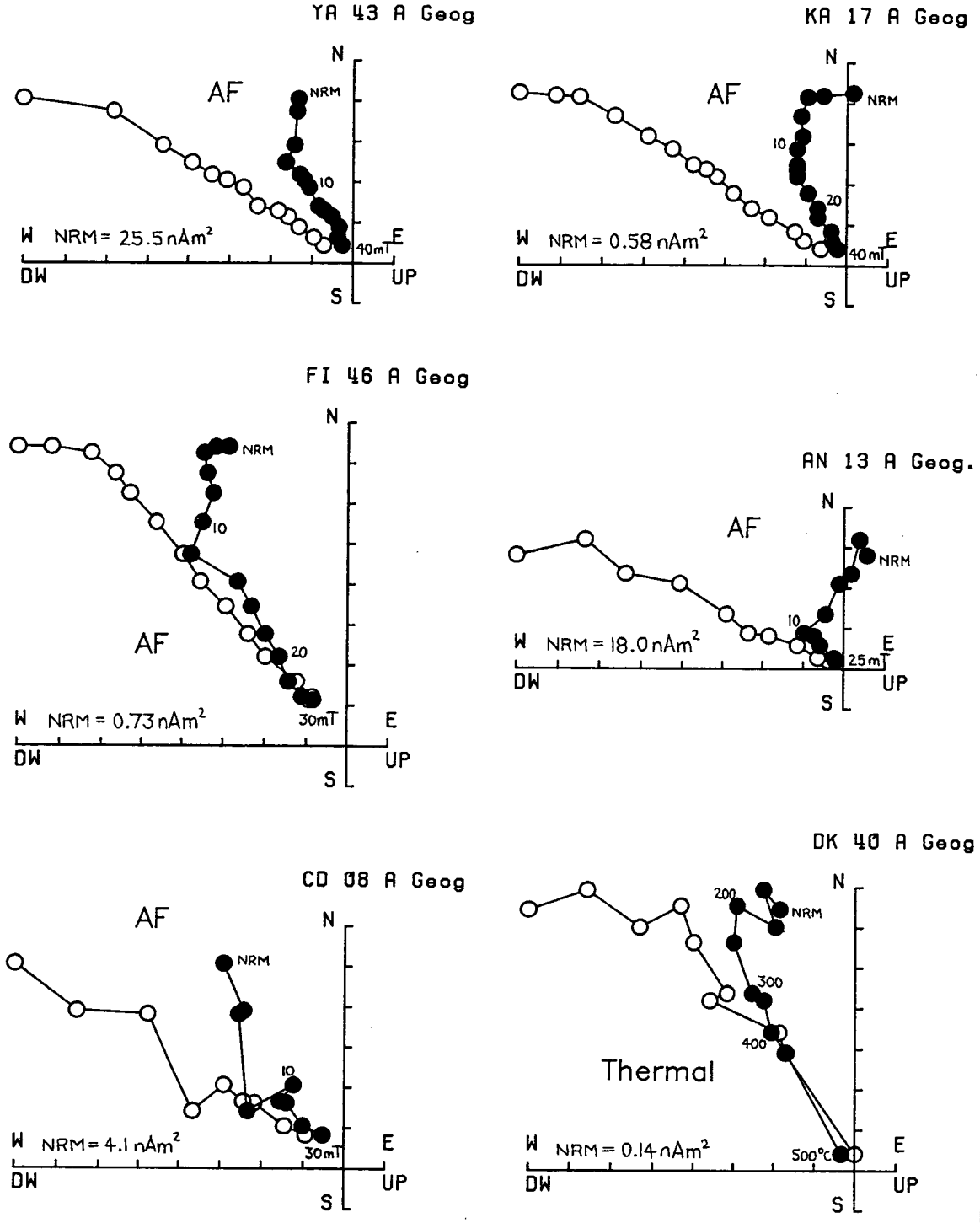

Figure 6.06. Examples of both alternating field and thermal demagnetisation of the natural remanence carried by the Tauride platform carbonates. Note that AF demagnetisation is effective in removing all the natural remanence, even in samples where haematite was identified. Also note that the vertical projections are on the horizontal axes.

conjunction with the effectiveness of AF demagnetisation in reducing NRM intensities to zero, demonstrate that only magnetite carries a natural remanence in these samples.

6.3.2 Palaeomagnetic results.

Reliable palaeomagnetic results with directions unrelated to the present geomagnetic field direction at the sampling site were obtained from nine sites within the Tauride platform units. Only data from those samples which showed stable demagnetisation paths were used in calculating site mean directions. The direction of the cleaned remanence vector for each of these samples was found by drawing best-fit lines through the last four or more points on Zijderveld demagnetisation diagrams (Zijderveld, 1967). The cleaned site mean directions are reported in Table 6.1, both before and after the application of standard structural tilt corrections (i.e. in both geographic and stratigraphic coordinates).

At five sites within the platform sequences of the Bey Daglari massif (Table 6.1), the characteristic remanence directions cluster in the northwest quadrant in geographic coordinates. At some of these sites, demagnetisation has resulted in a slight increase in within-site dispersion compared with the NRM directions. An example of this is shown in Figure 6.08 from site YA (Bayatbademlisi), located in the Palaeocene sequence at the top of the Bey Daglari platform (Figure 6.01). The lower dispersion of the NRM directions is attributed to the presence of viscous components acquired in the present geomagnetic field at the sites (for example, see the Zijderveld demagnetisation diagram for sample YA 043 A shown in Figure 6.06). These viscous components have a biasing effect on the sampling of secular variation of the geomagnetic field inherent at each site.

At site CD (Çamlidere), again located in the top part of the Bey Daglari platform (Figure 6.01), the application of a standard tilt correction to the cleaned characteristic remanences results in an increase in the α_{95} cone of confidence from 10.2° to 16.9° and a decrease in the precision parameter from 57.0 to 21.5 (Table 6.1). The site mean direction moves away from a northwest azimuth and becomes more northerly after application of the tilt correction (Figure 6.09). The increased dispersion in stratigraphic coordinates *may* indicate that the magnetisation of these samples was acquired after folding had occurred at the site. However, this is not statistically significant using the F-test of McElhinny (1964), since $K_1/K_2 = 2.651$ but must exceed 3.44 for significance at the 95% confidence level.

More conclusive evidence for the post-folding age of the magnetisation identified at these sites comes from a comparison of the cleaned remanence directions at sites YA (Bayatbademlisi) and FI (Finike). At both sites, the application of a tilt correction

Table 6.1. Palaeomagnetic results from the Tauride platform units.

Site	Age	N	Geographic				Stratigraphic			
			Dec	Inc	α_{95}	K	Dec	Inc	α_{95}	K
Bey Daglari										
DA	Palaeocene	4	314	27	13.2	50	344	44	14.7	40
FI	Palaeocene	12	316	50	7.2	38	354	40	7.9	30
DK	Palaeocene	8	334	20	12.3	21	349	45	12.3	21
YA	U.Cre-L.Tert	27	313	50	7.0	17	312	39	7.4	15
CD	U.Cre-L.Tert	5	325	50	10.2	57	352	42	16.9	21
Barla Dag										
BA	U.Triassic	9	323	19	9.4	31	320	25	12.1	19
LE	Pal/Eoc flysch	6	331	49	10.0	46	335	29	10.0	46
Anamas Dag										
AN	Pre-mid Jur	13	331	56	4.1	103	320	68	6.9	37
Karacahisar platform										
KA	U.Cre	4	340	47	13.6	47	015	17	13.6	47

N = number of samples; α_{95} = semi-angle of 95% cone of confidence; K = Fisher precision parameter

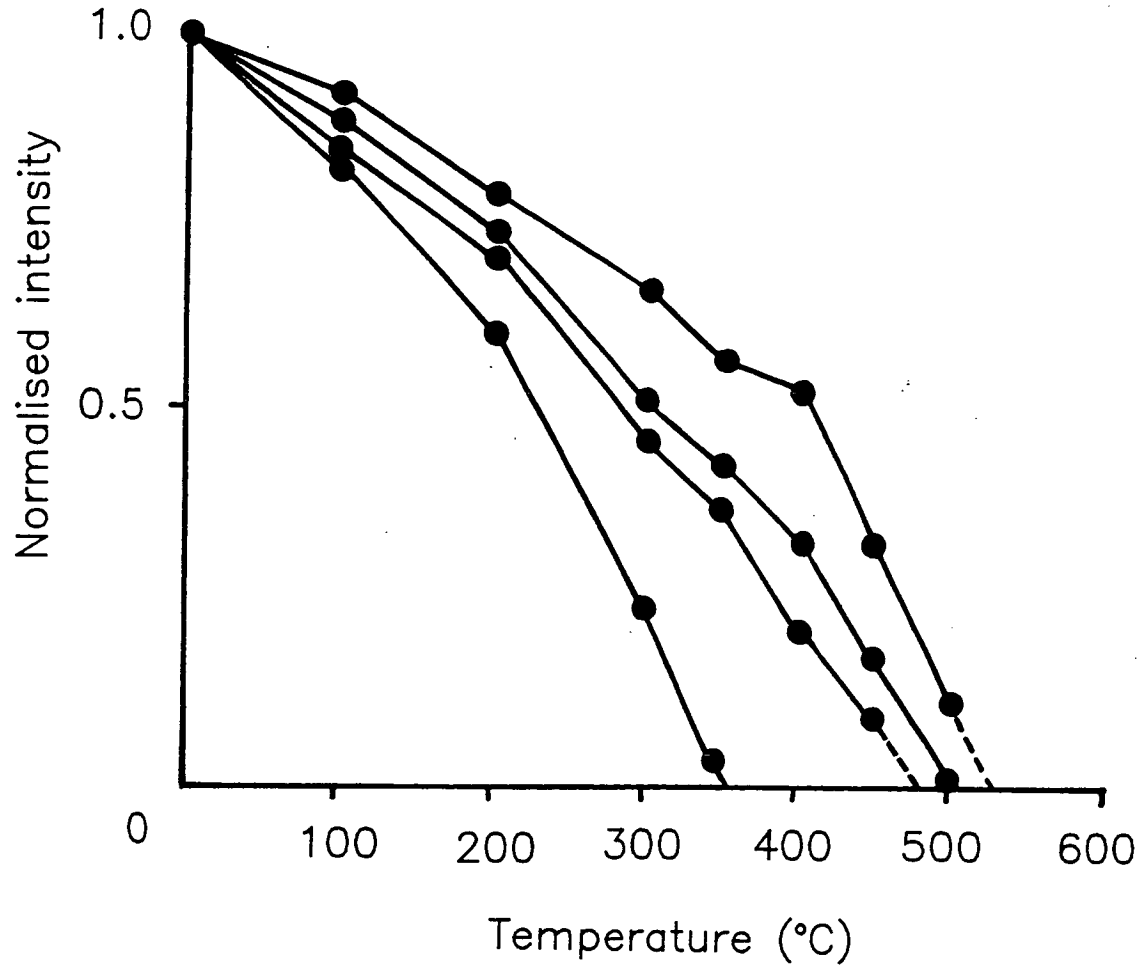

Figure 6.07. The decay of NRM intensity with increasing temperature for various platform samples. The maximum unblocking temperatures are between 350°C and 500°C. Together with the AF demagnetisation data illustrated in Figure 6.06, these data indicate that only magnetite carries a natural remanence in these samples.

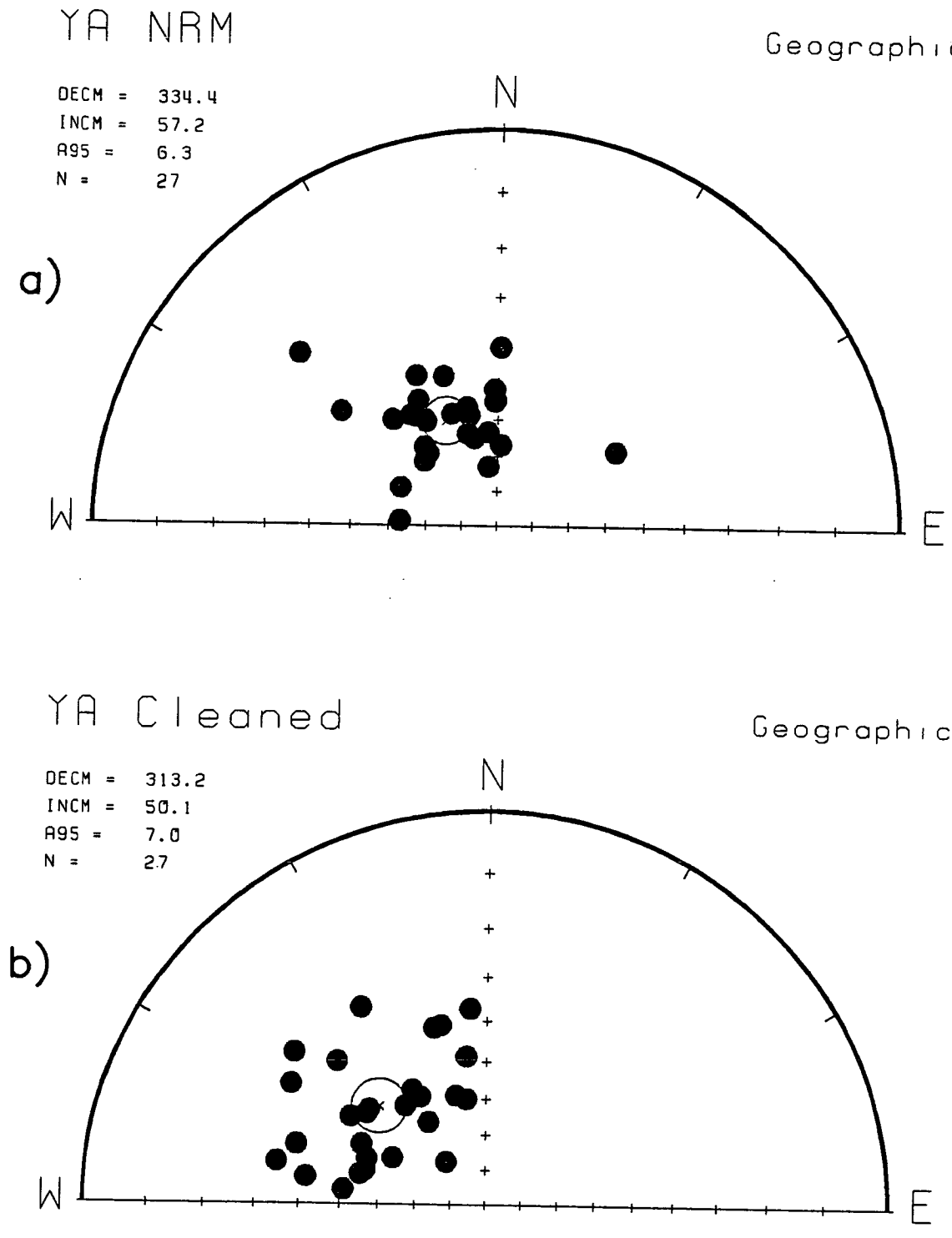

Figure 6.08. The distribution of (a) NRM directions, and (b) cleaned remanence directions at site YA within the Upper Cretaceous to Lower Tertiary sequences of the Bey Daglari platform massif. Note the slight increase in dispersion caused by removal of a common north-dipping viscous component.

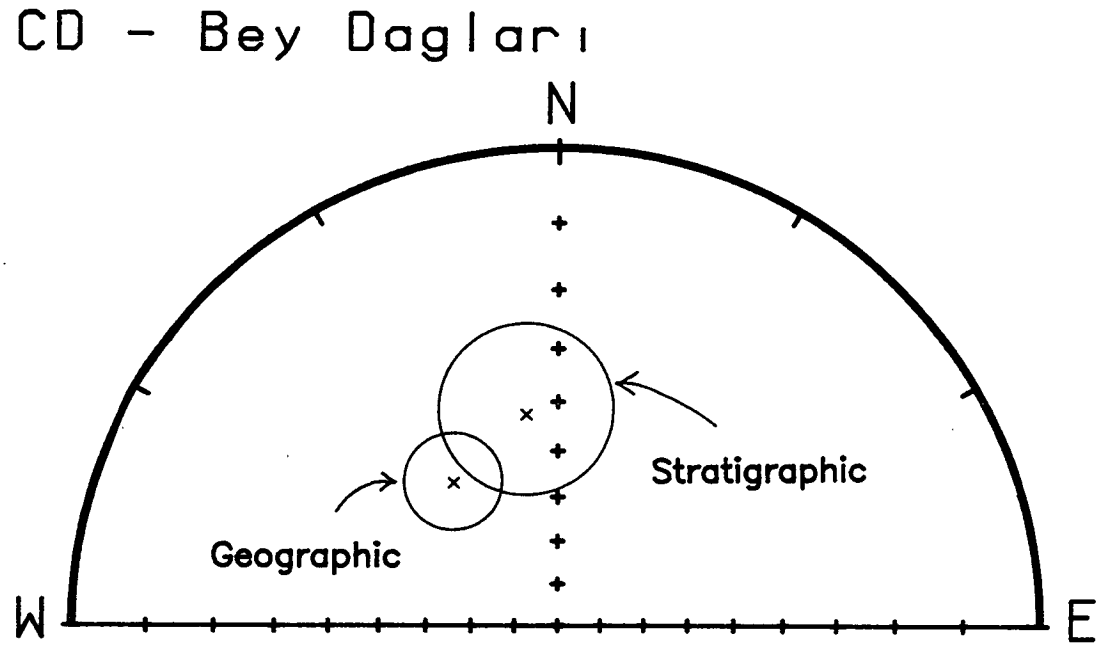

Figure 6.09. The within-site negative fold test at site CD within the Upper Cretaceous to Lower Tertiary sequences of the Bey Daglari platform massif. The application of stratigraphic corrections to the cleaned remanence directions at the site results in an increase in the within-site dispersion.

increases within-site dispersion slightly (Table 6.1). More importantly, however, the α_{95} cones of confidence at the sites overlap almost completely in geographic coordinates, but become distinct and move apart in stratigraphic coordinates (Figure 6.10). This negative fold test (Graham, 1949) is significant at the 99% confidence level (see Appendix A), using the statistical test of McFadden and Jones (1981), and proves that the magnetisation carried by the topmost sequences of the Bey Daglari was acquired after folding took place.

The only stable endpoints with reversed polarity identified in the Isparta angle study area were found at site BA, located in Upper Triassic calciturbidites of the Barla Dag unit (Figure 6.01). The NRM directions at this site were all of normal polarity and formed two distinct groups; one in the northwest quadrant, and the second with a southerly azimuth. However, an important northward dipping viscous component was removed from both groups during the initial stage of magnetic cleaning (using both AF and thermal demagnetisation methods on different samples). The samples in the southerly-directed group then became of reversed polarity with southeasterly-directed declinations, to produce a normal-reverse polarity couple (Figure 6.11). Such antipodal normal and reverse polarity groupings are normally cited as indicating the stability and primary nature of the measured remanence at a site (e.g. Kissel and Laj, 1988). However, in view of the secondary nature of the remanences identified at other sites in this study, there are two possible explanations for the two groups observed at site BA: i) the magnetisation recorded at the site is a primary remanence acquired at or close to the time of deposition of the strata, and that the sampled section covers at least one reversal of the geomagnetic field; or ii) the magnetisation represents a secondary overprint similar to that identified at other sites, in which case the remagnetisation event must span the time period of at least one reversal.

The application of a reversal test to this site does not allow us to choose between these explanations. In both geographic and stratigraphic coordinates, the mean directions of the normal and reversed polarity groups (after inverting the reversed group through the origin) are indistinguishable statistically (using the test of McFadden and Jones, 1981; see Appendix A). The angle between the mean directions of the two groups increases from 3.6° to 16.8° after removal of the bedding tilt, which may indicate that the magnetisation is of post-folding age. However, countering this is the observation that the normal and reversed polarity groups conform to stratigraphic layering, which suggests that the magnetisation is primary. It is difficult to see how a remagnetisation event could produce such magnetostratigraphic layering. Additionally, the cleaned remanence directions from site LE (Figure 6.01) support a primary origin for the magnetisation at site BA. The former site is located in flysch of Palaeocene/Eocene age,

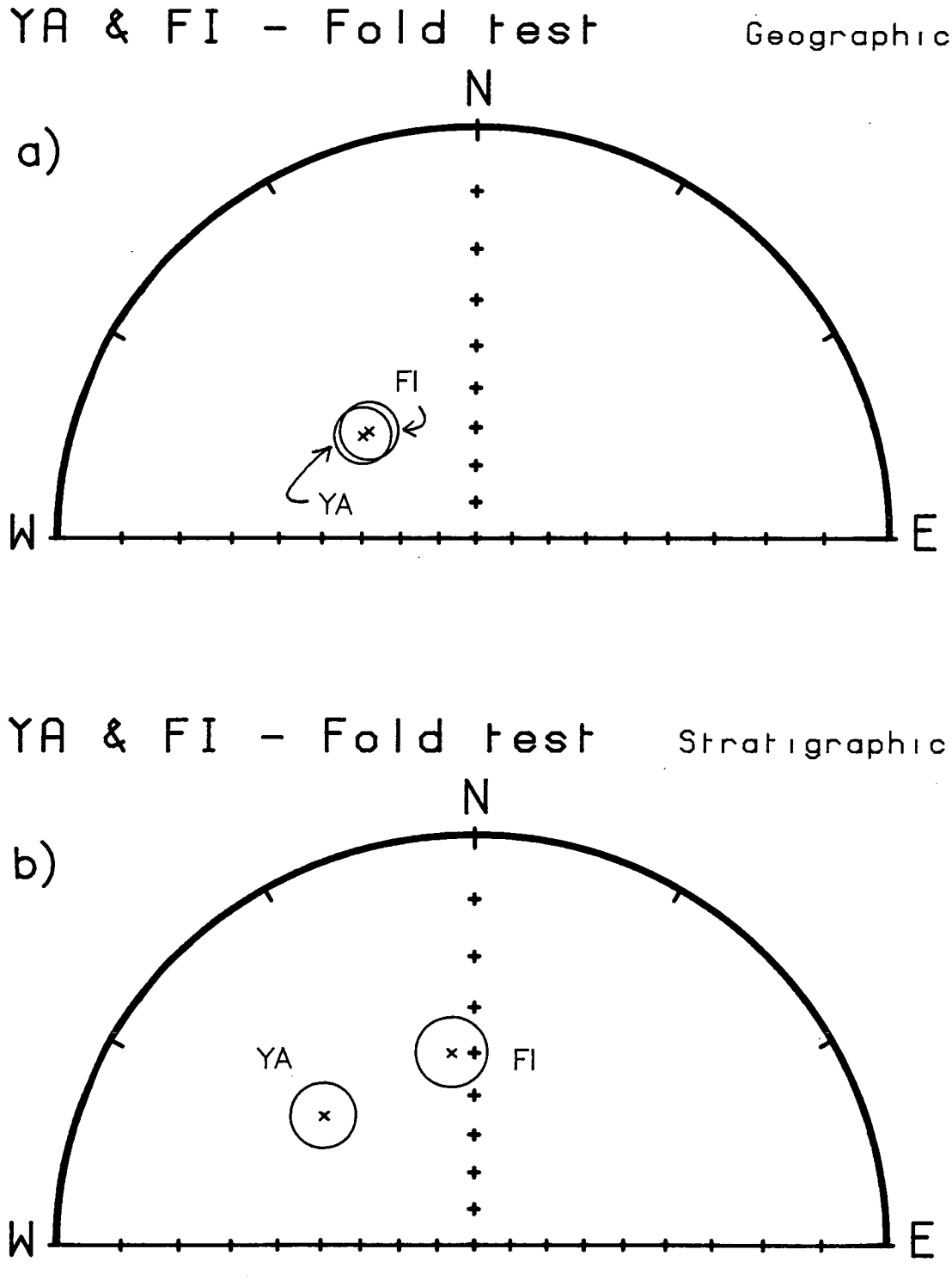

Figure 6.10. The between-site negative fold test at sites YA and FI, within the Upper Cretaceous to Lower Tertiary sequences of the Bey Daglari platform massif: (a) in geographic coordinates the α_{95} cones of confidence associated with the cleaned site mean directions at the sites overlap almost completely, whereas (b) in stratigraphic coordinates they become separated. There is less than a 5% chance that the two site populations share a common mean direction in stratigraphic coordinates.

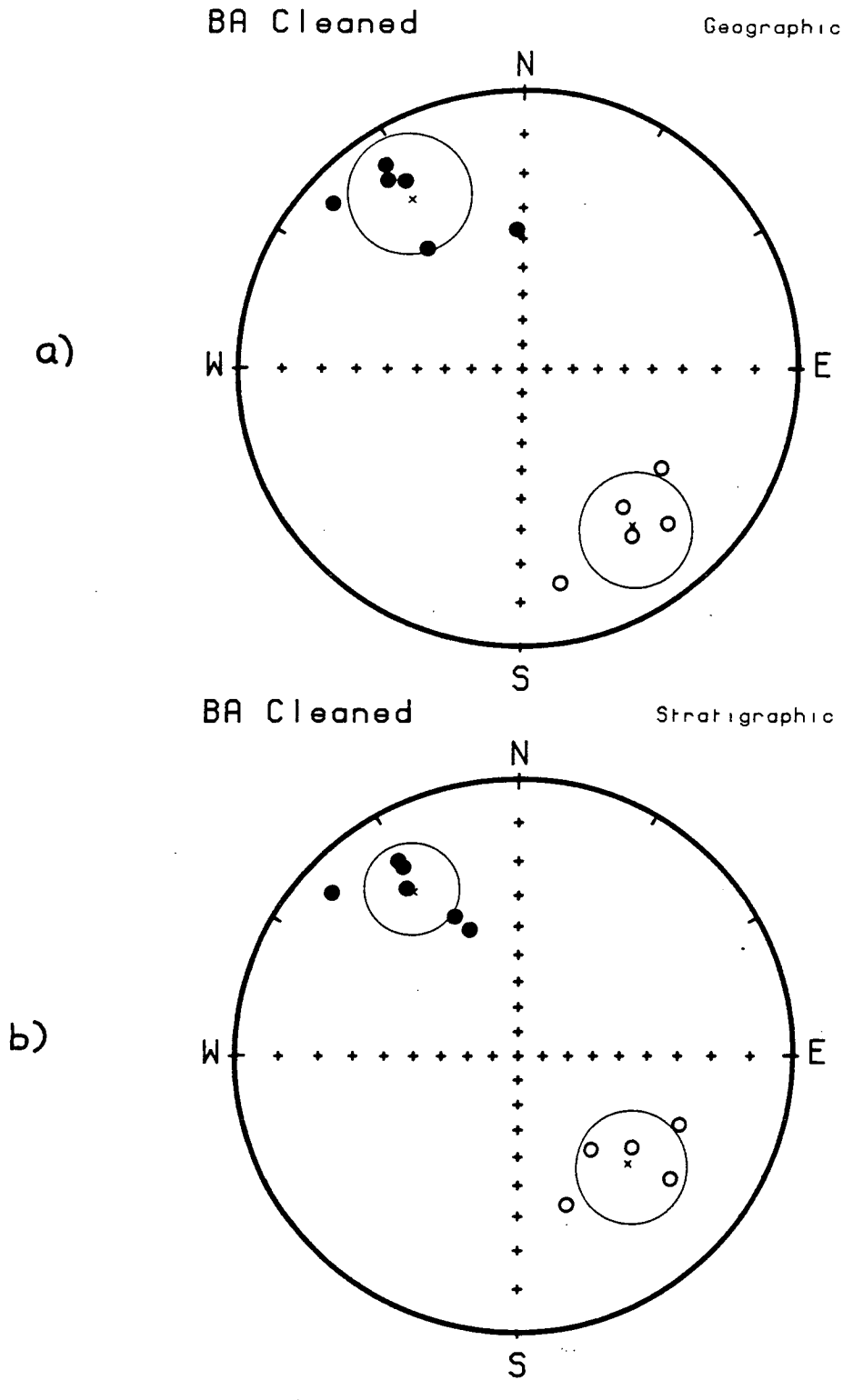

Figure 6.11. The cleaned remanence directions obtained at site BA, located within Upper Triassic carbonates of the Barla Dag platform massif. In both geographic (a) and stratigraphic (b) coordinates, the mean directions of the normal and reversed polarity groups are antiparallel. The normal and reversed groups conform to stratigraphic layering at the site, which indicates that the magnetisation is probably of primary, depositional origin.

which rests *in situ* upon the platform carbonates of the Barla Dag massif. The α_{95} cones of confidence for the two sites are distinct in geographic coordinates; they are significantly different at a greater than 99% confidence level using the test of McFadden and Jones (1981; see Appendix A)). In stratigraphic coordinates, however, the α_{95} cones of confidence for the two sites overlap partially and the two sample populations share a common mean direction. This suggests that primary depositional remanent magnetisations are preserved at both site BA and site LE. Any valid remagnetisation mechanism proposed to explain the post-folding magnetisations seen at other sites must be capable of accounting for the preservation of these primary remanences. This point will be discussed in Section 6.6.1 below.

Only two reliable sites occur within the autochthonous platform sequences on the eastern side of the Isparta angle (Table 6.1). The first of these sites is located in the Upper Cretaceous section of the Karacahisar platform (site KA), which has been correlated with the much larger Anamas-Akseki platform (Robertson *et al.*, in press; see Chapter 5, Section 5.3.4). A limited number of samples at this site yielded high quality demagnetisation data (see Figure 6.06 for an example). Cleaned remanence directions plot in the northwest quadrant in geographic coordinates, but the application of a tilt correction brings these vectors into the northeast quadrant and makes the inclination much shallower.

The second site is located in pre-Mid Jurassic limestones of a para-autochthonous slice (the Zindan sequence), close to the main Anamas-Akseki platform (site AN). This unit is separated from the platform itself by a fault zone. Again, the cleaned vectors from this site (Table 6.1) cluster in the northwest quadrant in geographic coordinates. Removing the bedding tilts at this site makes the site mean inclination become steeper than the present field inclination at the site (68°, compared with 56°). Also, within-site dispersion is increased by the application of the tilt corrections, with the cleaned vectors dividing into two distinct groups. This provides a within-site negative fold test (Figure 6.12; see Appendix A) which is significant at the 99% confidence level and which indicates that magnetisation was acquired here after the development of folding.

The data from sites KA and AN also provide an intra-site negative fold test (Figure 6.13), which is significant at better than the 99% confidence level, using the test of McFadden and Jones (1981; see Appendix A).

The results from these sites suggest that the post-folding remagnetisation identified in the sequences of the Bey Daglari platform to the west was the result of a widespread event. The negative fold tests from both limbs of the Isparta angle indicate that an area-wide test may be possible. I shall return to this point after examining the palaeomagnetic results obtained from the Antalya Complex.

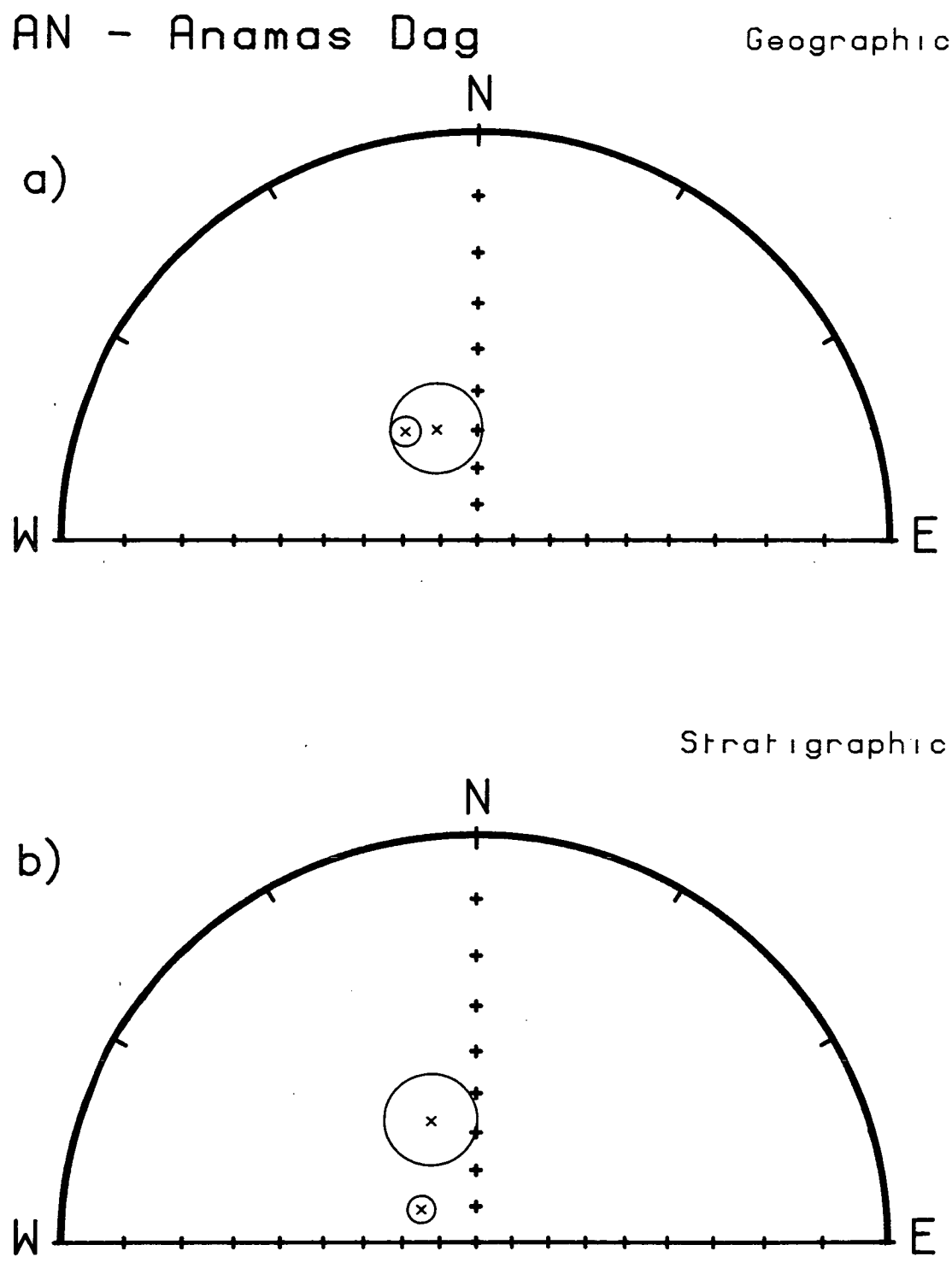

Figure 6.12. The negative within-site fold test at site AN, Anamas-Akseki Dag. (a) Cleaned remanence vectors from the limbs of a small fold have overlapping α_{95} cones of confidence in geographic coordinates, but (b) become distinct upon the application of structural tilt corrections. In stratigraphic coordinates, there is less than a 5% chance that the two groups come from the same population.

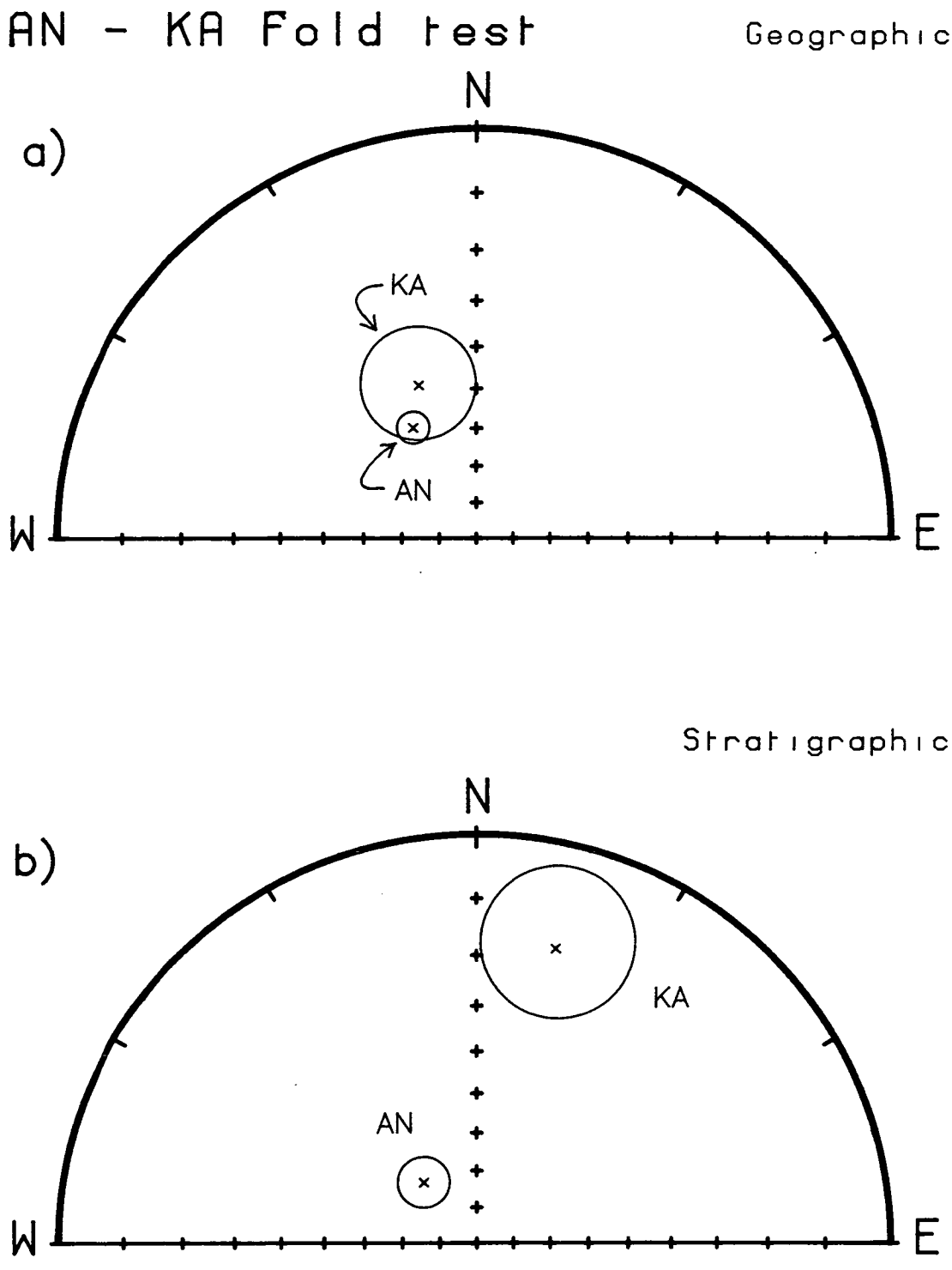

Figure 6.13. The negative intra-site fold test at sites AN and KA, within the Anamas-Akseki-Karacahisar platform. (a) In geographic coordinates, the site mean directions are in close agreement, whereas (b) in stratigraphic coordinates, they become widely separated. In stratigraphic coordinates, there is less than a 1% chance that the two sites share a common mean direction.

In summary, the palaeomagnetic results described here from the autochthonous units of the Isparta angle indicate that, in the majority of cases, a strong secondary overprint has completely replaced the primary depositional remanence. This pervasive remagnetisation took place after the development of folding at the sites. I shall discuss the tectonic rotation implied by these data in Section 6.6.2 below.

6.4 Palaeomagnetic results from the Antalya Complex.

6.4.1 Rock magnetic characteristics.

The frequency distribution of the NRM intensities of carbonate samples from within the allochthonous Antalya Complex are shown in Figure 6.14. The intensities fall naturally into two groups. The first group consists of platform limestones and carbonates of passive margin affinities, and has a mean intensity of 5.4×10^{-5} Am^{-1}. This is comparable to the mean intensity of the Tauride platform carbonates (7.6×10^{-5} Am^{-1}; Section 6.3.1). The same problems were encountered when analysing these samples as in the case of the autochthonous units, outlined in Section 6.3.1. The second group consists of samples from a complete Ordovician to Upper Cretaceous section within the off-margin carbonate sliver of the Kemer Zone. These samples have a mean intensity of 2.3×10^{-3} Am^{-1}, which is two orders of magnitude greater than the other limestones measured. The effects of instrumental and other noise on the measurement of these samples were significantly reduced because of the higher NRM intensities involved. All measurements of the carbonates of the Antalya Complex were made using the CCL cryogenic magnetometer.

Two sites were located in the Upper Triassic lavas of the Gödene Zone (Robertson and Woodcock, 1981c), at Cirali (site CI) and Sayrun (site SM). The mean NRM intensity of samples from these sites is 8.7 Am^{-1}, which is of the same order of magnitude as the mean intensity of the Upper Cretaceous pillow lavas sampled in the Limassol Forest area in Cyprus (1.3 Am^{-1}; Chapter 4, Section 4.3.1). All measurements were made on these samples using the Molspin spinner magnetometer (Chapter 1, Section 1.5).

The same procedures have been followed to determine the magnetic mineralogy of the Antalya Complex samples as those described in Section 6.3.1 for the Tauride platform units.

Typical results of studies of the rate of acquisition of IRM in fields up to 1.0 - 2.0 T for at least two samples per site are shown in Figure 6.15. As in the case of the platform units, the majority of samples exhibit a rapid initial rise and subsequent flattening off of curves below 0.3 T, indicating that magnetite is the dominant magnetic mineral present.

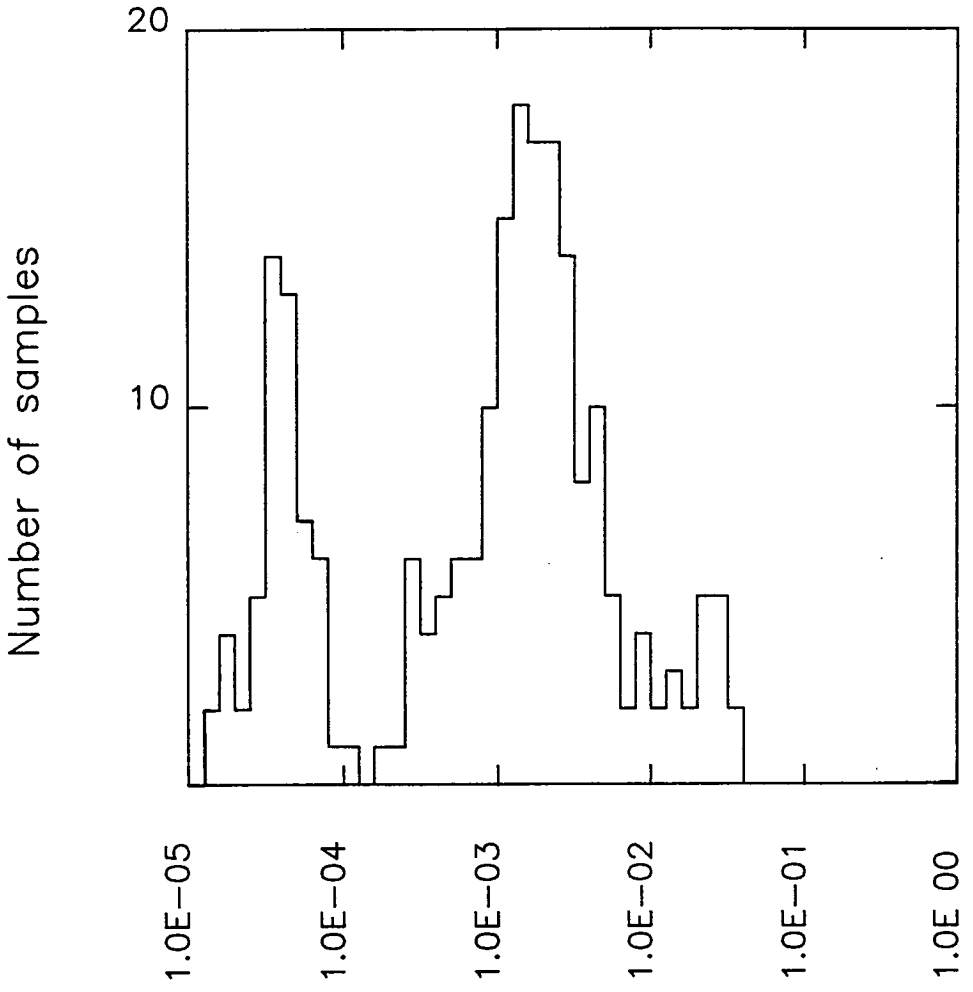

Figure 6.14. Histogram showing the frequency distribution of the NRM intensities of the carbonates analysed from the Antalya Complex.

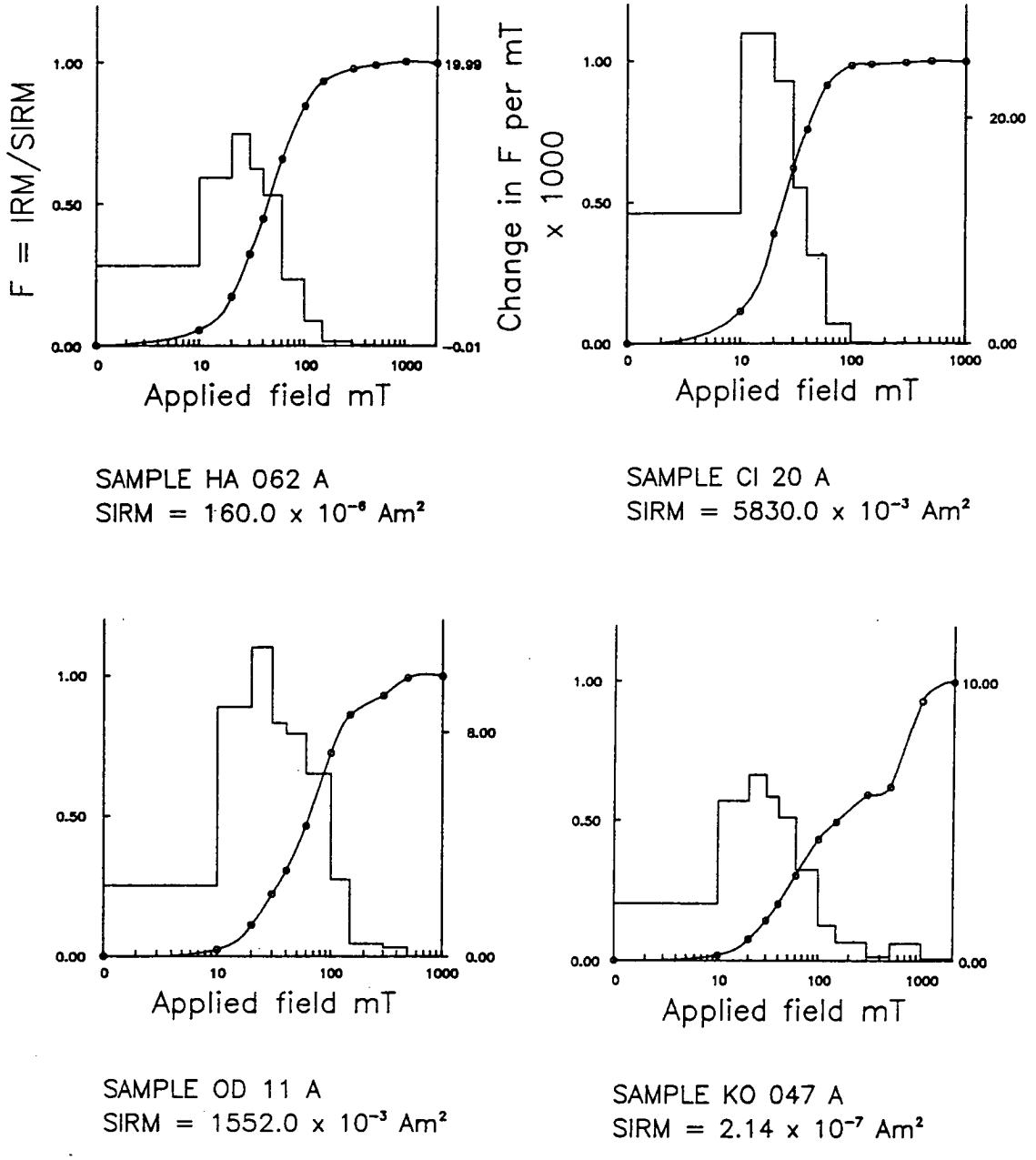

Figure 6.15. Typical IRM acquisition curves for the sampled lithologies within the Antalya Complex units, again indicating the dominance of magnetite as a potential remanence carrier. At two sites a magnetic mineral with a coercivity higher than that of magnetite is also present in some samples.

However, some samples showed an additional continuous increase in the IRM for fields above 0.3 T, demonstrating the presence of a mineral with a coercivity higher than that of magnetite (e.g. KO 47 A in Figure 6.15). The thermal demagnetisation of a composite IRM in these samples confirmed the presence of magnetite, with Curie temperatures of between 530°C and 580°C, and identified the higher coercivity fraction as haematite.

The application of the domain size test of Jonhson *et al.* (1975) to samples from the Antalya Complex sites gave results which are identical to those obtained from the Tauride platform units; i.e. in all cases, weak-field ARMs were found to be more resistive to AF demagnetisation than IRMs, indicating the dominance of single-domain-sized grains in the magnetite fraction of the samples.

Stepwise AF demagnetisation of a minimum of ten samples per site was carried out up to peak fields of 100 mT. In the case of the sedimentary sites, many samples did not reach stable endpoint directions before the intensity of magnetisation decreased below the minimum measurable level (approximately 10.0×10^{-6} Am^{-1}). Sufficient high quality demagnetisation paths to define reliable site mean directions were obtained at three sites within the sedimentary successions (see the next section).

Stable endpoints were identified in all the samples studied from the two sites located in the Upper Triassic pillow lavas of the Gödene Zone. However, at site SM the directions of the cleaned vectors were widely separated and a reliable site mean direction was not obtained. The data from this site are not discussed further.

In all samples where stable components of magnetisation were recovered, AF demagnetisation was found to be effective in reducing the intensity of magnetisation down to the noise level of the magnetometer used. This indicates that, as in the case of the Tauride platform samples, the haematite fraction identified by the IRM acquisition and thermal demagnetisation experiments does not carry any significant natural remanence. Typical Zijderveld demagnetisation diagrams are shown in Figure 6.16. Single stable components of magnetisation were identified after demagnetisation at less than 10 mT.

6.4.2 Palaeomagnetic results.

Reliable palaeomagnetic results with directions unrelated to the present geomagnetic field direction at the sampling site were obtained from four sites within the Antalya Complex units. Again, only data from those samples which showed stable demagnetisation paths were used in calculating mean directions of magnetisation at these sites, and cleaned remanence vectors for these samples were found by drawing best-fit lines through the last four or more points on Zijderveld demagnetisation

Table 6.2. Palaeomagnetic results from the Antalya Complex.

Site	Age	N	Geographic				Stratigraphic			
			Dec	Inc	α_{95}	K	Dec	Inc	α_{95}	K
Passive margin sequences of Bey Daglari)										
HA		37	033	47	4.5	29	037	12	6.9	13
Çayköy Ridge (correlated with the Davras Dag massif)										
KO	U.Cre	7	349	64	8.9	47	328	44	8.9	47
Sutculer Limestones										
YU	Mid-U.Cre (Present field direction)	39	005	57	4.8	18	-	-	-	-
Gödene Zone										
CI	U.Tri	18	334	49	5.6	40	309	-46	11.8	10
	Sub-site 1	7	328	45	10.7	32	325	-20	10.7	32
	Sub-site 2 (overturned)	11	338	51	6.4	52	289	-60	6.4	52
Kemer Zone										
KK	Ord-U.Cre	123	321	36	3.2	17	056	34	5.4	7
	Ordovician	27	320	39	7.9	13	112	29	7.9	13
	Permian	49	321	36	4.6	21	049	26	5.3	15
	Triassic	7	305	56	22.0	8	055	20	22.0	8
	Jur-U.Cre	40	322	29	4.6	25	030	40	4.5	27
Tektrova Zone										
OD	U.Cre (Present field direction)	12	354	55	2.8	238	-	-	-	-

N = number of samples; α_{95} = semi-angle of 95% cone of confidence; K = Fisher precision parameter

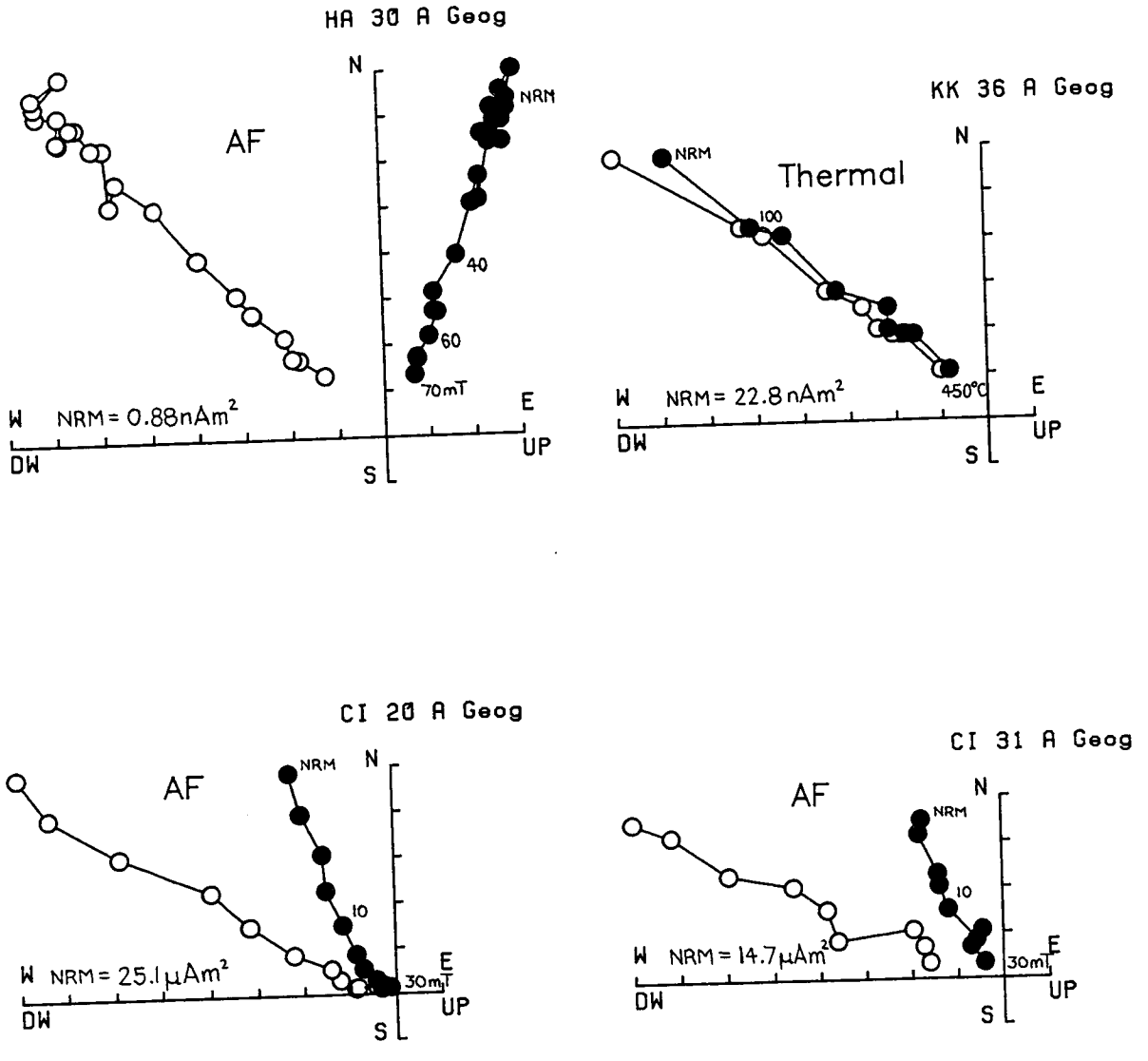

Figure 6.16. Examples of alternating field demagnetisation of the natural remanence carried by the Antalya Complex samples. Note that the vertical projections are on the horizontal axes.

diagrams (Zijderveld, 1967). The cleaned site mean directions are reported in Table 6.2, both in geographic and stratigraphic coordinates.

At a further two sites within the Antalya Complex (sites OD and YU, Figure 6.01), only present field components were identified (Figures 6.17 and 6.18), indicating that chemical remanent magnetisations acquired during subaerial weathering and/or viscous remanent magnetisations acquired during the last few hundred thousand years dominate the remanences (Tarling, 1983). The mean NRM directions at these sites are also given in Table 6.2.

NRM directions obtained from samples at a series of small sites located along a transverse through the imbricate thrust stack of the Kumluca Zone, collectively known as site LB, were widely dispersed and showed no grouping within individual sheets (Figure 6.19a). During alternating field demagnetisation, the sample vectors became even more dispersed; for example, Figure 6.19b shows the directions obtained after the 20 mT demagnetisation step. No stable endpoints were identified at this site.

Of the four reliable sites, three are located in the southwestern segment of the Antalya Complex.

Site HA exhibits the only northeasterly-directed cleaned remanence directions (in geographic coordinates) identified with the Isparta angle area (Figure 6.20a). This site is located within Upper Triassic, *Halobia*-bearing limestones which represent the platform edge facies of the Bey Daglari massif (Çatal Tepe unit; Robertson and Woodcock, 1982). The unit is separated from the massif by a low-angle thrust of Upper Cretaceous to Palaeocene age. After the application of structural corrections to the data from this site, the cleaned remanence directions diverge and form two groups; one with shallow inclinations and northeasterly-directed declinations, and a second with steeper inclinations and easterly-directed declinations (Figure 6.20b). This may indicate that the observed magnetisation was acquired after the development of folding at the site, in agreement with the post-folding age of the magnetisations identified at the Bey Daglari sites (Section 6.3.2). However, the northeasterly site mean declination in geographic coordinates is difficult to explain, and suggests that the sampled unit may represent a detached block.

More conclusive evidence for the secondary nature of the remanence carried by the Antalya Complex units comes from the remaining two sites in the southwestern area.

Site CI is located within the Upper Triassic pillow lavas of the Gödene Zone (Robertson and Woodcock, 1981c) at Cirali (Figure 6.01). Samples were collected at this site from two separate fault-bounded blocks. At one of these sub-sites, the morphology of the pillow lavas indicates that the block has been overturned. The cleaned remanence directions obtained from both blocks cluster in the northwest quadrant before

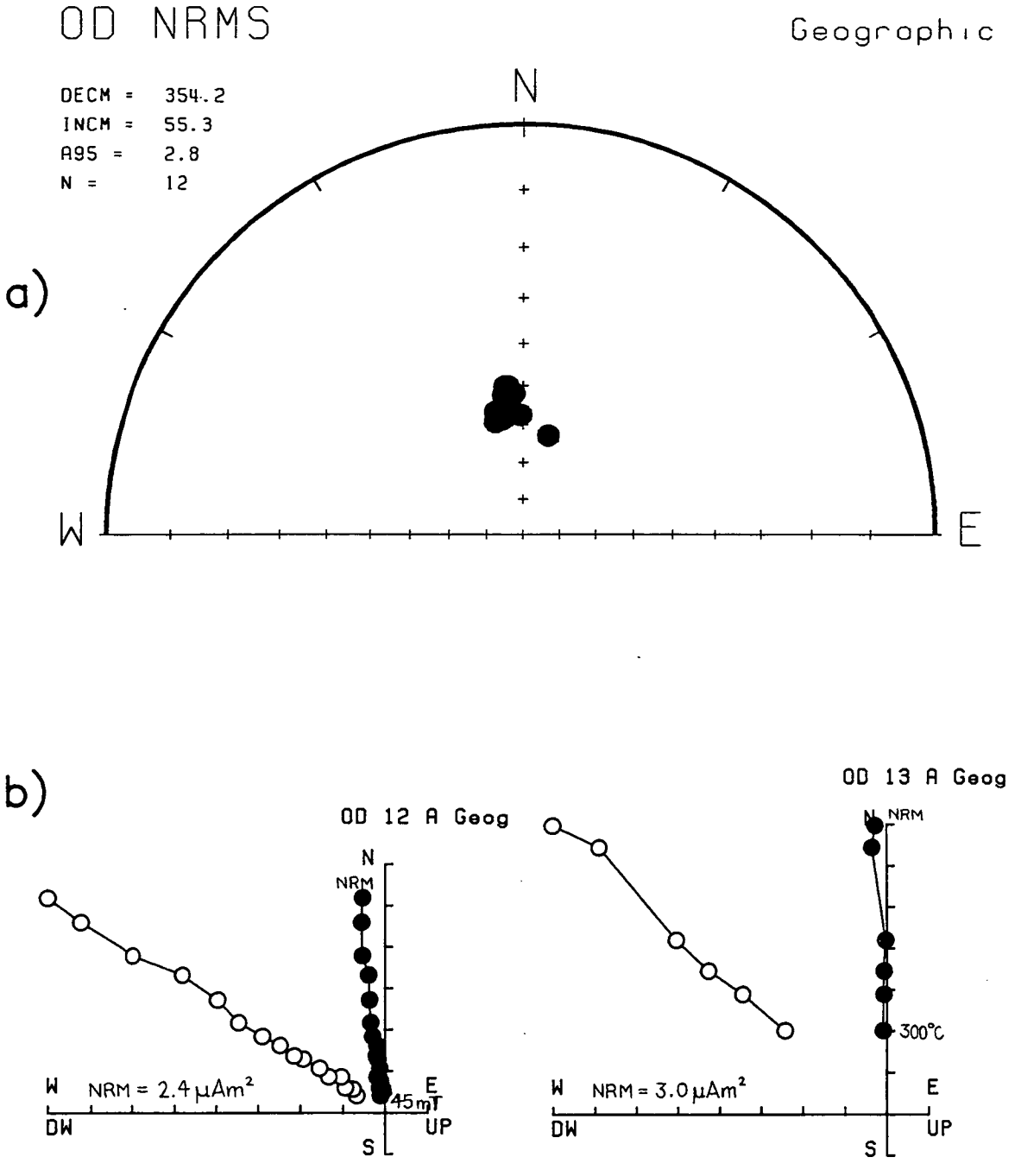

Figure 6.17. (a) the distribution of NRM directions at site OD, located within Upper Cretaceous ophiolite-derived sandstones of the Tekirova Zone. The remanence here is dominated by viscous magnetisations acquired during the last few hundred thousand years; (b) examples of both AF and thermal demagnetisation of samples from this site, showing that only present-field direction components are present. Note that the vertical projections are on the horizontal axes.

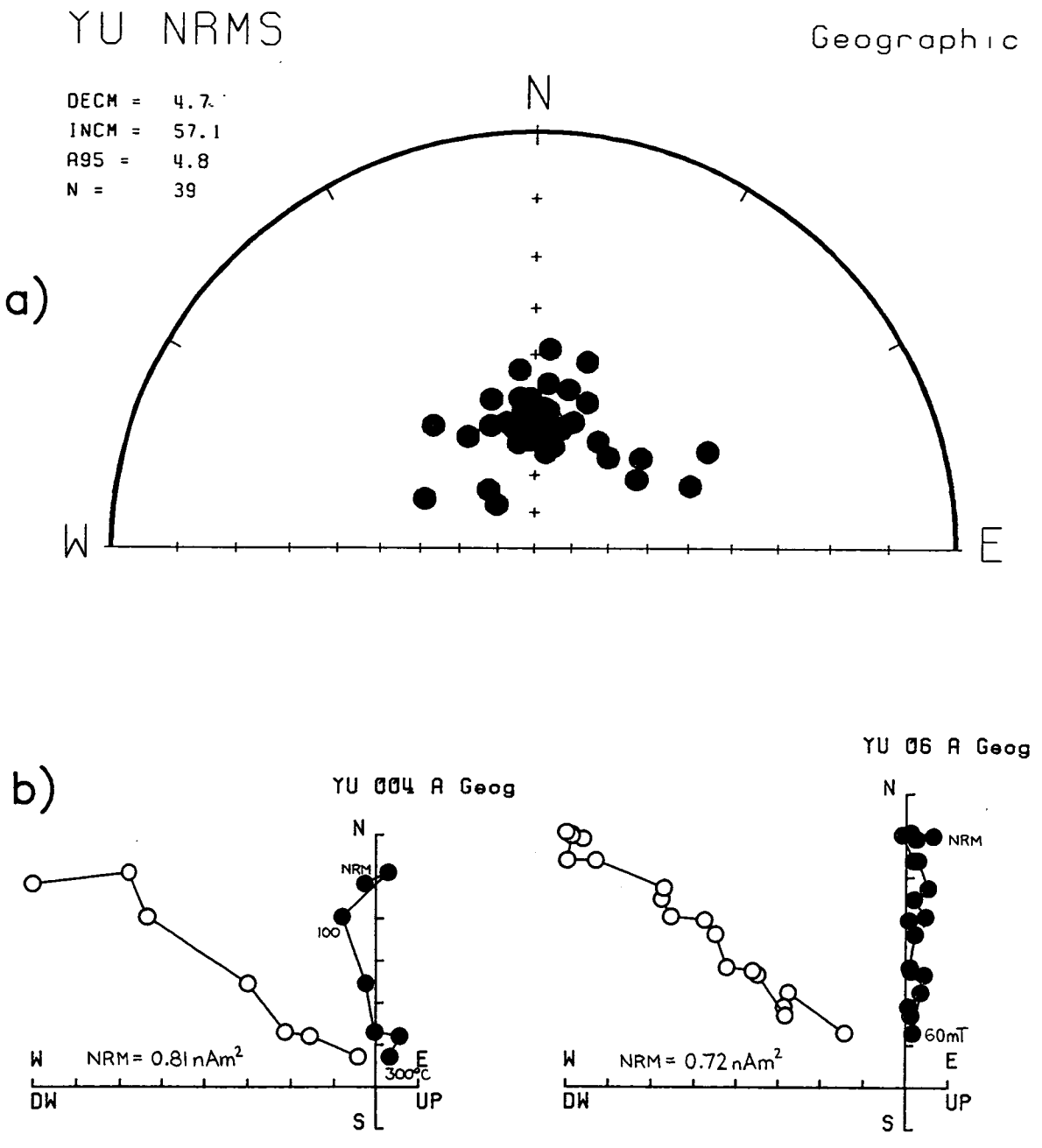

Figure 6.18. (a) the distribution of NRM directions at site YU, located in the Sutculer Limestones of Mid-Upper Cretaceous age. As at site OD, the remanence here is dominated by viscous magnetisations acquired during the last few hundred thousand years; (b) examples of both AF and thermal demagnetisation of samples from this site, showing that only present-field direction components are present. Note that the vertical projections are on the horizontal axes.

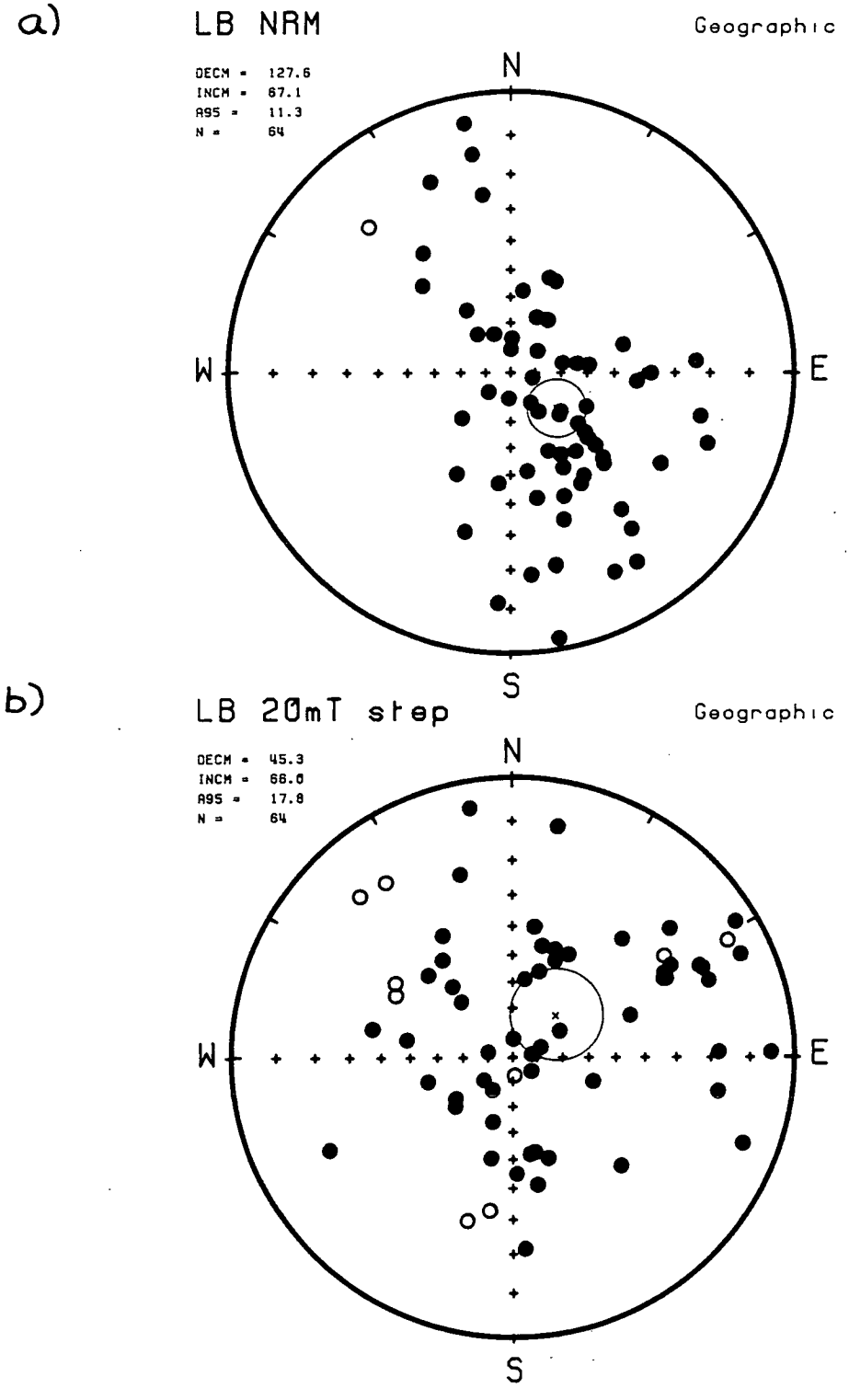

Figure 6.19. (a) The widely dispersed NRM directions observed at site LB, within the imbricate thrust stack of the Kumluca Zone; (b) Remanence directions obtained at this site after demagnetising at 20 mT are more widely dispersed than the NRM directions. No stable endpoints were identified at this site.

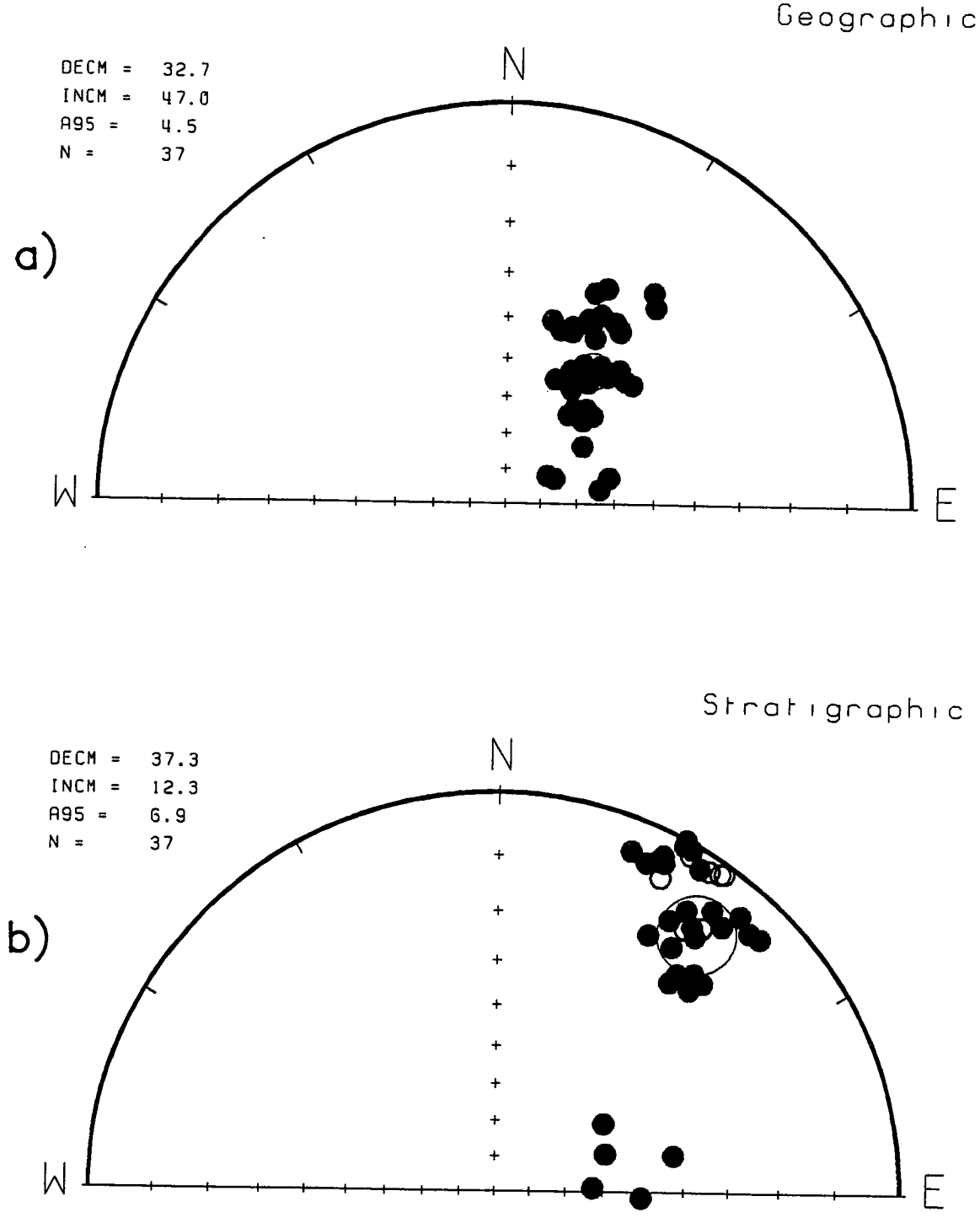

Figure 6.20. The cleaned remanence directions observed at site HA, within the Upper Cretaceous limestones of the Çatal Tepe unit (Robertson and Woodcock, 1982), both before (a) and after (b) the application of stratigraphic corrections. Note the northeasterly-directed vectors and the increased dispersion in stratigraphic coordinates.

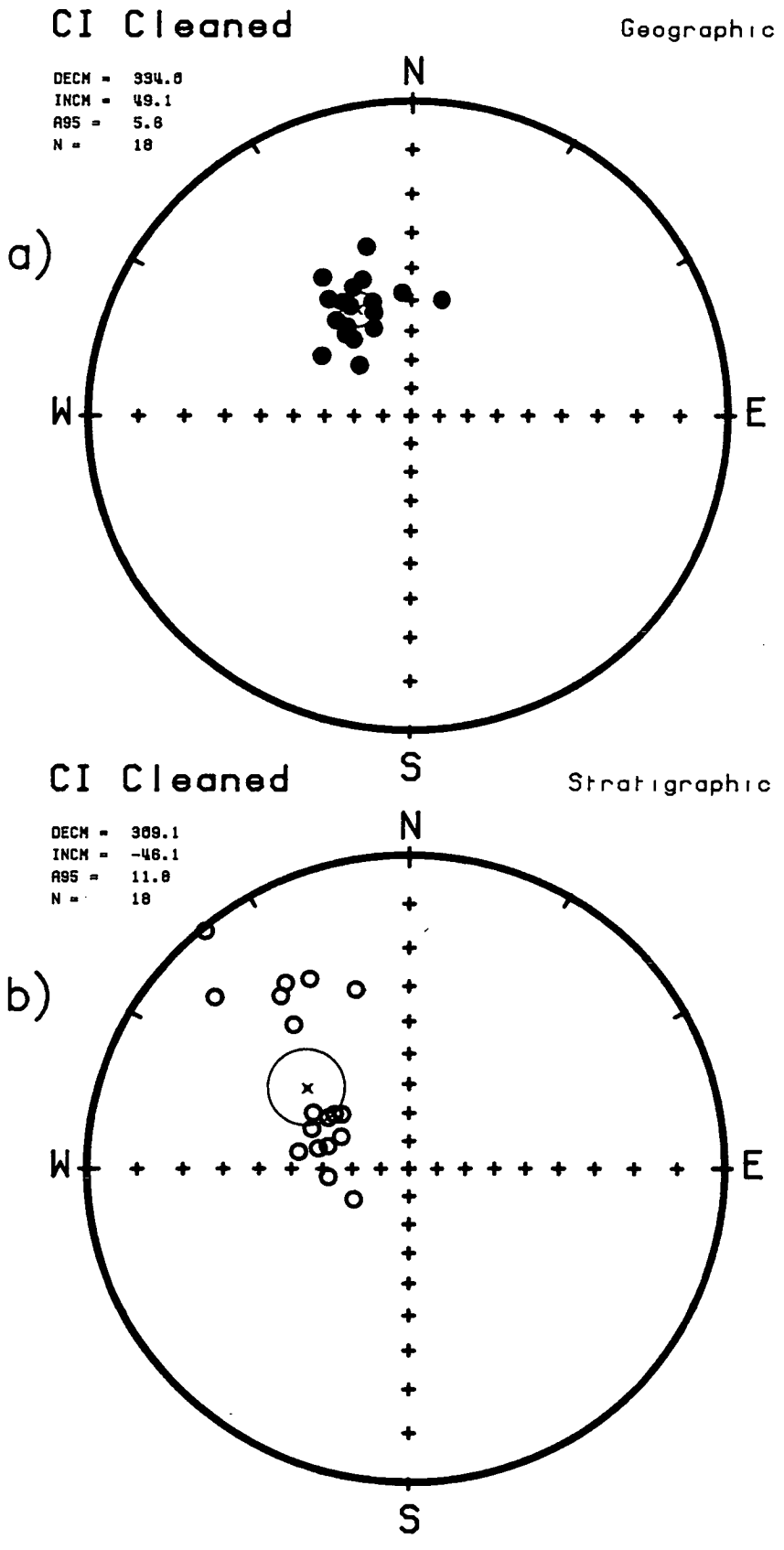

Figure 6.21. The cleaned remanence directions observed at site CI, within the Upper Triassic lavas of the Gödene Zone (Robertson and Woodcock, 1981c), both before (a) and after (b) the application of stratigraphic corrections. Note the separation of vectors into two groups associated with the two sampled fault-blocks (one of which is inverted) after correction to the palaeohorizontal.

correction to the palaeohorizontal (Figure 6.21a). The mean direction for the blocks is in close agreement with those described in Section 6.3.2 from the platform units. After correcting for the observed tilt of the palaeohorizontal at each block, the remanence directions diverge into two groups, both with negative inclinations (Figure 6.21b). If we examine the mean directions for each block separately, we see that their α_{95} cones of confidence overlap in geographic coordinates (Figure 6.22a), but become distinct in stratigraphic coordinates (Figure 6.22b). This negative fold test is significant at the 99% confidence level (McFadden and Jones, 1981; see Appendix A), and demonstrates the post-folding age of the magnetisation at the site.

The samples from site KK were collected from a 100 metre long continuous section within the Kemer Zone, inferred to be an off-margin, carbonate-capped microcontinental sliver (Chapter 5, Section 5.3.2). The sampled section covers the complete Ordovician to Upper Cretaceous interval. Table 6.2 gives a breakdown of the number of samples analysed in each time period. A large number of stable endpoints were obtained at this site, partly because of the significantly higher NRM intensities involved (Section 6.4.1 above). Two lines of evidence point to the secondary nature of the remanence at site KK:
a) No reversed polarity samples have been identified, even though the sampled section covers such a broad stratigraphic interval (Figure 6.23a). In particular, over one third of the samples analysed are of Permian age, and the Permo-Carboniferous represents a reversed polarity bias superchron (Harland *et al.* 1982).
b) The site mean direction in geographic coordinates is in close agreement with those obtained at site CI and the Tauride platform sites (Figure 6.23a). The removal of the stratigraphic tilt along the section results in a increase in the dispersion of remanence directions (Figure 6.23b). If we examine the data in four 'time-slices' corresponding to the Ordovician, Permian, Triassic and Jurassic to Upper Cretaceous (Table 6.2), then we see that the α_{95} cones of confidence for these groups overlap in the northwest quadrant in geographic coordinates (Figure 6.24a), but become widely separated in stratigraphic coordinates (Figure 6.24b). This negative fold test is significant at the 99% confidence level (McFadden and Jones, 1981; see Appendix A).

The only reliable site mean direction obtained in the northern outcrop areas of the Antalya Complex comes from site KO (Table 6.2). This site is situated in a small, elongate outcrop of platform carbonates known as the Çayköy Ridge (Figure 6.01). This unit has been interpreted by Waldron (1984a, b) as a continuation of the larger Davras Dag carbonate platform to the west. The sampled section is of Upper Cretaceous age. The cleaned remanences at this site have a mean inclination in geographic coordinates which is steeper than the inclination of the present geomagnetic field at the site (64°, compared with 56° for an axial geocentric dipole field). After application of a tilt

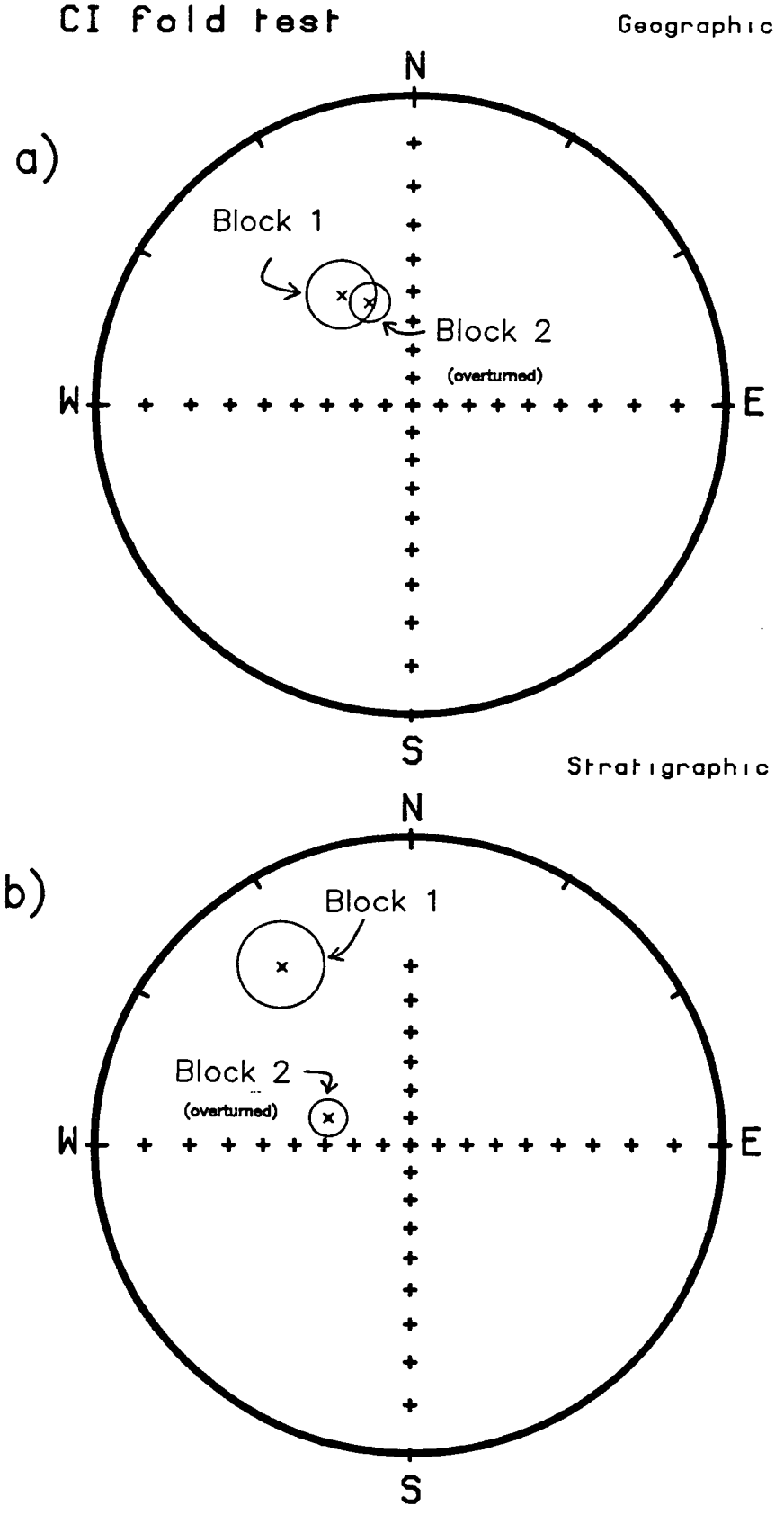

Figure 6.22. The within-site fold test provided by the fault-bounded blocks sampled at site CI; (a) in geographic coordinates the α_{95} cones of confidence for the two groups overlap, whereas (b) in stratigraphic coordinates they become distinct. This negative fold test is significant at the 5% confidence level.

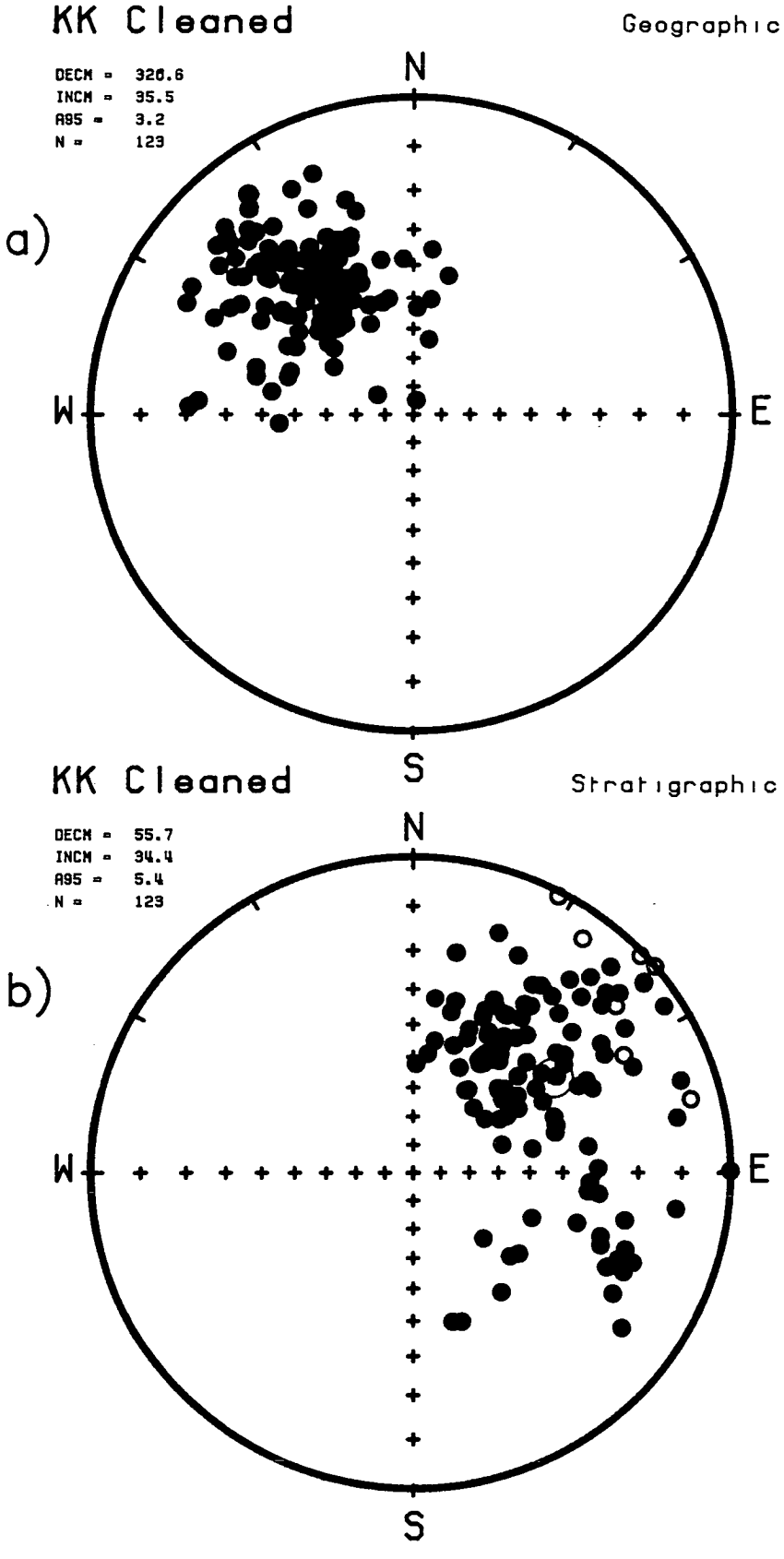

Figure 6.23. The cleaned remanence directions observed at site KK, which consists of a continuous Ordovician to Upper Cretaceous section. (a) The site mean direction in geographic coordinates lies in the northwest quadrant and matches closely with those obtained from site CI and the Tauride platform sites. (b) After removing the bedding tilt along the section, the remanence directions become more dispersed. Note the absence of reversed polarity samples.

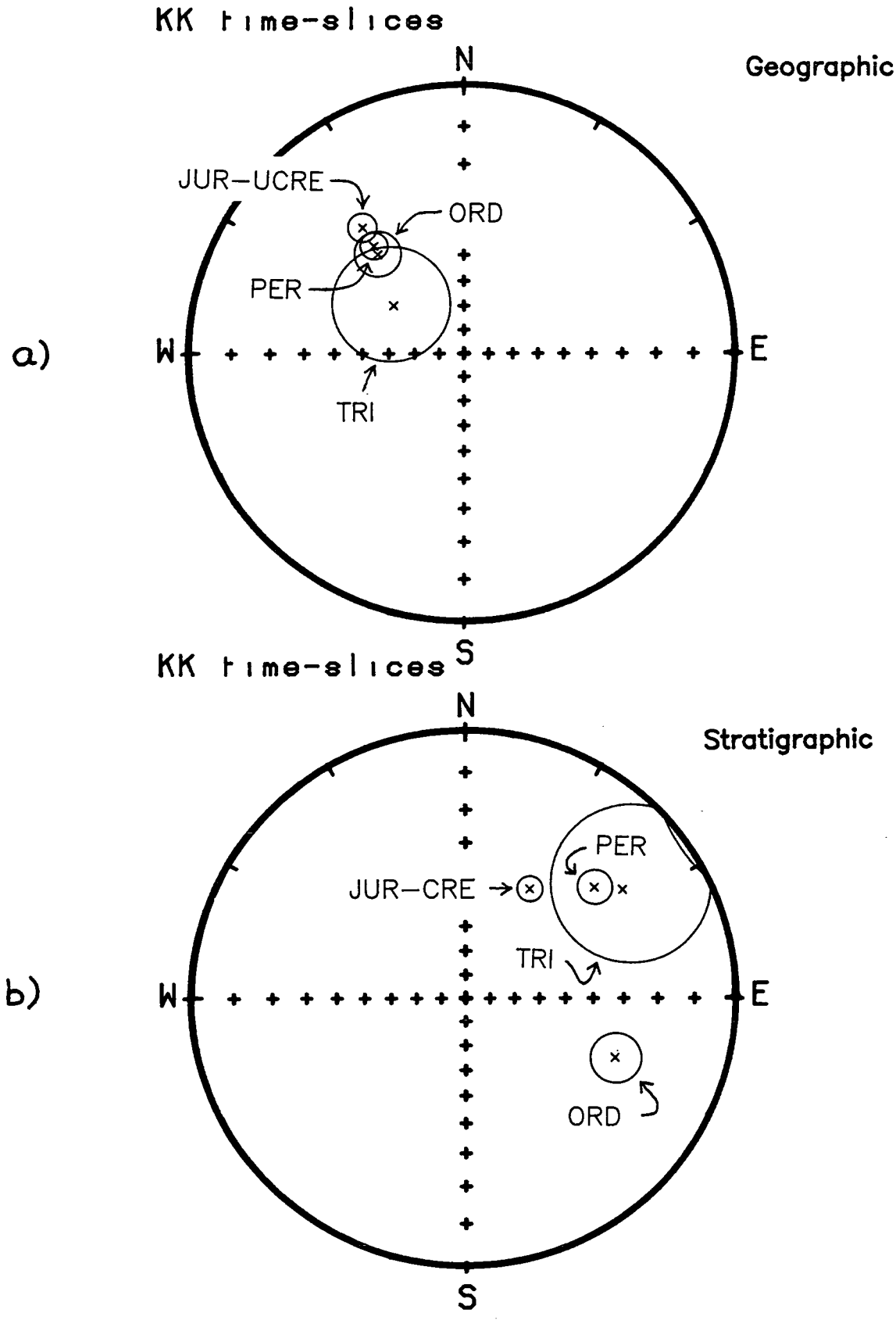

Figure 6.24. The within-site fold test provided by the data at site KK, when divided into time-slices corresponding to the Ordovician, Permian, Triassic, and Jurassic to Upper Cretaceous; (a) in geographic coordinates the α_{95} cones of confidence for the four groups overlap, whereas (b) in stratigraphic coordinates they become distinct. This negative fold test is significant at the 1% confidence level.

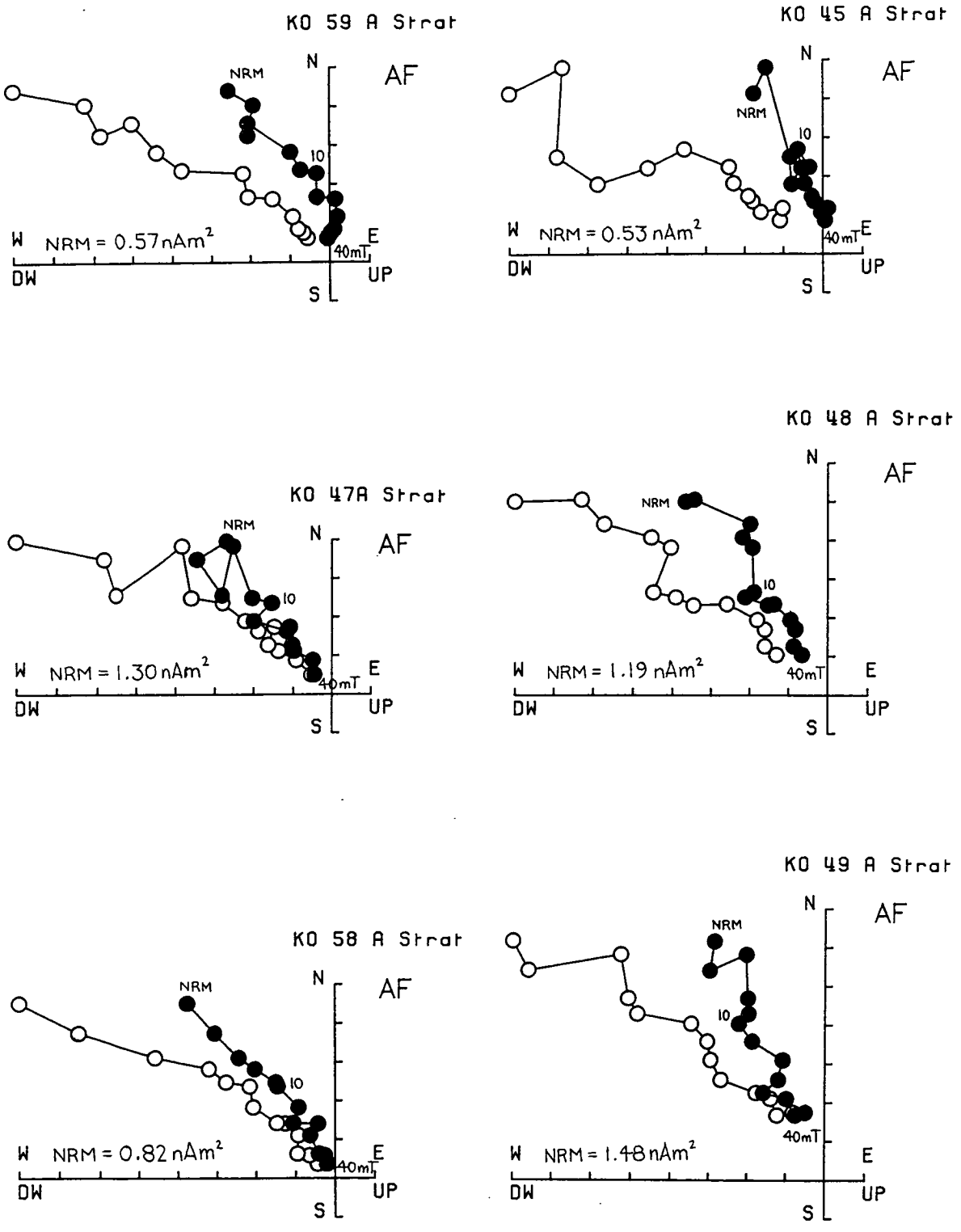

Figure 6.25. Examples of alternating field demagnetisation of the natural remanence carried by the samples from site KO, located in the Çayköy Ridge. Note that AF demagnetisation is effective in removing all the magnetisation, even though haematite is present in these samples. This demonstrates that only magnetite carries a significant natural remanence at this site. Note that the vertical projections are on the horizontal axes.

correction to the data, however, the site mean direction becomes indistinguishable from the remagnetised directions described at other sites (Table 6.2; Figure 6.25). Although there is a possibility that the magnetisation at this site is a primary depositional remanence, I therefore prefer to interpret this result as a secondary remanence acquired prior to the minor tilting which has occurred at the site (mean dip = 21°).

In summary, the results here indicate that the remagnetisation which has affected the platform sequences has also resulted in the destruction of the primary remanence carried by the sampled units of the Antalya Complex. This secondary magnetisation has been shown to reside purely in magnetite grains.

6.5 Summary of the evidence for extensive remagnetisation.

In both the Tauride platform units and the Antalya Complex there is a substantial body of data which indicate that the sampled units have been subjected to an extensive remagnetisation event *after* the development of folding at the sites. To recap, the evidence for the secondary nature of the measured remanent magnetisations includes:
i) within-site negative fold tests at sites CD and AN in the autochthons and sites HA, CI and KK in the Antalya Complex, where either the within-site dispersion is increased or the cleaned remanences divide into two or more well-defined groups upon application of stratigraphic corrections;
ii) negative fold tests between sites YA and FI within the Bey Daglari and between sites KA and AN in the Anamas-Akseki-Karacahisar platform;
iii) the lack of reversed polarity samples throughout the area, and in particular within the complete Ordovician to Upper Cretaceous section at site KK in the Kemer Zone;
and iv) the area-wide agreement between the site mean directions in geographic coordinates (Figure 6.26; Tables 6.1 and 6.2).

The directions of the secondary magnetisation at all sites listed in Tables 6.1 and 6.2 are unrelated to the present geomagnetic field direction in the study area. The results cannot reflect viscous components of magnetisation acquired in the ambient field in the laboratory during storage, as samples were not stored in orientated positions. The common northwesterly-directed remanence directions must therefore represent ancient magnetisations acquired during some remagnetisation event. The possible causes of this remagnetisation are discussed in the next section.

It should be noted that the Bey Daglari sites sampled by Lauer (1981) and Kissel and Poisson (1987) probably retain primary depositional remanences. These sites are of Palaeocene to Miocene age (Chapter 5, Section 5.4) and record both normal and

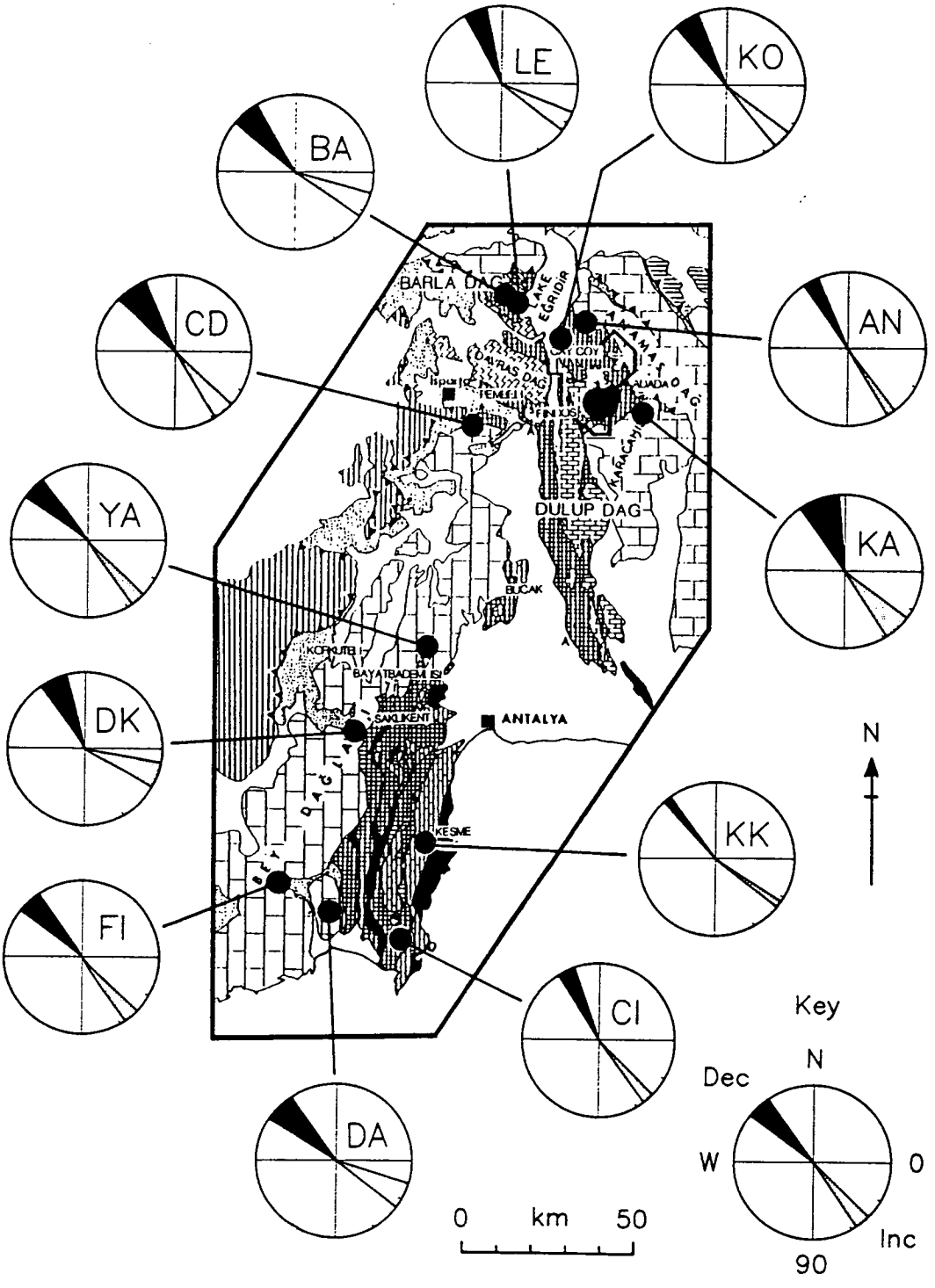

Figure 6.26. 'Clock' diagrams showing the 95% confidence limits associated with the mean declination and inclination at each of the remagnetised sites in geographic coordinates, and at the Barla Dag sites which probably retain a primary remanence. The confidence limits have been calculated from each α_{95} using the method of Demarest (1983) (see Chapter 4, Section 4.3.2). Note the area-wide consistency of the site mean declinations.

reversed polarities of magnetisation. In particular, at two sites of Kissel and Poisson (op. cit.) an antiparallel alignment of both polarities within each site indicates the stability and primary nature of the remanence (sites EL 71 and EL 67, of Eocene and Oligocene age respectively; Figure 5.10). It is significant that these sites are located along the western flank of the Bey Daglari massif. I shall return to this point in Section 6.6.3 below.

6.6 Discussion of results.

6.6.1 Assessment of mechanisms of remagnetisation.

Many palaeomagnetic studies of ancient limestones have identified stable magnetisations carried by magnetite. In most cases, such magnetisations have been interpreted as post-depositional remanences acquired soon after initial deposition. In the present study, however, negative fold tests demonstrate the secondary nature of the characteristic magnetisation identified at many sites. The area-wide consistency of the site mean directions in geographic coordinates indicates that remagnetisation was widespread. We therefore have a situation where a stable, ancient secondary magnetisation is carried exclusively by magnetite. This secondary magnetisation has completely obscured any pre-existing primary remanence carried by the units sampled in the Antalya Complex. However, components of magnetisation of possible primary origin may be retained by some of the successions of the adjacent carbonate platforms.

There are two possible explanations for the origin of the pervasive remagnetisation identified in this study: i) it represents a thermally activated remagnetisation due to burial and subsequent uplift; or ii) it represents a chemical magnetisation acquired by the growth of authigenic magnetite.

Two main problems are associated with the first of these explanations. Firstly, thermal demagnetisation experiments carried out on samples from several of the carbonate platform sites reveal maximum unblocking temperatures of between 350°C and 500°C (Figure 6.07). The units sampled have only been subjected to sub-greenschist facies metamorphism and are unlikely to have been buried to depths greater than 1-3 km (A. H. F. Robertson, pers. comm., 1990). Assuming an average geothermal gradient of 25°C/km, these burial depths suggest that the units have been heated to a maximum of 75°C. The theoretical curves for magnetite of Pullaiah *et al.* (1975, Figure 1a) suggest that even an exposure to such a temperature for a period in excess of 4.5 b.y. could not produce the observed unblocking temperatures. Secondly, it is difficult to see how a burial and uplift event could result in the pattern of remagnetisation observed here, where the southwestern segment of the Antalya Complex and the eastern margin

of the Bey Daglari have been completely remagnetised, whereas the western margin of the Bey Daglari and the Barla Dag probably retain primary remanences.

The alternative explanation is that the secondary magnetisation represents a chemical remanent magnetisation (CRM), produced by the precipitation of authigenic magnetite from fluids migrating through the orogen during the final stages of emplacement of the Antalya Complex onto the adjacent continental margin. It is well known that when continental margins in zones of crustal convergence are buried beneath thrust sheets, fluids containing abundant hydrated minerals are expelled towards the foreland basin and continental interior. Huge volumes of fluid are involved, perhaps one-third to one-half of the volume of the overthrust units (Oliver, 1986). Such fluids may be expected to react with the host lithologies, possibly releasing iron into solution, which may then contribute to the formation of authigenic magnetite. Elmore *et al.* (1987) have demonstrated that the precipitation of authigenic magnetite may be linked to the migration of hydrocarbon-related fluids. It should be noted in this respect that drilling by the Turkish geological survey (MTA) has established the existence of heavy oil in the core of the Finike Anticline (Bey Daglari). Also, methane (of uncertain origin) is currently escaping from the Tekirova ophiolite (A. H. F. Robertson, pers. comm., 1990). If the orogenic fluids were also hot, then the remagnetisation could have been due to both chemical and thermal magnetisation processes.

This model would explain elegantly the pattern of remagnetisation observed in this study (Figure 6.27). Tectonic fluids forced thorough the orogen would be expected to have the greatest geochemical effect upon the overthrust and tectonised Antalya Complex units and the adjacent parts of the platform. Pervasive remagnetisation would be expected to occur within these units. On the other hand, the more distal, inboard parts of the carbonate platform would experience little or no remagnetisation, and may be expected to retain a primary magnetisation signal. Also, the sequences of the Barla Dag escaped remagnetisation because this unit has never been covered by overthrust ophiolitic units (the platform here is covered by Eocene flysch which contains no ophiolite-derived detritus).

In recent years it has become established that a similar process was responsible for remagnetisation of Palaeozoic carbonates in the Appalachian Basin of eastern North America. In a study of the Devonian Helderberg and Onondaga carbonates of New York State, Jackson *et al.* (1988) and McCabe *et al.* (1989) demonstrated that magnetite concentration along the outcrop belt of the formations varied in a regular fashion. A striking correlation was found between the magnetite concentration and the degree of diagenetic illitisation of clay minerals in a Devonian bentonite horizon, which took place during the Alleghenian orogeny (Carboniferous). Jackson *et al.* and McCabe *et al.* (op.

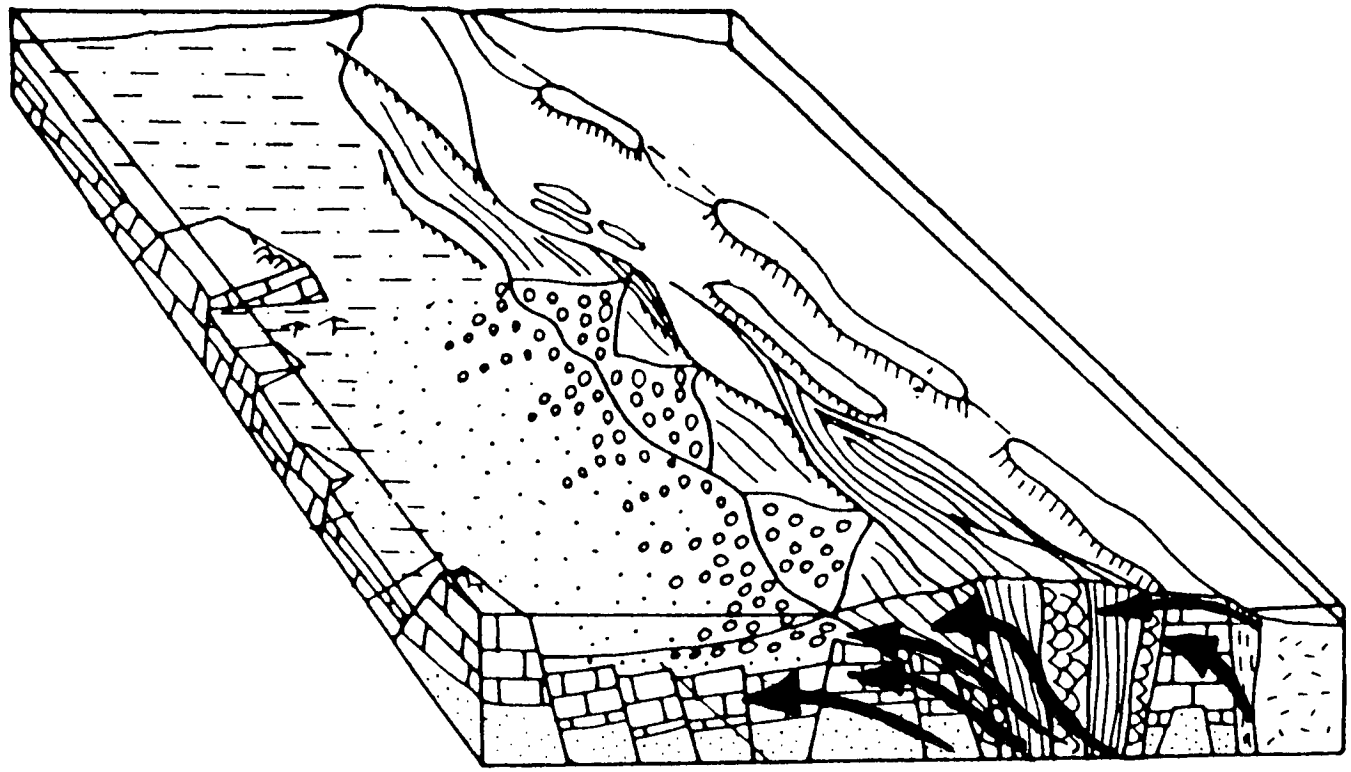

Figure 6.27. Block diagram to illustrate the concept of the expulsion of tectonic brines towards the foreland during convergence and the emplacement of the Antalya Complex onto the Bey Daglari carbonate platform (modified from Haywood, 1984).

cit.) concluded that most of the magnetite in these carbonates is of authigenic origin, and that clay mineral alteration and magnetite authigenesis were coeval, late Palaeozoic events that were controlled by the same diagenetic factors. They noted that authigenic potassium-feldspars and potassium-bentonites of Alleghenian age had previously been reported in the basin, giving evidence for potassium-rich orogenic fluids. McCabe *et al.* (op. cit.) concluded that, since the illitisation of detrital smectite requires potassium and that the process may release iron, the introduction of exotic, potassium-rich brines may have triggered both magnetite authigenesis and the illitisation of detrital clays within the limestones.

6.6.2 Geotectonic interpretation of the results.

I interpret the secondary remanence carried by the majority of the sampled units in the Isparta angle area as a chemical remanent magnetisation, residing in authigenic magnetite. Although the youngest remagnetised units sampled in the present study are parts of the Palaeocene of the Bey Daglari, the remagnetisation event is constrained to be post-folding in age by the various negative fold tests. This folding was related to Miocene regional compression. It is possible, therefore, that the authigenic magnetite formed in the Early to Middle Miocene as a result of a short-lived geochemical event related to the migration of orogenic fluids ahead of the emplacing Antalya Complex. The short duration of the event is indicated by the lack of reversed polarities of magnetisation in the remagnetised units, since the Miocene forms part of the Cretaceous-Tertiary-Quaternary mixed polarity superchron (Harland et al., 1982) where reversals of the geomagnetic field were frequent. The longest normal polarity chron in the Miocene was of approximately 1 Ma duration (polarity chron 6; Harland et al., 1982).

The most northerly sampled unit, the Barla Dag, escaped remagnetisation and probably retains a primary remanence. The western parts of the Bey Daglari massif further to the south, where reversed polarity site mean directions have been identified (Lauer, 1981; Kissel and Poisson, 1987; Chapter 5, Section 5.4) were also unaffected by the remagnetisation event.

Since it has been demonstrated that, in the majority of cases, the remanence directions described above represent secondary magnetisations acquired after tectonic folding, it is appropriate to calculate a regional mean direction based on the site mean directions in geographic coordinates*:

---

*also including the tilt corrected mean direction from site KO.

Dec = 326°, Inc = 43°, K = 37, A_{95} = 8.1°, N = 10.

This indicates that, subsequent to the growth of authigenic magnetite grains through the critical blocking volume, the Bey Daglari platform and the overthrust southwestern segment of the Antalya Complex, the Çayköy Ridge, and at least the northern part of the Anamas-Akseki-Karacahisar platform were all subjected to a *c.* 30° anticlockwise rotation (with respect to present north). This rotation was probably driven by the overall convergence and the bending of the Aegean arc in the Miocene (see Chapter 7, Section 7.3.1). This also drove the final stages of the emplacement in the Middle to Late Miocene of the Lycian Nappes onto the western margins of the Tauride platform units, which form the western limb of the Isparta angle. Orogenic fluids related to this later thrusting event may not have affected the Bey Daglari massif because of the presence of an extensive foreland basin, filled with impermeable muds, located between the platform and the Lycian Nappes to the west.

The close agreement between the declination data at the two Barla Dag sites (BA and LE) demonstrates that no significant tectonic rotation of this massif occurred between the Upper Triassic and the Palaeocene/Eocene. The 30°-40° anticlockwise tectonic rotation of the Barla Dag platform (with respect to the present north), suggested by the data at these sites, agrees well with that suggested by the regional mean direction calculated from the remagnetised sites. This implies that the Middle Miocene regional rotation affected both areas to the same extent.

Finally, the Aksu phase of thrusting in the Upper Miocene (Poisson, 1977) transported the entire eastern limb of the Isparta angle over the northeastern edge of the Bey Daglari (Waldron, 1984b). This final convergence may have been responsible for slightly tilting the sequence sampled at site KO (Çayköy), and may also be responsible for some of the minor variations in site mean inclinations between the remagnetised sites. The post-remagnetisation tilting at site KO may also be related to the development of the Neotectonic Kovada graben.

One of the original aims of this work was to constrain the palaeolatitude of formation of the Isparta angle units. The strong Middle Miocene magnetic overprint which has been identified has severely restricted the usefulness of the sampled successions for this purpose. However, components of magnetisation of assumed primary origin have been recovered from the sequences of the Barla Dag massif, at sites BA and LE. The inclination data from these sites imply a similar palaeolatitude of approximately 13-17°N for the Barla Dag during both the Upper Triassic and the Palaeocene/Eocene. This is in agreement with the palaeolatitudes calculated from the African polar wander path of Westphal *et al.* (1986), assuming sites in the Isparta angle

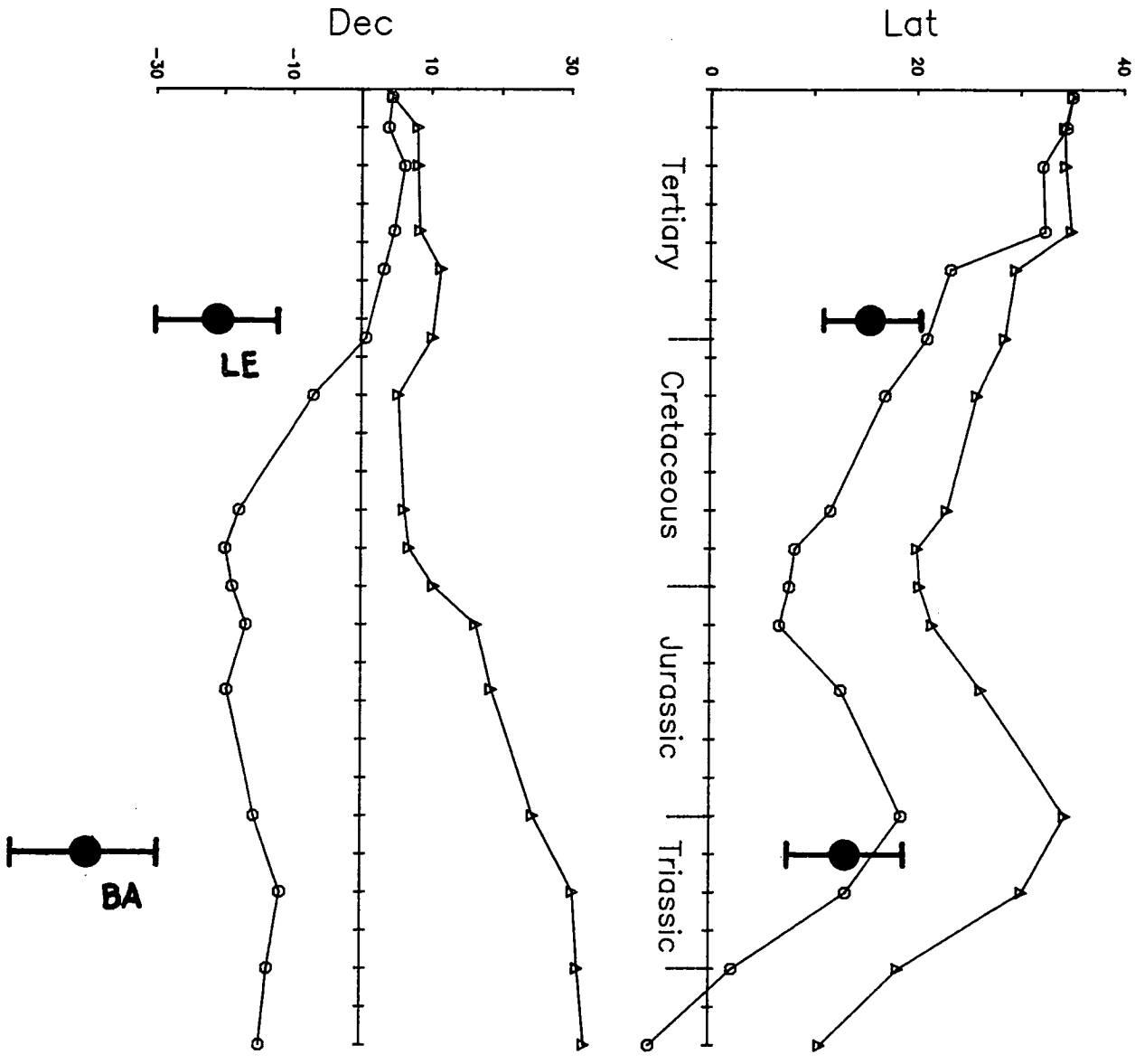

Figure 6.28. Reference declination and palaeolatitude curves calculated from Westphal *et al.*'s (1986) Eurasian and African polar wander curves (triangles and circles respectively) for a site in the centre of the Isparta angle (lat.= 37°N, long.= 31°E). Also shown are the declination and palaeolatitude, derived from the site mean directions at sites BA and LE (within the Barla Dag massif), together with their 95% confidence limits determined using the method of Demarest (1983). Note the African affinity of the sampled block.

were rigidly attached to Africa (Figure 6.28). This demonstrates the Gondwanan affinities of this unit. The inclination data from site BA is discussed further in Section 6.6.3, in relation to the hypothesis of Lauer (1981, 1984).

Additionally, the regional mean inclination of 43° of the remagnetised sites implies a palaeolatitude of 25°N for the sampled units during the Middle Miocene. This is similar to the palaeolatitudes obtained in other studies of Miocene sediments in the Aegean region (e.g. Kissel *et al.*, 1985; Kissel and Poisson, 1986, 1987; Horner and Freeman, 1983). At face value this suggests that the Aegean region as a whole has undergone a northward drift of over 1000 km since the Miocene. This is unreasonable geologically. However, Westphal et al. (1986) have pointed out that low inclination values during the Tertiary are not confined to the Aegean area, but have been obtained over a large part of the Mediterranean region, from Iberia to Iran. As yet this phenomenon has no consistent explanation (Kissel and Laj, 1988).

6.6.3 Reassessment of previous palaeomagnetic studies within the Isparta angle.

The recognition that in many cases the remanent magnetisation recorded by successions along the western limb of the Isparta angle represents a remagnetisation acquired during the final emplacement of the Antalya Complex has several implications for the data previously obtained in the area by Kissel and Poisson (1987) and Lauer (1981, 1984). These data were discussed previously in Chapter 5.

The main conclusion reached by Kissel and Poisson (1987) was that the Bey Daglari platform has experienced a *c.* 30° anticlockwise rotation since the Middle Miocene (Langhian). The reversed polarity of some of their sites may attest to the primary nature of the magnetisations identified. As discussed in Sections 6.6.1 and 6.6.2 above, this does not affect the validity of the remagnetisation hypothesis proposed here. If sites located along the western margin of the Bey Daglari massif do record depositional remanent magnetisations, then the similarity between the declinations of the site mean directions identified by Lauer (1981) and Kissel and Poisson (1987) with that of the regional direction found from the remagnetised sites in the present study implies that no significant rotation of the massif occurred prior to the Middle Miocene. This is in agreement with the results from the Barla Dag obtained here.

When assessing the geological significance of their data, Kissel and Poisson (1987) state that the rotation of the Bey Daglari must die out in the Antalya Complex. They reached this conclusion because the data obtained by them from the Neogene sequences of the Antalya basin indicate that of these sediments have been subjected to no rotation since at least the Langhian (Middle Miocene) (Kissel and Poisson, 1986).

However, the data from sites KK and CI of the present study, from the Kemer Zone and Gödene Zone of the southwestern segment of the Antalya Complex respectively, indicate that these units have been rotated along with the Bey Daglari itself.

At face value the various data imply that the tectonic rotation occurred in a very short time interval in the Langhian, before the end of deposition of Langhian-aged sediments within the Antalya Basin. However, an examination of the site mean directions reported by Kissel and Poisson (1986) (see Figure 5.08 of this study) shows that only two sites were located in the Langhian part of the succession. The better defined of these site means (in terms of within-site dispersion) has a declination of 347°. This may indicate that the regional rotation occurred over a slightly longer time interval and was not complete by the time of deposition of the strata sampled at this site.

At Site CI of the present study, located in the Upper Triassic lavas of the Gödene Zone (Robertson and Woodcock, 1981c) at Cirali (Figure 6.01), a negative fold test establishes that the identified characteristic magnetisation is of post-folding age. After remagnetisation, this site was subjected to the same anticlockwise tectonic rotation as the Bey Daglari platform to the west and Kemer Zone off-margin carbonate build-up to the east. This has important implications for the data obtained by Lauer (1981) at 11 sites located in the Çalbali Dag lava massif to the north (see Chapter 5, Section 5.4.1). *After* the application of standard structural tilt corrections to the data from these sites, Lauer (op. cit.) obtained mean directions which clustered in the northwest quadrant and were of predominantly reversed polarity. However, the pervasive remagnetisation identified in the present study, together with the negative fold test obtained at site CI, suggests that Lauer (op. cit.) was *not* justified in removing the structural tilt at these sites. Luckily, Lauer (op. cit.) lists the corrections applied to these data, and so it is possible to recover the following site mean directions prior to application of these corrections:

	Dec	Inc	K	α_{95}	n
Site 43	351°	19°	33	10.7°	7
Site 44	330°	46°	18	16.1°	6
Site 45	324°	14°	28	12.9°	6
Site 46	324°	-09°	72	7.1°	7
Site 47	321°	20°	47	13.5°	4
Site 48	321°	13°	55	16.8°	3
Site 49	338°	-06°	53	10.6°	5
Site 50	333°	06°	104	9.0°	4
Site 51	357°	16°	16	19.7°	5
Site 52	343°	03°	43	14.1°	4
Site 53	350°	31°	50	11.0°	5

The Fisherian mean of these sites directions is:

Dec = 336°, Inc = 14°, K = 16, α_{95} = 11.6°.

We can see that the mean declination of the Çalbali Dag sites before tilt correction is comparable to that of the lava blocks sampled at Cirali in the present study (site CI). The mean inclination becomes positive, but is not as high as that found at Cirali. Such variations in inclination might be expected if remagnetisation took place during the final stages of folding.

I reinterpret the mean directions identified by Lauer (1981) at these 11 sites as secondary magnetisations acquired during the Miocene. This interpretation has serious consequences for the hypothesis of Lauer (1981, 1984), in which the Turkish blocks originated close to the equator and subsequently reached their present position by drifting northwards around the Arabian margin. The proposed equatorial origin for block B of Lauer (op. cit.) relies heavily on the tilt-corrected inclination data obtained from the Çalbali Dag section. I have shown here that there is good evidence that the Upper Triassic lavas of the Gödene Zone do not retain any primary remanence, but instead carry only secondary components of magnetisation. It is the incorrect application of structural tilt corrections to these remagnetised units which leads Lauer (op. cit.) to position his block B so far to the south in the Upper Triassic. Perhaps it is unfair to speculate that this might be the case at other sites sampled by Lauer.

Additionally, it has been shown here that the Upper Triassic carbonates of the Barla Dag massif, sampled at site BA (Section 6.3.2; Figure 6.01), probably retain a primary depositional remanence. The presence of normal and reverse polarity groups which conform to stratigraphic layering indicates that this site has not been affected by the severe secondary overprint observed elsewhere. Although it is clearly dangerous to attach too much importance to the data from one site, the mean inclination at site BA can be used to estimate the palaeolatitude of the Barla Dag unit during the Upper Triassic. Assuming an axial geocentric dipole field, the mean tilt corrected inclination of 25° corresponds to a palaeolatitude of 13°N. The apparent polar wander path for Africa given by Westphal *et al.* (1986) indicates that during the Triassic Africa was moving in a sinistral sense with respect to Eurasia, and with a small northward component of motion. This means that Africa was slightly to the south and to the west of its position in the first of the palaeocontinental reconstructions of Savostin *et al.* (1986), shown in Figure 2.06a (Lias). An examination of the palaeolatitudes superimposed on this figure indicates that, with a palaeolatitude of 13°N, the Barla Dag unit may be placed comfortably within the embayment of the African margin, without resorting to positioning it in the proto-Indian ocean, to the east of the Arabian promontory, as required by Lauer (1981, 1984).

6.7 Conclusions.

The main conclusion of this section is that the units analysed for the present study within the Isparta angle provide compelling evidence for a widespread remagnetisation event which has completely replaced the primary magnetisation at the majority of sites. This remagnetisation event was probably triggered by the migration of orogenic fluids ahead of the Antalya Complex during its emplacement in the Early to Middle Miocene, and resulted in the formation of authigenic magnetite. Subsequent to the acquisition of remanent magnetisation by the newly formed magnetite grains by growth through the critical blocking volume, a large segment of the area underwent an anticlockwise rotation of 30°, probably related to the final emplacement of the Lycian Nappes onto the western limb of the Isparta angle during the Middle to Late Miocene.

A general conclusion which may be drawn from this section of the thesis is that considerable care must be exercised in applying standard structural tilt corrections to data obtained in complex orogenic regions. Unless the age of magnetisation can be constrained by suitable field stability tests, the application of such corrections can lead to the serious misinterpretation of data.

PART FOUR - GREECE.

CHAPTER SEVEN - GEOLOGY AND PALAEOMAGNETISM OF GREECE: A REVIEW.

7.1 General.

This part of the thesis is concerned with a palaeomagnetic study of the autochthonous and allochthonous units of the Peloponnesos of southern Greece. The area lies at the opposite end of the Hellenic arc and trench system to the Antalya area dealt with in the previous two chapters.

This research was shifted to the Argolis Peninsula of the Peloponnesos because of difficulties in following up the sampling carried out in Antalya. The choice of area was influenced by the identification by Pucher *et al.* (1974) and later by Turnell (1988) of a large clockwise rotation of part of the peninsula since the Jurassic. The exact timing and nature of this rotation were not known. Thus the principal aim of the sampling was to constrain both the size and age of the rotated unit by collecting samples from a wide area and from sequences spanning as much of the stratigraphic record as possible. Since it seemed unlikely that the Argolis rotation was an isolated event in an otherwise unrotated region, sampling was subsequently extended into the rest of the Peloponnesos.

Previously reported palaeomagnetic data from other parts of southern and central Greece, most notably the Ionian Islands off the west coast (e.g. Laj *et al.*, 1982), have indicated that the present curvature of the Hellenic arc and trench was acquired, at least in part, by Neotectonic bending and rotation in opposite senses at the two extremities (Kissel and Laj, 1988). The rotation of the Bey Daglari, detailed in the previous chapter, is the manifestation of this process in the east. In the next chapter I attempt to relate the rotation of the Argolis units, and other rotations identified within the Peloponnesos, to the Miocene to Recent deformation occurring at the other limit of the trench system.

This part of the thesis is divided into three chapters. The remainder of this chapter presents a brief review of the geology of southern Greece (drawing in part upon the earlier discussions of Chapter 2), and a discussion of the palaeomagnetic research within the area published to date. Chapter 8 concerns the results of the detailed sampling carried out in the Argolis Peninsula, and preliminary results obtained at additional sites located in the rest of the Peloponnesos. Chapter 9 then presents the results of a palaeomagnetic study of the Pindos thrust sheets, which tectonically overlie much of the platform sequences of the northern Peloponnesos.

Throughout the following two chapters, it should be borne in mind that this research is in an ongoing state. The database from the autochthonous platform

sequences is not extensive enough at present to enable a definite choice to be made between various rotation mechanisms. Many of the sites collected during the final field season of this research await measurement. It is hoped that this will be completed during the tenure of a post-doctoral fellowship at the University of Newcastle-upon-Tyne..

7.2 Regional geology.

7.2.1 Isopic/geotectonic zones.

The Hellenides are those Alpine ranges that constitute the greater part of Greece and Albania, together with the southeastern corner of Yugoslavia. They consist of a number of microcontinental and ophiolitic terranes, which formed during the complex closure of the various strands of the Neotethyan ocean.

The Hellenides have been subdivided into a number of tectonostratigraphic or *isopic* zones, based on large-scale facies differences and major tectonic features (Aubouin *et al.*, 1970). The arrangement of these isopic zones in Greece is shown in Figure 7.01. Those zones which are of interest in the present study are now briefly described.

The Pelagonian Zone consists of a sequence of Upper Palaeozoic metamorphic rocks, rift volcanics and locally metamorphosed Mesozoic platform carbonates (Celet and Ferriere 1978). It is interpreted as an elongate microcontinental sliver which rifted off of the Apulian promontory of Gondwanaland during the Triassic (Chapter 2, Section 2.4.4).

The Subpelagonian Zone lies to the west of the Pelagonian Zone, and consists of a belt of folded and thrusted platform carbonate units. These are overlain tectonically by ophiolitic nappes and associated thrust sheets of rift and deep-water sediments. The Subpelagonian Zone is considered to represent allochthonous ophiolitic and continental margin sequences which have been emplaced on to the relatively *in situ* Pelagonian microcontinent.

Further west still lies the Pindos Zone (Figure 7.01). This consists of an imbricated stack of deep-water sediments interpreted as the deposits of the western margin of the Neotethyan ocean (the Pindos basin; Chapter 2, Section 2.4.4) which formed by the separation of the Pelagonian microcontinent from the Gondwanan margin.

The thrust sheets of the Pindos Zone tectonically overlie the carbonate platform of the Apulian microcontinent (Chapter 2, Section 2.4.4), which is exposed in westernmost Greece and the southern part of Italy. The Ionian Zone is recognised as a major intra-platform basin within the Apulian margin. It separates the neritic platform of the Pre-Apulian Zone to the west from that of the Gavrovo-Tripolitza Zone to the east.

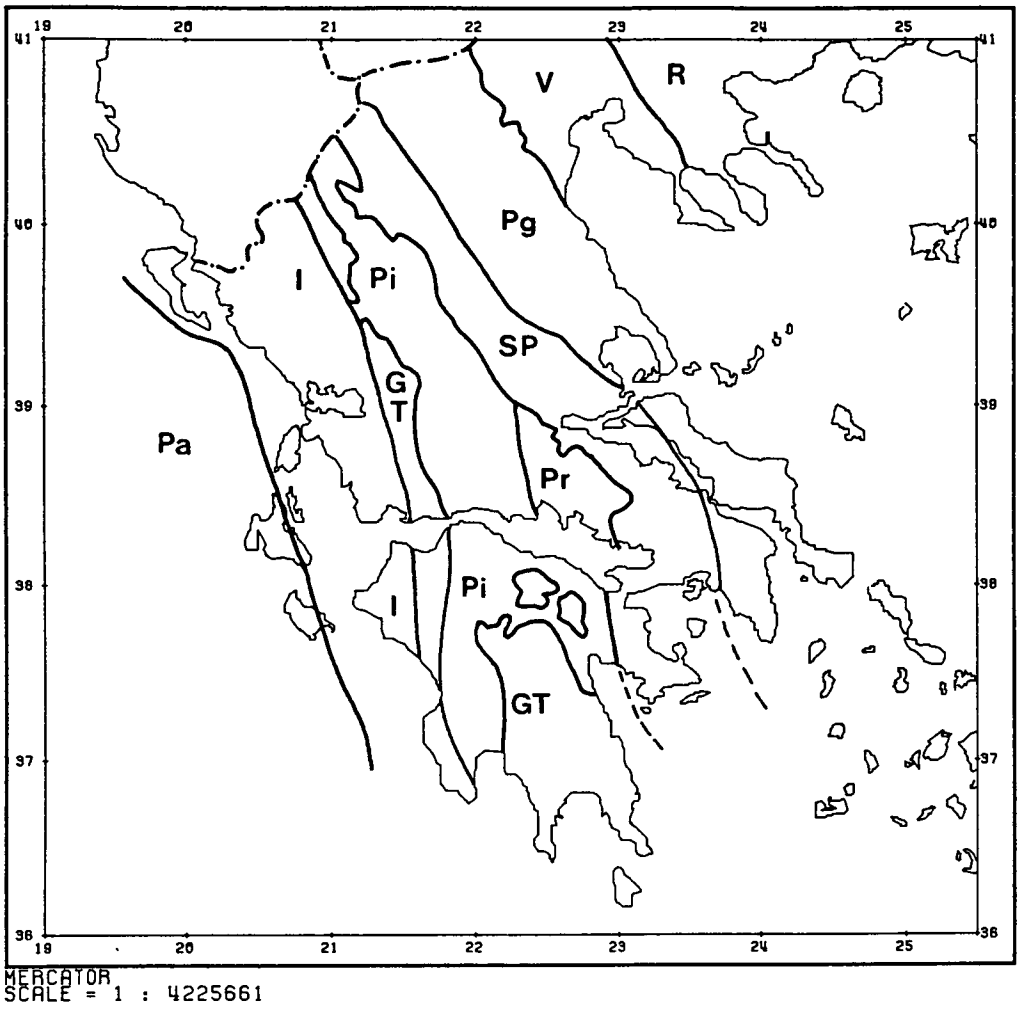

Figure 7.01. Map of the isopic zones of the Greek Hellenides. Key: Pa = Preapulian ; I = Ionian; GT = Gavrovo-Tripolitza; Pi = Pindos; Pr = Parnassos; SP = Subpelagonian; Pg = Pelagonian; V = Vardar; R = Rhodope.

To the east of the Pelagonian Zone, the ophiolitic rocks and deep-water sediments of the Vardar Zone represent the site of a second, more northerly branch of the Neotethys. This zone is exposed in northeastern Greece, but is submerged beneath the Aegean Sea in southern Greece. However, evidence for the southwards continuation of the Vardar basin is found in eastern Argolis in the form of a subduction-accretion complex (the Ermioni Complex; Clift and Robertson, 1989).

The palaeogeographic evolution of these zones is discussed in the following section.

7.2.2 Mesozoic to Early Tertiary palaeogeography of the southern Greek Neotethys.

A full description of the preferred model for the tectonic history of the Neotethys (that of Robertson and Dixon, 1984) has already been given in Chapter 2, Section 2.4.4. Here, I give a brief outline of the general history of the southern Greek Neotethys, to act as a basis for discussions of the geology of the Argolis Peninsula given in the next chapter, and of the Pindos Zone given in Chapter 9.

As discussed in Chapter 2, there is good evidence for the existence of a small Red Sea-type ocean basin floored by oceanic crust separating the Pelagonian microcontinental fragment from the Apulian margin in the Mesozoic and Early Tertiary. Formation of this Pindos ocean followed continental break-up in the Late Triassic to Early Jurassic. The palaeogeography of the Pindos ocean was relatively straightforward (Robertson *et al.*, in press; Figure 7.02). Passive continental margins can be identified along both the western and eastern edges of the ocean (Robertson *et al.*, in press). On the Apulian continental margin, represented by the Pre-Apulian and Gavrovo-Tripolitza Zones (Aubouin *et al.*, 1970), shallow-water carbonate deposition became established during the Late Triassic (Carnian) (Thiebault, 1982), in response to flexural subsidence as spreading began in the Pindos ocean (Robertson *et al.*, in press). The Gavrovo-Tripolitza platform passed westwards into an ensialic rift, the Ionian Zone (Aubouin *et al.*, 1970; Jenkins, 1972). Differential subsidence to form an intra-platform basin began in the Early Jurassic and peaked in the Late Jurassic.

The eastern margin of the basin comprised a several hundred kilometre-long, linear passive margin offset by inferred transform faults. The Pelagonian microcontinent was located some distance eastwards of Apulia, and extended from the Scutari-Pec transform (along the present northern border of Albania; Robertson and Dixon, 1984) as far south as the Argolis Peninsula. In the south, the Pelagonian sliver narrowed and fragmented into intra-platform rift basins (Clift and Robertson, 1990; see Chapter 8, Section 8.2.2).

During the Middle Jurassic, westward-dipping intra-oceanic subduction was initiated (Figure 7.02; Jones and Robertson, in press), in response to regional

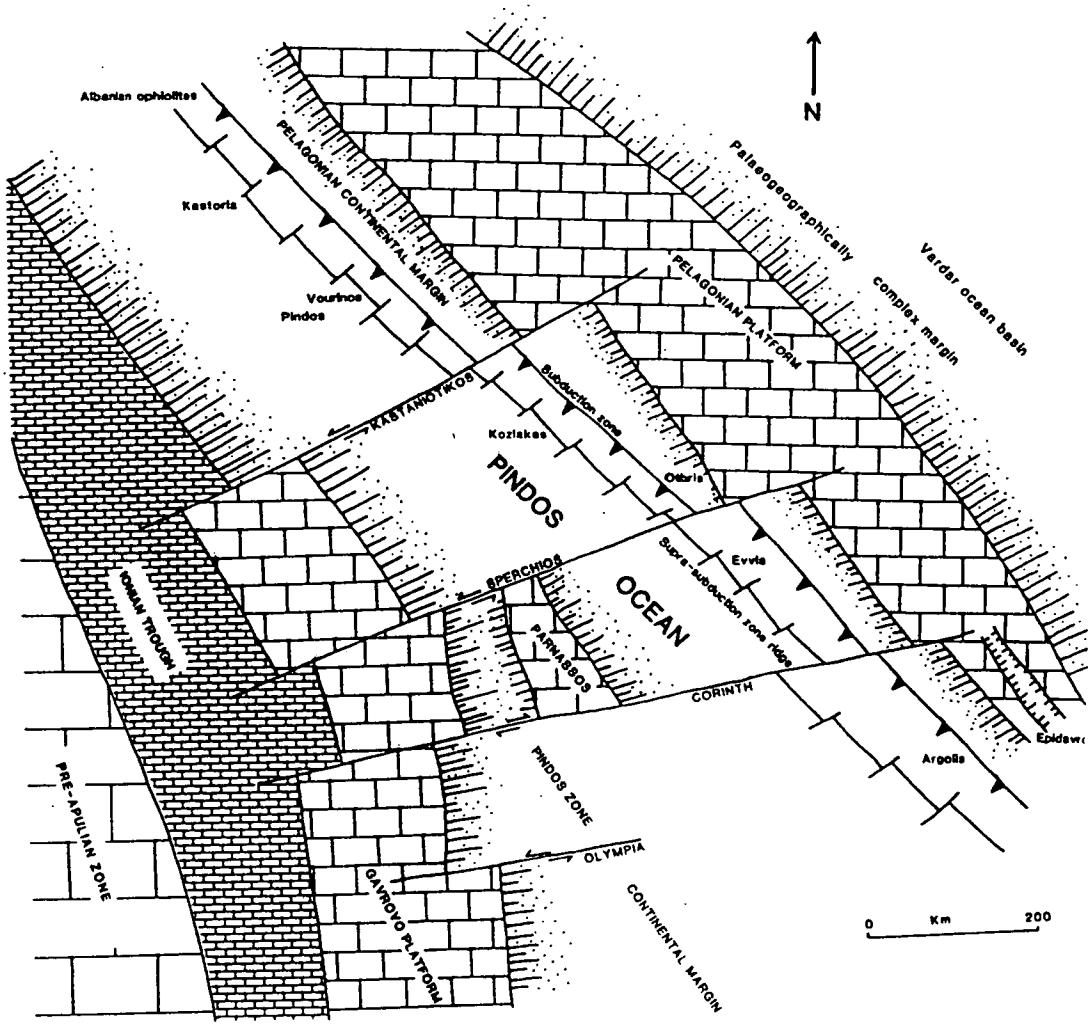

Figure 7.02. Palaeogeography of the Pindos ocean in the Middle Jurassic (*ca.* 160 Ma) according to Robertson *et al.* (in press). Spreading in the Late Triassic-Early Jurassic was followed by the death of the spreading ridge. Regional compression, related to the opening of the North Atlantic, then initiated a west-dipping intra-oceanic subduction zone near the former spreading axis. Ophiolites were generated above the subduction zone, and were emplaced in pre-Tithonian time (*ca.* 155 Ma), as a result of collision of the trench with the easterly passive margin of the Pelagonian microcontinent.

compression related to the opening of the North Atlantic. The major Jurassic ophiolites (e.g. Pindos, Vourinos) were generated above the subduction zone, and were emplaced in pre-Tithonian time (*ca.* 155 Ma) as a result of the collision of the trench with the easterly passive margin of the Pelagonian microcontinent. This was followed by complete closure of the Pindos ocean in the north, in the present area of Albania and Yugoslavia.

Further south the ocean basin remained open until the Early Tertiary (Robertson *et al.*, in press), when final closure occurred in response to regional compression and eastward-dipping subduction. This subduction phase was responsible for the emplacement of the Triassic to Early Tertiary deep-water sediments of the Pindos Zone as a huge stack of thrust sheets (the Pindos-Olonos nappes) over the margin of the Apulian continent to the west (the Gavrovo-Tripolitza Zone) (Aubouin *et al.*, 1970; Dercourt, 1964). The emplaced units represent the western parts of the Pindos ocean, adjacent to the Apulian microcontinent (Pe-Piper and Piper, 1984; Robertson *et al.*, in press).

The existence of a second, more northerly branch of the Neotethys (the Vardar basin) in southern Greece, to the east of the Pelagonian microcontinent, is indicated by the presence of a large body of Palaeocene-Eocene flysch tectonically overlying the Argolis platform. This unit, the Ermioni Complex, is interpreted as a subduction-accretion complex formed during the final stages of closure of the Vardar basin, and emplaced over the continental margin in the Eocene (Clift and Robertson, 1989).

7.2.3 Present tectonic setting.

a. The Hellenic arc and trench system.

After Early Tertiary continental collision and basin closure, only a remnant southern strand of the Neotethys still survived, to the south of Turkey, Crete and the Peloponnesos. The post-Miocene Neotectonic phase has been dominated by the later stages of collision between Africa and Eurasia. This has resulted in a tightening up of the pre-existing mosaic of continental blocks, together with subduction of the remains of this southern Neotethyan ocean crust (Robertson and Dixon, 1984). The overall pattern of deformation was established by the collision of the Adriatic/Apulian and Arabian promontories of Gondwanaland with Eurasia (Tapponnier, 1977). This collision resulted in the westward expulsion of the Anatolian block towards the Aegean along major transform faults (Sengör, 1979; see Chapter 2, Section 2.4.1). At the same time, up to several hundred kilometres width of Neotethyan oceanic crust in the Ionian Sea was subducted north-eastwards beneath Crete, forming the Hellenic arc and trench (Le Pichon and Angelier, 1979).

At present, seismic and volcanological studies indicate that subduction along the Hellenic arc and trench system is characterised by a well-defined downgoing slab, dipping northwards at 30-40° away from the trench (McKenzie, 1972). An active calc-alkaline volcanic arc is also observed (Fytikas *et al.*, 1984).

The horizontal projections of slip vectors associated with large shallow thrust faulting-type earthquakes along the Hellenic arc indicate that there is a transition from transform motion along the Strabo and Pliny trenches in the east to more compressive motion along the northwestern part of the arc, in the region of the Ionian islands (Le Pichon and Angelier, 1979; Figure 2.08 in Chapter 2). Neotectonic studies have shown that the compressional regime in this latter area has existed throughout the Pleistocene and the Pliocene. However, the exact timing of the beginning of subduction is still a matter of some debate. Le Pichon and Angelier (1979) argued that subduction started at 13 Ma ago (during the middle Miocene), on the basis of the age of extensional faulting in the southern Aegean and of the oldest known volcanic material in the active volcanic arc. McKenzie (1978) and Mercier *et al.* (1979) suggested a younger age of 5 Ma, based on the initiation of calc-alkaline volcanism in the late middle Miocene and the identification from studies of faults in the field of a 5-7 Ma compressive event. However, Sorel and Mercier (1988) have noted that this 5 Ma age does not refer to the onset of subduction beneath the central part of the arc, but rather concerns the time at which the arc achieved its present configuration. They suggest that subduction began in the Langhian, at about 16 Ma ago, in broad agreement with the age given by Le Pichon and Angelier (1979). However, a more recent estimate by Meulenkamp et al. (1988), based upon the length of the down-going slab deduced from seismic studies, suggests that subduction may have begun even earlier at 26 Ma ago.

A point raised by this discussion is that the frontal thrust of the arc has not been stationary with time. During the Langhian, a strong compressional tectonic phase initiated a new frontal thrust of the belt in northwestern Greece, to the east of the Ionian Islands (Mercier et al., 1979; Sorel and Mercier, 1988). In addition, a new frontal thrust was initiated at this time in southwestern Turkey, represented by the front of the Lycian Nappes onto the Bey Daglari massif (Poisson, 1977, 1984). In the Early Pliocene, the northwestern front of the arc jumped into the Pre-Apulian isopic zone, west of the Ionian Islands, probably because of the limited possibility of subducting light continental crust (Sorel and Mercier, 1988). This arc is still active today.

Whereas in the northwestern part of the arc a compressive regime has existed since at least the Late Miocene, by contrast the internal Aegean regions have experienced a large-scale extensional regime during the same period. This has given rise to extensive normal faulting and the formation of grabens (McKenzie, 1978). This regime has only

occasionally been interrupted by compressive events in the Late Miocene, Early Pliocene and Early Pleistocene periods (Mercier *et al.*, 1979). However, the significance of these compressive episodes is controversial, and Jackson *et al.* (1982) have suggested that the apparently reversed faults in the Aegean area may actually represent antithetic normal faults which have rotated above listric master faults.

The internal Aegean regions have also been affected by Tertiary and Quaternary calc-alkaline volcanism. Two distinct phases of volcanism are recognised of Oligocene-Miocene and Plio-Quaternary ages, separated by a period of quiescence of several million years (Fytikas *et al.*, 1984). The latter is related to subduction along the arc, which is still active today. It is unlikely that the older Oligocene-Miocene volcanic rocks are related to subduction around the Hellenic arc, since they are situated too far north to have been erupted above the newly subducting plate. They are more likely to represent the products of an older subduction episode and may be related to the final closure of the Pindos and Vardar basins.

b. The distributed shear zone.

The Anatolian block, which is being forced westwards towards the Aegean by the incipient collision between the Eurasian and Arabian plates in the Zagros thrust belt (Le Pichon and Angelier, 1979), is bounded on its northern edge by the North Anatolian transform fault (Sengör, 1979; Figure 2.08 in Chapter 2). It has been estimated that 25 km of dextral motion has been accommodated along the transform since the Late Miocene (Barka and Hancock, 1984). Strike-slip motion along the fault extends westwards into the North Aegean Trough. McKenzie (1972) suggested that the transform extended across Central Greece to join up with the Hellenic trench to the west. However, field studies failed to confirm the presence of this fault. Subsequently, McKenzie and Jackson (1983) have proposed that the motion of the North Anatolian Fault is taken up on a large active normal fault system, which forms a zone of distributed shear linking the North Anatolian Fault to the Hellenic trench. The model developed for this area by McKenzie and Jackson (1983, and later papers) has been dealt with in detail in Chapter 2, Section 2.5, in the discussion of tectonic rotations within deforming zones. The model predicts that fault-bounded blocks within the shear zone should be rotated in a clockwise sense about inclined axes, with the instantaneous rate of rotation being dependent on whether the fault blocks are attached to the boundaries of the shear zone or 'float' within it.

Deformation associated with this postulated distributed shear zone would be superimposed upon the deformation related to active subduction along the arc. In addition, as described below, substantial clockwise rotations have been documented

along the Hellenic arc, believed to be due to Neotectonic bending of the arc to accommodate back-arc extension in the Aegean Sea and/or roll-back of the Hellenic trench (Kissel and Laj, 1988; Le Pichon and Angelier, 1979). In Central Greece, we should therefore expect to observe large clockwise rotations, due to a combination of rotation of the arc and rotation of fault blocks within the shear zone. Palaeomagnetic studies provide a unique method for identifying such rotations.

7.3 Palaeomagnetic studies in Greece.

I now present a brief discussion of the palaeomagnetic research from within the Greek area which has been published to date and which is relevant to the present study. This is not intended to be a comprehensive review of all palaeomagnetic studies carried out in Greece, which is beyond the present scope. Instead, the aim is to provide a palaeomagnetic framework within which to interpret the data obtained in this study.

This discussion is divided into two sections. Firstly, I will examine a model for the geodynamic evolution of the Hellenic arc, mainly based on palaeomagnetic data from the Tertiary units of the Ionian Zone of western Greece, proposed by Kissel and Laj (1988). I will then move on to discuss two studies which have been carried out in the Argolis Peninsula (Pucher *et al.*, 1974; Turnell, 1988).

7.3.1 The geodynamic evolution of the Hellenic Arc deduced from palaeomagnetic studies: the work of Kissel, Laj and others.

Le Pichon and Angelier (1979) suggested that the Hellenic arc was originally more rectilinear in shape and had acquired its present curvature by tectonic rotation. For them, the Neotectonic movement over the last 13 Ma at the western end of the arc could be modelled to a first approximation by a clockwise rotation of approximately 30° of the consuming boundary about an Eulerian pole located in the southern Adriatic Sea (40°N, 18°E). They viewed this rotation as the necessary result of large-scale back-arc extension in the Aegean Sea and/or the westward expulsion of the Anatolian block away from a zone of continental collision to the east (see Chapter 2, Section 2.4.1, and Section 7.2.3b above).

In a series of papers (Laj *et al.*, 1982; Kissel and Poisson, 1986, 1987; Kissel *et al.*, 1984; Kissel *et al.*, 1985; Kissel *et al.*, 1986a.; Kissel *et al.*, 1986b; Kissel *et al.*, 1986c), the French research group based at Gif-sur-Yvette set out to test this model by examining Tertiary and Quaternary sequences exposed in key areas around the arc, both in Greece and Turkey (see Chapter 5 for a summary of the Turkish work). The palaeomagnetic data reported in these papers was synthesised by Kissel and Laj (1988), along with other data reported by Horner and Freeman (1983) and Kondopoulou and

Westphal (1986), into a model which attempted to explain the variations in rotational deformation observed around the arc. I will not present a detailed appraisal of the palaeomagnetic data gathered by this group, since these data are all of high quality. Instead, I will discuss the interpretation of the data given by Kissel and Laj (1988).

Figure 7.03 shows the regions from which the various palaeomagnetic results incorporated into the model of Kissel and Laj (*op. cit.*) were obtained.

Along the external sedimentary arc, samples were collected from blue-grey marine clay sections and fine-grained carbonates. Upper Miocene, Pliocene and Quaternary formations were sampled in both the Ionian and Preapulian Zones in the Ionian Islands, the Peloponnesos, Crete, Rhodes and the Antalya Basin (see Chapter 5, Section 5.4.2). Older Oligocene and Lower Miocene series were sampled in the mainland of Greece, between Epirus and Akarnania, and in the Bey Daglari massif (see Chapter 5, Section 5.4.2). The data obtained by Horner and Freeman (1983) from Palaeocene and Eocene limestones exposed in Epirus were also included.

Within the internal region, most sites were located in plutonic and volcanic formations. Included in the analysis were the data obtained by Kondopoulou and Westphal (1986) from the Chalkidiki Peninsula. The results from sedimentary and volcanic formations of Western Anatolia relate to the development of the major east-west trending graben system north of Izmir and will not be discussed here.

The results obtained along the external arc were found to be coherent, with sites in the Ionian Islands, the Peloponnesos, Epirus, Akarnania and the Mesohellenic Trough all being characterised by easterly declinations which varied systematically with the age of the studied formations. By contrast, only northerly declinations were found in the units sampled in Crete, whereas westerly declinations were recovered in the Bey Daglari (see Chapter 5, Section 5.4.2, and the results of the present study in Chapter 6).

In the internal regions, easterly declinations were found by Kondopoulou and Westphal (1986) in the Chalkidiki, whereas declinations from the western side of the Aegean Sea (Volos, Evvia, Skyros) were found to vary between north and northeast. The latter rotations were attributed by Kissel and Laj (1988) to the motion of fault-bounded blocks within the zone of distributed shear proposed by McKenzie and Jackson (1983) (see Section 7.2.3b).

An examination of the data from the Late Miocene and Plio-Quaternary formations of the external region led Kissel and Laj (*op. cit.*) to conclude that the northwestern part of the arc from Corfu to the Peloponnesos had undergone a clockwise rotation of 26°, whereas the southeastern part from Crete to Rhodes had not experienced any significant rotation since the Late Miocene (Tortonian). They assumed that the two areas were decoupled along a zone of intense deformation in the Strait of Kythira (Lyberis *et*

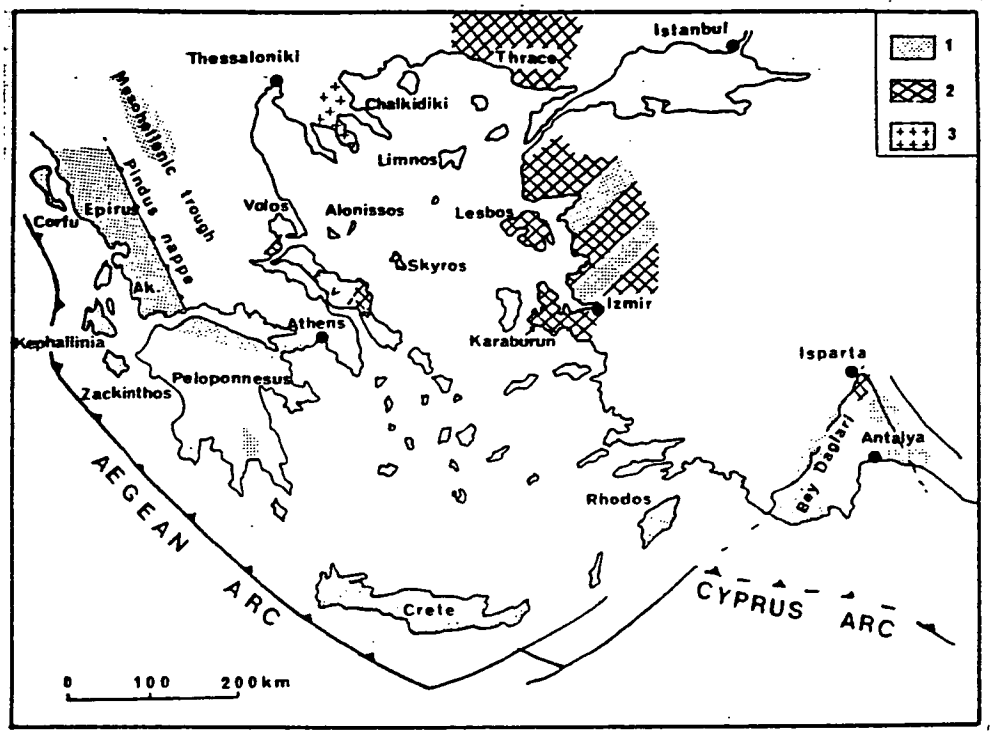

Figure 7.03. Present day configuration of the Aegean domain showing the locations of the regions where the palaeomagnetic data included in the model of Kissel and Laj (1988) were obtained. The type of rock in which the majority of sites have been sampled in each region is represented by symbols 1 to 3 (1 = sedimentary formations; 2 = volcanic products; 3 = plutons). Ak. = Akarnania
From Kissel and Laj (1988).

al., 1982). Since the three Ionian Islands studied had experienced essentially the same structural evolution during the Neotectonic period, Kissel and Laj (*op. cit.*) constructed a diagram for the islands which related the measured angle of rotation to the age of the corresponding formations (Figure 7.04). This diagram indicated a period between 12 and 5 Ma where no rotation occurred. This was followed by a total rotation of 26° which occurred progressively between 5 Ma and the present day. They noted that the beginning of this rotation overlapped in time with the Early Pliocene compressive phase, suggested by Mercier *et al.* (1979) to represent the time at which the external Aegean became an active continental margin.

In contrast, the palaeomagnetic results from Palaeocene to Upper Eocene limestones (Horner and Freeman, 1983) and from Lower to Upper Oligocene flysch sections (Kissel *et al.*, 1984, 1985) in Epirus and Akarnania suggested a total clockwise rotation of 45° for the northwestern arc. Since no major structural discontinuities exist between the mainland of Greece and the Ionian Islands, Kissel and Laj (1988) assumed that the Plio-Quaternary rotation of 26° described above had also affected the Epirus-Akarnania region. Thus, over half of the 45° post-Oligocene rotation was attributed to the Plio-Quaternary event. The remaining rotation was dated as between Early and Middle Miocene in age, and was related by Kissel and Laj (*op. cit.*) to the Langhian compressive phase.

Thus, Kissel and Laj (*op. cit.*) proposed a two-stage rotation history for the western end of the Aegean arc; an Early to Middle Miocene rotation of *ca.* 20°, followed by a progressive Lower Pliocene to Recent rotation totalling 26°. Data from the Bey Daglari in southwestern Turkey (Chapters 5 and 6) indicated that the first of these events also produced a 30° anticlockwise rotation of the eastern termination of the arc. These rotations were not considered to have affected the internal regions.

The acquisition of the curvature of the arc in two major phases, as proposed by Kissel and Laj (*op. cit.*), is consistent with the geological results of Mercier *et al.* (1979). The latter suggested that two different and successive orogenic systems occurred in this region; an earlier Ionian-Lycian arc and the present Hellenic arc, which formed by a sudden jump from the Miocene arc position at the Miocene-Pliocene boundary (see Section 7.2.3a).

The Miocene rotations may be interpreted in terms of the indentation of the Eurasian margin by the Adriatic and Arabian promontories of Africa, as proposed by Tapponnier (1977) (see Section 7.2.3a, and Chapter 2, Section 2.4.1). However, Kissel and Laj (1988) point out that in Tapponnier's model, the curvature is already established in the Early Eocene. This suggested to them that the time between the

indentation of Eurasia and the acquisition of the curvature of the arc had been considerably underestimated.

The Plio-Quaternary rotation of Kissel and Laj (*op. cit.*) is comparable to that suggested by Le Pichon and Angelier (1979) from geological and seismological evidence. This rotation can be described by the movement of a semi-rigid plate around an Eulerian pole located in the southern part of the Adriatic Sea. However, the palaeomagnetic data show that the movement is much more rapid than suggested by Le Pichon and Angelier (it takes place over a period of 5 Ma, compared with the 13.5 Ma in their model).

In the next chapter, I will show that the division of the Aegean region by Kissel and Laj (1988) into external and internal zones on the basis of the rotations defined by the palaeomagnetic data may not be fully justified. In particular, I suggest that their Pliocene rotation event affected both internal and external zones alike, and can therefore account for a large part of the rotations of Evvia and Skyros. Kissel and Laj (1988) considered these latter rotations to result wholly from the rotation of fault-blocks within the postulated shear zone crossing Central Greece (McKenzie and Jackson, 1983). This is an aspect which will be followed up in the future during the tenure of a post-doctoral fellowship at the University of Newcastle-upon-Tyne.

7.3.2 Palaeomagnetic studies within the Argolis Peninsula.

In addition to the palaeomagnetic sampling of Tertiary formations by the French group and others, two studies of relevance to the present work have been carried within older sequences of the Argolis Peninsula. The first of these, that of Pucher *et al.* (1974), attempted to determine whether an observed difference in strike of 100° between the Pindos mountains in northern Greece and the Argolis Peninsula was the result of a relative block rotation between the two areas. The aim of the more detailed study of Turnell (1988) was to constrain both the Mesozoic palaeolatitude and the amount of rotation of two crustal blocks within the Subpelagonian Zone. As I will show in the next chapter, although the units sampled within the Argolis Peninsula in both of these studies were Mesozoic in age, the rotations identified are probably of Tertiary origin and relate to the Neotectonic deformation of southern and central Greece.

a. The work of Pucher and others.

Pucher *et al.* (1974) observed that, whereas the Pindos Zone in northern Greece has a trend of NNW-SSE, the strike of the tectonic units in the Argolis Peninsula, within the Subpelagonian Zone of southern Greece, is E-W. They set out to test the hypothesis that this difference was due to a relative rotation between the two areas.

Although there does not appear to be a clear tectonic strike direction within Argolis, and also a comparison of isolated results which are widely separated geographically is questionable in such a tectonically complex area, the data collected by Pucher *et al.* (*op. cit.*) did give the first palaeomagnetic evidence for a large rotation of part of the Argolis area.

Within the peninsula, Pucher *et al.* (*op. cit.*) collected nine hand-samples from four sites within the Jurassic pillow lavas of the Migdhalitsa Ophiolite Unit (see next chapter, Sections 8.2.2 and 8.2.4f). The exact location of these sites is not given ("... various locations south of Lighourio.", see Figure 8.01). Both normal and reversed polarities were identified, but the overall mean direction of Dec = 082°, Inc = 19° was not well defined (Figure 7.05).

A comparison of this mean direction with that obtained from gabbro samples from the Pindos ophiolite in northern Greece led Pucher *et al.* (*op. cit.*) to suggest that the Argolis area had experienced a clockwise rotation of 108° with respect to the northern area. However, this conclusion may not have been warranted since: i) it is now recognised that the Migdhalitsa Ophiolite Unit is totally allochthonous with respect to the underlying carbonate platform; and ii) the gabbros of the Pindos ophiolite do not consist of any coherent outcrops but instead occur as highly dismembered thrust sheets (Jones and Robertson, *in press*). In addition, the data collected by Pucher (*op. cit.*) would not now be considered to be of sufficient quality to interpret, mainly because of the large sample dispersions.

b. The work of Turnell.

Over a decade after the initial study of Pucher *et al.* (1974), further palaeomagnetic sampling was carried out in the Argolis area by Turnell (1988). She examined the Middle Jurassic condensed limestones (Ammonitico Rosso) exposed at the top of the Argolis platform (the Pantokrator Unit) at a total of 9 sites. These pink and red nodular limestones were deposited during subsidence of the platform before the Migdhalitsa Ophiolite Unit was emplaced in the Upper Jurassic (Kimmeridgian). In contrast to the pillow lavas sampled by Pucher *et al.* (1974), these units are relatively *in situ**.

Of the nine sites sampled by Turnell (1988), the data from seven were combined to produce a formation mean direction of:

Dec = 250°, Inc = -36°, K = 23, A_{95} = 13°, N = 7 (Stratigraphic coordinates).

The application of a standard structural tilt correction was found to improve the grouping of the site means, indicating that the magnetisation predated folding.

---

*Note that the geology of Argolis is outlined in the next chapter.

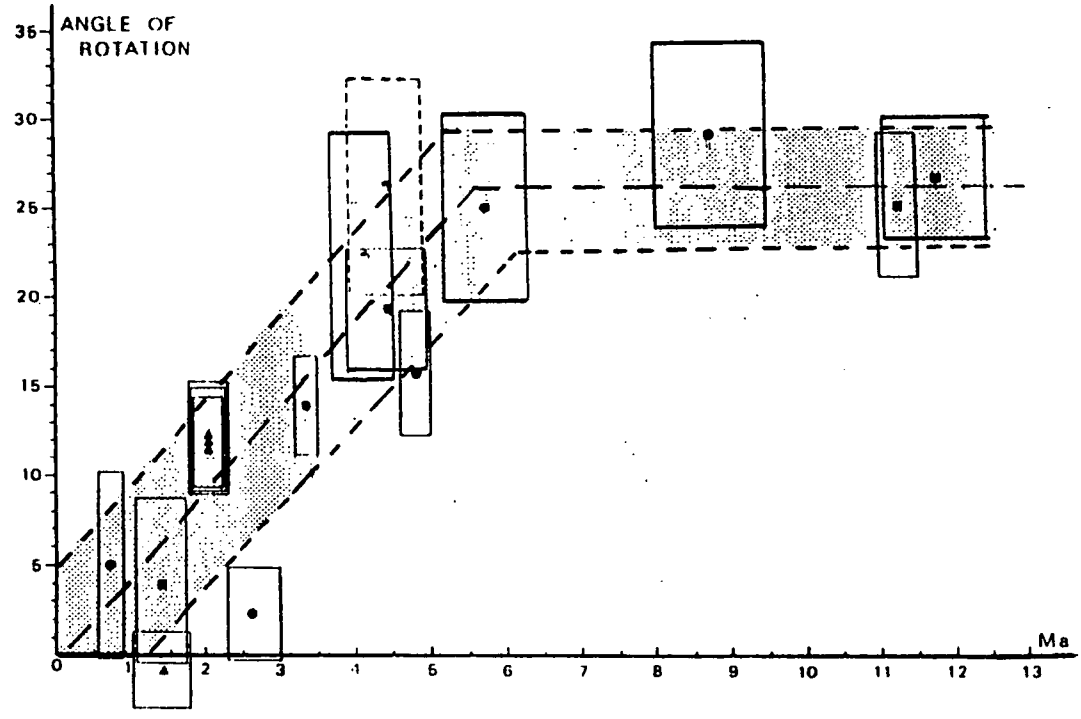

Figure 7.04. Plot of the measured angle of rotation versus the age of the corresponding formation for the Ionian Islands, according to Kissel and Laj (1988).

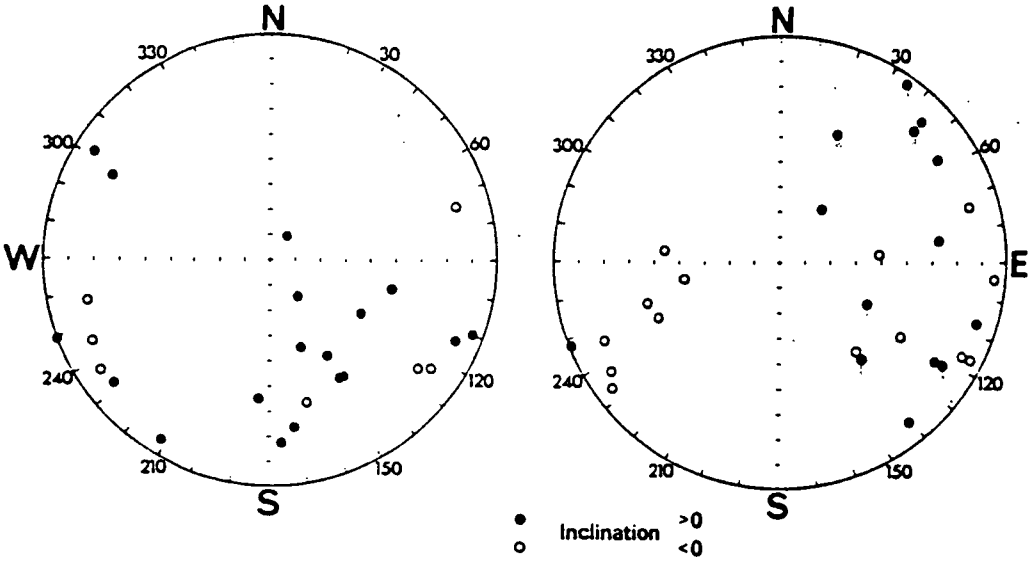

Figure 7.05. The distribution of cleaned remanence directions found by Pucher et al. (1974) within the pillow lavas of the Migdhalitsa Ophiolite Unit. Note the large dispersion of sample vectors.

The remaining two sites were excluded from the analysis because the application of a tilt correction moved the site mean directions away from those of the other sites. Turnell (*op. cit.*) suggested that this may be due to the anomalous sites belonging to a block with a different deformation history from the other sampling areas. In the next chapter, I confirm that this is the case.

The mean inclination found by Turnell (*op. cit.*) corresponds to a palaeolatitude of 20°N (the magnetisation must be of reversed polarity to avoid unacceptable overlaps with the African plate). This places the Argolis platform at a position midway between the north and south margins of the Tethys in the Middle Jurassic (see Figure 2.06a).

The mean declination reported by Turnell (*op. cit.*) indicates that the sampled part of the Argolis platform has experienced a clockwise rotation of 70° (with respect to present north) since the Middle Jurassic. In the next chapter, I confirm that at least 40° of this rotation, and possibly all of it, took place since the Lower Pliocene.

I shall return to the data of Turnell (*op. cit.*) in the next chapter, where I will combine it with that obtained in the present study to obtain a better estimate of the rotational deformation which has affected the Argolis Peninsula.

7.4 Summary.

The Hellenides consist of a mosaic of microcontinental and ophiolitic terranes which formed during the complex closure of the Neotethys. There is evidence for two separate Neotethyan strands in the Greek area; a Pindos ocean between the Apulian margin and the microcontinental sliver of the Pelagonian Zone, and a Vardar ocean further to the west. Final suturing of these basins took place in the Lower Tertiary.

Palaeomagnetic studies within the Greek area have identified large tectonic rotations in many areas. Studies of the Tertiary formations exposed around the Hellenic arc demonstrate that the arc has acquired its present curvature by opposing tectonic rotations at its western and eastern extremities. These rotations will be discussed again in the next chapter, in relation to the data obtained in the present study.

CHAPTER EIGHT - A PALAEOMAGNETIC STUDY OF THE RELATIVE AUTOCHTHONS OF THE PELOPONNESOS.

8.1 Introduction and aims.

In this chapter, I present the results of a palaeomagnetic study of the Mesozoic and Tertiary carbonate platforms and associated units exposed in the Peloponnesos of southern Greece. The field work for this study was carried out over a total period of three months during the summers of 1987 and 1988.

In the first field season, sampling was concentrated in the Argolis Peninsula, a critical area of the central southern Hellenides. Previous palaeomagnetic research in this area (Pucher *et al.*, 1974; Turnell, 1988; Chapter 7, Section 7.3.2) suggested that the peninsula had experienced a 70° clockwise rotation since the mid-Jurassic. The principal aim of the present study was to confirm the existence of this rotation and to attempt to constrain both the size of the rotated unit and the timing of rotation. To do this, samples were collected from a wide geographical area and from as many different lithologies of various ages as possible. Additionally, it was hoped that detailed palaeomagnetic sampling would help in assessing the validity of several tectonic models proposed for the Argolis area, in particular that of Baumgartner (1985).

As in the case of the study of the Isparta angle detailed in Part Three of this thesis, many of the platform carbonate lithologies sampled were not sufficiently magnetic to yield palaeomagnetic results. However, several lithologies were identified which are excellent recorders of the ancient geomagnetic field direction.

During the final days of the first field season, sampling was extended westwards from the Argolis Peninsula, along the main Argos to Tripolis road, to determine whether the postulated large rotation of the peninsula had affected this area too. Sampling in this area was concentrated in the pelagic limestones and calciturbidites of the Pindos Zone, which rest tectonically upon the platform carbonates of the Gavrovo-Tripolitza Zone. The results obtained from these samples are the subject of the next chapter.

The final field season of this research involved the collection of samples from a much wider area, covering almost the whole Peloponnesos. The aims of this sampling were to obtain an overall view of the rotational deformation affecting the region, and to determine whether variations in the amount of rotation (as seen in the Argolis Peninsula) could be detected. More sites were collected from the Pindos Zone (discussed in the next chapter). Also, the Gavrovo-Tripolitza platform and deeper water limestones of the Ionian Zone were sampled at as many localities as possible, avoiding the types of facies which were unsuccessful in the Argolis area. Across much of the Peloponnesos,

these units are only exposed in small windows through the thrust sheets of the Pindos Zone. Thus the choice of sampling sites was restricted. Many of the platform sites have not been analysed at the time of writing because of a lack of time, partially due to instrumental problems associated with the CCL magnetometer. However, interesting data have been obtained from a limited number of sites. These are described in the later part of this chapter.

The chapter is divided into three main sections. The first concerns the results of the detailed sampling carried out within the Argolis Peninsula. This is followed by the preliminary data obtained from the other autochthonous units of the Peloponnesos. The final section is a general discussion of the results from all the areas, and includes a comparison with other published palaeomagnetic data from Greece.

8.2 The Argolis Peninsula: a case study.

The Argolis Peninsula and the area to the west around Argos and Astros together form a key region for the unravelling of the complex tectonic history of the central southern Hellenides. Sequences belonging to three of the geotectonic (isopic) zones of Greece are exposed in a small geographic area. To the west of the Gulf of Argolikos, platform carbonates and flysch of the Gavrovo-Tripolitza Zone are tectonically overlain by the calciturbidites and pelagic limestones of the Pindos Zone. The latter unit is the subject of the next chapter. To the east of the gulf, Triassic to Tertiary shallow and deep water limestones of the southern-most Subpelagonian Zone occur, along with the remnants of a Late Jurassic ophiolite (the Migdhalitsa Ophiolite Unit) and an extensive area of Early Tertiary flysch (the Ermioni Complex) (Figure 8.01).

The allochthonous units of the region provide evidence for the existence of two Mesozoic/Tertiary ocean basins in southern Greece; the deep-water facies of the Pindos nappes were derived from a Pindos basin which separated the Pelagonian micro-continental sliver from the Apulian margin (see Chapter 2, Section 2.4.4, and Chapter 7, Section 7.2.2), whereas the Ermioni Complex represents a preserved accretionary prism derived from subduction of a more easterly Vardar basin (Clift and Robertson, 1989). The question of whether the Migdhalitsa Ophiolite Unit was derived from the Pindos or Vardar basins will be discussed in Section 8.2.6c.

This section of the chapter is devoted to a palaeomagnetic study of the various tectonic units exposed within the Argolis Peninsula. In view of the range of different lithologies and ages of the units sampled within the area, a different procedure will be followed in describing the results than that used in preceding chapters. Rather than outlining the magnetic mineralogy and the palaeomagnetic results separately, overall

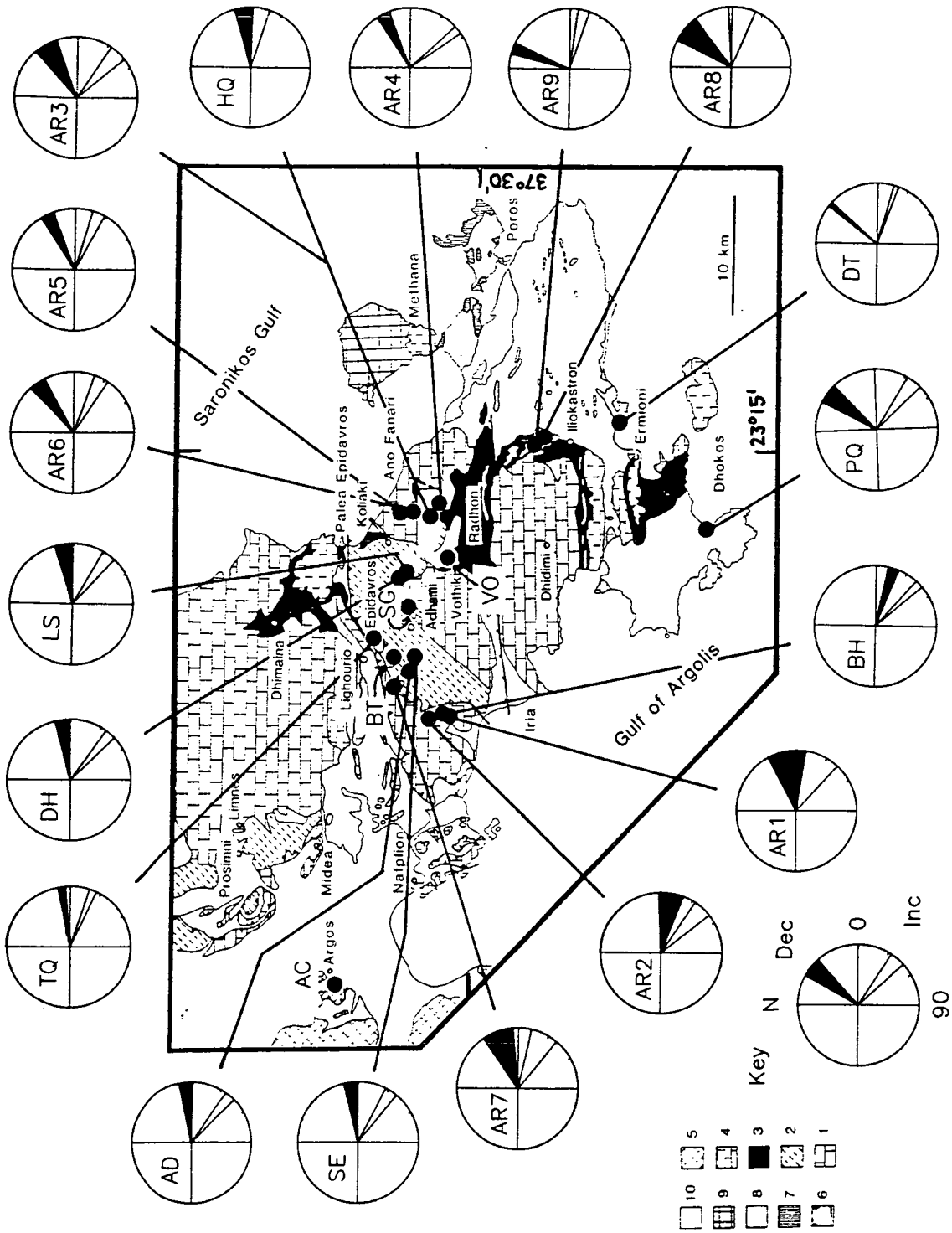

Figure 8.01. Geological map of the Argolis Peninsula (modified after Baumgartner (1985) by Clift (1990)) showing the location of all sampling sites and places mentioned in the text. The 'clock' diagrams show the 95% confidence limits associated with the mean declination and inclination in stratigraphic coordinates at each site. Also shown are the sites previously reported by Turnell (1988) from within the Middle Jurassic Ammonitico Rosso of the Pantokrator Unit (nine sites with the prefix AR). Note the significant difference between the site mean declinations on either side of the Migdhalitsa Graben. (Geological map of the Argolis Peninsula modified after Baumgartner (1985) by Clift (1990)).

Key to lithologies: 1. Pantokrator Limestone, neritic (Middle Triassic-Liassic); 2. Adhami Limestones, pelagic (Middle Triassic-Liassic); 3. Ophiolitic units (Upper Jurassic); 4. Akros Limestone, neritic (Lower-Upper Cretaceous); 5. Pindos limestones (Upper Cretaceous); 6. Ermioni Limestones, pelagic (Upper Cretaceous); 7. Poros limestones, pelagic (Lower-Upper Cretaceous); 8. Flysch (Eocene); 9. Volcanics (Quaternary); 10. Neogene-Recent deposits.

descriptions of the results from each of the units are presented in turn. I begin this section, however, with a brief review of the geology of the Argolis area.

8.2.2 The geology of the Argolis Peninsula.

The Argolis Peninsula lies within the Subpelagonian tectono-stratigraphic or isopic zone of the eastern ('internal') Hellenides (Aubouin *et al.*, 1970). The sequences exposed in the peninsula record the development, drowning and subsequent re-establishment of a carbonate platform situated between two strands of the Neotethys ocean.

The oldest rocks in the peninsula are Middle Triassic (Ladinian) rift-related tuffs and volcanics. After the initial rifting, a thick carbonate platform became developed (Bannert and Bender, 1968; Vrielynck, 1978a, b, 1980), ranging in age from Middle Triassic to Late Liassic. This is known as the Pantokrator Unit. A second major unit within the peninsula, the Asklipion Unit, consists of Middle Triassic (Anisian) andesitic tuffs and volcanics, and deep-water carbonates (the Adhami Limestone).

During the Lower Jurassic (Toarcian) the platform subsided to pelagic depths. This drowning event was marked by the deposition of condensed limestones (Ammonitico Rosso) of Toarcian to Bathonian age and of ribbon radiolarian cherts (Koliaki Chert). It was followed by the deposition of ophiolite-derived detritus (Dhimaina and Potami Formations) and the emplacement of ophiolitic rocks and mélange (Migdhalitsa Ophiolite Unit) over the platform in the Upper Jurassic (Kimmeridgian) (Baumgartner, 1985). During the Cretaceous (Barremian-Maastrichtian), a progressive marine transgression covered the subaerially weathered, emplaced ophiolite. This led to the re-establishment of platform conditions (Dercourt, 1964; Decrouez, 1977a, b; Clift, 1990).

Final closure of a Neotethyan ocean basin to the east during the Eocene resulted in thrust displacement of the Cretaceous limestones, re-thrusting of the Mesozoic nappe stack, and the emplacement of an accretion-subduction complex (Ermioni Complex; Clift and Robertson, 1989). During the Miocene-Recent period (i.e. the Neotectonic period), the area was subjected to normal faulting and calcalkaline volcanism, related to subduction of the African plate along the Hellenic trench (Mercier *et al.*, 1979; Le Pichon and Angelier, 1979; McKenzie, 1978; Fytikas *et al.*, 1984).

Within this geological framework, the relationship between the Pantokrator and Asklipion Units has been a matter of some debate. Bannert and Bender (1968) and Bachmann and Risch (1979) interpreted the various outcrops of the Asklipion Unit as a number of small, deep-water intra-platform basins within the shallow-water carbonate platform of the Pantokrator Unit (Figure 8.02a). According to this model, the Adhami Limestone represents the partial infill of these basins. This interpretation requires the

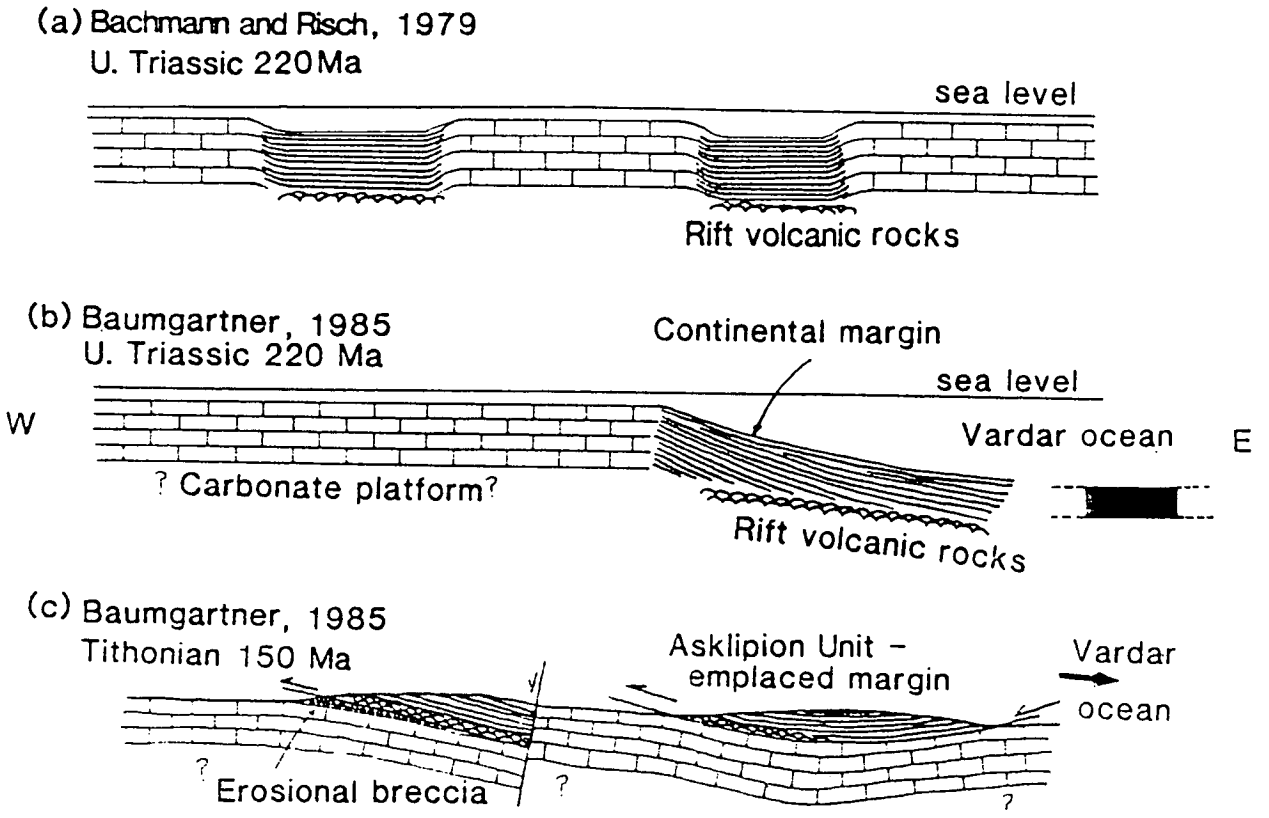

Figure 8.02. Various models proposed to explain the presence of deep-water Adhami Limestones within the Argolis Peninsula; a. after Bachmann and Risch (1979); b. and c. after Baumgartner (1985).
From Clift and Robertson (1990).

existence of a number of lateral sedimentary facies variations between the basinal and platform lithologies.

An alternative model has been proposed by Baumgartner (1985), in which the deep-water Adhami Limestones are totally allochthonous. Baumgartner (*op. cit.*) interpreted the Pantokrator Unit as a relatively autochthonous carbonate platform, in agreement with Bannert and Bender (1968). However, he considered the Adhami Limestone to represent the product of deep-water sedimentation at the base of a carbonate platform slope, situated far to the east, along the passive margin of the Vardar ocean (Figure 8.02b). This continental margin sequence was then thrust a substantial distance (up to 100 km) westwards, together with Vardar ocean crust (Migdhalitsa Ophiolite Unit), onto the Pantokrator platform in the Late Jurassic (during the 'Eohellenic' phase of deformation; Figure 8.02c).

The most recent addition to this debate has been the structural and sedimentological work of Clift (1990) and Clift and Robertson (1990), who have re-examined the critical contacts between the two units. They have demonstrated that at two key localities the deep-water redeposited carbonates of the Asklipion Unit pass laterally into the shallow-water platform carbonates of the Pantokrator Unit. This confirms the intra-platform origin of the Adhami Limestone proposed by Bannert and Bender (1968).

In the model of Clift and Robertson (1990), initial rifting and the formation of deep-water basins took place in the Late Triassic (Ladinian). During Late Triassic to Early Jurassic times, a carbonate platform developed on the subsiding rift margins (Pantokrator Limestone). Displaced carbonate was shed into the rifts, forming the 1000 metre-thick calciturbidite sequences of the Adhami Limestone (Figure 8.03a).

During the Late Jurassic, the Argolis area underwent regional compression, probably related to a change in the direction of relative motion between Africa and Eurasia when the central Atlantic began to open (Livermore and Smith, 1984; Robertson and Dixon, 1984; see Chapter 2, Sections 2.3 and 2.4.4). As a consequence, the thinned crust beneath the intra-platform basins was shortened and thrust over the adjacent, more rigid platform units (Clift and Robertson, 1990). The deep-water basins were then inverted and became imbricated within the Pantokrator Limestone platform (Figure 8.03b).

I shall discuss the opposing (allochthonous vs. autochthonous) models for the origin of the Asklipion Unit again in Section 8.2.6b below, in relation to the palaeomagnetic data of the present study.

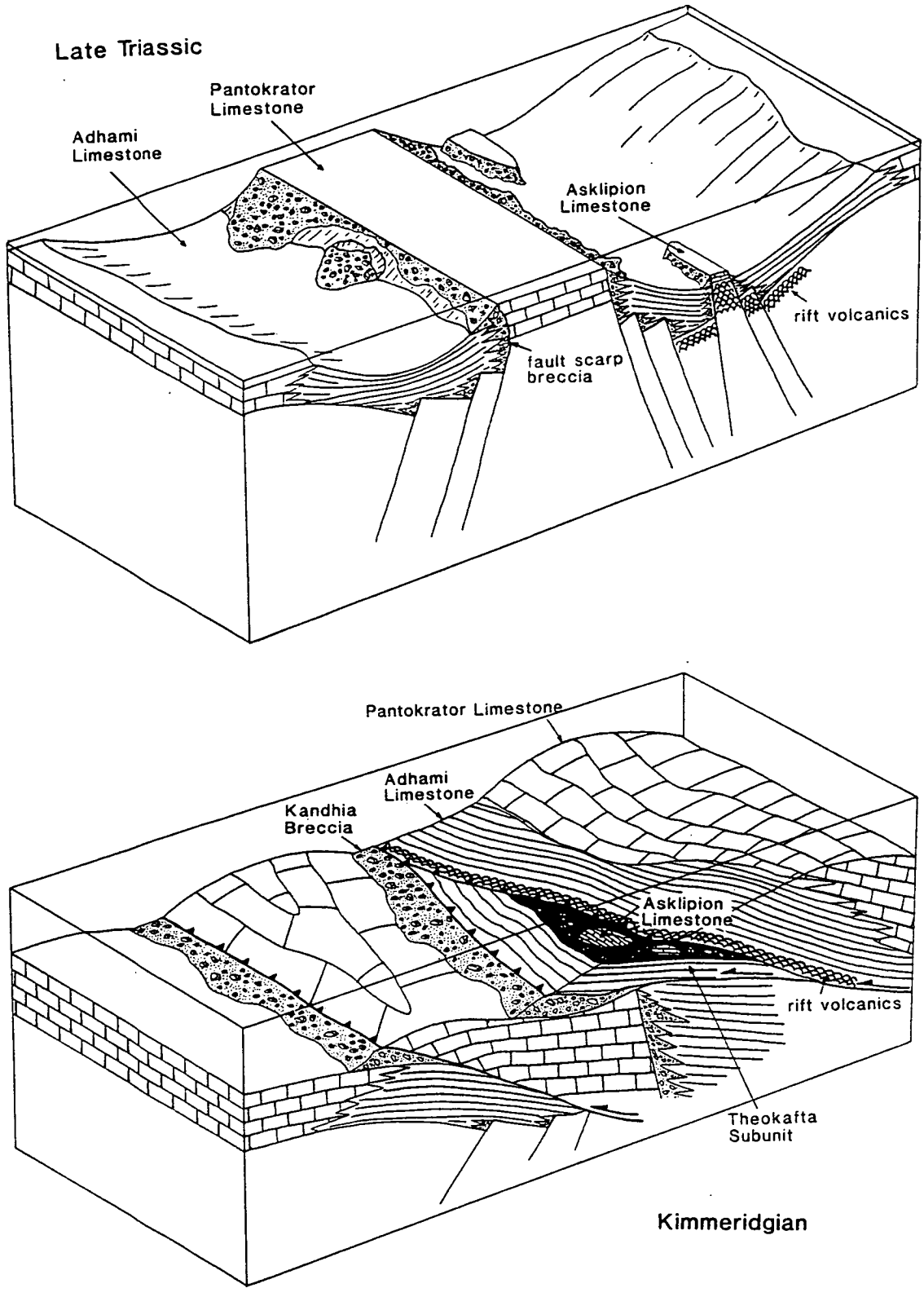

Figure 8.03. a. Block diagram showing the reconstructed Asklipion deep-water basins of the Argolis Peninsula during the Ladinian (Late Triassic), after initial rifting and basin formation; b. Block diagram of the Asklipion basins after inversion and imbrication with the Pantokrator Limestone platform during the Kimmeridgian (Late Jurassic).
From Clift and Robertson (1990).

8.2.3 Sampling and methods.

Samples were collected from all the main units exposed in the Argolis Peninsula, ranging from Middle Triassic to Plio-Quaternary in age. Sites were spread throughout the area to attempt to identify any variations in rotational deformation affecting the peninsula. Where possible two or more sites were located in each unit.

In general, sites with only minor structural tilt (normally less than 40°) and simple folding were preferred. It was hoped that collecting from such strata would minimise any declination errors due to tectonic rotation about inclined axes (MacDonald, 1980). Visibly weathered and altered exposures were avoided, together with sections close to major faults and zones of penetrative veining.

Sampling was carried out using a standard petrol-driven rock drill, with water cooled, 1" diameter diamond-tipped drill bits. Each sample was orientated with both magnetic and sun compasses (Creer and Sanver, 1967). Structural tilt corrections were based on the attitude of well-developed bedding planes within the carbonate sequences. A total of 29 sites were collected. The location of the sites from which reliable results were obtained are shown in Figure 8.01, along with the locations of the sites previously reported by Turnell (1988).

In the laboratory, 18 mm long subsamples were prepared from each core for analysis using the 2-axis CCL superconducting magnetometer. This is the maximum sample length which this magnetometer can accommodate with the sample inserted on its side (Chapter 1, Section 1.6.2).

For each site, two samples were subjected to stepwise AF demagnetisation in 2.5 mT intervals up to 20 mT, 5 mT intervals up to 50mT, and then 10 mT intervals up to a maximum field of 100 mT. A further two samples were demagnetised thermally in 50°C steps up to a maximum temperature of 700°C. With both techniques demagnetisation was stopped below the maximum field/temperature when the intensity of magnetisation decreased below a level at which accurate measurement could be made (approximately 10.0×10^{-9} Am^{-1}).

Although it is standard practice to monitor changes in the susceptibility of samples at each stage of thermal demagnetisation, to detect any changes in magnetic mineralogy induced by heating, this was not possible in the present study. This was because the available susceptibility meter was not sensitive enough to measure the susceptibility of the weakly magnetic carbonates. However, the consistency of the direction of remanent magnetisation between heating steps in these samples indicates that no new minerals

which contribute significantly to the sample remanence were formed during heating, before the intensity of magnetisation became too low to measure*.

The results of these demagnetisation experiments were used to decide which technique to apply to the rest of the samples at each site. The remaining samples were then stepwise demagnetised, but at a reduced number of steps. Cleaned sample directions were found by drawing best-fit lines through the last four or more points on Zijderveld demagnetisation diagrams (Zijderveld, 1967).

Of the original 29 sites sampled, 13 gave reliable palaeomagnetic results, of which 11 gave directions unrelated to the present geomagnetic field direction in Argolis. Sixteen sites were rejected because of either the very weak intensities of magnetisation, which made accurate measurement impossible, or unacceptably large within site dispersions (K<10). The following sections describe the reliable results from each unit, in order of decreasing stratigraphic age. The cleaned mean directions obtained from the reliable sites are reported in Table 8.1, both before and after the application of standard structural tilt corrections (i.e. in both geographic and stratigraphic coordinates).

8.2.4 Results.

a. The Middle Triassic rift-related tuffs of the Asklipion Unit.

The base of the Asklipion Unit consists of a 200-300 metre-thick succession of andesitic lavas and tuffs (Baumgartner, 1985; Pe-Piper, 1982). These were erupted during the Middle Triassic into the rift-basins proposed by Clift and Robertson (1990).

The tuffs have been sampled at two sites, BT and SG (Figure 8.01), along the Adhami road. Both sites consisted of exposures of medium- to coarse-grained trachytic to andesitic tuffs with graded bedding.

At both sites, the NRM directions were found to cluster around the present field direction (inclination = 56°). This suggests that the remanences are dominated by viscous components acquired during the last few hundred thousand years (Tarling, 1983), and/or recent CRM components generated by subaerial weathering. Alternating field (AF) demagnetisation of several samples failed to recover primary components of magnetisation. The ease with which AF treatment removed the magnetisation suggests that the viscous overprint is carried by magnetite. No further work was carried out on these sites.

---

* Note that the samples were always randomly orientated within the demagnetisation oven.

Table 8.1. Palaeomagnetic results from the Argolis Peninsula.

Site	Age	N	Geographic				Stratigraphic			
			Dec	Inc	α_{95}	K	Dec	Inc	α_{95}	K
Rift-related tuffs of the Asklipion Unit.										
BT	Triassic (Present field direction)	13	358	56	5.9	51	-	-	-	-
SG	Triassic (Present field direction)	7	351	57	9.4	42	049	59	13.6	21
Asklipion Limestone of the Asklipion Unit.										
TQ	Triassic	32	255	-44	4.4	34	262	-22	4.4	34
Adhami Limestones of the Asklipion Unit.										
SE	Triassic	13	242	-39	7.5	32	263	-33	7.5	32
LS	Triassic	12	240	-59	8.1	25	260	-36	8.1	25
DH	Triassic	31	256	-33	6.6	16	262	-41	6.5	17
AD	Triassic	18	240	-45	6.8	24	265	-40	6.3	27
Ammonitico Rosso of the Pantokrator Unit.										
BH	M. Jurassic	18	082	54	4.6	88	107	45	4.8	52
HQ	M. Jurassic	15	270	31	10.3	15	261	-2	10.3	15
The Migdhalitsa Ophiolite Unit.										
VO	U. Jurassic (Present field direction)	7	353	47	5.6	116	-	-	-	-
The Akros Limestone Formation.										
AC	Cretaceous	37	143	69	3.5	46	095	62	3.5	46
The Upper Cretaceous-Palaeocene pelagic limestones.										
DT	U.Cre-Pal	25	226	-27	3.0	96	220	-18	2.9	103
The Plio-Quaternary sediments.										
PQ	Plio-Quat	6	039	40	9.4	51	-	-	-	-

N = number of samples; α_{95} = semi-angle of 95% cone of confidence; K = Fisher precision parameter

b. The Middle-Late Triassic Asklipion Limestone.

Associated with the main outcrop of the Asklipion Unit, adjacent to the ancient theatre of Epidavros to the southeast of Lighourion (Figure 8.01), is the Theokafta Subunit. This is tectonically sandwiched between the mainly redeposited carbonates of the Asklipion Unit and the platformal limestones of the Pantokrator Unit (Clift and Robertson, 1990). The subunit consists of Late Triassic to Early Jurassic successions of cherty basinal limestone, capped by hardgrounds, neptunian dykes infilled with pelagic sediment and syn-sedimentary breccias. These are overlain by ribbon radiolarian cherts (Koliaki Cherts; Baumgartner, 1985) of Late Jurassic age. Within these cherts are 1-100 metre-sized blocks (olistoliths) of condensed pelagic limestone known as the Asklipion Limestone, dated as Anisian-Carnian (Middle-Late Triassic). These condensed limestones accummulated slowly on a seamount within one of the intra-platformal rifts basins after the end of volcanism (Clift and Robertson, 1990). During the Late Jurassic, regional compression led to the disintegration of the intra-platform basin seamounts, which were entrained as olistoliths within a tectonic mélange located between the Pantokrator basement and the overthrust Asklipion Unit (Clift, 1990). Samples have been collected from the main olistolith (site TQ; Figure 8.01).

The NRM directions at this site form a strung-distribution with westerly declinations and a range of inclinations (Figure 8.04a), suggesting the existence of two superimposed components of magnetisation. IRM acquisition curves for these samples (Figure 8.04b) show a sharp initial rise below 300 mT, indicative of the presence of magnetite. A further increase in isothermal moment up to the maximum applied field of 2.0 T indicates the presence of a second magnetic mineral with coercivities higher than that of magnetite. Thermal demagnetisation of a composite IRM (see Chapter 6, Section 6.3.1) demonstrated that this high coercivity mineral is haematite, presumably in the form of pigment, with a maximum blocking temperature close to the Curie point (Figure 8.04c). The application of the domain size test of Johnson *et al.* (1975) demonstrates that single-domain-sized particles dominate the magnetite fraction (Figure 8.04d).

Alternating field and thermal demagnetisation were found to be equally effective in recovering stable endpoints from these samples. However, AF treatment could not remove all of the magnetisation. The results suggest that both minerals carry the same direction of magnetisation. This would normally indicate that formation of the pigmentary haematite occurred soon after initial deposition.

The majority of the samples at this site have been demagnetised using the AF technique. The final cleaned site mean direction has a negative inclination and a westerly declination (Figure 8.05). Assuming that this magnetisation is of reversed polarity, the mean declination of 262° implies that this unit has experienced a clockwise

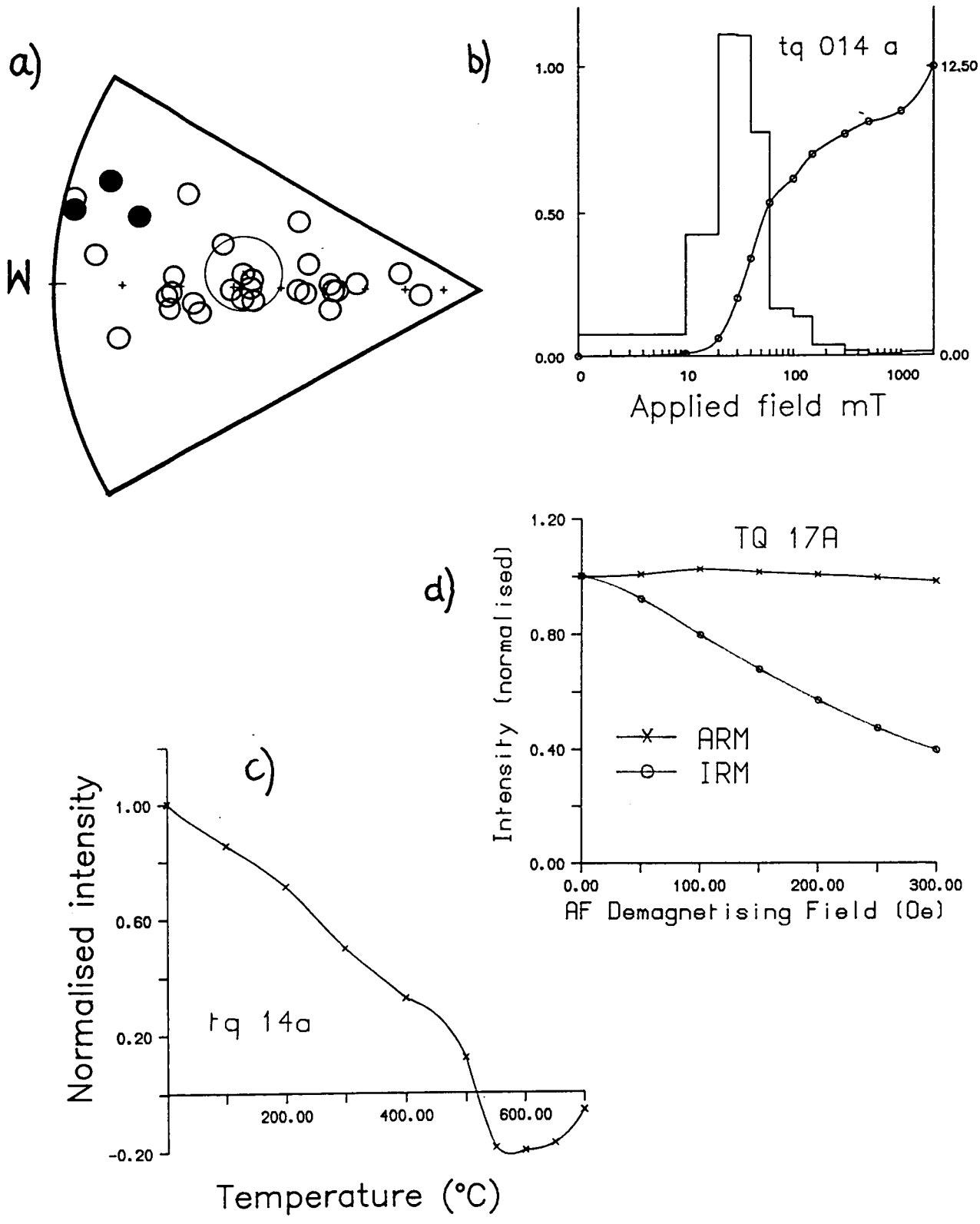

Figure 8.04. Site TQ within the Asklipion Limestone formation of the Theokafta Subunit: a. The distribution of NRM directions at the site; b. A typical result of the IRM acquisition experiments; c. An example of stepwise thermal demagnetisation of a composite IRM, for sample TQ 14 A. Low coercivity carriers have a positive magnetisation, and high coercivity carriers have a negative one. A decrease in the normalised intensity up to temperatures of 580°C indicates the presence of magnetite, whereas maximum unblocking temperatures of close to 700°C for the 2.0 T IRM indicate that haematite is also present; d. A typical result of the domain size test of Johnson *et al.* (1975) indicating the dominance of single-domain-sized grains in the magnetite fraction.

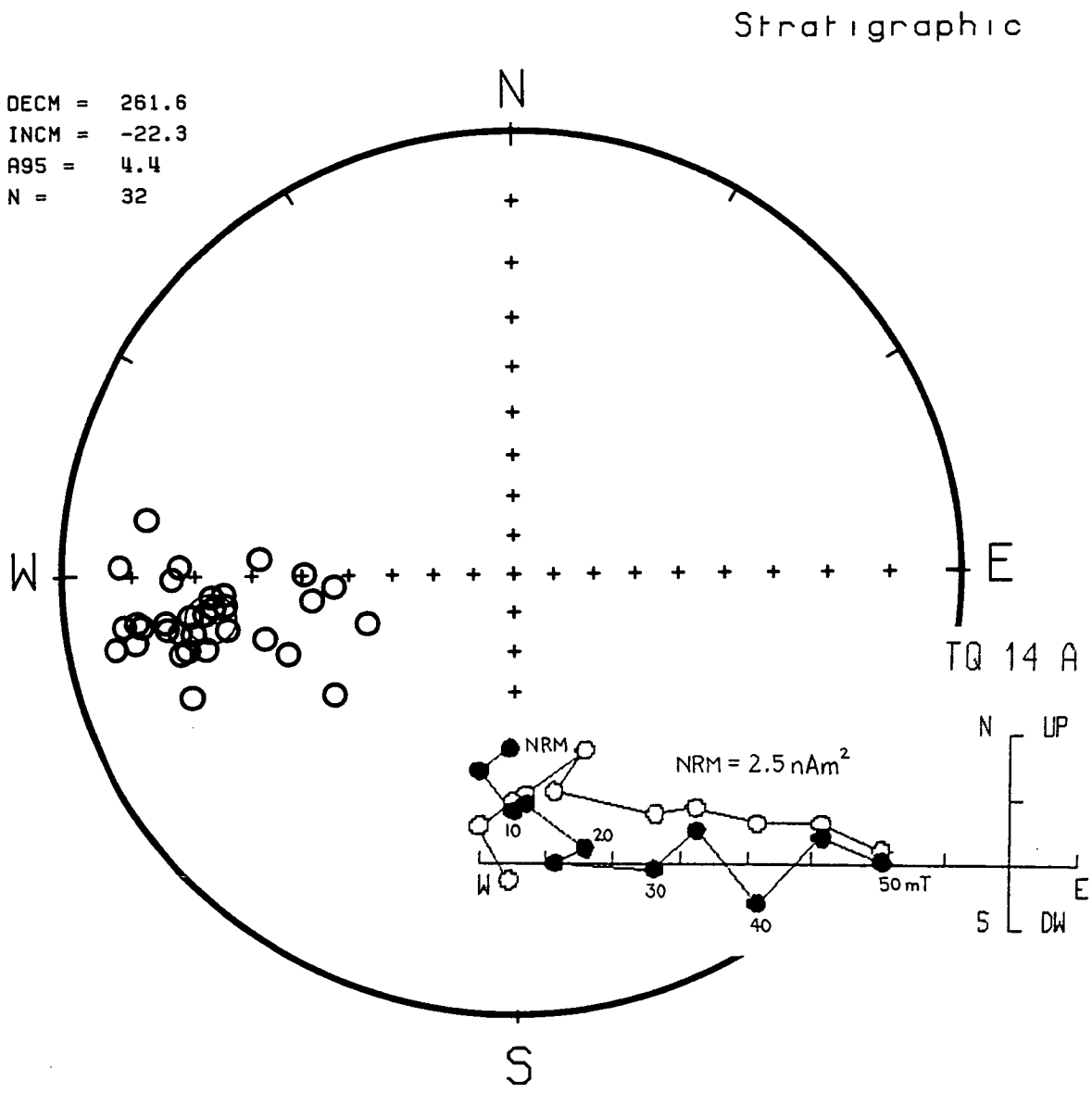

Figure 8.05. The cleaned sample directions at site TQ (stratigraphic coordinates), indicating an 82° clockwise rotation of the sampled unit, and a Zijderveld plot showing a typical alternating field demagnetisation result.

rotation of 82°. This result is in close agreement with those from the Triassic Adhami Limestones of the Asklipion unit and the Middle Jurassic Ammonitico Rosso of the Pantokrator Unit, described below. However, biostratigraphical studies at this site, reported by Krystyn and Mariolakos (1975), have indicated that the sampled block is overturned. This interpretation is based upon a sequence of ammonite zones preserved within the section. Also, the tuffs of the Asklipion Unit which occur stratigraphically beneath the Asklipion Limestone lie on top of the latter formation at the site, supporting the idea that the sampled block represents an overturned olistolith. The agreement between the tilt-corrected vectors at this site and the other sites in the northern half of Argolis may have resulted from a chance alignment of the azimuth of the magnetisation of the olistolith with that of the *in situ* units. Alternatively, the olistolith may have been remagnetised during the collapse of the intra-platform basin in the Late Jurassic, when the Asklipion Limestone was detached from its seamount basement and incorporated into a tectonic mélange. Such extreme deformation may have led to the acquisition of a strong secondary magnetic overprint in the direction of the geomagnetic field at the time. The site mean inclinations in geographic and stratigraphic coordinates (-44° and -22° respectively; Table 8.1) do not allow a choice to be made between these two alternatives, since they fall on either side of the mean inclination of the other units.

In either case, the data from this site indicate a large clockwise rotation of between 75° and 82°, with respect to the present north.

c. The Triassic Adhami Limestones of the Asklipion Unit.

The deep-water carbonates of the Adhami Limestones form a 1000 metre-thick succession, dated as Late Anisian to Early Ladinian (Middle Triassic) at the base (Vrielynck, 1978a, b), and as Early Jurassic near the top (Dercourt, 1964; Aubouin *et al.*, 1970; Vrielynck, 1978a, b). The succession is dominated by thin- to medium-bedded calciturbidites, and is interpreted as the sedimentary infill of intra-platform rift basins (Clift and Robertson, 1990; see Section 8.2.2 above).

The Triassic part of this sequence has been sampled at four localities (sites SE, LS, DH and AD, Table 8.1), along the Lighourio-Adhami-Trachia road (Figure 8.01).

At each of these sites, the NRM directions are strung out along a great circle girdle between steep positive inclinations to the north and shallow negative inclinations to the west (Figure 8.06). These great circle distributions suggest the presence of two superimposed components of magnetisation at the sites.

AF demagnetisation was found to be ineffective with these samples. The intensity of magnetisation was not reduced by fields of 50 mT. On the other hand, thermal treatment reduced the magnetisation below a level at which accurate measurement

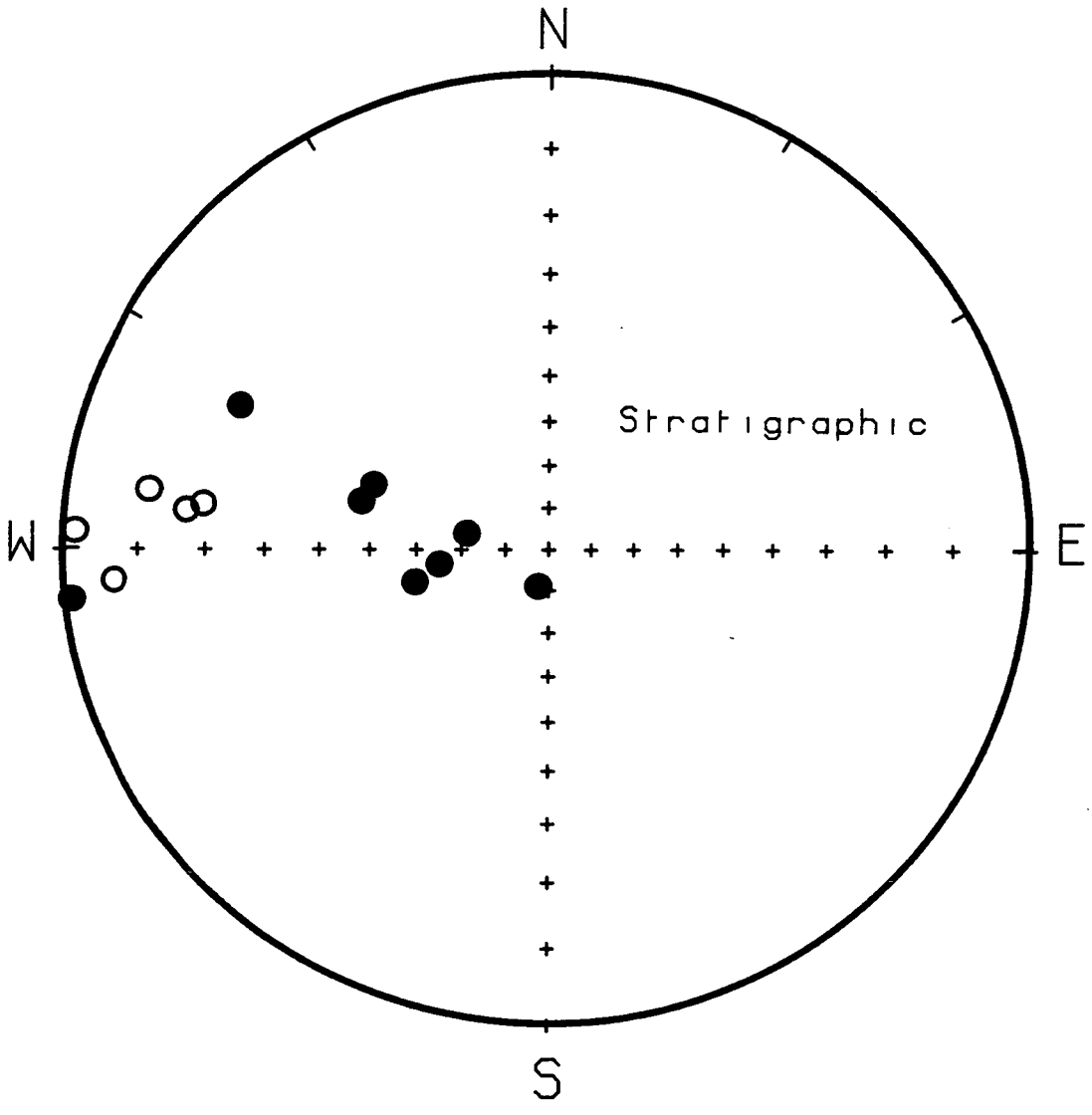

Figure 8.06. The distribution of NRM directions at site SE, within the Triassic Adhami Limestones of the Asklipion Unit.

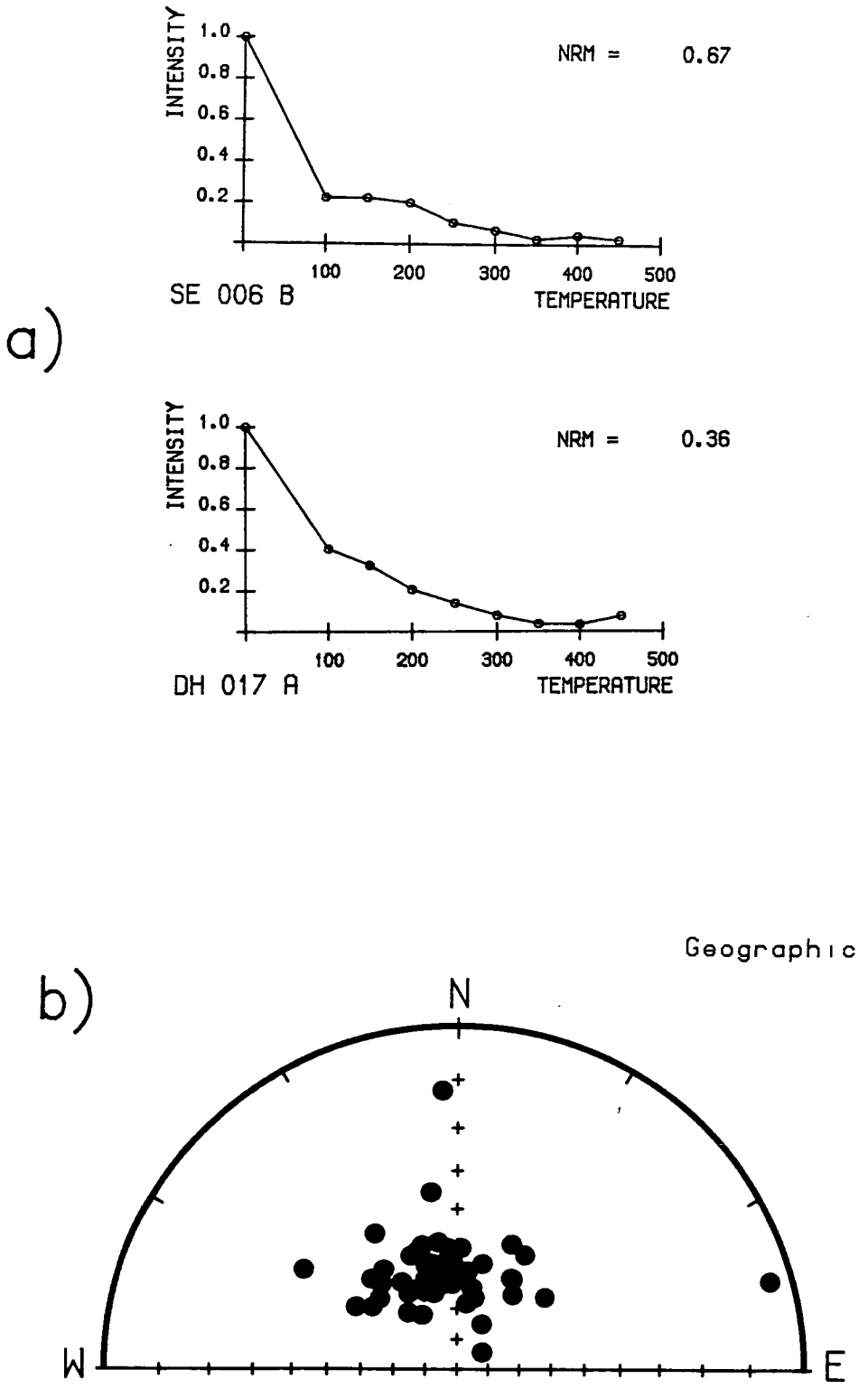

Figure 8.07. a. Thermal demagnetisation characteristics of the Adhami Limestone samples; b. The directions (in geographic coordinates) of the components of magnetisation removed by heating to 100°C at site DH. The tight clustering around the present field direction, combined with a marked decrease in the intensity of natural remanence, indicates the presence of a recent component of magnetisation carried by goethite.

could be made (approximately 10.0 x 10^{-9} Am^{-1}) by temperatures of 350°-550°C. In many cases, over half of the initial NRM was removed by 100°C (Figure 8.07a). When the directions (in geographic coordinates) of the components of magnetisation removed during this first step of demagnetisation are plotted on a stereonet (Figure 8.07b), they are found to cluster around the present field direction. The data indicate the presence of a recent component of magnetisation carried by goethite, which has maximum blocking temperatures typically in the range of 50°-90°C (Heller, 1977).

After removal of the recent components, the magnetisation vectors at each site migrate along great circles paths to reach stable endpoints, with west-southwesterly declinations and intermediate negative inclinations, by temperatures of 300°C (Figure 8.08).

The cleaned site mean directions reported in Table 8.1 for these four sites may be combined to form an overall mean as follows:

Geographic coordinates: Dec = 245°, Inc = -44°, A_{95} = 14.4, K = 42.

Stratigraphic coordinates: Dec = 263°, Inc = -38°, A_{95} = 4.6, K = 401.

The decrease in between-site dispersion after the application of structural tilt corrections indicates that the magnetisation predates folding at the sites. This positive fold test is significant at the 99% confidence level, using the F-test of McElhinny (1964; K_1/K_2 = 9.55, K_1/K_2 > 8.47 for significance at the 99% confidence level). The stable endpoints identified by the demagnetisation experiments are, therefore, interpreted as remanent magnetisations acquired at or shortly after the time of deposition and carried by haematite. Since detrital haematite has generally been found to be of minor importance in limestones (Lowrie and Heller, 1982), it seems likely that the haematite in these rocks formed during early diagenesis by the dehydration of goethite that had precipitated directly from seawater.

The need to avoid unacceptable overlaps with the inferred position of the African plate confirms that the magnetisation is of reversed polarity. After inverting the mean direction of magnetisation through the origin, the data indicate that these sites have been rotated clockwise by 83° (with respect to the present north).

d. The Middle Jurassic Ammonitico Rosso of the Pantokrator Unit.

During the Lower Jurassic (Toarcian), the Pantokrator platform subsided to pelagic depths. This drowning event led to the deposition of pink/red condensed pelagic limestones (Ammonitico Rosso facies) of Toarcian to Bathonian age, and of ribbon radiolarian cherts (Koliaki Chert; Baumgartner, 1985). The Ammonitico Rosso has been sampled at two localities (sites BH and HQ; Figure 8.01).

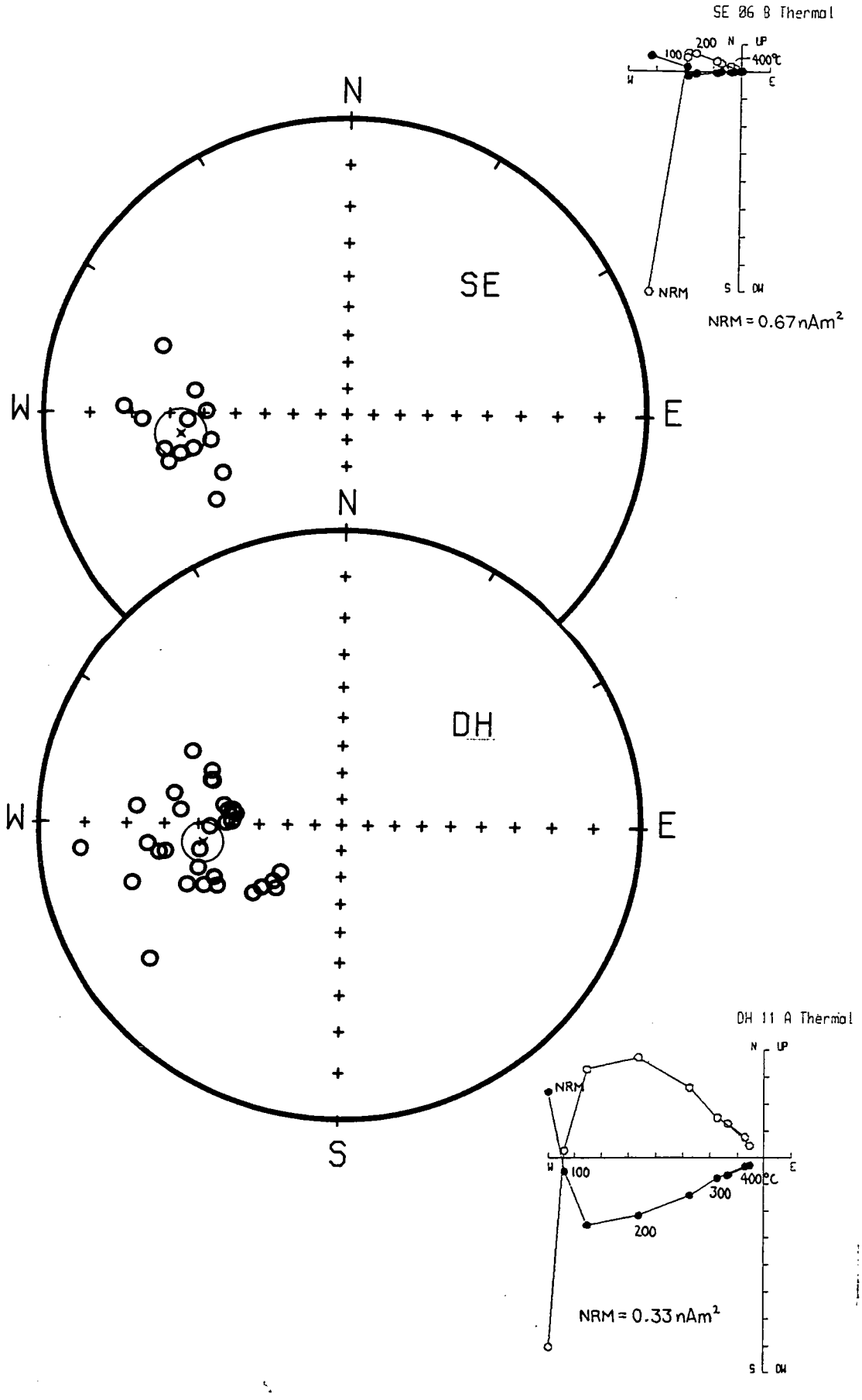

Figure 8.08. The cleaned sample directions at sites SE and DH, within the Adhami Limestones of the Asklipion Unit, together with typical examples of thermal demagnetisation.

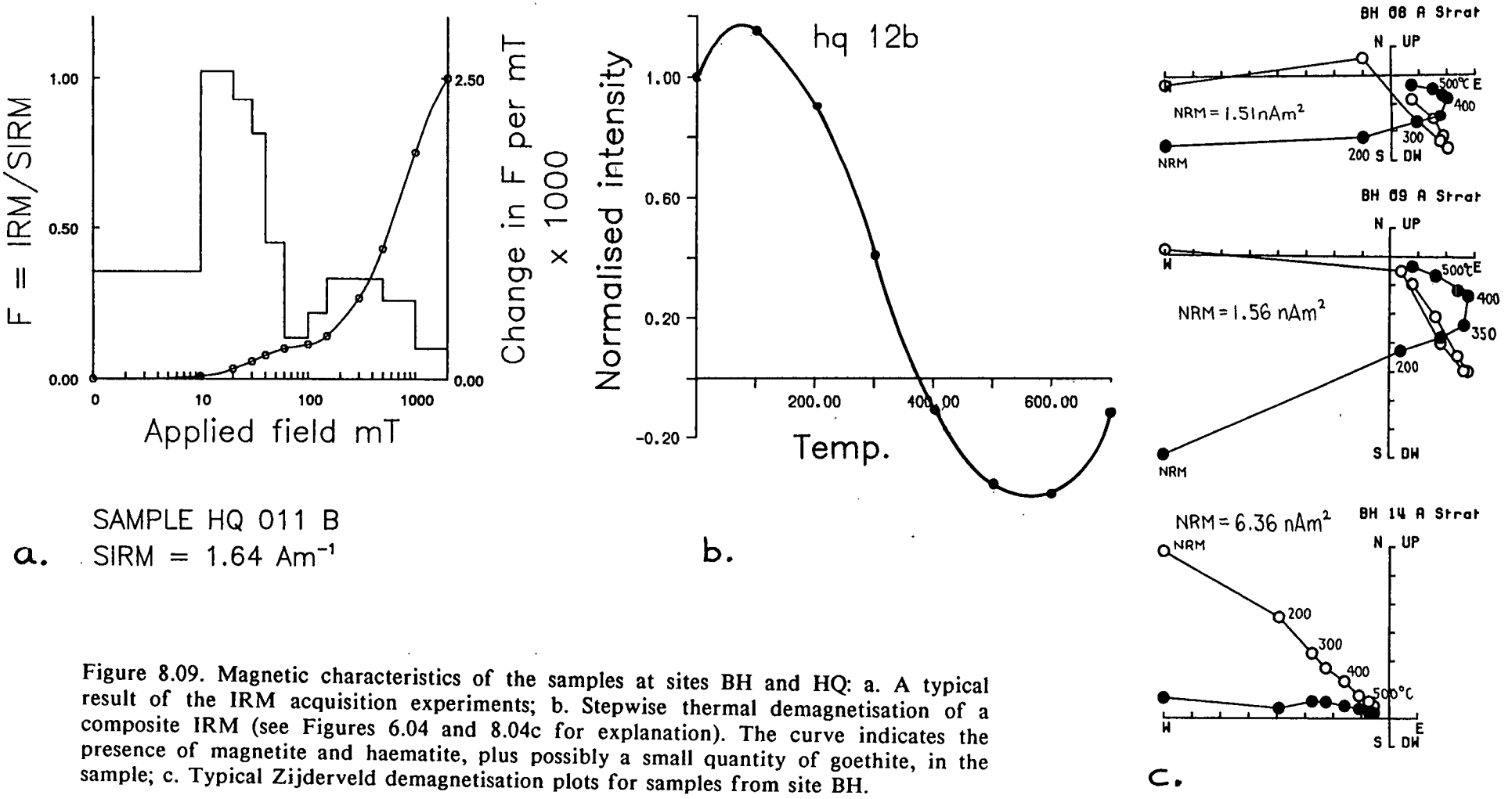

Figure 8.09. Magnetic characteristics of the samples at sites BH and HQ: a. A typical result of the IRM acquisition experiments; b. Stepwise thermal demagnetisation of a composite IRM (see Figures 6.04 and 8.04c for explanation). The curve indicates the presence of magnetite and haematite, plus possibly a small quantity of goethite, in the sample; c. Typical Zijderveld demagnetisation plots for samples from site BH.

The magnetic characteristics of the samples from these sites are very similar. Both normal and reversed polarities have been identified at site BH, on the western side of the peninsula, but only reversed polarities are observed at site HQ.

The NRM directions at both sites have westerly declinations and shallow to intermediately dipping inclinations. The rate of acquisition of IRM indicates that two main magnetic minerals are present in these samples; a low coercivity fraction which is probably detrital magnetite, and a higher coercivity mineral, which in view of the red colouration of this lithology is probably pigmentary haematite (Figure 8.09a). This haematite probably formed by the dehydration of a goethite precursor. Stepwise thermal demagnetisation of a composite IRM (see Chapter 6, Section 6.3.1) confirms the presence of haematite with a maximum unblocking temperature close to the Curie point of 680°C. However, a slight increase in the isothermal moment below 100°C in this experiment may indicate that a small goethite fraction is also present (Figure 8.09b).

Thermal demagnetisation was found to give better results that AF treatment. Upon demagnetisation, the samples at site BH divide into two groups. One group does not change in direction, whereas the other migrates towards the east and finally reaches a stable position antiparallel to the first group. These changes are illustrated in the Zijderveld demagnetisation diagrams of Figure 8.09c. A marked decrease in the intensity of the natural remanence below 100°C suggests that the 'secondary' magnetisation removed in this process is carried by goethite. The direction of the 'secondary' magnetisation is unrelated to the present geomagnetic field direction at the site, suggesting that the goethite formed before tectonic rotation took place, possibly by precipitation from seawater.

The final cleaned remanence directions at both sites are shown in Figure 8.10. The shallow inclinations at site HQ are difficult to explain. They may be due to an incomplete removal of a normal polarity overprint, to the application of a slightly erroneous structural tilt correction, or to post-depositional compaction of the sediment. Although no fold test is possible at these sites, the presence of normal and reversed polarity groups at site BH suggests that the primary depositional remanence has been identified. However, the alignment of the two groups is not precisely antiparallel (the data fail a reversal test at the 95% confidence limit; see Appendix A). This may indicate the presence of a persistent high blocking temperature component, probably carried by pigmentary haematite. The data from both sites indicate large (*ca.* 90°) clockwise rotations of the sampled units.

The rock type sampled at these sites is identical to that studied by Turnell (1988) in her preliminary study of the Argolis Peninsula (see Chapter 7, Section 7.3.2b). The results obtained here agree well with those reported by Turnell (*op. cit.*), which indicated

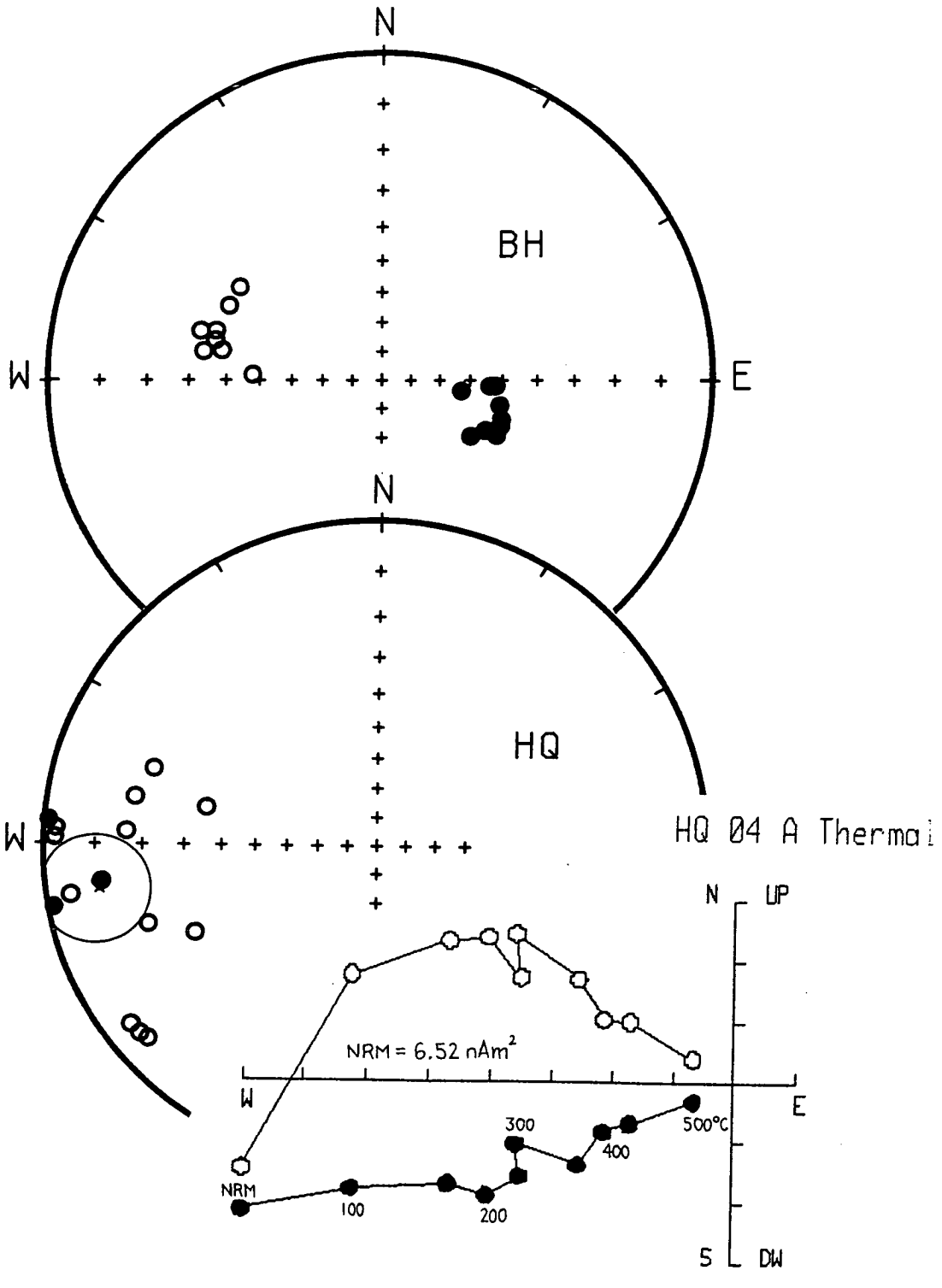

Figure 8.10. The cleaned sample directions at sites BH and HQ, within the Middle Jurassic Ammonitico Rosso facies of the Pantokrator Unit, together with a typical example of thermal demagnetisation of a sample from site HQ.

a 70° clockwise rotation of part of the peninsula since the Jurassic. Turnell's data will be combined with those of the present study in Section 8.2.5b below to obtain an improved estimate of this rotation.

e. The Late Jurassic ophiolite.

Site VO is the only place where the tholeiitic pillow lavas of the Migdhalitsa Ophiolite Unit were sampled. This site is located 500 metres to the north of the village of Vothiki (Figure 8.01). Baumgartner (1985) dated the overlying cherts as late Middle Jurassic in age, implying that the oceanic crust represented by the lavas formed in the Middle Jurassic. The Migdhalitsa Ophiolite Unit was emplaced over the Pantokrator platform in the Late Jurassic (Kimmeridgian) (Baumgartner, 1985). Emplacement was broadly from the present east or northeast (Baumgartner, 1985; Clift, 1990; Section 8.2.6c below). The ophiolite is now only preserved in structural lows within the Migdhalitsa Graben system. However, Clift and Robertson (1990) have observed ophiolitic olistostromes as far west as Argos Castle, suggesting that the ophiolite and/or its detritus originally covered the whole of the Argolis Peninsula.

The NRM directions of the samples at this site cluster around the present field direction, suggesting that the remanence is dominated by viscous components of magnetisation acquired over the last few hundred thousand years (Tarling, 1983), and/or a recent CRM component generated during subaerial weathering. AF demagnetisation was found to be effective in removing all the magnetisation, but revealed only single northwards-directed components. The low resistance of the samples to AF demagnetisation is consistent with the IRM acquisition characteristics, which indicate that magnetite is the only mineral present capable of carrying a remanent magnetisation. The decay of NRM intensity with AF demagnetisation was rapid, with median destructive fields of between 5 and 10 mT. This suggests that the magnetite is in the form of low coercivity multi-domain (MD) grains. However, the application of the domain size test of Johnson *et al.* (1975) demonstrates that single-domain-sized particles dominate the magnetite fraction.

The lack of a primary remanent magnetisation at this site makes the result geologically unimportant. However, the first palaeomagnetic study in the Argolis Peninsula, by Pucher *et al.* (1974), involved sampling similar pillow lavas within the Migdhalitsa Ophiolite Unit (see Chapter 7, Section 7.3.2a). Pucher *et al.* (*op. cit.*) identified both normal and reversed polarities of magnetisation at their sites, with directions unrelated to the present geomagnetic field direction. Although the dispersion of sample vectors was great, the mean remanence direction reported by this group (Dec = 082°, Inc = 19°, α_{95} = 17°, N = 24) was the first direct evidence that the Argolis

Peninsula had been tectonically rotated. Pucher *et al.*'s data suggest that, in general, the pillow lavas of the ophiolite record primary thermoremanent magnetisations and are not everywhere dominated by viscous components.

f. The Akros Limestone Formation.

The hiatus in sedimentation after ophiolite emplacement in the Late Jurassic was followed by a gradual marine transgression over the ophiolite and its debris during the Cretaceous. This transgression and the re-establishment of tectonic stability led to the redevelopment of carbonate platform conditions. The limestones so formed are exposed in many areas of the Argolis Peninsula, but most notably at Akros Mountain near Palea Epidavros (Figure 8.01; Decrouez, 1977a), and have been termed the Akros Limestone Formation by Clift (1990).

The Lower to Upper Cretaceous platform units have been sampled at several localities, including the Akros Mountain exposure. Unfortunately, these limestones are extremely weakly magnetised, with intensities at or below the noise level of the cryogenic magnetometer. At one site at Argos Castle hill (site AC; Figure 8.01), however, the samples were found to be sufficiently magnetic to enable both NRM measurements and demagnetisation experiments to be performed.

Site AC consists of thick-bedded, fine-grained, shallow-water bioclastic limestones, which form part of a thrust sheet of Akros Limestones overlying a second thrust sheet of pelagic limestones of the Pindos Zone (see Chapter 9). The samples at this site were collected from various parts of a single, 0.5 metre-thick bed. A greater spread of sampling was not possible because of the limited nature of the exposure and the near-horizontal attitude of the bedding.

The NRM directions at the site are tightly grouped and close to the vertical in both geographic and stratigraphic coordinates. No rock magnetic experiments have been carried out on these samples, but AF demagnetisation was effective in removing all the magnetisation by fields of 50 mT. This suggests that the remanence is carried by magnetite, of presumed detrital origin. Thermal demagnetisation was found to give better results than AF treatment, and indicated maximum unblocking temperatures of approximately 500°C, again consistent with a magnetite remanence carrier.

Upon demagnetisation, the magnetisation of the samples migrated away from the vertical and became slightly shallower to the east. The cleaned sample directions are shown in Figure 8.11. The mean direction of magnetisation has a similar declination to that of the Pantokrator platform sites to the east. However, the mean inclination is steeper than the inclination of the present geomagnetic field at the site (62° compared to 56° for an axial geocentric dipole field), and implies a palaeolatitude of 43°N which is

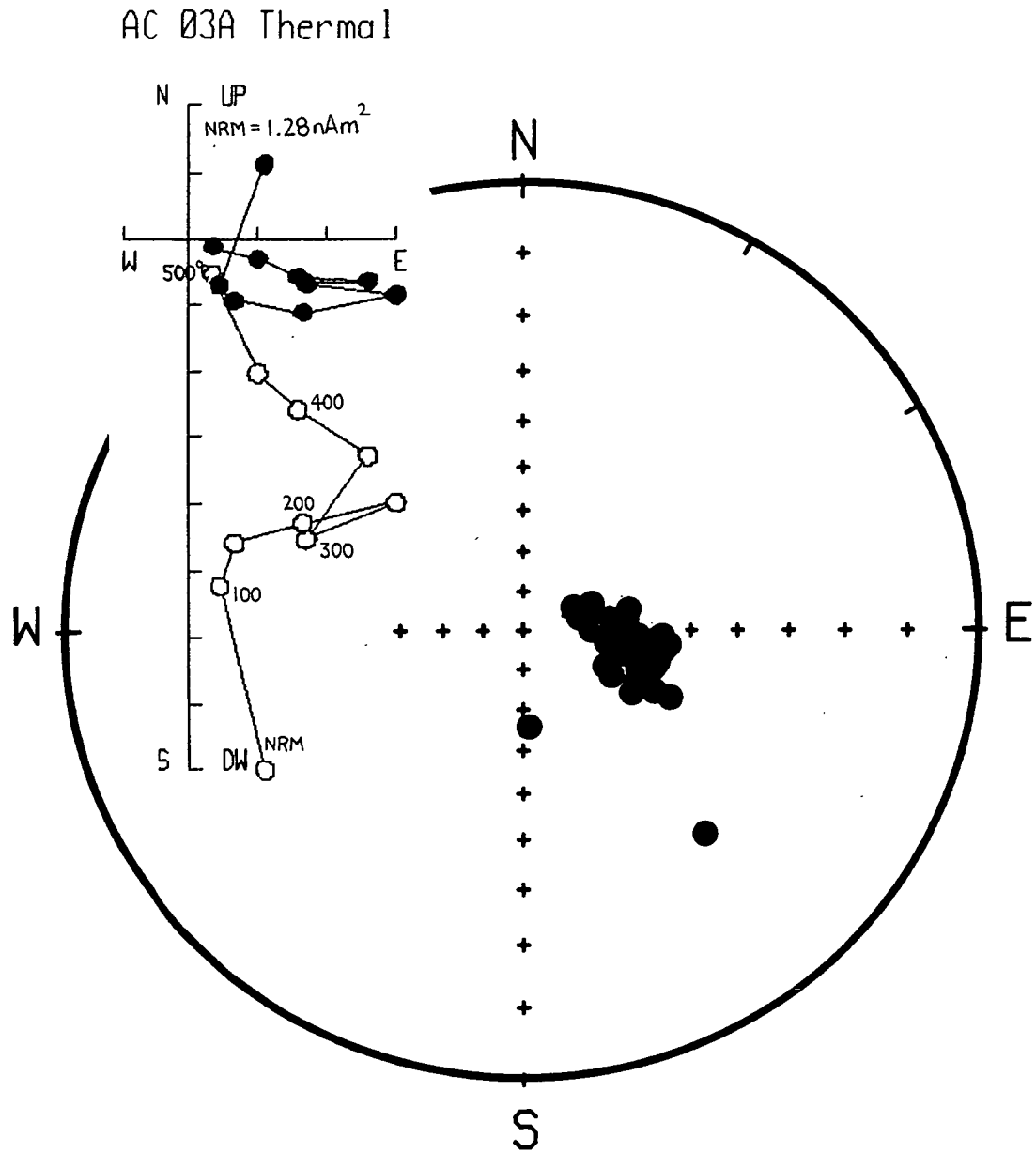

Figure 8.11. The cleaned sample directions at site AC, located within the Cretaceous neritic limestones of the Akros Limestone Formation, together with a typical example of thermal demagnetisation.

clearly unreasonable. The strike and dip of the bedding at this site was not easy to measure. However, an independent estimate of the structural tilt by P. D. Clift (pers. comm., 1990) matches closely with that found in the present study. This suggests that the steep inclination is not a product of the application of an invalid tilt correction. Instead, it is probable that palaeosecular variation has not been effectively averaged at this site, because of the limited sampling spread. Alternatively, the steep inclination may be due to the proximity of the sampled beds to the major thrust, separating the Pindos limestones below from the platform limestones above. Locally intense deformation may have affected the original direction of magnetisation. Studies of the anisotropy of magnetic susceptibility at this site may shed light on whether the remanence has been influenced by deformation during thrusting and folding. These have not been carried out at the time of writing.

The data from this site have been excluded from the calculation of the mean rotation affecting the northern half of the Argolis Peninsula (Section 8.2.5b).

g. The Upper Cretaceous-Palaeocene pelagic limestones.

During the Upper Cretaceous (Maastrichtian), the Argolis platform again subsided to pelagic depths under the influence of crustal extension. This was followed by the emplacement of a large body of Palaeocene-Eocene flysch over the eastern margin of the platform. This unit, known as the Ermioni Complex, consists of a tectonically thickened wedge of terrigenous flysch, interleaved with thin, tectonically disrupted sheets of basic lava, massive sulphides, and metalliferous and pelagic sediments (Robertson *et al.*, 1987; Clift and Robertson, 1989). It is interpreted as a subduction-accretion complex formed during the final stages of closure of the Neotethyan Vardar basin.

As subsidence occurred, pink, condensed pelagic limestones were deposited over the top of the platform during the Upper Cretaceous to Palaeocene. These have been sampled in a small quarry along the southern coast of the peninsula, to the east of Ermioni (site DT; Figure 8.01).

The NRM directions at this site fall in the southwest quadrant with shallow positive inclinations, in both geographic and stratigraphic coordinates. IRM acquisition curves for this lithology characteristically show a rapid initial rise in isothermal moment up to 100 mT (Figure 8.12a), followed by a further three-fold increase up to the maximum applied field of 2.0 T. This indicates the presence of both magnetite and a mineral with a higher coercivity. Stepwise thermal demagnetisation of a 2.0 T IRM carried out on one sample showed a progressive decrease in total moment up to a maximum temperature of 700°C (Figure 8.12b). No large decrease in total moment was observed below temperatures of 100°C. The high coercivity mineral identified by the IRM analysis is

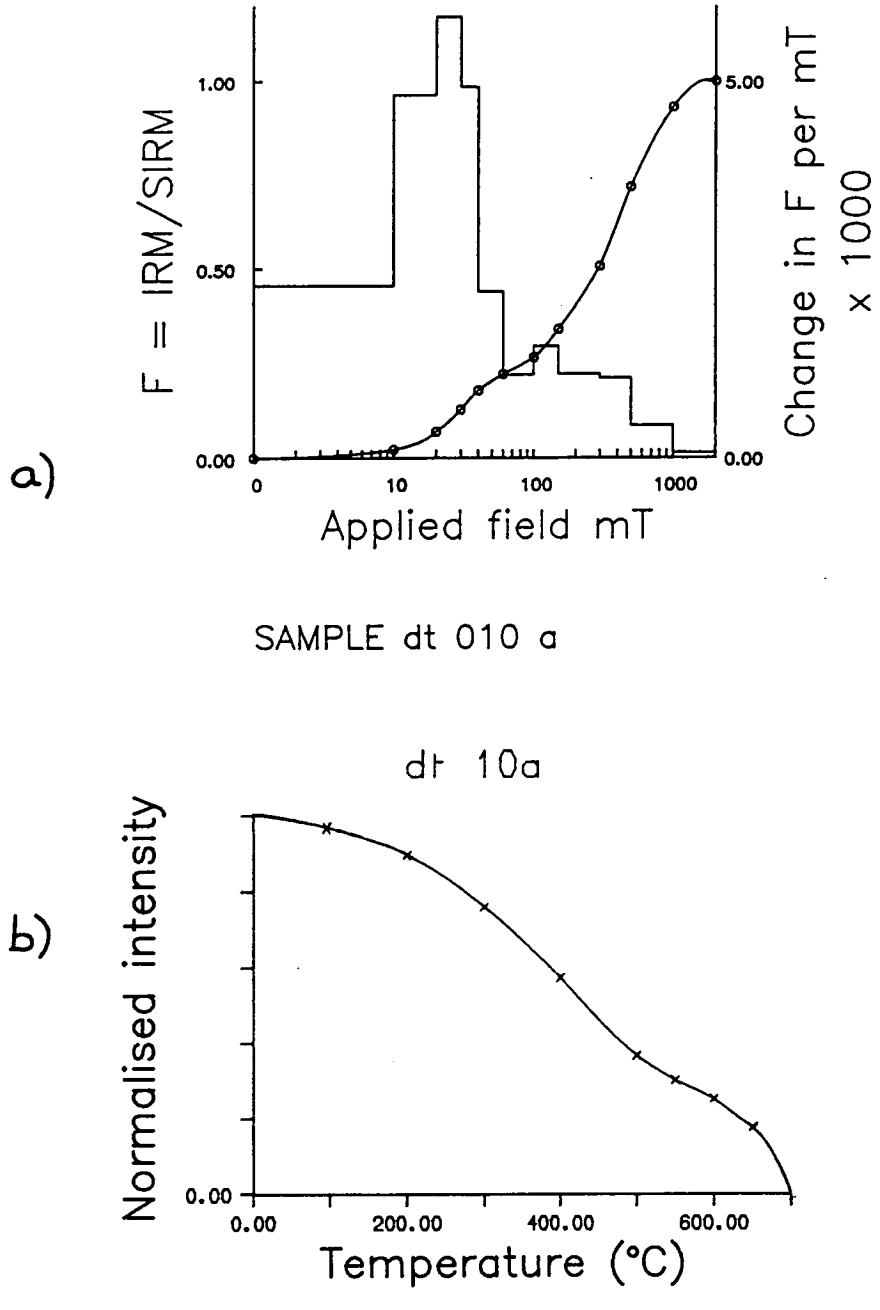

Figure 8.12. a. A representative IRM acquisition curve for the samples at site DT; b. Stepwise thermal demagnetisation of a 2.0 T IRM for sample DT 10 A. Note the progressive decrease in total moment up to a maximum temperature of 700°C indicating the presence of haematite.

therefore probably haematite, in the form of pigment. An inflexion in the thermal demagnetisation curve at approximately 500°C confirms the presence of magnetite. The application of the test of Johnson *et al.* (1975) shows that the magnetite fraction is dominated by single-domain-sized grains.

Stepwise AF and thermal demagnetisation experiments were carried out on four samples (2 AF, 2 thermal). A common northward-dipping viscous component was removed by fields of 15-20 mT and temperatures of 200°C, to leave single stable components of magnetisation. Both AF and thermal techniques identified the same stable directions, although AF treatment to 100 mT did not remove all the magnetisation. This suggests that the NRM is carried by a combination of the magnetite and pigmentary haematite, and that haematite formation occurred soon after the acquisition of a depositional remanence by the magnetite, possibly by the dehydration of a goethite precursor.

Since the AF method was found to be as effective as thermal treatment in recovering the presumed primary magnetisation, the remaining samples at the site were subjected to stepwise AF demagnetisation. Some typical results are shown in Figure 8.13a.

The final cleaned remanence directions for all samples are shown in Figure 8.13b. They form a tight cluster in the upper hemisphere of the southwest quadrant, in both geographic and stratigraphic coordinates. No fold test is possible at this site because of the near uniform dip of the sampled beds. However, the application of a standard tilt correction causes a very slight improvement in the within-site dispersion. This may support the assumption that the primary magnetisation at the site has been identified. This magnetisation must be of reversed polarity, to avoid unacceptably large overlaps with the inferred position of the African plate.

The mean declination in stratigraphic coordinates of 220° suggests that this site has experienced a clockwise rotation of 40° with respect to present north. The mean inclination of 18° is lower than that expected at the site from the African polar wander path of Westphal *et al.* (1986). This may be due to post-depositional compaction of the sediment.

h. The Plio-Quaternary sediments.

Pliocene to Quaternary sequences are only well exposed along the southern coast of the Argolis Peninsula. Only one exposure was found where these sediments were sufficiently fine-grained and indurated to allow samples to be collected (Site PQ; Figure 8.01). This was located in a small quarry off of the Ermioni to Porto Heli coastal road. Here, samples were drilled in several thin beds of calcite-cemented fine-grained

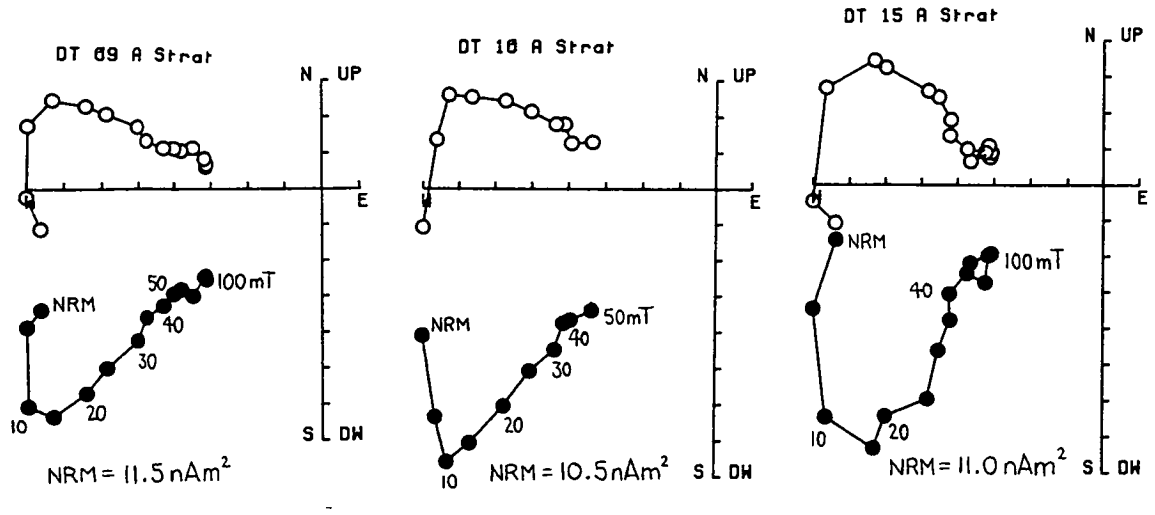

a.

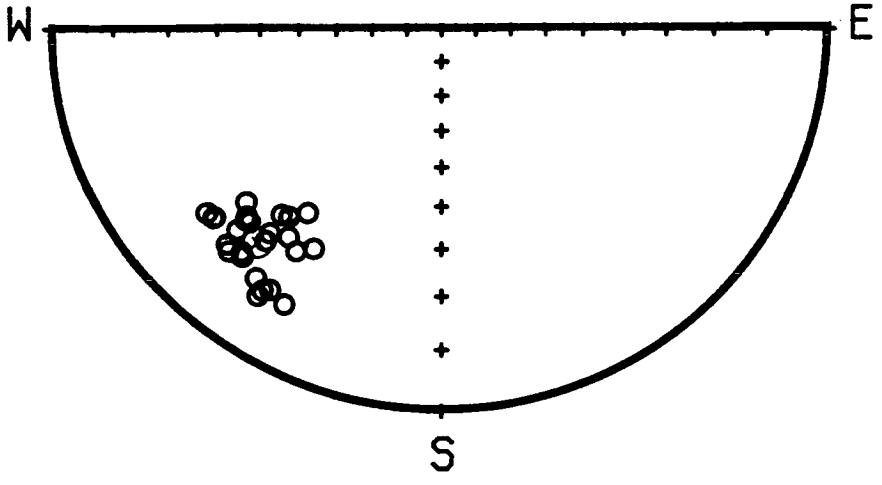

b.

Figure 8.13. a. Typical results of AF demagnetisation for samples from site DT.; b. The cleaned sample directions at site DT, located within the Upper Cretaceous-Palaeocene pink pelagic limestones of southern Argolis.

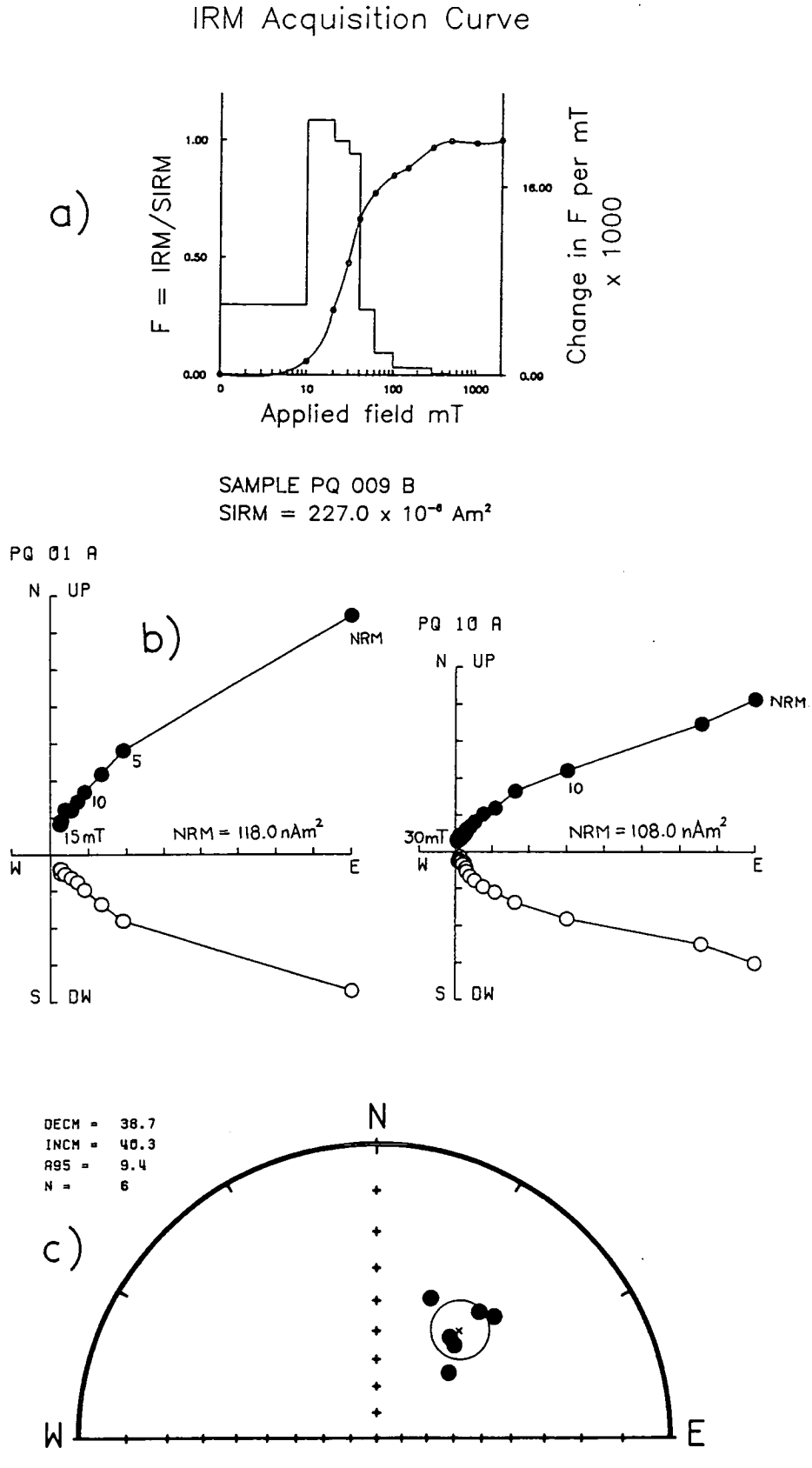

Figure 8.14. Results from the Plio-Quaternary sandstones of site PQ in southern Argolis: a. A typical IRM acquisition curve, indicating that magnetite is the only mineral capable of carrying a remanence in these samples; b. Representative AF demagnetisation curves; c. The cleaned sample directions at the site.

sandstones. In places these beds contain small well-rounded clasts of limestone and chert. These sediments represent the most recent phase of deposition in the peninsula, and are similar to the sediments being deposited off the coast at the present time.

Because of the soft nature of most of the exposure, only a limited number of samples were collected at this site. Furthermore, several samples disintegrated during subsample preparation in the laboratory. However, enough samples survived to give some interesting and important data.

A typical IRM acquisition curve for these samples is illustrated in Figure 8.14a. The rapid initial rise in isothermal moment and subsequent flattening off of the curve above 300 mT indicates that magnetite is the only mineral capable of carrying a remanence in these samples. This magnetite is of presumed detrital origin.

The NRM directions at this site show a tight grouping in the northeast quadrant (mean declination = 059°) with shallow positive inclinations (mean inclination = 21°). Alternating field demagnetisation was effective in removing all the magnetisation. No thermal demagnetisation was attempted because of the fragile nature of the samples. Figure 8.14b shows two representative Zijderveld demagnetisation diagrams. A soft component is removed by fields of less than 10 mT, to leave stable components of magnetisation. A final northward directed component with a higher coercivity is present in some samples, and may possibly represent a CRM associated with recent weathering.

The stable intermediate coercivity directions have a more northerly declination and a steeper inclination than the NRM directions. The site mean direction of these components is reported in Table 8.1 and shown in Figure 8.14c. This change in direction may indicate that the soft component removed during the initial stages of demagnetisation represents a small secondary magnetisation acquired during a reversed polarity period.

No fold test is possible at this site since the beds are currently horizontal. However, in view of the recent age of the sediments it seems unlikely that these sediments have been subjected to any major remagnetisation event, apart from recent weathering. The intermediate coercivity components are therefore interpreted as the primary depositional remanence.

The mean declination of the intermediate coercivity components of 039° indicates that this site has experienced a net clockwise rotation with respect to present north since the time of magnetisation. This declination is in close agreement with that obtained at site DT, located within the Palaeocene pelagic carbonates to the east. As discussed in Section 8.2.5a below, this *may* provide an important constraint on the age of the palaeorotation of the southern half of the Argolis Peninsula.

The mean inclination of 40° of the intermediate coercivity components (Table 8.1) corresponds to a palaeolatitude of 23°N. Taken at face value, this would imply that the site belongs to a block which has experienced a northward drift in excess of 1500 km over not more than the last 5 Ma. This is clearly unreasonable. Instead, the shallow inclination at this site may be attributed to an 'inclination error' produced during initial deposition of the sediments (King, 1955) and/or to a flattening of the inclination due to post-depositional compaction.

8.2.5 Rotations within the Argolis Peninsula.

The 'clock' diagrams of Figure 8.01 show the variations in the mean direction of magnetisation obtained at those sites in the peninsula where the remanence was unrelated to the present geomagnetic field direction. These diagrams show the 95% confidence limits associated with the mean declination and inclination at each site calculated using the method of Demarest (1983). Also included are the data previously obtained by Turnell (1988) from sites within the Middle Jurassic Ammonitico Rosso of the Pantokrator Unit (9 sites with the prefix AR).

A significant difference in the mean declination between sites located to the north and to the south of the Migdhalitsa Graben indicates that these areas have undergone different amounts of clockwise tectonic rotation. The data from the southern and northern 'units' are therefore discussed separately below.

a. Rotation of the southern Argolis Peninsula.

The mean declination of the intermediate coercivity components identified at site PQ, located in the Plio-Quaternary sediments exposed along the southern coast of the peninsula between Ermioni and Porto Heli (see Section 8.2.4h above), may indicate that this area has been rotated by 39° clockwise (with respect to present north) since the Pliocene (i.e during a period of no more than 5 Ma), providing that the interpretation of the intermediate coercivity components at the latter site is correct.

A further constraint on the rotational deformation in the area is provided by the data from site DT, located within the Upper Cretaceous to Palaeocene pelagic limestones exposed along the coast to the east. The agreement between the mean declination at this site (040°) and that found at site PQ (039°) suggests that no significant rotation occurred between the Palaeocene and the Pliocene (56.5-5.2 Ma).

Turnell (1988) reported data from two sites within the mid-Jurassic Ammonitico Rosso exposed in an area slightly to the north of site DT of the present study (sites AR8 and AR9 of Turnell, *op. cit.*; Figure 8.01). These results were excluded from the formation mean given by Turnell (*op. cit.*), because of the difference between the site

mean directions and those obtained from the rest of her sites to the north. However, the direction of magnetisation at both of these sites is statistically identical (using the comparison of means test of McElhinny, 1967) to that obtained at site DT in the present study. Thus the complete data set from the southern half of the Argolis Peninsula suggests that no significant rotation of the area occurred between the mid-Jurassic and the Pliocene, but that a clockwise rotation of *ca.* 40° then took place over at most the last 5 Ma. It must be stressed again however that this interpretation is based upon the limited dataset obtained at site PQ.

b. Rotation of the northern Argolis Peninsula.

To obtain the best estimate of the amount of rotation which has affected the sites located in the northern half of the peninsula, the data obtained here should be combined with that reported previously by Turnell (1988).

Turnell's seven sites and the Ammonitico Rosso sites from the Pantokrator Unit in the present study (BH and HQ) are dated as Toarcian to Middle Jurassic in age, by reference to the thorough palaeontological studies of Baumgartner (1985). Combining the data from these sites gives a formation mean of:

Dec = 075°, Inc = 33°, A_{95} = 13.7°, K = 15, N = 9 (Stratigraphic coordinates).

The remaining five northern sites analysed in the present study are from the Asklipion Limestone and the Adhami Limestone of the Asklipion Unit, dated as Anisian to Carnian (Middle to Late Triassic) in age (Vrielynck, 1978a, b). The overall mean direction of these sites (TQ, SE, LS, DH and AD) is:

Dec = 082°, Inc = 34°, A_{95} = 7.4°, K = 109, N = 5 (Stratigraphic coordinates).

The palaeolatitudes calculated from these mean directions of magnetisation are 18°N for the Jurassic sites, and 19°N for the Triassic sites. Figure 8.15 shows the palaeolatitudes expected at a site in the central Peloponnesos, calculated from the African and Eurasian polar wander paths of Westphal et al. (1986) (see Chapter 2, Section 2.2). The observed data agree well with the African path, which predicts similar palaeolatitudes during the Triassic and Jurassic. Both sets of data may therefore be combined to produce an overall mean direction of magnetisation for the northern Argolis unit of:

Dec = 077°, Inc = 33°, A_{95} = 8.7°, K = 22, N = 14 (Stratigraphic coordinates).

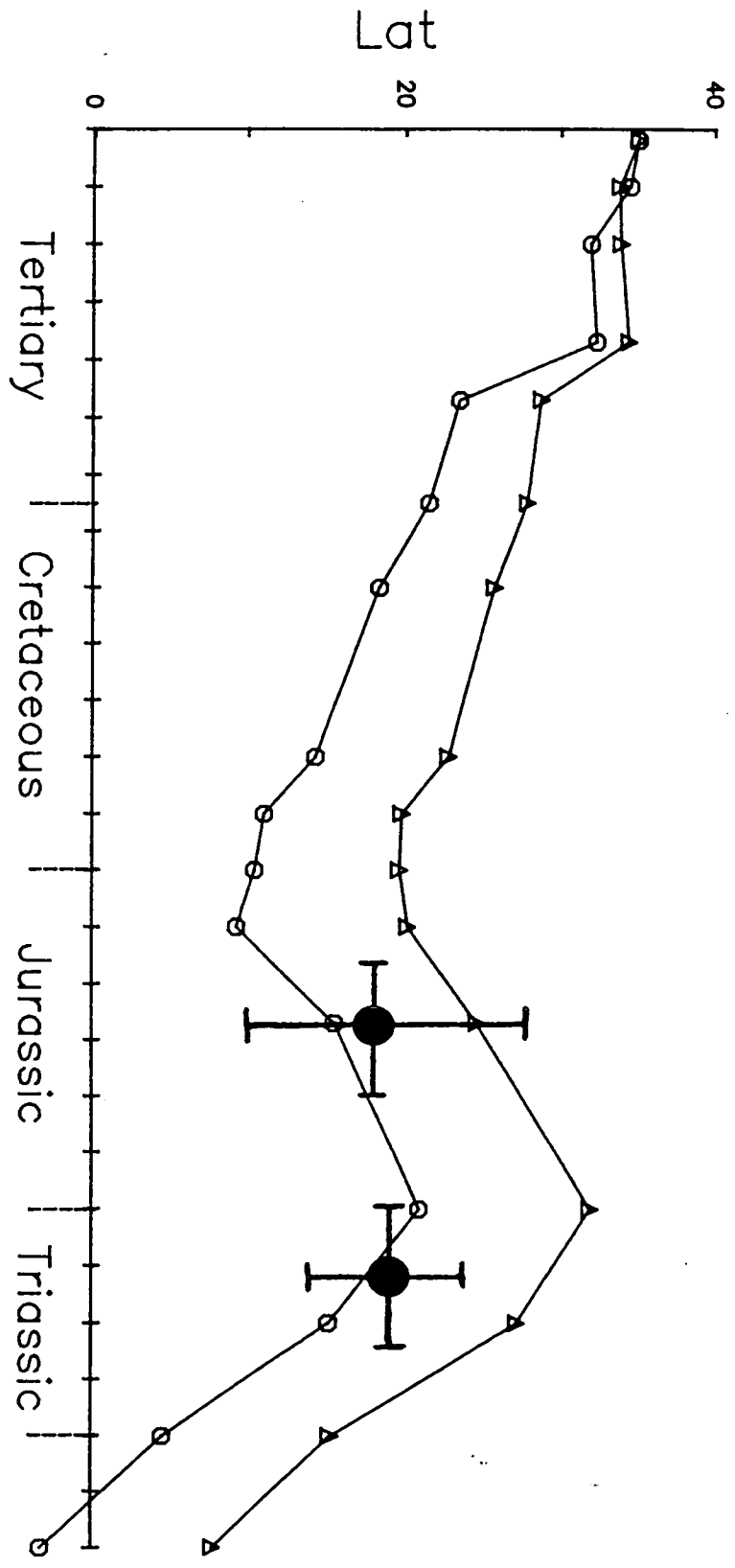

Figure 8.15. Reference palaeolatitude curves calculated from Westphal *et al.*'s (1986) Eurasian and African polar wander curves for a site in the central Peloponnesos (lat. = 37.5°N, long. = 22.5°E). Circles = African data, Triangles = Eurasian data. Superimposed are the palaeolatitudes calculated from the Triassic and Jurassic formation mean directions obtained from the Argolis dataset. Note the good agreement with the African data, and the similar palaeolatitudes predicted for the two time periods.

The data therefore indicate that the northern half of the Argolis Peninsula has experienced a clockwise rotation of 77° since the Middle Jurassic*. Furthermore, no rotation occurred between the Middle Triassic and the Middle Jurassic.

Since there is some evidence to suggest that the rotation of the southern half of the peninsula is Pliocene in age, I further suggest that a large part of the 77° rotation of the northern unit is also of Late Tertiary age.

8.2.6 Implications of the palaeomagnetic data for the geology of Argolis.

a. The Migdhalitsa Graben.

The most obvious tectonic feature within the Argolis Peninsula separating the northern sites, which have rotated by 77°, from those to the south, which have rotated by 40°, and which could have acted as a boundary between the two areas is the Migdhalitsa Graben.

Baumgartner (1985) proposed the existence of three Mesozoic or Early Tertiary strike-slip faults within the Argolis area. However, a recent re-examination of the main faults has led Clift (1990) and Clift and Robertson (1990) to contest Baumgartner's interpretation. They reinterpreted the northern-most fault of Baumgartner (1985) as a low-angle thrust plane, and found no evidence for his central fault. The southern-most fault identified by Baumgartner (*op. cit.*), which runs eastwards from Iria on the southwest coast of the peninsula (Figure 8.01), was confirmed as a high-angle fault by Clift (1990) and Clift and Robertson (1990). However, this structure has been reinterpreted by these workers as a Neotectonic fault forming the bounding fault to a major east-west, asymmetrical graben system, related to the north-south back-arc extension currently active in the Aegean region (McKenzie, 1978; Le Pichon and Angelier, 1979; Mercier *et al.*, 1979).

Figure 8.16 shows a detailed map of the Neotectonic faults of the complete graben system, compiled by Clift (1990) from a combination of field observations and satellite image analysis. The graben is approximately 8 km wide and can be traced along strike for 30 km. The main fault set has an east-west alignment, whereas a subsidiary north-south orientated set is observed in the east of the system. Slickenside striations exposed on all fault planes were found to indicate dip-slip motions, at least for the most recent movements. However, minor oblique slip displacements (in both sinistral and dextral shear senses) were found along the main, southern bounding fault of the graben and along associated faults. These were considered by Clift and Robertson (1990) as minor

* The data from site AC within the Akros Limestone Formation exposed at Argos Castle have been excluded from these calculations.

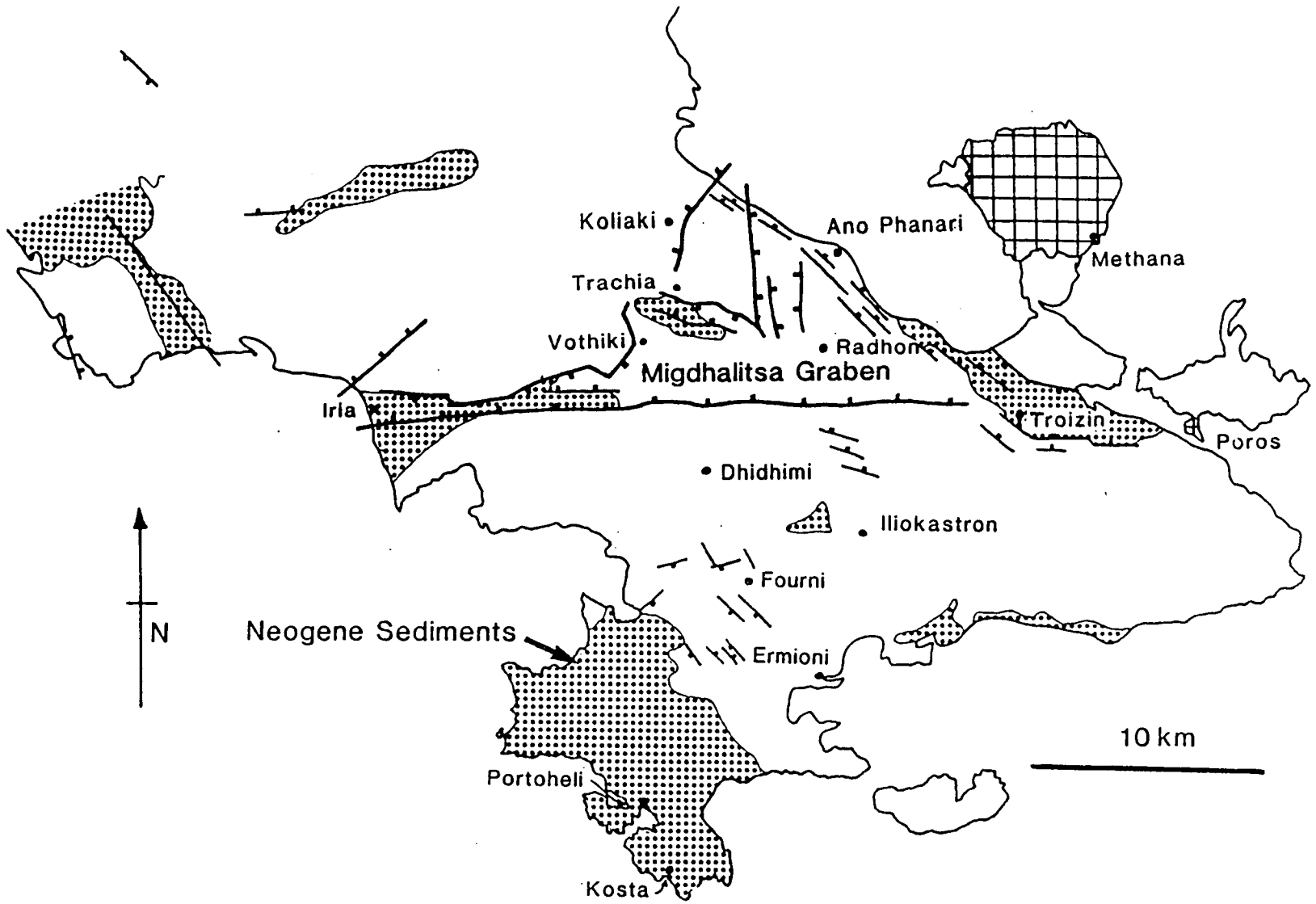

Figure 8.16. Simplified sketch map of the major Neotectonic faults of the Argolis Peninsula, compiled from satellite image and field observations by Clift (1990).

components which accommodate the transfer of extensional stress from the Migdhalitsa Graben to the next graben system to the north. They were not considered as indicative of motion along a true strike-slip fault zone.

The role of this graben system in the rotational deformation of the Peloponnesos is discussed in Section 8.4.2 below. In that discussion, I suggest that the graben may either have acted as the southern boundary of the zone of distributed shear proposed by McKenzie and Jackson (1983), or as a zone of decoupling between the southeastern part of the Peloponnesos and the area to the north. In both cases, the graben system must represent a major tectonic boundary. In this respect it is interesting to note that the graben may have already existed in the Upper Cretaceous (A. H. F. Robertson, pers. comm., 1990, suggesting that it represents a long-lived zone of crustal weakness.

b. The origin of the Asklipion Unit.

As discussed in Section 8.2.2, the deep-water redeposited carbonates of the Asklipion Unit (Adhami Limestone) have been interpreted as either the sedimentary infill of rift basins within the Pantokrator platform (Bannert and Bender, 1968; Bachmann and Risch, 1979; Figure 8.02a; Clift, 1990; Clift and Robertson, 1990; Figure 8.03), or as far-travelled thrust sheets which originated along the Vardar margin and were subsequently transported westwards during the Jurassic (Baumgartner, 1985; Figure 8.02b and c).

The palaeomagnetic data from within the sequences of the Asklipion Unit give an overall mean direction of magnetisation which is indistinguishable statistically from that obtained here and by Turnell (1988) from the Ammonitico Rosso of the Pantokrator Unit. If the Asklipion Unit did represent a completely allochthonous continental margin assemblage which was transported over the Pantokrator platform, we might expect to observe a significant difference between the direction of remanence within the two units. Therefore, the results obtained here appear to support the view of Clift and Robertson (1990), that the deep-water limestones of the Asklipion Unit were formed within intra-platformal rift basins, and are essentially *in situ*.

c. Emplacement direction of the Migdhalitsa Ophiolite Unit: Pindos vs. Vardar basin origin.

The identification of large clockwise rotations within the Argolis Peninsula (Pucher *et al.*, 1974; Turnell, 1988; this study), and the constraints on timing provided by the data here, have important implications for the sedimentological and structural data which have been used to determine the direction of emplacement of the Migdhalitsa Ophiolite Unit during the Jurassic 'Eohellenic' tectonic phase. In the present study, I have used the limited Plio-Quaternary dataset from site PQ to suggest that the

palaeorotation of the southern Argolis block is of Pliocene age, and have also suggested that the rotation of the northern unit is of Neotectonic age. Therefore, the effects of the later rotations must be removed from the geological data to recover the original Jurassic transport direction.

Baumgartner (1985) observed systematic lateral changes in the ophiolite-derived clastics (Potami and Dhimaina Formations) which overlie the cherts at the top of the Pantokrator Unit. He noted that the ophiolite detritus becomes finer-grained and thinner from east to west, implying that the ophiolite itself was emplaced from *east to west.*

A different direction of emplacement has been proposed by Clift (1990), who found evidence for southwestwards directed thrusting within duplexes of Adhami-type limestones in a small area to the north of Iliokastron. Also, a larger body of structural data gathered by Clift (*op. cit.*) from within the Migdhalitsa Graben, including early folds and small-scale duplexes in chert and pelagic limestone, together with folded radiolarites, indicated tectonic transport from *northeast to southwest.* This is in agreement with independent work carried out by S. K. Matthai (Tubingen, West Germany; P. D. Clift, pers. comm., 1990). The evidence presented by Baumgartner (1985) for eastward emplacement of the ophiolite has been contested by P. D. Clift and A. H. F. Robertson (pers. comm., 1990). They suggest that the thinning of ophiolitic debris observed by Baumgartner (1985) is the result of post-emplacement Cretaceous and Recent erosion, while the presence of coarse debris as far west as Argos Castle does not support a systematic decrease in grain-size from east to west.

In section 8.2.6a, I suggested that the Migdhalitsa Graben forms a boundary between the two blocks, which have experienced a relative rotation of 37°. The structural data of Clift (1990) from the duplexes of Adhami-type limestones were obtained from the area to the south of the graben. After removing the 40° rotation of the southern unit, this data indicates emplacement from the present north.

The close agreement between the transport directions obtained by Clift (1990) from the Migdhalitsa Graben and from the Iliokastron area suggests that the units examined by Clift within the graben have been rotated as part of the southern Argolis block. However, as this area falls on the proposed boundary between the northern and southern blocks, the possibility that it has been rotated with the northern unit (or has experienced more complex local rotations) cannot be excluded. If this were so, the removal of the effects of a 77° clockwise rotation from the structural data would indicate tectonic transport from the present northwest.

Do the combined structural and palaeomagnetic data enable us to decide whether the Migdhalitsa Ophiolite originated in the Vardar or Pindos strands of the southern

Greek Neotethys? The palaeomagnetic data obtained previously by Kissel and Laj (1988) indicate that the Hellenic Arc was originally more rectilinear in shape and has acquired its present curvature by tectonic rotations in opposite senses at each end of the arc. This is consistent with the model of Le Pichon and Angelier (1979), and suggests that the isopic zones of Greece initially had a northwest-southeast trend. The inferred Vardar basin would then have been located to the northeast of the Pelagonian micro-continental sliver, with the Pindos basin to the southwest. The north to south emplacement direction implied by the structural data obtained by Clift (1990) from the southern Argolis block (after removing the effects of the Pliocene rotation), suggests that the ophiolite was rooted in the Vardar basin. However, the larger body of data obtained by Clift (1990) from the Migdhalitsa Graben may suggest that ophiolite emplacement was directed along the strike of the Pelagonian microcontinental sliver (i.e. with a strike-slip mode of emplacement), in which case it may have originated in either basin. Thus the database at present is insufficient to enable a definite choice to be made between root-zone models.

It is worth noting, however, that there is growing evidence from other Jurassic ophiolites, exposed in northwestern and central Greece, for eastwards or northeastwards emplacement onto the Pelagonian microcontinent (see Chapter 2, Section 2.4.4). After taking the overall clockwise sense of rotation identified by palaeomagnetic studies in Greece (e.g. Kissel and Laj, 1988), these emplacement directions become more towards the north, confirming that they were derived from the Pindos Basin. Since it seems unlikely that ophiolites were emplaced onto the Pelagonian microplate from different directions from both the Pindos and Vardar basins at the same time, I prefer a model in which the Migdhalitsa Ophiolite Unit originated in the Pindos ocean. The unusual transport direction of this unit with respect to the strike of the continental margin may be due to complications arising from the anomalous position of the Argolis area, at the southern tip of the Pelagonian Zone, which must have been in close proximity to a triple junction.

8.3 The Gavrovo-Tripolitza and Ionian Zones.

Before attempting to interpret the data from Argolis in terms of possible rotation mechanisms and the regional tectonic setting, it is first necessary to examine the preliminary data found from the other sites located in the autochthons of the Peloponnesos. The database compiled to date can then be combined with other previously published palaeomagnetic data to attempt to obtain an overall view of the pattern of rotational deformation affecting Greece.

Table 8.2. Palaeomagnetic results from the Peloponnesos.

Site	Age	N	Geographic				Stratigraphic			
			Dec	Inc	α_{95}	K	Dec	Inc	α_{95}	K
Rift-related tuffs.										
SJ	Triassic (Present field direction)	11	359	51	2.3	413	027	32	2.3	413
Platform carbonate units of Gavrovo-Tripolis Zone.										
OM	U. Cretaceous (Present field direction)	10	004	58	11.0	16	-	-	-	-
EL	U. Cretaceous (Present field direction)	15	356	66	12.1	11	-	-	-	-
LA	Palaeocene	7	257	-07	12.3	25	251	-22	12.3	25
GH	U. Triassic	9	026	53	10.1	21	029	46	10.1	21
WD	Jurassic	10	040	42	9.3	23	044	42	9.3	23
Deep-water limestones of Ionian Zone.										
DS	U. Cretaceous	7	214	-54	4.7	166	240	-42	5.2	136
RT	U. Cretaceous	5	216	-54	11.7	44	254	-35	11.7	44
Pindos and Ionian flysch.										
CN	Mid-U. Eocene (Present field direction)	14	004	58	4.8	69	-	-	-	-
TM	U. Oligocene (Present field direction)	21	355	59	5.8	31	-	-	-	-

N = number of samples; α_{95} = semi-angle of 95% cone of confidence; K = Fisher precision parameter

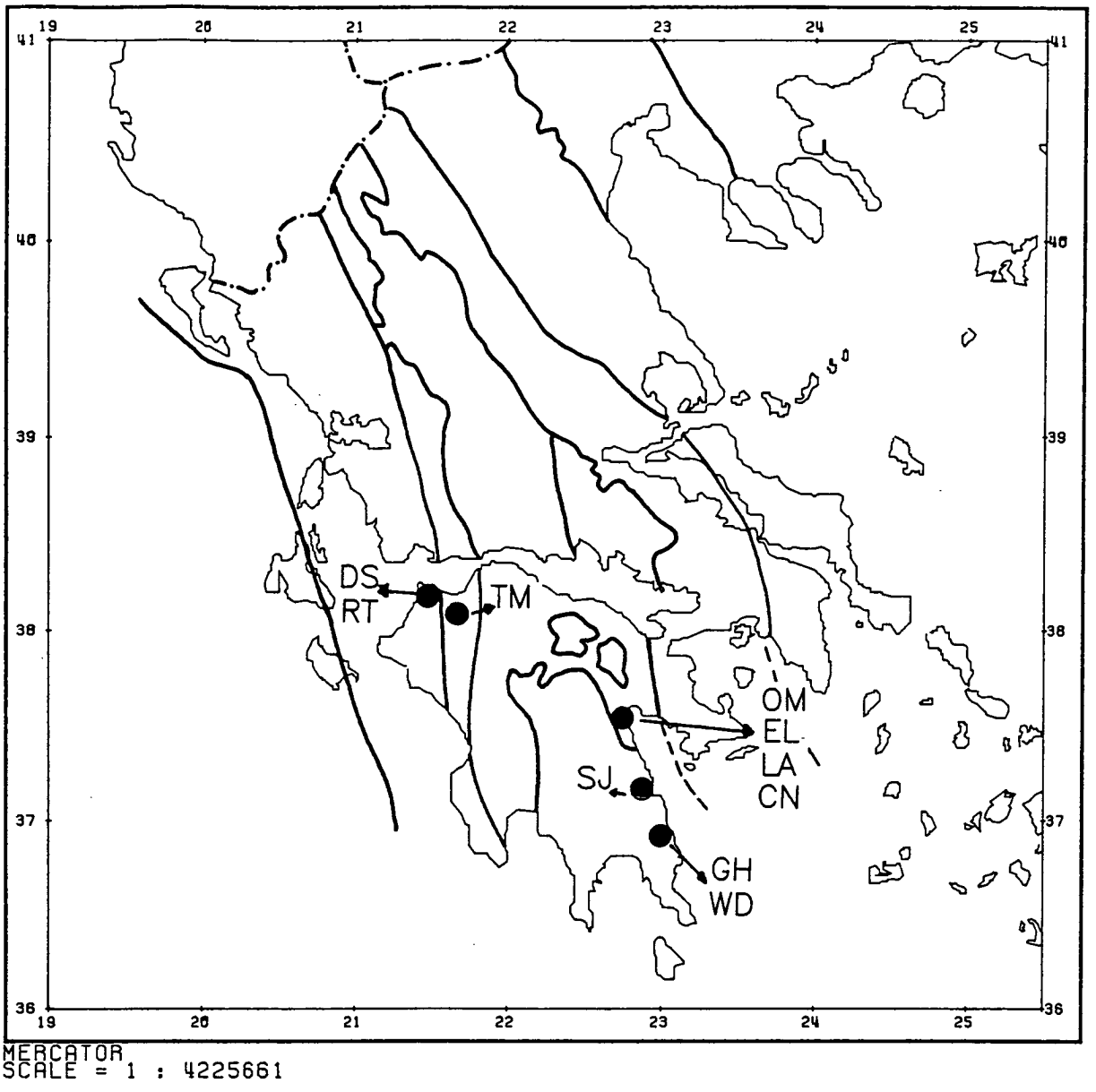

Figure 8.17. The location of the sites in the Peloponnesos described in the text, in relation to the isopic zones of the Hellenides. The location of the sites which are awaiting measurement are not shown.

As mentioned in the introduction to this chapter, many of the sites collected within the sequences of the Gavrovo-Tripolitza and Ionian Zones have not been analysed at present. This back-log is due to a break-down of the CCL magnetometer for over six months, due to a faulty SQUID and a helium leak. It is my intention to measure the samples from these sites at a later date.

The data presented here come from eight sites within Triassic tuffs, Upper Triassic and Jurassic platform limestones, Palaeocene hemipelagic limestones, and Tertiary flysch of the Gavrovo-Tripolitza Zone, exposed along the eastern side of the Peloponnesos, and from two sites within Upper Cretaceous pelagic limestones of the Ionian Zone, exposed at the northwestern corner of the Peloponnesos. Magnetisations with directions unrelated to the present geomagnetic field direction were obtained at five of these ten sites. The results from all ten sites are reported in Table 8.2, and the locations of the sites with respect to the isopic zones are shown in Figure 8.17. Other sites, awaiting examination, are not shown.

8.3.1 The Lower-Middle Triassic rift-related tuffs.

This unit was sampled along the eastern coast of the Peloponnesos (site SJ; Figure 8.17). The site was located within water-lain andesitic tuffs which exhibit graded bedding. The sampled lithology was similar to that described earlier from the Argolis Peninsula (see Section 8.2.4a).

The NRM directions from this site form a tight cluster around the present geomagnetic field direction (Table 8.2), indicating that the remanence is dominated by viscous components acquired during the last few hundred thousand years (Tarling, 1983). AF demagnetisation was unable to recover primary magnetisations at this site. The ease with which AF treatment removed the magnetisation suggests that the viscous overprint is carried by magnetite. No further work was carried out on this site.

8.3.2 The carbonate units of the Gavrovo-Tripolitza and Ionian Zones.

a. The Upper Triassic to Jurassic sequences of the Gavrovo-Tripolitza platform of the southeastern Peloponnesos.

A total of 14 sites have been collected in the complete Triassic to Cretaceous sections of the Gavrovo-Tripolitza platform exposed in the southeastern part of the Peloponnesos. Four of these sites have been analysed at the time of writing, of which two have given reliable results (sites GH and WD; Figure 8.17; Table 8.2).

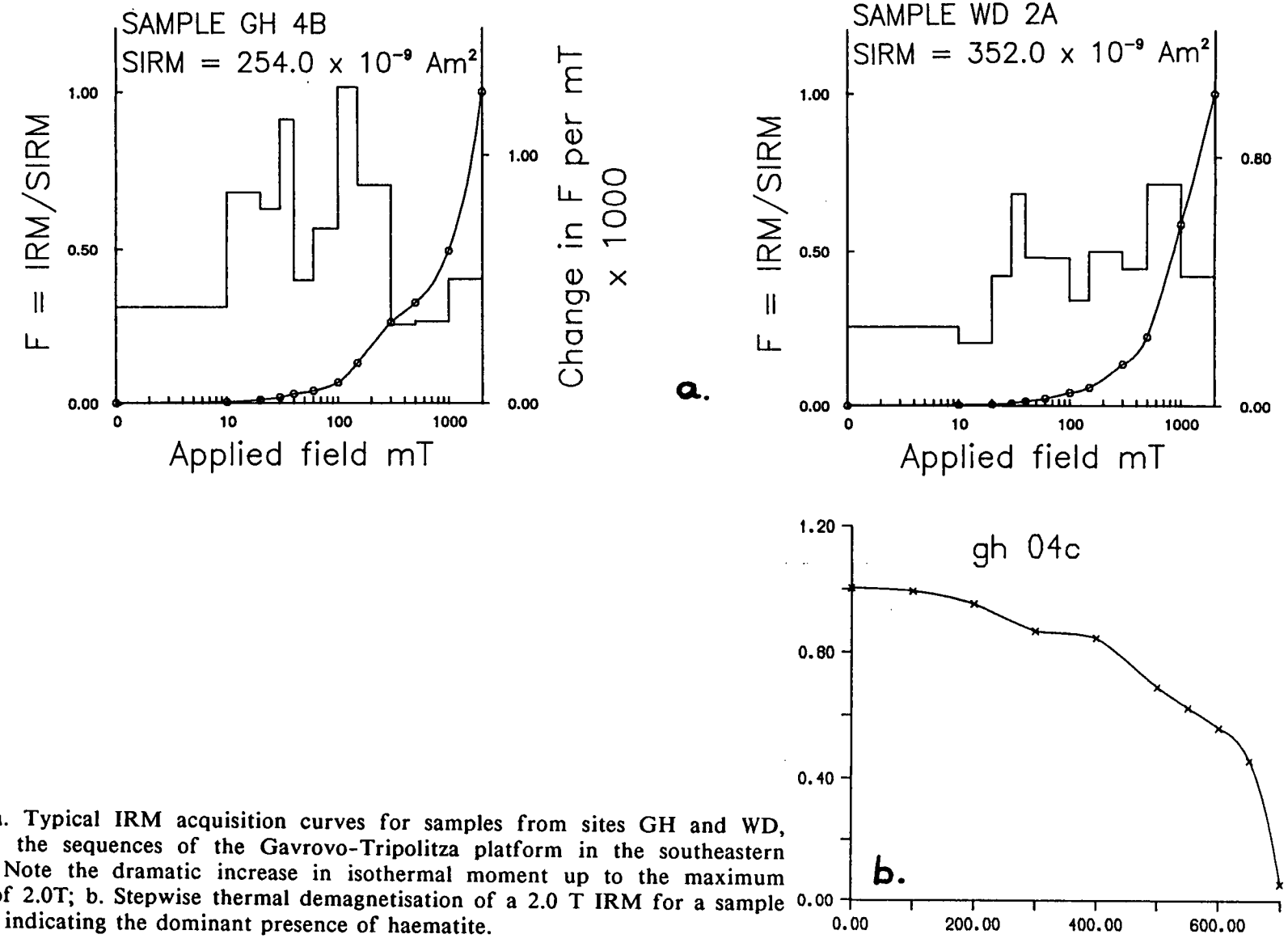

Figure 8.18. a. Typical IRM acquisition curves for samples from sites GH and WD, located within the sequences of the Gavrovo-Tripolitza platform in the southeastern Peloponnesos. Note the dramatic increase in isothermal moment up to the maximum applied field of 2.0T; b. Stepwise thermal demagnetisation of a 2.0 T IRM for a sample from site GH, indicating the dominant presence of haematite.

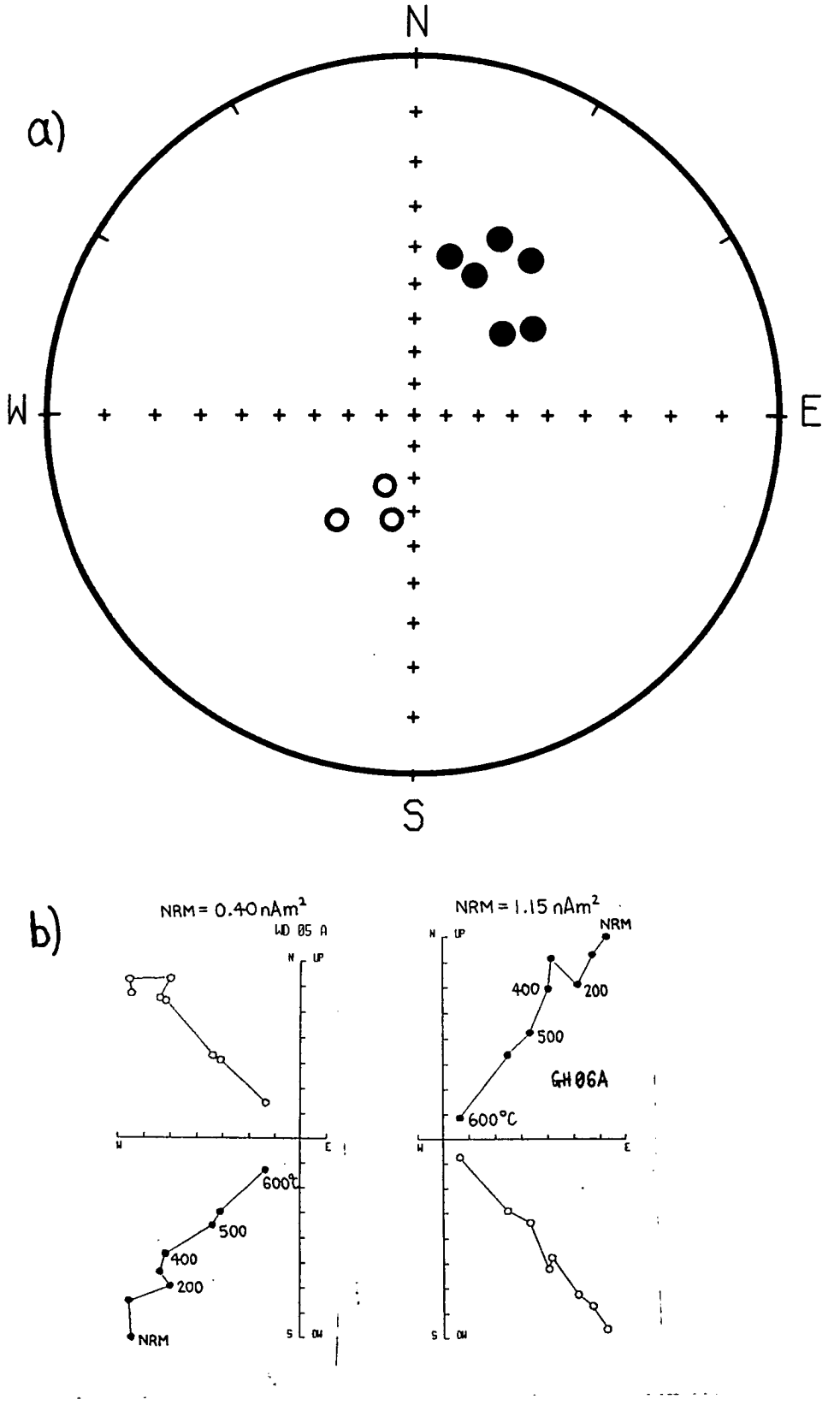

Figure 8.19. a) The distribution of cleaned remanence directions at site GH. Note the opposing normal and reversed polarity groups; b) Typical examples of thermal demagnetisation at sites WD and GH.

Site GH is located in muddy, bitumenous limestones of the Upper Triassic part of the sequence, whereas site WD is within micritic limestones of the Jurassic section (but is not dated any more accurately). The magnetic characteristics of both sets of samples are very similar.

At both sites the NRM directions fall into two distinct antiparallel normal and reversed polarity groups. The NRM is very resistant to AF demagnetisation, and IRM acquisition experiments indicate the presence of magnetite plus a very significant amount of a high coercivity mineral (Figure 8.18a). Stepwise thermal demagnetisation of a 2.0 T IRM reveals maximum unblocking temperatures of between 650°C and 700°C, indicative of haematite (Figure 8.18b). The origin of the haematite in these carbonates is difficult to determine. There is no notable red colouration in the samples. This suggests that the haematite does not exist in the form of pigment. Also, since detrital haematite or specularite seems to be of negligible importance in limestones generally (Lowrie and Heller, 1982), it seems likely that the haematite present in these samples formed diagenetically from a goethite precursor. The identification of both normal and reversed polarities at the sites indicates that haematite formation spanned at least one reversal period of the geomagnetic field.

Thermal demagnetisation was found to be effective in reducing the natural remanent intensities down to the noise level of the cryogenic magnetometer. Demagnetisation resulted in an improvement in the clustering of the normal and reversed polarity groups. The distribution of cleaned remanence vectors at site GH is shown in Figure 8.19.

The site mean declinations at these sites (Table 8.2) indicate that the sampled sections have experienced a 29°-44° clockwise rotation since the acquisition of remanence by the haematite. In Section 8.4.2 below, I suggest that this rotation is of recent Neotectonic origin.

b. The Upper Cretaceous sequences of the Gavrovo-Tripolitza platform of the northeastern Peloponnesos.

Two sites have been analysed within this part of the platform sequence at the time of writing (sites EL and OM; Figure 8.17). These sites occur in small tectonic windows through the overlying Pindos thrust sheets (see Chapter 9, Section 9.2), and consist of medium to thickly bedded, dark grey bitumenous limestones.

At both sites, the NRM directions coincide with the present geomagnetic field direction (Table 8.2), indicating that, again, the remanence is dominated by recent viscous components. Stepwise thermal demagnetisation of several samples from site EL did not succeed in recovering primary remanences. At site OM, thermal demagnetisation

reveals a dramatic decrease in NRM intensity below 100°C, due to the presence of goethite. This is confirmed by the stepwise thermal demagnetisation of a 2.0 T IRM, which further indicates the presence of magnetite with a blocking temperature close to the Curie point (580°C).

The lack of a primary remanent magnetisation at these sites make the results geologically unimportant, and may indicate that these dark grey limestones of Upper Cretaceous age are not suitable for palaeomagnetic analysis.

c. The Palaeocene of the Gavrovo-Tripolitza platform of the northeastern Peloponnesos.

The topmost Palaeocene section of the Gavrovo-Tripolitza platform is exposed in a small tectonic window through the overlying pelagic limestones of the Pindos nappes, at a locality along the main Argos-Tripolis road. Site LA is located within the thin-bedded hemipelagic limestones of this unit (Figure 8.17). These limestones pass upwards into Eocene flysch lying beneath the Pindos thrust sheets.

The NRM directions at site LA have westerly declinations and positive inclinations. IRM acquisition curves for this lithology characteristically show a rapid initial rise in isothermal moment up to 300 mT and a subsequent flattening off. This indicates that magnetite is the only mineral capable of carrying a remanence in these rocks. This conclusion is supported by the ease with which AF demagnetisation reduced the NRM intensities to zero. No thermal demagnetisation was carried out at this site.

A common north-dipping secondary component, attributed to viscous magnetisation in the present field direction, was removed by fields of 25 mT. Thereafter, only single stable components were observed.

The cleaned sample directions at this site are shown in the stereonet of Figure 8.20. Upon demagnetisation, the site mean direction migrates into the upper hemisphere (in both stratigraphic and geographic coordinates). No fold test is possible at this site because of the uniform dip of the sampled beds. However, the site mean inclination in geographic coordinates (-7°; Table 8.2) would place this unit too far to the south during the Palaeocene, and would cause unacceptable overlaps with the inferred position of the African plate at that time (see Figure 2.06g). This is not the case with the tilt corrected inclination, as long as the magnetisation is considered to be of reversed polarity. I therefore assume that the magnetisation identified at this site represents the primary depositional remanence.

The site mean declination (in stratigraphic coordinates) of 251° indicates that this unit has experienced a clockwise rotation of 71°, with respect to present north.

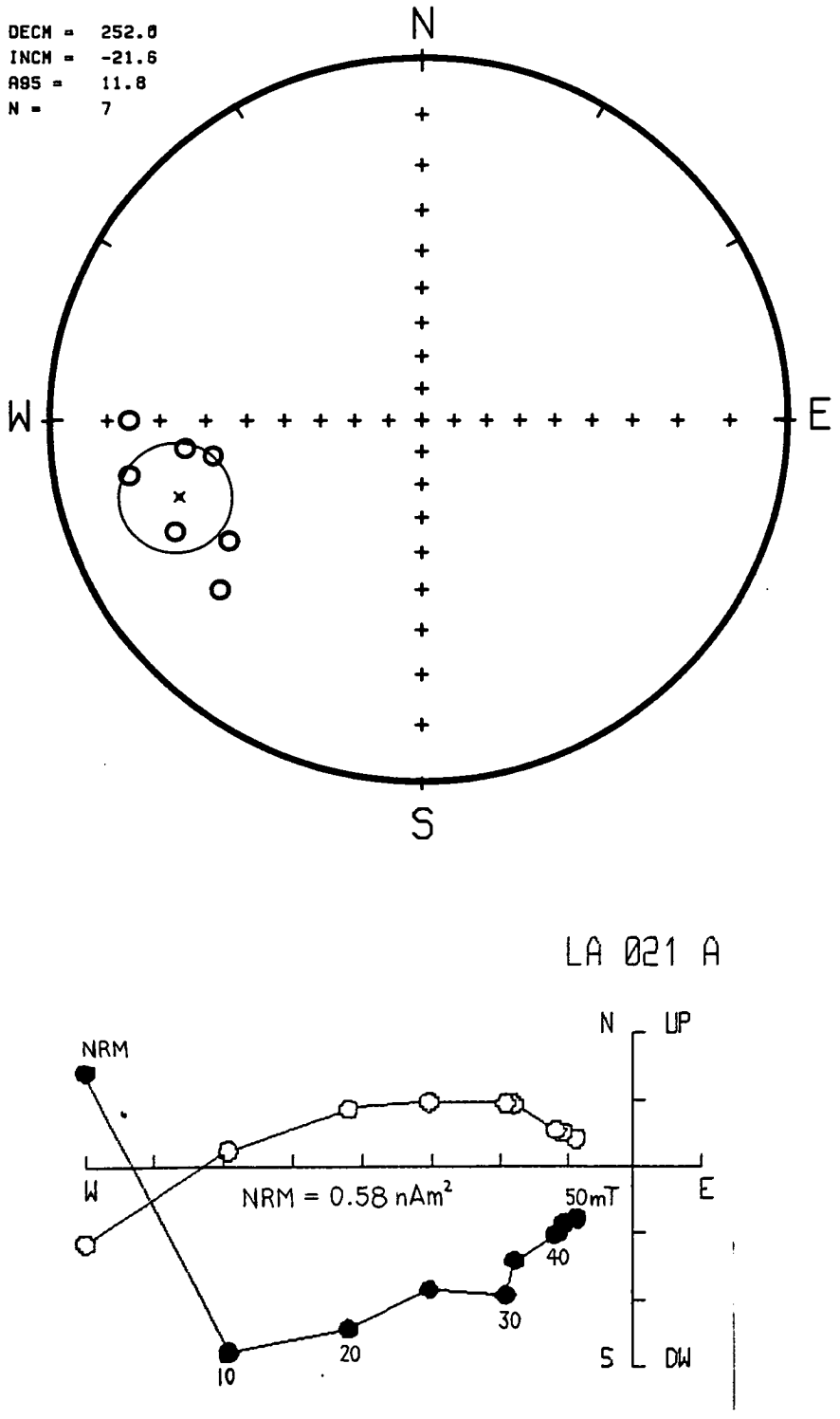

Figure 8.20. The cleaned sample directions at site LA, located within the Palaeocene part of the Gavrovo-Tripolitza platform, together with a typical example of AF demagnetisation.

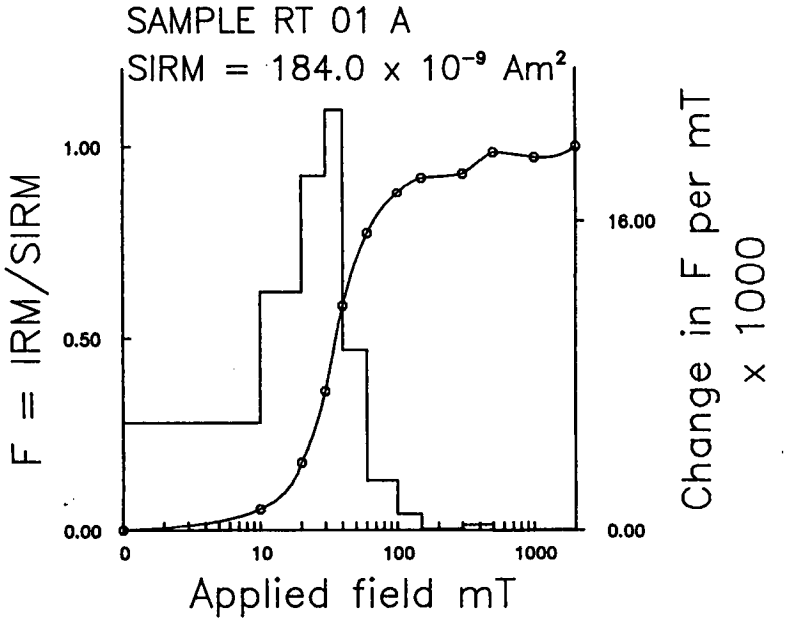

a.

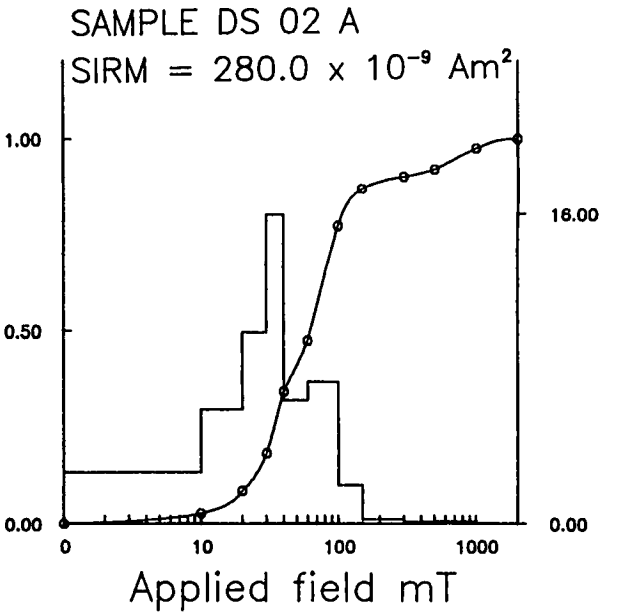

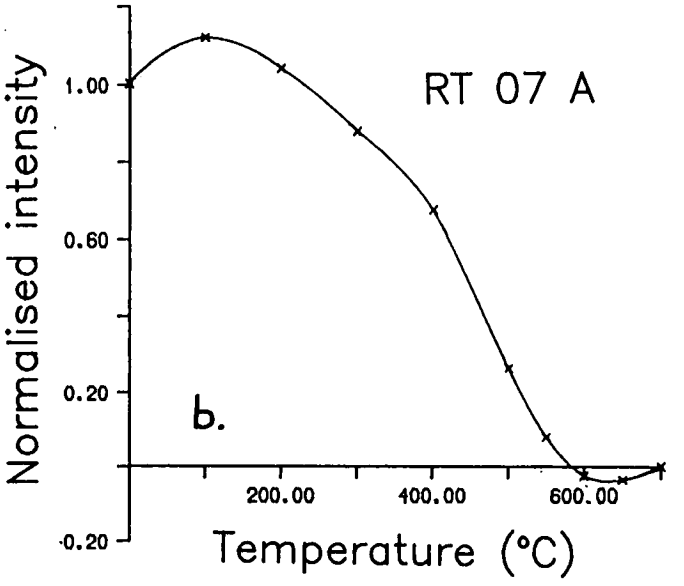

Figure 8.21. a. Typical IRM acquisition curves for the Upper Cretaceous pelagic limestones of the Ionian Zone sampled at sites DS and RT; b. The stepwise thermal demagnetisation of a composite IRM (see Figure 6.04) indicates that the high coercivity mineral identified by the IRM acquisition analysis is haematite.

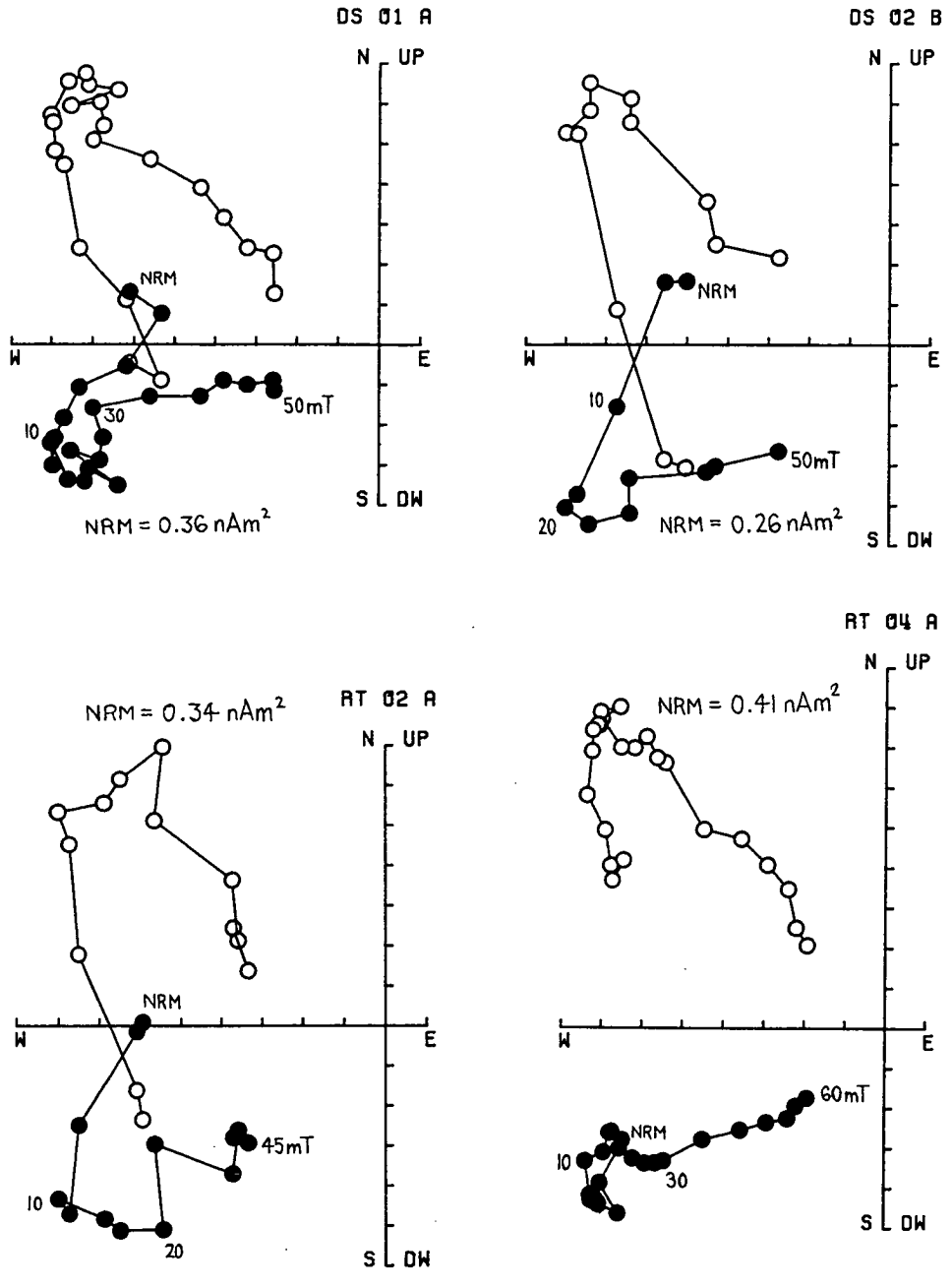

Figure 8.22. Representative AF demagnetisation plots for samples from sites DS and RT, located within the Upper Cretaceous pelagic limestones of the Ionian Zone.

d. The Upper Cretaceous pelagic limestones of the Ionian Zone.

The carbonates of the Ionian Zone have been sampled at six sites in three areas of the western Peloponnesos. Of these, two sites located within Upper Cretaceous pelagic limestones exposed along a peninsula to the west of Patras have yielded reliable results at the time of writing (sites DS and RT; Figure 8.17; Table 8.2).

The lithology sampled at these sites is a fine-grained, buff coloured, micritic pelagic limestone, very similar to the limestones of the Pindos nappes exposed to the east (see Chapter 9).

The magnetic characteristics of the two sites are identical. IRM acquisition curves for these samples show an initial rapid rise in isothermal moment up to 100 mT, indicating the presence of magnetite. A subsequent very gradual rise up to the maximum applied field of 2.0 T suggests the presence of a small quantity of a mineral with a higher coercivity (Figure 8.21a). Stepwise thermal demagnetisation of a composite IRM (see Chapter 6, Section 6.3.1) indicates that this second mineral is haematite (Figure 8.21b). However, AF demagnetisation was found to effectively remove all of the magnetisation in these samples. This suggests that the haematite fraction does not contribute significantly to the natural remanence.

A northward-directed secondary component of magnetisation, attributed to viscous magnetisation in the present geomagnetic field, was removed by AF demagnetising fields of less than 20 mT. AF treatment revealed single, stable components of magnetisation thereafter (Figure 8.22).

The cleaned sample directions at the two sites are in close agreement. No fold test is possible either within or between the sites because of the uniform dip of the bedding. The magnetisation is assumed to be of primary, depositional origin, and again, must be of reversed polarity to avoid unacceptable overlaps with the inferred position of the African plate in the Upper Cretaceous.

The mean declinations (in stratigraphic coordinates) at these sites (see Table 8.2) indicate that the pelagic limestones of the Ionian Zone exposed west of Patras have been subjected to a clockwise rotation of 60° to 74°.

8.3.3 The Tertiary flysch.

Two sites have been analysed within the Tertiary flysch overlying the topmost sequences of the Gavrovo-Tripolitza platform (sites CN and TM; Figure 8.17; Table 8.2).

Site CN is located in fine-grained sandstones of the Eocene flysch which separates the platform from the overlying thrust sheets of the Pindos Zone, in the region to the northwest of Argos. Site TM on the other hand is within flysch of Upper Oligocene age

located in the western Peloponnesos, adjacent to a prominent ridge of Upper Cretaceous hemipelagic limestones. Several sites from this latter unit await measurement. The flysch at site TM consists of fine-grained, calcite-cemented turbiditic sandstones.

As in the case of the Triassic tuffs, the NRM directions at both sites coincide with the present geomagnetic field direction. This indicates that the remanences are dominated by recent viscous components of magnetisation. Kissel *et al.* (1985) have reported very reliable palaeomagnetic data from sites located in the Ionian flysch of northwestern Greece. The flysch sampled by this group consisted of blue-grey marls, whereas the lithology sampled here was brown in colour. This suggests that the lack of primary magnetisations at sites CN and TM may be due to the destruction of primary titanomagnetite phases by subaerial weathering and oxidation.

8.4 Discussion of rotations within the Peloponnesos.

8.4.1 Preliminary pattern of rotation within the Peloponnesos.

The data described above demonstrate that clockwise rotations of a magnitude approaching that of the northern half of the Argolis Peninsula (77°) appear to have affected the Ionian sequences of the western Peloponnesos (60-74°), and the platform underlying the Pindos nappes in the Argos-Astros area (71°). This suggests that the large rotation of the Argolis unit does not represent an anomalous rotation of a small fault-bounded block, but rather we must account for a *ca.* 70° rotation of at least the northern half of the Peloponnesos, and possibly an even larger area (see next section). However, we must also bear in mind the possibility that this rotation is not uniform throughout the area and that we may have just sampled parts of the autochthon with similar declinations by chance.

The clockwise rotation of between 29° and 44° implied by the data at sites GH and WD, located in the platform sequences of the southeastern Peloponnesos, is comparable to the rotation which has affected the southern unit in Argolis (40°). The implications of this are discussed in the next section.

There appears then to be a significant difference between the amount of clockwise rotation observed in the northern and southern parts of the Peloponnesos. It must be stressed that, with the exception of the data from Argolis, these results are of a very preliminary nature. However, we may still attempt to explain the observed pattern of rotation by considering the data in conjunction with that previously obtained in Greece, most notably by the French group headed by Catherine Kissel and Carlo Laj.

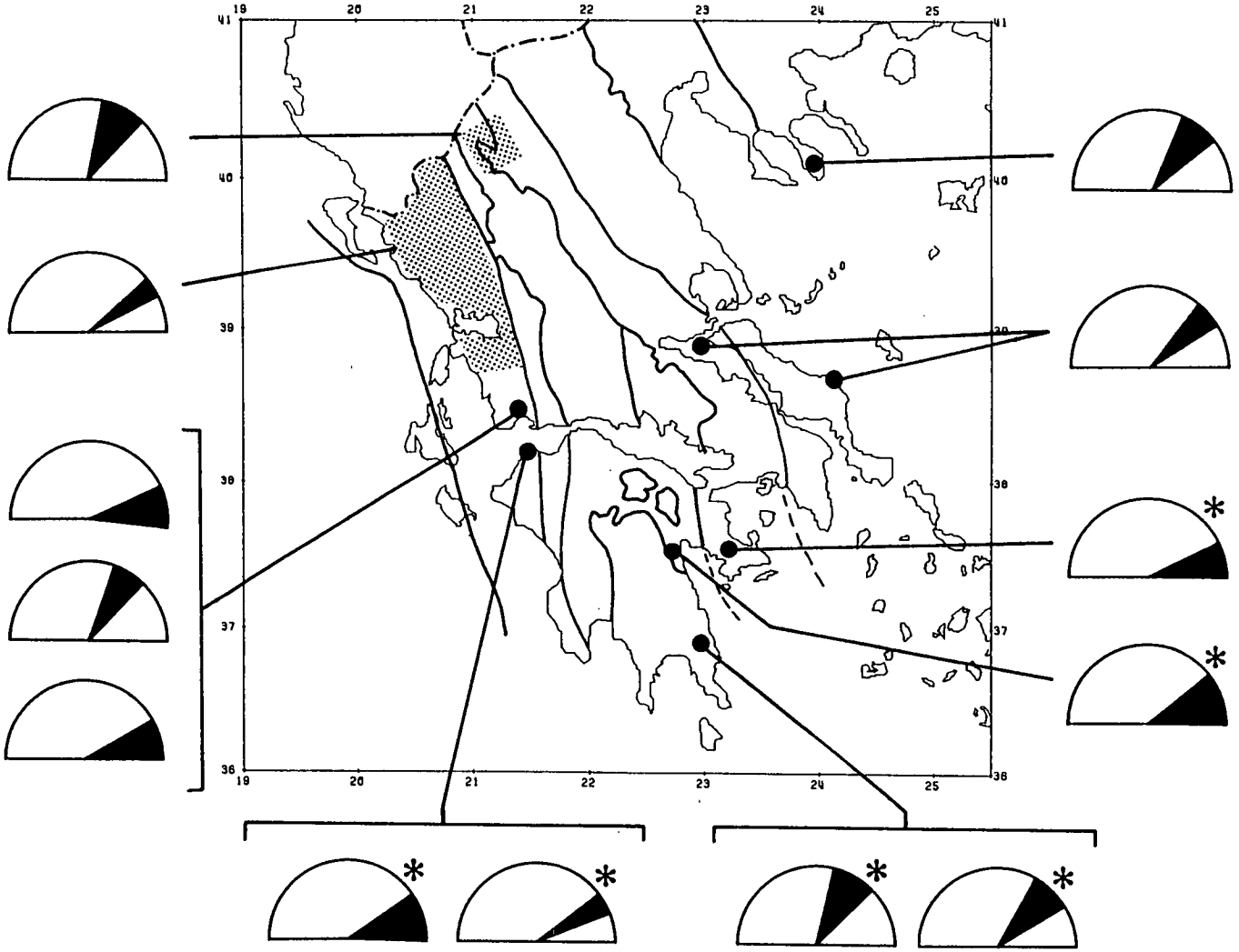

Figure 8.23. The combined database for Greece showing the variations in mean declination at all pre-Middle Miocene sites.

Data obtained in the present study are marked with an asterisk. The remaining data are from Kissel and Laj (1988, and references therein), Horner and Freeman (1983) and Kondopoulou and Westphal (1986). The data from the northern Argolis Peninsula have been combined to form one mean direction. Also, the result from the Ionian Zone represents an average of 27 sites. Note the large ca. 70° clockwise rotations on either side of the Gulfs of Patras and Argolikos.

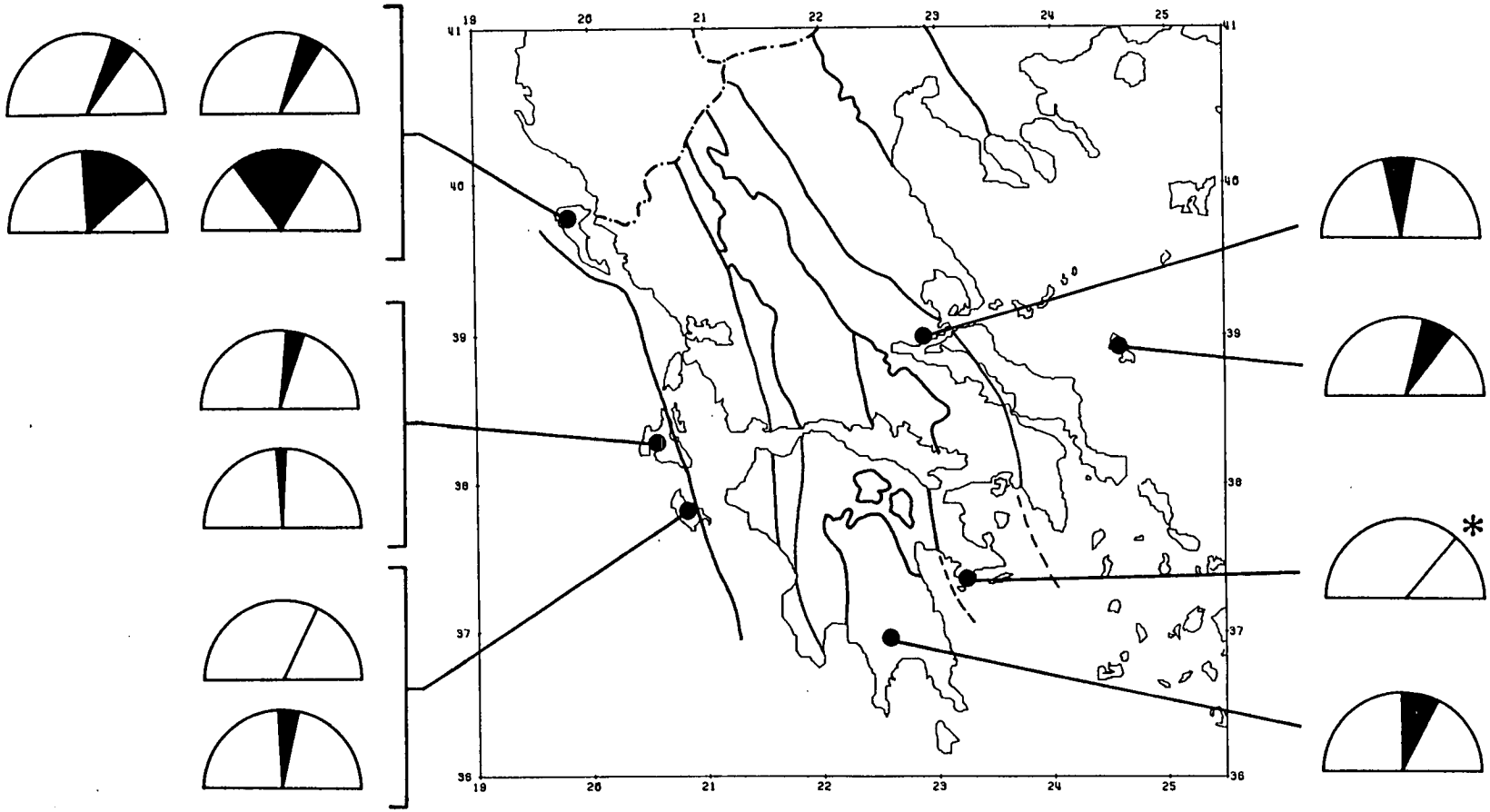

Figure 8.24. The combined database for Greece showing the variations in mean declination at all Middle Miocene or younger sites.

Data obtained in the present study are marked with an asterisk. The remaining data are from Kissel and Laj (1988, and references therein). Variations in declination within the Ionian Zone have been attributed to a progressive rotation beginning in the Lower Pliocene and still active today; the oldest rocks shown the greatest rotation. There is no clear distinction between the declinations observed in the Ionian Zone and those seen further eastwards. Note that a rotation of the same magnitude as that identified by Kissel and Laj (1988) in the Ionian Islands has affected the Chalkidiki Peninsula of northern Greece since the Pliocene (Westphal et al., 1990). This rotation is not shown here.

8.4.2 Comparison with previously reported palaeomagnetic data.

In the previous chapter, I presented a brief review of a model for the geodynamic evolution of the Aegean arc developed by Kissel and Laj (1988) on the basis of palaeomagnetic data obtained by them and other workers in the Greek area over the last decade (Laj *et al.*, 1982; Kissel and Poisson, 1986, 1987; Kissel *et al.*, 1984; Kissel *et al.*, 1985; Kissel *et al.*, 1986a.; Kissel *et al.*, 1986b; Kissel *et al.*, 1986c; Horner and Freeman, 1983; Kondopoulou and Westphal, 1986). These data are illustrated in the 'clock' diagrams of Figures 8.23 and 8.24, along with the data found in the present study. For simplification only the overall mean direction of magnetisation for the 15 sites located in the northern half of the Argolis Peninsula is shown (average of the 8 sites reported in this study and the 7 sites reported by Turnell, 1988). Also, the clearly consistent data given by Kissel and Laj (1988, and references therein) for the Ionian Zone are combined to form one average. This average does not, however, include their data from Southern Akarnania, which I believe is significantly different from the data from the north.

Before considering the various interpretations which can be placed on the data obtained in the Peloponnesos in the present study, it is necessary to reconsider the model proposed by Kissel and Laj (1988).

Kissel and Laj (1988) divided the western Aegean area into the two domains of the external (western) and internal (eastern) regions, which they considered to have had significantly different rotational histories. They suggested that the external Ionian Zone had experienced a clockwise rotation of approximately 50° which occurred in two distinct phases; a Middle Miocene rotation of 25°, followed by a second rotation of 25° between the Lower Pliocene and the present day. This conclusion was mainly based on studies of Oligocene rocks located in the Epirus region and mainland Greece between Corfu and Kephallinia, and Middle Miocene to Quaternary sequences of the Ionian Islands (Corfu, Kephallinia, Zackinthos).

In contrast, the rotations reported by Kissel and Laj (1988) from the internal region were considered to result from the rotation of fault-bounded blocks in a shear zone connecting the North Anatolian Fault/North Aegean Trough to the external arc (McKenzie and Jackson, 1983; see Chapter 2, Section 2.5, and Chapter 7, Section 7.2.3b). This conclusion was based on studies of the Lower to Middle Miocene volcanic rocks of the islands of Evvia and Skyros.

Since all the data included by Kissel and Laj (1988) in their reconstruction are from formations of Oligocene or younger age, their data have not been influenced by any possible rotations caused by final closure of the Neotethyan basins in the Eocene. Thus, their division of the western Aegean area into external and internal zones implies that

these regions have been decoupled from each other, presumably by the reactivation of pre-existing major thrusts. However, an examination of Figures 8.23 and 8.24, which show those data from pre-Middle Miocene formations and from Middle Miocene or younger formations respectively, suggests that other possibilities have to be taken into account, since there is *no* clear difference between the rotations implied by the data in the external and internal regions.

Four situations may be envisaged:

1. Both the Middle Miocene and the Lower Pliocene rotation events identified by Kissel and Laj (1988) within the Ionian Zone were restricted to the external area and did not affect the areas to the east;
2. Both events affected the whole region, external and internal zones alike;
3. The Middle Miocene event was restricted to the external area, whereas the Lower Pliocene event affected the whole area;
4. The Middle Miocene event affected the whole area, whereas the Lower Pliocene event was restricted to the external region.

These possibilities are hereafter referred to as Options 1-4.

If Options 2, 3 or 4 apply then it is obvious that we do not need to attribute *all* of the rotation described by Kissel and Laj (1988) from the islands of Evvia and Skyros to the effects of fault block rotation within the postulated distributed shear zone.

The limited data obtained in the present study from site PQ, located in the Plio-Quaternary sandstones of the southern Argolis Peninsula, suggest that this area may have experienced a 40° clockwise rotation since the Pliocene. Also, new data reported by Westphal *et al.* (1990) from Plio-Pleistocene formations of the Chalkidiki, northern Greece, indicate that this area has undergone a recent rotation of the same magnitude as that identified by Kissel and Laj (1988) in the Ionian Islands (the new data of Westphal *et al.* (*op. cit.*) have not been incorporated into Figure 8.24). There is, therefore some evidence for a Pliocene rotation event affecting the Ionian Islands (Kissel and Laj, 1988 and references therein), the Chalkidiki Peninsula (Westphal *et al.*, 1990), and southern Argolis (this study). This suggests that the Lower Pliocene event proposed by Kissel and Laj (1988) cannot be restricted to the external region alone. Instead, a 25°-40° Pliocene rotation appears to have affected almost the whole of Greece (excluding Crete). Therefore, Options 1 and 4 above may be discarded, although clearly a larger Pliocene database is required to confirm this rotation.

Thus we are left with two scenarios according to whether the Middle Miocene rotation of Kissel and Laj (1988) has or has not affected the internal zones (Options 2 and 3 respectively).

It should be noted that the remaining discussion in this section relies heavily on the limited data from the Plio-Quaternary section at site PQ, and in particular on the assumption that the intermediate coercivity component at that site represents the primary depositional magnetisation.

A further consideration of the data obtained in the present study from the southern Argolis Peninsula enables a preliminary choice to be made between these remaining possibilities in the region of the southeastern Peloponnesos. The Palaeocene pelagic limestones studied at site DT have a declination which is identical to that at site PQ (Plio-Quaternary sandstones), suggesting that no rotation has affected this area between the Palaeocene and the start of the Pliocene. This would exclude a Middle Miocene rotation for the southern Argolis area. Also, the data from sites GH and WD, of Upper Triassic and Jurassic age respectively, indicate a rotation of the southeasterly Peloponnesos of between 29° and 44°. This is comparable to the 40° rotation of southern Argolis. Kissel and Laj (1988) report data from Middle Pliocene to Quaternary sediments, exposed just to the west of sites GH and WD, which indicate a 13° rotation (average of 5 sites). This suggests that a large part of the rotation identified at sites GH and WD is also of Pliocene age, while the agreement between the total amount of rotation in this area and in southern Argolis suggests that the whole of the southeastern Peloponnesos was unaffected by the Middle Miocene event of Kissel and Laj (1988).

I therefore suggest that the southeastern corner of the Peloponnesos (southern Argolis and the southeastern part of Laconia) has experienced no rotation prior to the Pliocene, and a *ca.* 40° clockwise rotation thereafter. While it is tempting to extrapolate this interpretation to the rest of the Greek mainland and to conclude that the Middle Miocene rotation of Kissel and Laj (1988) was restricted to the external regions (Option 3), such an extrapolation would be clearly unreliable given the complex nature of deformation in Greece and the sparsity of palaeomagnetic data. Instead we must consider the implications of both Options 2 and 3 for the remaining data.

As discussed in the previous section, the data obtained in the present study indicate that the northern Peloponnesos has experienced a large, but possibly variable clockwise rotation (77° in northern Argolis, 71° of the Gavrovo-Tripolitza platform exposed along the Tripolis road, and 60°-74° of the Ionian pelagic limestones exposed to the west of Patras). Birch (1989) also reports a large clockwise rotation of 60°-90° from pelagic limestones of Upper Cretaceous to Lower Tertiary age within the Parnassos Zone (to the north of the Gulf of Corinth). This result is not illustrated in Figure 8.23, since Birch (1989) does not give the exact location of his sampling sites. Additionally, data reported by Kissel *et al.* (1985) from three sites within an Oligocene section in the Ionian flysch in Southern Akarnania (to the north of the Gulf of Patras) indicate rotations of

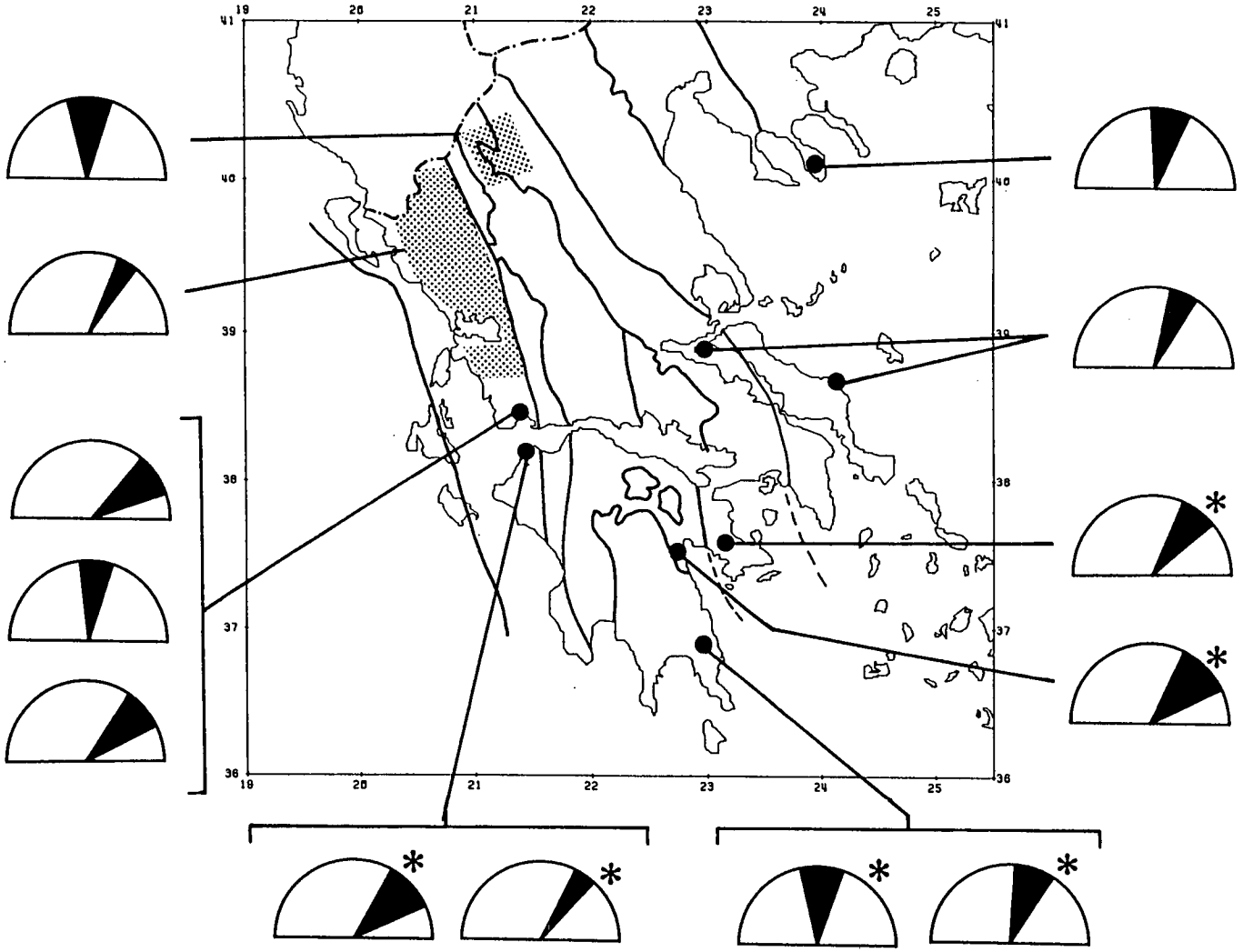

Figure 8.25. The data of Figure 8.33 after the removal of a 26° to 40° rotation of Pliocene age. Note that large clockwise rotations still remain on both sides of the Gulfs of Patras and Argolikos. These may be due to a combination of an earlier Miocene event and rotation of fault blocks within a distributed shear zone, or wholly to the latter mechanism.

75°, 31° and 81° (see Figure 8.23). These data were excluded from the mean direction shown in Figure 8.23 for the Ionian Zone, but were included in the mean given by Kissel and Laj (1988). Thus, the available data suggest that large clockwise rotations of *ca.* 70° occur throughout the northern Peloponnesos and to the north of the Gulfs of Corinth and Patras.

In the preceding part of this discussion, I suggested that the available data indicates that a *ca.* 25°-40° rotation has affected the entire area between the Chalkidiki and the southern Peloponnesos. Thus we must remove the effects of this event from the data in the region where large rotations are observed, to recover the amount of pre-Pliocene rotation*. Because the data related solely to the Pliocene rotation are limited, all we are able to do is strip-off the average rotation of 26° given by Kissel and Laj (1988). This clearly introduces an extra element of uncertainty into the database. An possible exception is in the Argolis area, where the close agreement between the data from sites DT and PQ of this study enables us to remove a 40° Pliocene rotation with more confidence. The effects of removing the Pliocene event from the database are shown in Figure 8.25.

Firstly, I will consider the possibility that the Middle Miocene rotation identified by Kissel and Laj (1988) has not affected the region where large rotations are observed (Option 3). This would be consistent with the model of Kissel and Laj (1988), i.e. that the external and internal zones have experienced a different rotation history. If this were the case, the large rotations remaining in the central area after removing the Pliocene rotation cannot be attributed to the tectonic bending of the arc. The most obvious alternative explanation for these rotations is that they are due to the rotation of fault-bounded blocks within a zone of distributed deformation, as proposed by McKenzie and Jackson (1983). This was the mechanism which Kissel and Laj (1988) invoked to explain the large rotations of Evvia and Skyros. This would imply that the zone of distributed shear extends across Central Greece and has affected areas as far south as southern Argolis and as far west as the Ionian Zone.

There are several points in favour of this model. Firstly, there is no need to decouple the northern Peloponnesos from southern Argolis and southeastern Peloponnesos during rotation associated with the bending of the arc. Secondly, we do not need to invoke large amounts of strike-slip motion along the Migdhalitsa Graben to account for the differential rotation of the Argolis units. Slickensides on the faults of the

---

* or more strictly the declinations which would be observed if the Pliocene rotation had not taken place. This is subtly different from the pre-Pliocene rotation since it does not exclude the possibility of additional, more localised rotations of Pliocene or younger age.

graben system do not support such strike-slip motion but instead indicate a predominance of dip-slip movements (Clift and Robertson, 1990; Section 8.2.6a). In this model, the graben may represent the southern boundary of the shear zone, and we might therefore expect more complex deformation than in the fault block zone to the north. This may explain the non-systematic occurrence of small dextral and sinistral components indicated by the slickenside data (Clift and Robertson, 1990; Section 8.2.6a). Finally, the strike of the imbricate fan of the western Pindos Zone in the Peloponnesos appears to be deflected in a clockwise sense with respect to the strike of the equivalent unit to the north. By effectively invoking an additional rotation for the northern Peloponnesos, this model may explain this observation.

There are however two points which argue against this model. Firstly, the palaeomagnetic database suggests that the later Lower Pliocene rotation affected a large area between the Chalkidiki and southeastern Peloponnesos. Since both the Middle Miocene and Pliocene events have been causally related to changes in the geometry of the Aegean arc through time (Kissel and Laj, 1988), it is difficult to see how one event could be restricted to the external zones whereas the other affected the whole area. Secondly, the Neotectonic faults in the Argolis area appear to have been inactive throughout the Late Quaternary (P. D. Clift, pers. comm., 1990), whereas the faults in the postulated shear zone to the north (e.g. in the east of the Gulf of Corinth) have been active in historical times (McKenzie and Jackson, 1983). However, this does not exclude an extension of the zone of distributed deformation into northern Argolis at an earlier time. It should be noted that the North Anatolian Fault has been active since at least the earliest Pliocene (Barka and Hancock, 1984).

The second alternative (Option 2) is that *both* the Middle Miocene and Lower Pliocene events were of regional extent. A substantial part of the large rotations identified in the central area may then be attributed to the Miocene rotation. However, since Kissel and Laj (1988) have identified only a 25° rotation of this age, an additional small rotation of 15° to 20°, attributed to activity within the shear zone, would still be required to account for the observed declinations. This model is more consistent with the evidence for the Pliocene rotation, which may have affected the entire region, and avoids the need for a different pattern of rotation in events which are causally linked to the same process.

The available database is not extensive enough to enable a definite choice to be made between these two alternative models. Hopefully, additional data from the platform sites collected in the present study which still await measurement will extend our knowledge of the pattern of rotation within the Peloponnesos, and may lead to a better understanding of this critical zone.

8.5 Conclusions

Although the discussion above is necessarily open-ended until further data are available, some general conclusions can be made:

1. The division by Kissel and Laj (1988) of the Aegean region into external and internal zones on the basis of the palaeomagnetic results from the area does not appear to be wholly justified. At least their Lower Pliocene event may have affected both external and internal zones alike. This is evidenced by the identification of rotations of Pliocene age in southern Argolis (this study) and in the Chalkidiki peninsula (Westphal *et al.*, 1990). This event could therefore account for a large part of the rotation of the islands of Evvia and Skyros identified by Kissel and Laj (1988).

2. The rotation of the northern half of the Argolis Peninsula does not appear to represent the isolated rotation of a small fault-bounded block. Instead, preliminary evidence for large (*ca.* 70°) clockwise rotations in areas both to the north and south of the Gulfs of Corinth and Patras suggests that the Argolis rotation is the result of a more widespread phenomenon. These rotations may not be completely attributed to the Neotectonic bending of the Aegean arc suggested by Kissel and Laj (1988) and Le Pichon and Angelier (1979). The data indicate that, whether or not the Middle Miocene rotation of Kissel and Laj (1988) affected the internal regions, a further rotation is required to explain the observed declinations. This amplified rotation is probably related to fault block activity within a distributed shear zone linking the North Anatolian Fault with the Hellenic trench to the west.

3. On a more local scale, the palaeomagnetic data from the northern half of the Argolis Peninsula support the idea that the deep-water facies of the Asklipion Unit do not represent the far-travelled remnants of the continental margin of the Vardar basin, as suggested by Baumgartner (1985). Instead, the agreement between the directions of magnetisation of the Asklipion and Pantokrator Units supports the suggestion of Bannert and Bender (1968), Bachmann and Risch (1979), Clift (1990) and Clift and Robertson (1990) that the deep-water Adhami limestones represent the essentially *in situ* sedimentary infill of intra-platform basins within the Pantokrator platform.

4. The rotations within the Argolis area must be taken into account when interpreting structural data relating to the Jurassic emplacement of the Migdhalitsa Ophiolite Unit. Unfortunately, the pre-rotation transport directions do not allow a definite choice to be made between different root-zone models (Pindos or Vardar basins).

It is hoped that further work on the platform limestones of the Peloponnesos to be carried out in the near future will shed more light on the complex rotational deformation which has affected southern Greece during the Tertiary.

CHAPTER NINE - A PALAEOMAGNETIC STUDY OF THE PINDOS THRUST SHEETS.

9.1 Introduction and aims.

In the previous chapter, I suggested that the large *ca.* 70° clockwise rotations observed in the northern half of the Argolis Peninsula and the northernmost Peloponnesos resulted from a regional rotation in the Pliocene of 25°-40° and an additional rotation related to the zone of distributed deformation and/or the Miocene rotation of the arc proposed by Kissel and Laj (1988).

During sampling of the autochthonous platform units, samples were also collected from the overlying deep-water sediments of the Pindos thrust sheets. The principal aim of this sampling was to test whether significant rotation of the allochthonous units took place during overthrusting, or whether the remanence directions recorded by these units reflect rotation of the underlying platform units.

As described below, the calciturbidites and pelagic limestones of the Pindos Series proved to be one of the most palaeomagnetically stable carbonate facies sampled in the present study. Significant variations in the declination of cleaned remanence directions between sites in the thrust sheets have been found. These data are described in detail below.

I begin this chapter with a brief description of the sedimentology and structure of the Pindos rocks in the Peloponnesos.

9.2 The geology of the Pindos Zone in the Peloponnesos.

The classical palaeogeographical interpretation of the external Hellenides, developed in detail by Aubouin (1958, 1965), interprets the Pindos Zone as a Mesozoic trough, flanked to the west by the carbonate platform of the Gavrovo-Tripolitza Zone and to the east by that of the Pelagonian Zone. This model was developed in continental Greece, but has also been applied to the interpretation of similar Pindos rocks in the Peloponnesos by Dercourt (1964). In the more recent palaeogeographical synthesis of Dercourt *et al.* (1986), the Pindos Zone basin was interpreted as an intra-continental rift within a single Apulian microplate. However, as discussed in Chapter 2 (Section 2.4.4), the presence of tholeiitic basaltic blocks within the tectonic mélange underlying the Pindos sediments, together with the growing body of evidence for eastwards emplacement of Jurassic ophiolites onto an adjacent Pelagonian microcontinental sliver from a Pindos root-zone, indicates that the Pindos basin is more likely to have been a small ocean basin floored by oceanic crust (Figure 7.02).

In either case, it is clear that the Pindos Series is entirely allochthonous. It occurs as a series of thrust sheets which form part of the Central Hellenic nappe sequence (Jacobshagen *et al.*, 1978) and which cover much of the northern half of the Peloponnesos and extend into the southeastern Peloponnesos. The western boundary of the zone consists of an imbricate fan of thrust slices resting tectonically on flysch of Upper Eocene to Oligocene age, which in turn overlies the Gavrovo-Tripolitza platform basement (Temple, 1968). The thrust sheets in this area are steeply inclined and repeat the entire Triassic to Palaeocene/Eocene Pindos sequence (see below). To the east, behind the main thrust front, are several tectonic windows where Mesozoic and Lower Tertiary shallow and deeper marine carbonates of the Gavrovo-Tripolitza Zone are exposed, beneath the age-equivalent deep-water carbonates of the Pindos Series (Figure 7.01). In this area (the Table d'Achladi), the basal thrust occurs at a stratigraphically higher position and generally lies within the Upper Cretaceous part of the sequence. The Upper Cretaceous sediments are multiply imbricated but are generally gently inclined. The basal thrust only occasionally cuts through to the older parts of the sequence.

The oldest Pindos rocks in the Peloponnesos are a Late Triassic (Carnian) flysch facies, overlain by Upper Triassic limestones and shales (Dercourt *et al.*, 1973). They pass up into the Radiolarite Series, which consists of several hundred metres of cherts and red shales of Jurassic to Lower Cretaceous age. A period of influx of terrigenous sediment in the mid-Cretaceous is represented by the 'First Flysch', which comprises a few tens of metres of turbidites associated with red shales and calciturbidites. The 'First Flysch' is overlain by a sequence of Upper Cretaceous calciturbidites and interbedded pelagic micrites up to 250 metres thick. These pass up into a 100 metre series of calciturbidites interbedded with terrigenous turbidites, shales and marls, and pelagic limestones known collectively as the Passage Beds. The youngest unit of the zone is the Pindos Flysch, an entirely terrigenous flysch sequence of Palaeocene to Eocene age, which is rarely more than 20 metres thick (Piper and Pe-Piper, 1980).

9.3 Sampling and methods.

Samples were collected mainly from the Upper Cretaceous pelagic limestone interval of the Pindos Series, although some sites were located in the older parts of the sequence. A limited number of sites were collected during the first field season in Greece. Preliminary analyses of the samples from these sites showed that the best results were obtained from pale buff to pale pink/purple lithologies. During the second field season, therefore, sampling was concentrated on beds of these colours. Cores were

taken using a standard petrol-driven rock drill, with water cooled, 1" diameter diamond-tipped drill bits.

The choice of sampling sites was limited by the severity of the deformation to which these strata have been subjected. The imbricate fan zone in the west of the outcrop area of the Pindos Zone was avoided completely because of the complexity of the structure (sites located in the structurally similar Kumluca Zone imbricate fan within the Antalya Complex gave no reliable data; Chapter 6). The densest sampling was carried out in the less-disturbed and near-horizontally layered sections of the thrust sheets to the east, in the area around Argos and Astros (Table d'Achladi). Sites were located away from zones of intense shearing and brecciation. Such pervasive deformation is particularly common close to the sole thrusts of the nappes. Visibly weathered and altered exposures were avoided. Structural tilt corrections were based on the attitude of well-developed bedding planes within the deep-water facies. Sites with only minor structural tilt (normally less than 40°) and simple folding were preferred. It was hoped that collecting from such strata would minimise any declination errors due to tectonic rotation about inclined axes (MacDonald, 1980).

In general, between 6 and 15 samples were drilled at each site, although more samples were collected per site during the first field season in Greece. Each sample was orientated with both magnetic and sun compasses (Creer and Sanver, 1967). A total of 25 sites were collected. The location of the sites discussed in the text are shown in Figure 9.01.

In the laboratory, 18 mm long subsamples were prepared from each core, for analysis using the 2-axis CCL superconducting magnetometer. This is the maximum sample length which this magnetometer can accommodate with the sample inserted on its side (Chapter 1, Section 1.6.2). Additionally, the samples from some sites were cut to a length of 22 mm for measurement on the 3-axis 2-G superconducting magnetometer, which has a wider access tube (Chapter 1, Section 1.6.3).

9.4 Palaeomagnetic results.

9.4.1 Rock magnetic characteristics.

The frequency distribution of the natural remanent magnetisation (NRM) intensities of the Pindos samples is shown in Figure 9.02. Although these samples are weakly magnetised, with a mean intensity of 4.0×10^{-5} Am^{-1}, reliable measurements could be made using both of the available cryogenic magnetometers. In the majority of samples, the NRM intensity was high enough to enable full demagnetisation experiments to be carried out.

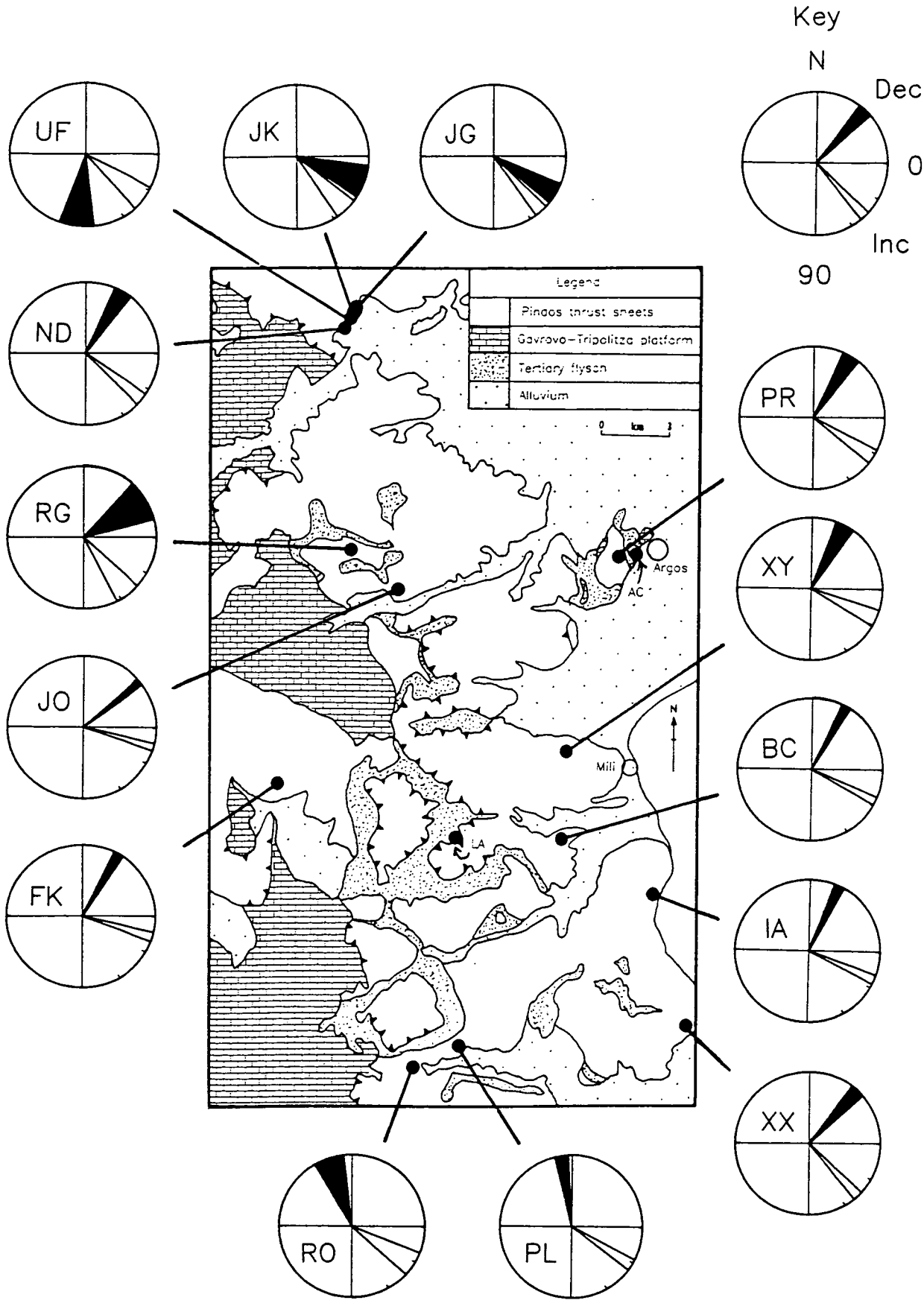

Figure 9.01. Generalised geological map of Argos and Astros areas, showing the locations of the sampling sites discussed in the text. The 'clock' diagrams show the 95% confidence limits associated with the mean declination and inclination in stratigraphic coordinates at each site.

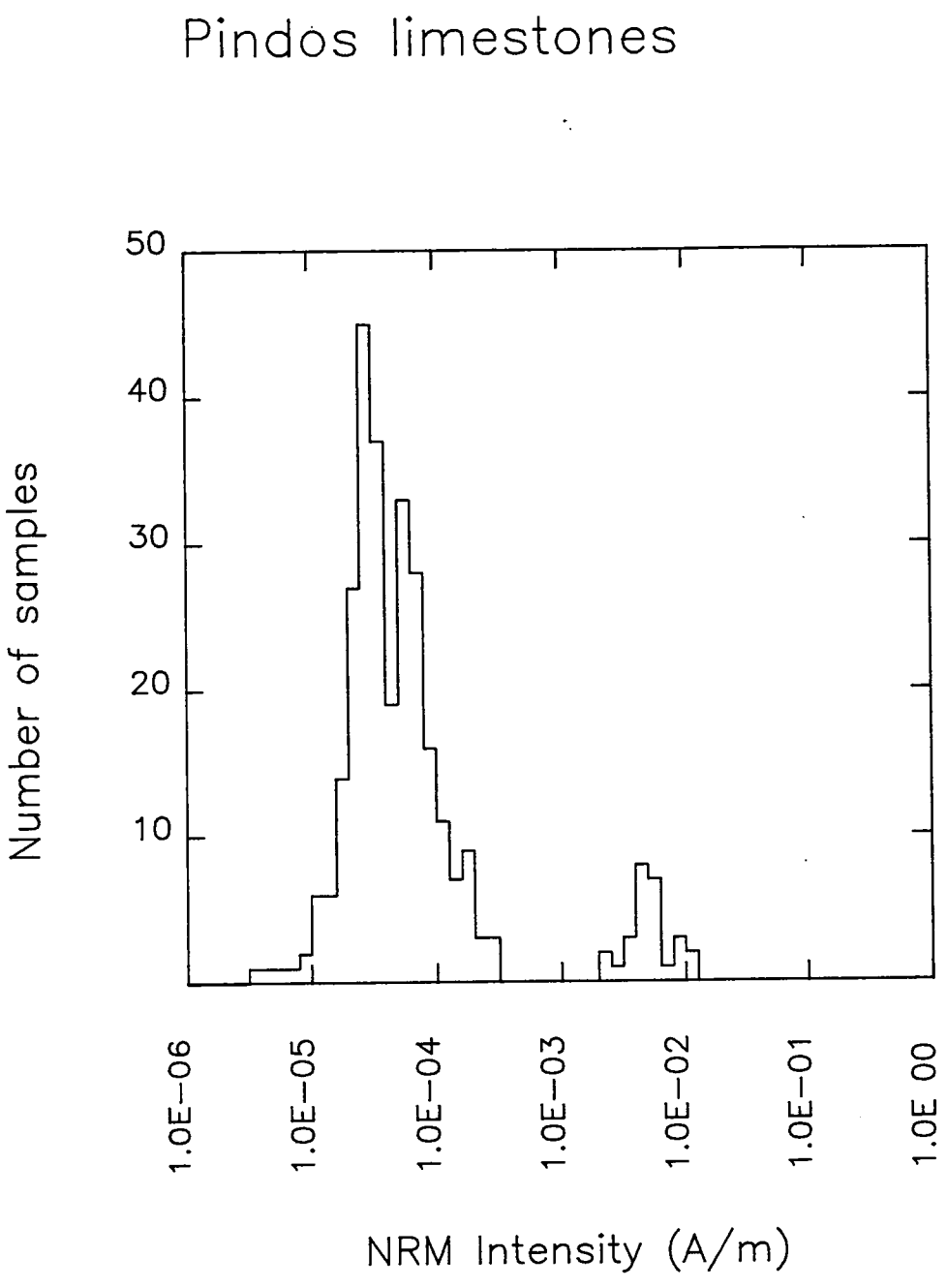

Figure 9.02. Histogram of illustrating the frequency distributions of the NRM intensities of the Pindos limestones.

Again, no attempt has been made to obtain magnetic extracts from these limestones because of the low concentration of magnetic minerals implied by the low NRM intensities. Instead, the magnetic mineralogy of the Pindos samples has been determined from the coercivity and blocking temperature characteristics of both natural and laboratory-grown remanences.

For at least two samples per site, the rate of acquisition of isothermal remanence (IRM) in fields up to 2.0 T has been studied. Details of the experimental procedure involved have been previously given in Chapter 4, Section 4.3.1. Figure 9.03 shows typical results of these analyses. In each graph the solid curve represents the stepwise increase in isothermal remanent moment produced by successively increasing applied fields, while the histogram shows the incremental coercivity spectrum (Dunlop, 1972). In all cases, a rapid increase in isothermal moment up to fields of 100 to 300 mT indicates the presence of magnetite, of presumed detrital origin. In those samples which were off-white/pale buff in colour, this initial rise is followed by a slower increase in IRM up to the maximum applied field of 2.0 T (e.g. sample JK 01 A in Figure 9.03). This indicates that a significant amount of a mineral with coercivity higher than that of magnetite is also present. The importance of this high coercivity fraction is greater in those samples which were light pink/purple in colour (e.g. sample RG 04 A in Figure 9.03), where inflexions at approximately 100 to 200 mT separate those parts of the IRM acquisition curves attributable to the presence of magnetite and those attributable to the higher coercivity fraction. This colour-dependence suggests that the high coercivity mineral present is haematite in the form of pigment.

To determine the blocking temperature spectra of these deep-water carbonates, one sample from each site was given an IRM in a field of 2.0 T along the sample Z axis and was then subjected to stepwise thermal demagnetisation. Figure 9.04 shows typical normalised intensity against temperature curves obtained from these experiments. The IRM's are destroyed progressively up to maximum temperatures of between 470°C and 600°C. No steep decrease in IRM intensity is observed after heating to 100°C, indicating that the high coercivity mineral identified by the IRM acquisition experiments is not goethite. The range of unblocking temperatures found is consistent with the remanence being carried by a combination of titanomagnetite with low Ti content and haematite containing a small but significant quantity of Ti in the lattice (Tarling, 1983). The haematite pigment may have formed during early diagenesis by dehydration of goethite that had precipitated directly from seawater (Lowrie and Heller, 1982).

The domain structure of the titanomagnetite carriers has been examined using the test of Johnson *et al.* (1975), outlined in Chapter 6, Section 6.3.1. In every instance, weak-field anhysteretic remanence was found to be more resistive to alternating field

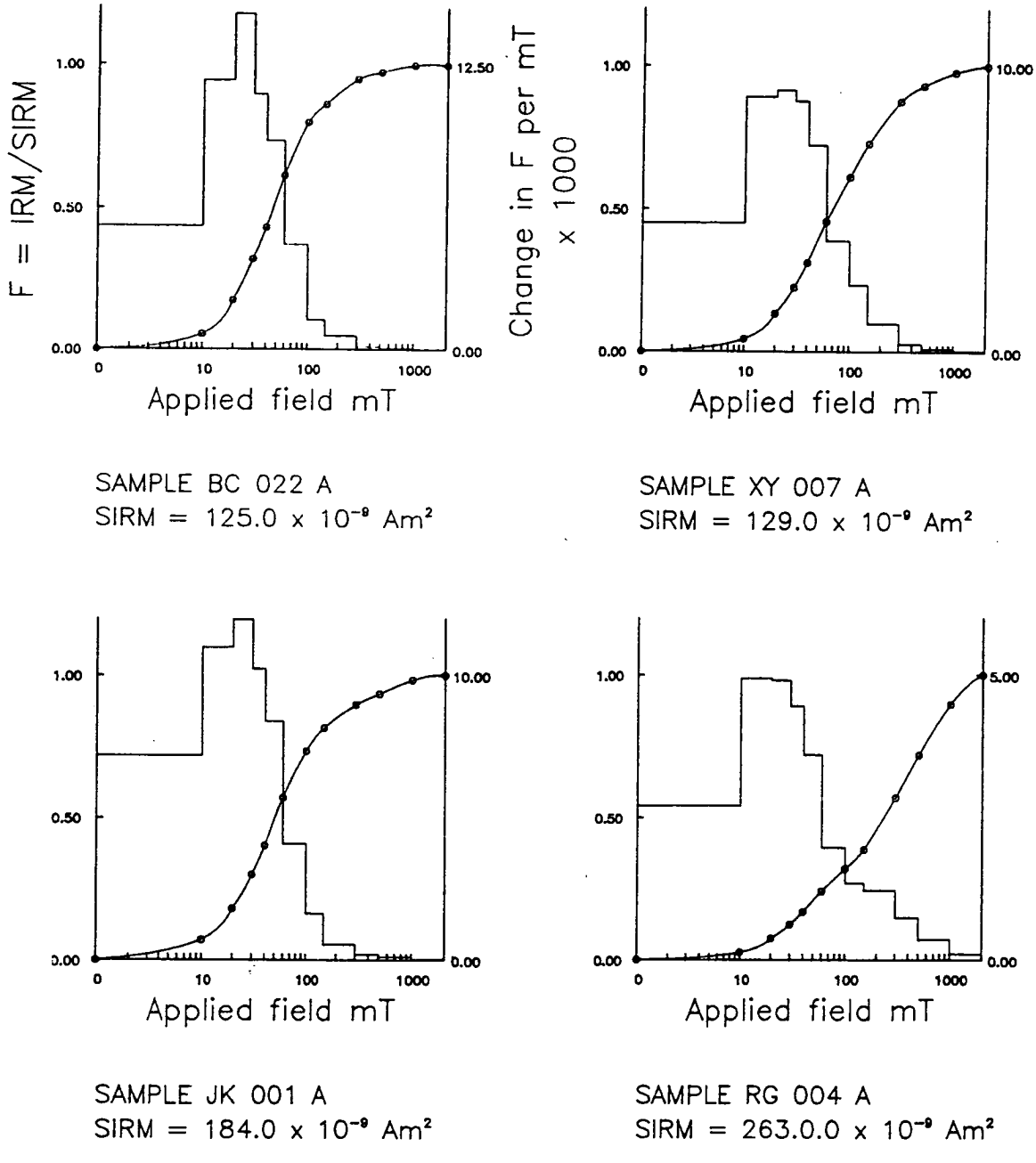

Figure 9.03. Typical examples of IRM acquisition curves for the Pindos samples.

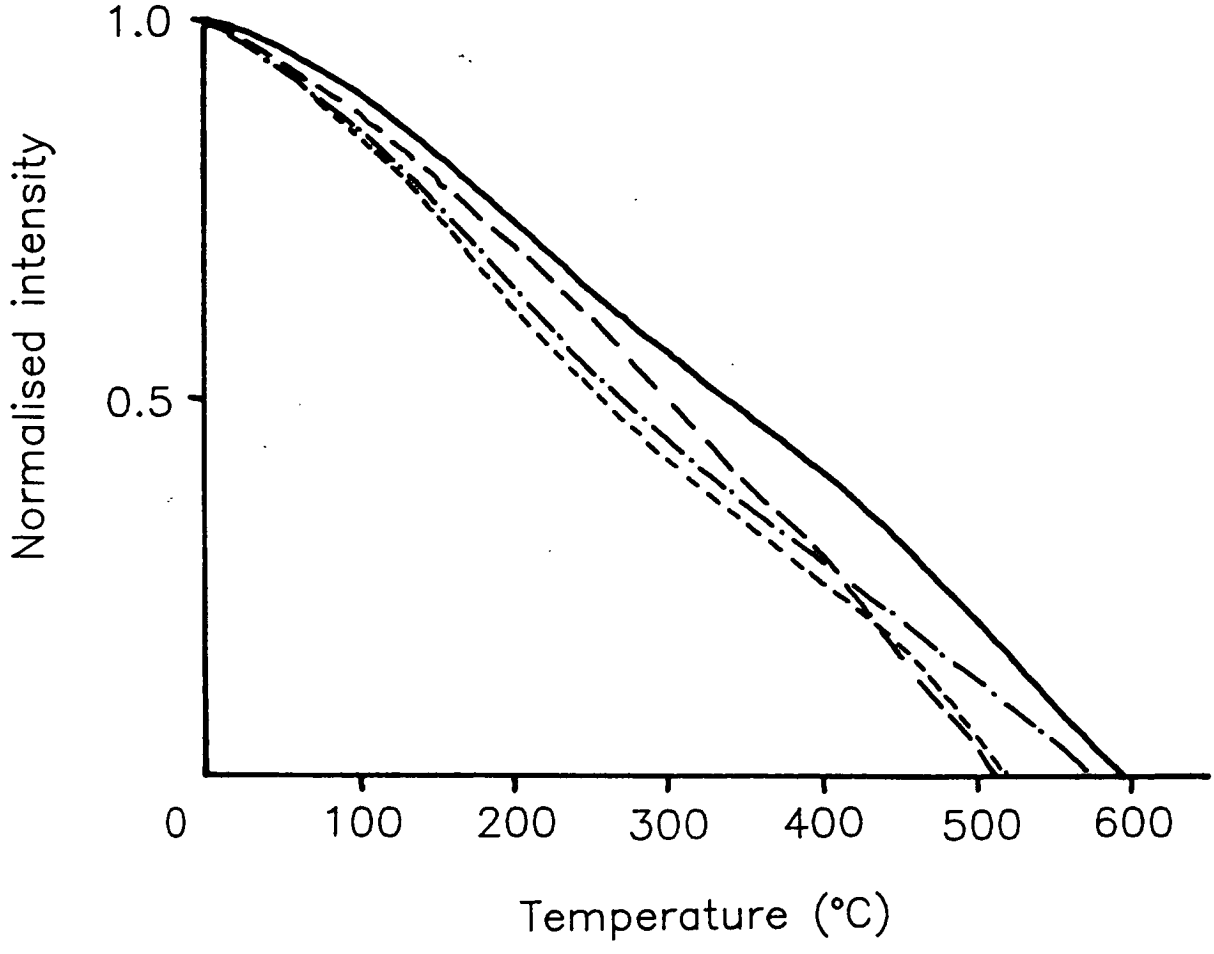

Figure 9.04. Typical normalised intensity against temperature curves obtained by stepwise thermal demagnetisation of a 2.0 T IRM for the Pindos samples.

(AF) demagnetisation that IRM. This indicates that single-domain-sized grains dominate the magnetite fraction of the samples.

At each site, one sample was subjected to stepwise AF demagnetisation in 2.5 mT intervals up to 20 mT, 5 mT intervals up to 50mT, and then 10 mT intervals up to a maximum field of 100 mT. A second sample was demagnetised thermally in 50°C steps up to a maximum temperature of 700°C. With both techniques demagnetisation was stopped below the maximum field/temperature when the intensity of magnetisation decreased below a level at which accurate measurement could be made (approximately 10.0×10^{-9} Am^{-1}).

Although changes in the susceptibility of samples at each stage of thermal demagnetisation were not monitored, the consistency of the direction of remanent magnetisation between heating steps in these samples indicates that no new minerals which contribute significantly to the sample remanence were formed during heating, before the intensity of magnetisation became too low to measure*.

The results of these demagnetisation experiments were used to decide which technique to apply to demagnetise the rest of the samples at each site. The remaining samples were then stepwise demagnetised, but at a reduced number of steps.

Typical results of both AF and thermal demagnetisation are shown in Figure 9.05. In general, AF demagnetisation was found to produce slightly noisier results than thermal treatment. However, AF demagnetisation was preferred over thermal demagnetisation, where it proved to be effective in recovering stable components of magnetisation, because of the reduced time required to magnetically clean the samples. A common north-dipping component, attributed to viscous magnetisation in the present field direction, was removed by fields of 20-30 mT and temperatures of 200°C. Thereafter, only single stable components of magnetisation were identified. This suggests that any natural remanence carried by the haematite in these samples has the same direction of magnetisation as that carried by the magnetite. This may indicate that the acquisition of a chemical remanence by the pigmentary haematite occurred more or less contemporaneously with the acquisition of a PDRM by the presumed detrital magnetite.

The maximum unblocking temperatures identified by thermal demagnetisation of the natural remanence carried by these samples were between 450°C and 500°C, which corresponds with those found from studies of the decay of IRM described above.

---

* Note that the samples were always randomly orientated within the demagnetisation oven.

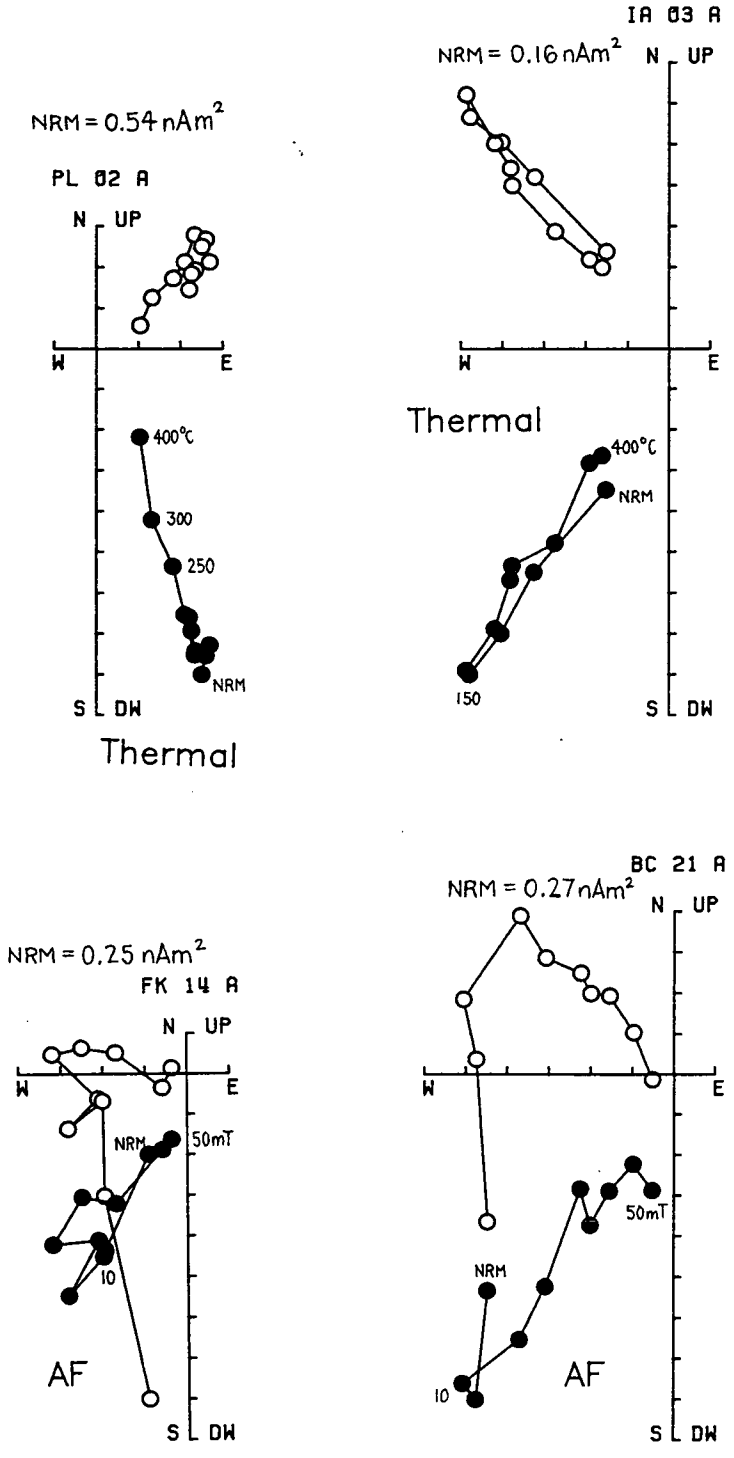

Figure 9.05. Typical results of both AF and thermal demagnetisation experiments for the Pindos samples.

9.4.2 Palaeomagnetic results.

Reliable palaeomagnetic results were obtained from 15 of the 20 sites measured to date (several sites have not been analysed at the time of writing due to lack of time). Five sites were rejected because stable endpoints were not reached before the intensity of magnetisation dropped below the noise level of the cryogenic magnetometer. Only data from samples exhibiting stable demagnetisation paths were used in calculating site mean directions. The direction of the cleaned remanence vector for each of these samples was found by drawing best-fit lines through the last four or more points on Zijderveld demagnetisation diagrams (Zijderveld, 1967). The cleaned site mean directions are reported in Table 9.1, both before and after the application of standard structural tilt corrections (i.e. in both geographic and stratigraphic coordinates). Within-site dispersion is small. Typical distributions of sample vectors are shown in the stereographic projections of Figure 9.06.

The age of magnetisation of these carbonates can be determined by examining the data from three sites (BC, IA, and XY; Table 9.1) located in a small area to the south of the village of Mili (Figure 9.01; Argos and Astros sheets; Papastamatiou *et al.*, 1970; Tartaris *et al.*, 1970). These sites are all within the Upper Cretaceous (Turonian to Maastrichtian) calciturbidites and pelagic micrites of the Pindos Series. The bedding at these sites varies between strikes of 330° to 054° and dips of 10° to 31°. These variations enable an inter-site fold test to be carried out (Figure 9.07). The site mean directions all fall in the upper hemisphere of the southwestern quadrant of a stereoplot, in both geographic and stratigraphic coordinates. These directions must represent magnetisations formed during a period when the geomagnetic field had a reversed polarity. An origin to the south of the equator is ruled out by the need to avoid unacceptable overlaps with the African plate. The directions shown in Figure 9.07 have, therefore, been inverted through the origin. In geographic coordinates (Figure 9.07a) the mean directions from the four sites are spread out with mean inclinations ranging from 21° to 46°. In stratigraphic coordinates, however, the grouping of the site means is improved. This positive fold test is significant at the 99% confidence level (McFadden and Jones, 1981; see Appendix A), and demonstrates that the stable endpoint directions identified in the demagnetisation experiments represent components of magnetisation acquired before the development of folding at the sites. The only significant folding event which has affected these strata was associated with the final closure of the Pindos Basin and the westwards emplacement of the thrust sheets onto the adjacent carbonate platform of the Gavrovo-Tripolitza Zone. Thus, it seems probable that the magnetisation recorded at these sites represents a primary depositional or post-depositional remanence acquired at or soon after the time of initial deposition.

Table 9.1. Palaeomagnetic results from the Pindos Series thrust sheets.

Site	Age	N	Geographic				Stratigraphic			
			Dec	Inc	α_{95}	K	Dec	Inc	α_{95}	K
BC	Upper Cretaceous	39	205	-21	5.2	21	208	-26	4.3	29
IA	Upper Cretaceous	13	189	-46	4.9	71	204	-23	4.9	71
XY	Upper Cretaceous	13	189	-36	9.0	22	207	-24	8.9	22
FK	Upper Cretaceous	22	199	-27	5.3	35	209	-17	4.7	45
PR	Upper Cretaceous	15	045	29	7.8	22	031	33	7.6	23
XX	Upper Cretaceous	10	181	-38	5.8	89	222	-47	5.1	114
RO	Upper Cretaceous	6	016	66	10.3	43	341	32	13.2	27
PL	Upper Cretaceous	12	010	57	4.6	88	351	32	6.0	54
JO	Upper Cretaceous	14	230	-4	3.7	115	230	-16	3.8	109
RG	Upper Cretaceous	6	205	-39	13.1	27	238	-53	13.1	27
ND	Upper Jurassic	6	305	50	7.0	93	030	40	7.0	93
UF	Lr-Mid Cretaceous	7	195	47	13.5	21	187	38	13.5	21
JG	Upper Cretaceous	8	139	45	9.3	31	123	47	9.3	31
JK	Upper Cretaceous	7	104	54	11.6	30	111	47	11.6	30
NA	Upper Cretaceous	6	096	24	15.2	20	092	47	12.8	28

N = number of samples; α_{95} = semi-angle of 95% cone of confidence; K = Fisher precision parameter

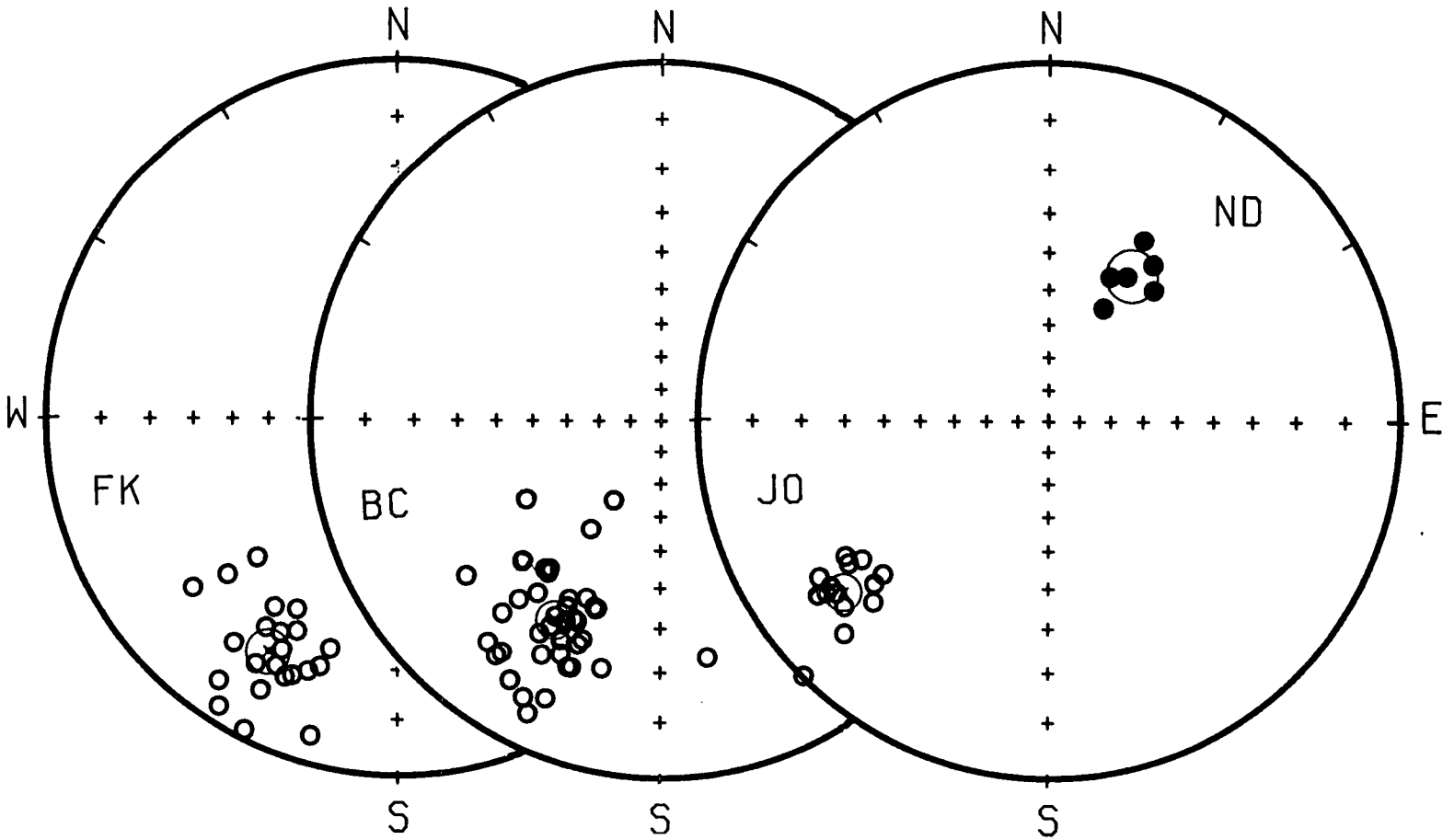

Figure 9.06. Stereographic projections showing typical distributions of cleaned sample vectors at the Pindos sites. Note the small within-site dispersions.

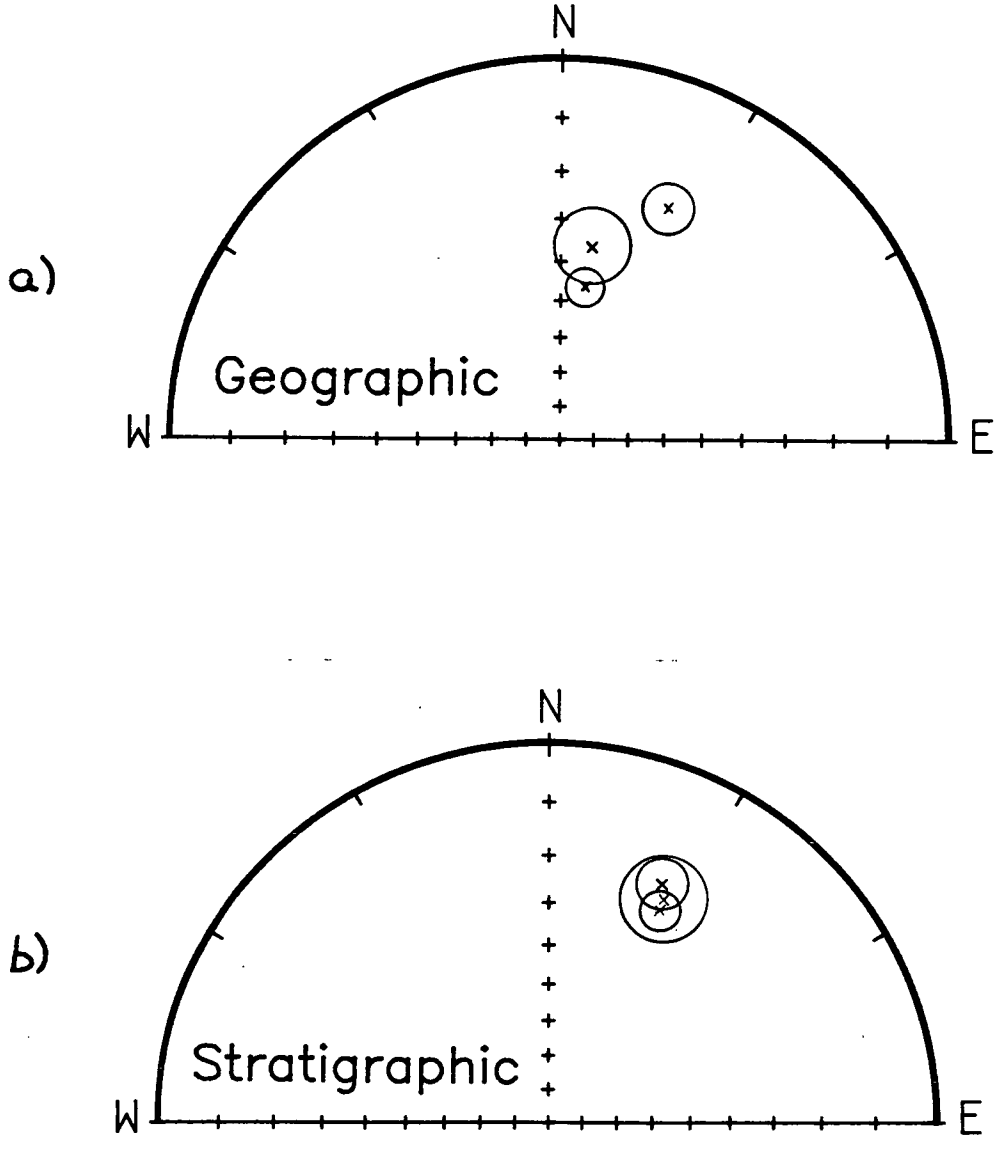

Figure 9.07. The inter-site positive fold test at sites BC, IA, and XY, demonstrating that the magnetisation of the Pindos limestones was acquired before emplacement of the thrust sheets.

Since the lithology and the magnetic characteristics of the samples at the rest of the sites are identical to those analysed at sites BC, IA, and XY, it is justified to assume that these sites also record primary remanent magnetisations. Supporting evidence for this assumption comes from sites RO and PL (Table 9.1) where both normal and reversely magnetised samples are found with anti-parallel directions of magnetisation. This indicates the stability and primary nature of the remanences at these sites.

The site mean directions in stratigraphic coordinates are shown in the "clock" diagrams of Figure 9.01. These diagrams show the 95% confidence limits associated with the mean declination and inclination at each site, calculated using the method of Demarest (1983) (see Chapter 4, Section 4.3.2).

9.5 Discussion.

It can be seen from Figure 9.01 that significant variations in the declination of the mean direction of magnetisation occur between sites. However, these directions are in general different from those identified in the underlying platform in the previous chapter. For instance, the Palaeocene limestones at the top of the Gavrovo platform exposed along the Tripolis road (site LA) gave a mean declination of 071°, compared to the average declination of approximately 030° of the overlying Pindos units in this area. This suggests that a significant rotation of the thrust sheets took place during their emplacement over the platform in the Eocene. We can obtain an estimate of this thrust-related rotation if we assume a value for the average rotation of the underlying platform, since the latter rotation almost certainly took place during the Neotectonic phase (i.e after emplacement of the Pindos nappes in the Eocene). We must remember, however, that this may not be justified since undetected but significant variations in the rotation affecting the platform may have occurred.

Since the majority of sites are located reasonably close to site LA, I will assume an average rotation of the autochthon in this area of 71° clockwise. This is very close to the average declination of the sites in the northern Peloponnesos. The effects of removing this rotation are shown by the clock diagrams of Figure 9.08.

If our assumptions concerning the rotation of the autochthon hold, then the generally northwesterly declinations shown in Figure 9.08 suggest that the thrust sheets experienced an overall anticlockwise rotation during emplacement. It is now believed that oceanic crust persisted in the south of the Pindos basin after initial suturing occurred in the north (Robertson *et al.*, in press). It is possible that the net anticlockwise rotation of the thrust pile could be related to this diachronous closure of the basin.

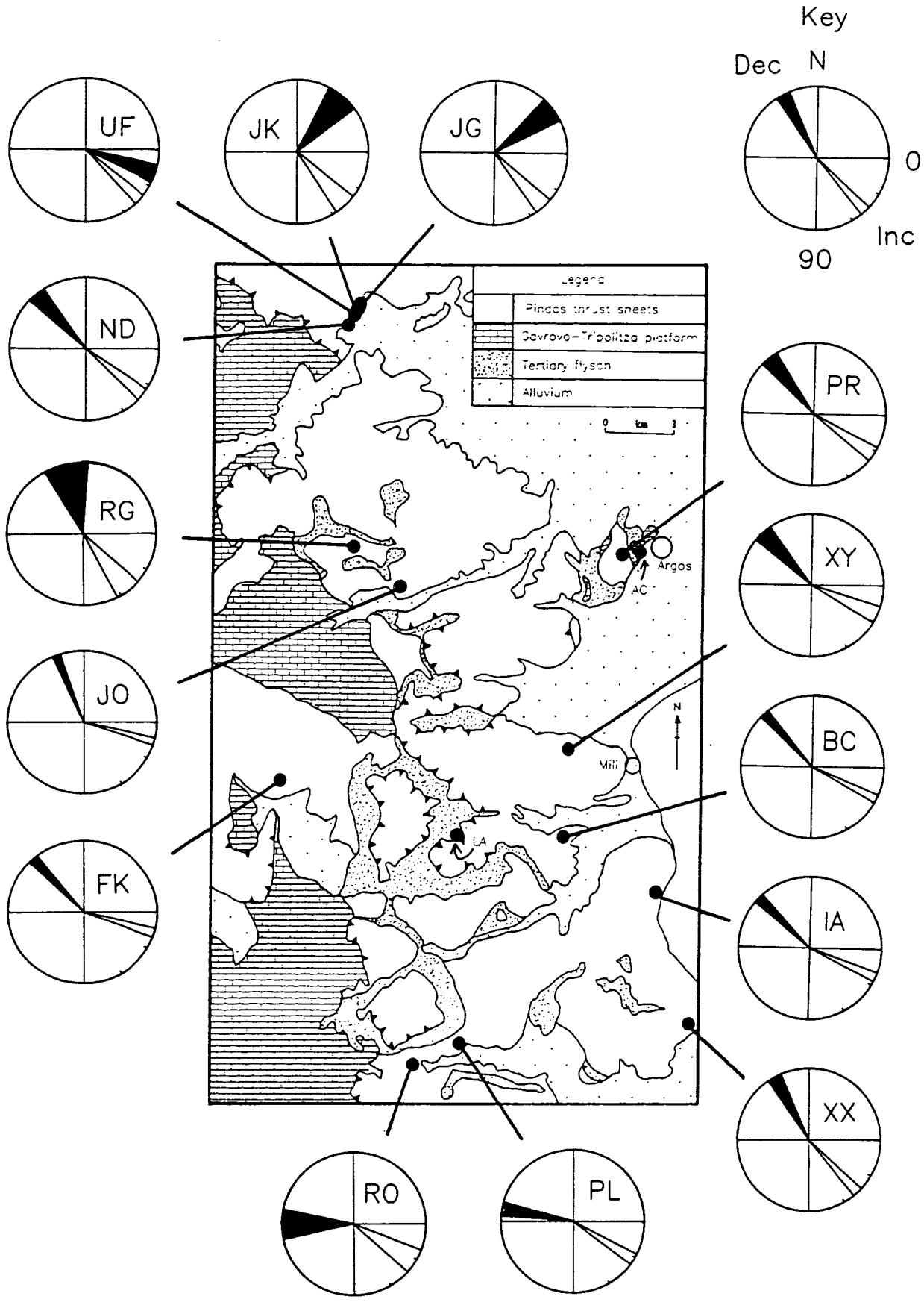

Figure 9.08. The data of Figure 9.01 after removal of an average clockwise rotation of 71° of the underlying autochthon.

The variations in declination identified earlier are still present after removing the effects of rotation of the underlying autochthon, since we have removed the same rotation from all sites. These variations can be interpreted in two ways:

1. They are related to local rotations of the thrust sheets during emplacement. This implies that the Pindos units fragmented during thrusting and were affected by variations in the footwall topography.

2. They are related to local variations in the amount of rotation affecting the autochthon during the Late Tertiary.

Obviously, these possibilities represent end-members in the interpretation; the actual variations in declination could be due any combination of 1. and 2. above. A more definite interpretation of the data would require greater constraints on the rotation affecting the Gavrovo-Tripolitza platform.

The mean inclination of the Pindos sites in stratigraphic coordinates is 35°, after inverting all reversed polarity samples through the origin. Assuming an axial geocentric dipole field, this inclination corresponds to a palaeolatitude of 19.3°. As discussed in Section 9.4.2 above, these rocks could not have originated to the south of the equator in the Upper Cretaceous, since their position would then overlap with that of the African plate (see the palaeolatitudes indicated in Figure 2.06g). Also, a position to the south of the equator would require large parts of the thrust sheets to have been rotated by nearly 180°.

A palaeolatitude of 19°N is consistent with an origin for the deep-water carbonates within a Pindos basin located mid-way between the African and Eurasian plate margins (Figure 2.06g).

9.6 Conclusions.

The pelagic limestones and calciturbidites of the Pindos nappes were emplaced over the platform units of the Gavrovo-Tripolitza Zone during the final closure of the Pindos ocean in the Eocene. The sparsity of data from the underlying autochthon makes any interpretation of the palaeomagnetic results obtained from Pindos series difficult. However, the present database suggests that the thrust sheets experienced an anticlockwise rotation during Eocene emplacement. Variations in declination between sites may reflect a combination of rotation due to break-up of the thrust sheets during emplacement over a topographically uneven footwall, and local variations in the Late Tertiary rotation of the underlying autochthon. The inclination data obtained from the allochthonous units are consistent with formation in an Neotethyan ocean basin located between Africa and Eurasia.

PART FIVE - CONCLUSIONS.

CHAPTER TEN - CONCLUSIONS AND SUGGESTIONS FOR FURTHER WORK.

10.1 General.

This research has identified block rotations in a variety of geological settings. These range from rotations occurring during the genesis of oceanic crust (Limassol Forest area of Cyprus), to those associated with the closure of small ocean basins (Isparta angle of Turkey, and the Pindos nappes of Greece) and to the final stages of continental collision (carbonate platforms of Greece).

An important general point is that these rotations would be impossible to identify by means of field structural studies alone, since these frequently only tell us about horizontal crustal movements and provide little information about rotations around steeply inclined axes. A unique property of the palaeomagnetic technique is that it can be used to document such rotations.

The following sections give a brief summary of the conclusions reached in each of the three study areas. Some suggestions for further palaeomagnetic research within each area are also outlined.

10.2 The Southern Troodos Transform Zone of Cyprus.

The Troodos massif of Cyprus represents an uplifted fragment of Neotethyan oceanic crust which formed above a northward dipping intra-oceanic subduction zone in the Upper Cretaceous, and which subsequently underwent a 90° anticlockwise rotation. The Limassol Forest Complex and Arakapas fault belt sub-terranes exposed along the southern margin of the massif were formed within a 'leaky' oceanic fracture zone, termed the Southern Troodos Transform Zone.

A palaeomagnetic study of the extrusives and sediments exposed along the Arakapas fault belt and around the periphery of the Limassol Forest block, detailed in Part Two of this thesis, indicates that significant intra-crustal rotations of small fault-bounded blocks have taken place within the inferred transform zone. These rotations are considered to represent primary features of crustal genesis and can not be attributed simply to post-oceanic disruption of the fracture zone. The predominantly clockwise sense of block rotation suggests that the Troodos ridge system had a sinistral offset configuration. This is supported by original north-west dyke strikes found along the Arakapas fault belt which are consistent with a stress field operating across a dextrally slipping transform.

Additional palaeomagnetic data obtained from the umbers and radiolarites of the Perapedhi Formation, overlying the extrusives of the Eastern Limassol Forest Complex, confirm that the Campanian period was a time of rapid rotation of the Troodos microplate, with up to 45° of rotation occurring over 15 Ma.

The palaeomagnetic database within the Troodos ophiolite is now very extensive. The timing of the 90° anticlockwise rotation of the Troodos microplate is sufficiently well-constrained. Further sampling within Western Limassol Forest Complex, where few sites exist, may provide a more detailed picture of the pattern of rotation within the Southern Troodos Transform Zone.

A more important objective of future research within Cyprus would be to carry out a palaeomagnetic study of the Mesozoic carbonates of the Kyrenia terrane (northern Cyprus). This unit is interpreted as a fragment of the northern continental margin of the Neotethyan Troodos ocean basin. Data provided by such a study would determine whether the Kyrenia Range has been affected by the 90° anticlockwise rotation of the Troodos microplate, and may shed light on the role of the Kyrenia terrane in the tectonic evolution of the eastern Mediterranean.

10.3 The Isparta angle of southwestern Turkey.

The palaeomagnetic study of both the autochthonous Tauride platform units and allochthonous Antalya Complex units of the Isparta angle, detailed in Part Three, has provided compelling evidence for a widespread Neogene remagnetisation event in the area. This event was probably triggered by the migration of orogenic fluids ahead of the Antalya Complex during its emplacement on to the adjacent platforms in the Early to Middle Miocene, and resulted in the formation of authigenic magnetite. The secondary magnetisation produced by this event has completely obscured the primary magnetisation at the majority of sites studied.

Subsequent to the acquisition of remanent magnetisation by the newly formed magnetite grains by growth through the critical blocking volume, a large segment of the Isparta angle area underwent an anticlockwise rotation of 30°. This rotation was probably driven by the overall convergence and bending of the Aegean arc in the Miocene, and was related to the emplacement of the Lycian Nappes onto the western limb of the Isparta angle.

The identification of this remagnetisation event has serious implications for the equatorial origin for the Turkish blocks proposed by Lauer (1981, 1984). This model relied heavily upon structurally corrected data from the Upper Triassic lavas of the Çalbali Dag section of the Gödene Zone, which indicated shallow negative inclinations. However, the *in situ* data from this section are consistent with the remagnetisation

hypothesis proposed here, and in particular match closely with data obtained in the present study from Upper Triassic lavas exposed to the south, where a negative fold test proves the secondary nature of the remanence. Thus, the equatorial position inferred by Lauer (op. cit.) for one of his three Turkish blocks is due to the inappropriate application of structural tilt corrections.

Future work in the Isparta angle clearly needs to take into account the need for adequate fold tests. Such fold tests may be able to further constrain the age of the remagnetisation event by using partial unfolding techniques. The pattern of remagnetisation within the major Bey Daglari carbonate platform needs to be investigated in more detail. Further sampling of this unit should concentrate upon the Upper Cretaceous-Palaeocene part of the sequence, where the best results were obtained in the present study. The Barla Dag platform massif, which appears to have escaped remagnetisation requires a more detailed study. Condensed, red pelagic limestones (Ammonitico Rosso) of Triassic age are known to occur within this unit, but have not been sampled to date. Additionally, more data are required from the overthrust Antalya Complex units, and in particular from the intensely magnetised and easily measurable Triassic lavas of the Gödene Zone.

There is also a need to extend sampling into the Lycian and Beysehir-Hoyran-Hadim Nappes, to the northwest and northeast of the Isparta angle respectively, to determine whether the remagnetisation and subsequent rotation identified in the present study have affected an even greater area.

10.4 The Peloponnesos of Greece.

A detailed palaeomagnetic study of the Mesozoic and Tertiary units of the Argolis Peninsula of the Peloponnesos has demonstrated that the northern and southern halves of this area have undergone significantly different tectonic rotations. The southern area has experienced a 40° clockwise rotation which may have occurred since the Pliocene (i.e over at most the last 5 Ma). The exact age of the 77° clockwise rotation identified in the northern area is not known. The youngest unit sampled is of Cretaceous age, but it is likely that this rotation is also of Neotectonic origin. The detailed results support the suggestion that the Asklipion Unit exposed within Argolis represents the sedimentary infill of intra-platformal deep-water basins and not a far-travelled continental margin assemblage. The data also indicate that the emplacement of the Jurassic Migdhalitsa Ophiolite Unit may have had a strong strike-slip component.

A combination of the palaeomagnetic database compiled to date within the autochthons of the Peloponnesos with previously reported data from the other Greek areas suggests that a 25-40° clockwise rotation affected much of the Greece in the

Pliocene. This event does not appear to be limited to the external Hellenides as suggested by Kissel and Laj (1988, and references therein), and could therefore account for a large part of the rotations of the islands of Evvia and Skyros identified by these authors. The combined database also suggests that the large rotation of the northern half of the Argolis Peninsula does not represent the isolated rotation of a small fault-bounded block. Instead, there is evidence for large (*ca.* 70°) clockwise rotations in areas both to the north and south of the Gulf of Corinth. A widespread Pliocene event can not account for all of these rotations, even in conjunction with the earlier Miocene event reported by Kissel and Laj (op. cit.). The large rotations may in part be related to fault block activity within a distributed shear zone linking the North Anatolian Fault with the Hellenic trench to the west.

Results from the Pindos thrust sheets, which overlie the Gavrovo-Tripolitza platform, indicate varying amounts of rotation with respect to the present north. These variations may be related to local rotations due to break-up of the thrust sheets during emplacement over a topographically uneven footwall and/or to local variations in the Late Tertiary rotation of the underlying autochthon. Removal of an average rotation of the basement suggests that the thrust sheets experienced an overall anticlockwise rotation during their emplacement, which may relate to the diachronous closure of the Pindos basin in the Eocene.

The palaeomagnetic research within the Peloponnesos carried out for this thesis is in an on-going state. The remaining sites within the Gavrovo-Tripolitza and Ionian Zones await measurement. It is hoped that data from these units will allow firmer conclusions to be drawn concerning the rotational deformation which has affected the area during the Tertiary. Such data may also make possible a more detailed interpretation of the results obtained in the present study from the Pindos thrust sheets.

Finally, the question of whether the large rotations observed in Central Greece can be attributed to deformation within a distributed shear zone will be investigated in a new project, to be carried out under the tenure of a University of Newcastle-upon-Tyne post-doctoral research fellowship. This project will also extend palaeomagnetic sampling into the North Anatolian Fault Zone of Turkey.

APPENDIX A - FOLD AND REVERSAL TEST STATISTICS.

APPENDIX A - FOLD AND REVERSAL TEST STATISTICS.

Chapter 6 - The Isparta angle.

Sites FI & YA.

		Geographic				Stratigraphic			
	N	Dec	Inc	K	R	Dec	Inc	K	R
FI	12	316	50	38	11.71	354	40	30	11.63
YA	27	313	50	17	25.47	312	39	15	25.27

Testing for common precision parameters (F-test of McElhinny, 1964):

Geographic coords. $K_1/K_2 = 2.24$
Stratigraphic coords. $K_1/K_2 = 2.00$
Critical value $K_1/K_2 > 2.67$ for 99% confidence

Therefore, in both cases we may accept the hypothesis that the 2 sites share a common K.

Fold test of McFadden and Jones (1981):

Geographic coords. Test value = 0.0025
Stratigraphic coords. Test value = 0.5806
Critical value = 0.1325 for 99% confidence

Therefore, we can reject the hypothesis that the 2 sites share a common mean direction in stratigraphic coordinates, but not in geographic coordinates. i.e. negative fold test at 99% confidence level.

Sites BA & LE.

		Geographic				Stratigraphic			
	N	Dec	Inc	K	R	Dec	Inc	K	R
BA	9	323	19	31	8.74	320	25	19	8.58
LE	6	331	49	46	5.89	335	29	46	5.89

Testing for common precision parameters (F-test of McElhinny, 1964):

Geographic coords. $K_1/K_2 = 1.48$
Stratigraphic coords. $K_1/K_2 = 2.42$
Critical value $K_1/K_2 > 4.55$ for 99% confidence

Therefore, in both cases we may accept the hypothesis that the 2 sites share a common K.

Fold test of McFadden and Jones (1981):

Geographic coords. Test value = 1.3436
Stratigraphic coords. Test value = 0.1941
Critical value = 0.4251 for 99% confidence

Therefore, we can reject the hypothesis that the 2 sites share a common mean direction in geographic coordinates, but not in stratigraphic coordinates. i.e. positive fold test at 99% confidence level.

Site AN.

		Geographic				Stratigraphic			
	N	Dec	Inc	K	R	Dec	Inc	K	R
Gp1	9	327	55	184	8.96	302	73	184	8.96
Gp2	4	340	58	63	3.95	340	55	63	3.95

Testing for common precision parameters (F-test of McElhinny, 1964):

Geog/Strat coords. $K_1/K_2 = 2.92$
Critical value $K_1/K_2 > 4.20$ for 99% confidence

Therefore, in both cases we may accept the hypothesis that the 2 limbs share a common K.

Fold test of McFadden and Jones (1981):

Geographic coords. Test value = 0.2758
Stratigraphic coords. Test value = 2.5435
Critical value = 0.5199 for 99% confidence

Therefore, we can reject the hypothesis that the 2 limbs share a common mean direction in stratigraphic coordinates, but not in geographic coordinates. i.e. negative fold test at 99% confidence level.

Sites AN & KA.

		Geographic				Stratigraphic			
	N	Dec	Inc	K	R	Dec	Inc	K	R
AN	13	331	56	103	12.88	320	68	37	12.68
KA	4	340	47	47	3.94	015	17	47	3.94

Testing for common precision parameters (F-test of McElhinny, 1964):

Geographic coords. $K_1/K_2 = 2.19$
Stratigraphic coords. $K_1/K_2 = 0.79$
Critical value $K_1/K_2 > 3.67$ for 99% confidence

Therefore, in both cases we may accept the hypothesis that the 2 sites share a common K.

Fold test of McFadden and Jones (1981):

Geographic coords. Test value = 0.2843
Stratigraphic coords. Test value = 4.0503
Critical value = 0.3594 for 99% confidence

Therefore, we can reject the hypothesis that the 2 sites share a common mean direction in stratigraphic coordinates, but not in geographic coordinates. i.e. negative fold test at 99% confidence level.

Site CI.

		Geographic				Stratigraphic			
	N	Dec	Inc	K	R	Dec	Inc	K	R
Sub-site 1	7	328	45	32	6.81	325	-20	32	6.81
Sub-Site 2	11	338	51	52	10.81	289	-60	52	10.81

Testing for common precision parameters (F-test of McElhinny, 1964):

Geog/Strat coords. $K_1/K_2 = 1.63$
Critical value $K_1/K_2 > 3.23$ for 99% confidence

Therefore, in both cases we may accept the hypothesis that the 2 sub-sites share a common K.

Fold test of McFadden and Jones (1981):

Geographic coords. Test value = 0.1346
Stratigraphic coords. Test value = 3.5612
Critical value = 0.3335 for 99% confidence

Therefore, we can reject the hypothesis that the 2 sub-sites share a common mean direction in stratigraphic coordinates, but not in geographic coordinates. i.e. negative fold test at 99% confidence level.

Site KK.

		Geographic				Stratigraphic			
	N	Dec	Inc	K	R	Dec	Inc	K	R
Ordovician	27	320	39	13	25.00	112	29	13	25.00
Permian	49	321	36	21	46.71	049	26	15	45.80
Jur-U.Cre	40	322	29	25	38.44	030	40	27	38.56

Testing for common precision parameters (McFadden and Lowes, 1981):

Geographic coords. E = 2.40
Stratigraphic coords. E = 8.56
Critical value = 9.21 for 99% confidence

Therefore, in both cases we may accept the hypothesis that the 3 time-slices share a common K.

Fold test of McFadden and Jones (1981):

Geographic coords. Test value (f) = 3.44
Stratigraphic coords. Test value (f) = 93.30
Critical value = 3.32 for 99% confidence

Therefore, we can reject the hypothesis that the 3 time-slices share a common mean direction in both geographic and stratigraphic coordinates. i.e. negative fold test at 99% confidence level. However, the directions are only just significantly different in geographic coordinates at this confidence level, whereas in stratigraphic coordinates the test value is very much greater than the critical value. This indicates that the magnetisation at this site predates folding.

Site BA Reversal test.

		Geographic				Stratigraphic			
	N	Dec	Inc	K	R	Dec	Inc	K	R
Norm	6	328	19	18	5.73	328	21	29	5.83
Rev	5	145	-21	24	4.83	134	-32	20	4.80

Testing for common precision parameters (F-test of McElhinny, 1964):

Geographic coords. $K_1/K_2 = 1.32$
Stratigraphic coords. $K_1/K_2 = 1.44$
Critical value $K_1/K_2 > 3.35$ for 95% confidence

Therefore, in both cases we may accept the hypothesis that the normal and reversed groups share a common K.

Using the fold test of McFadden and Jones (1981) to test for significant differences between the mean directions of the normal and reversed groups (inverting the reversed group through the origin):

Geographic coords. Test value = 0.0108
Stratigraphic coords. Test value = 0.2925
Critical value = 0.3950 for 95% confidence

Therefore, we must accept the hypothesis that the normal and reversed groups share a common mean direction in both geographic and stratigraphic coordinates. i.e. positive reversal test at 95% confidence level.

Chapter 8 - The relative autochthons of the Peloponnesos.

Site BH Reversal test.

		Geographic				Stratigraphic			
	N	Dec	Inc	K	R	Dec	Inc	K	R
Norm	10	075	59	109	9.92	108	52	109	9.92
Rev	5	269	-48	81	4.95	286	-37	77	4.95

Testing for common precision parameters (F-test of McElhinny, 1964):

Geographic coords. $K_1/K_2 = 1.35$
Stratigraphic coords. $K_1/K_2 = 1.42$
Critical value $K_1/K_2 > 2.51$ for 95% confidence

Therefore, in both cases we may accept the hypothesis that the normal and reversed groups share a common K.

Using the fold test of McFadden and Jones (1981) to test for significant differences between the mean directions of the normal and reversed groups (inverting the reversed group through the origin):

Geographic coords. Test value = 0.7466
Stratigraphic coords. Test value = 0.8736
Critical value = 0.2059 for 95% confidence

Therefore, we must reject the hypothesis that the normal and reversed groups share a common mean direction in both geographic and stratigraphic coordinates. i.e. negative reversal test at 95% confidence level.

Chapter 9 - The Pindos thrust sheets.

Sites BC, IA and XY.

		Geographic				Stratigraphic			
	N	Dec	Inc	K	R	Dec	Inc	K	R
BC	39	205	-21	21	37.19	208	-26	29	37.69
IA	13	189	-46	71	12.83	204	-23	71	12.83
XY	13	189	-36	22	12.45	207	-24	22	12.45

Testing for common precision parameters (McFadden and Lowes, 1981):

Geographic coords. E = 12.40
Stratigraphic coords. E = 8.70
Critical value = 9.21 for 99% confidence

Therefore, we may accept the hypothesis that the 3 sites share a common K in stratigraphic coordinates, but not in geographic coordinates.

Fold test of McFadden and Jones (1981):

Geographic coords. Test value (f) = 17.80
Stratigraphic coords. Test value (f) = 0.46
Critical value = 3.48 for 99% confidence

Therefore, we must accept the hypothesis that the 3 sites share a common mean direction in stratigraphic coordinates. Although strictly we should not use the McFadden and Jones (1981) test in geographic coordinates in this case, because the sites do not share a common precision parameter, the results suggest that there are significant differences between the site mean directions before tilt correction. i.e. a positive fold test at the 99% confidence level.

BIBLIOGRAPHY.

BIBLIOGRAPHY.

ABRAHAMSEN, N., & SCHÖNHARTING, G., 1987, Palaeomagnetic timing of the rotation and translation of Cyprus. *Earth Planet. Sci. Letts.*, **81**, 409-418.

ALLASINAZ, A., GUTNIC, M., & POISSON, A., 1974, La formation de L'Isparta Cay: calcaires à Halobies, grès à plantes, et radiolarites d'âge Carnien (?) Norien (Taurides-Région d'Isparta-Turquie). *Schr. Erdwiss. Komm. Oster. Akad.*, **2**, 11-21.

ALLERTON, S., 1988a, Palaeomagnetic and structural studies of the Troodos ophiolite, Cyprus. *Unpubl. PhD Thesis, Univ. East Anglia*, 232pp.

ALLERTON, S., 1988b, Fault block rotations in ophiolites: Results of palaeomagnetic studies in the Troodos Complex, Cyprus. in: C. KISSEL & C. LAJ (eds.), *Palaeomagnetic rotations and continental deformation*. NATO ASI Series C, **254**, 393-410.

ALLERTON, S., 1989, Distortions, rotations and crustal thinning at ridge-transform intersections. *Nature*, **340**, 626-628.

ALLERTON, S., 1990, Palaeomagnetic and structural studies of the Troodos ophiolite, Cyprus. in: *Ophiolites and oceanic lithosphere*, Proceedings of International Conference, Nicosia, Cyprus 1988, in press.

ALLERTON, S., *in prep.*, Palaeomagnetic and structural studies of the south-eastern part of the Troodos Complex.

ALLERTON, S., & VINE, F. J., 1987, Spreading structure of the Troodos ophiolite, Cyprus: Some paleomagnetic constraints. *Geology*, **15**, 593-597.

ANONYMOUS, 1972, Penrose field conference on ophiolites. *Geotimes*, **17**, 24-25.

ARGAND, E., 1924, La tectonique de l'Asie. *Proc. Int. Geol. Congr.*, **13**, 171-372.

AUBOUIN, J., BONNEAU, M., CELET, P., CHARVET, J., CLEMENT, B., DEGARDIN, J. M., DERCOURT, J., FERRIERE, J., FLEURY, J. J., GUERNET, C., MAILLOT, H., MANIA, J., MANSY, J. L., TERRY, J., THIEBAULT, P., TSOFLIAS, P., & VERRIEUX, J. J., 1970, Contribution a la géologie des Héllenides: Le Gavrovo, Le Pinde et la Zone Ophiolitique Subpelagonian. *Annales de la Societié Géologique du Nord*, **90**, 277-306.

BACHMANN, G. H., & RISCH, H., 1979, Die geologische Entstehung der Argolis-Halbinsel (Peloponnesus, Greichenland). *Geologie Jahrbuch, Reihe B*, **32**, 160pp.

BANNERT, D., & BENDER, H., 1968, Zur Geologie der Argolis-Halbinsel (Peloponnes, Greichenland). *Geologica et Palaeontologica*, **2**, 151-162.

BARKA, A. A., & HANCOCK, P. L., 1984, Neotectonic deformation patterns in the convex-northwards arc of the North Anatolian fault zone. in: DIXON, J. E., & ROBERTSON, A. H. F. (eds.), The geological evolution of the Eastern Mediterranean, *Spec. Pub. Geol. Soc. Lond.* **17**, 763-774.

BAUMGARTNER, P. O., 1985, Jurassic sedimentary evolution and nappe emplacement in the Argolis Peninsula (Peloponnesus, Greece). *Memoire de la Societé Helvetique pour la Science Naturelle*, 111pp.

BECK, M. E., 1976, Discordant palaeomagnetic pole positions as evidence for regional shear in the western Cordillera of North America. *Am. J. Sci.*, **276**, 694-712.

BERNOULLI, D., GRACIANSKY, P. C., & MONOD, O., 1974, The extension of the Lycian Nappes (SW Turkey) into the southeastern Aegean islands. *Eclogae Geologicae Helvetiae*, **67**, 39-90.

BESKE-DIEHL, S., & BANERJEE, S. K., 1980, Metamorphism in the Troodos ophiolite: Implications for marine magnetic anomalies. *Nature*, **285**, 563-564.

BLOME, C. D., & IRWIN, W. P., 1985, Equivalent radiolarian ages from ophiolite terrains of Cyprus and Oman. *Geology*, **13**, 401-404.

BONHOMMET, N., ROPERCH, P., & CALZA, F., 1988, Paleomagnetic arguments for block rotations along the Arakapas Fault (Cyprus). *Geology*, **16**, 422-425.

BOYLE, J. F., 1984, The origin and geochemistry of the metalliferous sediments of the Troodos massif, Cyprus. *Unpubl. PhD Thesis, Univ. Edinburgh*, 277pp.

BOYLE, J. F., & ROBERTSON, A. H. F., 1984, Evolving metallogenesis at the Troodos spreading axis. in: GASS, I. G., LIPPARD, S. J., & SHELTON, A. W. (eds.), Ophiolites and Oceanic Lithosphere, *Spec. Publ. Geol. Soc. Lond.*, **13**, 169-181.

BRUNN, J. H., DE GRACIANSKY, P. CH., GUTNIC, M., JUTEAU, T., MARCOUX, R., MONOD, O., and POISSON, A., 1970, Structures majeures et corrélations stratigraphiques dans les Taurides occidentales. *Bull. Soc. géol. Fr.*, **12**, 515-556.

BRUNN, J. H., DUMONT, J. F., GRACIANSKY, P. C. DE, GUTNIC, M., JUTEAU, T., MARCOUX, J., MONOD, O., & POISSON, A., 1971, Outline of the geology of the western Taurids. in: CAMPBELL, A. S. (ed), *Geology and History of Turkey*. Petrol. Explor. Soc. Libya, Tripoli, 225-252.

BRUNN, J. H., RICOU, L. E., POISSON, A., MARCOUX, J., & GRACIANSKY, P. C. DE, 1976, Eléments majeurs de liason entre Taurides et Hellénides. *Bull. géol. Soc. France*, **18**, 481-497.

BULLARD, E. C., EVERETT, J. E., & SMITH, A. G., 1965, The fit of the continents around the Atlantic. *Phil. Trans. R. Soc. Lond.*, **A258**, 41-51.

CAMERON, W. E., 1985, Petrology and origin of primitive lavas from the Troodos ophiolite, Cyprus. *Contrib. Mineral. Petrol.*, **89**, 239-255.

CAREY, W. S., 1955, The orocline concept in geotectonics. *Pap. Proc. R. Soc. Tasmania*, **89**, 255-288.

CELET, P., & FERRIERE, J., 1978, Les Hellénides internes: Le Pélagonien. *Eclogae Geologicae Helvetiae*, **73**, 467-495.

CHANNELL, J. E. T., 1977, Palaeomagnetism of limestones from the Gargano Peninsula, (Italy), and the implications of these data. *Geophys. J. R. astr. Soc.*, **51**, 605-616.

CHANNELL, J. E. T., D'ARGENIO, B., & HORVATH, F., 1979, Adria, the African promontory, in Mesozoic Mediterranean palaeogeography. *Earth Sci. Rev.*, **15**, 213-292.

CHANNELL, J. E. T., FREEMAN, R., HELLER, F., & LOWRIE, W., 1982, Timing of diagenetic haematite growth in red pelagic limestones from Gubbio (Italy). *Earth Planet. Sci. Letts.*, **58**, 189-201.

CLIFT, P. D., 1990, Mesozoic/Cenozoic sedimentation and tectonics of the southern Greek Neotethys (Argolis Peninsula). *Unpubl. PhD Thesis, Univ. Edinburgh*, 337pp.

CLIFT, P. D., & ROBERTSON, A. H. F., 1989, Evidence of a late Mesozoic ocean basin and subduction-accretion in the southern Greek Neo-Tethys. *Geology*, **17**, 559-563.

CLIFT, P. D., & ROBERTSON, A. H. F., 1990, Mesozoic intraplatform basins in Argolis, Southern Greece. *J. Geol. Soc. Lond.*, in press.

CLUBE, T. M. M., 1986, The palaeorotation of the Troodos microplate. *Unpubl. PhD Thesis, Univ. Edinburgh*, 275pp.

CLUBE, T. M. M., CREER, K. M., & ROBERTSON, A. H. F., 1985, The palaeorotation of the Troodos microplate. *Nature*, **63**, 522-525.

CLUBE, T. M. M., & ROBERTSON, A. H. F., 1986, The palaeorotation of the Troodos microplate, Cyprus, in the Late Mesozoic - Early Cenozoic plate tectonic framework of the Eastern Mediterranean. *Surveys in Geophysics*, **8**, 375-437.

COLLINSON, D. W., 1983, *Methods in Palaeomagnetism and Rock Magnetism*. Chapman & Hall, London, 500pp.

CREER, K. M. , & SANVER, M., 1967, The use of the sun compass. in: COLLINSON, D. W., CREER, K. M., & RUNCORN, S. K. (eds.), *Methods in Palaeomagnetism*. Elsevier, Amsterdam, 11-15.

DECROUEZ, D., 1977a, Etude stratigraphique du Crétacé d'Argolide (Péloponnèse septentrional, Grèce). 1 - Introduction générale et la Formation de l'Akros (domaine ophiolitique éxterne). *Note du Laboratoire de Paleontologie de l'Université de Genève*, **No. 3.**, 8pp.

DECROUEZ, D., 1977b, Etude stratigraphique du Crétacé d'Argolide (Péloponnèse septentrional, Grèce). 2 - La Formation de la Palamède (sous-zone de Trapezona). *Note du Laboratoire de Paleontologie de l'Université de Genève*, **No. 4.**, 6pp.

DELAUNE-MAYERE, M., MARCOUX, J., PARROT, J.-F., & Poisson, A., 1977, Modèle d'évolution Mésozoïque de la paléomarge Téthysienne au niveau des nappes radiolaritiques et ophiolitiques du Taurus Lycien, d'Antalya et du Baër Bassit. in: B. BIJU-DUVAL & L. MONTADERT (eds.), *Structural history of the Mediterranean Basins*, Editions Technip, Paris, 79-94.

DEMAREST Jnr, H. H., 1983, Error analysis for the determination of tectonic rotation from paleomagnetic data. *J. Geophys. Res.*, **88**, 4321-4328.

DERCOURT, J., 1964, Contribution a l'étude géologique d'un secteur du Peloponnèse septentrional. *Annales des Pays Hélleniques*, **15**, 417-467.

DERCOURT, J., ZONENSHAIN, L. P., RICOU, L.-E., KAZMIN, V. G., LE PICHON, X., KNIPPER, A. L., GRANDJACQUET, C., SBORTSHIKOV, I. M., GEYSSANT, J.,

LEPVRIER, C., PECHERSKY, D. H., BOULIN, J., SIBUET, J.-C., SAVOSTIN, L. A., SOROKHTIN, O., WESTPHAL, M., BAZHENOV, M. L., LAUER, J. P., & BIJU-DUVAL, B., 1986, Geological evolution of the Tethys belt from the Atlantic to the Pamirs since the Lias. *Tectonophysics*, **123**, 241-315.

DEWEY, J. F., PITMAN, W. C. 3rd, RYAN, W. B. F., & BONNIN, J., 1973, Plate tectonics and the evolution of the Alpine System. *Bull. Geol. Soc. Am.*, **84**, 3137-3180.

DUMONT, J. F., 1976, Etudes géologiques dans les Taurides Occidentales: Les formations paléozoiques et mésozoiques de la cupole de Karacahisar (Province d'Isparta, Turquie). *Unpubl. Ph.D Thesis, Université Paris Sud, France.*

DUMONT, J.-F., GUTNIC, M., MARCOUX, J., MONOD, O., & POISSON, A., 1972, Le Trias des Taurides occidentales (Turquie). Definition du bassin pamphylien: un nouveau domain à ophiolites à la marge externe de la chaîne taurique. *Zeit. Deutsch. Geol. Ges.*, **123**, 385-409.

DUNLOP, D. J., 1972, Magnetic mineralogy of unheated and heated red sediments by coercivity spectrum analysis. *Geophys. J. R. astr. Soc.*, **27**, 37-55.

EATON, S., 1986, The sedimentology of mid to Late Miocene carbonates and evaporates in southern Cyprus. *Unpubl. PhD Thesis, Univ. Edinburgh*, 240pp.

ELMORE, R. D., ENGEL, M. H., CRAWFORD, L., NICK, K., IMBUS, S., & SOFER, Z., 1987, Evidence for a relationship between hydrocarbons and authigenic magnetite. *Nature*, **325**, 428-430.

ENGLAND, P., & MOLNAR, P., 1990, Right-lateral shear and rotation as the explanation for strike-slip faulting in eastern Tibet. *Nature*, **344**, 140-142.

EVANS, I., HALL, S. A., CARMAN, M. F., SENALP, M., & COSKUN, S., 1982, A palaeomagnetic study of the Bilecik limestone (Jurassic), North-western Anatolia. *Earth Planet. Sci. Letts.*, **61**, 399-411.

FOX, P. J., & GALLO, D. G., 1984, A tectonic model for ridge-transform-ridge plate boundaries: implications for the structure of oceanic lithosphere. *Tectonophysics*, **104**, 205-242.

FREUND, R., 1970, Rotation of strike-slip faults in Sistan, southeastern Iran. *Jour. Geol.*, **78**, 188-200.

FYTIKAS, M., INNOCENTI, F., MANETTI, P., MAZZOULI, R., PECCERILLO, A., & VILLARI, L., 1984, Tertiary to Quaternary evolution of volcanism in the Aegean region. in: DIXON, J. E., & ROBERTSON, A. H. F. (eds.), The geological evolution of the Eastern Mediterranean, *Spec. Pub. Geol. Soc. Lond.* **17**, 687-699.

GASS, I. G., 1968, Is the Troodos Complex, Cyprus, formed by sea-floor spreading?. *Nature*, **220**, 39-42.

GASS, I. G., 1980, The Troodos massif: its role in the unravelling of the ophiolite problem and its significance in the understanding of constructive plate margin processes. in: PANAYIOTOU, A. (ed.), *Ophiolites*, Proceedings of International Ophiolite Symposium, Nicosia, Cyprus, 1979, 23-35.

GASS, I. G., & SMEWING, J. D., 1973, Intrusion, extrusion and metamorphism at constructive margins: evidence from the Troodos Massif, Cyprus. *Nature*, **242**, 26-29.

GLENNIE, K. W., BOEUF, M. G. A., HUGHES-CLARKE, M. W., MOODY-STUART, M., PILAAR, W. F. H., & REINHARDT, B. M., 1973, Late Cretaceous nappes in the Oman Mountains and their geological evolution. *Bull. Am. Ass. Petrol. Geol.*, **57**, 5-27.

GOREE, W. S., & FULLER, M., 1976, Magnetometers using RF-driven SQUIDs and their applications in rock magnetism and paleomagnetism. *Revs. Geophys. Space Phys.*, **14**, 591-608.

GRAHAM, J. W., 1949, The stability and significance of magnetism in sedimentary rocks. *J. Geophys. Res.*, **54**, 131-167.

GREGOR, C. B., & ZIJDERVELD, J. D. A., 1964, Palaeomagnetism and Alpine tectonics of Eurasia, part 1. The magnetism of some Permian red sandstones from northwestern Turkey. *Tectonophysics*, **1**, 189-306.

HALLS, H. C., 1976, A least-squares method to find a remanence direction from converging remagnetisation circles. *Geophys. J. R. astr. Soc.*, **45**, 297-304.

HARLAND, W. B., COX, A. V., LLEWELLYN, P. G., PICKTON, C. A. G., SMITH, A. G., & WALTERS, R., 1982, *A geologic time scale*. Cambridge Univ. Press, 131pp.

HARRISON, C. G. A., 1980, Analysis of the magnetic vector in a single rock specimen. *Geophys. J. R. astr. Soc.*, **60**, 489-492.

HAYWOOD, A. B., 1984, Miocene clastic sedimentation related to the emplacement of the Lycian Nappes and the Antalya Complex, S. W. Turkey. in: DIXON, J. E., & ROBERTSON, A. H. F. (eds.), The geological evolution of the Eastern Mediterranean, *Spec. Pub. Geol. Soc. Lond.* **17**, 287-300.

HAYWOOD, A. B., & ROBERTSON, A. H. F., 1982, Direction of ophiolite emplacement inferred from Tertiary and Cretaceous sediments of an adjacent autochthon; the Bey Daglari, S. W. Turkey. *Bull. geol. Soc. Am.*, **93**, 68-75.

HELLER, F., 1977, Palaeomagnetism of the Upper Jurassic limestones from Southern Germany. *J. Geophys.*, **42**, 475-488.

HORNER, F., & FREEMAN, R., 1983, Palaeomagnetic evidence from pelagic limestones for clockwise rotation of the Ionian zone, western Greece. *Tectonophysics*, **98**, 11-27.

IRVING, E., 1957, The origin of the palaeomagnetism of the Torridonian Sandstones of north-west Scotland. *Phil. Trans. R. Soc. Lond.*, **A250**, 100-110.

IRVING, E., 1977, Drift of the major continental blocks since the Devonian. *Nature*, **270**, 304-309.

JACKSON, J. A., KING, G., & VITA-FINZI, C., 1982, The neotectonics of the Aegean: an alternative view. *Earth Planet. Sci. Letts.*, **61**, 303-318.

JACKSON, M., MCCABE, C., BALLARD, M. M., & VAN DER VOO, R., 1988, Magnetite authigenesis and diagenetic paleotemperatures across the northern Appalachian basin. *Geology*, **16**, 592-595.

JENKINS, D. A. L., 1972, Structural development of Western Greece. *Bull. Am. Ass. Petrol. Geol.*, **56**, 128-149.

JOHNSON, H. P., LOWRIE, W., & KENT, D. V., 1975, Stability of anhysteretic remanent magnetisation in fine and coarse magnetite and maghemite particles. *Geophys. J. Roy. astr. Soc.*, **41**, 1-10.

JONES, G., 1990, Tectono-stratigraphy and evolution of the Mesozoic Pindos Ophiolite and associated units, northwest Greece. *Unpubl. PhD Thesis, Univ. Edinburgh.*

JONES, G., & ROBERTSON, A. H. F., 1990, Tectono-stratigraphy and evolution of the Mesozoic Pindos ophiolite and related units in northwest Greece: an integrated

supra-subduction zone spreading and subduction-accretion model. *J. Geol. Soc. Lond.*, in press.

JUTEAU, T., 1975, Les ophiolites des Nappes d'Antalya (Taurides occidentales, Turquie). Pétrologie d'un fragment de l'ancienne croûte océanique téthysienne. *Sciences de la Terre, Nancy, Mém.*, **32**, 692pp.

KING, R. F., 1955, The remanent magnetism of artificially deposited sediments. *Monthly Notices R. astr. Soc, Geophys. Supp*, **7**, 115-134.

KISSEL, C., & LAJ, C., 1988, The Tertiary geodynamical evolution of the Aegean arc: a palaeomagnetic reconstruction. *Tectonophysics*, **146**, 183-201.

KISSEL, C., & POISSON, A., 1986, Etude paléomagnétique préliminaire de formations néogènes du bassin d'Antalya (Taurides occidentales, Turquie). *C. R. Acad. Sci. Paris*, **302**(II-10), 711-716.

KISSEL, C., & POISSON, A., 1987, Etude paléomagnétique des formations cénozoïques des Bey Daglari (Taurides occidentales). *C. R. Acad. Sci. Paris*, **304**, 343-348.

KISSEL, C., KONDOPOULOU, D., LAJ, C., & PAPADOPOULOS, P., 1986b, New paleomagnetic data from Oligocene formations of Northern Aegea. *Geophys. Res. Letts.*, **13**, 1039-1042.

KISSEL, C., LAJ, C., & MAZAUD, A., 1986c, First palaeomagnetic results from Neogene formations in Evia, Skyros and the Volos region and the deformation of central Aegea. *Geophys. Res. Lett.*, **13**, 1446-1449.

KISSEL, C., LAJ, C., & MULLER, C., 1985, Tertiary geodynamical evolution of Northwestern Greece: palaeomagnetic results. *Earth Planet. Sci. Letts.*, **72**, 190-204.

KISSEL, C., LAJ, C., POISSON, A., & SIMEAKIS, K., 1988, A pattern of block rotations in central Aegea. in: C. KISSEL & C. LAJ (eds.), *Palaeomagnetic rotations and continental deformation*. NATO ASI Series C, **254**, 115-129.

KISSEL, C., LAJ, C., POISSON, A., SAVAŞÇIN, Y., SIMEAKIS, K., & MERCIER, J. L., 1986a, Paleomagnetic evidence for Neogene rotational deformations in the Aegean domain. *Tectonics*, **5**, 783-796.

KISSEL,. C., JAMET, M., & LAJ, C., 1984, Paleomagnetic evidence of Miocene and Pliocene rotational deformations of the Aegean area. in: DIXON, J. E., &

ROBERTSON, A. H. F. (eds.), The geological evolution of the Eastern Mediterranean, *Spec. Pub. Geol. Soc. Lond.* **17**, 669-679.

KONDOPOULOU, D., & WESTPHAL, M., 1986, Paleomagnetism of the Tertiary intrusives from Chalkidiki (Northern Greece). *J. Geophys.*, **59**, 62-66.

KRYSTYN, L., & MARIOLAKIS, I., 1975, Stratigraphie und Tektonik der Halstatter Scholle von Epidavros (Greichenland). *Sitzungberichte der Akademie der Wissenschaften in Wien. Mathematisch-naturwissenschaftliche. Klasse (1)*, **184**, 181-195.

LAJ, C., JAMET, M., SOREL, D., & VALENTE, J. P., 1982, First palaeomagnetic results from the Mio-Pliocene series of the Hellenic sedimentary arc. *Tectonophysics*, **86**, 45-67.

LAUER, J. P., 1981, L'evolution geodynamique de la Turquie et de la Chypre deduite de l'etude paleomagnetique. *Unpubl. Doctorat-Es-Sciences These, Univ. Strasbourg, France*, 292pp.

LAUER, J. P., 1984, Geodynamic evolution of Turkey and Cyprus based on palaeomagnetic data. in: DIXON, J. E., & ROBERTSON, A. H. F. (eds.), The geological evolution of the Eastern Mediterranean, *Spec. Pub. Geol. Soc. Lond.* **17**, 483-491.

LAUER, J. -P., & BARRY, P., 1976, Etude paleomagnetique des ophiolites de Chypre. *4eme Reunion Ann. Sci. Terre Paris*, 205.

LE PICHON, X., 1968, Sea-floor spreading and continental drift. *J. Geophys. Res.*, **73**, 3661-3697.

LE PICHON, X., & ANGELIER, J., 1979, The Hellenic Arc and Trench system: a key to the neotectonic evolution of the eastern Mediterranean area. *Tectonophysics*, **60**, 1-42.

LEFEVRE, R., 1967, Un nouvel element de la geologie du Taurus lycien: les nappes d'Antalya (Turquie). *C. R. Seances Acad. Sci. Paris*, **165**, 1365-1368.

LIVERMORE, R. A., & SMITH, A. G., 1984, Some boundary conditions for the evolution of the Mediterranean region. in: *Proc. NATO A.R.I., Erice, Sicily, Volume on Mediterranean tectonics.*

LOWRIE, W., & FULLER, M. D., 1971, On the alternating field demagnetisation characteristics of multi-domain thermoremanent magnetisation in magnetite. *J. Geophys. Res.*, **76**, 6339-6349.

LOWRIE, W., & ALVAREZ, W., 1975, Palaeomagnetic evidence for the rotation of the Italian Peninsula. *J. Geophys. Res.*, **80**, 1579-1592.

LOWRIE, W., & HELLER, F., 1982, Magnetic properties of marine limestones. *Revs. Geophys. Space Phys.*, **20**, 171-192.

LOWRIE, W., CHANNELL, J. E. T., & HELLER, F., 1980, On the credibility of remanent magnetization measurements. *Geophys. J. R. astr. Soc.*, **60**, 493-496.

LYBERIS, N., ANGELIER, J., BARRIER, E., & LALLEMANT, S., 1982, Active deformation of a segment of arc: the strait of Kythira, Hellenic arc, Greece. *J. Structural Geol.*, **4**, 299-311.

MACDONALD, W. D., 1980, Net tectonic rotation, apparent tectonic rotation, and the structural tilt correction in palaeomagnetic studies. *J. Geophys. Res.*, **85**, 3659-3669.

MACLEOD, C. J., 1988, The tectonic evolution of the Eastern Limassol Forest Complex, Cyprus. *Unpubl. PhD Thesis, Open Univ.*, 231pp.

MACLEOD, C. J., 1990, Role of the Southern Troodos Transform Fault in the rotation of the Cyprus microplate: evidence from the Eastern Limassol Forest Complex. in: *Ophiolites and oceanic lithosphere*, Proceedings of International Conference, Nicosia, Cyprus 1988, in press.

MAKRIS, J., BEN-AVRAHAM, Z., BEHLE, A., GINZBURG, A., GIESE, P., STEINMETZ, A., ELEFTHERION, S., & WHITMARSH., B., 1983, Deep seismic soundings between Cyprus and Israel and their interpretation. *Geophys. J. R. astr. Soc.*, **75**, 575-591.

MANTIS, M., 1970, Upper Cretaceous - Tertiary foraminiferal zones in Cyprus. *Epitiris*, **3**, 227-241.

MARCOUX, J., RICOU, L. E., BURG, J. P., & BRUN, J. P., 1989, Shear-sense criteria in the Antalya and Alanya thrust system (southwestern Turkey): evidence for a southward emplacement. *Tectonophysics*, **161**, 81-91.

MCCABE, C., JACKSON, M., & SAFFER, B., 1989, Regional patterns of magnetite authigenesis in the Appalachian basin: implications for the mechanism of Late Paleozoic remagnetisation. *J. Geophys. Res*, **94**, 10429-10443.

MCCULLOCH, M. T., & CAMERON, W. C., 1983, Nd-Sr isotopic study of primitive lavas from the Troodos ophiolite, Cyprus: evidence for a subduction-related setting. *Geology*, **11**, 727-731.

MCELHINNY, M. W., 1964, Statistical significance of the fold test in palaeomagnetism. *Geophys. J. Roy. astr. Soc.*, **8**, 338-340.

MCELHINNY, M. W., 1967, Statistics of a spherical distribution. in: COLLINSON, D. W., CREER, K. M., & RUNCORN, S. K. (eds.), *Methods in Palaeomagnetism*. Elsevier, Amsterdam, 313-321.

MCFADDEN, P. L., & JONES, D. L., 1981, The fold test in palaeomagnetism. *Geophys. J. Roy. astr. Soc.*, **67**, 53-58.

MCFADDEN, P. L., & LOWES, F. J., 1981, The discrimination of mean directions drawn from Fisher distributions. *Geophys. J. Roy. astr. Soc*, **67**, 19-33.

MCKENZIE, D., 1972, Active tectonics of the Mediterranean region. *Geophys. J. Roy. astr. Soc*, **30**, 109-185.

MCKENZIE, D., 1978, Active tectonics of the Alpine-Himalayan Belt: The Aegean sea and surrounding regions. *Geophys. J. Roy. astr. Soc*, **55**, 217-254.

MCKENZIE, D., 1982, Active tectonics of the Alpine-Himalayan belt: the Aegean Sea and surrounding regions. *Geophys. J. R. astr. Soc.*, **55**, 217-254.

MCKENZIE, D., 1990, Spinning continents. *Nature*, **344**, 109-110.

MCKENZIE, D., & JACKSON, J. A., 1983, The relationship between strain rates, crustal thickening, palaeomagnetism, finite strain and fault movements within a deforming zone. *Earth Planet. Sci. Letts.*, **65**, 182-202.

MCKENZIE, D., & JACKSON, J. A., 1986, A block model of distributed deformation by faulting. *J. Geol. Soc. Lond.*, **143**, 349-353.

MCKENZIE, D., & JACKSON, J. A., 1988, The kinematics and dynamics of distributed deformation. in: C. KISSEL & C. LAJ (eds.), *Palaeomagnetic rotations and continental deformation.* NATO ASI Series C, **254**, 17-31.

MERCIER, J., DELIBASSIS, N., GAUTHIER, A., JARRIGE, J., LEMEILLE, F., PHILIP, H., SEBRIER, M., & SOREL, D., 1979, La néotectonique de l'arc Egéen. *Révue Geographie physique et Géologie dynamique*, **21**, 67-92.

MEULENKAMP, J.E, WORTEL, M. J. R., VAN WAMEL, W. A., SPAKMAN, W., & HOOGERDUYN STRATING, E., 1988, On the Hellenic subduction zone and the geodynamic evolution of Crete since the late Middle Miocene. *Tectonophysics*, **146**, 203-215.

MOLNAR, P., & TAPPONNIER, P., 1975, Cenozoic tectonics of Asia: effects of a continental collision. *Science*, **189**, 419-426.

MONOD, O., 1977, Recherches géologiques dans le Taurus occidental au Sud de Beysehir (Turquie). *Unpubl. PhD Thesis, Univ. Paris-Sud, Orsay, France*, 511pp.

MONOD, O., 1978, Guzelsu Akseki bölgesindeki Antalya Naplari üzerine aciklama (Orta Bati Toroslar-Türkiye) - Precisions upon the Antalya Nappes in the region of Güzelsü-Akseki (Western Taurus, Turkey). *Bull. Geol. Soc. Turkey*, **21**,27-29.

MOORES, E. M., ROBINSON, P. T., MALPAS, J., & XENOPHONTOS, C., 1984, A model for the origin of the Troodos Massif, Cyprus and other mideast ophiolites. *Geology*, **12**, 500-503.

MOORES, E. M., & VINE, F. J., 1971, The Troodos massif, Cyprus and other ophiolites as oceanic crust: evaluation and implications. *Phil. Trans. Roy. Soc. Lond. A.*, **268**, 443-466.

MORRIS, A., CREER, K. M., & ROBERTSON, A. H. F., 1990, Palaeomagnetic evidence for clockwise rotations related to dextral shear along the Southern Troodos Transform Fault, Cyprus. *Accepted by Earth Planet. Sci. Letts.*

MUKASA, S. B., & LUDDEN, J. N., 1987, Uranium-lead ages of plagiogranites from the Troodos ophiolite, Cyprus, and their tectonic significance. *Geology*, **15**, 825-828.

MURTON, B. J., 1986, Anomalous oceanic lithosphere formed in a leaky transform fault: evidence from the Western Limassol Forest Complex, Cyprus. *J. geol. Soc. London*, **143**, 845-854.

MURTON, B. J., 1987, Suprasubduction transform activity along the southern Troodos ophiolite: a microplate margin. *Abstracts of papers accepted for oral and poster presentation; Symposium, Troodos 87, 'Ophiolites and oceanic lithosphere', Nicosia, Cyprus, 4-10 October, 1987, Geological Survey Department, Nicosia*, p27.

MURTON, B. J., & GASS, I. G., 1986, Western Limassol Forest complex, Cyprus: part of an Upper Cretaceous leaky transform fault. *Geology*, **14**, 255-258.

NUR, A., RON, H., & SCOTTI, O., 1988, Mechanics of distributed fault and block rotation. in: C. KISSEL & C. LAJ (eds.), *Palaeomagnetic rotations and continental deformation*. NATO ASI Series C, **254**, 209-228.

OKAY, A. I., & ÖZGÜL, N., 1984, HP/LT metamorphism and the structure of the Alanya Massif, Southern Turkey: an allochthonous composite tectonic sheet. in: DIXON, J. E., & ROBERTSON, A. H. F. (eds.), The geological evolution of the Eastern Mediterranean, *Spec. Pub. Geol. Soc. Lond.* **17**, 429-439.

OLIVER, J., 1986, Fluids expelled tectonically from orogenic belts: their role in hydrocarbon migration and other geological phenomena. *Geology*, **14**, 99-102.

PE-PIPER, G., 1982, Geochemistry, tectonic setting and metamorphism of mid-Triassic volcanic rocks of Greece. *Tectonophysics*, **85**, 253-272.

PE-PIPER, G., & PIPER, D. W. J., 1984, Tectonic setting of the Mesozoic Pindos basin of the Peloponnese, Greece. in: DIXON, J. E., & ROBERTSON, A. H. F. (eds.), The geological evolution of the Eastern Mediterranean, *Spec. Pub. Geol. Soc. Lond.* **17**, 563-568.

PEARCE, J. A., 1975, Basalt geochemistry used to investigate past tectonic environments on Cyprus. *Tectonophysics.*, **25**, 41-67.

PIPER, J. D. A., 1987, *Palaeomagnetism and the continental crust*. Open University Press, Milton Keynes, 434pp.

PITMAN, W. C. 3rd, & TALWANI, M., Sea-floor spreading in the North Atlantic. *Geol. Soc. Am. Bull.*, **83**, 619-646.

POISSON, A., 1977, Recherches géologiques dans les Taurides occidentales, Turquie. *Unpubl. PhD Thesis, Univ. Paris-Sud, Orsay, France*, 790pp.

POISSON, A., 1984, The extension of the Ionian trough into southwestern Turkey. in: DIXON, J. E., & ROBERTSON, A. H. F. (eds.), The geological evolution of the Eastern Mediterranean, *Spec. Pub. Geol. Soc. Lond.* **17**, 241-249.

PUCHER, R., BANNERT, D, & FROMM, K., 1974, Palaeomagnetism in Greece: indications for relative block movement. *Tectonophysics*, **22**, 31-39.

PULLAIAH, G., IRVING, E., BUCHAN, K. L., & DUNLOP, D. J., 1975, Magnetization changes caused by burial and uplift. *Earth Planet. Sci. Letts.*, **28**, 133-143.

REUBER, I, 1984, Mylonitic ductile shear zones within tectonites and cumulates as evidence for an oceanic transform fault in the Antalya ophiolite, S. W. Turkey. in: DIXON, J. E., & ROBERTSON, A. H. F. (eds.), The geological evolution of the Eastern Mediterranean, *Spec. Pub. Geol. Soc. Lond.* **17**, 319-334.

RICOU, L. E., MARCOUX, J., & POISSON, A., 1979, L'allochthonie des Bey Daglari orientaux. Reconstruction palinspastiques des Taurides occidentales. *Bull. Soc. Geol. Fr.*, **21**, 125-133.

RICOU, L. E., MARCOUX, J., & WHITECHURCH, H., 1984, The Mesozoic organization of the Taurides: one or several ocean basins? in: DIXON, J. E., & ROBERTSON, A. H. F. (eds.), The geological evolution of the Eastern Mediterranean, *Spec. Pub. Geol. Soc. Lond.* **17**, 349-359.

ROBERTSON, A. H. F., 1975, Cyprus umbers: basalt-sediment relationships on a Mesozoic ocean ridge. *J. geol. Soc. Lond.*, **131**, 511-531.

ROBERTSON, A. H. F., 1976, Pelagic chalks and calciturbidites from the Lower Tertiary of the Troodos Massif, Cyprus. *J. Sediment. Petrol.*, **46**, 1007-1016.

ROBERTSON, A. H. F., 1977a, The Kannaviou Formation, Cyprus: volcaniclastic sedimentation of a probable Late Cretaceous volcanic arc. *J. geol. Soc. Lond.*, **134**, 269-292.

ROBERTSON, A. H. F., 1977b, Tertiary uplift history of the Troodos Massif, Cyprus. *Geol. Soc. Am. Bull.*, **88**, 1763-1772.

ROBERTSON, A. H. F., 1978, Metallogenesis along a fossil oceanic fracture zone: Arakapas fault belt, Troodos Massif, Cyprus. *Earth Planet. Sci. Letts.*, **41**, 317-329.

ROBERTSON, A. H. F., 1990, Tectonic evolution of Cyprus. in: *Ophiolites and oceanic lithosphere*, Proceedings of International Conference, Nicosia, Cyprus 1988, in press.

ROBERTSON, A. H. F., & DIXON, J. E., 1984, Introduction: aspects of the geological evolution of the Eastern Mediterranean. in: DIXON, J. E., & ROBERTSON, A. H. F. (eds.), The geological evolution of the Eastern Mediterranean, *Spec. Pub. Geol. Soc. Lond.* **17**, 1-74.

ROBERTSON, A. H. F., & HUDSON, J. D., 1974, Pelagic sediments in the Cretaceous and Tertiary history of the Troodos Massif, Cyprus. *Spec. Publ. Int. Assoc. Sedimentol.*, **1**, 403-436.

ROBERTSON, A. H. F., & WOODCOCK, N. H., 1980a, Tectonic setting of the Troodos Massif in the East Mediterranean. in: PANAYIOTOU, A. (ed.), *Ophiolites*, Proceedings of International Ophiolite Symposium, Nicosia, Cyprus, 1979, 36-49.

ROBERTSON, A. H. F., & WOODCOCK, N. H., 1980b, Strike-slip related sedimentation in the Antalya Complex, S. W. Turkey. *Spec. Publ. int. Ass. Sediment.*, 4, 127-145.

ROBERTSON, A. H. F., & WOODCOCK, N. H., 1981a, Bilelyeri Group, Antalya Complex: deposition on a Mesozoic continental margin in S. W. Turkey. *Sedimentology*, **28**, 381-399.

ROBERTSON, A. H. F., & WOODCOCK, N. H., 1981b, Alakir Çay Group, Antalya Complex, S. W. Turkey: a deformed Mesozoic carbonate margin. *Sediment. Geol.*, **30**, 95-131.

ROBERTSON, A. H. F., & WOODCOCK, N. H., 1981c, Gödene Zone, Antalya Complex: volcanism and sedimentation along a Mesozoic continental margin, S. W. Turkey. *Geol. Rundschau.*, **70**, 1177-1214.

ROBERTSON, A. H. F., & WOODCOCK, N. H., 1982, Sedimentary history of the south-western segment of the Mesozoic-Tertiary Antalya continental margin, south-western Turkey. *Eclogae Geologicae Helvetiae*, **75**, 517-562.

ROBERTSON, A. H. F., & WOODCOCK, N. H., 1984, The S. W. segment of the Antalya Complex, Turkey as a Mesozoic-Tertiary Tethyan continental margin. in: DIXON, J. E., & ROBERTSON, A. H. F. (eds.), The geological evolution of the Eastern Mediterranean, *Spec. Pub. Geol. Soc. Lond.* **17**, 251-271.

ROBERTSON, A. H. F., CLIFT, P. D., DEGNAN, P., & JONES, G., in press, Palaeoceanography of the Eastern Mediterranean Neotethys.

ROBERTSON, A. H. F., VARNAVAS, S. P., & PANAGOS, A. G., 1987, Ocean ridge origin and tectonic setting of Mesozoic sulphide and oxide deposits of the Argolis Peninsula of the Peloponnesus, Greece. *Sedimentary Geol.*, **53**, 1-32.

ROBINSON, P. T., 1987, The Troodos ophiolite of Cyprus: new perspectives on its origin and emplacement. *Abstracts of papers accepted for oral and poster presentation; Symposium, Troodos 87, Ophiolites and oceanic lithosphere, Nicosia, Cyprus, 4-10 October, 1987, Geological Survey Department, Nicosia*, p3.

ROBINSON, P. T., MELSON, W. G., O'HEARN, T., & SCHMINCKE, H. U., 1983, Volcanic glass compositions of the Troodos ophiolite, Cyprus. *Geology*, **11**, 400-404.

RON, H., FREUND, R., GARFUNKEL, Z., & NUR, A., 1984, Block rotation by strike-slip faulting: structural and palaeomagnetic evidence. *J. Geophys. Res.*, **89**, 6256-6270.

SARIBUDAK, M., SANVER, M., & PONAT, E., 1989, Location of the western Pontides, NW Turkey, during Triassic time: preliminary palaeomagnetic results. *Geophys. J.*, **96**, 43-50.

SAVOSTIN, L. A., SIBUET, J.-C., ZONENSHAIN, L. P., LE PICHON, X., & ROULET, M.-J., 1986, Kinematic evolution of the Tethys Belt from the Atlantic Ocean to the Pamirs since the Triassic. *Tectonophysics*, **123**, 1-35.

SCHMINCKE, H. U., RAUTENSCHLEIN, M., ROBINSON, P.T., & MEHEGAN, J. M., 1983, Troodos extrusive series of Cyprus: a comparison with oceanic crust. *Geology*, **11**, 405-409.

SEARLE, R. C., 1983, Multiple closely spaced transform faults in fast-slipping fracture zones. *Geology*, **11**, 607-610.

SENGÖR, A. M. C., 1979, The North Anatolian transform fault: its age, offset and tectonic significance. *J. Geol. Soc. Lond.*, **136**, 269-282.

SENGÖR, A. M. C., & YILMAZ, Y., 1981, Tethyan evolution of Turkey: a plate tectonic approach. *Tectonophysics*, **75**, 181-241.

SENGÖR, A. M. C., YILMAZ, Y., & SUNGURLU, O., 1984, Tectonics of the Mediterranean Cimmerides: nature and evolution of the western termination of

Palaeo-Tethys. in: DIXON, J. E., & ROBERTSON, A. H. F. (eds.), The geological evolution of the Eastern Mediterranean, *Spec. Pub. Geol. Soc. Lond.* **17**, 77-112.

SHELTON, A. W., & GASS, I. G., 1980, Rotation of the Cyprus microplate. in: PANAYIOTOU, A. (ed.), *Ophiolites*, Proceedings of International Ophiolite Symposium, Nicosia, Cyprus, 1979, 61-66.

SIMONIAN, K. A., & GASS, I. G., 1978, Arakapas Fault Belt Cyprus: A fossil transform belt. *Geol. Soc. Am. Bull.*, **89**, 1220-1230.

SMEWING, J. D., SIMONIAN, K. O., & GASS, I. G., 1975, Metabasalts from the Troodos Massif, Cyprus: genetic implication deduced from petrography and trace element geochemistry. *Contrib. Min. Petrol.*, **55**, 49-64.

SMITH, A. G., 1971, Alpine deformation and the oceanic areas of the Tethys, Mediterranean, and Atlantic. *Geol. Soc. Am. Bull.*, **82**, 2039-2070.

SMITH, A. G., & WOODCOCK, N. H., 1982, Tectonic syntheses of the Alpine-Mediterranean region: a review. *Alpine Mediterranean Geodynamics. Geodyn. Ser., Am. Geophys. Union*, **7**, 15-38.

SMITH, A. G., WOODCOCK, N. H., & NAYLOR, M. A., 1979, The structural evolution of a Mesozoic continental margin. *J. Geol. Soc. Lond.*, **136**, 589-603.

SMITH, G. C., & VINE, F. J., 1990, Physical property sections through the Troodos Ophiolite, Cyprus; a geophysical analogue of oceanic crust?. in: *Ophiolites and oceanic lithosphere*, Proceedings of International Conference, Nicosia, Cyprus 1988, in press.

SMITH, G. M., 1985, Source of marine magnetic anomalies: Some results from DSDP Leg 83. *Geology*, **13**, 162-165.

SMITH, G., 1985, Late Glacial palaeomagnetic secular variations from France. *Unpubl. PhD Thesis, Univ. Edinburgh*, 308pp.

SNAPE, C., 1971, An example of anhysteretic moments being induced by alternating field demagnetisation apparatus. *Geophys. J. R. astr. Soc.*, **23**, 361-364.

SOREL, D., & MERCIER, J. L., 1988, The onset of oceanic lithosphere subduction beneath the Aegean arc: data on its age from structural geology. palaeomagnetism and marine geology. *Abstracts of papers accepted for oral and poster presentation;*

Joint BSRG/TSG meeting, 'The structural and sedimentary evolution of the Neotectonic Aegean basins', London, 5-6 April, 1988.

STROOP, J. B., & FOX, P. J., 1981, Geological investigations in the Cayman trough: evidence for thin oceanic crust along the Mid-Cayman Rise. *J. Geol.*, **89**, 395-420.

SUESS, E., 1904-24, *The Face of the Earth*, Clarendon Press, Oxford.

TAPPONNIER, P., 1977, Evolution tectonique du Systéme Alpin en Méditerranée: poinçonnement et écrasement rigide-plastique. *Bull. Geol. Soc. Fr.*, **19**, 437-460.

TARLING, D. H., 1983, *Palaeomagnetism: principles and applications in geology, geophysics and archaeology.* Chapman and Hall, London, 379pp.

THIEBAULT, F., 1982, Evolution géodynamique des Héllenides externes en Peloponnese meridional (Grèce). *Societé Géologique du Nord*, **Publ. No. 6**, 2 vols, pp574.

TURNELL, H. B., 1988, Mesozoic evolution of Greek microplates from palaeomagnetic measurements. *Tectonophysics*, **155**, 307-316.

VAN DER VOO, R., 1968, Palaeomagnetism and Alpine tectonics of Eurasia, part 4. Jurassic, Cretaceous, and Eocene pole positions from NE Turkey. *Tectonophysics*, **6**, 251-269.

VAN DER VOO, R., 1969, Palaeomagnetic evidence for the rotation of the Iberian Peninsula. *Tectonophysics*, **7**, 5-56.

VAN DER VOO. R., & FRENCH, R. B., 1974, Apparent polar wandering for the Atlantic-bordering continents: Late Carboniferous to Eocene. *Earth Science Reviews*, **10**, 99-119.

VANDENBERG, J., & ZIJDERVELD, H., 1982, Palaeomagnetism in the Mediterranean area. *Alpine Mediterranean Geodynamics. Geodyn. Ser., Am. Geophys. Union*, **7**, 83-112.

VARGA, R. J., & MOORES, E. M., 1985, Spreading structure of the Troodos ophiolite, Cyprus. *Geology*, **13**, 846-850.

VEROSUB, K. L., & MOORES, E. M., 1981, Tectonic rotations in extensional regimes and their palaeomagnetic consequences for oceanic basalts. *J. Geophys. Res.*, **86**, 6335-6349.

VINE, F. J., 1966, Spreading of the ocean floor: new evidence. *Science*, **154**, 1405-1415.

VINE, F. J., & MOORES, E. M., 1969, Palaeomagnetic study of the Troodos igneous massif. *EOS*, **50**, 131.

VINE, F. J., & MOORES, E. M., 1972, A model for the gross structure, petrology, and magnetic properties of oceanic crust. *Geol. Soc. Am. Mem.*, **132**, 195-205.

VINE, F. J., POSTER, C. K., & GASS, I. G., 1973, Aeromagnetic survey of the Troodos Igneous Massif, Cyprus. *Nature (Phys. Sci.)*, **244**, 34-38.

VRIELYNCK, B, 1978a, Données nouvelles sur les zones internes du Péloponnèse, Grèce. Les massifs a l'ést de la Plaine d'Argos. *Unpubl. PhD Thesis, Université des Sciences et Téchniques de Lille*, 137pp.

VRIELYNCK, B, 1978b, Données nouvelles sur les zones internes du Péloponnèse. Les massifs a l'ést de la Plaine d'Argos (Grèce). *Annales de la géologie des pays Hélleniques*, **29**, 440-462.

VRIELYNCK, B, 1980, Précisions sur la stratigraphie du Trias d'Argolide (Péloponnèse, Grèce) et consequences structurales. *Bull. Geol. Soc France*, **7**, t.XXII, no. 3, 345-382.

WALDRON, J. W. F., 1984a, Structural history of the Antalya Complex in the 'Isparta angle', Southwest Turkey. in: DIXON, J. E., & ROBERTSON, A. H. F. (eds.), The geological evolution of the Eastern Mediterranean, *Spec. Pub. Geol. Soc. Lond.* **17**, 273-278.

WALDRON, J. W. F., 1984b, Evolution of carbonate platforms on a margin of the Neotethys ocean; Isparta angle, southwestern Turkey. *Eclogae Geologicae Helvetiae*, **77**, 553-581.

WATSON, G. S., 1956, A test for randomness of directions. *Monthly Notices R. astr. Soc, Geophys. Supp*, **7**, 160-161.

WESTPHAL, M., 1977, Comments on: "Postulated rotation of Corsica not confirmed by new palaeomagnetic data", by K. M. Storetvedt & N. Petersen. *J. Geophys.*, **42**, 399-401.

WESTPHAL, M., BAZHENOV, M. L., LAUER, J. P., PECHERSKY, D. M., & SIBUET, J.-C., 1986, Palaeomagnetic implications on the evolution of the Tethys Belt from the Atlantic Ocean to the Pamirs since the Triassic. *Tectonophysics*, **123**, 37-82.

WOODCOCK, N. H., & ROBERTSON, A. H. F., 1977a, Imbricate thrust belt tectonics and sedimentation as a guide to emplacement of part of the Antalya Complex, S. W. Turkey. *Abstracts 6th Colloquiem on the Geology of the Aegean Region, Izmir, Turkey.* p. 98.

WOODCOCK, N. H., & ROBERTSON, A. H. F., 1977b, Origins of some ophiolite-related metamorphic rocks of the 'Tethyan' Belt. *Geology*, **5**, 373-376.

WOODCOCK, N. H., & ROBERTSON, A. H. F., 1982, Wrench and thrust tectonics along a Mesozoic-Cenozoic continental margin: Antalya Complex, S. W. Turkey. *J. Geol. Soc. Lond.*, **139**, 147-163.

YOUNG, K. D., JANCIN, M., VOIGHT, B., & ORKAN, N. I., 1985, Transform deformation of Tertiary rocks along the Tjörnes Fracture Zone, North Central Iceland. *J. Geophys. Res.*, **90**, 9986-10010.

ZIJDERVELD, J. D. A., 1967, A. C. demagnetisation of rocks: analysis of results. in: COLLINSON, D. W., CREER, K. M., & RUNCORN, S. K. (eds.), *Methods in Palaeomagnetism.* Elsevier, Amsterdam, 254-286.